UNIVERSITY OF OKLAHOMA

GRADUATE COLLEGE

REGRESSION AND NEURAL NETWORK MODELING OF RESILIENT MODULUS BASED ON ROUTINE SOIL PROPERTIES AND STRESS STATES

A DISSERTATION

SUBMITTED TO THE GRADUATE FACULTY

in partial fulfillment of the requirements for the

Degree of

Doctor of Philosophy

By

ALI HONARMAND-EBRAHIMI
Norman, Oklahoma
2006

UMI Number: 3238559

UMI Microform 3238559

ProQuest Information and Learning Company
300 North Zeeb Road
P.O. Box 1346
Ann Arbor, MI 48106-1346

REGRESSION AND NEURAL NETWORK MODELING OF
RESILIENT MODULUS BASED ON ROUTINE SOIL PROPERTIES
AND STRESS STATES

A DISSERTATION APPROVED FOR THE
SCHOOL OF CIVIL ENGINEERING AND ENVIRONMENTAL SCIENCE

BY

Dr. Musharraf Zaman

Dr. Joakim G. Laguros

Dr. Gerald A. Miller

Dr. Kianoosh Hatami

Dr. Luther White

ACKNOWLEDGMENTS

I would like to express my deepest gratitude to my committee chairman, Dr. Musharraf Zaman for his patience, understanding, and believing in me for the past twenty-two years. This work would not have been completed without Dr. Zaman's guidance. My sincere appreciation and thanks goes to Dr. Joakim Laguros, Dr. Gerald Miller, Dr. Kianoosh Hatami and Dr. Luther White for serving in my committee and providing me with the information I needed during my dissertation work.

I would like to thank Mr. Chau Yih Cheong for his assistance in completing this work. My sincere appreciation also goes to the staff and engineers of Burgess Engineering and Testing, Inc., especially to Mr. Hai Ming Lim and Mr. Cheong Fung Ting for their assistance.

Finally, I would like to thank my wife Ronessa for standing by me no matter how rough the sea and the journey has been. Thank you for all your support and the two beautiful children, Esther and Ali. My appreciation also goes to my parents, Issa and Mehri, for their help and support.

TABLE OF CONTENTS

LIST OF TABLES

LIST OF FIGURES

ABSTRACT

Resilient modulus (M_R) is one of the fundamental material properties in the mechanistic analysis and structural design of roadway pavements. In the current and the proposed mechanistic-empirical design guides by AASHTO, M_R is used to characterize subgrade soils. Resilient modulus of subgrade soils are generally determined by conducting repeated load triaxial tests in the laboratory on remolded or undisturbed specimens. In the proposed AASHTO design guide, three hierarchical design levels are suggested. In Level 1, the required input values for M_R are obtained from laboratory or field tests. For Level 2 and Level 3 designs, however, the M_R values are either obtained from the agency database or from estimation through correlations with other material properties. To this end, a combined laboratory and modeling study was undertaken to develop a database for subgrade soils in Oklahoma and to develop relationships or models that could be used to estimate M_R from commonly used subgrade soil properties in Oklahoma. Specifically, two categories of models, namely statistical models and Artificial Neural Network (ANN) models, are employed for the determination of M_R based on routine laboratory test results.

Sixty-three (63) soil samples from fourteen (14) different sites throughout Oklahoma were collected and tested for the development of the database and the statistical models and the ANN models. These sites were located in Adair, Alfalfa, Choctaw, Delaware, Greer, Jefferson, Kingfisher, Lincoln, Major, McClain, Noble, Okfuskee, Osage, and Rogers counties. Additionally, thirty-four (34) soil samples from three different sites, located in Rogers and Woodward counties, were collected and tested to evaluate the developed models. The parent materials for these soil samples

were a variation of shale, alluvium, sandstone, and limestone, with a majority from alluvium and shale.

Bulk samples were collected primarily from the B-horizon and the C-horizon. These samples were hand augured according to the Oklahoma Department of Transportation (ODOT) standard sampling method from each horizon. The bulk samples were bagged and transported to the Burgess Engineering and Testing, Inc. laboratory for the routine tests. The following routine laboratory tests were conducted: Atterberg limits, wet sieving (excluding hydrometer tests), dry sieving, and moisture-density. These tests are routinely used by ODOT to characterize subgrade soils. Resilient modulus (M_R) and unconfined compression tests were also conducted.

The laboratory results from the fourteen sites from fourteen counties were used to develop the relationships or models. Data from these sites are collectively referred to as the Development Dataset. Test data from the remaining three sites are used to evaluate the developed models. These test data are collectively referred to as the Evaluation Dataset. Consequently, the development dataset contained test data from 63 soil samples, while the evaluation dataset contained test data from 34 soil samples.

The routine material parameters selected in the development of the models include moisture content (w), dry density (γ_d), plasticity index (PI), percent passing No. 200 sieve (P_{200}), and unconfined compressive strength (U_c). Bulk stress (θ) and deviatoric stress (σ_d) were used to identify the state of stress. The choice for the selection of these parameters was partly based on the ODOT requirements for conducting pedagogical soil survey. The influence of these parameters in the Mechanistic-Empirical pavement design also played a role in this selection.

Based on the ODOT specifications, two specimens were prepared and tested for resilient modulus (M_R) for each soil. One of the M_R specimens was prepared at the Optimum Moisture Content (OMC) and 95% of the maximum dry density, while the other specimen was prepared at maximum dry density and 2% wet of the OMC. This yielded one hundred twenty six M_R specimens tests for the development dataset. The M_R test results were evaluated for quality assurance. Based on the high standard deviation of M_R (in excess of 340 Mpa) and high measurement error (in excess of 30%) for loading sequences 1, 6 and 11, the M_R values corresponding to these sequences were not included in the model development. Consequently, the development dataset consisted of 1512 M_R values. A similar approach was followed in the test program for the evaluation dataset. At the conclusion of each M_R test, an unconfined compression test was performed on the same specimen. Although this test is not required by the ODOT specifications, it was included in the present study because a number of previous studies have indicated a strong correlation between M_R and unconfined compression.

Several statistical models were developed in this study. These models include: stress-based, multiple regression, polynomial, and factorial. Each model was ranked based on its R^2 (goodness of fit) and F values (significance of the model) for the development dataset. Based on the R^2 and F values, the second order polynomial and factorial models were further considered for the evaluation dataset. An evaluation of the two models indicated that for the combined development and evaluation datasets neither a second order polynomial nor a factorial model is a good statistical model for evaluating M_R from the selected routinely determined properties.

As a result, a more complex modeling technique, Artificial Neural Network (ANN), was employed. Six different models were considered in this phase, namely, Linear Network (LN), Generalized Regression Neural Networks (GRNN), Radial Basic Function Networks (RBFN), and Multi-Layer Perceptrons Networks (MLPN) with one, two and three hidden layers (MLPN-1, MLPN-2, and MLPN-3). The degree of complexity of these models increases from LN being the simplest model with no hidden layers to MLPN models. The models were ranked based on their R^2 (goodness of fit) values. Based on the R^2 values, the MLPN-2 was determined to be the best model. The back-predictions of the development dataset for the ANN models were better than their statistical counterparts. Also, a sensitivity study of the ANN models was performed. It was determined that the unconfined compression was a major contributor to the relationship between R_M and routinely determined material parameters, as reported in some previous studies. The MLPN-2 model was further evaluated to examine the effect of different moisture and density condition on the model. At this stage two additional MLPN-2 models were developed and evaluated by separating the development and evaluation datasets according to the specimens moisture content and dry density (OMC and 95% of the maximum dry density, and OMC+ 2% moisture content and maximum dry density). A careful evaluation of these two new MLPN-2 models indicated that even though these models did a reasonably good job for their respective datasets, they were incapable of extrapolation (i.e., the MLPN-2 model developed on the basis of OMC and 95% maximum dry density is unable to back predict the M_R values from the OMC+2% and maximum dry density dataset, and vice versa). Furthermore, during the sensitivity analysis it was evident that the effect of moisture content, dry density, and plasticity index were masked by the unconfined compression. However, since the thrust of this study was to develop models to be used for Level 2 and Level 3 pavement designs for Oklahoma subgrade, the MLPN-2 model that includes both moisture contents and dry densities was considered the best.

In order to illustrate the application of the developed model, the AASHTO flexible pavement design methodology was used to design asphalt concrete pavement sections. The design M_R values from three soil specimens from the evaluation dataset were calculated from the MLPN-2 model. The pavement sections determined from the experimental M_R values were compared with the pavement sections determined from the M_R values predicted by the MLPN-2 model.

The models developed in this study are expected to be useful in the Level 2 and Level 3 designs of pavements in Oklahoma. The datasets developed may be enhanced by adding additional soils from other locations in Oklahoma. Also, field studies may be undertaken to correlate laboratory and in-situ resilient moduli.

CHAPTER 1

INTRODUCTION

1.1 Background

Surface transportation plays an important role in everyday life. It is the economic lifeline between cities, states, and countries. A dependable transportation network is a key factor in increasing trade and commerce. The nation's highways reached an estimated 2.7 trillion vehicle miles in 2000 (FHWA, 2000; NCHRP, 2004). This is four times the 1960 level. This amounts to 7.4 billion vehicle miles of travel every day. Truck travel has increased 231 percent since 1970 (FHWA, 2000; NCHRP, 2004). The four million miles of U.S. roadways (with approximately two million miles of paved roads) that were constructed and rehabilitated in the past century represent a significant investment (NCHRP, 2004). With increasing population and changing life style, the need for trade has increased significantly. This in turn has led to heavier trucks and ever-increasing demand on the durability of the existing roadways (Croney and Croney, 1991; Huang, 2003). Our transportation networks are increasingly getting overburdened, and consequently the conditions of many existing roadways are deteriorating rapidly.

According to the Federal Highway Administration's 1995-1997 National Pavement Design Review, approximately eighty percent of the transportation agencies use the 1972, 1986, or 1993 versions of the American Association of State Highway and Transportation Officials (AASHTO) design guides (NCHRP, 2004). These pavement design guides are primarily based on empirical equations that were developed largely from the AASHO Road Tests conducted in the 1950's. However, since the publication of 1986 design guides, increasing efforts have been made to introduce mechanistic elements in pavement design. Introduction of mechanistic elements requires different material properties than those used before.

In an attempt to improve and streamline the design procedures, the AASHTO published the "AASHTO Guide for Design of Pavement Structure" for both flexible and rigid pavements (AASHTO, 1986). In these publications, *Resilient Modulus* (M_R) rather than subgrade support value (SSV) was recommended as a fundamental material parameter for mechanistic analysis of a multi-layered pavement system. Since then M_R has been used frequently in characterization of materials for both pavement design and evaluation. M_R is a measure of the elastic modulus of subgrade soils at a given stress level, and is defined as the ratio of an applied deviatoric stress (σ_d) to the recoverable strain (ε_r):

$$M_R = \sigma_d / \varepsilon_r \qquad (1\text{-}1)$$

Among major advantages, M_R accounts for cyclic nature of vehicular traffic loading and inelastic behavior that are particularly important for subgrade soils (AASHTO, 1986). M_R also became the fundamental parameter in the 1993 AASHTO Design Guide to describe subgrade soils. The 1993 AASHTO Design Guide is currently used by the Oklahoma Department of Transportation (ODOT) in designing roadway pavements. The 1993 AASHTO Design Guide lists four methods for determining a design M_R value. These methods are:

(a) Direct laboratory measurements of M_R;

(b) Back calculation from non-destructive testing (NDT);

(c) Estimating M_R from correlations with other material properties; and

(d) Estimating M_R from original design and construction data.

In the direct laboratory measurement of M_R, different types of laboratory testing equipment and techniques have evolved during the past two decades including resonant column, torsional shear, gyratory, and cyclic triaxial testing (AASHTO, 1986; Kim and Stokoe, 1992; George, 1992; Kim et al., 1997). The most frequently used laboratory testing, however, is the cyclic triaxial testing, which is the standard method specified by AASHTO to determine the M_R of base, subbase, and subgrade materials. Historically, even the standard method for M_R testing has undergone changes (AASHTO, 1986; 1991; 1992; 1994; 1999; NCHRP1-28, 2003). These changes have included procedural details regarding loading duration, frequency, number of cycles, loading waveform, applied stress sequence, and location of linear variable differential transformers (LVDTs) (AASHTO, 1986; 1991; 1992; 1994; 1999; NCHRP1-28, 2003).

For design of new pavement, M_R is generally determined by conducting repeated load triaxial tests in the laboratory on remolded or undisturbed samples according to the AASHTO T-307-99 test method (AASHTO, 2003). The AASHTO T-307-99 test method is a complex, time consuming and expensive test method not, particularly well suited for small projects. For the rehabilitation designs, the M_R of the existing pavement is generally determined by conducting in-situ tests according to the ASTM D4694 test method (Deflections with a Falling Weight Type Inpulse Load Device) and the D4695 test method (Guide for General Pavement Deflection Measurements). The M_R values are backcalculated from the deflection measurements according to the ASTM D5858 test method (Guide for Calculating In-situ Equivalent Elastic Moduli of Pavement materials Using Layered Elastic Theory). The in-situ tests for determination of M_R can be climatologically sensitive, such as variations in moisture content of subgrade soil. Alternatively, M_R can be determined from correlation equations involving stress state and physical properties of soils (Chen et al., 1995; Zhu, 1997; Tian et al., 1998; George, 2004; Hopkins et al., 2004), which is the subject of the current study.

Since the AASHO Road Test during the 1950's, the AASHTO Joint Task Force on Pavement (JTFP) has been responsible for development and implementation of pavement design technologies. The JTFP has been responsible for many changes and their implementations in the design guide. In response to deficiencies in the 1986 and 1993 Design Guides, the JTFP embarked on developing a new design guide based as fully as possible on mechanistic principles (NCHRP, 2004).

The 1986 and 1993 AASHTO Guide for Design of Pavement Structures has several deficiencies. Some of these deficiencies are listed below, as per a recent NCHRP report (NCHRP, 2004):

(a) Traffic loading: The heavy truck traffic volume has increased significantly and the AASHTO Design Guides may not be used with reliability to model the traffic loads.

(b) Climatic loading: The AASHTO Design Guides are based on the AASHO climatic loading conditions and do not consider the national variations in this loading condition.

(c) Truck characterization: The vehicular characterization such as axle distribution, loading or tire pressures has changed since the AASHO Road Test of 1950's. Such changes have affected the traffic loading and the level of reliability in the overall design.

(d) Rehabilitation: The AASHO Test Road did not consider pavement rehabilitation. The 1993 AASHTO Design Guide uses a very limited and completely empirical procedure for pavement rehabilitation.

(e) Subgrade material: The AASHO Road Test was conducted on one type of subgrade material and did not consider possible changes in subgrade materials nationwide.

(f) Surface material: The AASHO Road Test used one type of hot mix asphalt (HMA) and one type of Portland cement concrete (PCC) mix. There has been an explosion in introduction and use of new materials as surface materials.

(g) Base course: The AASHO Road Test used only two types of unbound dense granular bases/subbases. Today there are various methods and types of stabilization available for heavily traveled roadways.

(h) Construction and drainage: The AASHO Road Test used the design, material and construction practices of the late 1950's with no subdrains. In today's construction practice, subdrains are used routinely for many projects.

(i) Design life: The AASHO Road Test was conducted for two years and did not consider the long term effect of climatic loading or aging of materials. Today pavements are routinely designed for 20 years.

(j) Performance: The AASHTO Design Guides relate the thickness of the pavement surface layer to serviceability. It has been determined that many pavements need surface layer rehabilitation due to thermal cracking or faulting. These types of failures were not considered in the AASHTO Design Guides.

(k) Reliability: The 1986 AASHTO Design Guide provides a procedure for design reliability. This procedure applies a large multiplier to the traffic load to achieve the reliability level. This procedure has never been validated.

As a result of these deficiencies and the empirical nature of the current AASHTO Design Guide, the 2002 AASHTO Guide for Design of Pavement Structures was proposed and is currently in the evaluation stage. The 2002 AASHTO Design Guide is based on mechanistic-empirical procedures, and it addresses some of the deficiencies of the current AASHTO Design Guide. Specifically, it includes three hierarchical design levels to match the inputs with the level of project importance. The following hierarchical design levels are included (NCHRP, 2004):

(a) Level 1: Inputs provide for the highest level of accuracy and the lowest level of uncertainty or error. This level would be used for designing heavily traveled pavements. Level 1 material inputs require laboratory or field testing, site specific axle load spectrum data collection, or non-destructive deflection testing.

(b) Level 2: Inputs provide an intermediate level of accuracy and is the closest to the current procedures adopted by the AASHTO design guides. Level 2 inputs would be user selected, possibly from agency database or from limited testing program or could be estimated through correlations. The present study is intended to address this issue.

(c) Level 3: Inputs provide the lowest level of accuracy. The inputs are based on typical regional averages.

The 2002 Design Guide recommends the following three methods for determination of M_R for analysis and design of pavements:

(a) Laboratory repeated load M_R test;

(b) Analysis or backcalculation of NDT data; and

(c) Correlation with other material properties.

The present study is conducted to evaluate and develop correlations between the M_R and other routine soil properties. The results from this study could be used for both the currently used 1986 and 1993 AASHTO Design Guides and the level 2 and level 3 recommendations of the 2002 AASHTO Design Guide.

1.2 Objectives and Study Tasks

As pointed out in the 1993 AASHTO Design Guide and the proposed 2002 AASHTO Design Guide for level 2 and level 3 design efforts, M_R can be determined from models or correlation equations involving commonly used soil properties. As discussed in Chapter 2, Farrar and Turner (1991), Santha (1994), Dai and Zollars (2002), Yau and Von Quintus (2002), and Rahim and George (2004) have developed correlation equations to predict M_R from conventional soil properties. The objective of the present study is to develop similar models for some commonly encountered subgrade soils in Oklahoma. The models developed in this study consider both stresses (deviatoric stress and bulk stress) and commonly used properties (unconfined compressive strength, dry density, moisture content, gradation, and Atterberrg limits) to predict the M_R of subgrade soils in Oklahoma. These parameters were selected partly because in the past decade the

Oklahoma Department of Transportation (ODOT) has been collecting these data in conjunction with the M_R values on different subgrade soils throughout the State. The author, through Burgess Engineering and Testing, Inc., has conducted many geotechnical projects for ODOT and has played a key role in the development of a useful database for the implementation of level 2 and level 3 in the 2002 Design Guide. The models developed in this study are based on the M_R test results and aforementioned soil properties evaluated by the author. The more specific tasks of the present study include the following:

(a) Conduct statistical analyses to develop correlations between the M_R values and deviatoric stress, bulk stress, unconfined compressive strength, dry density, moisture content, gradation, and plasticity index. Models of different complexities are explored as part of this task.

(b) Examine the strengths and the weaknesses of the developed statistical models using additional M_R test results that are not used in the development of these models.

(c) Develop Artificial Neural Network (ANN) based models to predict resilient modulus of subgrade soils as a function of factors that are used in the development of the statistical models.

(d) Verify the strengths and the weaknesses of the ANN models using additional M_R test results that are not used in the development of these models.

(e) Make a relative comparison between the statistical models and the ANN models and perform sensitivity studies.

(f) Demonstrate application of the developed models in a typical pavement design project in Oklahoma.

1.3 Format of the Dissertation

This dissertation is divided into eight chapters. Following introduction and objectives in Chapter 1, Chapter 2 provides a detailed literature review focusing on M_R, its influential factors, and the existing statistical and ANN models that attempted to correlate M_R with different variables. Chapter 2 also includes a review of the statistical and ANN models that are used in the present study. The procedures used in laboratory tests are presented in Chapter 3. The laboratory tests employed in the present study consist of routine soil property tests as well as M_R tests. Chapter 4 presents the results of the laboratory tests. Statistical analyses for the laboratory test results are also presented in this chapter. Chapter 5 presents the development and evaluation of the statistical models. The development and evaluation of the ANN models along with the sensitivity analysis are presented in Chapter 6. A demonstration of a developed ANN model in typical pavement design is presented in Chapter 7. Finally, the conclusions and recommendations of this study are presented in Chapter 8. The laboratory test data and the results of the analyses from the statistical and the ANN models are presented in Appendices.

CHAPTER 2

LITERATURE REVIEW

2.1 Introduction

Pavement design provides a combination of materials that serves the traffic load for the design period over existing soils and environmental conditions. Failure to properly characterize the traffic and environmental loads and existing soil strength will lead to improperly designed pavements. The traffic loads are determined based on present and future growth (Huang, 2003). Climatic conditions are included in the design based on their effect on the material parameters, and the strength of subgrade soils is determined based on laboratory and/or field tests (George, 2004). As noted by Yoder and Witczak, (1975) "all pavements derive their ultimate support from the underlying subgrade, therefore, knowledge of basic soil mechanics is essential."

In 1986, the American Association of State Highway and Transportation Officials (AASHTO) proposed a pavement design procedure. This procedure incorporated a new material parameter, called *Resilient Modulus* (M_R), to describe the deformation characteristics of pavement materials under repeated traffic loading. M_R was to replace the soil support value (SSV) that was proposed in the AASHTO guide for design of pavement structures in 1961 and in the later revision of 1972. The 1986 AASHTO guide introduced M_R as a design parameter since it indicates a basic material property that may be used in mechanistic analysis of multi-layered systems (Huang, 2003).

The 1993 AASHTO Design Guide retained M_R as the fundamental parameter to describe the subgrade soil characteristics. The 1993 AASHTO Design Guide is currently used by the Oklahoma Department of Transportation (ODOT) in pavement design. The 1993 AASHTO Design Guide lists four methods for determining a design M_R value. These methods are:

(e) Direct laboratory measurements of M_R;

(f) Backcalculation of M_R from non-destructive testing (NDT);

(g) Estimating M_R from correlations with other material properties; and

(h) Estimating M_R from original design and construction data.

In the direct laboratory measurement, M_R is usually determined by conducting repeated load triaxial tests on remolded or undisturbed samples according to the AASHTO T-307-99 test method (AASHTO, 2003). The direct laboratory measurement of M_R is normally used in the design of new pavements. For designs involving rehabilitation, the M_R of the existing pavement is determined by conducting in-situ testing along the existing roadway according to the ASTM D4694 (Deflections with a Falling Weight Type Inpulse Load Device) and the ASTM D4695 (Guide for General Pavement Deflection Measurements) test methods. The M_R values are backcalculated from the deflection measurements according to the ASTM D5858 (Guide for Calculating In-situ Equivalent Elastic Moduli of Pavement materials Using Layered Elastic Theory) test method. Alternatively, M_R can be determined from correlation equations involving stress state and physical properties of subgrade soils.

In response to deficiencies of the 1986 and 1993 Design Guides listed in Chapter 1, the AASHTO Joint Task Force on Pavement (JTFP) embarked on developing a new design guide based as fully as possible on mechanistic principles. As a result, the 2002 AASHTO Guide for Design of Pavement Structure was proposed and is currently in the evaluation stage. The proposed design guide will have three hierarchical design levels to match the inputs with the project importance level. The following hierarchical design levels are considered (NCHRP, 2004):

(d) Level 1: Inputs provide for the highest level of accuracy and the lowest level of uncertainty or error. This level would be used for designing heavily traveled pavements. Level 1 material inputs require laboratory or field testing, site specific axle load spectrum data collection, or non-destructive deflection testing.

(e) Level 2: Inputs provide an intermediate level of accuracy and is the closest to the current procedures adopted by the AASHTO design guides. Level 2 inputs would be user selected, possibly from an agency database or from limited testing program or could be estimated through correlations.

(f) Level 3: Inputs provide the lowest level of accuracy. The inputs are based on typical regional averages.

The proposed design guide recommends three methods for determination of the layered M_R for pavement design and analysis. The following three methods are suggested:

(d) Repeated load M_R testing in the laboratory;

(e) Analysis or backcalculation of NDT data; and

(f) Correlations with other properties of the associated materials.

The three methods of obtaining M_R in the 2002 AASHTO Design Guide are similar to those specified in the 1993 AASHTO Design Guide. The primary difference is the correlation of M_R with other material properties, for level 2 and level 3 designs (NCHRP, 2004).

2.2 Resilient Modulus

The AASHTO design guide treats M_R as an indicator of material behavior under repeated vehicular loading (AASHTO, 1986). When a pavement is subjected to a repeated vehicular load, a dynamic stress pulse is transmitted to the base, the subbase, if any, and to the subgrade. Under a given applied stress, the base, subbase, and subgrade deform as a layered system, causing total deformation of the pavement. The total deformation of a pavement can be divided into two parts, namely a resilient or recoverable deformation and a permanent deformation, as shown in Figure 2-1[†]. The recoverable deformations of the associated materials are characterized by their M_R values. Specifically, it is a measure of the elastic property of the subgrade soil recognizing certain nonlinear characteristics (AASHTO, 1986). The M_R can be mathematically defined as the deviatoric stress (σ_d) divided by the recoverable strain (ε_r).

$$M_R = \frac{\sigma_d}{\varepsilon_r} \qquad (2\text{-}1)$$

A pictorial representation of Equation 2-1 is shown in Figure 2-1.

2.3 Determination of Resilient Modulus From Laboratory and In-situ Testing

Although the concept of M_R is relatively simple, its determination is not as straightforward. Researchers have developed several methods to determine the M_R value for a given subgrade soil. The M_R of a pavement material may be determined using either laboratory testing or in-situ testing, as outlined below.

[†] Figures are presented at the end of each chapter

2.3.1 Laboratory Test

As noted earlier, the 1986 AASHTO Guide and the subsequent 2002 Guide utilize M_R for characterizing behavior of subgrade soils under vehicular traffic (AASHTO, 1986; 1991; 1992; 1994; 1999; NCHRP1-28, 2003). One of the most widely used test methods for the determination of M_R in the laboratory is cyclic triaxial testing. AASHTO proposed a series of cyclic triaxial testing procedures for the determination of M_R of base, subbase, and subgrade materials under repeated vehicular loading. Different versions of the M_R test procedures were released by AASHTO in 1986, 1991, 1992, 1994, and 1999.

Major modifications were introduced to address the findings of many studies in the following order: AASHTO T292-91I in 1991, AASHTO T294-92I in 1992, AASHTO T294-94 in 1994, and AASHTO T307-99 in 1999. The AASHTO T307-99 test method was used in the present study for the determination of M_R of subgrade soils. The basic differences among these testing procedures are applied loading sequences, method of measurement of axial deformation and confining pressure, and number of loading cycles (Pandey, 1996; AASHTO, 2003). A comparison of the applied loading sequences in AASHTO T292-91I, T294-92I, T294-94, and T307-99 test methods, for granular materials, is summarized in Table 2-1. The AASHTO T292-91I test method started from a confining stress of 138 kPa (20 psi) and decreased to 21 kPa (3 psi), but in the latest version (T307-99 (2003)) the confining stress sequence was reversed (i.e. low to high). Also, the AASHTO T292-91I test method only required 50 loading cycles for each loading sequence, while the latest version (T307-99 (2003)) required 100 loading cycles for each loading sequence. Moreover, the loading sequences for base and subbase materials are significantly different from the loading sequences for subgrade materials, as evident from Table 2-2. For base or subbase materials the test starts with a confining stress of 21 kPa (3 psi) and increases to 138 kPa (20 psi), in five different levels of confining stress. However, for subgrade materials, the test starts with a confining stress of 41 kPa (6 psi) and decreases to 14 kPa (2 psi), in three different confining stress levels instead of five. Also the base or subbase materials are subjected to higher axial stress levels than subgrade materials. The axial stress levels in base or subbase materials range from 21 kPa (3 psi) to 276 kPa (40 psi), while for subgrade materials the axial stress levels range from 14 kPa (2 psi) to 69 kPa (10 psi).

2.3.2 In-situ Test

In addition to laboratory testing, the M_R values can be determined using in-situ testing. The most common method for the determination of M_R in the field involves the use of Falling Weight Deflectometer (FWD). It FWD is a non-destructive test method. It uses a backcalculation approach to determine the M_R values of each pavement layer from the deformation profile data. FWD is a very useful test procedure for the health monitoring of existing flexible and rigid pavements (Ashraf and George, 2003; George et al., 2004). Due to the nature of the test, it collects a significant amount of data along the segment of the roadway being tested. One of the advantages of this test method is that it does not require any costly sample collection and laboratory testing, except thickness of each layer. This method is also used on a new roadway alignment to determine the M_R values of the base and the subgrade materials for use in pavement design. The FWD is performed when the roadway dirt work is completed. The results from the FWD is the analyzed and the pavement is designed based on the subgrade condition.

Among drawbacks, FWD requires that the backcalculation approach be calibrated by determining the layer thicknesses (Pandey, 1996; George et al., 2004). The results from the FWD test apply only to a particular condition at which the test is performed, namely the season, the surface temperature, and the moisture condition of the base and subgrade materials (Pandey, 1996; George, 2003; George et al., 2004). Other factors affecting the FWD test results include asphalt pavements less than 3 inches in thickness or shallow bedrock (Gurp et al., 2000; Chen et al., 2001; Nazzal, 2003).

2.3.3 Comparison of Laboratory and In-situ Test Results

Ping and Ge (1996) conducted a study to compare the M_R values obtained from the field testing with the laboratory testing on subgrade soils. In their study, the field results were obtained from the plate load test, whereas the cyclic triaxial tests were performed according to the AASHTO T292-91I test method to obtain the laboratory results. Remolded soil samples simulating the field moisture and density conditions were used in the laboratory tests. From the results of that study, the average values of the layer modulus backcalculated from the field plate test were in reasonable agreement with the M_R values from the laboratory test, based on the average applied stress in the elastic range of the load-deflection curve (Ping and Ge, 1996).

George and Uddin (1996) examined the application of a gyratory testing machine (GTM) to verify the M_R of soils from the GTM with backcalculated values from the FWD test. The GTM is a combination of kneading and compaction in order to simulate the abrasion effects caused by moving load and inter-granular movement within the mass of material in a flexible pavement structure, while permitting any desired gyratory angle (degree of shear strain) (George and Uddin, 1996). Evaluation of the application was accomplished by testing fine grained and coarse grained subgrade soils using both the conventional cyclic triaxial testing and the GTM testing. Dynaflect and falling weight deflectometer (FWD) were also used for backcalculation. The experimental results showed the M_R values from the GTM to be considerably lower than the M_R values from the repeated load triaxial test. Conversely, the zero-degree kneading M_R values for coarse grained soils were greater than the triaxial RM but were lower than or equal to the kneading M_R values for fine grained soils (George and Uddin, 1996). Additionally, the in-situ backcalculated values for both the Dynaflect and FWD were larger than the triaxial resilient modulus values. Overall, George and Uddin (1996) found that the GTM modulus compared poorly with the triaxial modulus and no significant correlation between the kneading M_R and the backcalculated moduli was evident. These researchers, however, believed that 0.1 degree GTM test could be modified for possible use in the resilient characterization of subgrade soils.

Overall, most researchers consider the cyclic triaxial testing to be appropriate for pavement design since the tests are conducted under controlled conditions (Uzan, 1985; Thompson and Smith, 1990; Pandey, 1996; Zhu, 1997; Russell and Hossain, 2000). It has been pointed out that cyclic triaxial testing is time consuming and expensive, and not particularly well suited for small projects.

2.4 Variability in Resilient Modulus Testing

The accuracy and precision in the measurement of M_R is very important in the design and analysis of a pavement. To examine the variability in M_R results, duplicate tests are often conducted, at least on selected samples. A number of studies have examined the effect of stress states, load sequences, number of cycles, placement of the linear variable differential transducers (LVDT), and other pertinent factors.

The effect of stress level and stress path on M_R values can be significant. As presented in Table 2-1 and Table 2-2, comparing the T292-91I and T294-94 test methods, the T292-91I test starts at a high stress level and terminates at a lower stress level. The T294-94 test method, on the other hand, starts at a low stress level and terminates at a higher stress level. According to Chen et al. (1995), keeping other factors constant, the M_R values of granular materials may change by as much as 55 percent due to different stress paths.

Houston et al. (1994) investigated the effect of laboratory-imposed stress state on M_R values of subgrade specimens. Also, they examined the effect of overstressing and insufficient preconditioning in the AASHTO T274-82 test method. The overstressing of the normal and shear stresses was found to have different effects on a soil specimen. If the normal stress of a specimen is overstressed, the measured M_R will generally be higher than the in-situ value (Houston et al., 1994). On the other hand, overstressing of the shear stress caused an opposite effect, producing a lower M_R value than the overloading with respect to normal stress. It should be noted that the normal and shear stress levels in the AASHTO T274-82 test method are well beyond the stress levels anticipated in the field (Houston et al., 1994).

Besides overstressing, the number of loading cycles in M_R testing has been studied by several researchers. For example, Khedr (1985) investigated the M_R values versus the number of load repetitions up to 10,000 cycles. It was reported that the M_R

values reached a stable value after approximately 100 loading cycles (Zhu, 1997). According to Zhu (1997), the M_R values from the first fifty cycles and the last five cycles were very close, indicating that the M_R values stabilize after a few loading cycles. Houston, et al. (1994) discussed the problem of preconditioning in the AASTHO T274-82 test method. Houston et al. (1994) recommended 1000 cycles of loading per stress state for preconditioning at low to moderate stress levels. For a high stress level, 2000 cycles of each stress state were recommended. Later, the AASHTO T292-91I and the latest version of the test methods required 500 to 1000 loading cycles in preconditioning and 100 loading cycles for each stress sequence.

The measurement of deformation using LVDT is another important issue in M_R testing. Mohammad et al. (1994) used an internal LVDT system to study the effect of LVDT location on the M_R values. The LVDTs were placed at the end and in the middle one third of the test specimens. The M_R values were higher for the LVDTs located in the middle one third than at the end of a specimen. The study by Ping and Ge (1996) also reported similar results. Ping and Ge (1996) used two LVDTs positioned in the middle half of a specimen, and the other two LVDTs were placed at the top of the specimens. The results from the middle half LVDTs showed higher M_R values than those from the top LVDTs. One of the reasons for the lower M_R values from the top LVDTs is the error induced by the LVDT measurements. These errors could be caused by the air gaps between the specimen and accessories such as porous stones and platens, as well as imprecise sample alignments and bedding problems. These problems are often called the end effects (Ping and Ge, 1996).

2.5 Influence of Resilient Modulus on Pavement Performance

The M_R is an indicator of pavement performance. A stronger pavement has higher layer coefficient, meaning higher M_R values. There are several factors that influence the overall M_R of a pavement structure. As such, these factors are important in the design of a pavement. A number of previous studies have examined the factors that influence the M_R values of pavement layers.

Long, Hossain, and Gisi (1996) studied the seasonal variation of backcalculated subgrade moduli at four selected sites in Kansas with monthly variations in temperature, subgrade moisture, and FWD deflection data. Subgrade moduli were backcalculated using the elastic layer theory in a commercially available software, MODULUS 6.0, and using the AASHTO calculation schemes. The subgrade layer was subdivided into a compacted subgrade layer and a natural soil subgrade layer. This scheme resulted in compacted subgrade moduli that were more sensitive to the seasonal variations in moisture and temperature for all sites, while the natural subgrade modulus did not vary significantly with season. However, the magnitude of variation of natural subgrade moduli was similar to that of the combined subgrade moduli. Both the MODULUS 6.0 and the AASHTO backcalculation schemes exhibited lower subgrade moduli for FWD testing in unusually higher pavement surface temperatures, especially for cohesive subgrade soils. This study suggests that the most decisive factor with respect to subgrade response is moisture content.

Subsequently, Drumm et al. (1997) published the results of a study on the changes in M_R as a function of saturation. A series of M_R tests were conducted on soils with different moisture contents to investigate the variation in M_R due to the increase in post compaction water content. Triplicate specimens were prepared for eleven soils throughout Tennessee, with each specimen prepared at optimum moisture content and maximum dry density. One specimen was tested at optimum saturation, and the other two were tested at increasing levels of saturation. The increase in the degree of saturation was achieved by backpressure. Test results showed that the M_R decreased with an increase in saturation. The magnitude of reduction in M_R was found to depend on the soil type. The soils with the highest M_R values were found to decrease the most. A method was proposed to correct the resilient modulus for increasing degree of saturation and the method supports the procedure described by AASHTO (Drumm et al., 1997).

Ping, Yang, and Ho (1998) discussed the results of an experimental program utilizing a test-pit facility to determine the M_R of compacted granular subgrades under various moisture conditions. The primary objective of their study was to evaluate the resilient moduli of subgrade materials in Florida under various moisture conditions in the test–pit (Ping et al., 1998). Five typical subgrade soils were tested under various moisture conditions, namely optimum, soaked, and drained. The results showed that the moisture conditions had significant effects on the M_R values. A high M_R could be obtained under the drained condition (with low degree of saturation), whereas the M_R under soaked condition (high degree of saturation) could be reduced to as low as 20% of the M_R values under the drained condition. A degree of saturation of approximately 80% to 90% for granular materials may be sufficient to take the most critical moisture condition into consideration for determining the M_R values from laboratory tests (Ping et al., 1998).

Mohammad et al. (1996) also studied the influence of moisture content variations on the M_R of subgrade soils. Emphasis was placed on the variation in moisture content as a result of seasonal and environmental fluctuations. These researchers also attempted to identify the properties of specimens that are prepared on the drier or wetter side of the optimum moisture content (OMC) because of prevalent field conditions. Two soil types, sand and silty clay, compacted at above and below the OMC, were tested using the AASHTO T-294 test method (Mohammad et al., 1996). Two internal LVDTs were used to measure the displacement. The LVDTs were placed at the ends of the specimens and at the middle one-third of the specimen. It was observed that the sand specimens exhibited higher M_R values at both dry and wet sides of the optimum than at OMC. The high M_R values at dry side of OMC contributed to higher strength. However, these researchers believed that high M_R values at wet side of optimum were due to some leakage problems. Overall, the statistical variations in M_R due to change in moisture content in clay were more predominant. Mohammed et al. (1996) concluded from their tests that clay had low M_R when the moisture content was on the higher side of optimum. This was due to the smaller cohesion and friction angle and high positive pore pressure that would decrease the effective stresses and the shear strength of clay specimens. Conversely, the variations among three moisture contents for sand specimens were relatively small because of high permeability of these specimens (Mohammed et al., 1996).

In a number of studies conducted on clayey subgrade soils in Kentucky, it was observed that the M_R can change significantly due to the change in moisture contents (Hopkins and Beckham, 2000; Hopkins et al., 2002; Hopkins et al., 2004). Based on the in-situ California Bearing Ratio (CBR) values measured over a 12-year period on a route in Kentucky, Hopkins et al. (2002, 2004) showed that the clayey subgrade soils tend to increase in overall moisture content and decrease in bearing strength with increasing time. Hence, the M_R decreased from the initial values obtained immediately after compaction to a lower value obtained after a period of time. In the study by Hopkins and Beckham (2000), the CBR values of soaked and unsoaked clayey soil specimens were compared. It was shown that the CBR values differed significantly between the soaked and unsoaked specimens. The M_R values decreased as the specimens were soaked in water for a period of time.

In a study conducted by Kamal et al. (1996), the mechanical behavior of unbound granular materials in pavements was investigated through field and laboratory evaluations of M_R. From their study, it was evident that the M_R values increased from a finer to a coarser mix. Conversely, the shear strain and the volumetric strain exhibited a reduction. A slight increase in M_R with increasing deviatoric stress was also observed. This observation was more noticeable at higher M_R values. With respect to plastic behavior, resistance to permanent deformation for a well-graded sample was found to increase as the gradation shifted from finer to coarser. In the course of the failure test, the shear strength was found to increase as the gradation changed from finer to coarser (Kamal et al., 1996). Full scale pavement tests using in-situ dynamic cone penetrometer, FWD, and deflectograph testing showed that materials with more fines have a higher deflection. Also, the elastic modulus was found to increase as the gradation became coarser (Kamal et al., 1996).

Swelling is another important property to characterize soil behavior. The soil swelling is defined as the changes in volume when the moisture contents increase (Annamalai et al., 1975; Kariuki and Van Der Meer, 2004). The swelling potential or swelling index is often used to characterize the swelling characteristics of soil. Several researchers have developed equations to determine the swelling index. Annamalai et al. (1975) examined twenty-four Oklahoma shales to find possible correlations for the volume change in terms of moisture-density, clay content, liquid limit, plasticity index, and reaction potential. Based on that study, the reaction potential and plasticity index were found to correlate well with volume change (Annamalai et al., 1975). A more recent study by Kariuki and Van Der Meer (2004) used correlations between various indices and the potential volume change to determine a unified swelling potential index for expansive soils. These indices include Atterberg limits, coefficient of linear extensibility (COLE), cation exchange capacity (CEC), and saturated moisture content (SP). The results showed that the most highly correlated indices were closely associated with clay type; these indices, namely CEC, PI, SP, and LL, are an indicator of the potential volume change a clay-type soil is expected to exhibit (Kariuki and Van Der Meer, 2004).

2.6 Determination of Resilient Moduli from Correlations with Other Soil Properties

Determination of M_R from laboratory and/or in-situ test results may be too expensive and time consuming for certain applications, particularly for small projects. As outlined in the 1993 AASHTO Guide for Design of Pavements, several researchers have attempted to develop empirical correlations to estimate resilient moduli in terms of other soil properties. Different models have been developed to represent M_R as a function of stresses. One of the commonly used models is the power model (Dunlap, 1963; Seed et al., 1967; Moossazadeh and Witczak, 1981; May and Witczak, 1981; Yau and Von Quintus, 2002; NCHRP, 2003; Hopkins et al., 2004). In this model, the M_R is expressed as a function of the deviatoric stress (σ_d) and the bulk stress ($\theta = \sigma_1 + \sigma_2 + \sigma_3$) as follows:

For cohesive soil,

$$M_R = a(\sigma_d)^b \quad (2\text{-}2)$$

For granular soil,

$$M_R = k_1(\theta)^{k2} \quad (2\text{-}3)$$

$$\theta = \sigma_d + 3(\sigma_3) \quad (2\text{-}4)$$

where a, b, k_1, and k_2 are regression constants, and θ is the bulk stress, σ_3 being the confining pressure. A number of experimental studies have shown that k_1 and k_2 are inversely correlated, as shown in Figure 2-2 (Rada and Witczak, 1981; FHWA, 2002).

According to Dunlap (1963), the confining pressure (σ_3) is correlated with the M_R as follows:

$$M_R = k_1(\sigma_3/P_a)^{k2} \quad (2\text{-}5)$$

where P_a is a reference pressure (e.g., atmospheric pressure) and k_1 and k_2 are the regression coefficients.

Seed et al. (1967) suggested that the M_R could be correlated with the bulk stress, as follows:

$$M_R = k_1(\theta/P_a)^{k2} \quad (2\text{-}6)$$

Note that this is a non-dimensional equation. Equations (2.3) and (2-6) are essentially the same, one is dimensional while the other is dimensionless.

Another model proposed by May and Witczah (1981) and by Uzan (1985) includes the principal stresses and deviatoric stress in the M_R function, as shown below:

$$M_R = k_1(\theta/P_a)^{k2}(\sigma_d/P_a)^{k3} \quad (2\text{-}7)$$

Besides the power model, Thompson and Robnett (1976) proposed a bi-linear model to correlate M_R of subgrade soils with deviatoric stress using two linear lines having different slopes, as given below:

$$M_R = k_1 + k_2\,\sigma_d \qquad \text{when } \sigma_d < \sigma_{di} \quad (2\text{-}8)$$

$$M_R = k_3 + k_4\,\sigma_d \qquad \text{when } \sigma_d > \sigma_{di} \quad (2\text{-}9)$$

where σ_{di} is deviatoric stress at which the slope of M_R versus σ_d changes and k_1, k_2, k_3, and k_4 are regression constants (k_2 and k_4 are usually negative). A typical bi-linear model is shown in Figure 2-3. The breakpoint M_R, the M_R value at σ_{di}, was often used to characterize the resilient properties of subgrade soils (Thompson and Robnett, 1976).

Other researchers utilized other soil property indices to estimate M_R. For example, Yau and Von Quintus (2002) studied the M_R data obtained from the LTPP test sections. It was observed that the physical properties of the unbound materials and soils could be correlated with the M_R values. They developed different equations for different soil types using a nonlinear regression technique. The equations proposed by these researchers could be generically expressed as follows:

$$M_R = k_1\,P_a\,(\theta/P_a)^{k2}\,[(\tau_{oct}/P_a)+1]^{k3} \quad (2\text{-}10)$$

where τ_{oct} is the octahedral shear stress, and k_1, k_2, and k_3, are the regression constants that are related to physical properties of soils, as below.

For coarse-grained sandy soils:

$$k_1 = 3.2868 - 0.0412\ P_{3/8} + 0.0267\ P_4 + 0.0137\ (\%Clay) + 0.0083\ LL - 0.0379\ w_{opt} - 0.0004\ \gamma_s \quad (2\text{-}11)$$

$$k_2 = 0.5670 + 0.0045\ P_{3/8} - 2.98\text{x}10^{-5}\ P_4 - 0.0043\ (\%Silt) - 0.0102\ (\%Clay) - 0.00411\ LL + 0.0014\ w_{opt} - 3.41\text{x}10^{-5}\ \gamma_s - 0.4582\ (\gamma_s/\gamma_{opt}) + 0.1779\ (w/w_{opt}) \quad (2\text{-}12)$$

$$k_3 = -3.5677 + 0.1142\ P_{3/8} - 0.0839\ P_4 - 0.1249\ P_{200} + 0.1030\ (\%Silt) + 0.1191\ (\%Clay) - 0.0069\ LL - 0.0103\ w_{opt} - 0.0017\ \gamma_s + 4.3177\ (\gamma_s/\gamma_{opt}) - (\gamma_s/\gamma_{opt}) - 1.1095\ (w/w_{opt}) \quad (2\text{-}13)$$

For Fine-grained silty soils:

$$k_1 = 1.0480 + 0.0177\ (\%Clay) + 0.0279\ PI - 0.0370\ w \quad (2\text{-}14)$$

$$k_2 = 0.5097 - 0.0286\ PI \quad (2\text{-}15)$$

$$k_3 = -0.2218 + 0.0047\ (\%Silt) + 0.0849\ PI - 0.1399\ w \quad (2\text{-}16)$$

For Fine-grained clayey soils:

$$k_1 = 1.3577 + 0.0106\ (\%Clay) - 0.0437\ w \quad (2\text{-}17)$$

$$k_2 = 0.5193 - 0.0073\ P_4 + 0.0095\ P_{40} - 0.0027\ P_{200} - 0.003\ LL - 0.0049\ w_{opt} \quad (2\text{-}18)$$

$$k_3 = 1.4258 - 0.0288\ P_4 + 0.0303\ P_{40} - 0.0521\ P_{200} + 0.0251\ (\%Silt) + 0.0535\ LL - 0.0672\ w_{opt} - 0.0026\ \gamma_{opt} + 0.0025\ \gamma_s - 0.6055\ (w/w_{opt}) \quad (2\text{-}19)$$

where $P_{3/8}$ = Percent passing 9.5 mm (3/8″) sieve,

P_4 = Percent passing 4.75 mm (No. 4) sieve,

P_{40} = Percent passing 0.425 mm (No. 40) sieve,

P_{200} = Percent passing 0.075 mm (No. 200) sieve,

%Clay = Percent clay,

%Silt = Percent silt,

LL = Liquid limit,

w = Moisture content of the sample,

w_{opt} = Optimum moisture content ,

γ_s = Dry density of the sample, kg/m^3, and

γ_{opt} = Optimum dry density, kg/m^3.

Dai and Zollars (2002) suggested a different model to correlate the M_R to physical properties of subgrade soils. Shelby tube samples were collected from six different pavement sections of the Minnesota Road Research project. Soil properties and M_R tests were conducted. Based on the test results, the following equations were developed:

$$M_R = k_1 \, \theta^{\,k2} \, \sigma_d^{\,k3} \qquad (2\text{-}20)$$

where k_1, k_2, and k_3, are regression constants that are related to physical properties of the soils as follows:

$$k_1 = 5770.8 - 520.98\,(\gamma_s)^{0.5} - 3941.8\,(w_c)^{0.5} + 33.1\,PI - 36.62\,LL - 17.93\,P_{200} \qquad (2\text{-}21)$$

$$k_2 = -5.334 + 0.000316\,(\gamma_s)^3 + 9.686\,(w_c) - 0.054\,PI + 0.046\,LL + 0.022\,P_{200} \qquad (2\text{-}22)$$

$$k_3 = 409.9 - 306.18\,(\gamma_s)^{0.1} - 82.63\,(w_c) + 0.033\,PI + 0.138\,S - 0.041\,LL \qquad (2\text{-}23)$$

where PI = Plastic index, and

S = Degree of saturation.

However, the relationships presented in the study by Dai and Zollars (2002) were based on soils with physical index properties within a narrow range. Therefore, the predictability of their model for other soils may be questionable (George, 2004).

Li and Selig (1994) proposed another approach to estimate the M_R values of fine-grained soils using the effect of physical state, stress state, and soil type. The following equations were proposed:

$$R_{m1} = 0.98 - 0.28(w - w_{opt}) + 0.029(w - w_{opt})^2 \qquad (2\text{-}24)$$

where $R_{m1} = M_R / M_{R\,(opt)}$ for the case of constant dry density; M_R = resilient modulus at a given moisture content, and w (%), and $M_{R\,(opt)}$ represent resilient modulus at maximum dry density and optimum moisture content, w_{opt} (%), respectively.

$$R_{m2} = 0.96 - 0.18(w - w_{opt}) + 0.0067(w - w_{opt})^2 \qquad (2\text{-}25)$$

where $R_{m2} = M_R/M_{R\,(opt)}$ for the case of constant compactive effort and M_R = resilient modulus at a given moisture content

Equation (2-24) accounts for the constant dry density, while Equation (2-25) accounts for constant compactive effort. The effect of stress state is determined by a set of equations that relate M_R at optimum moisture content to deviatoric stress so that the parameters of the equation represent the effect of soil type. A comparison of the tested and the estimated M_R values showed that their approach is simple and straightforward, and yet, accurately estimated the M_R of compacted fine-grained subgrade soils (Li and Selig, 1994).

Lee et al. (1997) studied the M_R of cohesive soils, mainly clayey subgrade soils, with repeated loading triaxial test. The test specimens were compacted with the custom-compaction method. To evaluate the custom-compaction method, the specimens were compacted with standard and modified Proctor methods. The results demonstrated that the custom-compaction results were in close agreement with the maximum dry unit weight and optimum moisture content from the standard and modified Proctor tests. The M_R test was performed according to the AASHTO T274-82 test method. Regression analyses were conducted to obtain a relationship between M_R and the stress in unconfined compression test causing 1% strain for laboratory compacted specimens. The relationship between M_R and stress in unconfined compression test causing 1% strain ($S_{U1.0\%}$) for a given soil was unique regardless of moisture content and compaction effort (Lee et al., 1997). The results showed that the M_R and $S_{U1.0\%}$ vary with the moisture content in a similar manner. Furthermore, four different compactive efforts were used in that study, but a single relationship between M_R and $S_{U1.0\%}$ was obtained as presented in Equation (2-26).

$$M_R = 695.4\ (S_{U1.0\%}) - 5.93\ (S_{U1.0\%})^2 \qquad \text{(2-26)}$$

Moreover, the relationship was similar for different cohesive soils, indicating that it may be applicable for different types of clayey soils. The limited data suggested that the same correlation might be used to estimate the M_R for both laboratory and field compacted conditions.

In a study conducted by Tian et al. (1998), a multiple linear regression model was developed to correlate the M_R value with cohesion (C), friction angle (ϕ), bulk stress (θ), major principal stress (σ_1), unconfined compressive strength (U_c), and the moisture content (w).

$$M_R \text{ (in kPa)} = 289{,}717 - 1113\ C + 127\ \sigma_1 \tan\phi + 261\ \theta - 33{,}939\ w + 276\ U_c \qquad \text{(2-27)}$$

In this model, a total of 75 M_R values were obtained from the M_R tests conducted on Richard Spur aggregate, which is commonly used in Oklahoma as the base material of roadway pavements. The model fitted the experimental data fairly well ($R^2 = 0.85$) and it could be used to predict the M_R values of similar aggregates under similar compaction states (Tian et al., 1998). A summary of correlation equations proposed by various researchers is presented in Table 2-3.

2.7 Types of Generalized Linear Model

In the present study, the Generalized Linear Model (GLM) (Dobson, 1990; McCullagh and Nelder, 1989; StatSoft, 2003) was used to develop statistical models. The GLM is used to correlate the linear and non-linear effects of the continuous and categorical independent variables to a discrete or continuous dependent variable. The GLM differs from the linear models in two major respects. First, the distribution of the dependent variable can be non-normal and discrete. Second, the dependent variable is related to a linear combination of independent variables through a link function (StatSoft, 2003). In the linear model, the dependent variable Y is linearly associated with the independent variables Xs, as shown below:

$$Y = a_0 + a_1 X_1 + a_2 X_2 + \ldots + a_n X_n \quad (2\text{-}28)$$

where a_i are the regression constants. On the other hand, the GLM relates the dependent and independent variables through a link function as follows:

$$Y = g(a_0 + a_1 X_1 + a_2 X_2 + \ldots + a_n X_n) \quad (2\text{-}29)$$

where *g* is a function and *f* is a link function which is the inverse function of g. Therefore,

$$f(\mu_y) = a_0 + a_1 X_1 + a_2 X_2 + \ldots + a_n X_n \quad (2\text{-}30)$$

where μ_y stands for the expected value of Y. The linear model is a special case of the GLM in which the dependent variable follows the normal distribution and the link function is a simple identity function (StatSoft, 2003).

In this study, STATISTICA 7.1, which is a commercially available statistical software developed by the StatSoft, Inc., was used in the development of the statistical models. The STATISTICA 7.1 provides different types of GLM features which include multiple regression, factorial regression, polynomial regression, response surface regression, mixture surface regression, analysis of covariance (ANCOVA), separate slopes designs, and homogeneity of slopes. A detail description of different types of GLM is presented in Chapter 5.

2.8 Artificial Neural Network

An artificial neural network (ANN) is a tool that imitates the function of a biological neural network. It provides some of the human characteristics of problem solving that are difficult to simulate using any of the logical, analytical, or standard computing techniques (Zurada, 1992; Fausett, 1994; Ripley, 1996). Some of the problems that can be solved by the ANN include classification, function approximation, forecasting, pattern association, and manufacturing process control (Zurada, 1992; Fausett, 1994; Ripley, 1996). The ANN has become an increasingly important tool due to its successes in many practical applications. Several geotechnical engineering problems solved using the ANN will be described in the next section.

The ANN modeling philosophy is similar to a number of traditional regression analyses (TRB, 1999; Shahin et al., 2001; Shahin et al., 2004). One of the objectives of the ANN models is to find a function that can relate the input variable to the output variable. For example, in linear regression model, a function is obtained by changing the slope and intercept so that the function fits the dataset. The same principle is applied to the ANN models. The ANN model is obtained by adjusting the weights between the processing elements. The ANN adjusts their weights by repeatedly presenting the input data to minimize the error between the historical and predicted output (TRB, 1999; Shahin and Maier, 2001). This phase is called "training" or "learning." The difference between an ANN model and a regression model is that a prior knowledge of the nature of the non-linearity is not required in ANN models (Shahin et al., 2001). The degree of non-linearity of the ANN models can be changed easily by varying the number of hidden layers, number of nodes in each layer, and the transfer functions. However, the traditional regression analysis may not be adequate when dealing with complex problems (Gardner and Dorling, 1998).

The architecture of ANN contains a number of simple, highly interconnected processing elements, known as "nodes" or "units". One of the most common ANNs in use currently is the feedforward networks, as shown in Figure 2-4. As evident from its name, a feedforward network only allows the data flow in the forward direction. The connections in the feedforward networks are only allowed from a node in the preceding layers. Moreover, there are no same layer connections (Zurada, 1992; Fausett, 1994; Ripley, 1996, StatSoft, 2003).

Based on the architecture, there are several types of feedforward networks, for example, multilayer perceptrons (MLP), radial basis function (RBF), probabilistic neural networks (PNN), generalized regression neural networks (GRNN), and linear networks.

The networks used in solving the regression problems are MLP, RBF, GRNN, and linear networks (TRB, 1999; StatSoft, 2003; Shahin et al., 2004).

In a typical processing element, as shown in Figure 2-5, each input connection has a weighting value. With the weighting value, input data and bias value, a net input is described into the processing element. Then, a transfer function provides an output from the net input. Finally, a single output is produced and transmitted to other processing elements (Skapura, 1996; Najjar et al., 2000; Shahin et al., 2001).

The main objective of the neural network approach is to find the weights through training a set of input data until the network reaches a minimum error. In the training process, a number of checks are performed in the network. After each epoch, the weights are adjusted and a sum of mean squared error between target and output values is calculated. The training process stops when the sum of mean squared error is minimized or falls within an acceptable range (Shahin et al., 2001; Shahin et al., 2004).

Different training algorithms can be used to train a network. The function of a training algorithm is to adjust the weights and thresholds using the training dataset. The training algorithms can be divided into two types: supervised and unsupervised algorithms. The supervised algorithms adjust the weights and the thresholds using the input and target output values, while the unsupervised algorithms only use the input values. The supervised training algorithms include back propagation, conjugate gradient descent, Levenberg-Marquardt, Pseudo-inverse, etc. (Mehrotra et al., 1996; StatSoft, 2003, Shahin et al., 2004).

2.9 Artificial Neural Network Model

Several researchers have utilized the advantages of the ANN modeling in solving various geotechnical engineering problems. Shahin et al. (2002) used the ANN technique to predict settlement of shallow foundations. A backpropagation neural network was used in that study. A database having 189 actual field measurements for settlements of shallow foundations on cohesionless soils was developed. The prediction results from the ANN models were then compared with three traditional methods for settlement prediction of shallow foundations. These include the methods proposed by Meyerhof (1965), Schultze and Sherif (1973), and Schmertmann et al. (1978). The results demonstrated that the ANN models have better predictive capabilities than the traditional regression models.

Ali and Najjar (2000) used the ANN modeling technique to simulate the consolidated drained stress-strain responses of Nevada sand. The study tried to characterize both extension and compression stress paths using one ANN model. The network had eight input parameters, namely, the initial relative density, total confining stress at current and futuristic loading state, axial stress at current and futuristic loading state, stress path parameter, and volumetric and axial strain values in current loading state. The stress path parameter was included to allow the network to distinguish between extension and compression stress paths. The outputs of the network were the volumetric and axial strain values in futuristic loading state. From the training of the network, the optimal network architecture (8-6-2) was found at 6 hidden nodes. The results showed that the model was able to accurately simulate the volumetric and axial strain behavior. The results also indicated that the model was able to capture the effects of the initial density on both volumetric and axial strain responses. However, small discrepancy between predicted and experimental values was noted in the early loading stages. According to these researchers, this discrepancy may be attributed to the variability in the testing procedure. Moreover, it is difficult for a single model to accurately simulate both extension and compression stress paths. Even with this discrepancy, Ali and Najjar (2000) concluded that the ANN modeling approach has an excellent potential for use in simulating the deformational behavior of sandy soils, in particular, and all geometerials, in general.

Park et al. (2006) used the ANN to predict the M_R values of subgrade and subbase materials. In predicting the M_R of subgrade soils, their study used three basic parameters, namely maximum dry unit weight, uniformity coefficient, and percent passing sieve No. 200, and two stress parameters, namely confining stress and deviatoric stress. However, only two material parameters (maximum dry density and uniformity coefficient) and one stress parameter (confining stress) were used in the prediction of subbase M_R. That study showed that the ANN models provided excellent predictions (M_R) for the subgrade and subbase materials. In the parametric studies, the results showed that the M_R was more dependent on the deviatoric stress than the confining stress in the subgrade model. While in the subbase model, the M_R was only slightly dependent on the deviatoric stress but the dependency increased considerably as the confining stress increased (Park et al., 2006).

The present study used the ANN models to develop correlations between the M_R values of subgrade soil and routine soil properties. The routine soil properties used in the present study were unconfined compressive strength, dry density, moisture content, percent passing 0.075 mm (No. 200) sieve, and plasticity index. The deviatoric stress and bulk stress were used as the stress state to identify the state of the specimens during the testing process.

The current study will attempt to demonstrate that stress or statistical based models are not capable of determining the complex relationship among the material properties and M_R. Therefore, more complex analysis methods such as Artificial Neural Networks (ANN), Recurrent Neural Network (RNN) or data mining. To this end this will imperative to collect a database large enough to accommodate this type of studies and analysis. It is the intention of this study to develop an ANN model, capable of predicting the M_R values that could be used for both the currently used 1993 AASHTO Design Guides and the level 2 and 3 design efforts of 2002 AASHTO Design Guides.

Table 2-1 Comparison of Different AASHTO Test Methods for Resilient Modulus Testing of Granular Base/Subbase Materials

	AASHTO T292-91I			AASHTO T294-92I and T294-94			AASHTO T307-99		
	σ_c (kPa)	σ_d (kPa)	No.of Cycles	σ_c (kPa)	σ_d (kPa)	No.of Cycles	σ_c (kPa)	σ_d (kPa)	No.of Cycles
Conditioning	138	103	1000	103	103	500-1000	103.4	103.4	500 - 1000
Test	138	69	50	21	21	100	20.7	20.7	100
	138	138	50	21	41	100	20.7	41.4	100
	138	207	50	21	62	100	20.7	62.1	100
	138	276	50	34	34	100	34.5	34.5	100
	103	69	50	34	69	100	34.5	68.9	100
	103	138	50	34	103	100	34.5	103.4	100
	103	207	50	69	69	100	68.9	68.9	100
	103	276	50	69	138	100	68.9	137.9	100
	69	34	50	69	207	100	68.9	206.8	100
	69	69	50	103	69	100	103.4	68.9	100
	69	138	50	103	103	100	103.4	103.4	100
	69	207	50	103	207	100	103.4	206.8	100
	34	34	50	138	103	100	137.9	103.4	100
	34	69	50	138	138	100	137.9	137.9	100
	34	103	50	138	276	100	137.9	275.8	100
	21	34	50						
	21	48	50						
	21	62	50						

σ_c = Confining stress, kPa
σ_d = Deviator stress, kPa
1 kPa = 0.145 psi

Table 2-2 Comparison of AASHTO Test Methods for Resilient Modulus Testing of Base/Subbase and Subgrade Materials

	AASHTO T307-99 for Base/ Subbase			AASHTO T307-99 for Subgrade		
	σ_c (kPa)	σ_d (kPa)	No.of Cycles	σ_c (kPa)	σ_d (kPa)	No.of Cycles
Conditioning	103.4	103.4	500 - 1000	41.4	27.6	500 - 1000
Test	20.7	20.7	100	41.4	13.8	100
	20.7	41.4	100	41.4	27.6	100
	20.7	62.1	100	41.4	41.4	100
	34.5	34.5	100	41.4	55.2	100
	34.5	68.9	100	41.4	68.9	100
	34.5	103.4	100	27.6	13.8	100
	68.9	68.9	100	27.6	27.6	100
	68.9	137.9	100	27.6	41.4	100
	68.9	206.8	100	27.6	55.2	100
	103.4	68.9	100	27.6	68.9	100
	103.4	103.4	100	13.8	13.8	100
	103.4	206.8	100	13.8	27.6	100
	137.9	103.4	100	13.8	41.4	100
	137.9	137.9	100	13.8	55.2	100
	137.9	275.8	100	13.8	68.9	100

σ_c = Confining stress, kPa
σ_d = Deviator stress, kPa
1 kPa = 0.145 psi

Table 2-3 Summary of Correlation Equations from Literature for Resilient Modulus

No.	**Equations** †	**References**	**Comments**
1	$M_R = k_1(\sigma_3)^{k2}$	Dunlap, 1963	--
2	$M_R = k_1 (\sigma_d)^{k2}$	Moossazadeh and Witczak, 1981	Cohesive Soil
3	$M_R = k_1(\theta)^{k2}$	Seed et al., 1967	Granular Soil
4	$M_R = k_1(\theta)^{k2} (\sigma_d)^{k3}$	May and Witczah, 1981	--
5	$M_R = k_1(\theta)^{k2} (\tau_{oct})^{k3}$	Uzan, 1985	All Types of Soils
6	$M_R = k_1(\sigma_3/P_a + 1)^{k2} (\sigma_d/P_a + 1)^{k3}$	NCHRP, 2003	--
7	$M_R = k_1(\theta/P_a)^{k2} (\tau_{oct}/P_a + 1)^{k3}$	Yau and Von Quintus, 2002	--
8	$M_R = k_1(\sigma_3/P_a + 1)^{k2} (\tau_{oct}/P_a + 1)^{k3}$	Hopkins et al., 2004	
9	$\log(M_R/P_a) = k_1 + k_2 \log(\theta/P_a) + k_3 \log(\tau_{oct} /P_a)$ $+ k_4 [\log(\tau_{oct} /P_a)]^2$	Stubstad et al., 2002	--
10	$M_R = k_1 + k_2 \sigma_d$ when $\sigma_d < \sigma_{di}$ $M_R = k_3 + k_4 \sigma_d$ when $\sigma_d > \sigma_{di}$	Thompson and Robnett, 1976	Fine-Grained Soil
11	$R_{m1} = 0.98 – 0.28(w - w_{opt}) + 0.029(w – w_{opt})^2$ $R_{m2} = 0.96 – 0.18(w - w_{opt}) + 0.0067(w – w_{opt})^2$	Li and Selig, 1994	Compacted Fine-Grained Soil
12	$M_R = 695.4 (S_{U1.0\%}) – 5.93 (S_{U1.0\%})^2$	Lee et al., 1997	Cohesive Soil
13	M_R (in kPa) $= 289,717 – 1113 C + 127 \sigma_1 \tan \phi$ $+ 261 \theta – 33,939 w + 276 U_c$	Tian, 1998	Aggregate Base
14	$M_R = 34280 – 359S – 325\sigma_d + 236\sigma_3 +86PI$ $+107P_{200}$	Farrar and Turner, 1991	Fine-Grain Wyoming Soil
15	$M_R = 16.75[(LL/w \gamma_{dr})^{2.06} + (P_{200}/100)^{-0.59}]$	Rahim and George, 2004	Fine-Grain Soil
16	$M_R = 307.4[(\gamma_{dr}/w)^{0.86} (P_{200}/\log c_u)^{-0.46}]$	Rahim and George, 2004	Coarse-Grain Soil
17	M_R (ksi) $= (a' + b'\sigma_d)/ \sigma_d$ $a' = 318.2 + 0.337U_c + 0.73(\%Clay)$ $+ 2.26PI – 0.915 \gamma_s – 2.19S – 0.304P_{200}$ $b' = 2.10 + 0.00039(1/a) + 0.104 U_c$ $+0.09LL – 0.10P_{200}$	Drumm et al., 1990	Cohesive Soil

† Definitions of variables are presented at the end of Table 2-3

Table 2-3 Summary of Correlation Equation for Resilient Modulus (Continued)

No.	Equations	References	Comments
18	$M_R = 37.431 - 0.4566PI - 0.6179w_c$ $- 0.1424P_{200} + 0.1791\sigma_3 - 0.3248\sigma_d$ $+36.722CH + 17.097MH$	Carmichael and Stuart, 1978	Fine-Grain Soil
19	$\text{Log } M_R = 0.523 - 0.025w + 0.544\log\theta +$ $0.173SM + 0.197GR$	Carmichael and Stuart, 1978	Coarse-Grain Soil
20	$M_R = k_1(\theta)^{k2}(\sigma_d)^{k3}$ $k_1 = 5770.8 - 520.98(\gamma_s)^{0.5} - 3941.8(w)^{0.5}$ $+ 33.1 PI - 36.62 LL - 17.93 P_{200}$ $k_2 = -5.334 + 0.000316(\gamma_s)^3 + 9.686 w$ $- 0.054 PI + 0.046 LL + 0.022 P_{200}$ $k_3 = 409.9 - 306.18(\gamma_s)^{0.1} - 82.63 w$ $+ 0.033 PI + 0.138 S - 0.041 LL$	Dai and Zollars, 2002	--
21	$M_R = k_1P_a(\theta/P_a)^{k2}[(\tau_{oct}/P_a) + 1]^{k3}$ $k_1 = 3.2868 - 0.0412 P_{3/8} + 0.0267 P_4$ $+ 0.0137(\%Clay) + 0.0083 LL$ $- 0.0379 w_{opt} - 0.0004 \gamma_s$ $k_2 = 0.5670 + 0.0045 P_{3/8} + 2.98x10^{-5} P_4$ $- 0.0043(\%Silt) - 0.0102(\%Clay)$ $- 0.0041 LL + 0.0014 w_{opt}$ $- 3.41x10^{-5} \gamma_s - 0.4582(\gamma_s/\gamma_{opt})$ $+ 0.1779(w/w_{opt})$ $k_3 = -3.5677 + 0.1142 P_{3/8} - 0.0839 P_4$ $- 0.1249 P_{200} + 0.1030(\%Silt)$ $+ 0.1191(\%Clay) - 0.0069 LL$ $- 0.0103 w_{opt} - 0.0017 \gamma_s$ $+ 4.3177(\gamma_s/\gamma_{opt}) - 1.1095(w/w_{opt})$	Mohammad et al., 1999	Coarse-Grained Sandy Soils
22	$M_R = k_1P_a(\theta/P_a)^{k2}[(\tau_{oct}/P_a) + 1]^{k3}$ $k_1 = 1.0480 + 0.0177(\%Clay) + 0.0279 PI$ $- 0.0370 w$ $k_2 = 0.5097 - 0.0286 PI$ $k_3 = -0.2218 + 0.0047(\%Silt) + 0.0849 PI$ $- 0.1399 w$	Mohammad et al., 1999	Fine-Grained Silty Soils
23	$M_R = k_1P_a(\theta/P_a)^{k2}[(\tau_{oct}/P_a) + 1]^{k3}$ $k_1 = 1.3577 + 0.0106(\%Clay) - 0.0437 w$ $k_2 = 0.5193 - 0.0073 P_4 + 0.0095 P_{40}$ $- 0.0027 P_{200} - 0.003 LL - 0.0049 w$ $k_3 = 1.4258 - 0.0288 P_4 + 0.0303 P_4$ $- 0.0521 P_{200} + 0.0251(\%Silt)$ $+ 0.0535 LL - 0.0672 w_{opt}$ $- 0.0026 \gamma_{opt} + 0.0025 \gamma_s$ $- 0.6055(w/w_{opt})$	Mohammad et al., 1999	Fine-Grained Clayey Soils

Table 2-3 Summary of Correlation Equation for Resilient Modulus (Continued)

No.	Equations	References	Comments
24	$M_R = k_1 P_a(\theta/P_a)^{k2} (\sigma_d/P_a)^{k3}$ $k_1 = 3.479 - 0.07\ w + 0.24\ w_r$ $+ 3.681\ COMP + 0.011\ (\%Silt)$ $+ 0.006\ (\%Clay) - 0.025\ SW - 0.039\ \gamma_s$ $+ 0.004\ (SW^2/\%\ Clay)$ $+ 0.003\ (\gamma_s{}^2 / P_{40})$ $k_2 = 6.044 - 0.053\ w_{opt} - 2.076\ COMP$ $+ 0.0053\ S - 0.0056\ (\%Clay)$ $+ 0.0088\ SW - 0.0069\ SH$ $- 0.027\ \gamma_s + 0.012\ CBR$ $+ 0.003\ (SW^2 / \%Clay)$ $- 0.31\ (SW+SH) / \%Clay$ $k_3 = 3.752 - 0.068\ w + 0.309\ w_r$ $- 0.006\ (\%Silt) + 0.0053\ (\%Clay)$ $+ 0.026\ SH - 0.033\ \gamma_s$ $- 0.0009\ (SW^2 / \%Clay)$ $+ 0.00004\ (S^2 / SH)$ $- 0.0026\ (CBR)(SH)$	Santha, 1994	Granular Soils
25	$M_R = k_1 P_a (\sigma_d/P_a)^{k3}$ $\log k_1 = 19.813 - 0.045\ w_{opt} - 0.131\ w$ $- 9.171\ COMP + 0.0337\ (\%Silt)$ $+ 0.015\ LL - 0.016\ PI - 0.021\ SW$ $- 0.052\ \gamma_s + 0.00001\ (P_{40})(S)$ $k_3 = 10.274 - 0.097\ w_{opt} - 1.06\ w_r$ $- 3.471\ COMP + 0.0088\ P_{40}$ $- 0.0087\ PI + 0.014\ SH - 0.046\ \gamma_s$	Santha, 1994	Cohesive Soils
26	$M_R = k_1 P_a(\sigma_{oct}/P_a)^{k2} (\tau_{oct}/P_a)^{k3}$ $\log k_1 = - 0.679 + 0.0922\ w + 0.00559\ \gamma_s$ $+ 3.54\ (\gamma_s / \gamma_{opt}) + 2.47\ w_r$ $+ 0.00676\ LL + 0.0116\ PL$ $+ 0.022\ (\%Sand) + 0.0182\ (\%Silt)$ $\log k_2 = - 0.887 + 0.0044\ w + 0.00934\ \gamma_s$ $+ 0.264\ (\gamma_s / \gamma_{opt}) + 0.305\ w_r$ $+ 0.00877\ LL + 0.00665\ PL$ $+ 0.0116\ (\%Sand) + 0.00429\ (\%Silt)$ $\log k_3 = - 0.638 + 0.00252\ w + 0.00207\ \gamma_s$ $+ 0.61\ (\gamma_s / \gamma_{opt}) + 0.152\ w_r$ $+ 0.00049\ LL + 0.00416\ PL$ $+ 0.00311\ (\%Sand) + 0.00143\ (\%Silt)$	Mohammad et al., 1999	--

Definition of variables used in table 2-3
γ_{dr} = Dry density/maximum dry density
γ_{opt} = Maximum dry density
γ_s = Dry density
ϕ = Friction angle

Table 2-3 Summary of Correlation Equation for Resilient Modulus (Continued)

θ = Bulk stress
σ_1 = Major principal stress
σ_3 = Confining stress
σ_d = Deviatoric stress
σ_{di} = Deviatoric stress at which the slope of M_R versus σ_d changes
σ_{oct} = Octahedral normal stress = $(\sigma_1 + \sigma_2 + \sigma_3)/3$
τ_{oct} = Octahedral shear stress = $(1/3)[(\sigma_1 - \sigma_2)^2 + (\sigma_2 - \sigma_3)^2 + (\sigma_3 - \sigma_1)^2]^{1/2}$
1/a = Initial tangent modulus
%Clay = Percent clay
%Sand = Percent sand
%Silt = Percent silt
C = Cohesion
CBR = California Bearing Ratio
CH = 1 for CH soil, 0 otherwise
COMP = Sample compaction
c_u = Uniformity coefficient
GR = 1 for GR soils, 0 otherwise
k_1, k_2, k_3, k_4 = Parameters
LL = Liquid limit
M_R = Resilient modulus
$M_{R\ (opt)}$ = Resilient modulus at maximum dry density and optimum moisture content
MH = 1 for MH soil, 0 otherwise
P_{200} = Percent passing #200 sieve
$P_{3/8}$ = Percent passing #3/8 sieve
P_4 = Percent passing #4 sieve
P_{40} = Percent passing #40 sieve
P_a = Atmospheric pressure
PI = Plasticity index
R_{m1} = M_R / $M_{R\ (opt)}$ for the case of constant dry density
R_{m2} = M_R / $M_{R\ (opt)}$ for the case of constant compactive effort
S = Degree of saturation
$S_{U1.0\%}$ = Stress causing 1% strain during a conventional unconfined compression test
SH = Percent shrinkage
SM = 1 for SM soils, 0 otherwise
SW = Percent swell
U_c = Unconfined compressive strength
w = Moisture content
w_r = w / w_{opt}
w_{opt} = Optimum moisture content

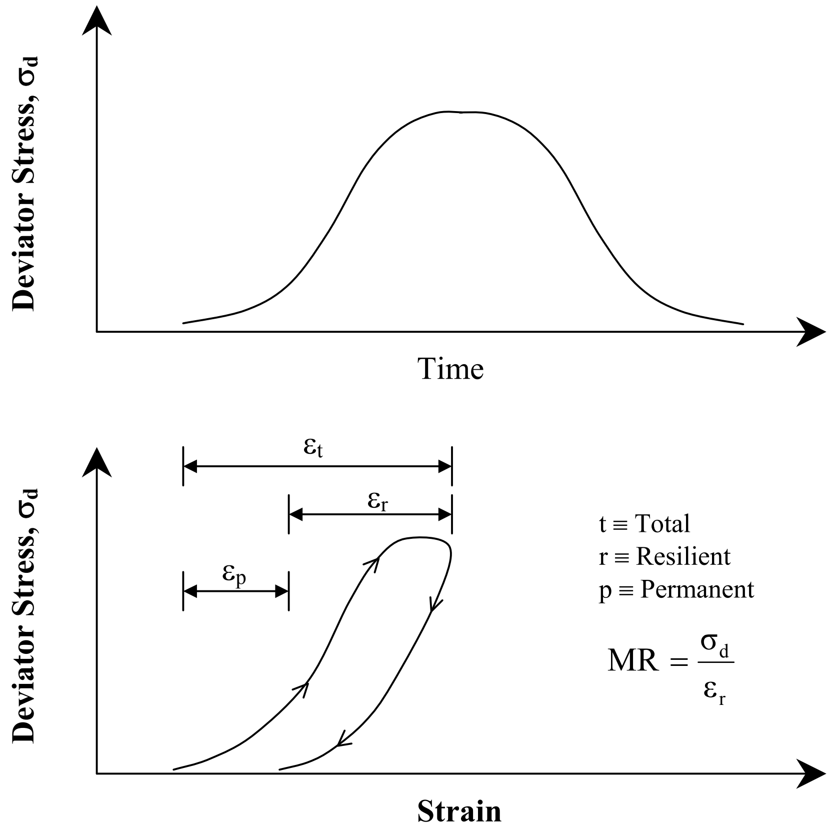

Figure 2-1 Typical Stress-Strain Response from Repeated Load Test (After Elliott and Thornton, 1988)

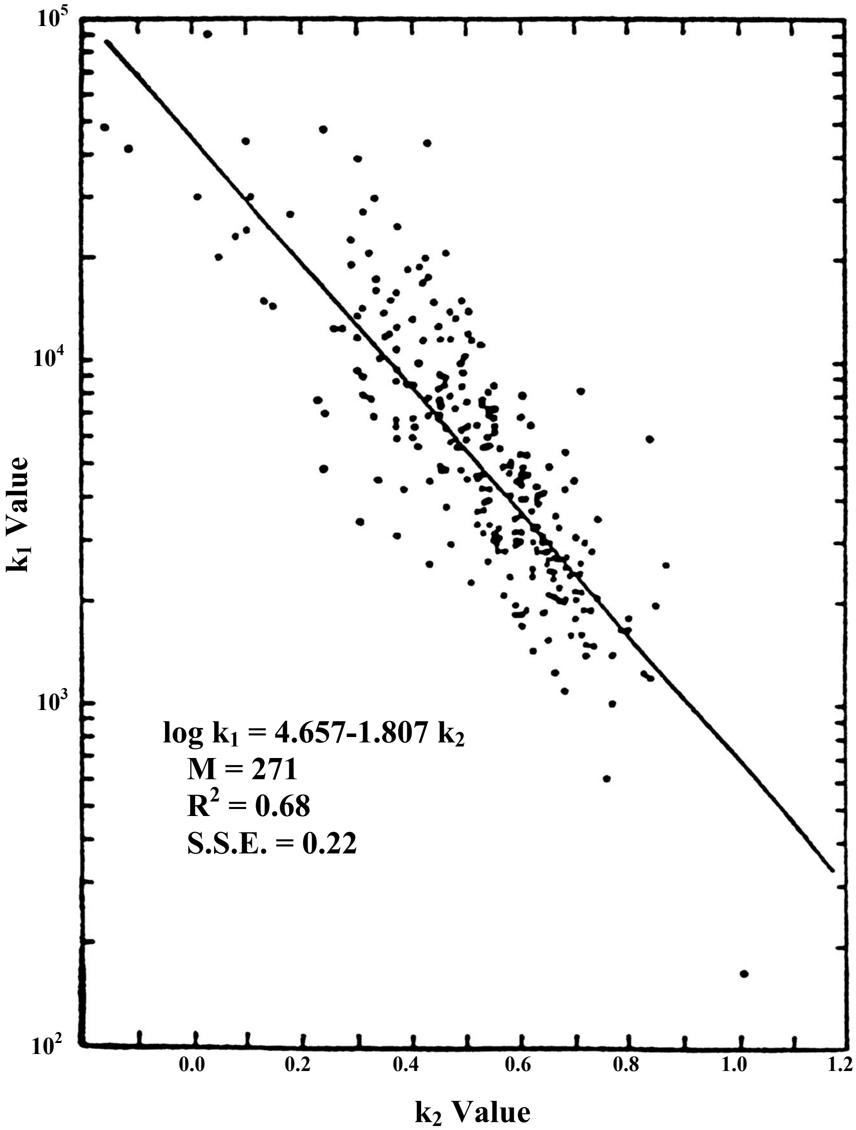

Figure 2-2 Range of k_1 and k_2 Values for Aggregates (After Rada and Witczak, 1981)

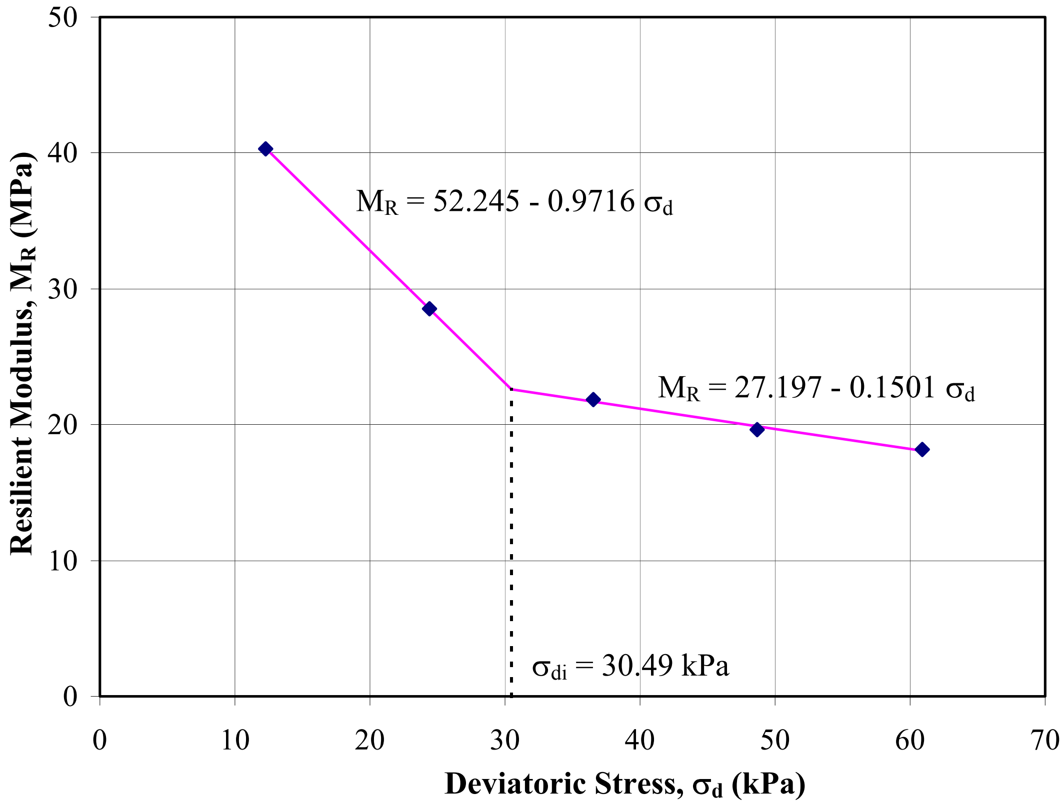

1 kPa = 0.145 psi

Figure 2-3 Typical Bi-linear Model

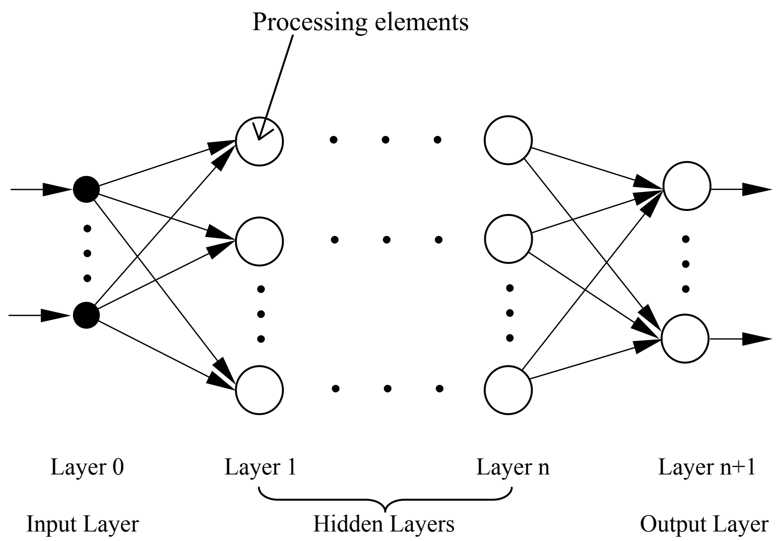

Figure 2-4 A General Feedforward Neural Network Architecture (StatSoft, Inc., 2006)

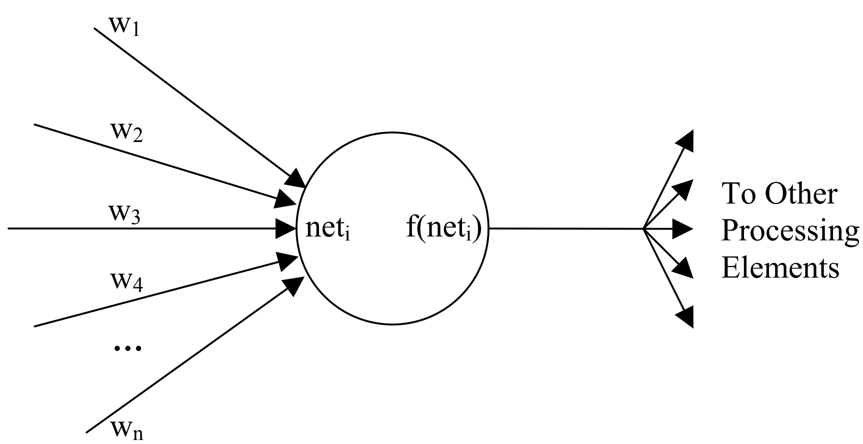

Figure 2-5 A Typical Processing Element (StatSoft, Inc., 2006)

CHAPTER 3

MATERIAL SOURCES AND EXPERIMENTAL METHODOLOGY

3.1 Introduction

This chapter describes the sources of material and the testing procedures adopted to achieve the objectives of this study enumerated in Chapter 1. The sampling locations and their geological information are presented along with the sampling method. The procedures for all laboratory tests performed are discussed along with the standard testing methods specified by AASHTO and ASTM. A flow chart of the sampling, testing schedule, and analysis are presented in Figure 3-1. The results from these laboratory tests will be discussed in Chapter 4.

3.2 Material Sources

3.2.1 Locations

Sixty-three (63) soil samples were collected from fourteen (14) different sites across Oklahoma. As depicted in Figure 3-2, these sites were located at Adair, Alfalfa, Choctaw, Delaware, Greer, Jefferson, Kingfisher, Lincoln, Major, McClain, Noble, Okfuskee, Osage, and Rogers counties in Oklahoma. Additionally, to evaluate the models developed in this study, thirty-four (34) soil samples were collected from three sites in Oklahoma. These sites, shown in Figure 3-3, were located in Rogers and Woodward counties. Sample ID's used in the laboratory testing program along with sample locations, parent material description and depth are shown in Table 3-1 and Table 3-2.

3.2.2 Geology

The geological information for the aforementioned locations is obtained from the county soil survey published by United States Department of Agriculture (USDA). The soils included in this study were developed mainly from the parent materials of Pennsylvanian, Mississippian, Permian, Quaternary and recent ages. These parent materials include sandstone, shale, limestone, colluvium and alluvium (Soil Conservation Services, 1952; 1956; 1962; 1963; 1965; 1966; 1967; 1968; 1970; 1973; 1975; 1978; 1979). Table 3-1 and Table 3-2 show the parent materials of soil samples collected from different locations in Oklahoma. The development and evaluation datasets were subdivided based on the parent materials of soil samples, and the results are presented in Table 3-3. A majority of the soil samples in the development dataset are from alluvium formations, followed by shale formations. There were 42 and 13 soil samples from alluvium and shale formations, respectively. There were only six and two soil samples having parent materials as sandstone and limestone, respectively. For the evaluation dataset, a majority of parent materials were from shale followed by alluvium formations. Fifteen soil samples were from shale formations, while only ten soil samples were from alluvium formations. In the evaluation dataset for Rogers County, the parent materials were from shale, alluvium, sandstone, and limestone, with a majority from shale formations. However, the soil samples from Woodward County were developed from alluvium and shale.

3.3 Sampling Method

Bulk samples of different soil series were collected from each site shown in Figure 3-2 and Figure 3-3. For each soil series, bulk sample was collected from each horizon, primarily from the B-horizon and the C-horizon, following the Oklahoma Department of Transportation (ODOT) standard sampling method for pedological and geological soil survey (FHWA, 2002; AASHTO, 2004). The sampling depth for each horizon is shown in Table 3-1 and Table 3-2. The bulk samples were hand augered according to the sampling locations and depths. The samples were transported to laboratory for processing and testing.

3.4 Soil Classification Tests

Atterberg limits and grain size distribution results were used in the soil classification. The Atterberg limit tests were performed to determine plastic limit (PL), liquid limit (LL), and Plasticity Index (PI) of the soil. The PL values were obtained using the "Hand Rolling Method", as described in AASHTO T90 (AASHTO, 2004). For the determination of LL, one point LL tests were conducted according to Method "B" in AASHTO T89 (AASHTO, 2004). The PI was determined by subtracting PL from LL. The grain size distribution was determined through wet sieving and dry sieving. The wet sieving was conducted according to the AASHTO T11 test method while the dry sieving was conducted according to the AASHTO T27 test method (AASHTO, 2004). After completion of the Atterberg limit tests and grain size distribution analyses, the soil samples were classified based on the Unified Soil Classification System according to ASTM D2487 and AASHTO Classification System according to AASHTO M145 (ASTM, 2005; AASHTO, 2004). The soil classification results for the present study are discussed in Chapter 4.

3.5 Proctor Test

In this study, standard Proctor tests were preformed to determine the relationship between the moisture content and dry density of compacted soils. These tests were conducted in accordance with Method A in ASTM D698 (ASTM, 2005). In this method, soil was compacted in a 101.6 mm (4 in) diameter mold with a 24.4 N (5.5 lbf) rammer dropped from a height of 305 mm (12 in). Each test specimen was compacted in 3 layers with 25 blows per layer. Four or five proctor samples were prepared for each soil type with each test specimen having a different moisture content. For each sample, the moisture content and dry density were calculated. Then, a compaction curve was prepared from the test results. A typical compaction curve is shown in Figure 3-4. The optimum moisture content and the maximum dry density were determined from the compaction curve.

3.6 Sample Preparation

Using the Proctor test results, two samples were prepared with different compaction conditions. One of these samples was compacted at the optimum moisture content (OMC) and 95% of the maximum dry density. For the other sample, the moisture content and dry density were set at 2% wet of OMC. Thus, a total of 126 M_R tests were conducted for 63 soils used in the development of models. In addition, 68 M_R tests were conducted for 34 soils for the evaluation of the developed models. The compaction method used in this study is a static compaction method (a modified version of the double plunger method) (AASHTO, 2004). First, the weight of soil required for a sample was calculated from the pertinent dry density-moisture content curve. After soil was mixed thoroughly with the desired amount of water, the mix was divided into five equal portions. A portion of the mix was placed into a mold between two large spacer plugs. The spacer plugs were pressed into the mold using a hydraulic jack until the spacer plugs were fully inside the mold. The pressure was maintained on the mold for at least one minute. Then, the mold was flipped over and the top spacer plug was removed. The next portion of the soil was placed on top of the compacted soil and a medium spacer was placed into the mold. The soil was compacted using the same compaction procedure for the first layer with a hydraulic jack. After the compaction, the mold was flipped over and the same procedure was repeated for the remaining three other layers with different sizes of spacer plugs as desired. The sequence of the layers is shown in Figure 3-5. The compacted sample had a diameter of 101.6 mm (4 in) and a height of 203.2 mm (8 in).

3.7 Resilient Modulus Test

The resilient modulus (M_R) tests were conducted in accordance with the standard testing procedures outlined in AASHTO T307 (AASHTO, 2004). There are two procedures described in AASHTO T307 for different types of materials: untreated subgrade soils and untreated base or subbase materials. The procedure recommended for subgrade soils was used in this study to conduct resilient modulus test. A summary of the test set up and test procedure is given in the following.

3.7.1 Testing Equipment and Setup

The M_R testing system used in this study was manufactured by Interlaken Technology Corporation. The system consists of a triaxial chamber, a loading frame, control and power electronics, and hydraulic power supply. The control and power electronics are located in the electronics bay. Figures 3-6 and 3-7 show the components of the M_R testing system. The control unit contains the control signal module, the data acquisition board, and the power control module. The control signal module supports the actuator stroke transducer, the load cell, the pressure transducers, and two external LVDTs. The LVDTs were fixed to opposite sides of the piston rod outside the test chamber (AASHTO, 2004). During the M_R test, all outputs were collected by the data acquisition board and then transferred to a personal computer for storing and post processing. The personal computer used in this study is a Dell Optiplex Pentium 3 with a 450 MHz microprocessor. The M_R testing system include a software that operates the system. This software was programmed to receive the test input including the desired load, frequency, confining pressure, and number of loading cycles for each sequence.

Before the M_R test began, the triaxial chamber was set up according to the AASHTO T307 test method. The triaxial chamber setup for this study is shown in Figure 3-8. The specimen to be tested was mounted in between a base and a cap in the triaxial chamber. Filter papers and porous stones were placed at each end of the specimen. Then, a membrane was placed around the specimen and sealed to the base and cap with O-rings. After the specimen was in place, the chamber was placed on the base plate. The cover plate with the chamber piston rod inserted at the center of the plate was placed on top of the chamber. The chamber was tightened with the tie rods. A solid bracket was attached to the piston rod and two LVDTs were attached to the bracket. Air supply and pressure transducer were connected to the triaxial chamber. The triaxial chamber was then placed under the load cell. Once the setup was completed, the M_R test was ready to begin.

3.7.2 Testing Procedures

As noted previously, the M_R tests in this study were conducted according to the standard method described in AASHTO T307 (AASHTO, 2003). The test method involves one sequence of conditioning and fifteen sequences of deviatoric stress loading. Specific confining pressure and axial stress were applied to the specimen during each sequence. The cyclic stress applied to the specimen involved a haversine-shaped pulse load, having a duration of 0.1 second followed by a rest period of 0.9 second, as shown in Figure 3-9. During the entire loading cycle, a constant contact stress, which is 10 % of maximum axial stress, was applied to the specimen.

At the beginning of the M_R testing, a confining pressure of 41.4 kPa (6 psi) and 500 to 1000 loading cycles with a maximum axial stress of 27.6 kPa (4 psi) were applied to the specimen during the sequence of conditioning. Then, the confining pressure and the maximum axial stress for each sequence were applied in accordance with the values in Table 3-4. During the M_R test, the recoverable deformations from each LVDT and each loading cycle were recorded. However, only the recovered deformations from the last five load cycles were used to calculate the M_R. Thus, an average M_R value was determined for each sequence. The M_R test results for Sample AL-8A are shown in Table 3-5 as an example.

3.8 Unconfined Compression Test

The unconfined compression test was conducted according to the AASHTO T208 test method. The specimen was placed in the center of the loading device. A load with an axial strain rate of 0.5 to 2 percent per minute was applied to the specimen. Load and time were recorded at every 0.25 mm (0.01 in) of deformation. The loading procedure continued until either the load values decreased with increasing strain or 15% strain was reached. A stress-strain curve for the specimen was plotted from the test results. The unconfined compressive strength of the specimen was the maximum compressive stress from the stress-strain curve. Figure 3-10 shows a typical stress-strain curve for Sample AL-8A. The unconfined compressive strength of this sample was approximately 238 kPa (34.5 psi). The unconfined compressive strength test was conducted on the same sample, following the M_R testing. It is assumed that since the M_R strain is in the range of ten thousands (mm/mm) (see Table 3-5) the influence of M_R test on the Unconfined Compression test would be negligible.

Table 3-1 Soil Series and Parent Materials for the Specimens Used in Model Development

Locations	Series	Parent Materials	Depth (in)	Sample I.D.
SH 59 from Westville to Watts in Adair County, Oklahoma, USA (8 Samples)	Bodine	Limestone	B-Horizon: 9 – 73	AD-1
	Etowah	Alluvium or Colluvium	B-Horizon: 7 – 70	AD-2
	Hector	Sandstone	B-Horizon: 6 – 15	AD-3
	Linker	Sandstone	B-Horizon: 5 – 35	AD-4
	Parsons	Shale	B-Horizon: 14 – 43 C-Horizon: 43 – 84	AD-5 AD-6
	Summit	Shale	B-Horizon: 13 – 89 C-Horizon: 89 – 116	AD-7 AD-8
SH 64 in Cherokee, Alfalfa County, Oklahoma, USA (10 Samples)	Brewer	Alluvium	B-Horizon: 12 – 80 C-Horizon: 80 – 90	AL-1 AL-2
	Dale	Alluvium	B-Horizon: 21 – 40 C-Horizon: 40 – 60	AL-3 AL-4
	Port	Alluvium	B-Horizon: 27 – 42 C-Horizon: 42 – 72	AL-5 AL-6
	Reinach	Alluvium	B-Horizon: 30 – 50 C-Horizon: 50 – 84	AL-7 AL-8
	Tabler	Alluvium	B-Horizon: 12 – 50 C-Horizon: 50 – 70	AL-9 AL-10
US 70, SE of Hugo, Choctaw County, Oklahoma, USA (4 Samples)	Bernow	Alluvium	B-Horizon: 15 – 68	CH-1
	Bosville	Alluvium	B-Horizon: 15 – 70	CH-2
	Kaufman	Alluvium	B-Horizon: 19 – 84	CH-3
	Lula	Limestone	B-Horizon: 10 – 52	CH-4
SH 59, NW of Grove, Delaware County, Oklahoma, USA (4 Samples)	Okemah	Alluvium or Colluvium	B-Horizon: 21 – 79	DE-1
	Sallisaw	Alluvium	B-Horizon: 10 – 60	DE-2
	Taloka	Alluvium or Colluvium	B-Horizon: 28 – 78	DE-3
	Woodson	Alluvium	B-Horizon: 20 – 97	DE-4
SH 6 at Granite, Greer County, Oklahoma, USA (3 Samples)	Hollister	Shale	B-Horizon: 6 – 70	GR-1
	Lawton	Alluvium	B-Horizon: 11 – 72	GR-2
	Spur	Alluvium	B-Horizon: 15 – 60	GR-3
US 70 near Ringling, Jefferson County, Oklahoma, USA (4 Samples)	Bunyan	Alluvium	C-Horizon: 16 – 62	JE-1
	Chickasha	Sandstone	B-Horizon: 12 – 58	JE-2
	Port	Alluvium	B-Horizon: 27 – 42	JE-3
	Zaneis	Sandstone and Shale	B-Horizon: 12 – 59	JE-4
SH 51 over Cimarron River, Kingfisher County, Oklahoma, USA (1 Sample)	Port	Alluvium	C-Horizon: 42 – 72	KI-1

Table 3-1 Soil Series and Parent Materials for the Specimens Used in Model Development (Continued)

Locations	**Series**	**Parent Materials**	**Depth (in)**	**Sample I.D.**
SH 66, SW of Wellston, Lincoln County, Oklahoma, USA (6 Samples)	Miller	Alluvium	B-Horizon: 14 – 35	LI-1
	Port	Alluvium	B-Horizon: 27 – 42 C-Horizon: 42 – 72	LI-2 LI-3
	Roebuck	Alluvium	B-Horizon: 10 – 45	LI-4
	Stephenville	Sandstone	B-Horizon: 15 – 33	LI-5
	Lucien	Sandstone or Sandy Shale	B-Horizon: 4 – 14	LI-6
US 412 in Major County, Oklahoma, USA (4 Samples)	St. Paul	Alluvium	B-Horizon: 12 – 56 C-Horizon: 56 – 70	MA-1 MA-2
	Weymouth	Shale	B-Horizon: 6 – 30 C-Horizon: 30 – 60	MA-3 MA-4
SH 39, S of Purcell, McClain County, Oklahoma, USA (1 Sample)	Miller	Alluvium	B-Horizon: 14 – 35	MC-1
SH 15 in Noble County, Oklahoma, USA (9 Samples)	Drummond	Alluvium	B-Horizon: 8 – 30 C-Horizon: 30 – 60	NO-1 NO-2
	Kirkland	Shale	B-Horizon: 8 – 82	NO-3
	Dale	Alluvium	B-Horizon: 21 – 40 C-Horizon: 40 – 60	NO-4 NO-5
	Port	Alluvium	B-Horizon: 27 – 42 C-Horizon: 42 – 72	NO-6 NO-7
	Renfrow	Shale	B-Horizon: 9 – 65 C-Horizon: 65 – 75	NO-8 NO-9
SH 56 over Nuyaka Creek and Yahola Creek, Okfuskee County, Oklahoma, USA (5 Samples)	Dennis	Shale	B-Horizon: 33 – 173 C-Horizon: 173 – 198	OK-1 OK-2
	Eram	Shale and Sandstone	B-Horizon: 25 – 76	OK-3
	Okemah	Alluvium or Colluvium	B-Horizon: 21 – 79	OK-4
	Verdigris	Alluvium	C-Horizon: 46 – 60	OK-5
SH 99, N of Hominy, Osage County, Oklahoma, USA (3 Samples)	Drummond	Alluvium	B-Horizon: 8 – 30	OS-1
	Lightning	Alluvium	B-Horizon: 11 – 60	OS-2
	Verdigris	Alluvium	C-Horizon: 46 – 60	OS-3
SH 88 in Roger County, Oklahoma, USA (1 Sample)	Parsons	Alluvium	C-Horizon: 58 – 80	RO-1

Table 3-2 Soil Series and Parent Materials for the Specimens Used in Model Evaluation

Locations	**Series**	**Parent Materials**	**Depth (in)**	**Sample I.D.**
SH 20, Claremore Bypass in Rogers County, Oklahoma, USA (10 Samples)	Apperson	Limestone	B-Horizon: 10 – 44	ROE-1
	Bates	Sandstone and Shale	B-Horizon: 9 – 33	ROE-2
	Catoosa	Limestone	B-Horizon: 10 – 20	ROE-3
	Choteau	Alluvium	B-Horizon: 22 – 65	ROE-4
	Claremore	Limestone	B-Horizon: 8 – 18	ROE-5
	Dennis	Shale	B-Horizon: 13 – 68	ROE-6
	Eram	Shale	C-Horizon: 30 – 40	ROE-7
	Kanima	Sandstone, Shale, and Limestone	C-Horizon: 6 – 72	ROE-8
	Riverton	Alluvium	B-Horizon: 7 – 44	ROE-9
	Verdigris	Alluvium	C-Horizon: 46 – 60	ROE-10
SH 88, N. of US 412 in Rogers County, Oklahoma, USA (19 Samples)	Apperson	Limestone	B-Horizon: 10 – 44	ROE-11
	Bates	Sandstone and Shale	B-Horizon: 9 – 33 C-Horizon: 33 – 37	ROE-12 ROE-13
	Choteau	Alluvium	B-Horizon: 22 – 65	ROE-14
	Collinsville	Sandstone	C-Horizon: 7 – 9	ROE-15
	Dennis	Shale	B-Horizon: 13 – 68 C-Horizon: 68 – 78	ROE-16 ROE-17
	Endsaw	Colluvium and Shale	B-Horizon: 14 – 42 C-Horizon: 42 – 60	ROE-18 ROE-19
	Eram	Shale	B-Horizon: 10 – 30 C-Horizon: 30 – 40	ROE-20 ROE-21
	Okemah	Shale	B-Horizon: 21 – 79	ROE-22
	Osage	Alluvium	B-Horizon: 13 – 80	ROE-23
	Parsons	Shale	B-Horizon: 12 – 58 C-Horizon: 58 – 80	ROE-24 ROE-25
	Taloka	Alluvium	B-Horizon: 28 – 78	ROE-26
	Verdigris	Alluvium	C-Horizon: 46 – 60	ROE-27
	Woodson	Shale	B-Horizon: 8 – 38 C-Horizon: 38 – 60	ROE-28 ROE-29
SH 3, SE of Woodward, Woodward County, Oklahoma, USA (5 Samples)	Carey	Shale	B-Horizon: 14 – 44 C-Horizon: 44 – 61	WOE-1 WOE-2
	Dale	Alluvium	C-Horizon: 46 – 84	WOE-3
	St. Paul	Alluvium	B-Horizon: 12 – 56 C-Horizon: 56 – 70	WOE-4 WOE-5

Table 3-3 Distribution of Parent Materials in Development and Evaluation Datasets

Parent Material	Development Dataset	Evaluation Dataset		
		Overall	Roger County	Woodward County
Alluvium	42	10	7	3
Shale	13	15	13	2
Sandstone	6	5	5	0
Limestone	2	4	4	0

Table 3-4 Resilient Modulus Testing Sequence for Subgrade Soil (AASHTO, 2004)

Sequence No.	Confining Pressure, S_3		Max. Axial Stress, S_{max}		Cyclic Stress, S_{cyclic}		Constant Stress, 0.1 S_{max}		No. of Load Applications
	kPa	psi	kPa	psi	kPa	psi	kPa	psi	
Conditioning	41.4	6	27.6	4	24.8	3.6	2.8	0.4	500-1000
1	41.4	6	13.8	2	12.4	1.8	1.4	0.2	100
2	41.4	6	27.6	4	24.8	3.6	2.8	0.4	100
3	41.4	6	41.4	6	37.3	5.4	4.1	0.6	100
4	41.4	6	55.2	8	49.7	7.2	5.5	0.8	100
5	41.4	6	68.9	10	62.0	9.0	6.9	1.0	100
6	27.6	4	13.8	2	12.4	1.8	1.4	0.2	100
7	27.6	4	27.6	4	24.8	3.6	2.8	0.4	100
8	27.6	4	41.4	6	37.3	5.4	4.1	0.6	100
9	27.6	4	55.2	8	49.7	7.2	5.5	0.8	100
10	27.6	4	68.9	10	62.0	9.0	6.9	1.0	100
11	13.8	2	13.8	2	12.4	1.8	1.4	0.2	100
12	13.8	2	27.6	4	24.8	3.6	2.8	0.4	100
13	13.8	2	41.4	6	37.3	5.4	4.1	0.6	100
14	13.8	2	55.2	8	49.7	7.2	5.5	0.8	100
15	13.8	2	68.9	10	62.0	9.0	6.9	1.0	100

Table 3-5 Resilient Modulus Testing Results for Sample AL-8A

Sequence No.	Confining Pressure, S_3 (kPa)	Max. Axial Stress, S_{max} (kPa)	Cycle No.	Recovery Deformation (mm)		Average Recovery Deformation (mm)	Resilient Strain (mm/mm)	Resilient Modulus (MPa)
				LVDT 1	LVDT 2			
1	41.4	13.8	96	0.01472	0.01438	0.01455	0.00007	104.3
			97	0.01288	0.01224	0.01256	0.00006	112.3
			98	0.01240	0.01208	0.01224	0.00006	114.0
			99	0.01323	0.01291	0.01307	0.00006	110.7
			100	0.01357	0.01327	0.01342	0.00007	109.1
			Average	**0.01336**	**0.01298**	**0.01317**	**0.00006**	**110.1**
2	41.4	27.6	96	0.06275	0.06138	0.06207	0.00031	77.0
			97	0.06330	0.06182	0.06256	0.00031	76.2
			98	0.06226	0.06064	0.06145	0.00030	76.1
			99	0.06399	0.06259	0.06329	0.00031	76.2
			100	0.06285	0.06136	0.06211	0.00031	76.0
			Average	**0.06303**	**0.06156**	**0.06230**	**0.00031**	**76.3**
3	41.4	41.4	96	0.09290	0.09181	0.09235	0.00045	77.9
			97	0.09269	0.09169	0.09219	0.00045	77.7
			98	0.09266	0.09159	0.09213	0.00045	77.8
			99	0.09324	0.09235	0.09279	0.00046	77.7
			100	0.09274	0.09159	0.09216	0.00045	77.5
			Average	**0.09285**	**0.09181**	**0.09232**	**0.00045**	**77.7**
4	41.4	55.2	96	0.12020	0.11871	0.11945	0.00059	78.6
			97	0.12011	0.11852	0.11931	0.00059	78.2
			98	0.12021	0.11877	0.11949	0.00059	78.3
			99	0.11953	0.11808	0.11881	0.00058	78.5
			100	0.11981	0.11828	0.11905	0.00059	78.7
			Average	**0.11997**	**0.11847**	**0.11922**	**0.00059**	**78.5**
5	41.4	68.9	96	0.15645	0.15519	0.15582	0.00077	76.7
			97	0.15618	0.15459	0.15538	0.00076	76.7
			98	0.15672	0.15519	0.15596	0.00077	76.4
			99	0.15599	0.15455	0.15527	0.00076	76.4
			100	0.15544	0.15414	0.15479	0.00076	76.5
			Average	**0.15616**	**0.15473**	**0.15544**	**0.00076**	**76.5**

Table 3-5 Resilient Modulus Testing Results for Sample AL-8A (Continued)

Sequence No.	Confining Pressure, S_3 (kPa)	Max. Axial Stress, S_{max} (kPa)	Cycle No.	Recovery Deformation (mm)		Average Recovery Deformation (mm)	Resilient Strain (mm/mm)	Resilient Modulus (MPa)
				LVDT 1	LVDT 2			
6	27.6	13.8	96	0.01622	0.01593	0.01607	0.00008	98.1
			97	0.01592	0.01556	0.01574	0.00008	100.1
			98	0.01669	0.01624	0.01647	0.00008	98.3
			99	0.01597	0.01562	0.01579	0.00008	100.2
			100	0.01728	0.01677	0.01702	0.00008	97.4
			Average	**0.01642**	**0.01602**	**0.01622**	**0.00008**	**98.8**
7	27.6	27.6	96	0.06174	0.06081	0.06127	0.00030	77.1
			97	0.06127	0.06040	0.06083	0.00030	77.0
			98	0.06290	0.06180	0.06235	0.00031	76.6
			99	0.06221	0.06122	0.06171	0.00030	76.4
			100	0.06120	0.06025	0.06073	0.00030	76.6
			Average	**0.06186**	**0.06090**	**0.06138**	**0.00030**	**76.7**
8	27.6	41.4	96	0.09392	0.09251	0.09321	0.00046	76.9
			97	0.09358	0.09211	0.09285	0.00046	76.7
			98	0.09300	0.09154	0.09227	0.00045	76.8
			99	0.09289	0.09142	0.09216	0.00045	77.1
			100	0.09279	0.09143	0.09211	0.00045	76.8
			Average	**0.09324**	**0.09180**	**0.09252**	**0.00046**	**76.8**
9	27.6	55.2	96	0.12053	0.11893	0.11973	0.00059	77.9
			97	0.12147	0.11985	0.12066	0.00059	77.7
			98	0.12067	0.11896	0.11982	0.00059	77.2
			99	0.12005	0.11858	0.11931	0.00059	77.9
			100	0.12036	0.11876	0.11956	0.00059	77.8
			Average	**0.12062**	**0.11902**	**0.11982**	**0.00059**	**77.7**
10	27.6	68.9	96	0.15371	0.15210	0.15290	0.00075	77.4
			97	0.15385	0.15233	0.15309	0.00075	77.3
			98	0.15380	0.15229	0.15305	0.00075	77.3
			99	0.15378	0.15238	0.15308	0.00075	77.3
			100	0.15393	0.15252	0.15322	0.00075	77.3
			Average	**0.15381**	**0.15232**	**0.15307**	**0.00075**	**77.3**

Table 3-5 Resilient Modulus Testing Results for Sample AL-8A (Continued)

Sequence No.	Confining Pressure, S_3 (kPa)	Max. Axial Stress, S_{max} (kPa)	Cycle No.	Recovery Deformation (mm)		Average Recovery Deformation (mm)	Resilient Strain (mm/mm)	Resilient Modulus (MPa)
				LVDT 1	LVDT 2			
11	13.8	13.8	96	0.01375	0.01340	0.01358	0.00007	113.4
			97	0.01388	0.01351	0.01370	0.00007	111.9
			98	0.01416	0.01367	0.01392	0.00007	110.0
			99	0.01458	0.01413	0.01435	0.00007	109.4
			100	0.01408	0.01368	0.01388	0.00007	111.0
			Average	**0.01409**	**0.01368**	**0.01389**	**0.00007**	**111.1**
12	13.8	27.6	96	0.05858	0.05736	0.05797	0.00029	81.9
			97	0.05856	0.05742	0.05799	0.00029	81.5
			98	0.05804	0.05703	0.05754	0.00028	82.0
			99	0.05891	0.05780	0.05836	0.00029	81.7
			100	0.05952	0.05807	0.05880	0.00029	81.4
			Average	**0.05872**	**0.05754**	**0.05813**	**0.00029**	**81.7**
13	13.8	41.4	96	0.08964	0.08767	0.08865	0.00044	80.1
			97	0.08946	0.08791	0.08869	0.00044	80.2
			98	0.08914	0.08716	0.08815	0.00043	79.9
			99	0.09029	0.08874	0.08951	0.00044	80.1
			100	0.08983	0.08804	0.08893	0.00044	79.6
			Average	**0.08967**	**0.08790**	**0.08879**	**0.00044**	**80.0**
14	13.8	55.2	96	0.11846	0.11668	0.11757	0.00058	79.6
			97	0.11779	0.11596	0.11688	0.00058	79.6
			98	0.11718	0.11564	0.11641	0.00057	78.9
			99	0.11751	0.11564	0.11658	0.00057	79.6
			100	0.11768	0.11589	0.11678	0.00057	79.4
			Average	**0.11772**	**0.11596**	**0.11684**	**0.00058**	**79.4**
15	13.8	68.9	96	0.15010	0.14792	0.14901	0.00073	79.0
			97	0.15081	0.14856	0.14968	0.00074	78.9
			98	0.15077	0.14885	0.14981	0.00074	78.8
			99	0.15095	0.14895	0.14995	0.00074	78.8
			100	0.15054	0.14829	0.14941	0.00074	78.8
			Average	**0.15063**	**0.14851**	**0.14957**	**0.00074**	**78.9**

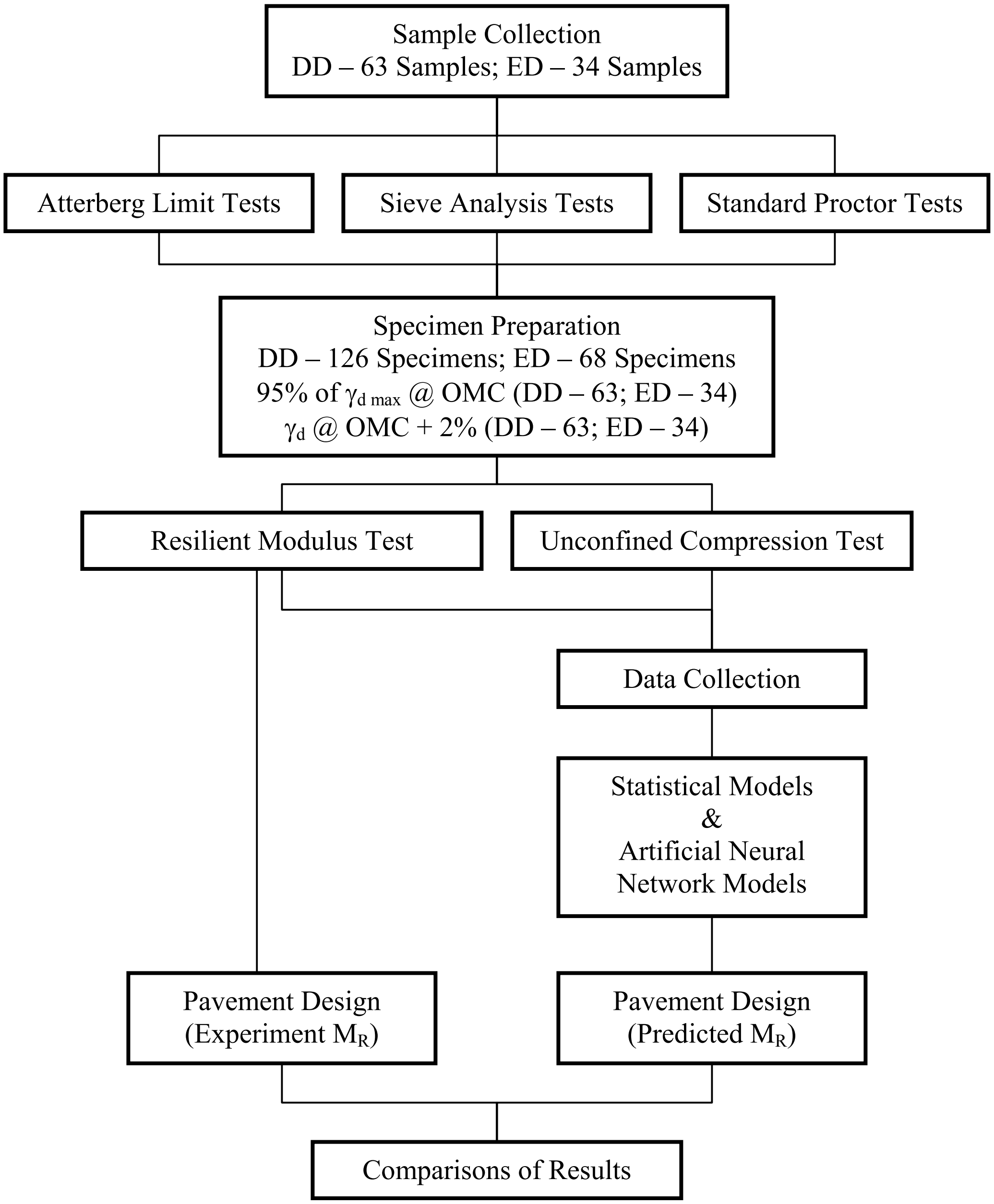

ED = Evaluation Dataset
DD = Development Dataset
M_R = Resilient Modulus
OMC = Optimum Moisture Content
γ_d = Dry Density
$\gamma_{d\,max}$ = Maximum Dry Density

Figure 3-1 Flow Chart of Operations

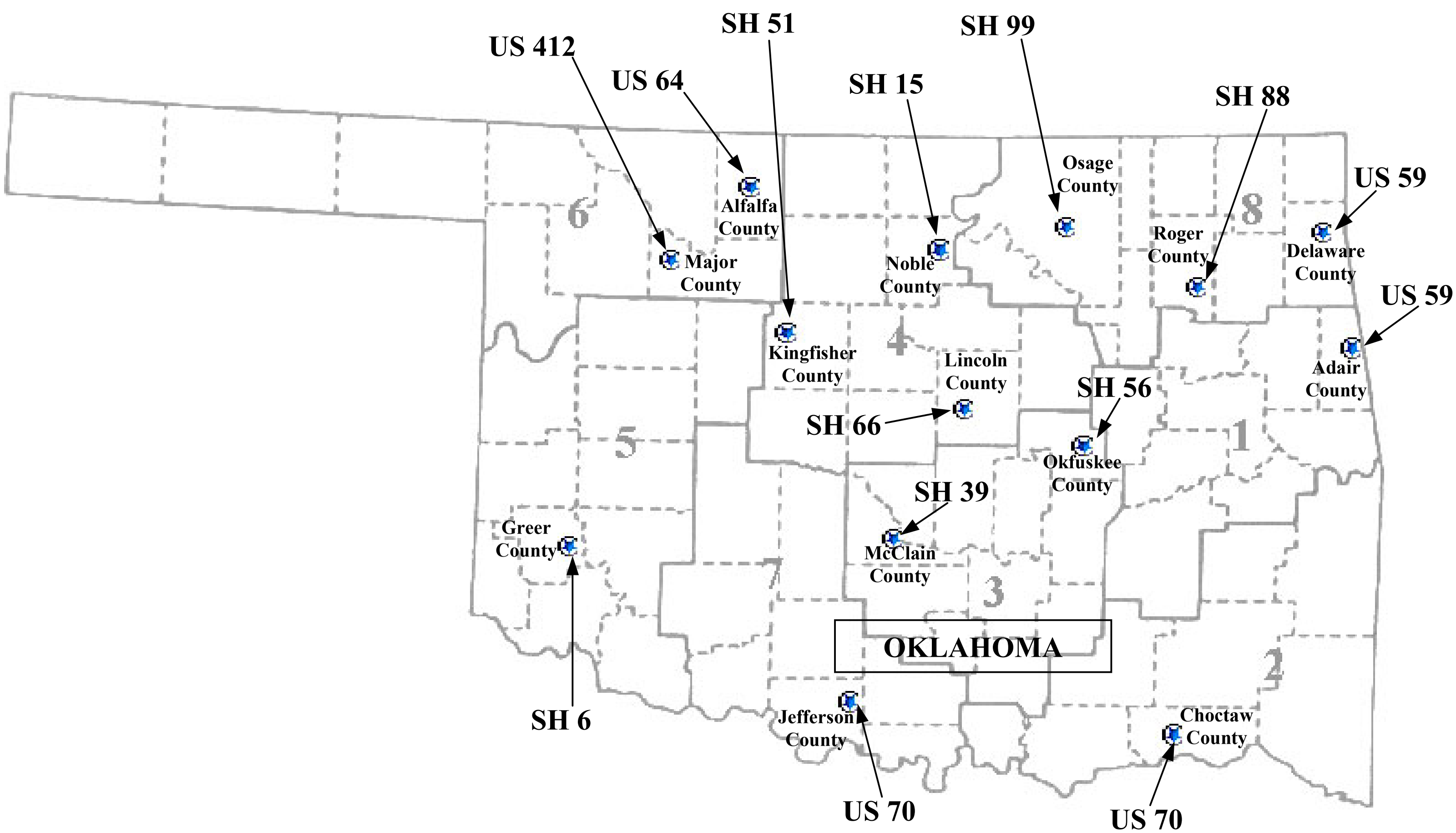

Figure 3-2 Location Map for Soil Samples Used in Laboratory Testing and Model Development

Figure 3-3 Location Map for Additional Soils Samples Used in Model Evaluation

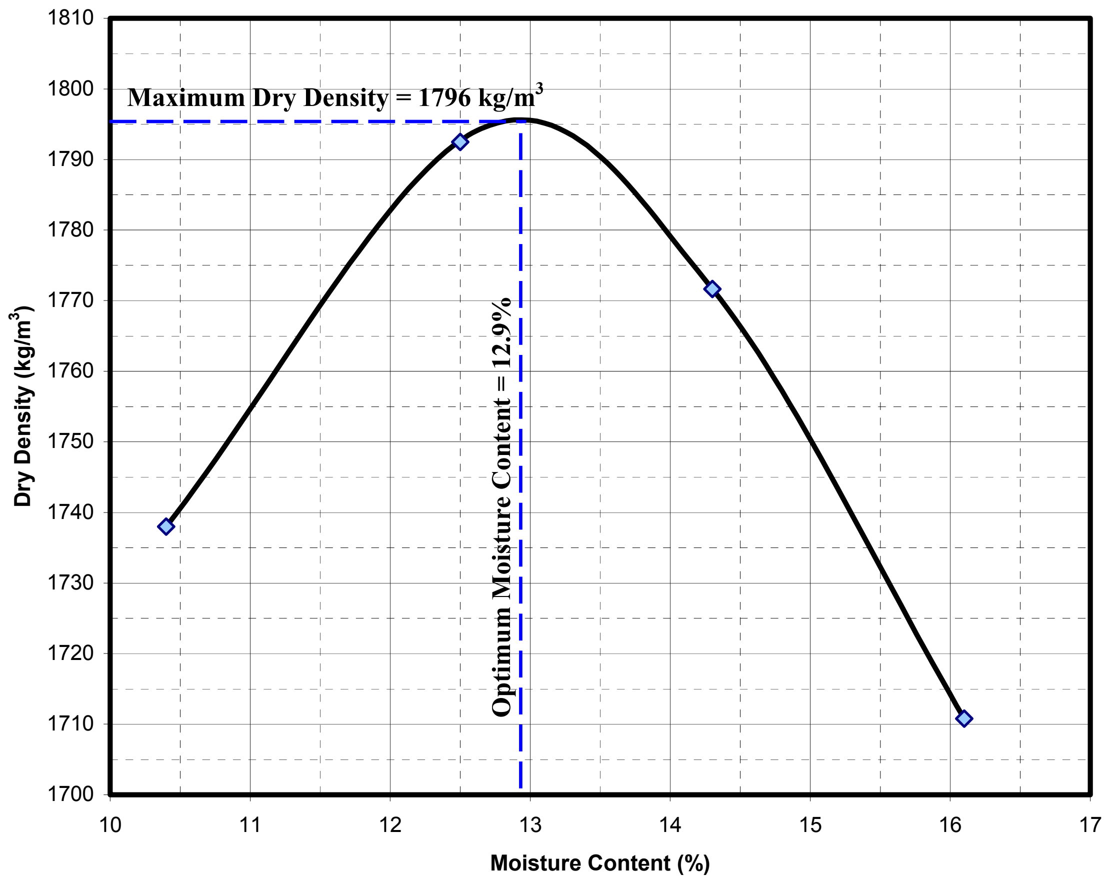

1 kg/m^3 = 0.06243 pcf

Figure 3-4 Moisture-Density Relationship Curve for Sample AL-10

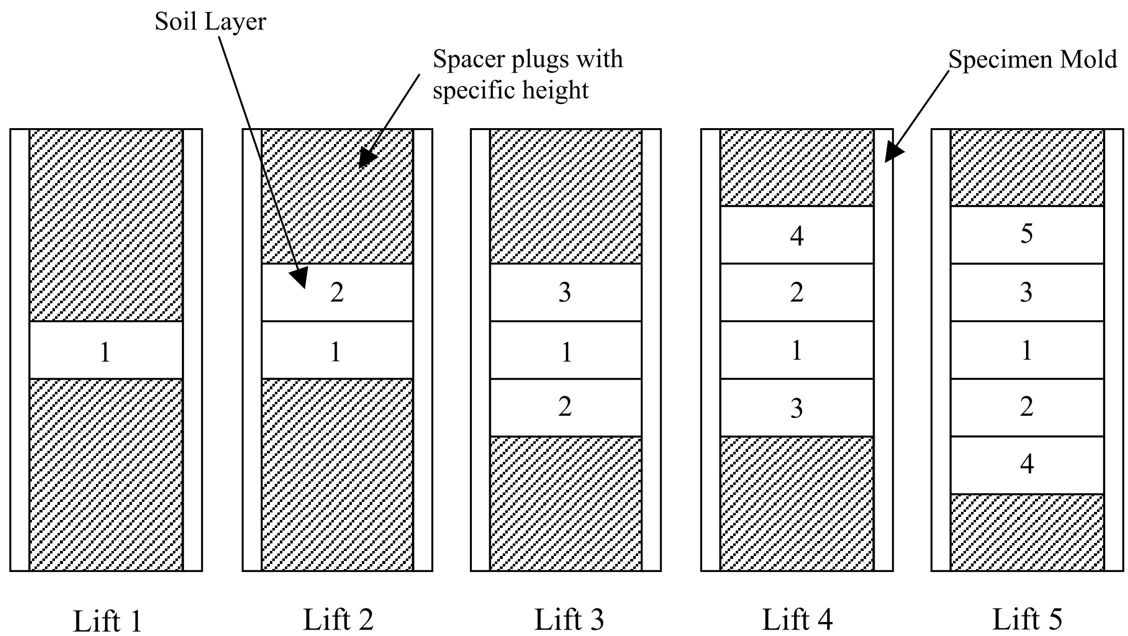

Figure 3-5 Static Compaction Process (AASHTO, 2004)

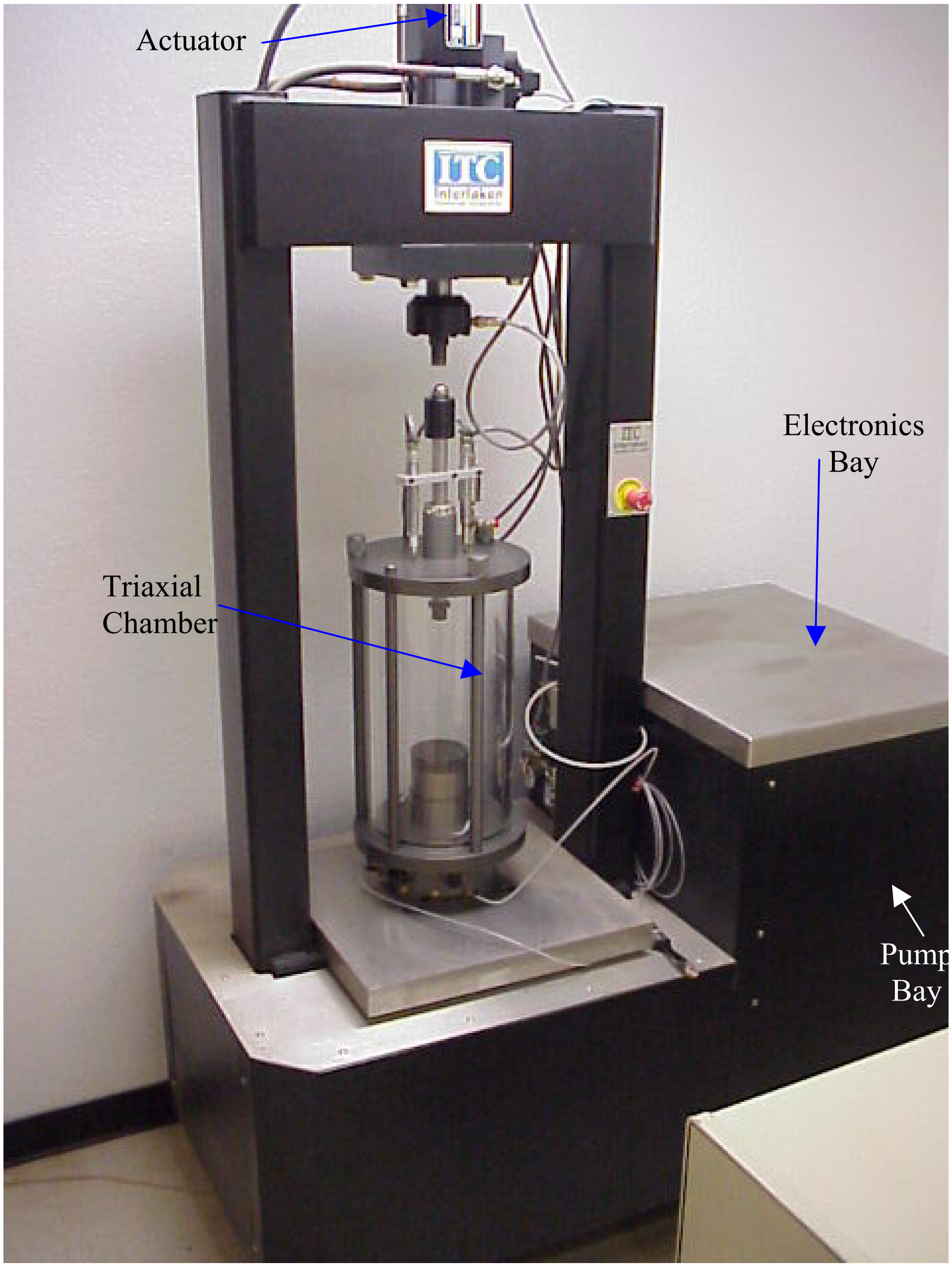

Figure 3-6 Resilient Modulus Testing System

Figure 3-7 Detail Illustration of Electronics Bay and Pump Bay

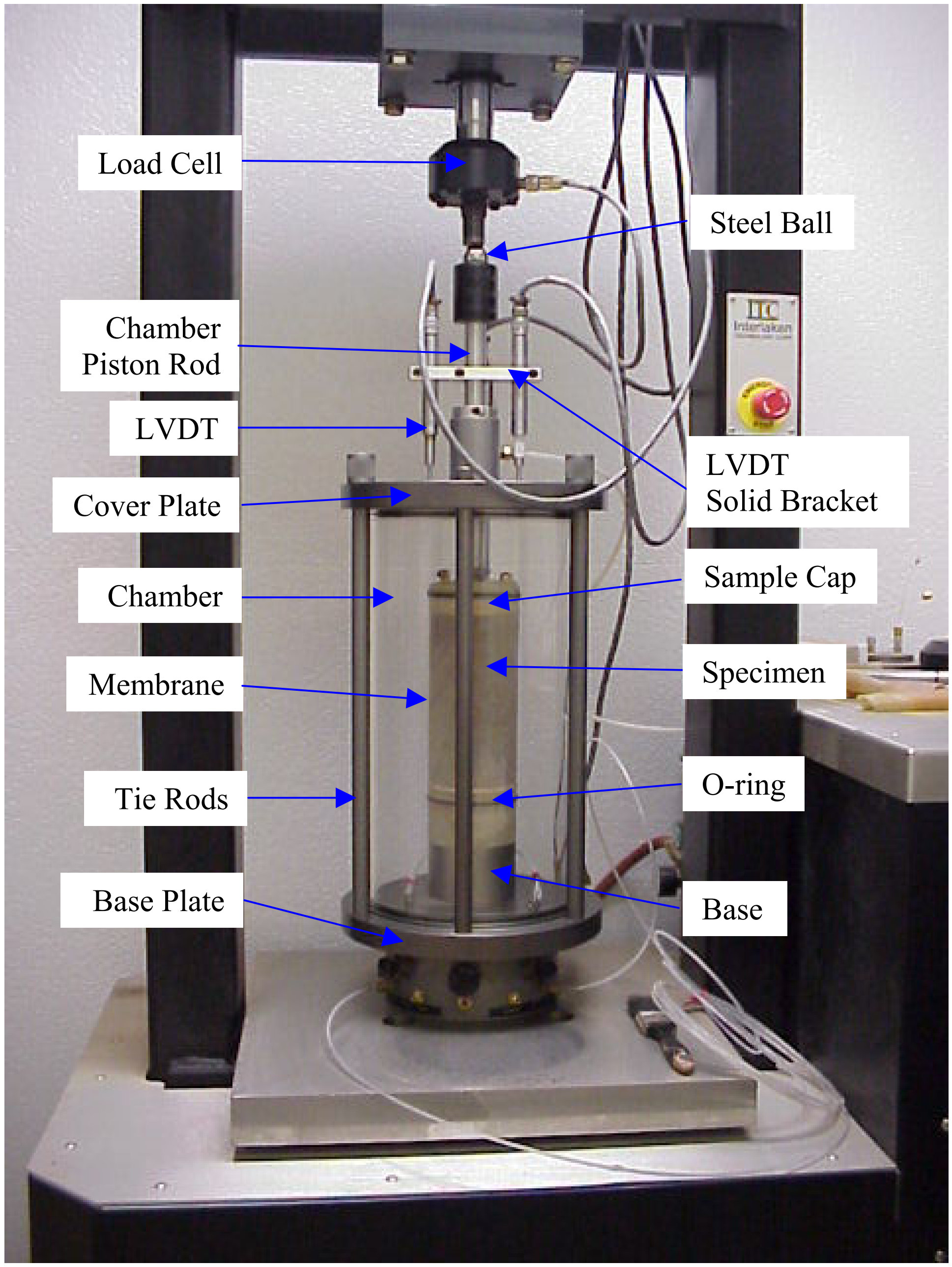

Figure 3-8 Triaxial Chamber Setup for Resilient Modulus Test

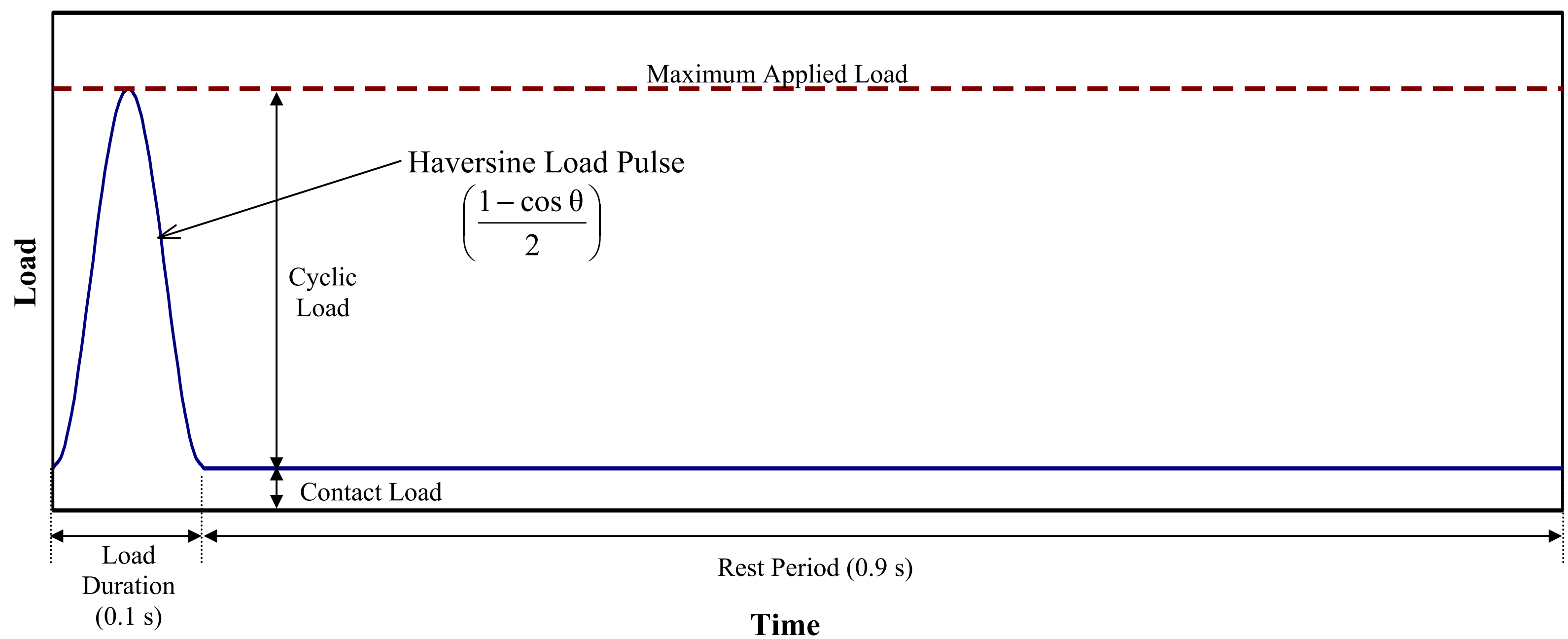

Figure 3-9 Haversine-shaped Load Pulse in a Loading Cycle

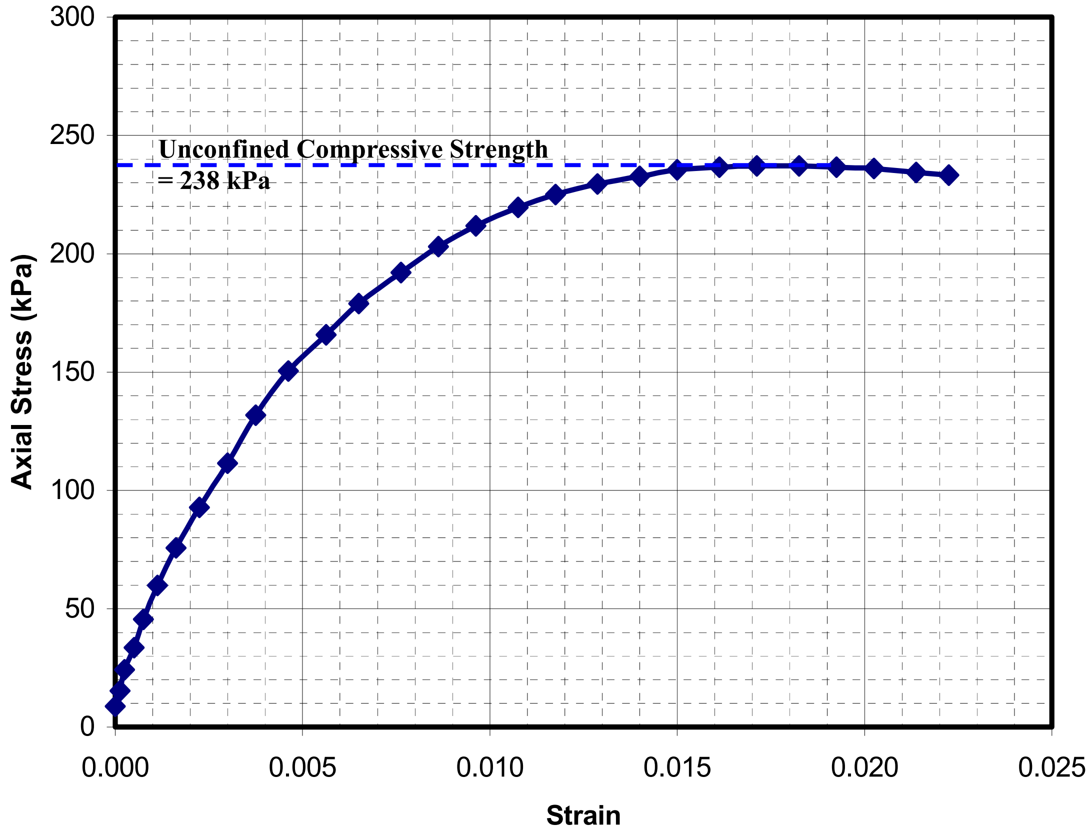

1 kPa = 0.145 psi

Figure 3-10 Unconfined Compression Test Results for Sample AL-8A

CHAPTER 4

PRESENTATION OF RESULTS

4.1 Introduction

A series of laboratory tests were conducted in this study to evaluate the properties of the soils collected from different roadway projects across Oklahoma. The following tests were conducted: Atterberg limits, grain size distribution, standard Proctor, unconfined compressive strength, and resilient modulus. These tests are part of the Oklahoma Department of Transportation (ODOT) testing specifications for evaluations of subsurface materials for design of roadways. As discussed in Chapters 1 and 2, the purpose of this study is to develop statistical and Artificial Neural Network (ANN) models that can be used to determine the M_R based on commonly used soil properties. As noted in Chapter 3, a rather significant number of soils from fifteen different counties in Oklahoma is used in this study. It is intended that the models developed in this study could be used in the implementation of both the currently used AASHTO 1993 Design Guide and the AASHTO 2002 Design Guide for levels 2 and 3 pavement designs. No previous studies have attempted to include that many soils from Oklahoma in developing correlations for resilient modulus for pavement design applications.

In this study, two sets of data were generated for the development (henceforth called "Development Dataset") and evaluation (henceforth called "Evaluation Dataset") of models. The data used in the evaluation of models were independent of those used in the development of models. The Development Dataset includes data from sixty-three (63) soil samples from fourteen (14) different sites. The Evaluation Dataset, on the other hand, contains data from thirty-four (34) soil samples from three (3) different sites. Thus, a total of one hundred and twenty-six (126) M_R tests were conducted for the development dataset and sixty-eight (68) tests were conducted for the evaluation of dataset. The laboratory test results and analysis of each set of data are presented in this chapter. The applications of these test data for development and evaluation of models for statistical models and ANN models are presented in Chapter 5 and Chapter 6, respectively.

4.2 Soil Parameters

This section discusses the results of the commonly used laboratory tests, and their influence on the mechanistic-empirical (M-E) pavement design. The material parameters selected for the study were plasticity index (PI), percent passing 200 (P200), specimen moisture content (w_c), specimen dry density (γ_d), and unconfined compression (UC) were used for model development. A brief description of Atterberg limits, grain size distribution, soil classification, group index, moisture content, dry density, unconfined compressive strength results, and resilient modulus test results are presented in the following sections.

4.2.1 Material parameters and their Relationship with M-E Pavement Design

The primary reason for the selection of the material parameters was to determine a relationship between M_R and routine soil properties. Furthermore, since the sampling and testing were performed according to ODOT specifications and the intension was to eventually incorporate the ODOT and other datasets pertaining to Oklahoma-based testing agencies, the selection of material parameters were limited to the above mentioned five parameters. It should, however, be noted that the selected parameters are influential in an M-E pavement design.

A mechanistic-empirical (M-E) pavement design method generally uses the layered elastic analysis to calculate the traffic-induced elastic strains (NCHRP, 2004). The critical strains are then empirically related to the rate at which pavement deteriorates by calibrating against observed performance of test pavements or in-service pavements (FHWA, 2000; NCHRP, 2004). M_R is a measure of stiffness of associated materials in the M-E design procedure. Fredlund et al. (1995) proposed prediction of shear strength of unsaturated soils using soil-water characteristic curves and Vanapalli et al. (1998) studied the effect of unsaturated shear strength on compacted clay at different initial water contents. These studies present the variation in soil suction due to soil structure as influenced by the initial compaction water content.

Vanapalli, (2000) employed PI to predict the shear strength of an unsaturated soil. Additionally, Lobbezzoo, et al. (2001) proposed techniques for estimating the coefficient of permeability of unsaturated soils and a fitting factor that is related to PI. Other researchers also have studied the effect of moisture-density relationship on elastic modulus and strength of soil (Swenson, et al., 2006). For example, Siekmeier and Robertson (2002) noted that the material properties that contribute to pavement distress include M_R and shear strength, which are influenced by moisture content, density and gradation. As a result, even though the material parameters selected for this study may not be directly correlated with $M_{R,}$ they do influence the stiffness of the specimens and may be used for determination of M_R

4.2.2 Liquid Limit (LL)

The results from the Liquid Limit (LL) tests for the development dataset range from 21 to 67 with a mean of 34.5 and a standard deviation of 10.0. The range of LL for evaluation dataset is from, 24 to 52 with a mean of 36.5 and a standard deviation of 8.4. Table 4-1 presents the basic statistical parameters for the two sets of data. Skewness is a measure of distribution of the data. A skewness of zero indicates perfectly normal distribution of data. Negative value of skewness indicates the data skewed left and positive value indicates the data skewed right. Based on the skewness parameter, the LL values for the evaluation dataset (i.e., 0.18) are more normally distributed than the development dataset (i.e., 1.11). Kurtosis parameter is an indicator of heaviness of the tail. A perfectly normal distribution of data has a Kurtosis of zero. A positive Kurtosis is an indication of more observations on the tail end of the distribution curve, while a negative Kurtosis is an indication of fewer observations on the tail end of the distribution curve. Based on the Kurtosis parameter, the LL data for development dataset and evaluation dataset are not distributed similarly (Figure 4-1). The development dataset has more data on the tail end with a Kurtosis of 1.20. On the other hand, the evaluation dataset has less data on the tail end with a Kurtosis of –1.16. These results indicate that the LL data are not perfectly normally distributed; however, the deviation is small and therefore, normally distributed theories may be applied in statistical analysis. Montgomery, (2006) has shown through Monte Carlo experiments that datasets deviating from normal distribution would not effect the outcome of the analysis and the results would not be critically affected.

The evaluation dataset is made up of soils from three (3) roadway sites. Two sites are located in northeast (Rogers County) Oklahoma and one site is located in northwest (Woodward County) Oklahoma. Closer look at these data indicate that the basic statistical parameters of the soils from Rogers County are different than the soils from Woodward County. The LL from Rogers County soils has wider range than Woodward County soils. The LL ranges from 24 to 52 for Rogers County. The corresponding range for Woodward County soils is 24 to 28. The mean and standard deviation of the LL from Rogers County are higher than those Woodward County. The Rogers County's LL has a mean of 38.3 and a standard deviation of 7.8, while the LL from Woodward County has a mean of 26.0 and standard deviation of 1.9. Furthermore, the basic statistical parameters (i.e., skewness and Kurtosis) for the Rogers County soils are closer to the soils from the development dataset (Table 4-1 and Figure 4-2). The difference in the mean values between the development dataset and the evaluation dataset for Rogers County soils is 2.0. However, the difference between the development dataset and the evaluation dataset from Woodward County is 8.5.

4.2.3 Plastic Limit (PL)

The Plastic Limit (PL) for the development dataset has a mean of 16.1 and a standard deviation of 3.5. The PL for the development dataset ranges from 9 to 27. The results for the evaluation dataset show a mean of 15.5 and a standard deviation of 2.7. The evaluation dataset ranges from 12 to 21 in PL values. The basic statistical parameters for the two sets of data are presented in Table 4-2. The distributions of the two sets of data are presented in Figure 4-3. The basic statistical parameters and the figure show that the distributions for both datasets are close to normally distributed. The skewness of the development and the evaluation datasets are 1.11 and 0.56, respectively, which are close to zero. Moreover, the Kurtosis of the development and the evaluation datasets are also close to zero. The Kurtosis of the development and the evaluation datasets are 1.48 and –1.00, respectively. The results also indicated that the distribution for the development dataset, the evaluation dataset for Rogers County, and the evaluation dataset for Woodward County are similar (Figure 4-4). Their largest differences in mean and standard deviation are 0.9 and 1.7, respectively.

4.2.4 Plasticity Index (PI)

The Plasticity Index (PI) values for the development dataset range from 7 to 43. The mean and standard deviation for the development dataset is 18.4 and 8.4. For the evaluation dataset, the mean of the PI values is 20.9 and the standard deviation is 8.9. The range of PI for the evaluation dataset is from 6 to 36. Table 4-3 presents the basic statistical parameters of the PI for the development and evaluation datasets. Figure 4-5 presents the distribution of the PI for both datasets. The results from the statistical parameters and figure show that the distributions of the PI for both datasets may be considered normal. The skewness and Kurtosis for both datasets are near zero. The development dataset has a skewness of 0.97 and a Kurtosis of 0.63. The evaluation dataset has a skewness of –0.03 and a Kurtosis of –1.22. A review of the evaluation data indicates that the soils from Rogers County and Woodward County have different PI distribution (Figure 4-4). The differences between Rogers County and Woodward County are 15.9 in the mean value and 5.4 in the standard deviation. Overall, the Rogers County soils are closer to the soils from the development data. The range of PI for the Rogers County soils is from 6 to 36, which is close to the range for the development data (i.e., 7 to 43). The standard deviations for both the development dataset and the evaluation dataset from Rogers County are similar at 8.4. Based on the data distribution and to capture the effect of the plasticity of the soils, the PI was selected as a soil parameter for development of the models.

4.2.5 Grain Size Distribution

Collection of grain size distribution data on ODOT projects involves the following sieves: 4.75 mm (No. 4), 2.00 mm (No. 10), 0.425 mm (No. 40), and 0.075 mm (No. 200). In the present study, the effect of percent silt and clay was included aggregately in the percent passing 0.075 mm (No. 200). As presented in Chapter 2, a number of researchers have separated the contribution of percent silt and clay in developing statistical models (Drumm et al., 1990; Santha, 1994; Mohammad et al., 1999). Since this was the first study in Oklahoma to investigate the contribution of the controlling material parameters on $M_{R,}$ it was decided to limit the scope to the current ODOT specifications. Following the analysis of laboratory test results and model development, a sensitivity study was performed to determine the effect of selected material parameters on M_R (see Tables 6-3 through 6-10). It was determined that the contribution of particle size and sieve analysis is limited and PI reflects the effect of clays. Tables 4-4 through 4-6 and Figures 4-7 through 4-12 present the grain size distribution results in terms of percent passing 4.75 mm (No. 4), 2.00 mm (No. 10), and 0.425 mm (No. 40) sieves. These results indicate that the grain size distribution for percent passing 4.75 mm (No. 4), 2.00 mm (No. 10), and 0.425 mm (No. 40) sieves are strongly skewed and are not normally distributed. The skewness for the development dataset from the three sieve sizes ranges from –3.27 to –3.64. The Kurtosis for the development dataset also is high, which ranges from 10.79 to 14.40. The evaluation dataset also shows similar skewness and Kurtosis. The skewness and Kurtosis for the evaluation dataset range from –1.82 to –2.77 and 3.05 to 7.89, respectively. These results are expected since the soils collected in the present study are relatively fine-grained soils. Thus, the theory of normal distribution may not be applied to these results. Furthermore, the high degree of skewness of data to one side reduces the contribution of data to the development of the models (Myers et al., 2001; Montgomery et al., 2006). As a result, these data (i.e., percent passing 4.75 mm (No. 4), 2.00 mm (No. 10), and 0.425 mm (No. 40) sieves) were not used in the development of the statistical and ANN models. Only the results from percent passing 0.075 mm (No. 200) sieve are used, from grain size distribution tests, in the model development.

The percent passing 0.075 mm (No. 200) sieve for the development dataset range from 36.5% to 98.0% with a mean of 83.0% and a standard deviation of 15.0%. The range for percent passing 0.075 mm (No. 200) sieve for the evaluation dataset is, on the other hand, from 37.9% to 94.2% with a mean of 94.2% and a standard deviation of 13.1%. Table 4-7 presents the basic statistical parameters for both datasets. These results indicate that the percent passing 0.075 mm (No. 200) sieve data are relatively normally distributed (Figure 4-13). The skewness is –1.05 for the development dataset and –0.49 for the evaluation dataset. The Kurtosis for the development and the evaluation datasets are 0.37 and 0.27, respectively. They are all close to the values for a normally distribution case (i.e., 0). Based on Table 4-7 and Figure 4-14, the percent passing 0.075 mm (No. 200) sieve data for the evaluation dataset from Rogers County and Woodward County soils are not distributed similarly. The standard deviations and

Kurtosis for Rogers County and Woodward County soils are different. The standard deviation for the Rogers County soils is 13.9%. The corresponding value for the Woodward County soils is 8.0%. The Kurtosis corresponding values are 0.16 and 3.89, respectively.

4.2.6 Soil Classification

The soils in this study were classified according to the Unified Soil Classification System (USCS) as per ASTM D2487 and AASHTO classification systems. The results for the development dataset and the evaluation dataset are presented in Tables 4-8 and 4-9, respectively. Based on the USCS, fifty-six (56) (i.e., 89%) soil samples from the development dataset and twenty-eight (28) (i.e., 82%) soil samples from the evaluation dataset are classified as low plastic lean clay (CL) (Figure 4-15). The rest of the soils, 11% for the development dataset and 18% for the evaluation dataset, are classified as fat clay (CH), silty clay (CL-ML), or clayey sand (SC). The USCS results for the evaluation dataset for Rogers County and Woodward County soils indicate that a majority of the soils are classified as lean clay (CL) (Figure 4-16).

According to AASHTO classification system, soils in the development dataset and the evaluation dataset fall in the A-4, A-6 or A-7-6 categories. The soils in the development dataset are classified as nineteen percent (19%) “A-4”, fifty-four percent (54%) “A-6”, and twenty-six percent (26%) “A-7-6”. The evaluation dataset are classified as twelve percent (12%) “A-4”, fifty-two percent (52%) “A-6”, and thirty-five percent (35%) “A-7-6” (Figure 17). The AASHTO classification results of the evaluation dataset for Rogers County and Woodward County indicate that a majority of the Rogers County soils are “A-6” and “A-7-6” type soils, while the soils from

Woodward County are primarily “A-4” and “A-6” type (Figure 4-18). This implies that Rogers County soils are more clayey than the Woodward County soils and resemble the development dataset more closely than the soils from Woodward County. These classification results could be used to explain the results presented in Chapters 5 and 6.

4.2.7 Group Index (GI)

The GI values for the development dataset range from 1 to 39. The mean and standard deviation for the GI values are 13.2 and 8.6. The range of GI for the evaluation dataset is from 1 to 31, with a mean of 14.6 and a standard deviation of 9.6. The basic statistical parameters for the two sets of data are presented in Table 4-10. The distribution of the GI values may be considered normally distributed since the deviation is small (Figure 4-19). The skewness of the development and the evaluation datasets are 0.81 and 0.29, respectively. The Kurtosis values of the development and the evaluation datasets are 0.58 and -1.36, respectively. These values are close to the normal distribution values (i.e. 0). Additionally, the distributions of GI data for the evaluation dataset from Rogers County and Woodward County are different (Figure 4-20). The results show that the mean of the evaluation dataset from Rogers County and Woodward County are 16.1 and 5.4, respectively. The corresponding standard deviations from Rogers County and Woodward County are also different, which are 9.5 and 2.6, respectively.

4.2.8 Moisture Content

After the completion of the M_R test, the moisture content of the tested specimen was determined. This moisture content is used as a parameter in the present study. The moisture contents for the development dataset range from 10.5% to 25.3% with a mean of 17.4% and a standard deviation of 3.0%. The range of moisture content for the evaluation dataset is from 11.4% to 22.4% with a mean of 17.3% and a standard deviation of 2.9%. Table 4-11 presents the basic statistical parameters for both datasets. These results indicate that the moisture content data are not perfectly normally distributed, but the deviation is small and may be considered normally distributed. The skewness and the Kurtosis of the datasets are close to zero, which indicated normal distribution. The skewness for moisture content for the development and the evaluation datasets are 0.39 and –0.24, respectively. The Kurtosis for the development and the evaluation datasets are -0.14 and –0.94, respectively. The mean, standard deviation, skewness, and Kurtosis of both datasets are close, thus, both datasets are similar in distribution (Figure 4-21). A review of "evaluation data" indicates that the basic statistical parameters of the soils from Rogers County are different than the soils from Woodward County. As indicated by the soil parameters, the Woodward County soils are less plastic than Rogers County soils. Therefore, a lower moisture content is required for the Woodward County soils to reach the OMC than the soils in Rogers County.

4.2.9 Dry Density

The dry density for the development dataset ranges from 1404.2 kg/m^3 (87.7 pcf) to 1872.6 kg/m^3 (116.9 pcf) with a mean of 1658.0 kg/m^3 (103.5 pcf) and a standard deviation of 106.7 kg/m^3 (6.7 pcf). The range of dry density for the evaluation dataset is from 1544.7 kg/m^3 (96.4 pcf) to 1862.9 kg/m^3 (116.3 pcf) with a mean of 1689.2 kg/m^3 (105.5 pcf) and a standard deviation of 74.8 kg/m^3 (4.7 pcf). Table 4-12 presents the basic statistical parameters for the two sets of data. These results indicate that the dry density data are distributed similarly for the development and the evaluation datasets

(Figure 4-23 and Figure 4-24). The mean and standard deviation are close to each other for the development and the evaluation datasets for Rogers County and Woodward County soils. The difference of the mean values is within 124 kg/m^3 (7.7 pcf). A review of the evaluation dataset also indicates that the distributions of the Rogers County and Woodward County soils are similar. As indicated by the soil parameters, the Woodward County soils are less plastic than Rogers County soils. Therefore, a higher specimen dry density and lower moisture content is obtained for the Woodward County soils.

4.2.10 Unconfined Compressive Strength

The ranges of the unconfined compression strength for the development and the evaluation dataset are from 50.9 kPa (7.38 psi) to 443.5 kPa (64.3 psi) and 56.5 kPa (8.2 psi) to 357.7 kPa (51.9 psi), respectively. The development dataset has a mean of 193.6 kPa (28.1 psi) and a standard deviation of 70.8 kPa (10.3 psi). The evaluation dataset has a mean of 159.9 kPa (23.2 psi) and a standard deviation of 64.4 kPa (9.3 psi). Table 4-13 presents the basic statistical parameters for both datasets. Based on the skewness and Kurtosis parameters, the unconfined compressive strength of the development and the evaluation datasets are normally distributed (Figure 4-25). The skewness and Kurtosis for the development dataset is 0.68 and 0.50, respectively. The corresponding skewness and Kurtosis for the evaluation dataset is 0.78 and 0.81, respectively. A review of the evaluation dataset indicates that the basic statistical parameters of the soils from Rogers County are different than the soils from Woodward County. The unconfined compression strength from the Rogers County soils starts from a lower range; from 56.5 kPa (8.2 psi) to 292.4 kPa (42.4 psi). On the other hand, the range for Woodward County is from 110.8 kPa (16.1 psi) to 357.7 kPa (51.9 psi). As indicated in the previous sections, the Woodward County specimens are denser with lower moisture content. This contributed to a higher minimum unconfined compressive strength. The basic statistical parameters of the Rogers County and Woodward County soils are similar to the soils from the development dataset (Table 4-13 and Figure 4-26). The means and standard deviations of the unconfined compressive strength are close for both the Rogers County and Woodward County soils.

4.3 Resilient Modulus Test

Two M_R specimens were prepared for each soil sample. One M_R specimen was compacted at the optimum moisture content (OMC) and 95% of maximum dry density, and the moisture content and dry density for the other specimen was set at 2% wet of OMC. Therefore, 126 M_R tests for the developmental dataset and 68 M_R tests for the evaluation dataset. According to the AASHTO specifications, there are fifteen sequences with different stress state in the M_R test. An average M_R value was determined at each sequence.

The M_R test results for the development dataset and the evaluation dataset are presented in Tables 4-14 and 4-15. A review of the M_R results from the development dataset indicates a very high standard deviation of M_R, which is in excess of 340 MPa (49.3 ksi) for the loading sequences 1, 6, and 11. This high standard deviation is attributed to the variation occurring in the M_R values at these loading sequences. The high standard deviation (more than 89 MPa or 12.9 ksi) for M_R values is also observed for the evaluation dataset in loading sequences 1, 6, and 11. In loading sequences 1, 6, and 11, the applied axial stress is 13.8 kPa (2 psi). This axial stress level may be too low to generate significant enough deformation relative to the accuracy of the deformation system. With small deformations, the M_R values will be high. Moreover, the small deformation values generated in these loading sequences may be electrical noise. As a result, the loading sequences 1, 6, and 11 were omitted and were not used in the study.

A review of the evaluation dataset for Rogers County soils, involving fifty-eight (58) specimens indicated a similarly high standard deviation (more than 86 MPa or 12.9 ksi) for loading sequences 1, 6, and 11; however, the test results for the ten (10) specimens from Woodward County soils did not indicate the same high standard deviation (more than 14 MPa or 2.0 ksi) for loading sequences 1, 6, or 11. According to NCHRP, (1997), this could be contributed to the sampling rate and/or the noise-level associated with the measurement accuracy of the deformation and applied stress. The LVDT used in the present study has ± 6.35 mm (± 0.25 in) stroke length with an accuracy of ± 0.001651 mm (± 0.000065 in). The 4448.22 Newton (1000 lb-force) load cell used here had an accuracy of ± 11.12 Newton (± 2.5 lb-force). Based on these levels of LVDT and load cell accuracies, the percent error for a typical M_R test (Table 3-5, specimen AL-8A) was evaluated. The percent error for the confining pressure of 41.4 kPa (6 psi) (the highest confining pressure and worse case scenario) for loading sequences 1, 2, 3, 4, and 5 were found to be (30.2% to –39.7%), (8.2% to –8.6%), (5.6% to –5.8%), and (3.4% to –3.5%), respectively. It was further determined that the relationship between the error of the LVDT and load cell is cumulative. The error for both load cell and LVDT is most significant for the lowest deviator stress condition. Consequently, it was decided to omit the 1, 6, and 11 loading sequences from further evaluations.

Table 4-1 Basic Statistical Parameters for Liquid Limit (LL)

Dataset	No. of Soils	Mean	Median	Min.	Max.	Std. Dev.	Skew-ness	Kurt-osis
Development	63	34.5	33.0	21	67	10.0	1.11	1.20
Evaluation: Overall	34	36.5	35.0	24	52	8.4	0.18	-1.16
Evaluation: Rogers County	29	38.3	37.0	24	52	7.8	0.03	-1.02
Evaluation: Woodward County	5	26.0	27.0	24	28	1.9	-0.38	-2.90

Table 4-2 Basic Statistical Parameters for Plastic Limit (PL)

Dataset	No. of Soils	Mean	Median	Min.	Max.	Std. Dev.	Skew-ness	Kurt-osis
Development	63	16.1	15.0	9	27	3.5	1.11	1.48
Evaluation: Overall	34	15.5	14.5	12	21	2.7	0.56	-1.00
Evaluation: Rogers County	29	15.6	15.0	12	21	2.9	0.50	-1.19
Evaluation: Woodward County	5	15.2	14.0	14	18	1.8	1.26	0.31

Table 4-3 Basic Statistical Parameters for Plasticity Index (PI)

Dataset	No. of Soils	Mean	Median	Min.	Max.	Std. Dev.	Skew-ness	Kurt-osis
Development	63	18.4	17.0	7	43	8.4	0.97	0.63
Evaluation: Overall	34	20.9	21.5	6	36	8.9	-0.03	-1.22
Evaluation: Rogers County	29	26.7	23.0	6	36	8.4	-0.32	-0.89
Evaluation: Woodward County	5	10.8	12.0	6	13	3.0	-1.43	1.58

Table 4-4 Basic Statistical Parameters for Percent Passing 4.75 mm (No. 4) Sieve

Dataset	No. of Soils	Mean	Median	Min.	Max.	Std. Dev.	Skew-ness	Kurt-osis
Development	63	98.0	100.0	73.4	100.0	6.4	-3.47	10.79
Evaluation: Overall	34	97.7	100.0	79.1	100.0	4.8	-2.77	7.89
Evaluation: Rogers County	29	97.3	99.6	79.1	100.0	5.1	-2.52	6.36
Evaluation: Woodward County	5	100.0	100.0	100.0	100.0	0.0	0.00	0.00

Table 4-5 Basic Statistical Parameters for Percent Passing 2.0 mm (No. 10) Sieve

Dataset	No. of Soils	Mean	Median	Min.	Max.	Std. Dev.	Skew-ness	Kurt-osis
Development	63	96.2	99.9	47.3	100.0	9.3	-3.64	14.40
Evaluation: Overall	34	95.6	99.3	74.6	100.0	6.7	-1.87	3.05
Evaluation: Rogers County	29	64.8	97.9	74.6	100.0	7.0	-1.66	2.22
Evaluation: Woodward County	5	100.0	100.0	100.0	100.0	0.0	0.00	0.00

Table 4-6 Basic Statistical Parameters for Percent Passing 0.425mm (No. 40) Sieve

Dataset	No. of Soils	Mean	Median	Min.	Max.	Std. Dev.	Skew-ness	Kurt-osis
Development	63	93.4	97.3	39.6	99.9	10.5	-3.27	12.38
Evaluation: Overall	34	88.8	92.2	49.3	100.0	11.4	-1.82	3.53
Evaluation: Rogers County	29	87.4	90.9	49.3	100.0	11.9	-1.61	2.76
Evaluation: Woodward County	5	96.3	96.5	95.1	97.7	1.0	0.22	0.26

Table 4-7 Basic Statistical Parameters for Percent Passing 0.075 mm (No. 200) Sieve

Dataset	**No. of Soils**	**Mean**	**Median**	**Min.**	**Max.**	**Std. Dev.**	**Skew-ness**	**Kurt-osis**
Development	63	78.5	83.0	36.5	98.0	15.0	-1.05	0.37
Evaluation: Overall	34	74.2	74.8	37.9	94.2	13.1	-0.49	0.27
Evaluation: Rogers County	29	74.6	75.2	37.9	94.2	13.9	-0.59	0.16
Evaluation: Woodward County	5	71.9	70.2	65.4	85.8	8.0	1.88	3.89

Table 4-8 Summary of Soil Classification Results for the Development Dataset

Soil Classification		**Number of Soils**
Unified Soil Classification System (USCS)		
Fat clay	CH	2
Sandy fat clay	CH	1
Lean clay	CL	23
Lean clay with sand	CL	22
Gravelly lean clay	CL	2
Sandy lean clay	CL	8
Silty clay with sand	CL-ML	1
Sandy silty clay	CL-ML	1
Clayey Sand	SC	1
Clayey Sand with gravel	SC	2
	Total :	**63**
AASHTO Classification System		
A-4		12
A-6		34
A-7-6		17
	Total :	**63**

Table 4-9 Summary of Soil Classification Results for the Evaluation Dataset

Soil Classification		**Number of Soils**
Unified Soil Classification System (USCS)		
Fat clay	CH	1
Fat clay with sand	CH	1
Lean clay	CL	8
Lean clay with sand	CL	8
Sandy lean clay	CL	10
Sandy lean clay with gravel	CL	2
Sandy silty clay	CL-ML	3
Clayey Sand	SC	1
	Total :	**34**
AASHTO Classification System		
A-4		4
A-6		18
A-7-6		12
	Total :	**34**

Table 4-10 Basic Statistical Parameters for Group Index (GI)

Dataset	No. of Soils	Mean	Median	Min.	Max.	Std. Dev.	Skew-ness	Kurt-osis
Development	63	13.2	13.0	1	39	8.6	0.81	0.58
Evaluation: Overall	34	14.6	13.0	1	31	9.6	0.29	-1.36
Evaluation: Rogers County	29	16.1	15.0	1	31	9.5	-0.02	-1.35
Evaluation: Woodward County	5	5.4	6.0	2	9	2.6	0.12	0.26

Table 4-11 Basic Statistical Parameters for Specimen Moisture Content

Dataset	No. of Soils	Mean (%)	Median (%)	Min. (%)	Max. (%)	Std. Dev. (%)	Skew-ness	Kurt-osis
Development	126	17.4	17.2	10.5	25.3	3.0	0.39	-0.14
Evaluation: Overall	68	17.3	17.5	11.4	22.4	2.9	-0.24	-0.94
Evaluation: Rogers County	58	17.9	18.3	11.4	22.4	2.6	-0.49	-0.37
Evaluation: Woodward County	10	13.7	13.3	11.5	15.1	1.2	-0.25	-0.88

Table 4-12 Basic Statistical Parameters for Specimen Dry Density

Dataset	No. of Soils	Mean (kg/m^3)	Median (kg/m^3)	Min. (kg/m^3)	Max. (kg/m^3)	Std. Dev. (kg/m^3)	Skew-ness	Kurt-osis
Development	126	1657.2	1658.0	1404.2	1872.6	106.7	-0.26	-0.44
Evaluation: Overall	68	1689.3	1676.3	1544.7	1862.9	74.8	0.40	-0.60
Evaluation: Rogers County	58	1672.8	1662.7	1544.7	1837.3	66.0	0.58	-0.02
Evaluation: Woodward County	10	1784.9	1783.7	1707.6	1862.9	46.0	0.13	-0.18

1 kg/m^3 = 0.06243 pcf

Table 4-13 Basic Statistical Parameters for Unconfined Compressive Strength

Dataset	No. of Soils	Mean (kPa)	Median (kPa)	Min. (kPa)	Max. (kPa)	Std. Dev. (kPa)	Skew-ness	Kurt-osis
Development	126	204.7	193.6	50.9	443.5	70.8	0.68	0.50
Evaluation: Overall	68	166.4	159.9	56.5	357.7	64.4	0.78	0.81
Evaluation: Rogers County	58	160.7	159.9	56.5	292.4	56.6	0.20	-0.57
Evaluation: Woodward County	10	199.1	161.9	110.8	357.7	95.9	0.99	-0.61

1 kPa = 0.145 psi

Table 4-14 Basic Statistical Parameters for Resilient Modulus at Each Sequence for Development Dataset (126 Specimens)

Sequence No.	Confining Pressure (kPa)	Axial Stress (kPa)	Resilient Modulus (MPa)			
			Mean	Minimum	Maximum	Standard Deviation
1	41.4	13.8	298.6	54.6	2042.3	347.6
2	41.4	27.6	86.8	34.5	229.0	31.7
3	41.4	41.4	72.3	24.6	163.8	28.2
4	41.4	55.2	63.4	24.3	155.7	28.0
5	41.4	68.9	57.9	20.7	152.6	26.8
6	27.6	13.8	269.4	41.9	2160.8	341.2
7	27.6	27.6	84.1	28.7	245.9	33.2
8	27.6	41.4	70.6	23.2	159.5	28.6
9	27.6	55.2	63.2	22.3	151.7	28.3
10	27.6	68.9	58.3	20.9	149.2	27.0
11	13.8	13.8	312.4	36.1	1892.2	393.3
12	13.8	27.6	93.3	23.7	979.9	87.9
13	13.8	41.4	76.9	19.8	727.9	65.9
14	13.8	55.2	63.9	19.6	159.8	29.6
15	13.8	68.9	59.4	18.2	190.9	29.3

1 kPa = 0.145 psi

Table 4-15 Basic Statistical Parameters for Resilient Modulus at Each Sequence for Evaluation Dataset (68 Specimens)

Sequence No.	Confining Pressure (kPa)	Axial Stress (kPa)	Resilient Modulus (MPa)			
			Mean	Minimum	Maximum	Standard Deviation
1	41.4	13.8	172.8	58.1	409.1	89.7
2	41.4	27.6	80.9	28.2	131.3	21.9
3	41.4	41.4	66.4	19.6	122.1	24.6
4	41.4	55.2	54.5	17.2	117.8	21.2
5	41.4	68.9	49.0	16.1	104.4	19.1
6	27.6	13.8	161.8	57.1	494.2	93.1
7	27.6	27.6	79.0	33.9	136.7	22.9
8	27.6	41.4	64.2	22.7	121.0	24.4
9	27.6	55.2	53.5	18.8	115.9	21.2
10	27.6	68.9	49.4	16.8	106.2	19.6
11	13.8	13.8	190.8	54.1	826.4	146.3
12	13.8	27.6	80.4	36.2	135.7	23.4
13	13.8	41.4	64.9	23.9	126.0	25.1
14	13.8	55.2	53.8	19.4	116.3	21.7
15	13.8	68.9	49.8	17.3	107.4	20.0

1 kPa = 0.145 psi

Table 4-16 Basic Statistical Parameters for Resilient Modulus at Each Sequence for Evaluation Dataset for Rogers County (58 Specimens)

Sequence No.	Confining Pressure (kPa)	Axial Stress (kPa)	Resilient Modulus (MPa)			
			Mean	Minimum	Maximum	Standard Deviation
1	41.4	13.8	189.7	75.5	409.1	86.3
2	41.4	27.6	83.1	28.2	131.3	22.4
3	41.4	41.4	66.8	19.6	122.1	25.6
4	41.4	55.2	53.7	17.2	117.8	21.3
5	41.4	68.9	47.6	16.1	104.4	18.4
6	27.6	13.8	176.3	77.7	494.2	93.2
7	27.6	27.6	80.9	33.9	136.7	23.2
8	27.6	41.4	64.7	22.7	121.0	25.2
9	27.6	55.2	52.6	18.8	115.9	21.1
10	27.6	68.9	48.0	16.8	106.2	19.0
11	13.8	13.8	210.4	83.0	826.4	149.7
12	13.8	27.6	82.4	36.2	135.7	23.7
13	13.8	41.4	65.4	23.9	126.0	25.9
14	13.8	55.2	52.9	19.4	116.3	21.6
15	13.8	68.9	48.3	17.3	106.5	19.3

1 kPa = 0.145 psi

Table 4-17 Basic Statistical Parameters for Resilient Modulus at Each Sequence for Evaluation Dataset for Woodward County (10 Specimens)

Sequence No.	Confining Pressure (kPa)	Axial Stress (kPa)	Resilient Modulus (MPa)			
			Mean	Minimum	Maximum	Standard Deviation
1	41.4	13.8	74.4	58.1	104.1	14.8
2	41.4	27.6	68.4	51.8	95.3	14.0
3	41.4	41.4	63.6	41.5	100.8	18.9
4	41.4	55.2	59.0	37.1	101.7	21.1
5	41.4	68.9	57.2	35.3	103.5	21.5
6	27.6	13.8	77.7	57.1	122.2	19.8
7	27.6	27.6	67.7	44.8	103.8	17.9
8	27.6	41.4	61.7	38.3	103.2	20.2
9	27.6	55.2	58.6	35.5	104.0	21.9
10	27.6	68.9	57.6	34.8	105.7	22.3
11	13.8	13.8	77.3	54.1	124.9	21.4
12	13.8	27.6	69.0	47.4	107.6	18.9
13	13.8	41.4	62.2	39.0	104.7	20.8
14	13.8	55.2	59.0	35.5	105.3	22.5
15	13.8	68.9	58.2	34.7	107.4	22.9

1 kPa = 0.145 psi

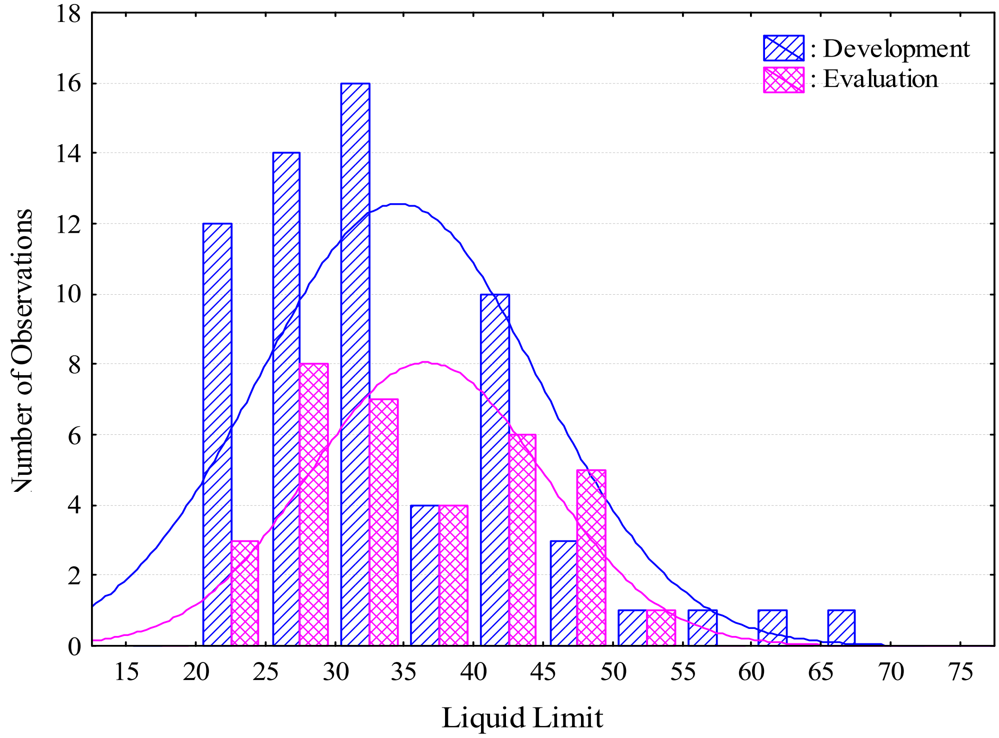

Figure 4-1 Distribution of Liquid Limits (LL) for the Development and the Evaluation Datasets

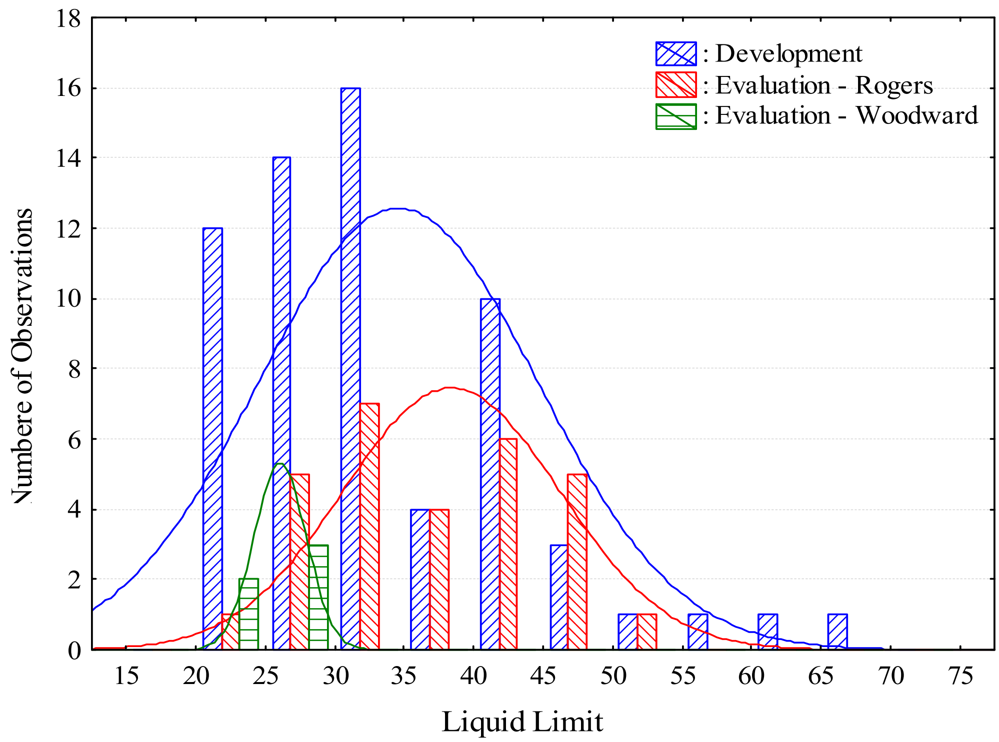

Figure 4-2 Distribution of Liquid Limits (LL) for the Evaluation Dataset for Rogers County and Woodward County Soils

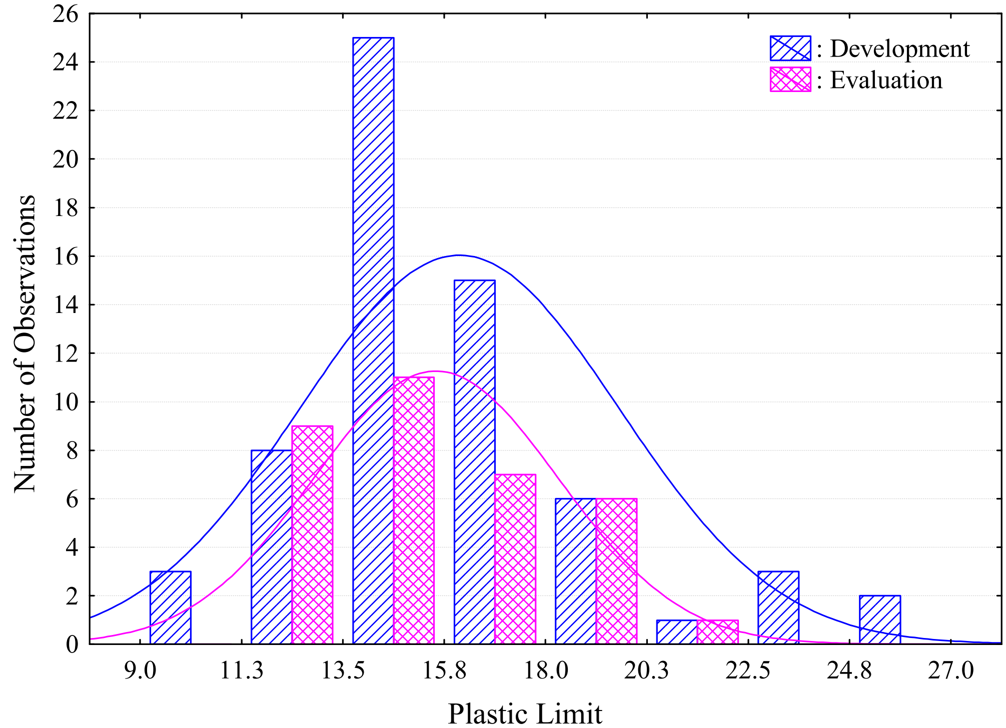

Figure 4-3 Distribution of Plastic Limits (PL) for the Development and the Evaluation Datasets

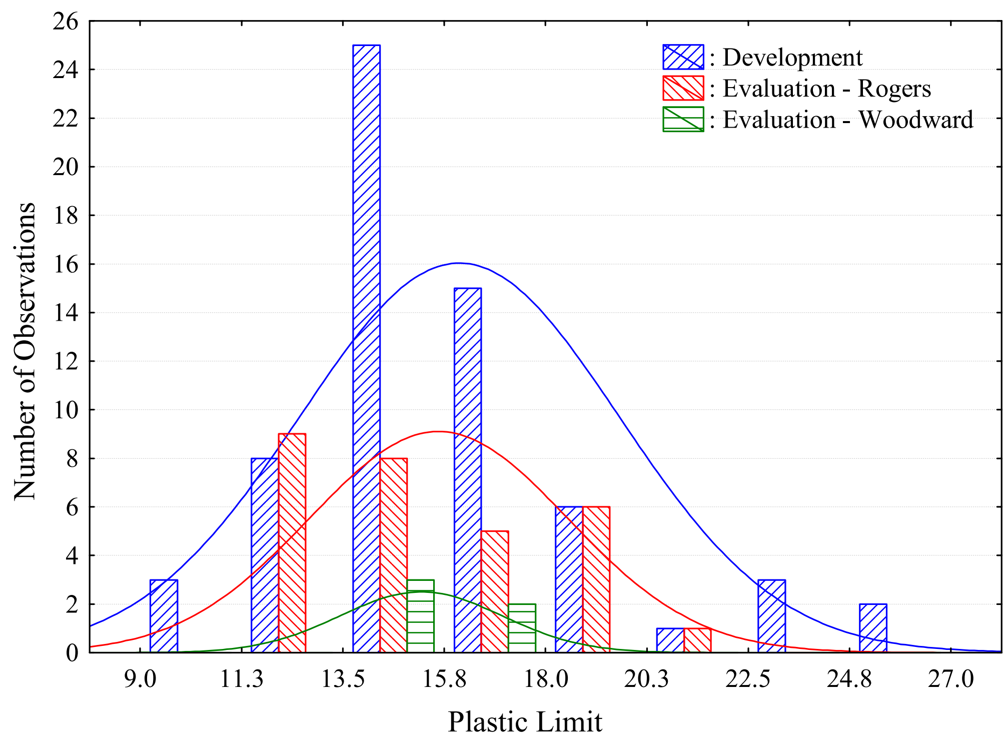

Figure 4-4 Distribution of Plastic Limits (PL) for the Evaluation Dataset for Rogers County and Woodward County Soils

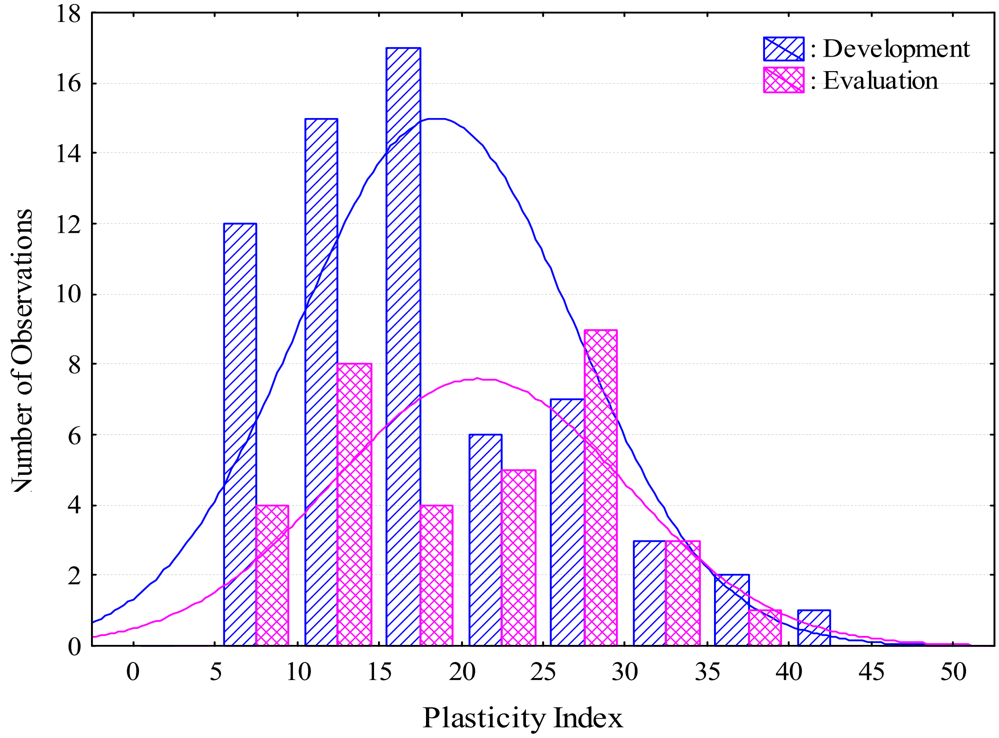

Figure 4-5 Distribution of Plasticity Index (PI) for the Development and the Evaluation Datasets

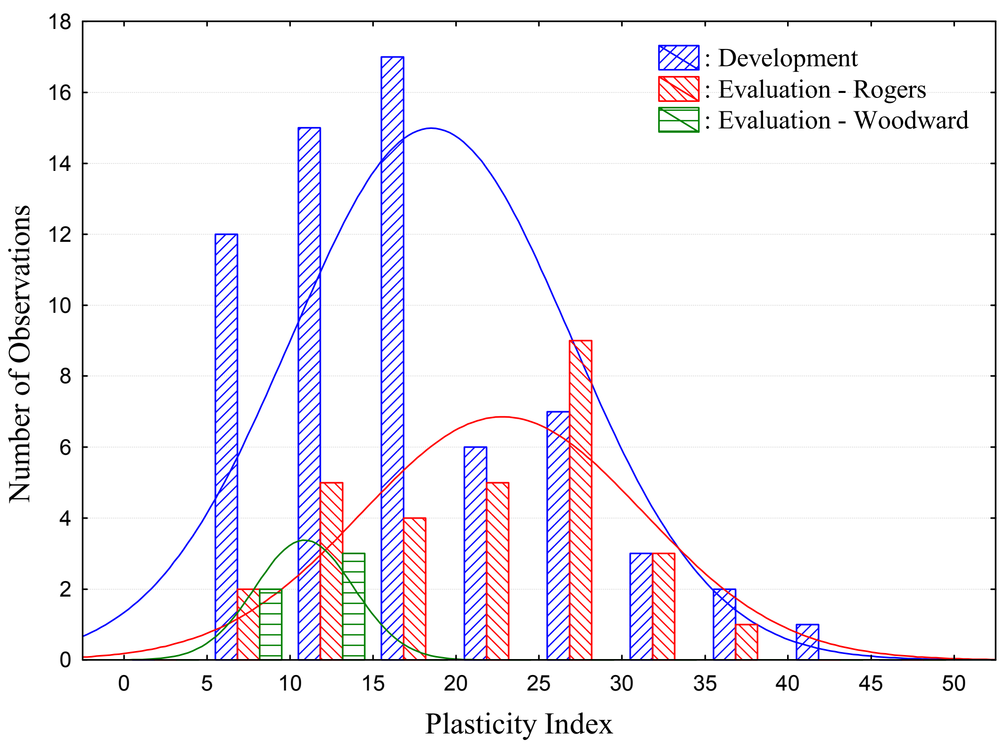

Figure 4-6 Distribution of Plasticity Index (PI) for the Evaluation Dataset for Rogers County and Woodward County Soils

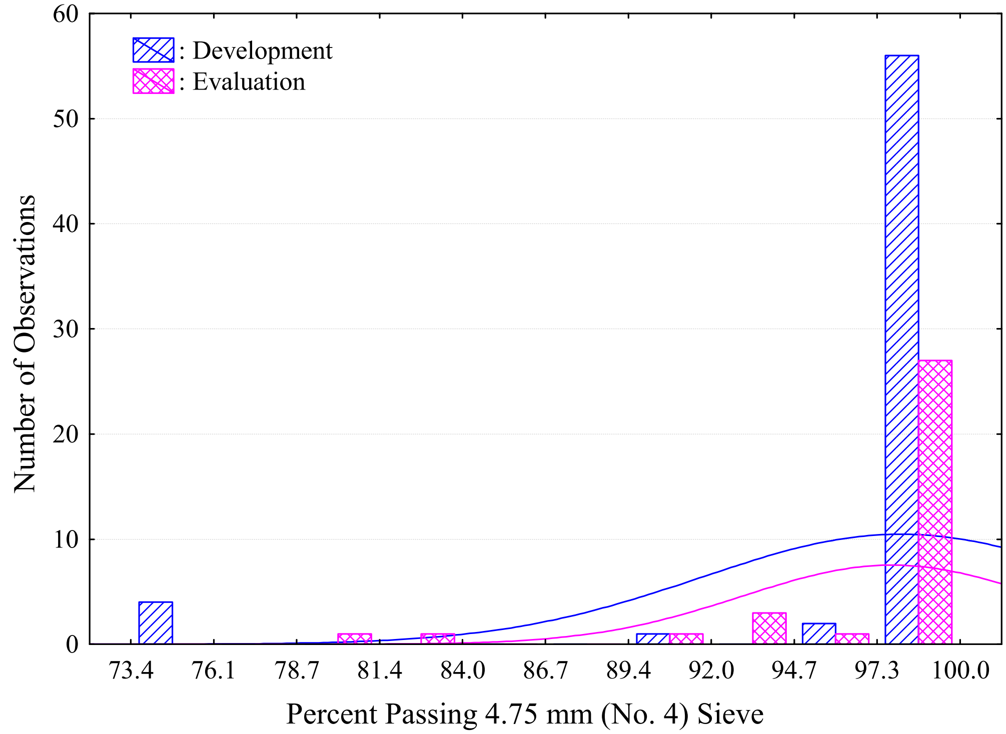

Figure 4-7 Distribution of Percent Passing 4.75 mm (No. 4) Sieve for the Development and the Evaluation Datasets

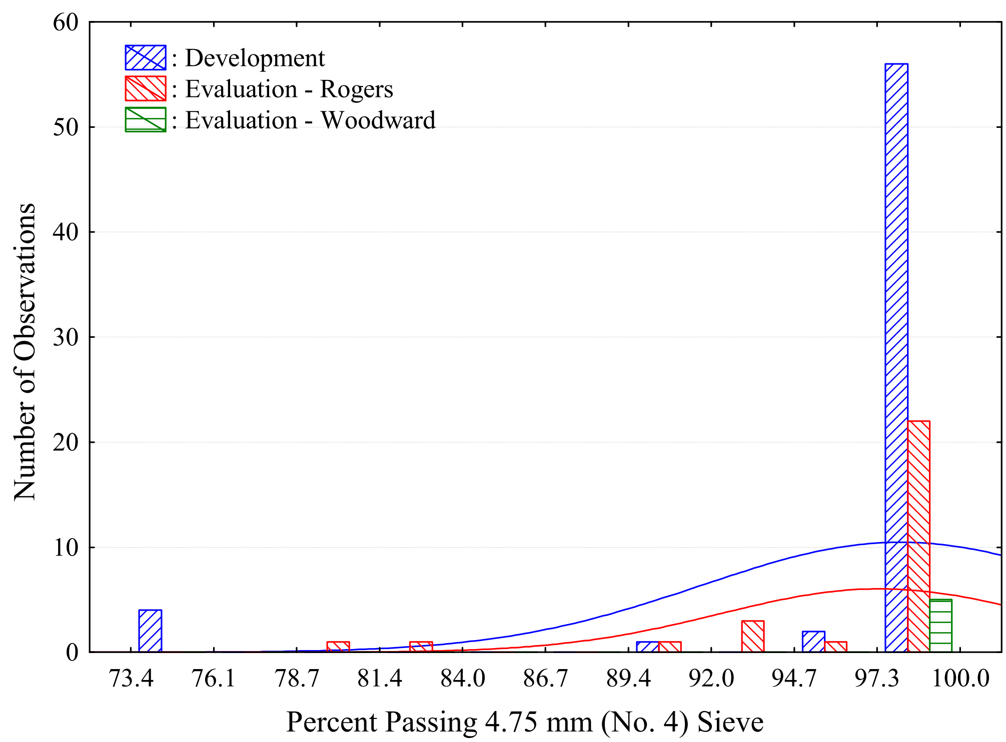

Figure 4-8 Distribution of Percent Passing 4.75 mm (No. 4) Sieve for the Evaluation Dataset for Rogers County and Woodward County Soils

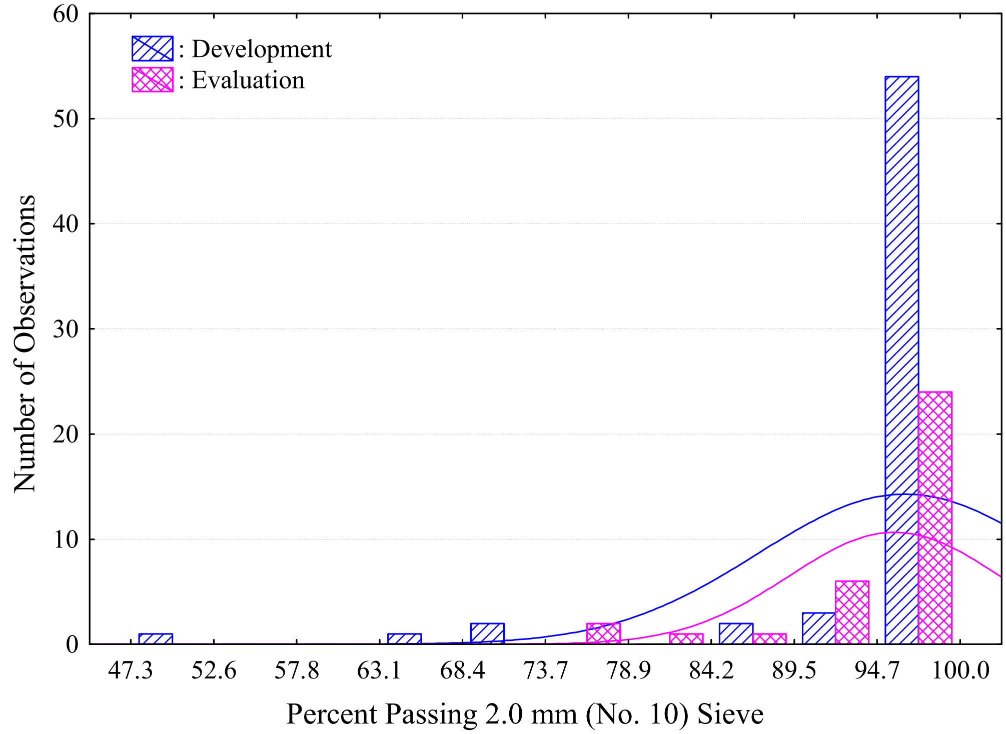

Figure 4-9 Distribution of Percent Passing 2.0 mm (No. 10) Sieve for the Development and the Evaluation Datasets

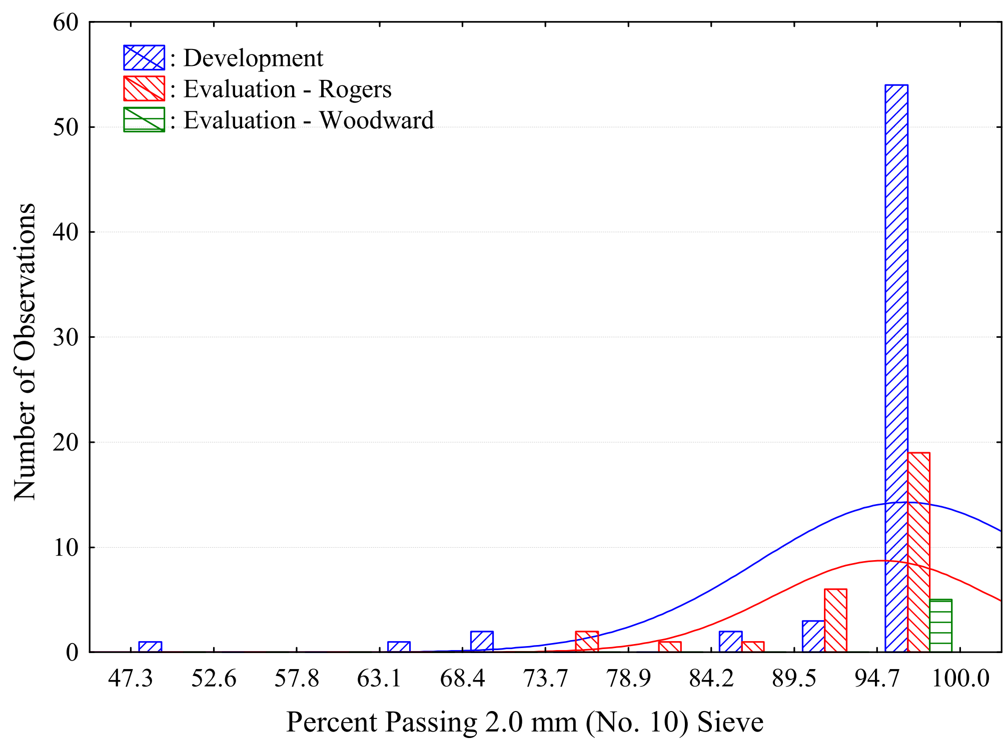

Figure 4-10 Distribution of Percent Passing 2.0 mm (No. 10) Sieve for the Evaluation Dataset for Rogers County and Woodward County Soils

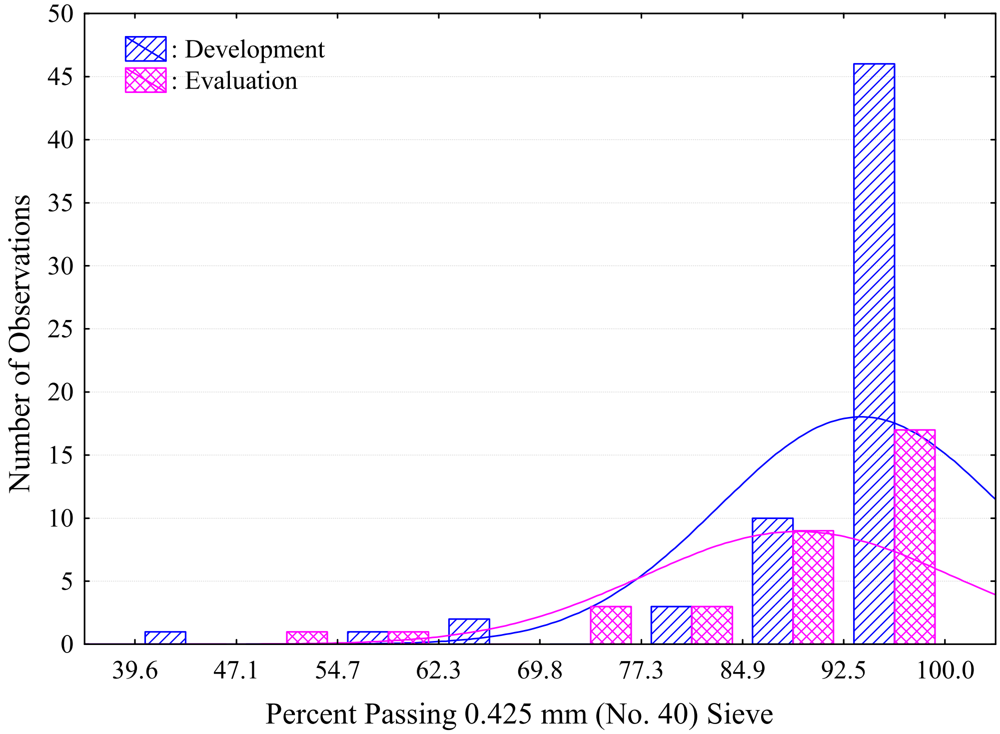

Figure 4-11 Distribution of Percent Passing 0.425 mm (No. 40) Sieve for the Development and the Evaluation Datasets

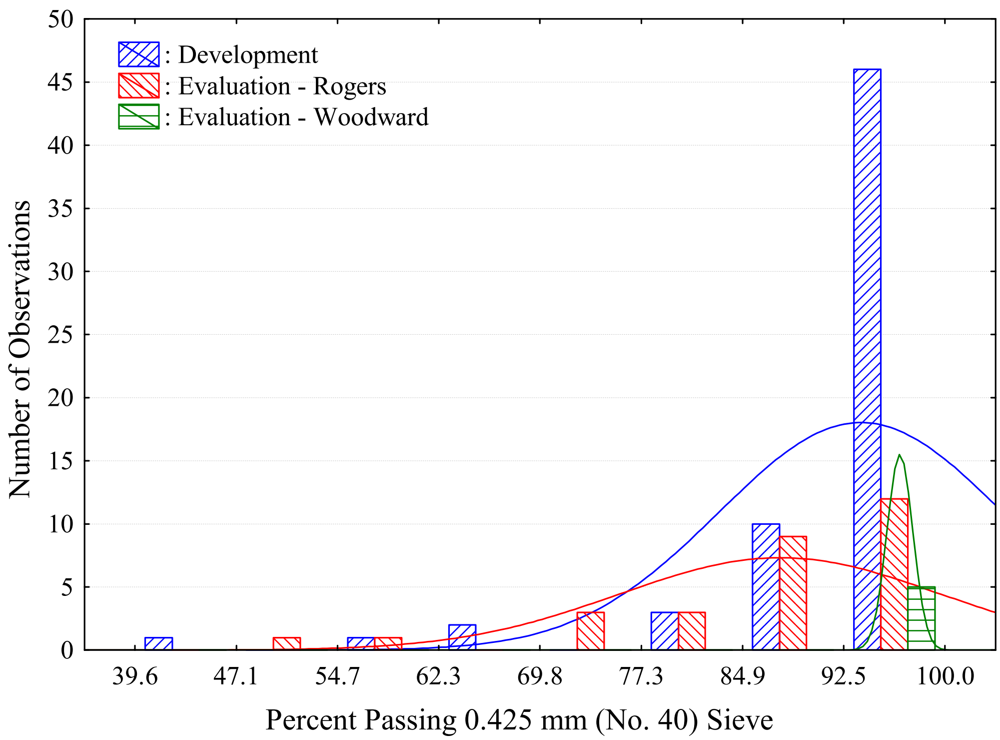

Figure 4-12 Distribution of Percent Passing 0.425 mm (No. 40) Sieve for the Evaluation Dataset for Rogers County and Woodward County Soils

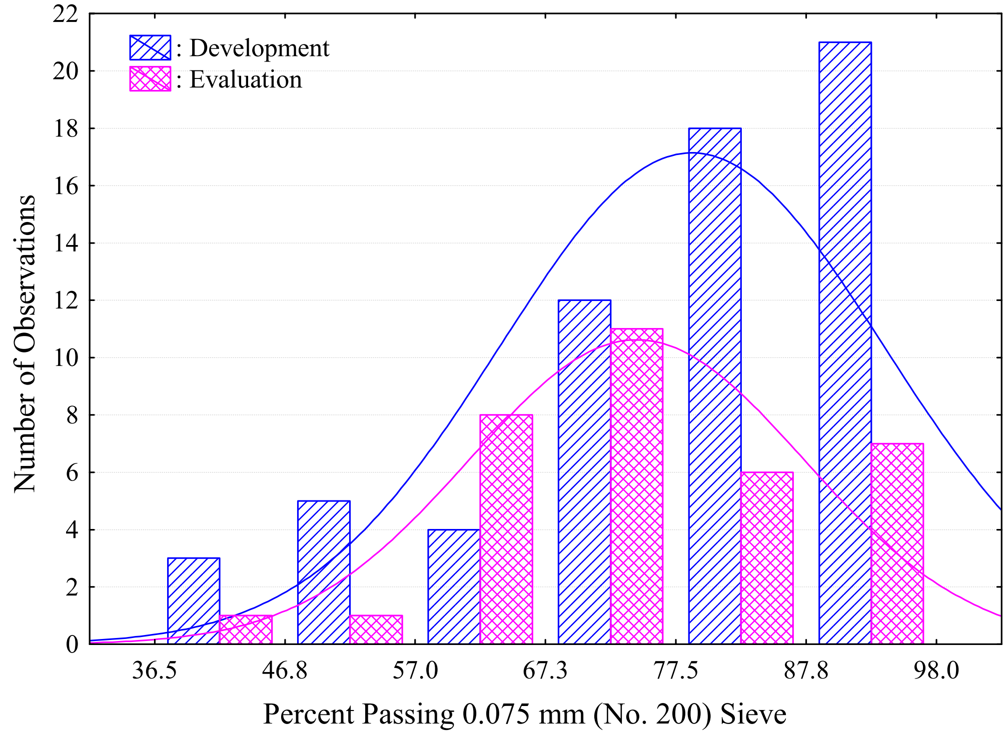

Figure 4-13 Distribution of Percent Passing 0.075 mm (No. 200) Sieve for the Development and the Evaluation Datasets

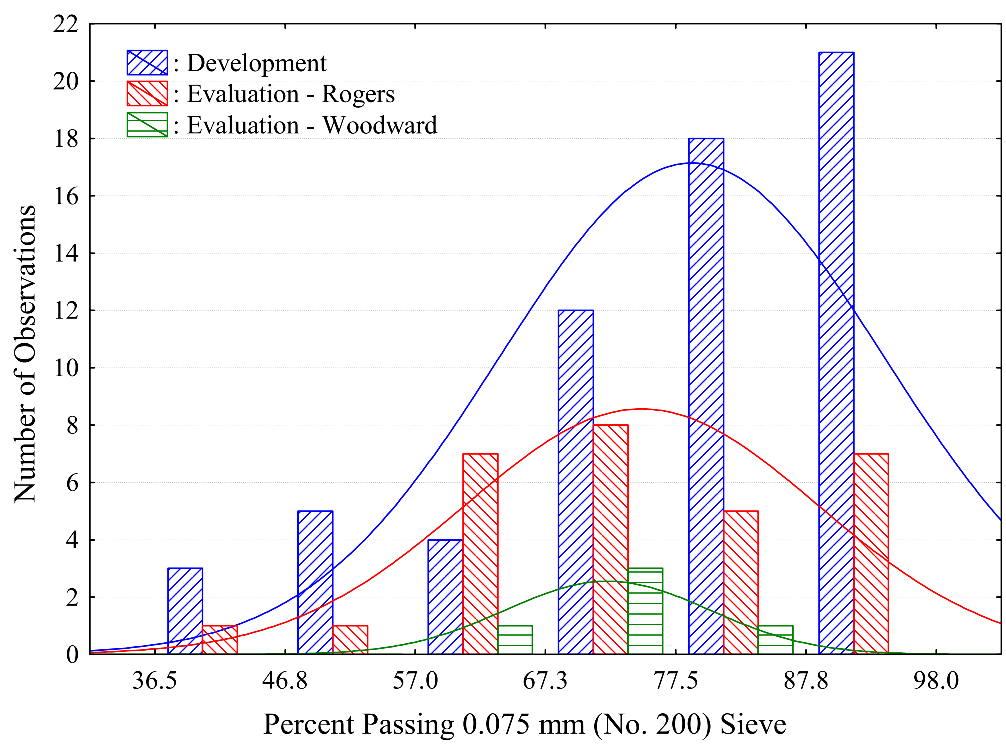

Figure 4-14 Distribution of Percent Passing 0.075 mm (No. 200) Sieve for the Evaluation Dataset for Rogers County and Woodward County Soils

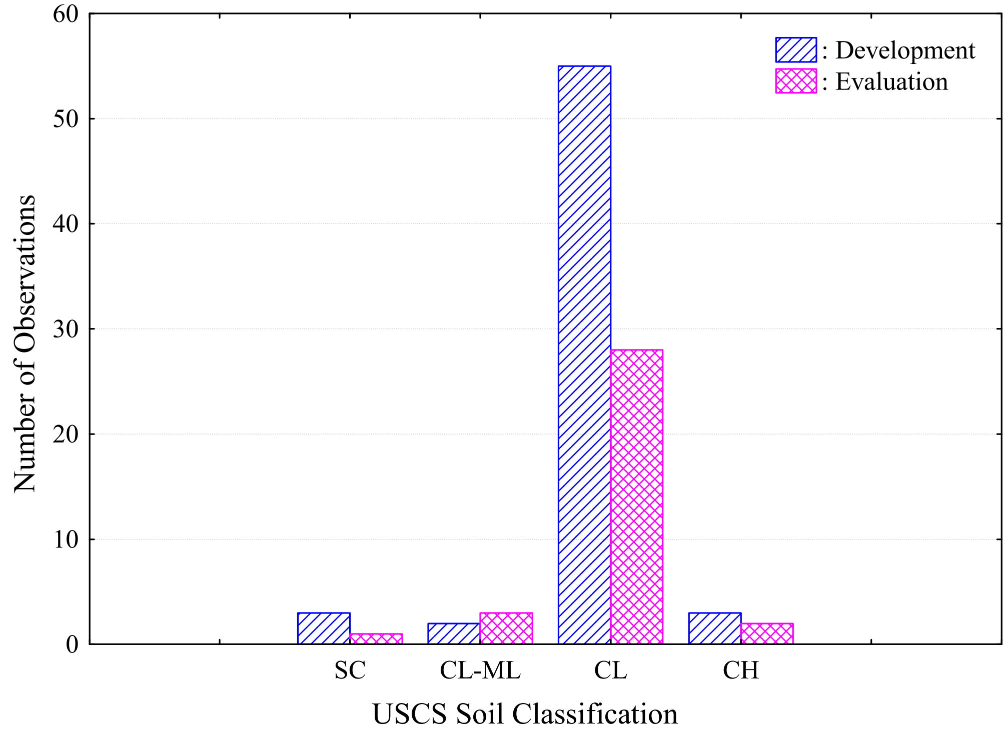

Figure 4-15 Distribution of USCS Soil Classification for the Development and the Evaluation Datasets

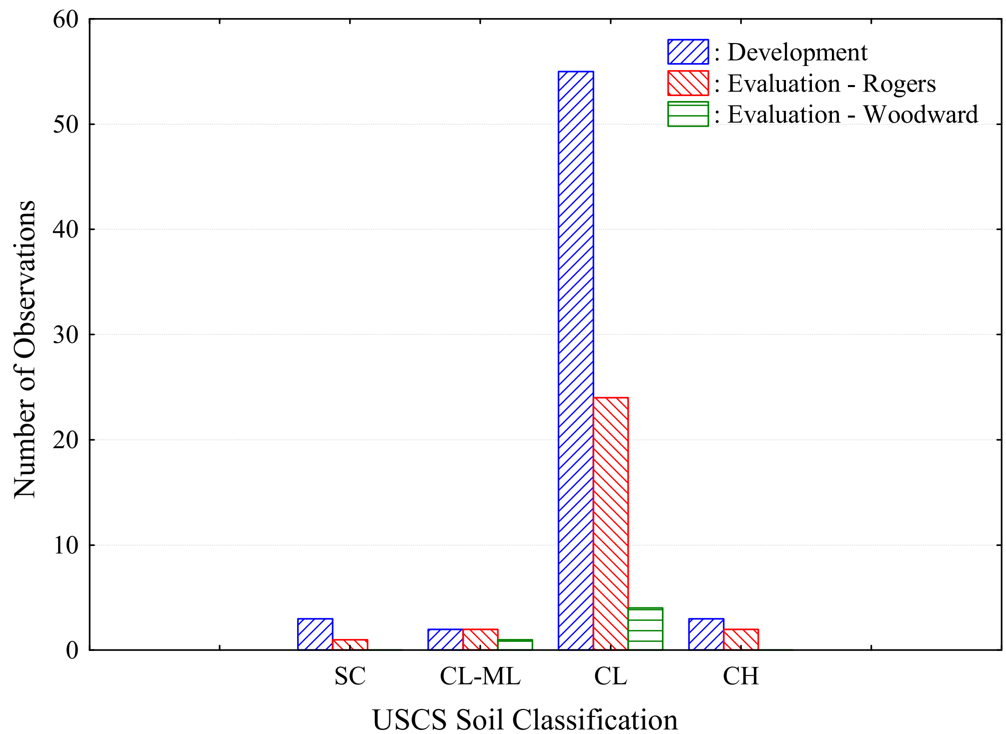

Figure 4-16 Distribution of USCS Soil Classification for the Evaluation Dataset for Rogers County and Woodward County Soils

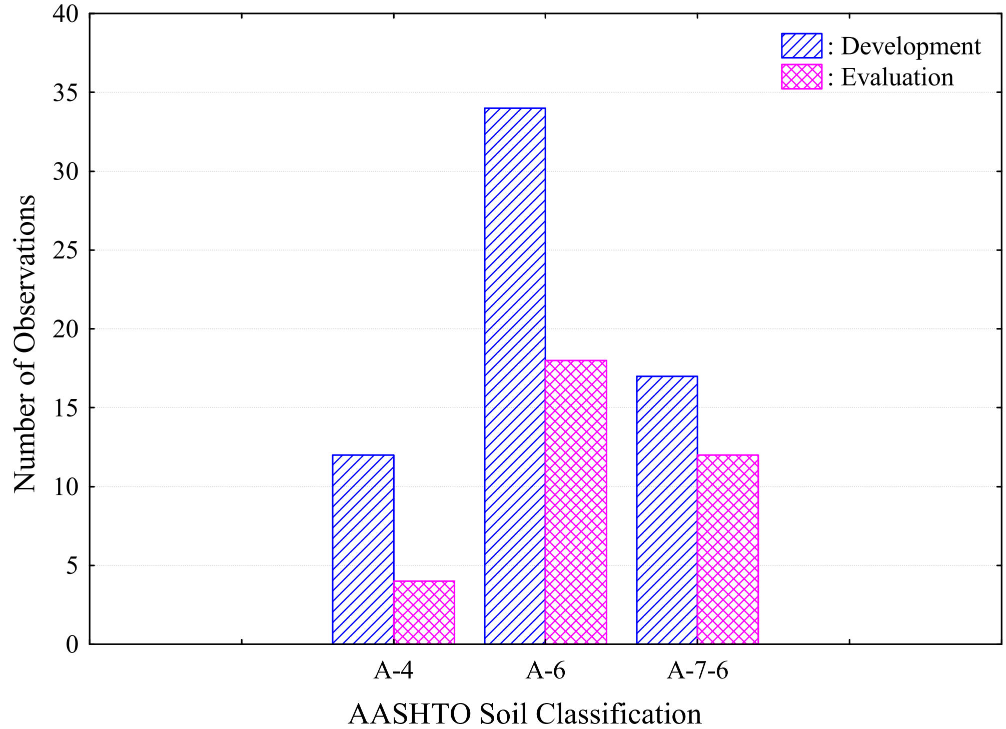

Figure 4-17 Distribution of AASHTO Soil Classification for the Development and the Evaluation Datasets

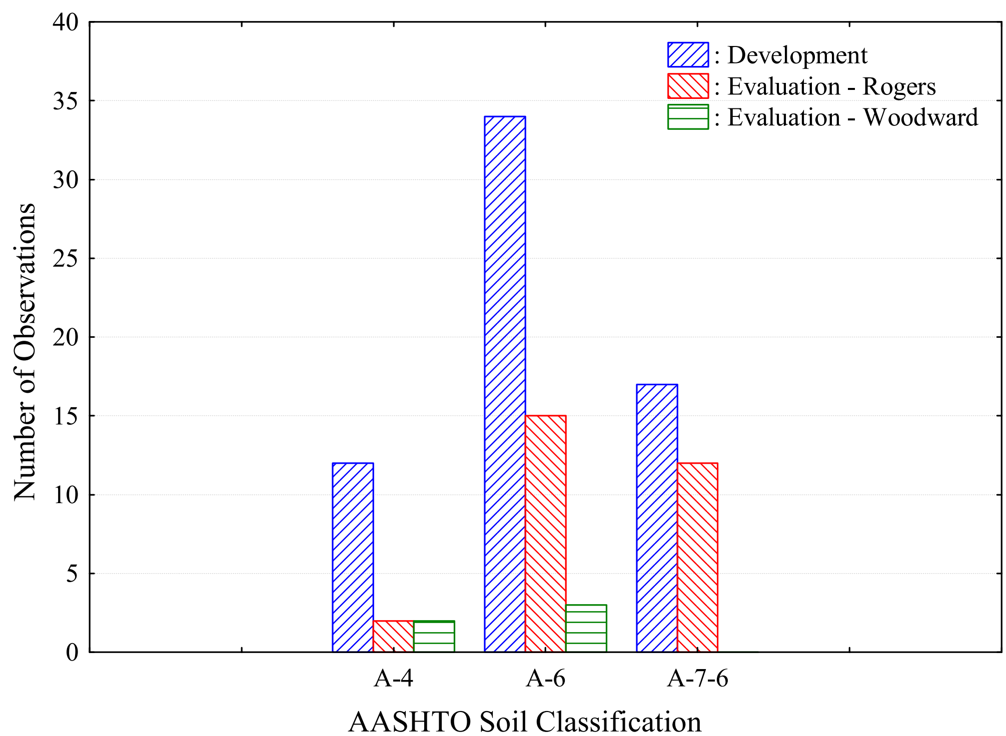

Figure 4-18 Distribution of AASHTO Soil Classification for the Evaluation Dataset for Rogers County and Woodward County Soils

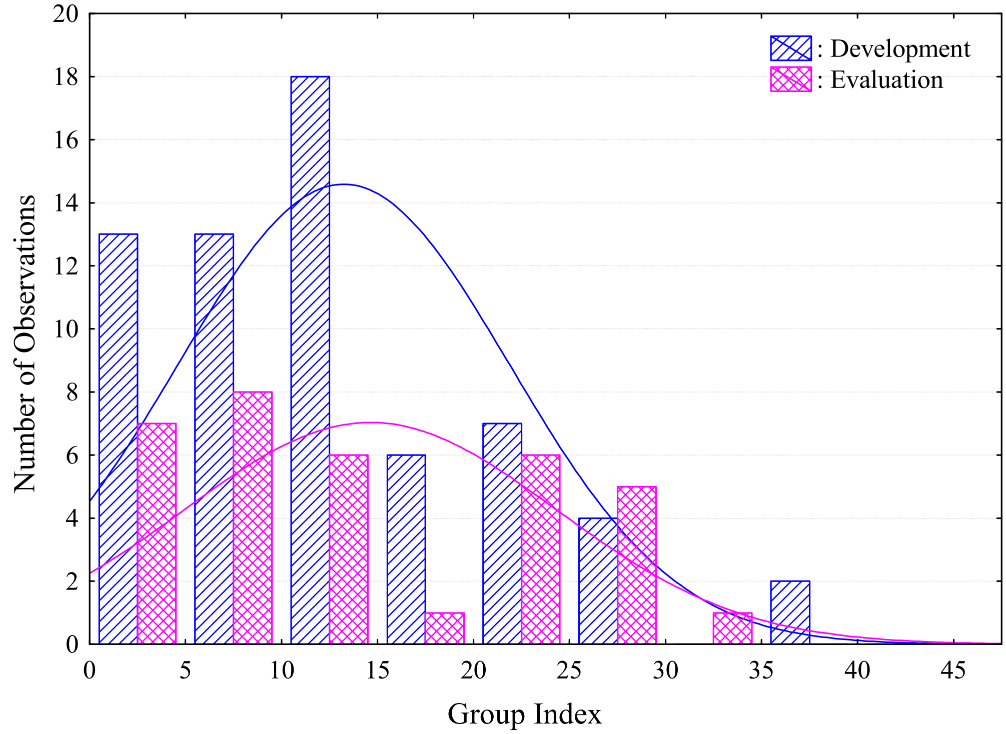

Figure 4-19 Distribution of Group Index (GI) for the Development and the Evaluation Datasets

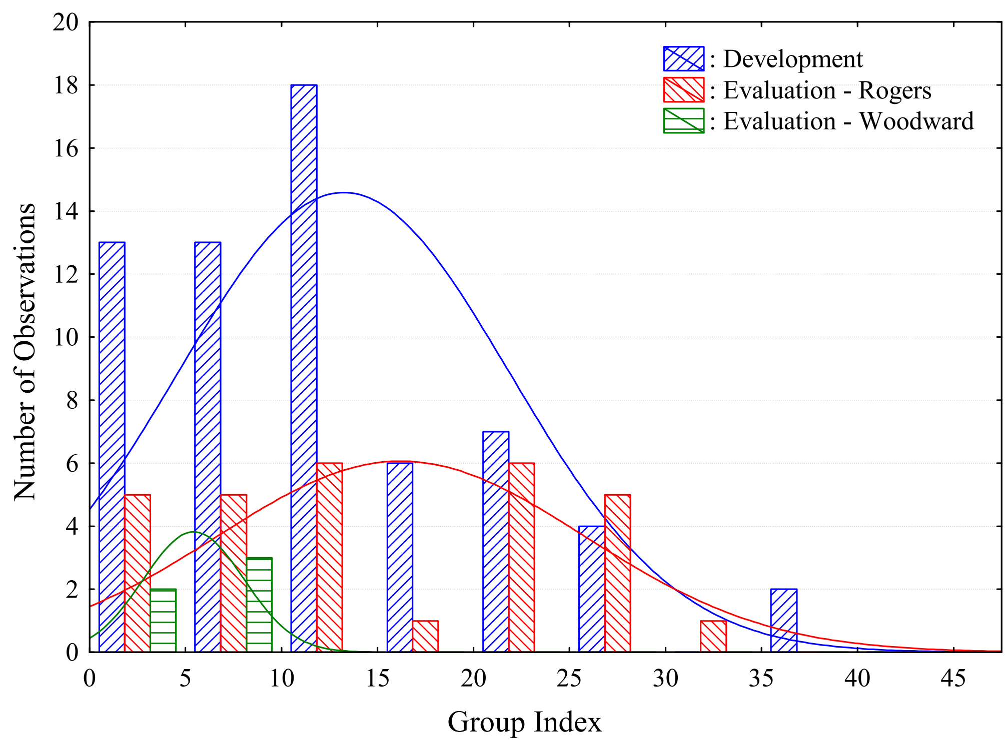

Figure 4-20 Distribution of Group Index (GI) for the Evaluation Dataset for Rogers County and Woodward County Soils

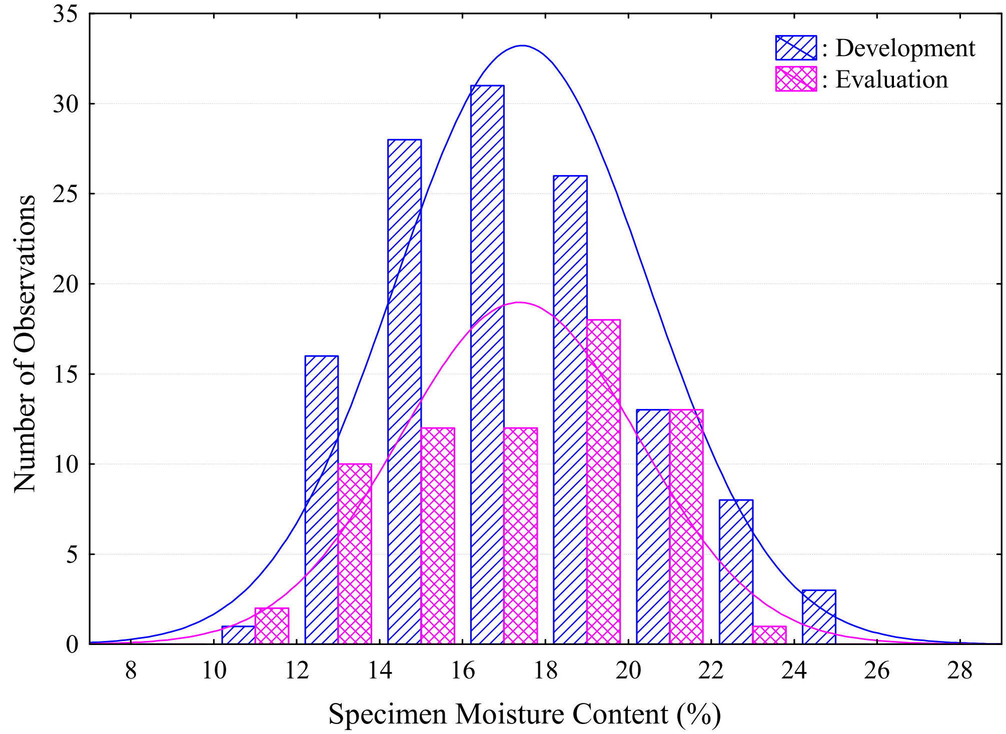

Figure 4-21 Distribution of Specimen Moisture Content for the Development and the Evaluation Datasets

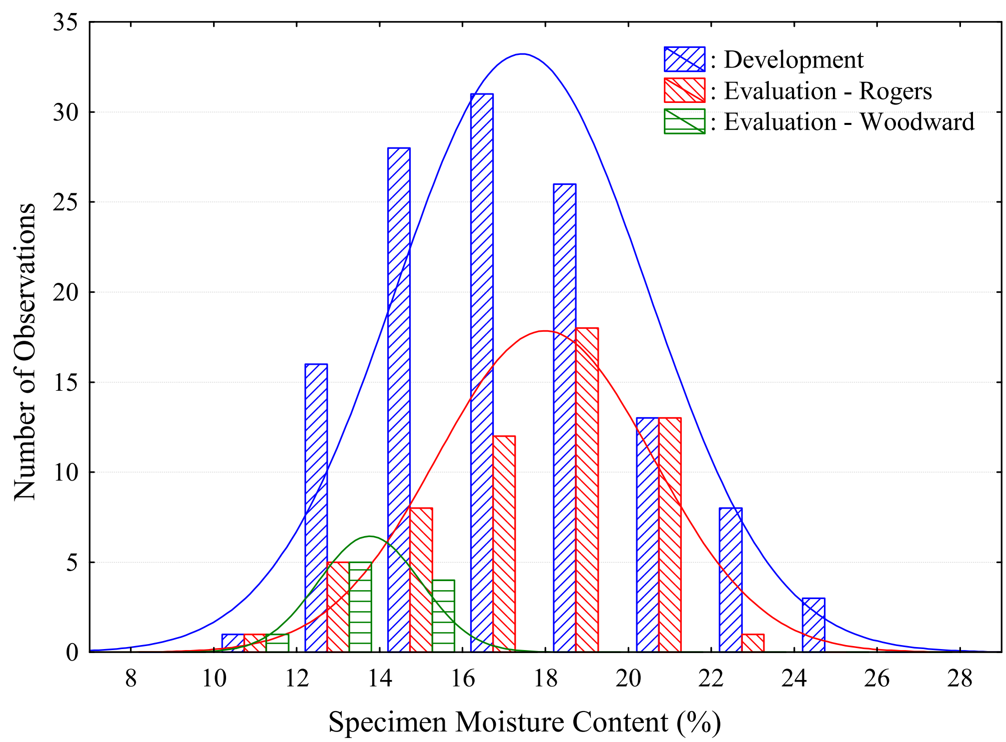

Figure 4-22 Distribution of Specimen Moisture Content for the Evaluation Dataset in Rogers County and Woodward County Soils

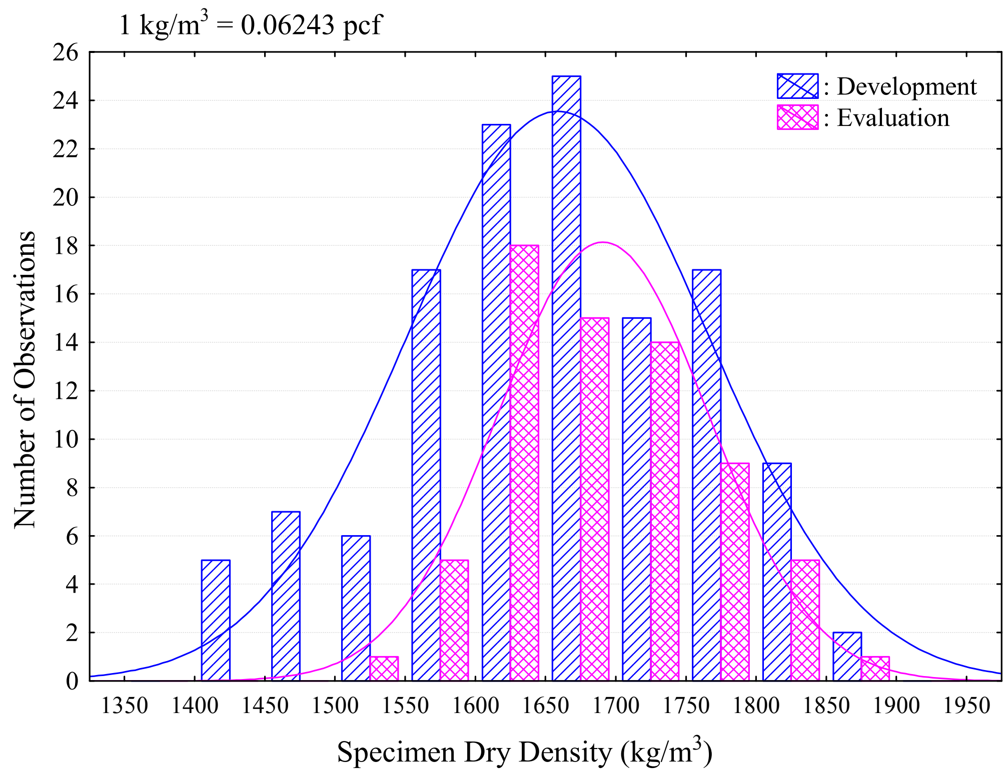

Figure 4-23 Distribution of Specimen Dry Density for the Development and the Evaluation Datasets

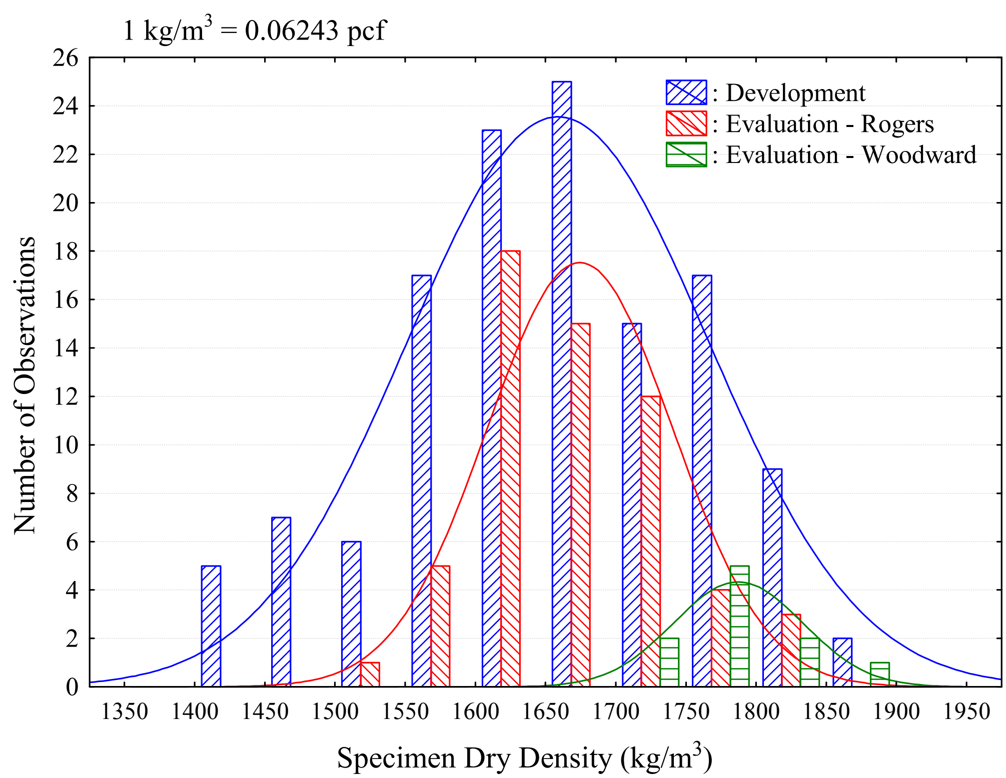

Figure 4-24 Distribution of Specimen Dry Density for the Evaluation Dataset for Rogers County and Woodward County Soils

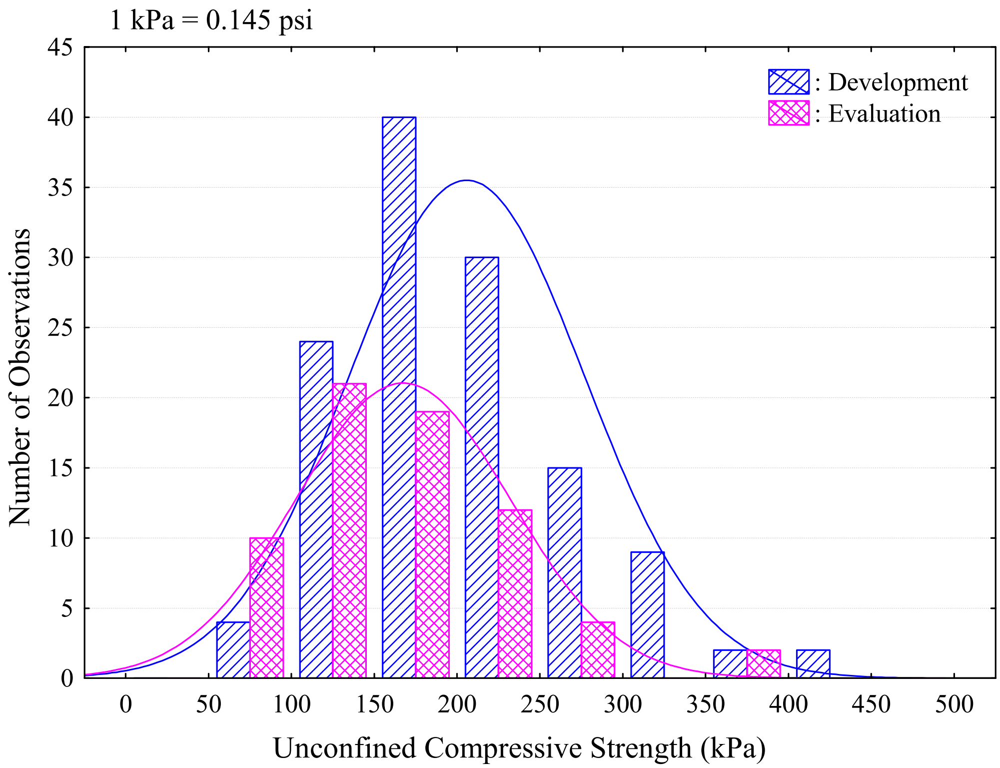

Figure 4-25 Distribution of Unconfined Compressive Strength for the Development and the Evaluation Datasets

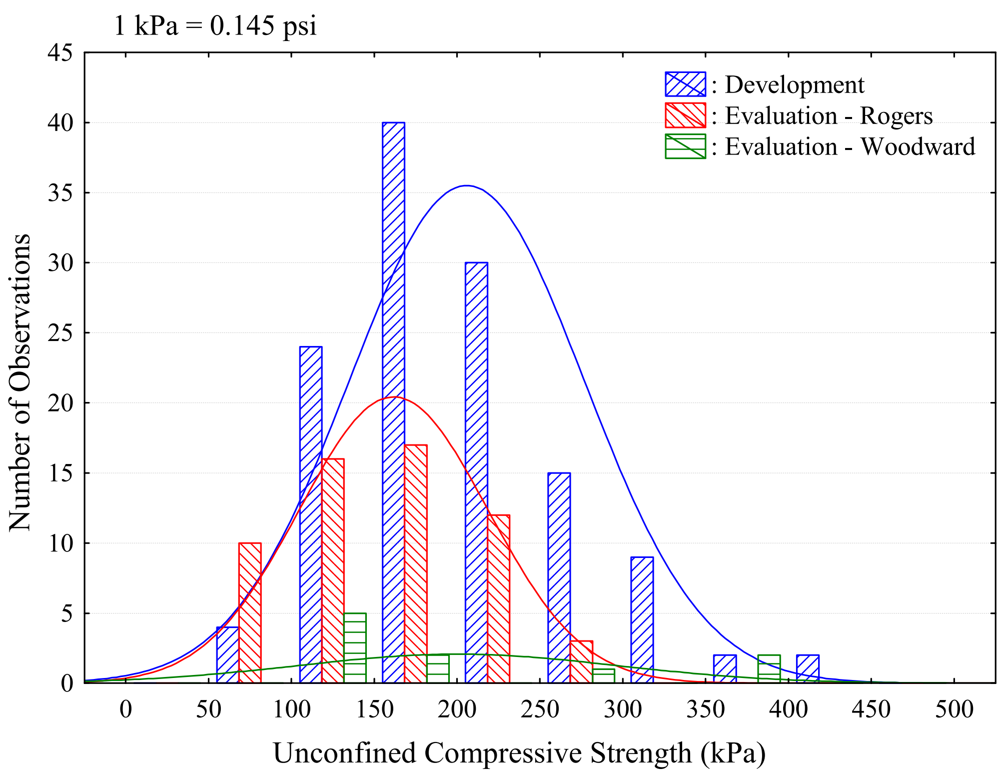

Figure 4-26 Distribution of Unconfined Compressive for the Evaluation Dataset for Rogers County and Woodward County Soils

CHAPTER 5

STATISTICAL MODELS

5.1 Introduction

This chapter presents the statistical models developed in this study for estimating resilient modulus from routine subgrade soil properties. The first statistical model developed is a stress-based model (NCHRP, 2003; Hopkins et al., 2004). The other statistical models are based on stress and subgrade soil properties determined from routine laboratory tests. A commercially available software, Statistica 7.1, is used in the development of these models (StatSoft, Inc., 2006). Several statistical models suitable for solving regression problems are available in Statistica 7.1. These models include multiple regression, polynomial, and factorial. An overview of these models is presented in this chapter.

Two sets of laboratory data were collected in this study. The first set of data is used in the development of the statistical models and is called "*development dataset*". The second dataset, called "*evaluation dataset,*" is not used for the development of the models; it is only used for the evaluation of the models by predicting the M_R values and comparing them with the experimental M_R values.

5.2 Application of Existing Models

In order to investigate the relevance of the present study, it was decided to use some of the existing models presented in Table 2-3 with the development dataset. The decision for the selection of the equation was based on the availability of the material parameters from the development dataset. After reviewing the 26 equations in Table 2-3, two equations were selected. These two equations were stress-based models, namely

Moossazadeh and witczak, 1981 and NCHRP, 2003. The corresponding equations and their R^2 values for the development dataset are presented in Table 5-1. Based on Table 5-1, the R^2 for the Moossazadeh and Witczak, 1981 and NCHRP, 2003 models when used to back predict the current dataset were 0.0605, and 0.0392, respectively. Figures 5-1 and 5-2 present the results of these two equations graphically in the form of back-predicted response for the development dataset. Based on these figures, it is clear that these models are incapable of back predicting the development dataset.

R^2 for one specimen subjected to any given confining pressure (and other material parameters kept the same) is close to 1. The correlation becomes weaker as more soil types and confining pressure magnitudes are included in the dataset. This effect is demonstrated in Figures 5.3 and 5.4.

Figures 5.3 shows M_R predictions for example soil specimen (i.e. Soil AD-1A) subjected to 41.4 Kpa confining pressure. It can be seen that the predicted and measured M_R values are in good agreement. Figure 5.4 shows predicted and measured M_R values for the same soils specimen when subjected to four confining pressure values of 41.4 Kpa, 27.6 Kpa, and 13.8 Kpa. It is observed that the data points start to deviate from a perfect correlation to a "banded" distribution as shown in Figure 5.4. The predicted R^2 value decreased from 0.9808 to 0.5839 when including additional confining pressure values. This phenomenon can also be concluded from other reported studies (e.g. FHWA 2002 and George 2004).

The effect is presented as a narrow band across indicating a poor back-prediction. However, if the results are observed as individual sets of data, the back-prediction for the individual test is good. As the number of M_R tests is increased the back-prediction quality decreases leading to the banding effect. Figure 5-3 and 5-4 present this effect.

5.3 Overview of Statistical Models

In the present study, four statistical models are developed, namely stress-based, multiple regression, polynomial, and factorial. In each model, the dependent variable, M_R, is correlated with seven independent variables, namely bulk stress (θ), deviatoric stress (σ_d), moisture content (w), dry density (γ_d), plasticity index (PI), percent passing No. 200 sieve (P_{200}), and unconfined compressive strength (U_c). As noted previously, of the seven independent variables used here only two (θ and σ_d) are stress-related. The five parameters (w, $\gamma_{d,}$ PI, P_{200}, and U_c) are determined from routine soil testing. An overview of these models is given in the following.

5.3.1 Stress-Based Model

There are several stress-based models available for prediction of M_R (Dunlap, 1963; Seed et al., 1967; Moossazadeh and Witczak, 1981; May and Witczak, 1981; Yau and Von Quintus, 2002; NCHRP, 2003; Hopkins et al., 2004). These models include such factors as bulk stress, deviatoric stress, principal stress, and octahedral shear stress. In the present study, bulk stress (θ) and deviatoric stress (σ_d) are used as the model parameters, and they are correlated with M_R as follows:

$$M_R/P_a = k_1 (\theta /P_a)^{k2} (\sigma_d /P_a)^{k3} \quad (5\text{-}1)$$

where P_a represents atmospheric pressure, and k_1, k_2, and k_3 are regression constants. The regression constants k_1, k_2, and k_3 are correlated with the selected soil properties or parameters w, γ_d, PI, P_{200}, and U_c. The dry density, γ_d, is normalized with respect to density of water and the unconfined compressive strength, U_c, is normalized with respect to the atmospheric pressure, P_a.

5.3.2 Multiple Regression Model

Multiple regression models represent a class of simple and widely used linear regression models for more than two continuous variables (Montgomery et al., 2006; StatSoft, Inc., 2006). The general equation for a multiple regression model for the independent variables utilized here could be expressed by the following equation:

$$M_R/P_a = b_0 + b_1\, w + b_2\, (\gamma_d/\,\gamma_w) + b_3\, PI + b_4\, P_{200} + b_5\, (U_c/\,P_a) + b_6\, (\sigma_d/\,P_a) + b_7\, (\theta/P_a) \qquad (5\text{-}2)$$

where b_i represents the regression constants.

5.3.3 Polynomial Model

A polynomial model includes the basic components of a multiple regression model with the addition of higher order effects for the independent variables. For the independent variables considered here, a second order polynomial model could be expressed as follows:

$$M_R/P_a = b_0 + b_1\, w + b_2\, w^2 + b_3\, (\gamma_d/\gamma_w) + b_4\, (\gamma_d/\gamma_w)^2 + b_5\, PI + b_6\, PI^2 + b_7\, P_{200} + b_8\, P_{200}^{\;2} + b_9\, (U_c/\,P_a) + b_{10}(U_c/\,P_a)^2 + b_{11}(\sigma_d/\,P_a) + b_{12}\, (\sigma_d/\,P_a)^{\,2} + b_{13}\, b_7\, (\theta/P_a) + b_{14}\, b_7\, (\theta/P_a)^2 \qquad (5\text{-}3)$$

where b_i represents the regression coefficients or models parameters. Although a second order model may be adequate for many problems, a general polynomial model can have higher than second order terms (Myers et al., 2001; Montgomery et al., 2006). In polynomial regression, higher order terms are added to the model to determine if they increase the associated R^2 significantly (Sokal and Rohlf, 1995; Myers et al., 2001;

Montgomery et al., 2006). Thus, a multiple regression model or a first order polynomial model is generally developed first, followed by a second order polynomial model. If the difference in the R^2 values between these two models is significant, then a third order polynomial model may be warranted (Fernandez-Juricic et al., 2003). In most cases, polynomial models of orders greater than three are not practical (Sokal and Rohlf, 1995).

5.3.4 Factorial Model

Similar to the polynomial model, a factorial model also includes the components of a multiple regression model. However, instead of considering higher order effects of the independent variables, it accounts for interactions among different variables in the model. Different levels of interactions may be incorporated such as interactions between two variables, among three variables, and so on (i.e. $w\times\gamma_d$, $PI\times U_c\times\sigma_d$, $w\times \gamma_d\times PI\times\sigma_d\times\theta$, etc.). A full-factorial regression model consists of all possible products of the independent variables. Moreover, a factorial regression model can be fractional (i.e., fractional exponent) (see e.g., Myers et al., 2001; Montgomery et al., 2006). Factorial regression designs can also be fractional, that is, higher-order effects can be omitted from the design. A fractional factorial design of degree two would include the main effects and all two-way interactions between the predictor variables. For example, the general equation for a fractional factorial design with second degree of interaction can be expressed as follows:

$$
\begin{aligned}
M_R/P_a = {} & b_0 + b_1\, w + b_2\, (\gamma_d/\gamma_w) + b_3\, PI + b_4\, P_{200} + b_5\, (U_c/ P_a) + b_6\, (\sigma_d/ P_a) \\
& + b_7\, (\theta/P_a) + b_8\, w\times(\gamma_d/\gamma_w) + b_9\, w\times PI + b_{10}\, w\times P_{200} + b_{11}\, w\times(U_c/ P_a) \\
& + b_{12}\, w\times(\sigma_d/ P_a) + b_{13}\, w\times(\theta/P_a) + b_{14}\, (\gamma_d/\gamma_w)\times PI + b_{15}\, (\gamma_d/\gamma_w)\times P_{200} \\
& + b_{16}\, (\gamma_d/\gamma_w)\times(U_c/ P_a) + \ldots + b_{26}\, U_c\times(\sigma_d/ P_a) + b_{27}\, (U_c/ P_a)\times(\theta/P_a)
\end{aligned}
$$

$$+ b_{28} (\theta/P_a) \times (\sigma_d / P_a) \quad (5\text{-}4)$$

5.4 Model Development

The aforementioned statistical models were developed in this study using the development dataset. Statistica 7.1 was utilized to determine the regression constants for all the statistical models. After the regression constants were determined, back-predicted M_R values were calculated and compared with the pertinent experimental values. The significance of each model is tested by calculating the R^2 and F values (Montgomery, 2006) of the model. The effectiveness of a model is assessed through a measure of goodness of fit, R^2. The R^2 value was calculated from the difference between the back-predicted values and the experimental values, and used as an indicator of the quality of the model. The R^2 values can range from 0 to 1, with 1 indicating a perfect fit. In some recent studies (e.g., Federal Highway Administration (2002), Stubstad, 2002; Dai and Zollars, 2002; Rahim and George, 2004), R^2 values have been used to measure the performance of statistical models.

The significance of a statistical model can be evaluated using the F value (Montgomery, 2006). In performing this test, one compares the sum-of-squares and the associated degrees of freedom. An F value of near one indicates that a simpler statistical model may be a reasonable choice. A much higher value is an indicator that a more complicated (e.g., a higher order) model may be desired. Also, random scatter in data can lead to higher F values (Motulsky, 2005).

5.4.1 Stress-Based Model Development

To develop the stress-based model, the regression constants in Equation (5-1) are determined for each M_R test in the development dataset (Appendix B). The R^2 for individual tests in the development dataset ranged from 0.512 to 0.996. Then, using the multiple linear regression option in Statistica 7.1, these regression constants are correlated with the specimen and soil parameters. The following expressions are obtained for k_1, k_2, and k_3 from the development dataset:

$$k_1 = 0.08789 + 0.1773\,(U_c/P_a) + 0.005048\,PI - 0.3967\,P_{200} + 1.2652\,w \qquad (5\text{-}5)$$

$$k_2 = 0.5074 - 0.01336\,PI + 2.3432\,w - 0.3868\,(\gamma_d/\gamma_\omega) \qquad (5\text{-}6)$$

$$k_3 = -0.6612 + 0.1589\,(U_c/P_a) - 0.2254\,P_{200} \qquad (5\text{-}7)$$

With this stress-based model (Equations 5-1, 5-5 to 5-7), the M_R can be predicted as a function of two specimen parameters (w and γ_d), three soil parameters (PI, P_{200}, and U_c) and two stress parameters (σ_d and θ). The overall R^2 value for this model was found to be as low as 0.3226. Figure 5-3 shows a plot of the experimental and predicted M_R/P_a values for this model. It is evident that overall the model did not back-predict the M_R/P_a values favorably. Significant scatter is observed for the entire data range, justifying a low R^2 value. From Table 5-1, the F value for this model is 253.37, which is an indicator that a more complicated model may be desired for the development dataset used here.

As noted in Chapter 2, a number of researchers in the past have developed stress based statistical models for resilient modulus using routine soil properties. For example, the Minnesota DOT developed a database of model parametes k_1, k_2, and k_3 (Dai and Zollars, 2002) for 23 fine grained soils from throughout Minnesota (Khazanovich et al., 2006). According to these researchers, a majority of these soils were classified as A-6 although there were some soils classified as A-7-5 and A-7-6. Based on an analysis of the k_1, k_2, and k_3 values it was concluded that these model parameters can vary significantly for soils located in the same state and having the same AASHTO classification. Furthermore, these researchers recommended that the range of the k_1, k_2, and k_3 may be used for an initial evaluation of the test quality. In another recent study, George (2004) reported that the correlations for M_R having good statistical significance were generally confined to specific soil types, with a relatively narrow band of material property indices. The studies that used a wide range of soils and test conditions generally resulted in poor correlations (Quintus and Killingsworth, 1998; George, 2004). Based on the R^2 and F values, as well as from the aforementioned findings, it is concluded that the stress-based model is not appropriate for prediction of M_R.

5.4.2 Multiple Regression Model Development

Using the same development dataset in Statistica 7.1, the regression constants for the multiple regression model, given by Equation (5-2), were evaluated. The resulting multiple regression model is given by Equation (5-8):

$$M_R/P_a = 1.8050 - 0.4904\ w - 0.5747\ (\gamma_d/\ \gamma_w) + 0.008083\ PI - 0.5123\ P_{200}$$
$$+ 0.2191\ (U_c/\ P_a) - 0.6401\ (\sigma_d/\ P_a) - 0.0009399\ (\theta/P_a) \qquad (5\text{-}8)$$

The R^2 and F values for the multiple regression model improved to 0.4357 and 165.88, respectively, which is a significant improvement over the stress based models. In a related study, based on a detailed literature survey, Carmichael and Stuart (1978) developed multiple regression models for cohesive and granular soils. These researchers reported R^2 values of 0.759 (418 observations) and 0.836 (583 observations) for cohesive and granular soils, respectively. Trials were performed with the current development dataset, where two sets of observations (240 and 480) were evaluated. The R^2 and F values for these trials were 0.9217, 390.01, and 0.7625, 216.53, respectively.

These values are in agreement with Carmichael and Stuart (1978) and indicate the importance of the size of the database.

Figure 5-4 shows a comparison between experimental and predicted M_R/P_a values for this model. It is evident that the level of scatter in data points reduced significantly for this model. Also, it is evident that the predicted values are closer to the equality line when the M_R/P_a values are less than 1,000. Figures 5-5, 5-6, and 5-7 present the back-prediction of the experimental M_R against the deviatoric stress for three selected specimens, MA-3B, NO-7A, and OS-1B, respectively. The M_R results from these specimens covered the full range of M_R response for the development dataset. Specimen NO-7A shows the best prediction (Figure 5-6), followed by specimen OS-1B (Figure 5-5). Specimen MA-3B shows the worst back-prediction (Figure 5-5). The soil classification results for these specimens indicate lean clay with AASHTO classification of A-6(10), A-6(16) and A-6(21) for OS-1B, NO-7A, and MA-3B, respectively (Appendix A1). The unconfined compression (U_c) results for OS-1B, NO-7A, and MA-3B were 161 kPa (23.3 psi), 272 kPa (39.4 psi), and 310 kPa (45.1 psi), respectively (Appendix A3). Thus, even though these soils are all classified as A-6 soils, their unconfined compressive strengths were quite different. Overall, it was observed that the M_R values increased with increasing unconfined compressive strength. This may have been a contributing factor for the three specimens exhibiting different levels of correlations between the experimental and predicted $M_{R.}$ Similar observations were made in previous studies. For example, Tian et al. (1998) developed a regression model to predict resilient modulus as a function of cohesion, angle of internal friction, moisture content and unconfined compressive strength of an aggregate base (see Table 2-3, Equation 13). In that study it was reported that the M_R was found to increase with increasing unconfined compressive strength.

5.4.3 Polynomial Model Development

The regression constants from Equation (5-3) are calculated using the polynomial modeling option in Statistica 7.1. The resulting model is given by the following equation:

$$M_R/P_a = 15.8002 + 2.9994\,w - 7.4142\,w^2 - 18.3291\,(\gamma_d/\gamma_w) + 5.4596\,(\gamma_d/\gamma_w)^2$$
$$+ 0.02191\,PI - 0.0003142\,PI^2 - 0.3705\,P_{200} - 0.009229\,P_{200}^2$$
$$+ 0.2628\,(U_c/P_a) - 0.01050(U_c/P_a)^2 - 2.0332(\sigma_d/P_a) + 1.62950(\sigma_d/P_a)^2$$
$$-0.01181\,(\theta/P_a) + 0.004735(\theta/P_a)^2 \qquad (5\text{-}9)$$

The R^2 and F values for this model were found to be 0.4858 and 101.02. These values were better than those of the multiple regression model (0.4357 for R^2 and 165.88 for F value). To examine if a higher order model was desired, a third order polynomial regression model was developed for the same development dataset. The R^2 and F values for the third order polynomial model changed to 0.4101 and 254.75, respectively. Specifically, the R^2 value for the third order polynomial regression model was worse than the corresponding values for both the multiple regression and the second order polynomial regression models. Also, the F value increased from the second order to the third order polynomial regression model indicating that the second order polynomial model was a better model (Sokal and Rohlf, 1995; Fernandez-Juricic et al., 2003).

Lee et al. (1997) developed a second order polynomial model with a single parameter, stress level causing 1% strain ($S_{u1.0\%}$). Their research was limited to only three cohesive soils from Indiana. The soils from South Bend and Washington were classified as CL according to USCS, while the soils from Bloomington were classified as CH. The R^2 for their model was very high (0.97), possibly due to small number of soils used. Unfortunately, Lee et al. (1997) did not report any other statistical parameters for comparison. It is worth noting that a very few higher order regression models have been reported previously correlating the M_R with other material parameters.

Figure 5-8 presents a comparison of experimental and the M_R/P_a values back-predicted by the second order polynomial model. The model's performance pertaining to specimens MA-3B, NO-7A, and OS-1B is illustrated in Figures 5-9, 5-10, and 5-11, respectively. As seen for the other statistical models in the preceding sections, prediction for specimen MA-3B appears to be the worst, while the prediction for specimen NO-7A appears to be the best. Prediction for the third specimen OS-1B appears to be intermediate. Similar observations are made in regard to other statistical models and the Artificial Neuron Network (ANN) models presented in Chapter 6. It will also become evident from Chapter 6 that the predictive capability of the ANN models are better than those of the statistical models.

5.4.4 Factorial Model Development

A full-factorial model is used in the present study. With seven independent variables and all possible products of the independent variables, the factorial model is a long equation with 128 terms. All the regression constants for this model were determined using Statistica 7.1. The resulting equation of the factorial model is presented in Appendix C.

The R^2 and F values for the factorial model were 0.6595 and 23.74, respectively. The R^2 is significantly higher than those for the previous models (0.4858). Significant observation was also made by the decrease of the F value from 101.02 for polynomial model to 23.74 for factorial model. Figure 5-12 shows a plot of experimental versus predicted M_R/P_a values for the factorial model. Figures 5-13, 5-14, and 5-15 present a comparison of the back-predicted M_R values against deviatoric stress for specimens MA-3B, NO-7A, and OS-1B, respectively. As expected, the factorial model back-predicted the resilient modulus values of specimen NO-7A very closely, while the prediction for specimen MA-3B is much worse. Furthermore, because of the improvement in R^2 and F values both the goodness of fit of the model and the significance model the observations between the experimental and back-predicted values are closer (Sokal and Rohlf, 1995; George, 2004; Hopkins et al., 2004). It may therefore be assumed at this point that since the F-value is 43.81 and it is the lowest F value, the factorial model is the most significant statistical model for the development dataset. Other complex regression models, such as separate slope, mixture surface, and homogeneity of slope models were considered in the present study. Even though the R^2 of these models increased to as high as 0.9429, the F values also increased and indicating that the complex models were not significant. Table 5-1 presents the R^2 and F values for these models. The limited literature review indicated no previous research in developing a factorial based model.

5.4.5 Comments On Comparative Performance of the Statistical Models

A summary of the R^2 and F values for the stress-based model and all the statistical models is presented in Tables 5-1 and 5-2. Based on the R^2 and F values, the stress-based model performs the worst in back-predicting the M_R values with a R^2 and F values of 0.3226 and 265.4, and the factorial model performs the best with a R^2 and F values of 0.6595 and 24.66, respectively. The performance of the multiple regression model and polynomial model are intermediate. As stated previously, the stress-based model does not appear to be an appropriate model for the dataset used in this study (George, 2004). Furthermore, since the second order polynomial model is a special case of multiple regression model and it performs better than the regression model, the two statistical models considered for further evaluation are the second order polynomial model and the full factorial model. Additional results on these two models are presented later in this chapter.

A common observation among all four statistical models is that better back-predictions of the M_R/P_a values are achieved in the lower range (up to 1,000). Similar observations will be evident from the results in Chapter 6 for the ANN models. When the M_R/P_a values increase beyond the 1,000, the differences between the experimental and model predicted M_R/P_a values increase. This observation may be due to the distribution of dataset. Only 140 M_R/P_a values out of 1512 M_R/P_a values (approximately 9%) are in the upper range of 1,000. The remaining 91% of the M_R/P_a values for this study are in the lower range of the development dataset. As a result statistical models appear to exhibit difficulty in back-predicting a majority of the resilient modulus values in the dataset that are in the lower range of the M_R/P_a values (Myers et al. 2001; Montgomery, 2006; Statsoft, Inc. 2006).

5.5 Evaluation of Models

As noted in the preceding section, only two statistical models, namely the second order polynomial model and the factorial model were considered for further evaluation. The M_R values were predicted using the evaluation dataset and then compared to the experimental M_R values. The R^2 value is utilized as the basis of comparing the developed models in regard to the goodness of fit and significance of the model (FHWA, 2002; Tarefder et al., 2005; Park et al., 2006). Furthermore, the evaluation dataset were separated into soils from Woodward County and Rogers County. Separate comparisons were made for Woodward County and Rogers County, and a comparison was made for both counties together (henceforth called "combined evaluation dataset"). This provides different views on the prediction quality and the importance of datasets on statistical analysis (Myers et al., 2001; Montgomery et al., 2006). Additionally, a comparison is made between the differences in the R^2 values of the development dataset and the evaluation dataset.

5.5.1 Evaluation of Factorial Model

The R^2 value of the combined evaluation dataset was only 0.3634. Figure 5-16 shows a comparison of the experimental and predicted M_R/P_a values for the combined evaluation dataset. Even though the overall R^2 value for the development dataset was 0.6595, it dropped significantly to 0.3634 for the evaluation dataset. Figures 5-17 and 5-18 compare experimental and predicted M_R/P_a values for the Woodward County and the Rogers County soils, respectively. The soils from Woodward County have the worst predictions among all the statistical models with a R^2 value of 0.0962. The full factorial model considered here contains 128 terms in the function, it may be considered a complex function among the four statistical models. Therefore, it is possible that the factorial model over-fited the development dataset and caused a poor prediction in the evaluation dataset (Hill and Lweicke, 2006; Montgomery et al., 2006). The concept of over fitting is similar to over training an Artificial Neuron Network (ANN). In the present study a full factorial model was considered. As stated previously a full factorial model with seven variables considers every form of permutation and has 128 terms. In the case of present dataset, it appears that the full factorial model has created a condition known as too much wiggle (Sokal and Rohlf, 1995; Fernandez-Juricic et al., 2003). Too much wiggle occurs when the equation has too many terms and tries to fit to as many data point as possible. This is an indication that when developing models, it is imperative to generate the model with a large dataset. Furthermore, any model should be evaluated by other datasets that were not used in the development of the model. The percent difference in the R^2 between the Development dataset and the Woodward County and Rogers County evaluation datasets are 85% and 39%, respectively. This is an indication that the predictions of factorial model are erratic and unreliable making the factorial model inappropriate for prediction of M_R values.

5.5.2 Evaluation of second order Polynomial Model

The second order polynomial model predicted the M_R/P_a values with an R^2 value of 0.5200. A plot of the experiment and predicted M_R/P_a values is illustrated in Figure 5-19. Comparisons of the experiment and predicted M_R/P_a values for the Woodward County and the Rogers County soils are presented in Figures 5-20 and 5-21, respectively. The results show that the Woodward County and the Rogers County soils have R^2 values of 0.6212 and 0.5523, respectively. The difference in the R^2 values for Woodward and Rogers Counties were approximately 27% and 6.2% higher than the R^2 value for the development dataset. This indicates that the second order polynomial model is capable of predicting the M_R values of the Rogers County soils, but is erratically predicting the M_R values of the Woodward County soils. It appears that even though the only viable statistical model is the second order polynomial model, the regression-based statistical models are not capable of capturing the relationship between M_R and material properties. An interesting observation of the similarities of regression models and ANN models in term of statistical modeling is the near identical R^2 values for the multiple regression (Table 5-2) and the Linear Network (LN) Table 6-1. The regression model and the simplest ANN model are predicating the same R^2 for both development dataset and evaluation datasets up to the Woodward County and Rogers County. As a result the more complex Artificial Neural Network modeling will be introduced and implemented in Chapter 6 in the hope that more complex modeling will be able to capture the relationship between the M_R and other soil material properties.

Table 5-1 Summary of R^2 and F Values for the Statistical Modeling

Statistical Model	R^2	**F**
*$M_R = k_1 (\sigma_d)^{k2}$	0.0605	98.38
**$M_R = k_1 (\sigma_3 + 1)^{k2} (\sigma_d + 1)^{k3}$	0.0392	30.81
Stress-based	0.3226	253.37
Multiple Regression	0.4357	165.88
Polynomial	0.4858	101.02
Factorial	0.6595	23.74
Separate Slope	0.8722	56.45
Mixture Surface	0.5522	67.79
Homogeneity of Slope	0.9430	83.38

* Moossazadeh and Witczak, 1981

** NCHRP, 2003

Table 5-2 Summary of the Statistical Modeling Results

Statistical Model	Development Dataset		Evaluation Dataset					
			Combined		Woodward County		Rogers County	
	R^2	R	R^2	R	R^2	R	R^2	R
Stress-Based	0.3226	0.5680	0.3569	0.5974	0.5776	0.7600	0.3666	0.6055
Multiple Regression	0.4357	0.6601	0.5403	0.7351	0.8077	0.8987	0.5370	0.7328
Polynomial	0.4858	0.6970	0.5200	0.7211	0.6212	0.7882	0.5523	0.7432
Factorial	0.6595	0.8121	0.3634	0.6028	0.0962	0.3102	0.4021	0.6341

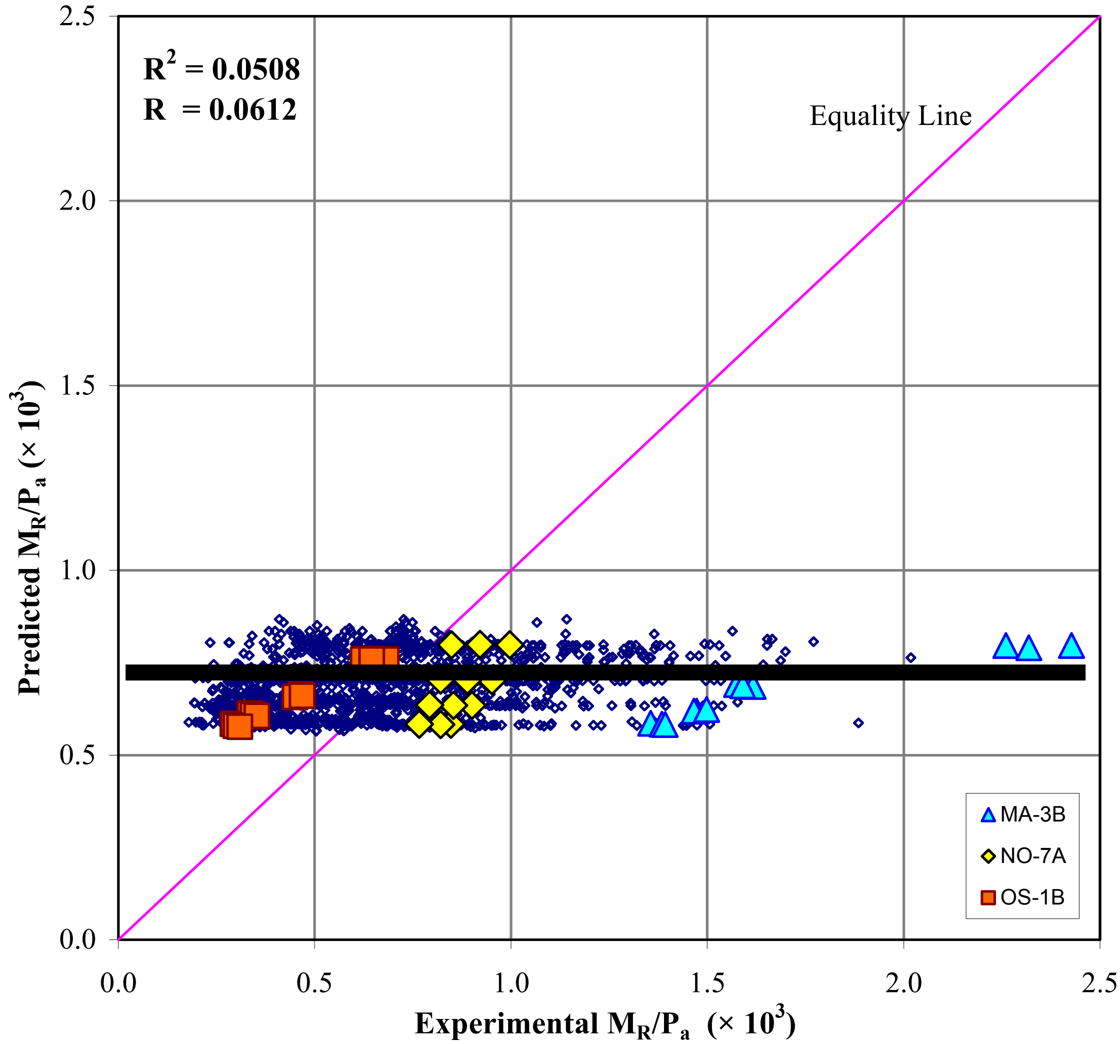

Figure 5-1 Comparison of Experimental and Predicted M_R/P_a for Development Dataset: Moossazadeh and Witczak, 1981 Stress-Based Model

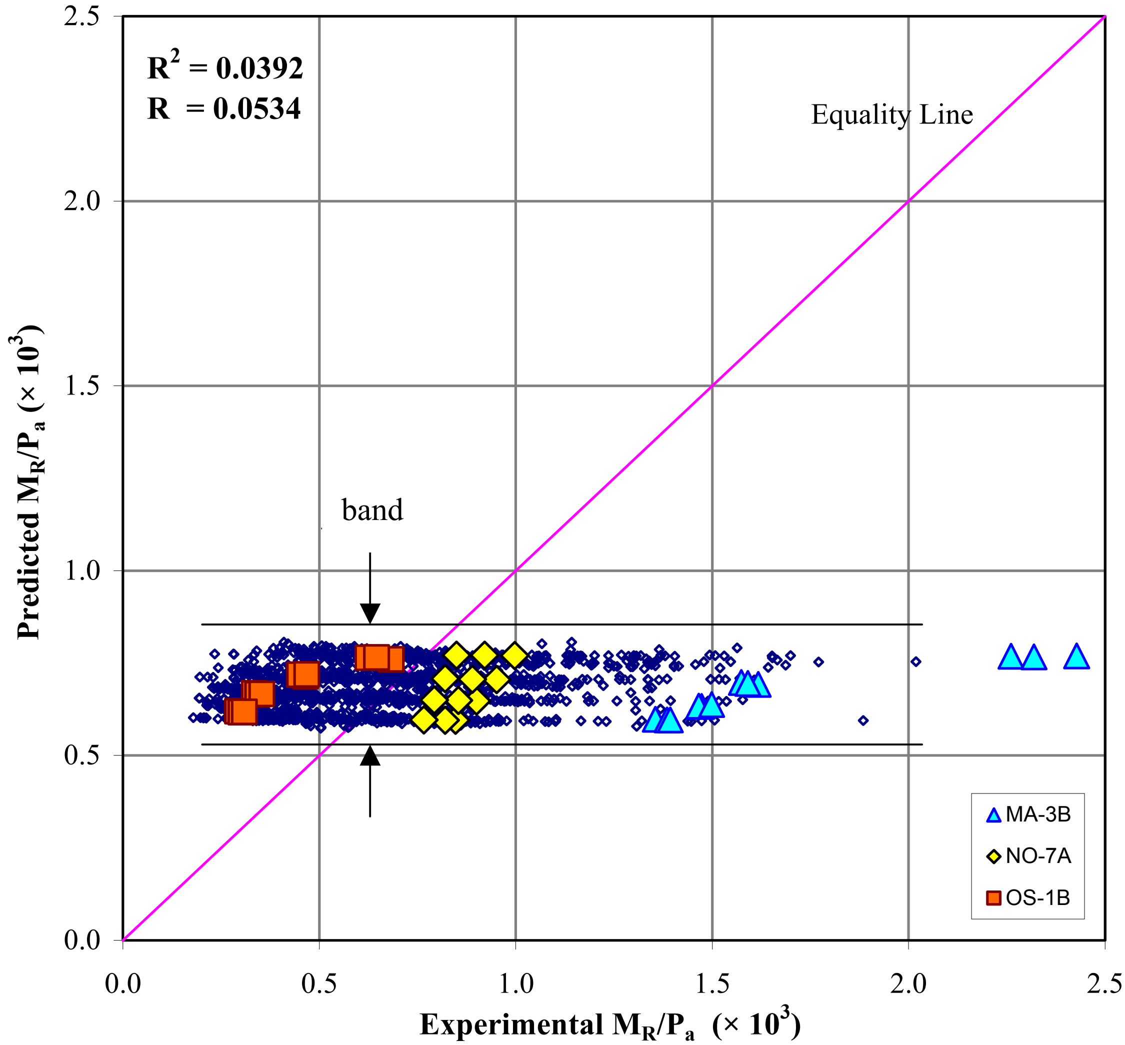

Figure 5-2 Comparison of Experimental and Predicted M_R/P_a for Development Dataset: NCHRP, 2003 Stress-Based Model

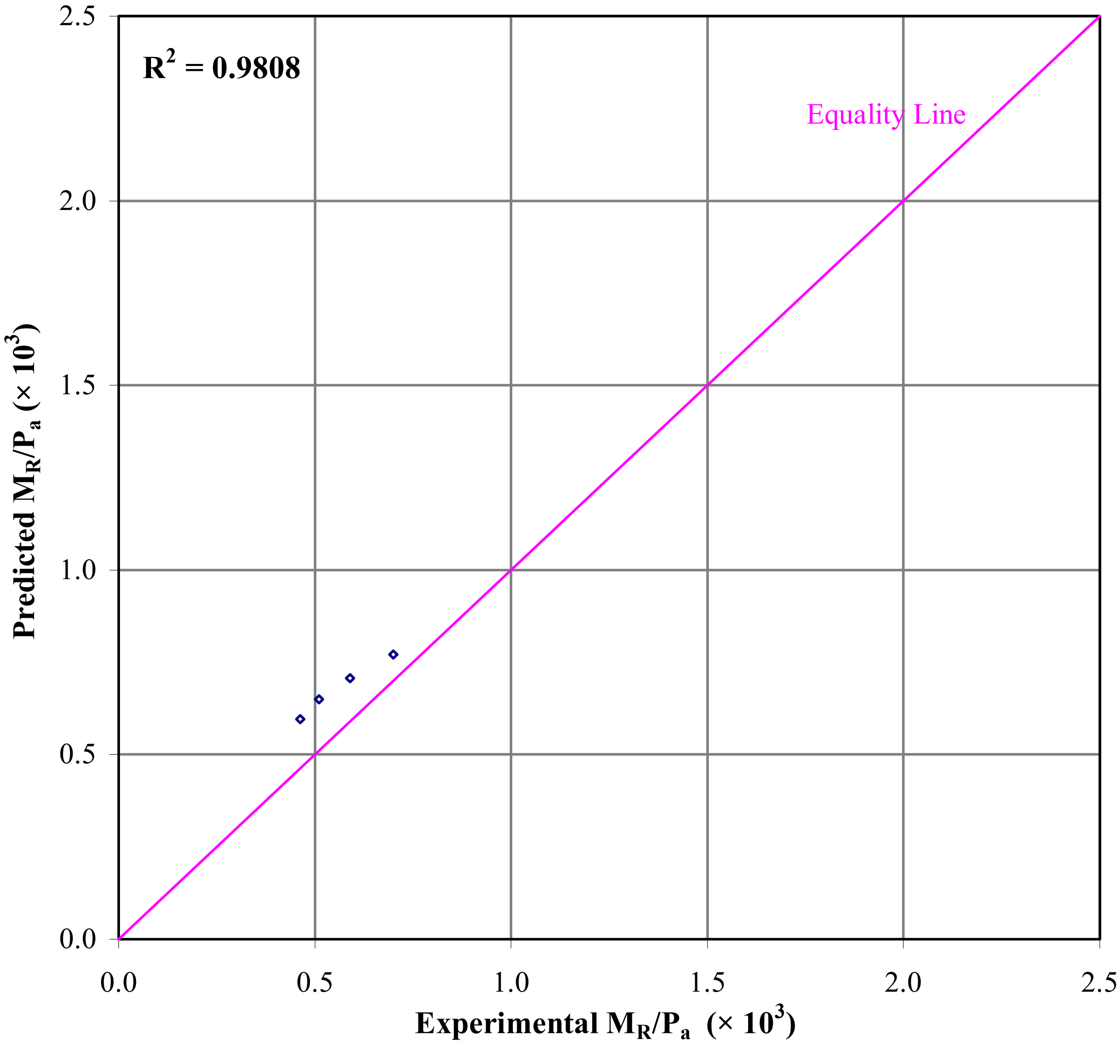

Figure 5-3 Comparison of Experimental and Predicted M_R/P_a for Development Dataset: NCHRP, 2003 Stress-Based Model for One Confining Pressure

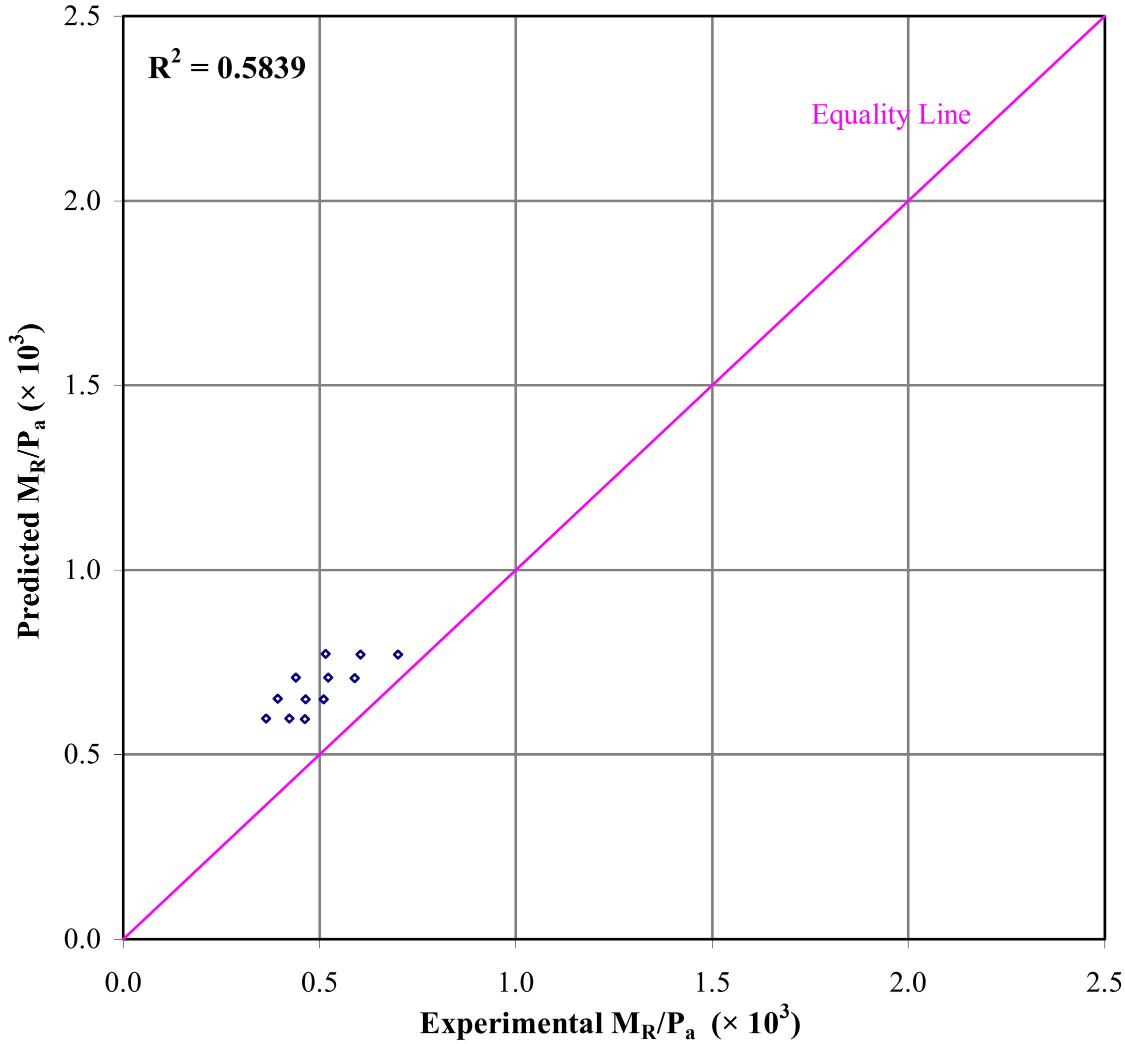

Figure 5-4 Comparison of Experimental and Predicted M_R/P_a for Development Dataset: NCHRP, 2004 Stress-Based Model for one M_R Test (Three Confining Pressures

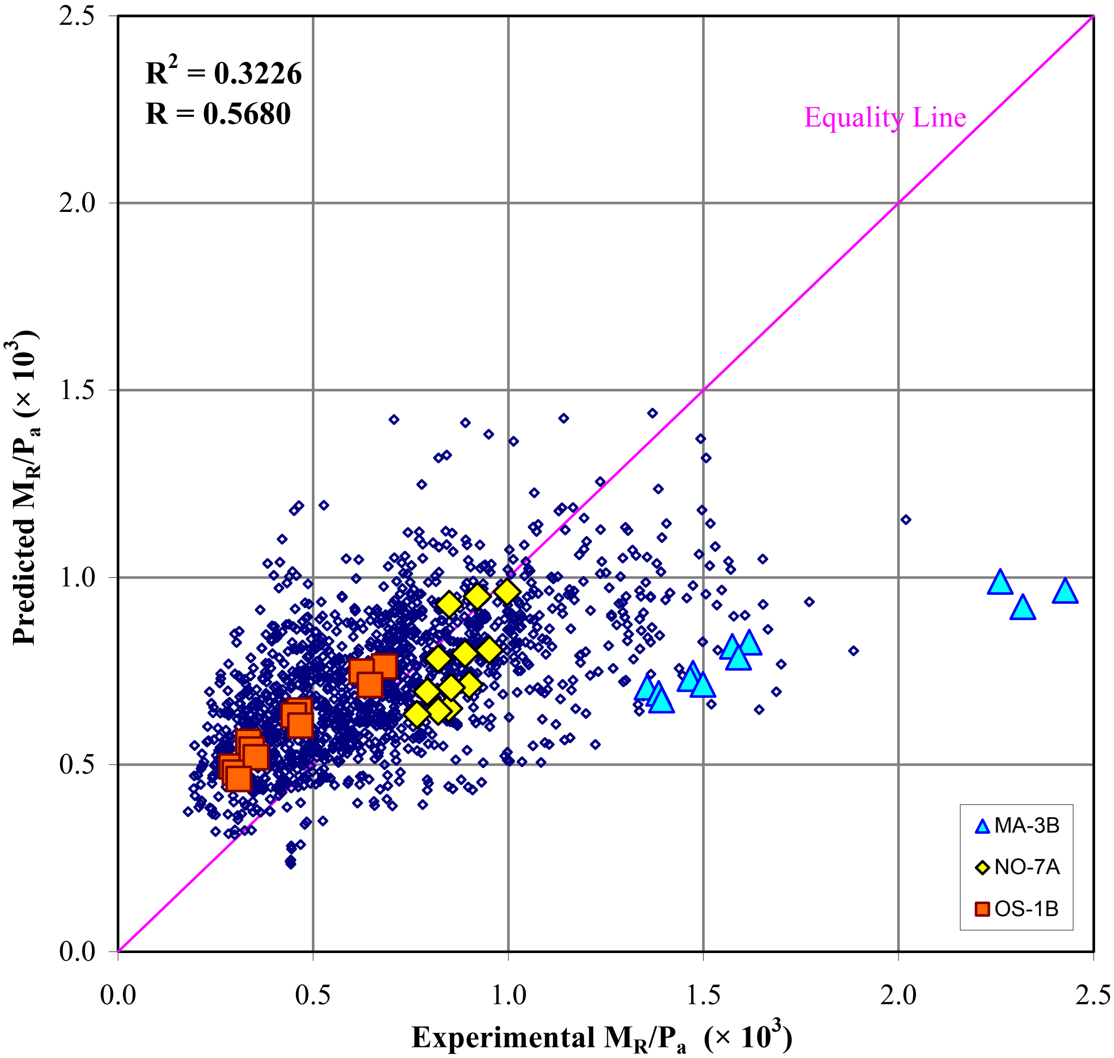

Figure 5-5 Comparison of Experimental and Predicted M_R/P_a for Development Dataset: Stress-Based Model

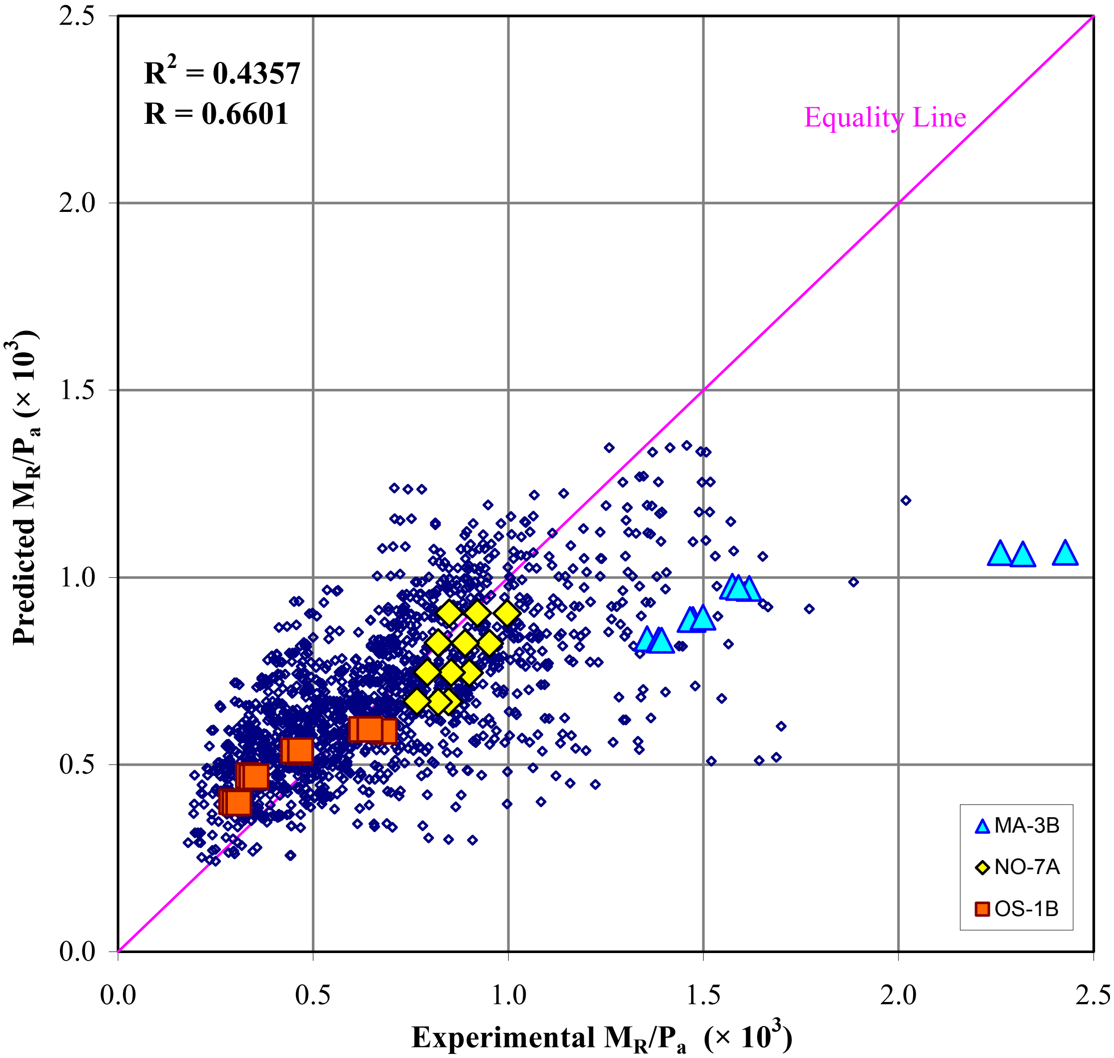

Figure 5-6 Comparison of Experimental and Predicted M_R/P_a for Development Dataset: Multiple Regression Model

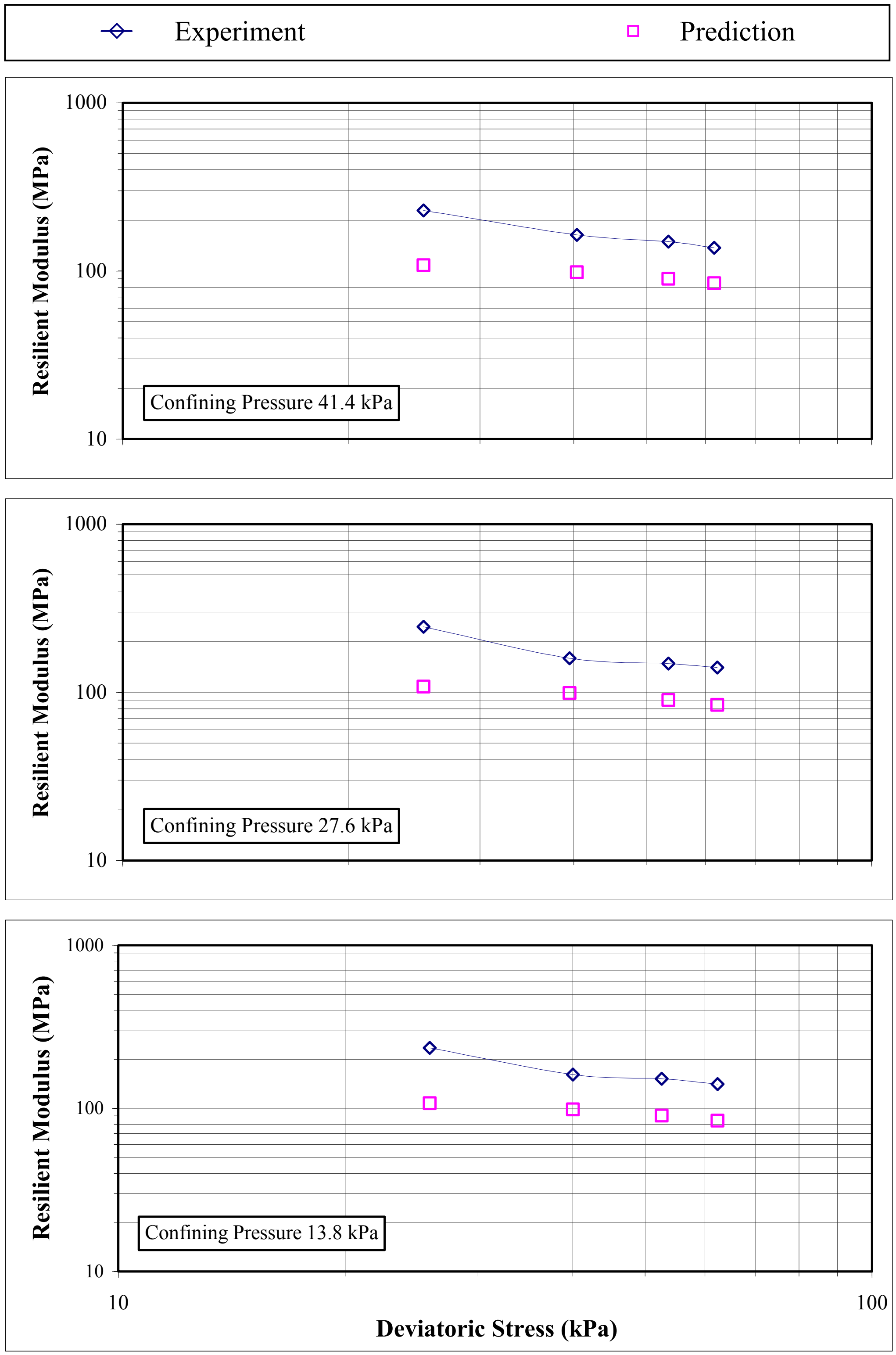

Figure 5-7 Resilient Modulus from Experiment and Multiple Regression Model: Specimen MA-3B

1 kPa = 0.145 psi

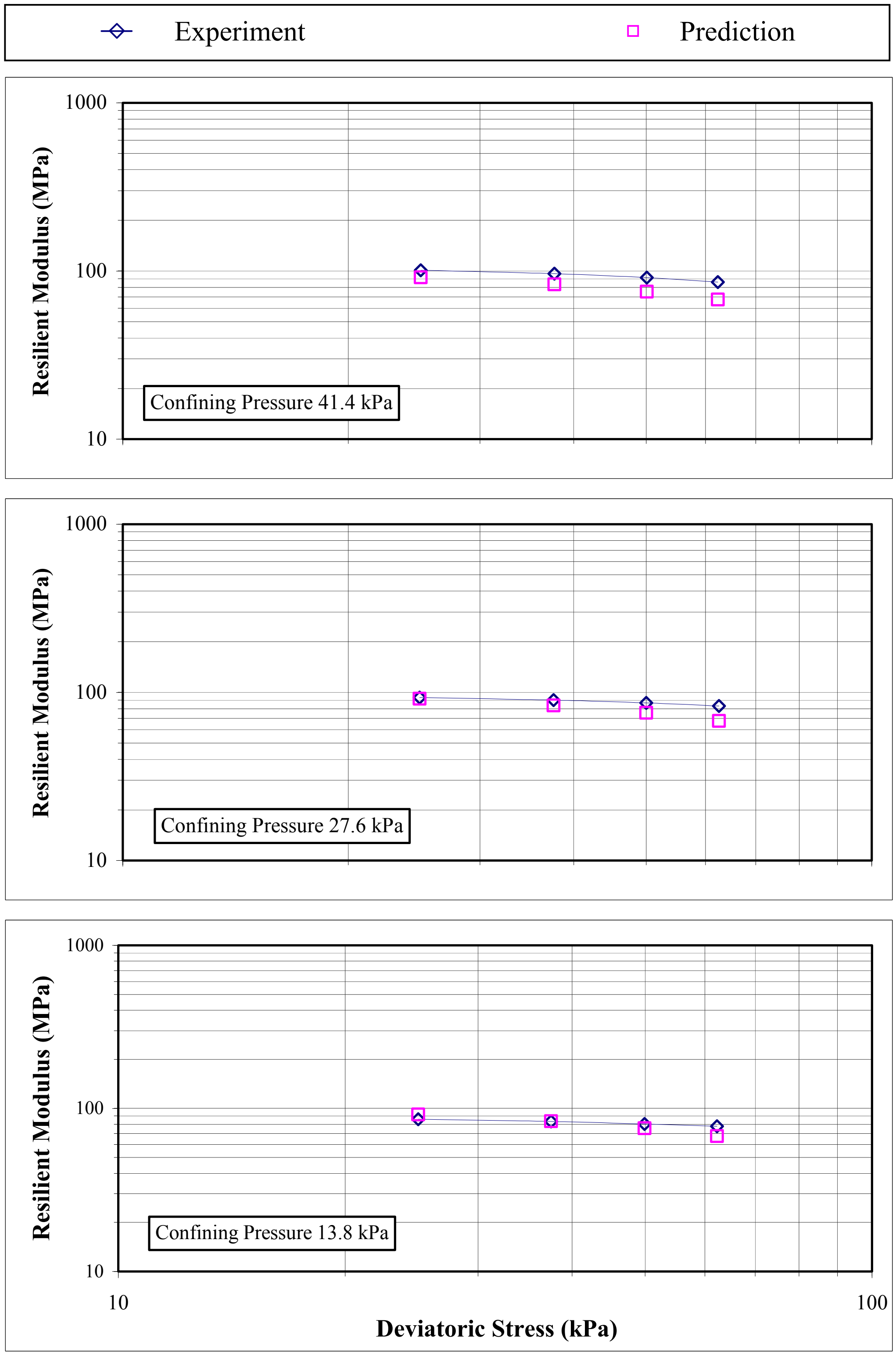

Figure 5-8 Resilient Modulus from Experiment and Multiple Regression Model: Specimen NO-7A

1 kPa = 0.145 psi

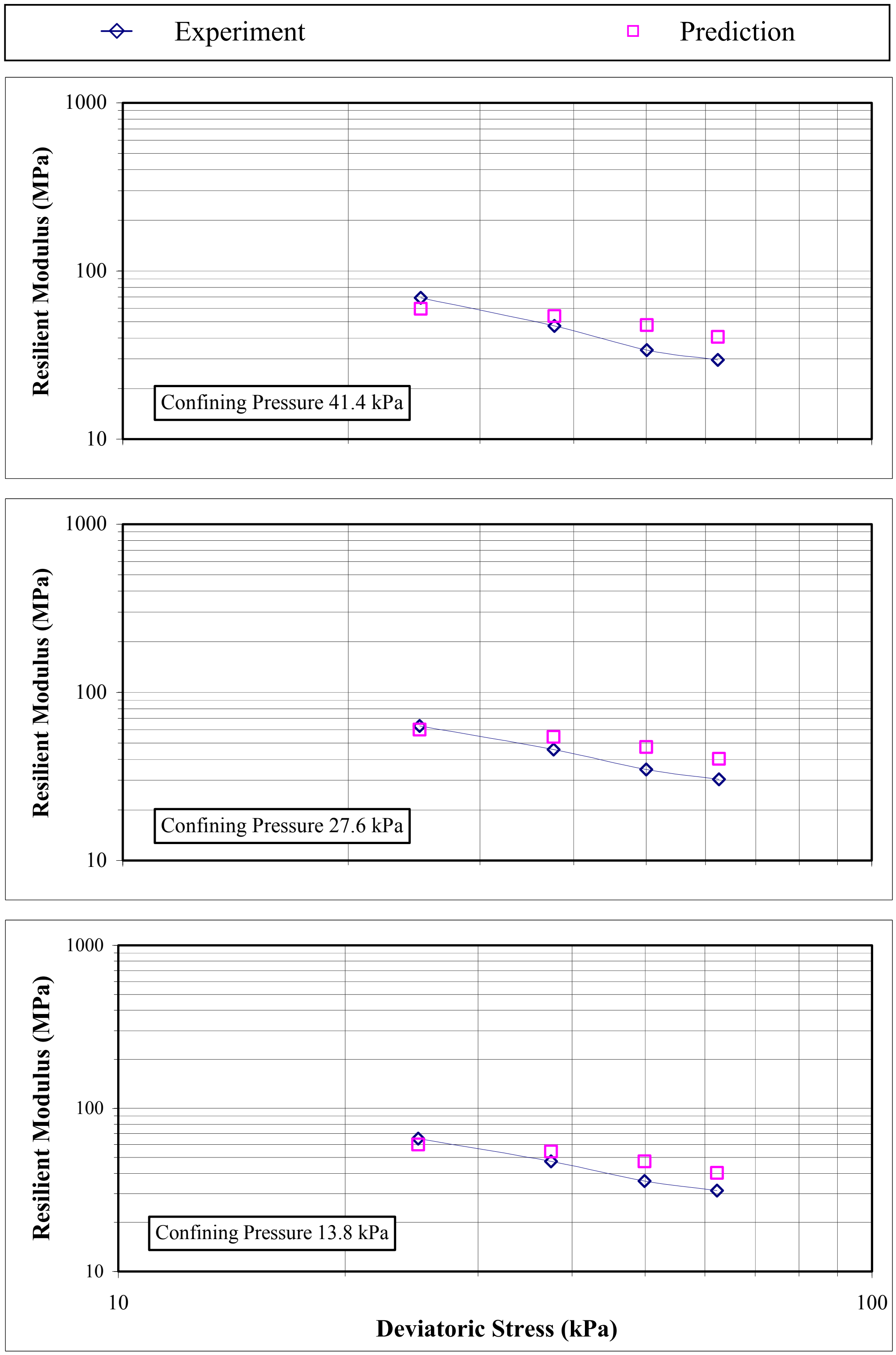

Figure 5-9 Resilient Modulus from Experiment and Multiple Regression Model: Specimen OS-1B

1 kPa = 0.145 psi

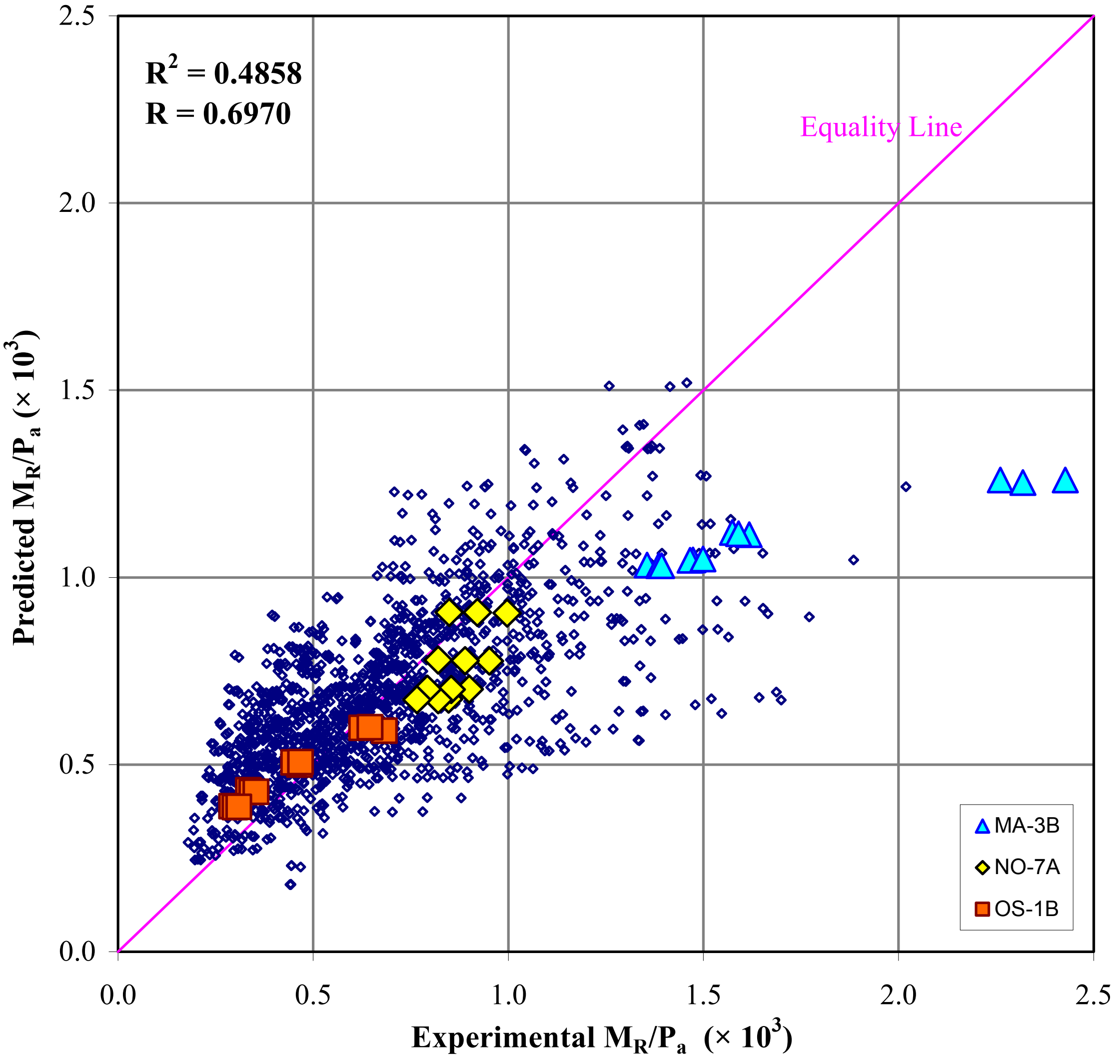

Figure 5-10 Comparison of Experimental and Predicted M_R/P_a for Development Dataset: Polynomial Model

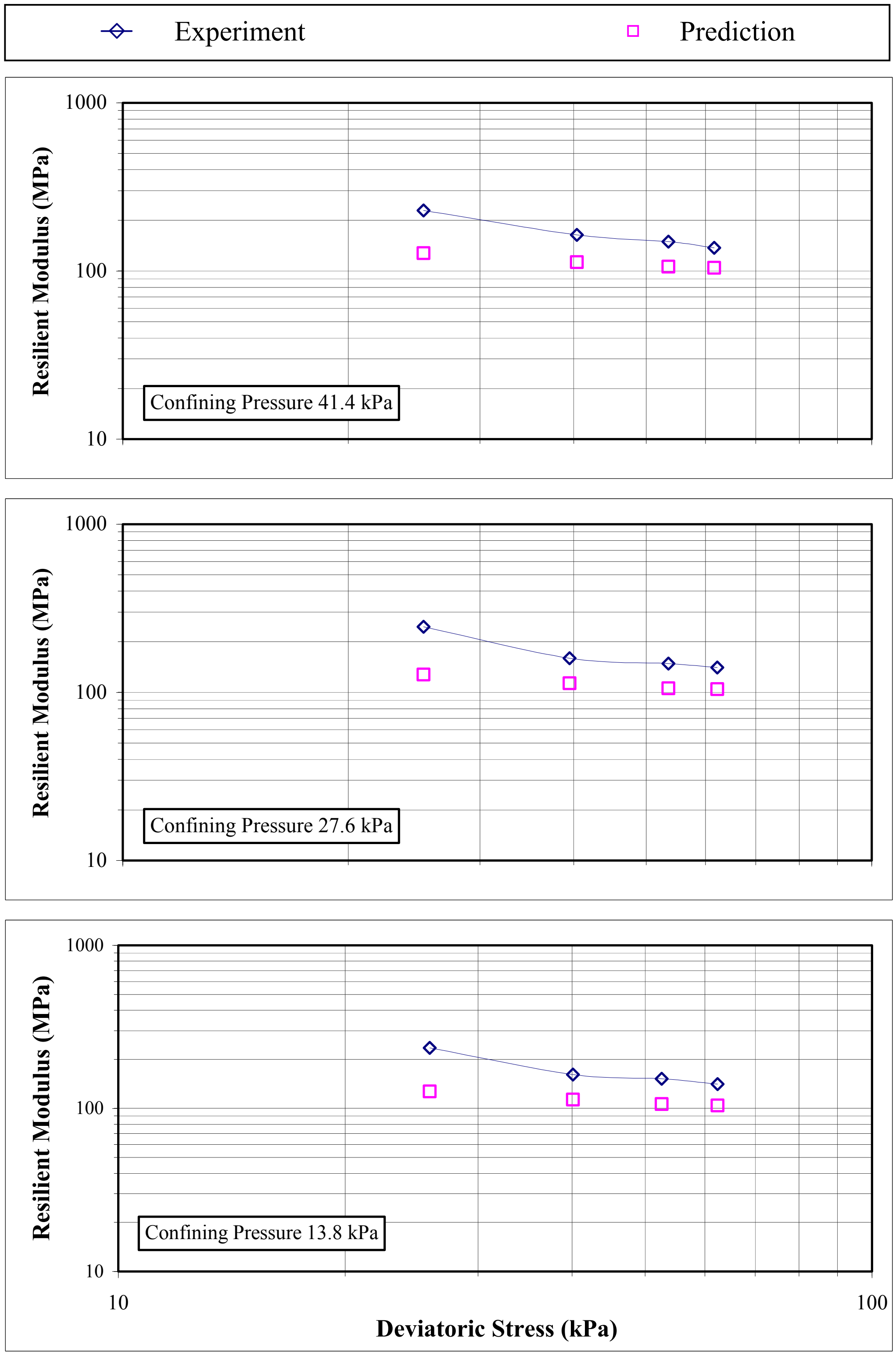

Figure 5-11 Resilient Modulus from Experiment and Polynomial Model: Specimen MA-3B

1 kPa = 0.145 psi

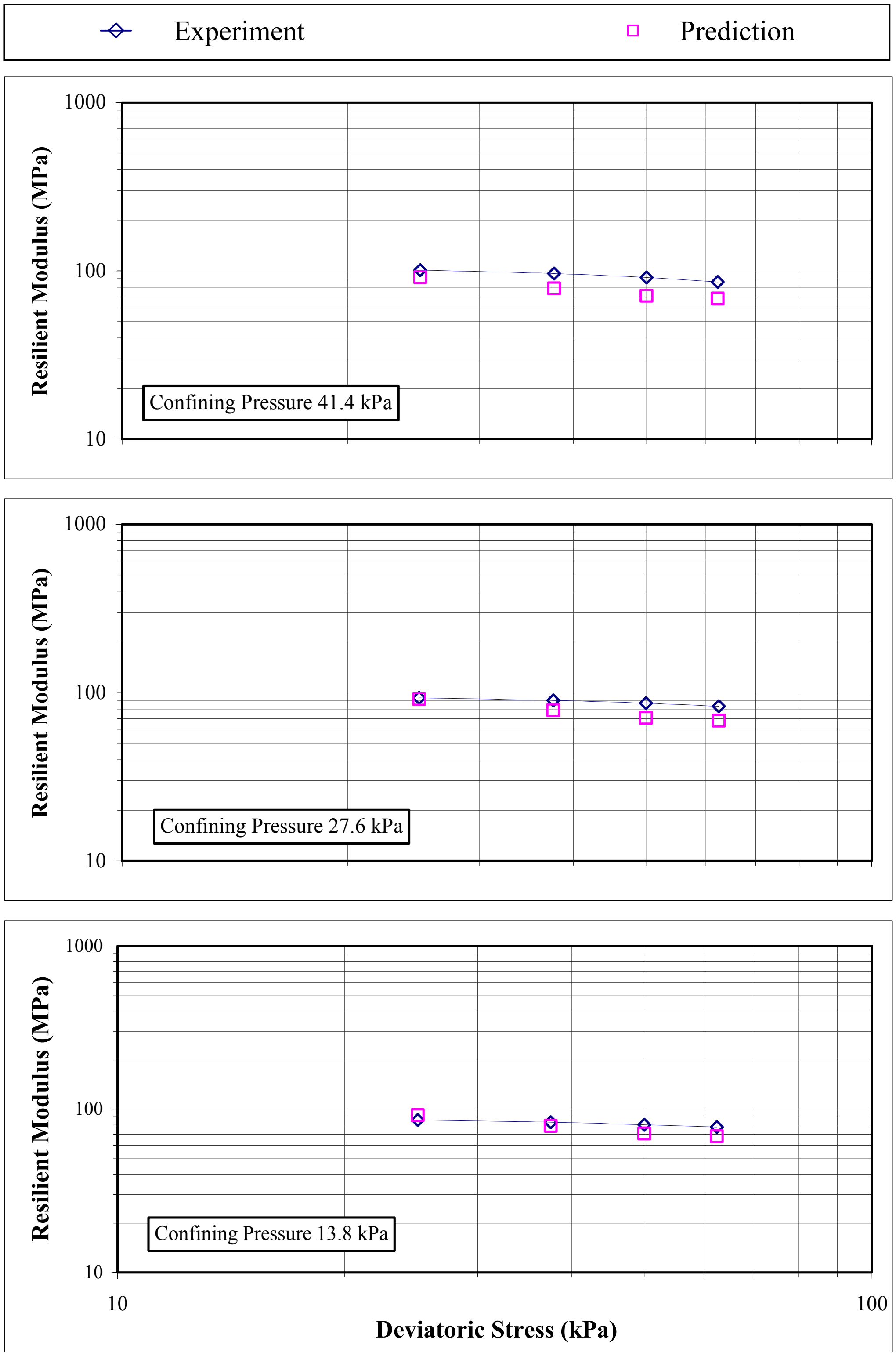

Figure 5-12 Resilient Modulus from Experiment and Polynomial Model: Specimen NO-7A

1 kPa = 0.145 psi

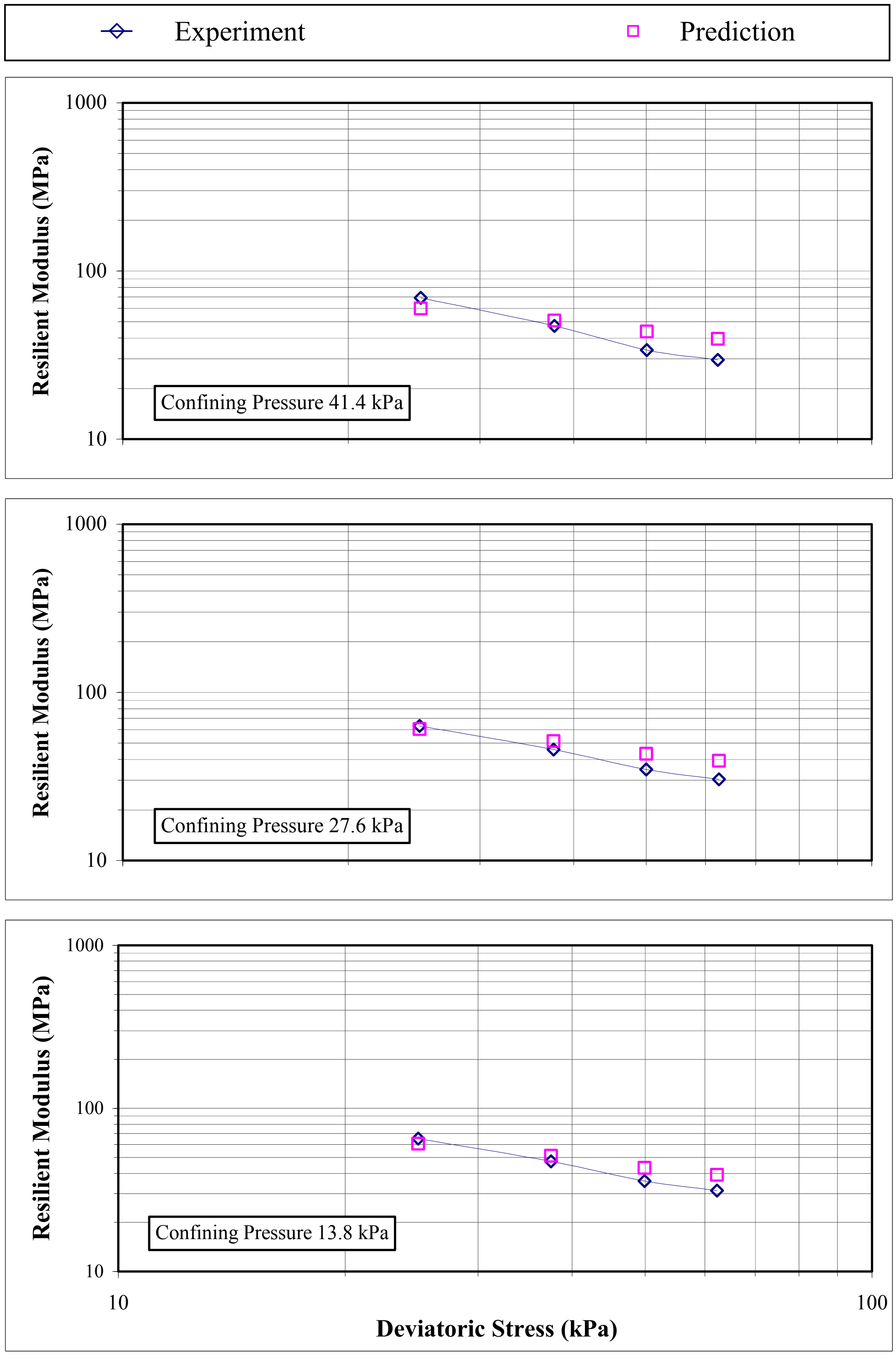

Figure 5-13 Resilient Modulus from Experiment and Polynomial Model: Specimen OS-1B

1 kPa = 0.145 psi

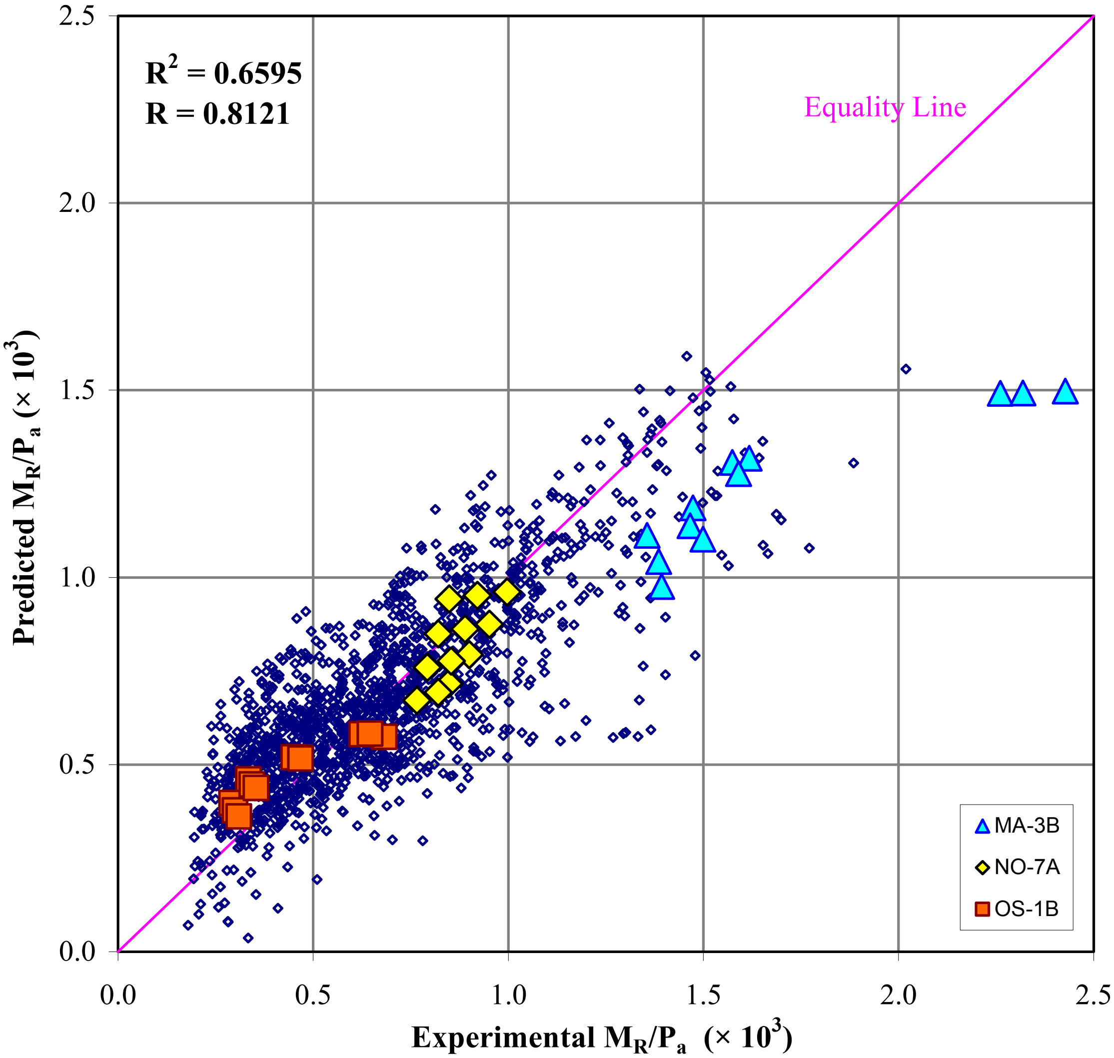

Figure 5-14 Comparison of Experimental and Predicted M_R/P_a for Development Dataset: Factorial Model

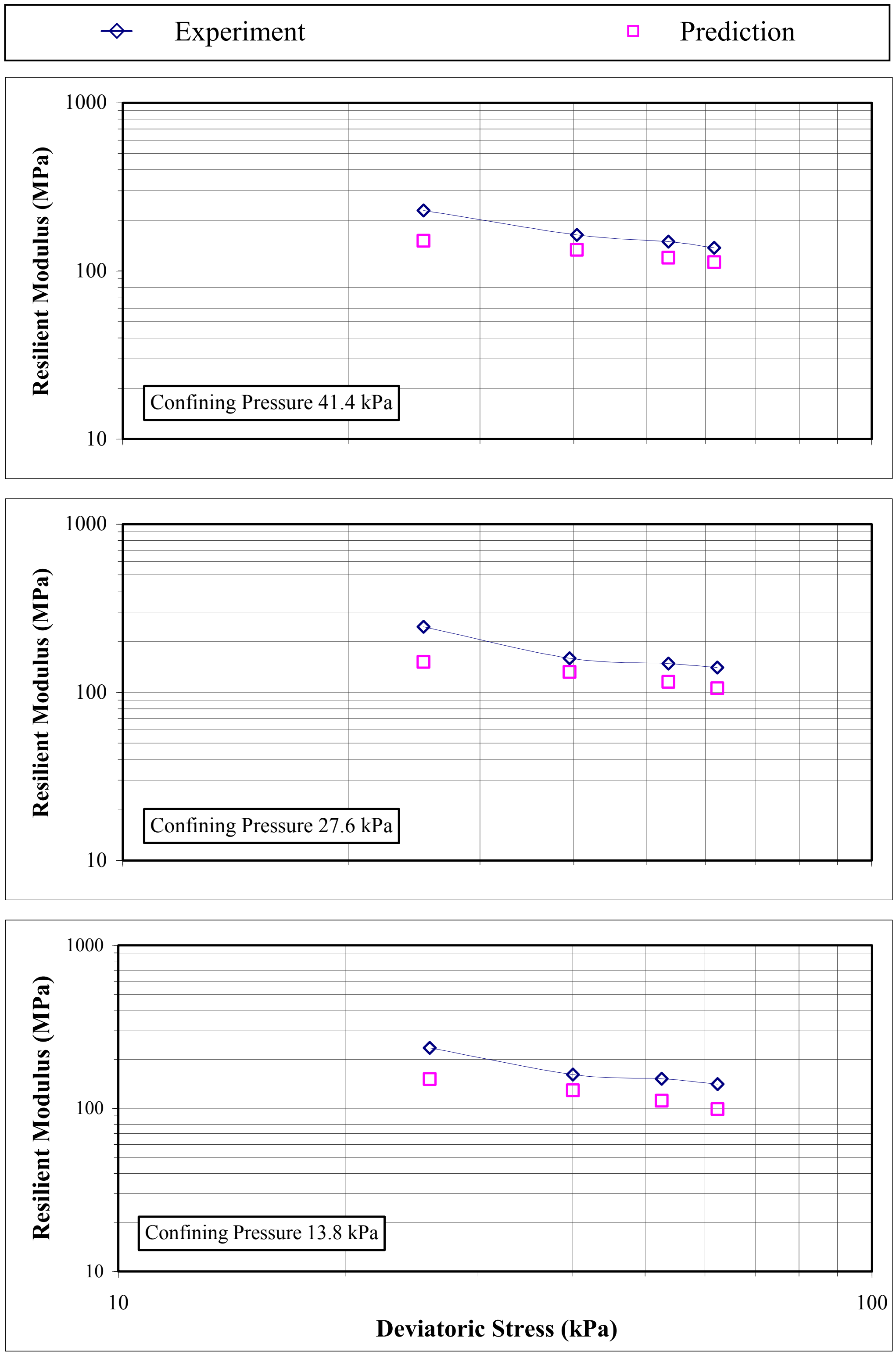

Figure 5-15 Resilient Modulus from Experiment and Factorial Model: Specimen MA-3B

1 kPa = 0.145 psi

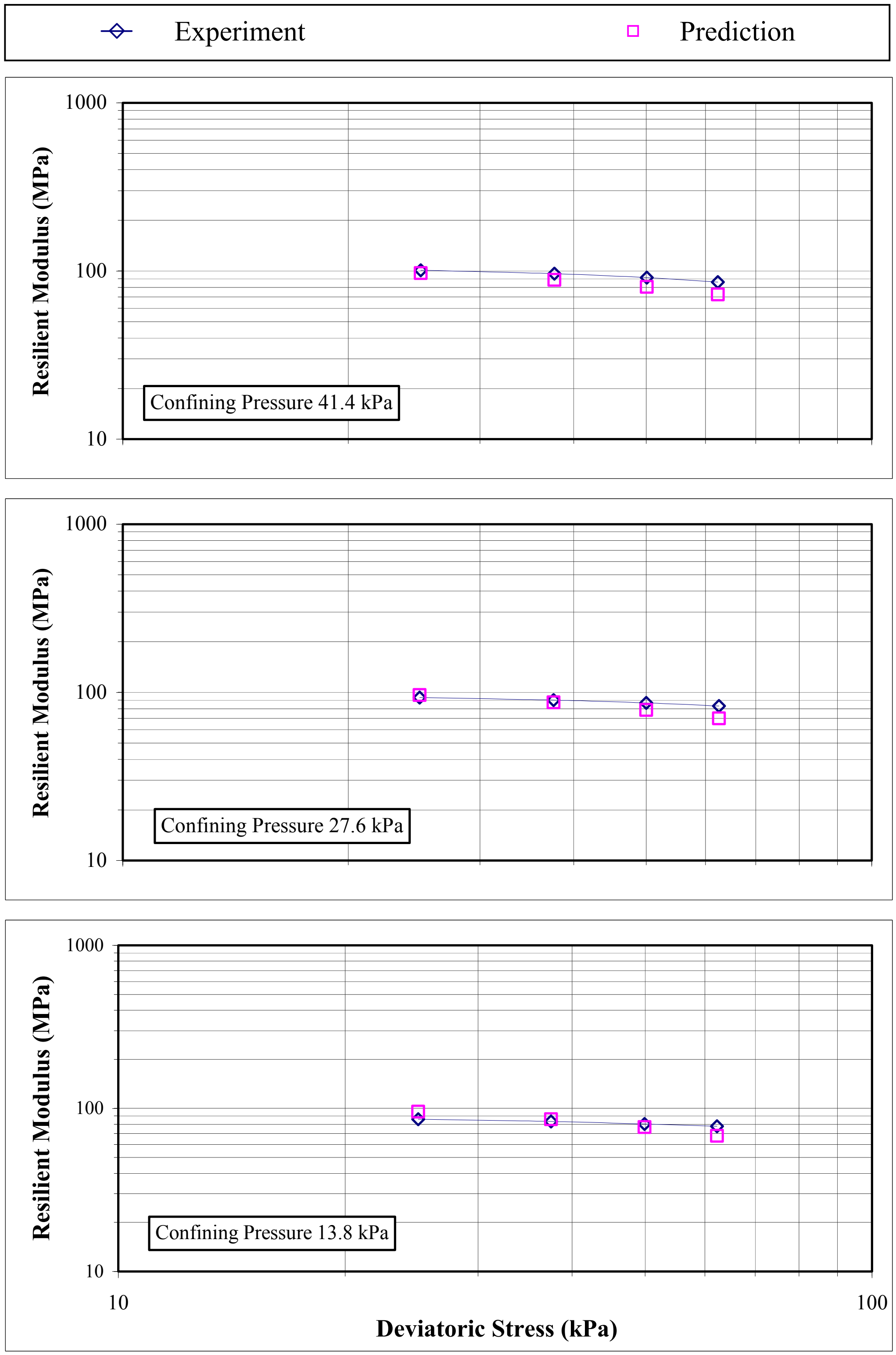

Figure 5-16 Resilient Modulus from Experiment and Factorial Model: Specimen NO-7A

1 kPa = 0.145 psi

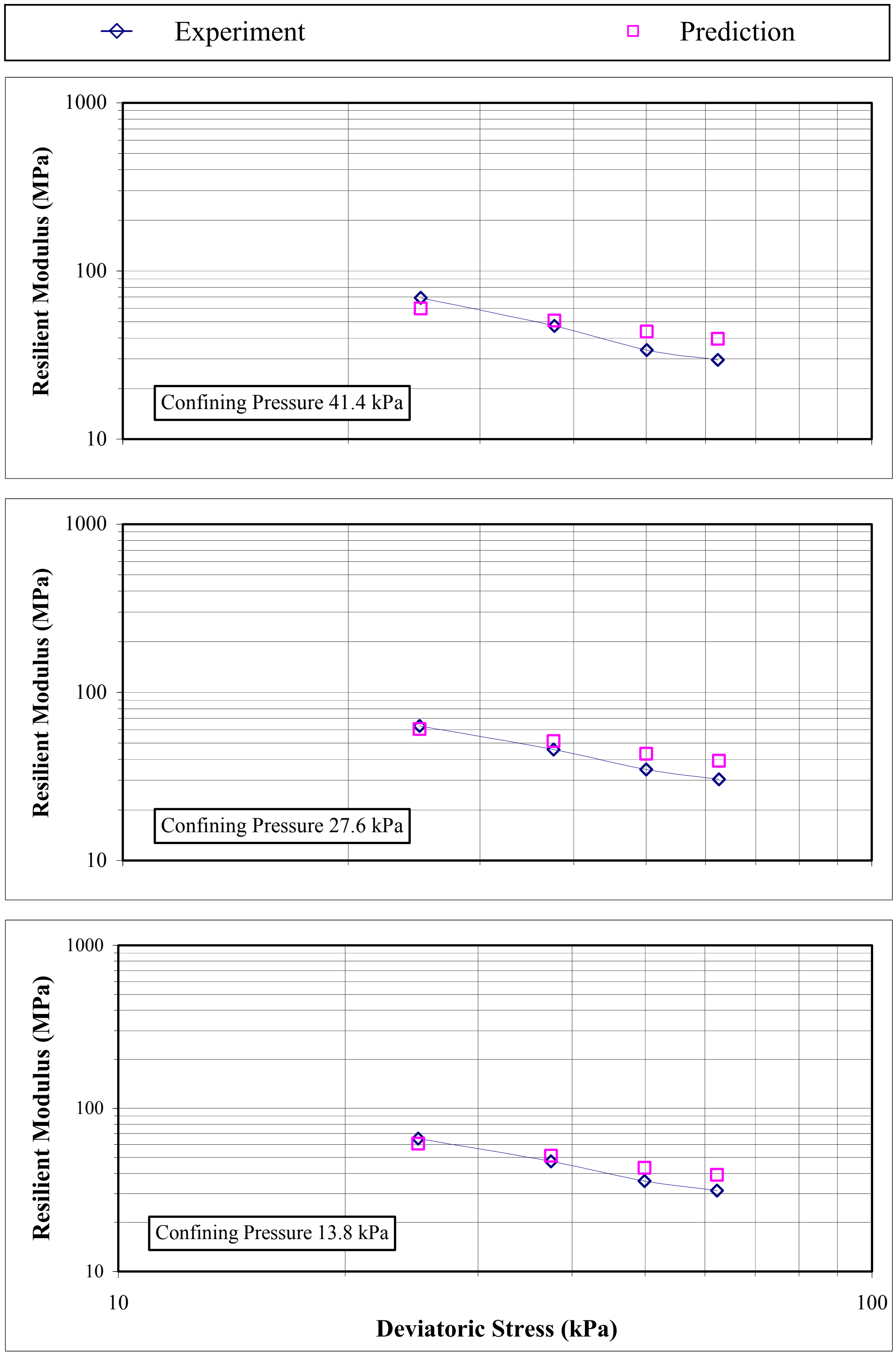

Figure 5-17 Resilient Modulus from Experiment and Factorial Model: Specimen OS-1B

1 kPa = 0.145 psi

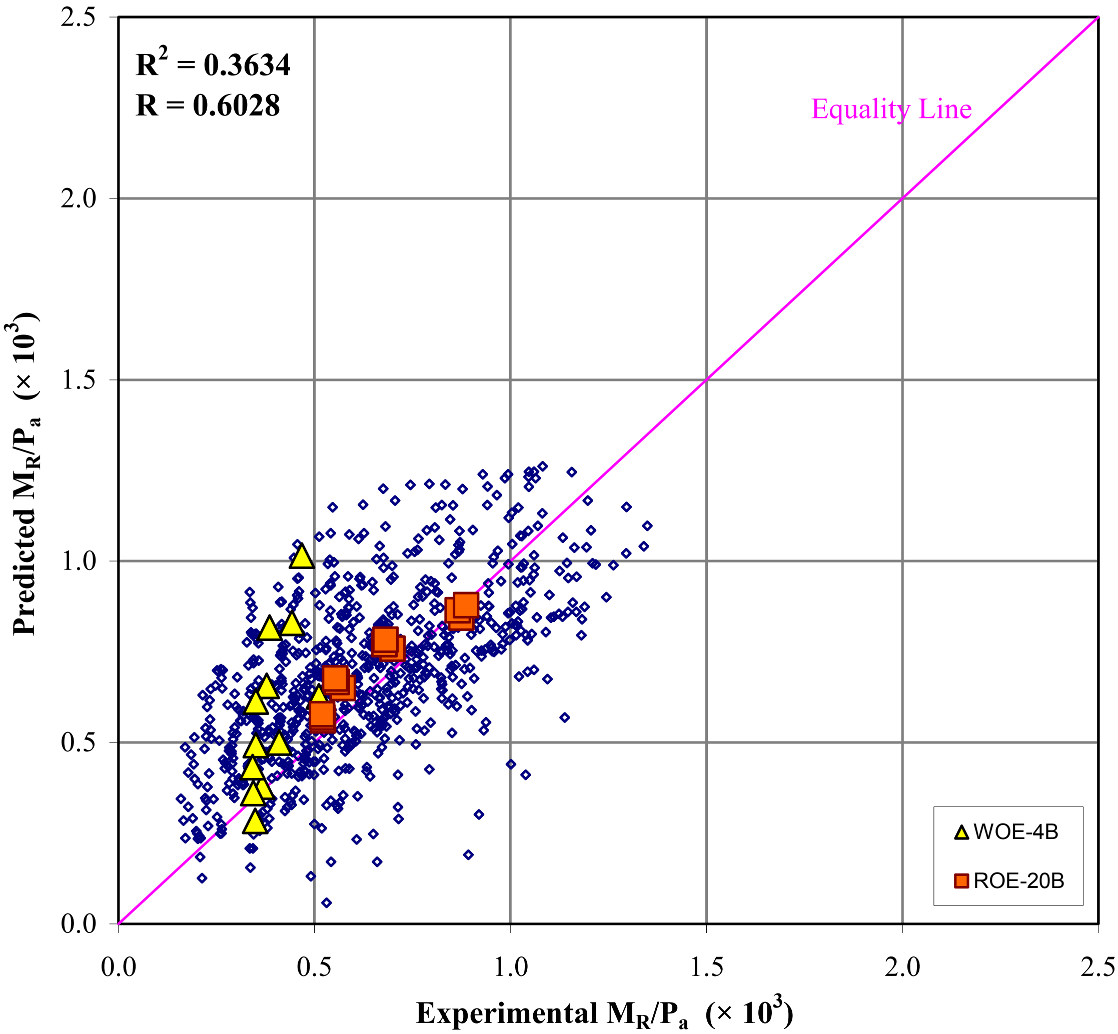

Figure 5-18 Comparison of Experimental and Predicted M_R/P_a for Combined Evaluation Dataset: Factorial Model

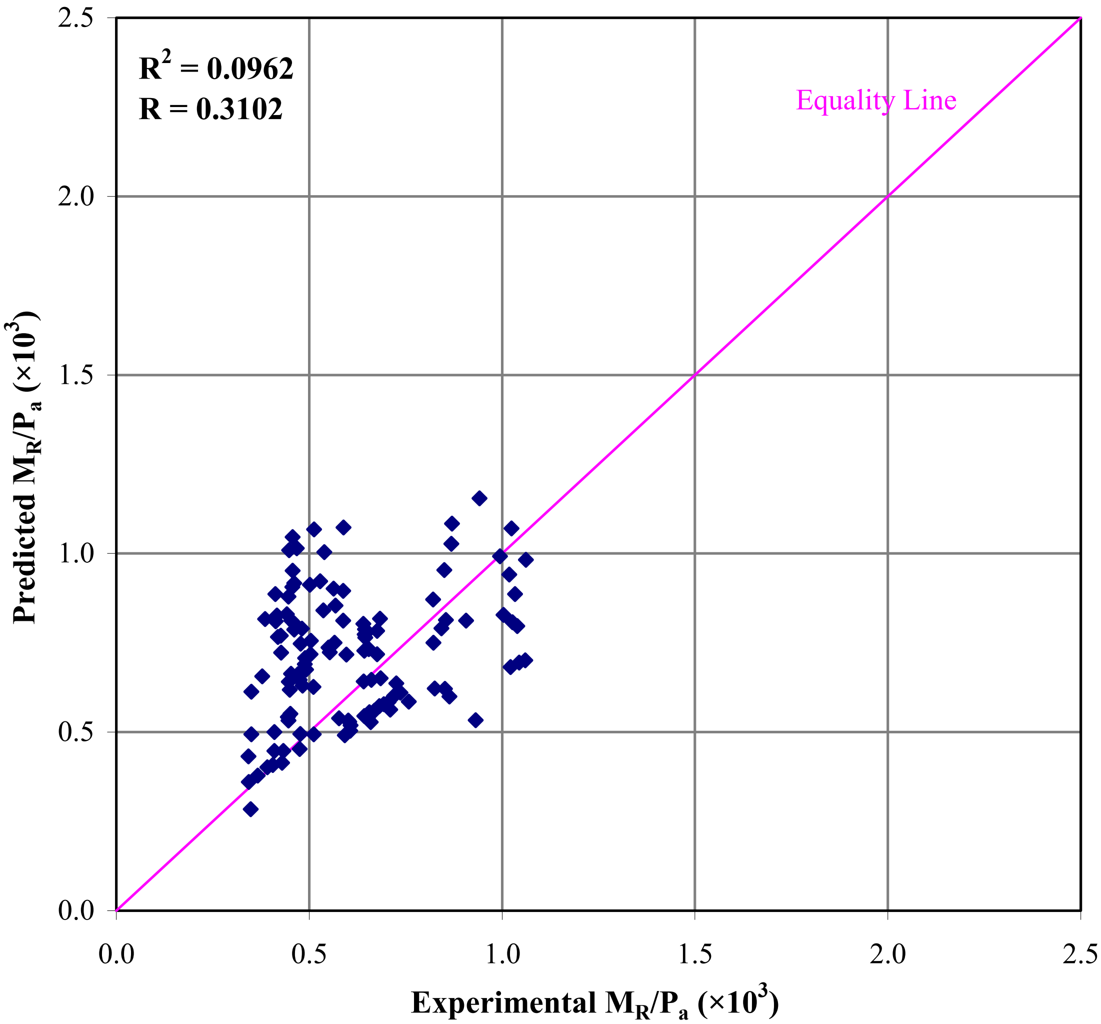

Figure 5-19 Comparison of Experimental and Predicted M_R/P_a for Evaluation Dataset from Woodward County: Factorial Model

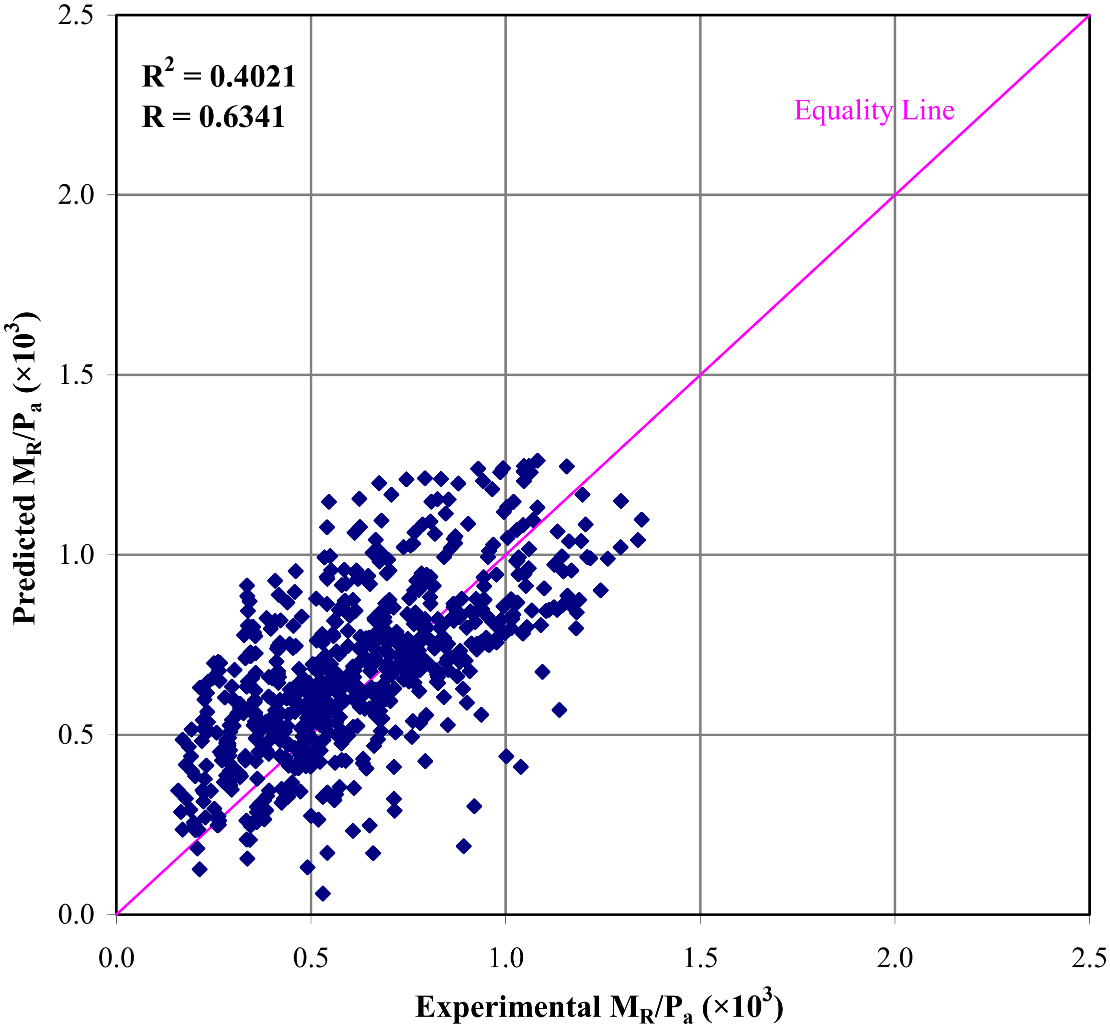

Figure 5-20 Comparison of Experimental and Predicted M_R/P_a for Evaluation Dataset from Rogers County: Factorial Model

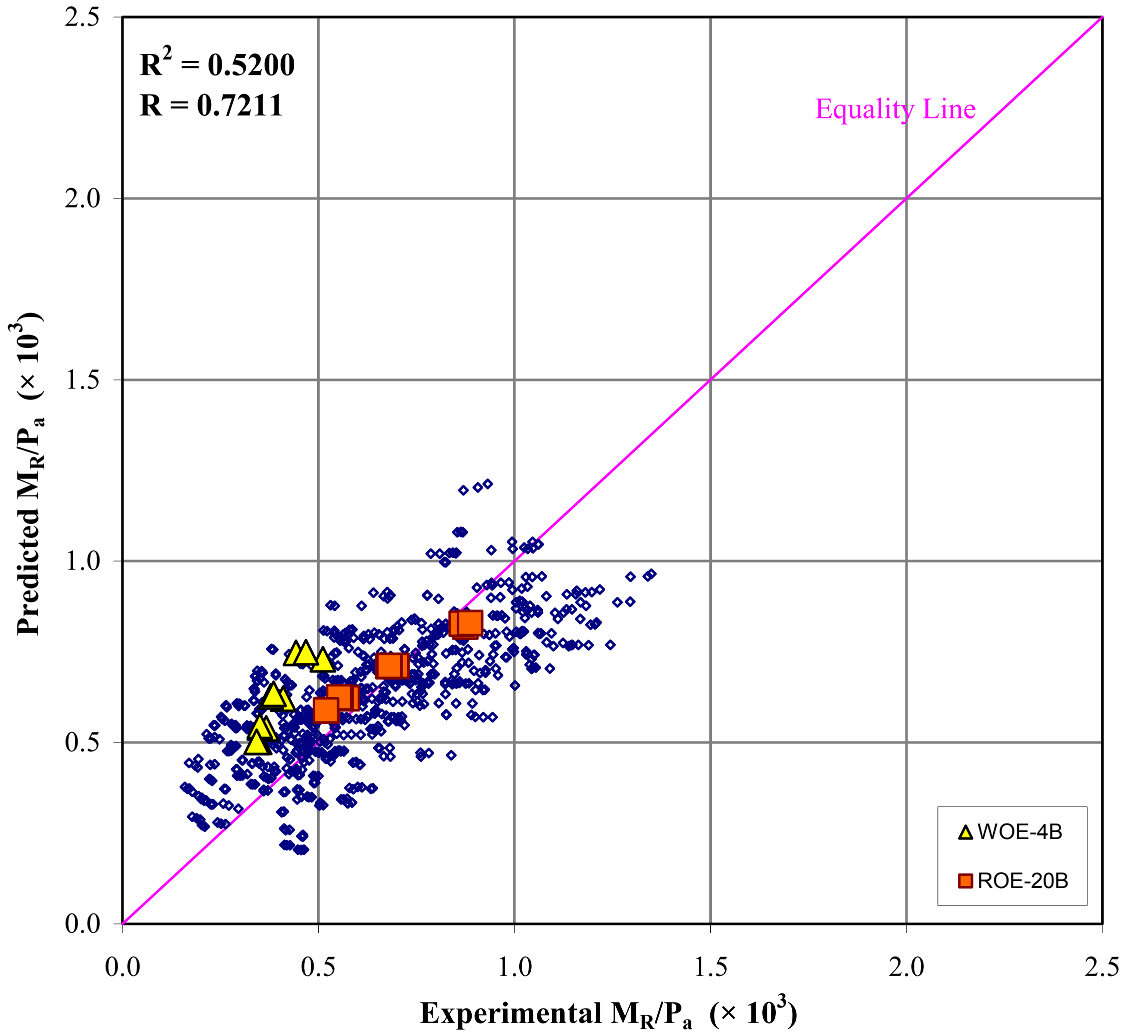

Figure 5-21 Comparison of Experimental and Predicted M_R/P_a for Combined Evaluation Dataset: Polynomial Model

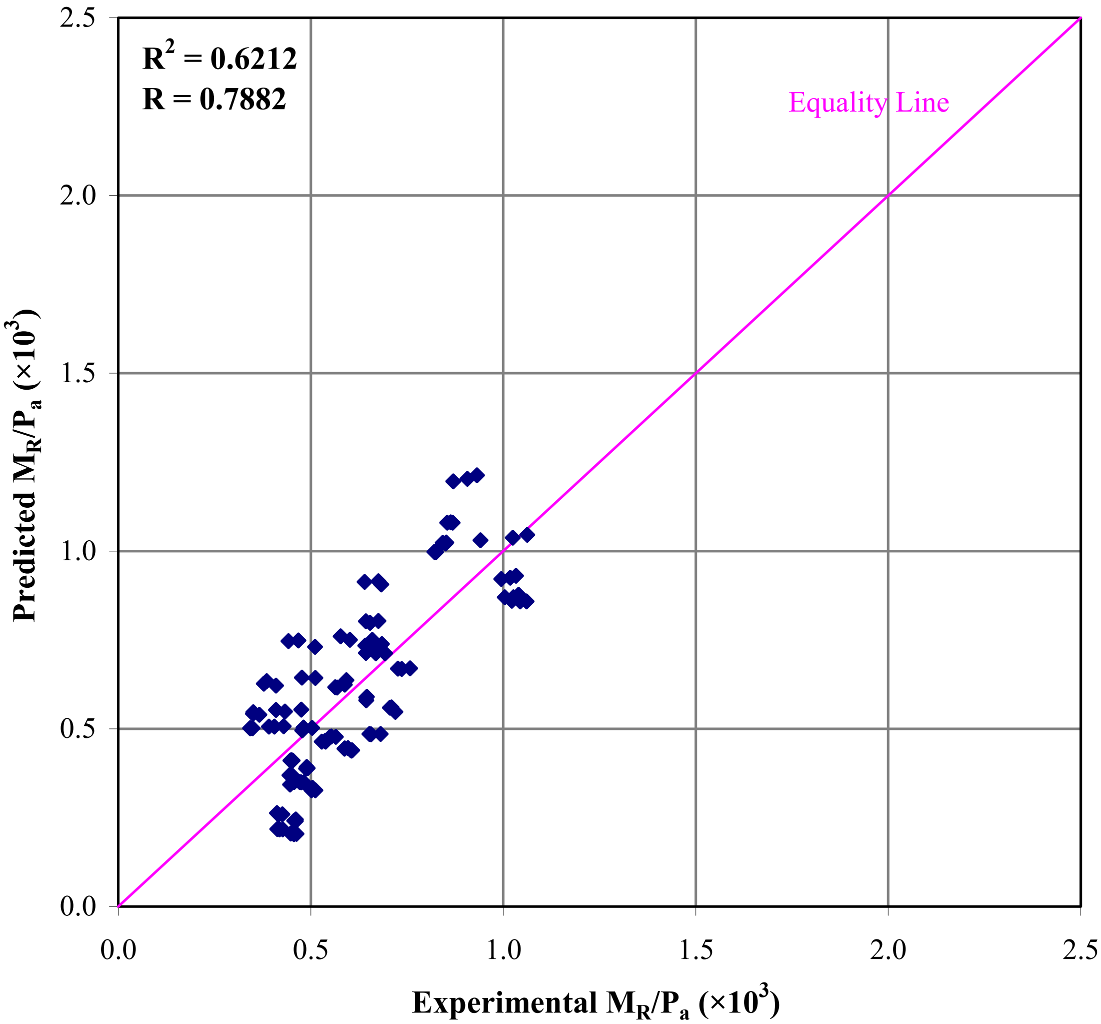

Figure 5-22 Comparison of Experimental and Predicted M_R/P_a for Evaluation Dataset from Woodward County: Polynomial Model

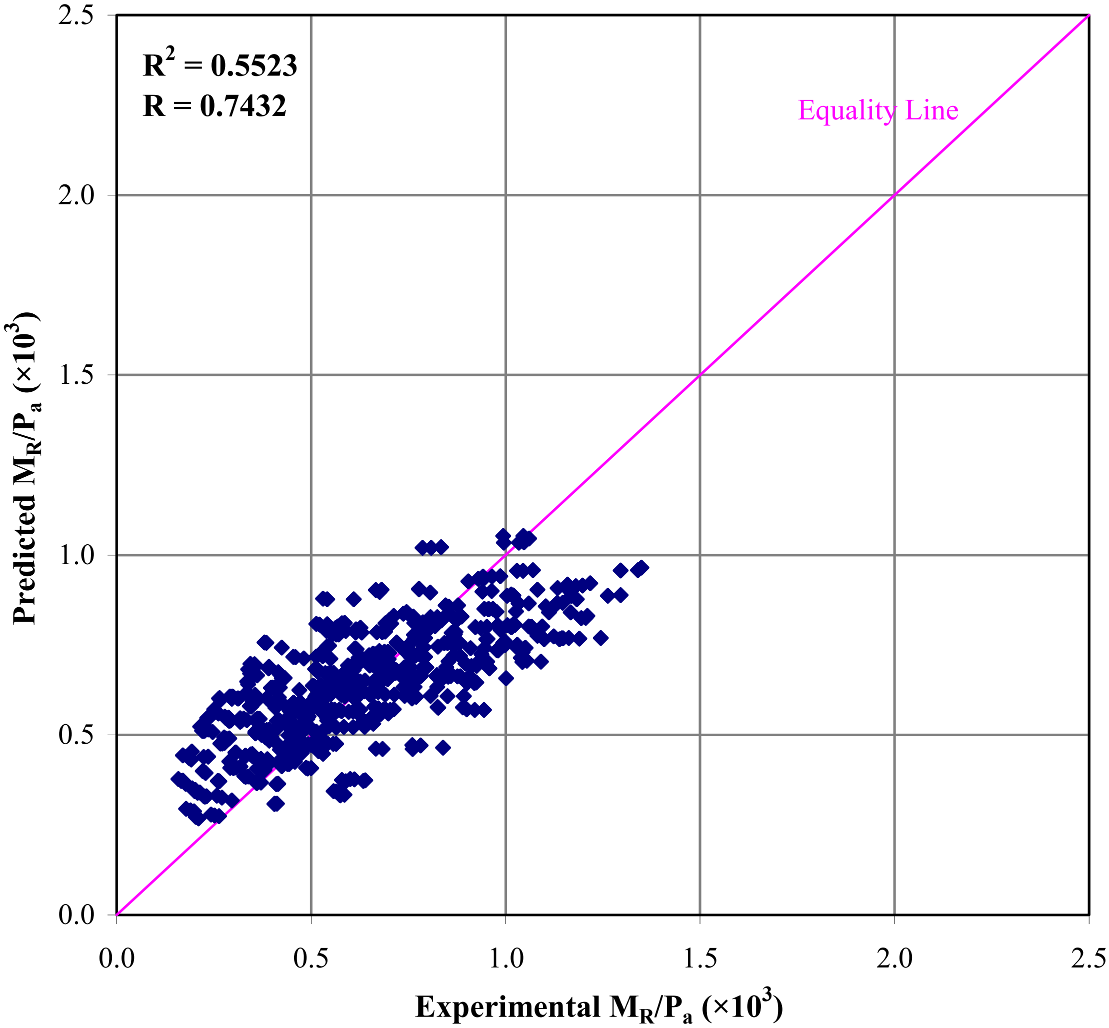

Figure 5-23 Comparison of Experimental and Predicted M_R/P_a for Evaluation Dataset from Rogers County: Polynomial Model

CHAPTER 6

ARTIFICIAL NEURAL NETWORK

6.1 Introduction

Artificial Neural Network (ANN) modeling is an alternative tool used in the present study (Carling, 1992). A commercially available software, STATISTICA 7.1, developed by the StatSoft, Inc., was used in the development of the ANN models. STATISTICA 7.1 has four ANN modeling options to solve regression problems, namely Linear Networks (LN), Generalized Regression Neural Networks (GRNN), Radial Basic Function Networks (RBFN), and Multi-Layer Perceptrons Networks (MLPN) (StatSoft, Inc., 2006). An overview of these ANN models, called "model type" in this chapter, is presented in the following sections. Similar to Chapter 5, this chapter presents the development of the ANN models. Moreover, a sensitivity study is conducted for each model parameter. A comparison of the models is presented in this chapter.

6.2 Artificial Neural Network Models

An Artificial Neural Network (ANN) is a tool that imitates the function of a biological neural network (Carling, 1992; Haykin, 1994; Hassoun, 1995; Patterson, 1996; Shanin et al., 2001; Hill and Lweicki, 2006). The architecture of ANN models contains a number of simple, highly interconnected processing elements. The STATISTICA 7.1, used in this study, utilizes the feedforward structure. In this architecture, signals move from inputs through hidden layers and eventually reach the output layer (Haykin, 1994; StatSoft, Inc., 2006). A feedforward structure is generally a simple network with stable behavior. Networks containing recurrent neurons may be unstable due to their complex dynamics and are of interest in neural network research

(Fausett, 1994; Haykin, 1994; Patterson, 1996; Steil, 1999; Wersing et al., 2001; StatSoft, Inc., 2006). The feedforward structures have proven useful in solving different types of problems (Tarefder et al., 2005; Park et al., 2006). In a feedforward network the neurons are arranged in distinct layers. The input layer introduces the values of the input variables, and the neurons in the hidden and the output layers have full connections to the preceding layer (Figure 2-4). Although it is possible to define networks with specific neurons connections, for most applications a fully connected network is desirable (StatSoft, Inc., 2006).

In the present application, the input layer consists of seven nodes, one node for each of the independent variables, namely moisture content (w), dry density (γ_d), plasticity index (PI), percent passing sieve No. 200 (P_{200}), unconfined compressive strength (U_c), deviatoric stress (σ_d), and bulk stress (θ). The output layer consists of one node for the dependent variable, which is the M_R. An overview of architecture of each type of ANN model used here is given in the following.

6.2.1 Linear Network (LN)

Linear Network (LN) has only two layers, an input layer and an output layer, but it does not have any hidden layers. A linear model is typically represented using an N×N matrix and a N×1 bias vector. "A neural network with no hidden layers, and an output with dot product synaptic function and identity activation function, actually implements a linear model. The weights correspond to the matrix, and the thresholds to the bias vector. When the network is executed, it effectively multiplies the input by the weight matrix then adds the bias vector." (Statsoft, Inc., 2006). Since the LN is the simplest ANN model available in STATISTICA 7.1, it is suggested that this network be created before trying other networks. This appears to be a logical step while using a hierarchical approach to ANN modeling.

6.2.2 General Regression Neural Network (GRNN)

The General Regression Neural Network (GRNN) is frequently used for estimating the probability density function (Speckt, 1991; Patterson, 1996; Bishop, 1995; Hill and Lweicki, 2006). "Gaussian Kernel functions are located at each training case. Each case can be regarded, in this case as evidence that the response surface is a given height at that point in input space, with progressively decaying evidence in the immediate vicinity. The GRNN copies that training cases into the network to be used to estimate the response on new points. The output is estimated using a weighted average of the output of the training cases, where the weighing is related to the distances of the point from the point being estimated (so that points nearby contributes most heavily to the estimate)" (Statsoft, Inc., 2006).

GRNN has four layers including the input layer, two hidden layers, and one output layer. The first hidden layer consists of the radial units. These radial units represent the clusters rather than each training case. The center of the clusters can be assigned using sub-sampling or Kohonen algorithm (Kohonen, 1989). The number of nodes in the first hidden layer can be as many as the number of cases. The second hidden layer consists of units that help estimate the weighted average. The second hidden layer always has exactly one more node than the output layer. Since only one output is considered in the present study (M_R), the second hidden layer has two nodes.

One of the advantages of the GRNN is that the output is probabilistic, allowing probabilistic interpretation of the output. Also, usually it is less time consuming to train this network. The disadvantage of the GRNN is that the network is large because of having two hidden layers and a large number of neurons or nodes in the first hidden layer. The large network makes the execution of the network slow, particularly for problems with a large dataset. Furthermore, this type of neural network does not extrapolate. Therefore, the predicted values stay within the range of the dataset.

6.2.3 Radial Basis Function Network (RBFN)

The radial basis function network (RBFN) uses an approach to divide the modeling space using hyperspheres. Their centers and radii characterize these hyperspheres. The RBFN units respond non-linearly to the distance of points from the center represented by a radial unit. The response surface of a single radial unit is the Gaussian (bell-shaped) function, peaked at the center, and descending outwards (Haykin, 1994; Bishop, 1995; TRB, 1999; Statsoft, Inc., 2006). Therefore, the RBFN has three layers, namely input, hidden, and output layers. The hidden layer consists of radial units. It models the Gaussian response surface. The two most common methods for assigning the center of the radial units are sub-sampling and K-Means algorithm (Bishop, 1995; Statsoft, Inc., 2006).

6.2.4 Multi-Layer Perceptrons Network (MLPN)

The multi-layer perceptrons network (MLPN) is one of the most popular network architectures in use today (Rumelhart and McClelland, 1986; Bishop, 1995; Narayan, 2002). The MLPN consists of an input layer, a number of hidden layers, and an output layer. In each of the hidden layers, the number of node can be varied. Due to the number of layers and the number of nodes in each layer, the MLPN can adjust the architecture of the network based on the complexity of a problem. In Statistica 7.1, the

MLPN has up to three hidden layers available. Each of the nodes in the network performs a biased weighted sum of their inputs and passes this activation level through a transfer function to produce its output. The weights and biases in the network are adjusted using a training algorithm. The training algorithms available in Statistica 7.1 are back propagation, conjugate gradient descent, quasi-Newton, and Levenberg-Marquardt (Statsoft, Inc., 2006).

6.3 Model Development

The general architectures of the ANN models were described in the previous section. In the present study, all the models have seven nodes in the input layer, one for each independent variable (w, γ_d, PI, P_{200}, U_c, σ_d, and θ), and one node for the output layer, dependent variable, M_R. The γ_d is normalized with the unit weight of water and U_c, σ_d, θ and the dependent variable M_R are expressed in a non-dimensional forms (U_c/P_a, σ_d/P_a, θ/P_a, and M_R/P_a), P_a being the atmospheric pressure. This non-dimensioning was done to ensure that all terms in the equations are non-dimensioned. The number of nodes in the hidden layers can be varied. A trial and error approach was used here in search of the optimum model. After the architectures of the models were set, the development dataset was fed into the models for training. To examine the strengths and weaknesses of the developed models, the predicted resilient modulus values were compared with the experimental values with respect to the R^2 values. The R^2 values indicated how well the ANN models fit the development dataset. Thus, a higher R^2 value was considered a better fit of the development dataset. Several researchers have used R^2 as an indicator of model performance (Tarefder et al., 2005; Rankine, and

Sivakugan, 2005; Park et. al., 2006). Other parameters such as mean square error have also been used (FHWA, 2002).

6.3.1 Linear Network (LN) Development

LN model was the first ANN network developed in this study. Since a LN model does not have any hidden layer, only one model was developed. The R^2 value for the linear network model was found to be 0.4323. Figure 6-1 shows a comparison of the experimental values and the predicted values of M_R/P_a. It is interesting to note that the R^2 for LN model is similar to the R^2 of the multiple regression model indicating that these two models are similar. Furthermore, it appears that the model back predicts the (M_R/P_a) better in the lower range of the dataset (up to 1,000). The differences between experimental and predicted M_R/P_a values beyond 1,000 increases with increasing M_R/P_a. A similar trend was observed in a study conducted by the Federal Highway Administration (FHWA, 2002). Figures 6-2, 6-3, and 6-4 present the back-prediction of the experimental M_R against the deviatoric stress for specimens MA-3B, NO-7A, and OS-1B, respectively. As noted previously, these specimens were selected since the M_R/P_a results from these specimens represents the range of the test results. Of these, specimens MA-3B exhibited relatively large differences (between measured and predicted M_R/P_a) in Figure 6-1, while specimen NO-7A exhibited much smaller differences. The third specimen (OS-1B) represents an intermediate case. Based on Figure 6-2, it may be observed that the LN model back predicts the M_R values well in the range of less than 100 MPa (i.e., M_R/P_a of about 1,000). From Figure 6-3, it is evident that the predicted M_R values follow the predicted M_R values fairly closely for the entire deviatoric stress range. This represents one of the best-case scenarios for this model. The back-prediction for the intermediate case is shown in Figure 6-4. It is seen that for both specimens MA-3B and NO-7A, the predicted M_R values are lower than the experimental values. For specimen OS-1B, however, an opposite trend is observed. Overall, the predicted M_R values for specimens NO-7A and OS-1B are within about 10 MPa.

6.3.2 General Regression Neural Network (GRNN) Development

As noted earlier, the GRNN model has two hidden layers. The optimum number of nodes in the first hidden layer was determined using a trial and error approach. The second hidden layer had two nodes for this study. From the trial and error approach, the best-fit GRNN model was found to have 1250 nodes in the first hidden layer. The R^2 value for the GRNN model was 0.6015, which was significantly better than the LN model (0.4323). This was expected due to the improved network architecture in the GRNN model (Bishop, 1995; Hill and Lweicki, 2006). To provide some specifics, a comparison of the experimental and the M_R/P_a values predicted by the GRNN model is presented in Figure 6-5. Overall, the prediction quality for this model is much better, having significantly less scatter, than the linear model (see Figure 6-1). The model fitted the M_R/P_a values well in the entire range of development dataset, although it appears that the entire dataset is clustered and rotated clockwise about the equality line at about 700 M_R/P_a. Figures 6-6, 6-7, and 6-8 present the back-prediction of the experimental M_R against the deviatoric stress for specimens MA-3B, NO-7A, and OS-1B, respectively; the same specimens that were used to examine the LN model. In case of specimen MB-3B, the back-predicted M_R values are within 80 MPa of the experimental values, in most cases. This is slightly better than the LN model, particularly considering that this is one of the worst-case scenarios. In case of specimen OS-1B both LN and GRNN models over estimated the experimental M_R values, particularly in high deviatoric stress range. Overall, the quality of back-predicted response for specimens NO-7A and OS-1B for both models is fairly comparable, with LN model doing a slightly better job.

The fact that the GRNN model treats data points as a cluster rather than individual training case, as noted in Section 6.2.2, is evident from a comparison of Figure 6-1 and Figure 6-5. In Figure 6-5, data points are much more densely clustered than in Figure 6-1. In addition to clustering, the orientation (with respect to the equality line) of the overall data seems to be different in the two models (see Figures 6-1 and 6-5). As a result, the back-predicted M_R values are lower than experimental values when M_R values are high (say over about 100 MPa). An opposite trend is observed for low M_R values.

6.3.3 Radial Basis Function Network (RBFN) Development

The RBFN model has one hidden layer. As in the case of the LN and GRNN models, a trial and error approach was used to determine the optimum number of nodes in the hidden layer. Following this approach, the optimum number of nodes in the hidden layer was found to be 100. The R^2 value of the RBFN model is 0.6284, which is slightly better than the GRNN model (0.6015) and much better than the LN model (0.4323). Figure 6-9 shows an overall comparison between experimental and predicted values of M_R/P_a for this model. This model appears to fit the overall dataset better than the LN and GRNN models. Figures 6-10, 6-11, and 6-12 present the back-prediction of the experimental M_R against the deviatoric stress for specimens MA-3B, NO-7A, and OS-1B, respectively. The results are much more encouraging for all three specimens than those of the LN and GRNN models. Also, unlike the LN and GRNN models, the RBFN model back-predicted the M_R values in both low and high range of M_R values. This improvement in back-prediction may be attributed to the use of hyperspheres in the RBFN model in the form of Gaussian (bell-shaped) function-type response surface (Haykin, 1994; Bishop, 1995; Bors, 2001; Yildirim and Ozyilmaz, 2002). GRNN is a special case of RBFN model. It uses the normalized version of the RBFN model. The same Gaussians (bell-shape) surface (Schioler and Hartmann, 1992; Monbet, 2004).

6.3.4 Multi-Layer Perceptrons Network (MLPN) Development

The number of hidden layers in the MLPN models can range from one to three. In the present study, three MLPN models henceforth referred to as MLPN-1, MPLN-2, and MLPN-3 models, were developed with different number of hidden layers in each model. The number of nodes in each of the three hidden layers was set at six nodes, based on the trial and error approach adopted. The R^2 values of the MLPN models were 0.5733, 0.5744, and 0.5587 for one, two and three hidden layers, respectively. These R^2 values indicate that all three MLPN models are expected to better correlate the M_R/P_a values than the LN model (0.4323). However, the MLPN models were worse than the GRNN (0.6015) and the RBFN (0.6284) models. Figures 6-13, 6-17, and 6-21 show comparisons between the experimental and predicted values of M_R/P_a values for each of the three MLPN models. Increasing of the number of hidden layers from one to two increased the R^2 slightly for the development dataset. But, increasing the hidden layers from two to three, causes the R^2 and the predictive capability of the model to decline. Overall, the results did not show any significant differences among the three MLPN models. Figures 6-14, 6-15, and 6-16 present the back-prediction of the experimental

M_R against the deviatoric stress for the MLPN-1 model for specimens MA-3B, NO-7A, and OS-1B, respectively. The corresponding comparisons for two and three hidden layers are shown in Figures 6-18 through 6-20 and in Figures 6-22 through 6-24, respectively. Based on these figures, the predictive capacity of the MLPN-2 model is better, in an overall sense, than the MLPN-1 or the MLPN-3 models for all three specimens. The MLPN-3 might have reached over-learning or over-fitting (Bishop, 1995). A network with three hidden layers involves more weights and more complex functions, leading to possible over-fitting of the development dataset (Bishop, 1995; Hill and Lweicki, 2006). Based on the R^2 values and the back-prediction (M_R vs. deviatoric stress) quality, the RBFN and the MLPN-2 models appear to be the two best ANN models. This statement, however, needs to be verified in light of the evaluation dataset, as will be done in Section 6.4.

6.3.5 Comments On Comparative Performance of the ANN Models

Table 6-1 presents a summary of the R^2 results for all the six models developed here (LN, GRNN, RBFN, MLPN-1, MLPN-2, and MLPN-3). The R^2 values ranged from 0.4323 to 0.6284, the LN model exhibiting the lowest R^2 value and the RBFN network model exhibiting the highest. Except for the LN model, the differences among the models, in terms of their R^2 values, were minor.

In general, better correlations are observed in the low range of the M_R/P_a values (say 1,000). With increased $M_R/P_{a,}$ values (beyond 1,000) the differences between the experimental and the predicted values increase. In the present study, a majority of the M_R/P_a values in the development dataset are in the lower range. Therefore, it is reasonable to expect that the ANN models would back-predict the experimental M_R/P_a

values more accurately in the lower range. In the process of lowering the overall error, the back-predicted values in the higher range of M_R/P_a values usually become less than the experimental values (i.e., under-prediction) and the back-prediction in the lower range increase (i.e., over-prediction). The most obvious example of the phenomenal is presented in Figure 6-5 where the entire development dataset is clustered and rotated clockwise. Similar observations were reported in the previous study conducted by the Federal Highway Administration (FHWA, 2002). The next step in the ANN study is to evaluate the developed models using a different set of data that were not used in the development phase (Bishop, 1995; Hill and Lweicki, 2006).

6.4 Evaluation of Models

Following the development of the ANN models, the evaluation dataset was introduced for evaluating the models. As noted before, the evaluation dataset were not included in the development dataset. Predictions of the M_R/P_a values were done using the developed models with the evaluation dataset. Then, a comparison of the predictions and the experimental M_R/Pa values was made for each model using the R^2 values as the basis of comparison (Tarefder et al., 2005; Rankine, and Sivakugan, 2005; Park et al., 2006). Three different comparisons were made: separate comparisons for soils from Woodward County and Rogers County, and a comparison for both the counties combined. This approach is similar to Chapter 5 where R^2 was used as a basis for comparison of prediction quality and the importance of datasets on statistical analysis, especially with respect to ANN modeling (Ripley, 1996; TRB, 1999; Myers et al., 2001; Montgomery et al., 2006).

6.4.1 Evaluation of LN Model

For the combined evaluation dataset, the LN model showed an R^2 value of 0.5503, which was higher than the R^2 (0.4323) for the development dataset. This is generally not expected (Runyon and Haber, 1976; Kachigan, 1986; Hays, 1988; Myers et al., 2001; Montgomery et al., 2006). One of the reasons for better prediction of the evaluation dataset could be the range of the M_R/P_a values (159 to 1,339), which corresponds to M_R values of about 16.1 MPa (2.3 ksi) to 135.7 MPa (19.7 ksi). As stated in the previous section, the ANN models appear to better suit for M_R/P_a for values lower than 1,000.

In order to further investigate the LN model, this model was used to separately predict the M_R/P_a values for soils from Woodward and Rogers counties. The R^2 value for the Woodward County soils was 0.8079, compared to 0.5443 for the Rogers County soils. Figures 6-25, 6-26, and 6-27 present a comparison of experimental and predicted M_R/Pa values for the evaluation dataset. Figure 6-28 is a plot of the M_R values against deviatoric stress for specimen WOE-4B (Woodward County). A similar plot for specimen ROE-20B (Rogers County) is shown in Figure 6-29. As noted in Table 3-3 in Chapter 3, the geology of the soils in Rogers County resembles the geology of the development dataset more closely than the soils from Woodward County. Furthermore, the analysis of development and evaluation dataset presented in Chapter 4 shows that the range of M_R values for the development dataset is from 20.7 MPa (3.0 ksi) to 979.9 MPa (142.1 ksi). Comparatively, the ranges of M_R values for Rogers and Woodward Counties are from 16.1 MPa (2.3 ksi) to 135.7 MPa (19.7 ksi) and from 34.7 MPa (5.0 ksi) to 107.6 MPa (15.6 ksi), respectively. Based on the range of M_R and the overall closeness of the Rogers County soils to the development dataset (see Chapter 4), the R^2 for Rogers County should have been higher than the Woodward County. However, the reverse is observed in the prediction analysis. The reason for this discrepancy could be attributed to the architecture of the LN model; other models (GRNN, RBFN, and MLPN) exhibited a different trend. In view of these observations, it was concluded that the LN model might not be an appropriate model for the prediction of M_R for the type of soils considered in this study.

6.4.2 Evaluation of GRNN Model

For the GRNN model, the overall prediction of M_R/P_a had a R^2 value of 0.4201 for the evaluation dataset (Table 6-1). There was a 43% difference between the R^2 for the evaluation dataset and the development dataset, indicating a problem with the model and the overall prediction. In the case of the Woodward County soils, the R^2 value decreased significantly (0.0515), while a much better R^2 (0.4791) was obtained for the Rogers County soils. Although the R^2 value of the Woodward County soils was very small, it did not have as much influence on the overall R^2 because of the fewer soils involved (five compared to 29 for Rogers County). In fact, in this case the R^2 value for the combined evaluation dataset appears misleading. This is because the prediction for the Woodward County soils (e.g., specimen WOE-4B, Figure 6-33) is expected to be much worse than the prediction for the Rogers County soils (e.g., ROE-20B, Figure 6-34), possibly due to the need for extrapolation. These figures indicate the possible problems in combining datasets or sites that are not comparable (Ripley, 1996).

It may, therefore, be concluded that the GRNN model developed here may not also be suitable for the overall dataset (development and evaluation combined), unless the model is retrained using the combined dataset (Statsoft, Inc., 2006).

6.4.3 Evaluation of RBFN Model

The RBFN model predicted the M_R/P_a values of the combined evaluation dataset with an R^2 value of 0.4938. Figures 6-35 through 6-37 compare the prediction quality of the RBFN model for the combined and individual evaluation datasets. The R^2 for the Rogers County soils is 0.5557, compared to 0.0251 for the Woodward County soils. These observations are similar to those for the GRNN model, as expected; the GRNN model is a special case of the RBFN model (Statsoft, Inc., 2006). Figures 6-38 and 6-39 show the predicted M_R values against the deviatoric stress for specimens WOE-4B (Woodward County) and ROE-20B (Rogers County), respectively. As expected, prediction for the Rogers County specimen is excellent, while that for the Woodward County shows significant differences.

6.4.4 Evaluation of MLPN Models

The R^2 values for the combined evaluation dataset for the MLPN-1, MLPN-2, and MLPN-3 models were found to be 0.5691, 0.5848 and 0.5500, respectively (Table 6-1). Although the R^2 values of the three models are similar, the MLPN-2 model shows the best prediction (see Figures 6-40, 6-41, and 6-42). As pointed out previously, the MLPN-3 involves more weights and more complex functions, leading to possible over-fitting (Bishop, 1995; Hill and Lweicki, 2006). Also, the MLPN-3 model predicts some negative M_R values in the low modulus range, making the usefulness of this model questionable for the current combined evaluation dataset. The R^2 values of the MLPN-1, MLPN-2, and MLPN-3 models for the Woodward County soils were found to be 0.1889, 0.6308, and 0.1795, respectively (see Figures 6-43, 6-44, 6-45). Comparatively, based on Figures 6-46, 6-47, and 6-48 the R^2 values of the MLPN-1, MLPN-2, and MLPN-3 models for the Rogers County soils were 0.6145, 0.6026, and 0.5899, respectively. A review of Table 6-1 indicates that based on the R^2 values, the MLPN-2 model appears to be the most accurate model for the present dataset.

Figures 6-49, 6-51, and 6-53 present the predicted M_R values against the deviatoric stress for specimen WOE-4B (Woodward County). A similar prediction for specimen ROE-20B (Rogers County) is presented in Figures 6-50, 6-52, and 6-54. As expected, the MLPN-2 model predicted the M_R values for the Rogers County soils very well. A troubling trend in Figures 6-49, 6-51, and 6-53 was the over prediction of the M_R values, with MLPN-2 model still exhibiting the best performance. In actual design cases this may lead to an under-designed pavement (Huang, 2003). This issue will be reviewed in Chapter 7 where the design of a typical pavement section is considered using the actual and the predicted M_R values, as an application.

6.5 Sensitivity Analysis

A sensitivity study was conducted on all the ANN models to evaluate the effect of each independent variable. In pursuing this sensitivity analysis, only one independent variable was changed at a time. First, the average and standard deviation of each independent variable were determined from the training and the evaluation datasets. The results of the mean and standard deviation of each independent variable are shown in Table 6-2. Then, M_R/Pa value was calculated by inputting the average values of each independent variable into the ANN models and this calculated value was called the "primary M_R/Pa value". A series of M_R/Pa values were then calculated by changing (within plus and minus of one standard deviation) one independent variable at a time, while the rest of the independent variables were kept at their mean values. The series of the M_R/Pa values thus obtained were compared with the primary M_R/Pa value.

6.5.1 Sensitivity Analysis For LN Model

The results (as percent difference) of the sensitivity analysis of the LN model are presented in Table 6-3. It is seen that unconfined compressive strength, deviatoric stress, dry density, and percent passing 0.075 mm (No. 200) sieve were more sensitive variables in the LN model. These four independent variables contributed to more than 10% differences in the comparison of M_R/Pa values. The unconfined compressive strength had the highest sensitivity followed by the deviatoric stress, dry density, and percent passing 0.075 mm (No. 200) sieve. The bulk stress contributed to less than 1% of difference for the dataset considered herein. Deviatoric stress, on the other hand, was found to be a much more significant variable, contributing to more than 12 percent difference in the prediction of M_R. As can be seen from the literature review in Chapter 2, some existing models only accounts for bulk stress, while disregarding deviatoric stress (See Table 2-3). Such models will be inappropriate to predict the resilient moduli of the soils considered here.

6.5.2 Sensitivity Analysis For GRNN Model

The results of the sensitivity analysis of GRNN model are presented in Table 6-4. Only deviatoric stress and unconfined compressive strength showed significant sensitivity in the GRNN model. These two independent variables had more than 10% differences in the comparison of M_R/Pa values. Dry density, moisture content, and plasticity index had only modest influence (6 ± 2 percent) on M_R. Percent passing 0.075 mm (No. 200) sieve and bulk stress had less than 1% difference in the comparison of M_R/Pa values. The rank of each independent variable considered here based on the sensitivity results is presented in Table 6-4. Once again, the unconfined compressive strength and deviatoric stress had the highest sensitivity and percent passing 0.075 mm (No. 200) sieve and bulk stress had the least sensitivity.

6.5.3 Sensitivity Analysis For RBFN Model

The results of the sensitivity analysis for the RBFN model are presented in Table 6-5. The results showed that six out of seven independent variables showed significant sensitivity in the RBFN model. The unconfined compressive strength had the highest sensitivity followed by dry density, moisture content, plasticity index, percent passing 0.075 mm (No. 200) sieve, and deviatoric stress. All these independent variables had more than 10% differences in the comparison of M_R/Pa values. The only independent variable that did not show significant sensitivity was bulk stress. Bulk stress exhibited less than 1% difference in the comparison of M_R/Pa values.

6.5.4 Sensitivity Analysis For MLPN Models

The results of the sensitivity analysis of MLPN-1, MLPN-2, and MLPN-3 models are presented in Table 6-6 through 6-8. Five independent variables showed significant sensitivity in the MLPN-1 model. The unconfined compressive strength had the highest sensitivity followed by dry density, deviatoric stress, plasticity index, and percent passing 0.075 mm (No. 200) sieve. All these independent variables had more than 10% of differences in the comparison of M_R/Pa values. Bulk stress and moisture content did not exhibit much sensitivity.

For the MLPN-2 model, four independent variables showed significant sensitivity (Table 6-7). The plasticity index had the highest sensitivity followed by unconfined compressive strength, deviatoric stress, and dry density. Once again, bulk stress showed the least significance in the sensitivity analysis. Moisture content and percent passing 0.075 mm (No. 200) sieve exhibited intermediate sensitivity (5% to 8%).

Finally, five independent variables showed significant sensitivity in the MLPN-3 model (Table 6-8). The unconfined compressive strength had the highest sensitivity, followed by dry density, plasticity index, deviatoric stress, and percent passing 0.075 mm (No. 200) sieve. Bulk stress and moisture content showed the least significance in the sensitivity analysis. The reason for the low effect of moisture content and bulk density may be that the influence of moisture content is over shadowed by other material parameters.

The overall sensitivity study showed that the sensitivity of independent variables was dependent on the type of ANN models. The sensitivity ranking of independent variables was different for each ANN model (Table 6-9). However, unconfined compressive strength and deviatoric stress consistently remained one of the most sensitive independent variables in all the ANN models developed here. The bulk stress, on the other hand, was always the least sensitive independent variable for the soils considered in this study. In a recent study, the bulk stress was found more significant for coarse grained soil, while the deviatoric stress was found more significant for fine grained soil (FHWA, 2002). Since a majority of soils used in this study was classified as fine-grained soil, the bulk stress did not show any recognizable significance in the sensitivity study.

6.6 Alternative MLPN-2 Models

Following the development and evaluation of models and selection of the MLPN-2 model, it was decided to evaluate the MLPN-2 model in more detail. This decision to evaluate this model further was based on the speculation that the effect of moisture content and density of samples might have been masked by the unconfined compression values. To that end, two new MLPN-2 models were developed based on the two sets of specimens used in the development dataset. These new models were called "dry" and "wet" models. As pointed out previously, the specimens were prepared at optimum moisture content (dry model) and two percent wet of optimum (wet model). Figures 6-55 and 6-56 present a comparison of the experimental and back predicted M_R values for the dry and wet models, respectively. The R^2 for these models and the predictions for the evaluation datasets are summarized in Table 6-2. The R^2 for the wet and dry models are 0.5491 and 0.5523, respectively. These values are slightly less than the R^2 value of 0.5744 for the MLPN-2 for the full development dataset. The R^2 values for the evaluation dataset are presented in Table 6-2. Based on these R^2 values, it is evident that the wet and dry models are capable of predicting their respective wet and dry evaluation datasets reasonably well but are not capable of predicting the opposite datasets (i.e., the wet model not predicting the dry dataset well, and vice versa). This is partly because the dry model predicting the wet dataset would require extrapolation. ANN models are generally not suitable for extrapolations (Haykin, 1994; Bishop, 1995; Hill and Lweicki, 2006. This is one of the shortcomings of these models. The sensitivity of the wet and dry models are presented in Table 6-11. Based on the results from this table, the effect of moisture content and density are no longer masked by the unconfined compression. However, as pointed out earlier, one of the primary objectives of this study was to develop a model that could be used to predict M_R for subgrade soils based on routine laboratory tests. It appears that this objective can be achieved by using both moisture content and density conditions (OMC and OMC+2). Based on these findings, it is recommended that a future study be undertaken to further explore this topic. Specimens capturing a full range of moisture content and density conditions may be included in that study.

6.7 Design Chart for Application of MLPN-2 Model

In order to implement the MLPN-2 model for design purposes, the predicted M_R/P_a against experimental chart was modified in to six zones (see Figure 6-57). Zones 3 and 4 are the two zones at either side of the equality line, limited by ± 0.25 deviation from the equality line. Zones 2 and 5 are bordered by the ± 0.25 and ± 0.50 deviation form the equality line and zones 1 and 6 are the areas with greater than ± 0.50 deviation from the equality line. These zones are further defined by the M_R/P_a values in the range of less than 500 M_R/P_a, greater than 500 and less than 1000 M_R/P_a, and finally greater than 1000 M_R/P_a. Based on these zones and the selected range of M_R/P_a values, Table 6-12 was developed. This table presents the percentage of occurrence of data in each zone. Using the MPLN-2 model a designer can predict the M_R/P_a for a certain soil, Figure 6-57 and Table 6-11 can then be used to either accept the predicted M_R/P_a or modify the prediction by increasing or decreasing the value, based on the designer judgment.

Table 6-1 Summary of the Artificial Neural Network (ANN) Modeling Results

Network Type	Network Architecture	Development Dataset		Evaluation Dataset					
				Combined		Woodward County		Rogers County	
		R^2	R	R^2	R	R^2	R	R^2	R
LN	7-1	0.4323	0.6575	0.5503	0.7418	0.8079	0.8988	0.5443	0.7378
GRNN	7-1250-2-1	0.6015	0.7755	0.4201	0.6482	0.0515	0.2268	0.4791	0.6922
RBFN	7-100-1	0.6284	0.7927	0.4938	0.7027	0.0251	0.1583	0.5557	0.7455
MLPN	7-6-1	0.5733	0.7571	0.5691	0.7544	0.1889	0.4346	0.6146	0.7840
MLPN	7-6-6-1	0.5744	0.7579	0.5848	0.7647	0.6308	0.7942	0.6026	0.7763
MLPN	7-6-6-6-1	0.5587	0.7474	0.5500	0.7416	0.1795	0.4237	0.5899	0.7680

Table 6-2 Summary of the Artificial Neural Network (ANN) Modeling Results For Separated Specimens Based on Moisture

Network Type	Network Architecture	Development Dataset		Evaluation Dataset					
				Combined		Woodward County		Rogers County	
		R^2	R	R^2 Wet	R^2 Dry	R^2 Wet	R^2 Dry	R^2 Wet	R^2 Dry
MLPN-2 (Wet)	7-6-6-1	0.5491	0.7410	0.5833	0.3121	0.6010	0.2512	0.6231	0.4032
MLPN-2 (Dry)	7-6-6-1	0.5523	0.7442	0.4092	0.5644	0.3305	0.7942	0.4360	0.5751

Table 6-3 Average and Standard Deviation of the Independent Variables from Development and Evaluation Datasets

Independent Variables	Average	Standard Deviation
Moisture Content (w)	0.1738	0.0303
Dry Density (γ_d) #	1.6572	0.1067
Plasticity Index (PI)	18.4	8.3
Percent Passing Sieve No. 200 (P_{200})	0.7854	0.1497
Unconfined Compressive Strength (U_c) *	2.025	0.6987
Deviatoric Stress (σ_d) *	0.4214	0.1294
Bulk Stress (θ) *	1.239	0.3586

Normalized by dividing γ_d to the density of water

* Normalized by dividing U_c, σ_d, and θ to the atmospheric pressure

Table 6-4 Sensitivity Study for the Linear Network (LN) Model

	M_R/Pa	Percent Different	Rank
Primary	0.6791	--	--
W + [#]	0.6644	-2.16	6
γ_d **+**	0.6048	-10.95	3
PI +	0.7245	6.69	5
P_{200}**+**	0.6102	-10.15	4
U_c **+**	0.8210	20.88	1
σ_d **+**	0.5952	-12.36	2
θ **+**	0.6814	0.34	7
w - [*]	0.6938	2.16	6
γ_d **-**	0.7535	10.95	3
PI-	0.6337	-6.69	5
P_{200}**-**	0.7481	10.15	4
U_c **-**	0.5373	-20.88	1
σ_d **-**	0.7630	12.36	2
θ **-**	0.6768	-0.34	7

[#] Independent variable plus one standard deviation

[*] Independent variable minus one standard deviation

Table 6-5 Sensitivity Study for the Generalized Regression Neural Network (GRNN) Model

	M_R/Pa	Percent Different	Rank
Primary	0.5897	--	--
w + [#]	0.5491	-6.88	3
γ_d +	0.5658	-4.05	5
PI+	0.6198	5.09	4
P_{200}+	0.5923	0.43	7
U_c +	0.6562	11.27	1
σ_d +	0.5410	-8.26	2
θ +	0.5928	0.51	6
w - [*]	0.6311	7.02	3
γ_d -	0.6228	5.61	4
PI-	0.5572	-5.52	5
P_{200}-	0.6103	3.48	6
U_c -	0.5428	-7.96	2
σ_d -	0.6711	13.79	1
θ -	0.5928	0.52	7

[#] Independent variable plus one standard deviation

[*] Independent variable minus one standard deviation

Table 6-6 Sensitivity Study for the Radial Basis Function Network (RBFN) Model

	M_R/Pa	Percent Different	Rank
Primary	0.6407	--	--
w + #	0.6530	1.91	6
DD+	0.5611	-12.43	4
PI+	0.7139	11.43	5
P_{200}+	0.5160	-19.47	2
U_c +	0.8044	25.54	1
σ_d +	0.5428	-15.29	3
θ +	0.6404	-0.05	7
w - *	0.8144	27.11	3
γ_d -	0.8225	28.37	2
PI-	0.4766	-25.62	4
P_{200}-	0.7216	12.62	6
U_c -	0.4540	-29.14	1
σ_d -	0.7596	18.56	5
θ -	0.6168	-3.73	7

Independent variable plus one standard deviation

* Independent variable minus one standard deviation

Table 6-7 Sensitivity Study for the Multilayer Perceptrons Network (MLPN-1) Model

	M_R/Pa	Percent Different	Rank
Primary	0.6343	--	--
w + [#]	0.5982	-5.68	6
γ_d **+**	0.5242	-17.34	3
PI+	0.7552	19.06	2
P_{200}**+**	0.5658	-10.79	5
U_c **+**	0.7811	23.15	1
σ_d **+**	0.5448	-14.11	4
θ **+**	0.6510	2.65	7
w - [*]	0.6715	5.87	6
γ_d **-**	0.7929	25.01	2
PI-	0.5289	-16.60	4
P_{200}**-**	0.7079	11.60	5
U_c **-**	0.4405	-30.55	1
σ_d **-**	0.7644	20.51	3
θ **-**	0.6178	-2.60	7

[#] Independent variable plus one standard deviation

[*] Independent variable minus one standard deviation

Table 6-8 Sensitivity Study for the Multilayer Perceptrons Network (MLPN-2) Model

	M_R/Pa	Percent Different	Rank
Primary	0.6415	--	--
w + [#]	0.6137	-3.23	5
γ_d +	0.6040	-4.77	4
PI+	0.7969	25.65	1
P_{200}+	0.6206	-2.15	6
U_c +	0.7650	20.62	2
σ_d +	0.5681	-10.43	3
θ +	0.6426	1.32	7
w - [*]	0.7006	10.47	6
γ_d -	0.7887	24.35	1
PI-	0.5568	-12.22	5
P_{200}-	0.7451	17.48	3
U_c -	0.4877	-23.10	2
σ_d -	0.7324	15.48	4
θ -	0.6516	2.74	7

[#] Independent variable plus one standard deviation

[*] Independent variable minus one standard deviation

Table 6-9 Sensitivity Study for the Multilayer Perceptrons Network (MLPN-3) Model

	M_R/P_a	Percent Different	Rank
Primary	0.6125	--	--
w + #	0.5965	-5.95	6
γ_d +	0.5492	-13.41	4
PI+	0.7339	15.72	2
P_{200}+	0.5418	-14.57	3
U_c +	0.7649	20.60	1
σ_d +	0.5607	-11.59	5
θ +	0.6161	-2.86	7
w - *	0.6032	-4.89	6
γ_d -	0.7428	17.12	2
PI-	0.5507	-13.17	3
P_{200}-	0.6866	8.25	5
U_c -	0.5004	-21.10	1
σ_d -	0.6991	10.23	4
θ -	0.6219	-1.95	7

Independent variable plus one standard deviation

* Independent variable minus one standard deviation

Table 6-10 Ranking of Independent Variables for ANN Models

Model \ Variables	w +	γ_d +	PI +	P_{200}+	U_c +	σ_d +	θ +	w -	γ_d -	PI -	P_{200}-	U_c -	σ_d -	θ -
LN	6	3	5	4	1	2	7	6	3	5	4	1	2	7
GRNN	3	5	4	7	1	2	6	3	4	5	6	2	1	7
RBFN	6	4	5	2	1	3	7	3	2	4	6	1	5	7
MLPN-1	6	3	2	5	1	4	7	6	2	4	5	1	3	7
MLPN-2	5	4	1	6	2	3	7	6	1	5	3	2	4	7
MLPN-3	6	4	2	3	1	5	7	6	2	3	5	1	4	7

Table 6-11 Ranking of Independent Variables for ANN Modeling Results for Separated Specimens Based on Moisture

Model \ Variables	w +	γ_d +	PI +	P_{200}+	U_c +	σ_d +	θ +	w -	γ_d -	PI -	P_{200}-	U_c -	σ_d -	θ -
MLPN-2 (Wet)	2	6	7	5	4	1	3	5	2	1	6	4	3	7
MLPN-2 (Dry)	3	6	7	5	4	1	2	3	2	1	6	5	4	7

Table 6-12 Percent Data Occurring in Each Zone Corresponding to the Range of M_R/P_a

	Zone 1	Zone 2	Zone 3	Zone 4	Zone 5	Zone 6
$M_R/P_a<500$	0.26	4.96	9.90	11.90	0.53	0.00
$500< M_R/P_a<1000$	0.99	2.31	22.88	27.38	4.49	0.13
$M_R/P_a>1000$	0.00	0.00	0.13	7.94	4.23	0.93

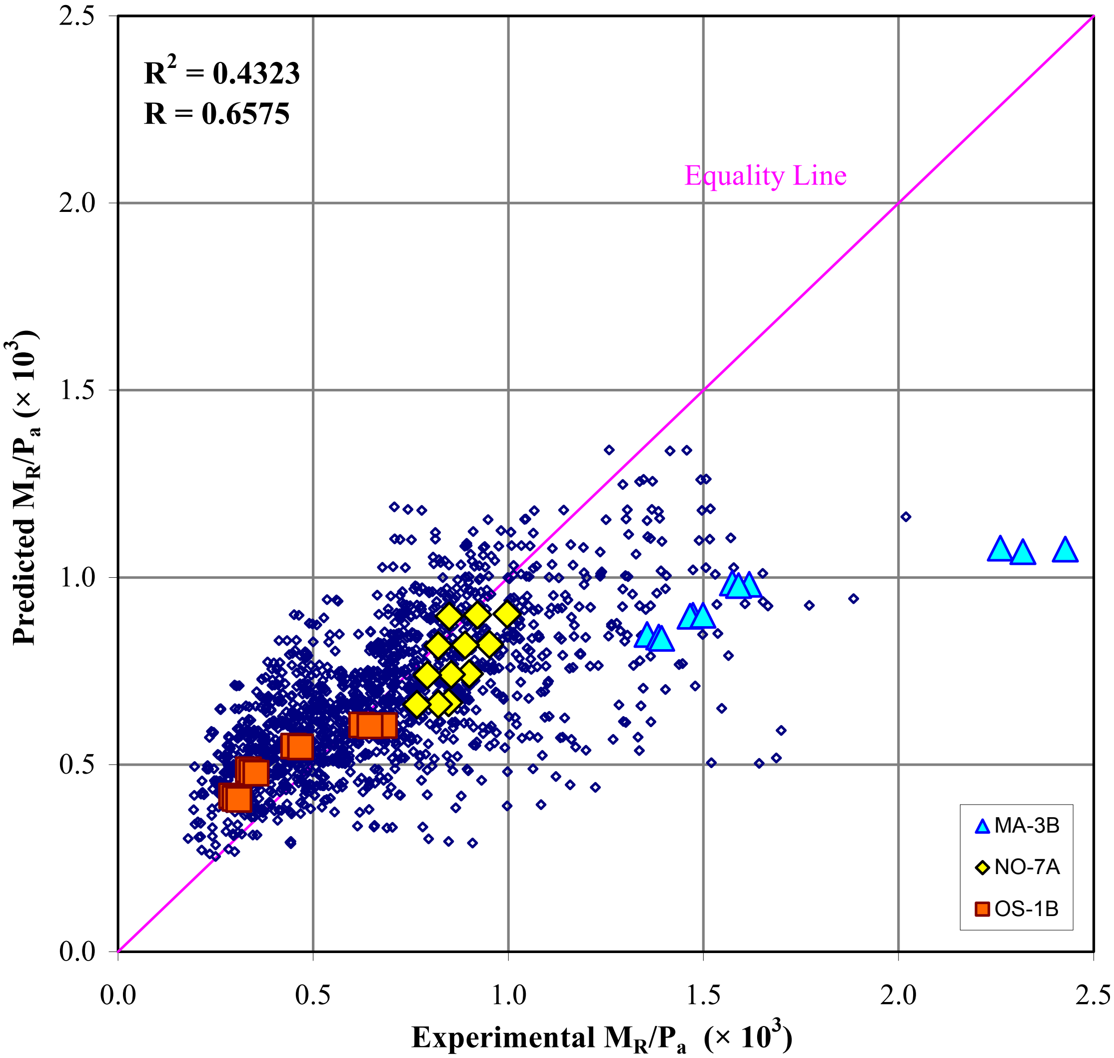

Figure 6-1 Comparison of Experimental and Predicted M_R/P_a for Development Dataset: Linear Network (LN) Model

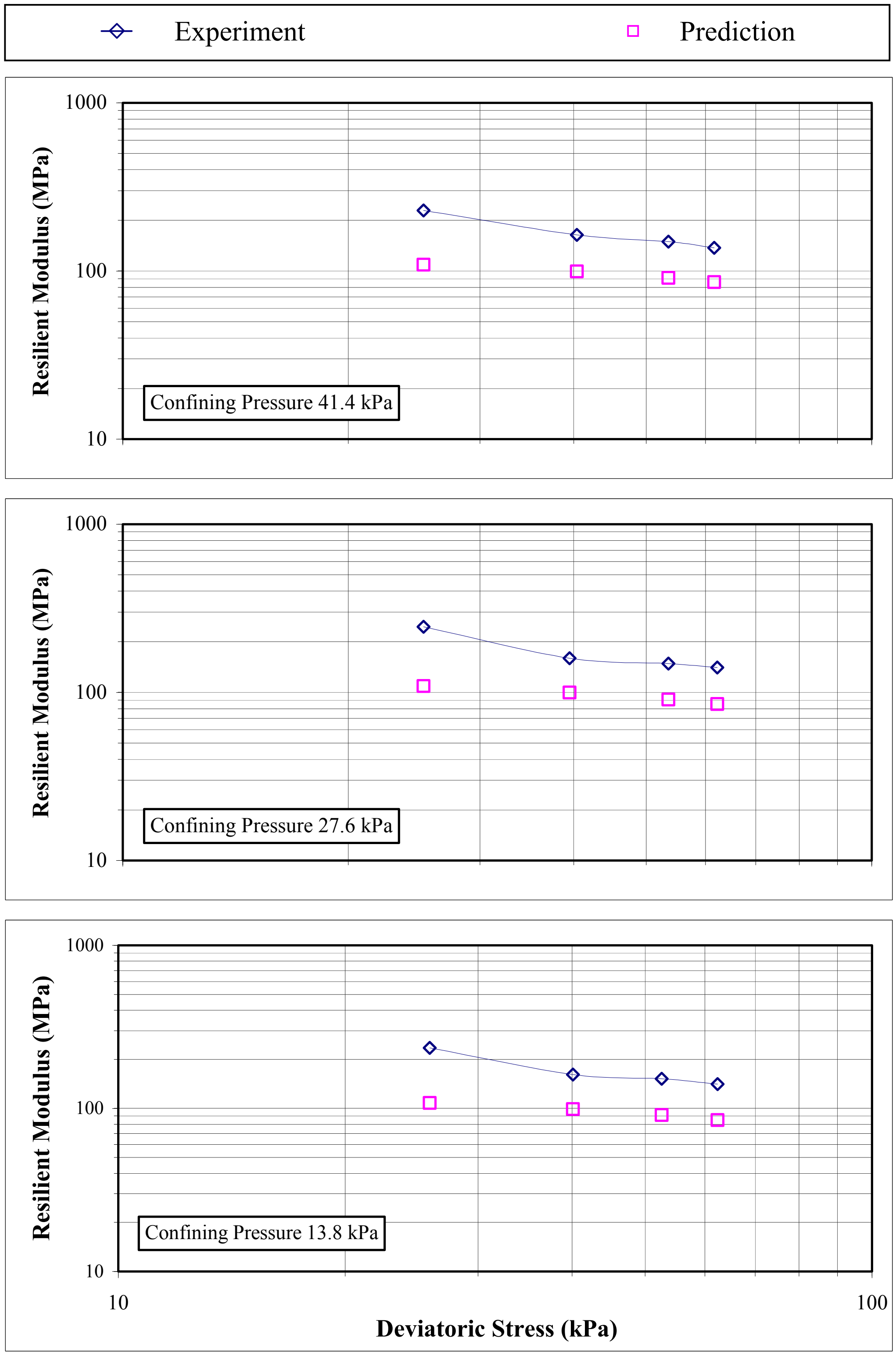

Figure 6-2 Resilient Modulus from Experiment and Linear Network (LN) Model: Specimen MA-3B

1 kPa = 0.145 psi

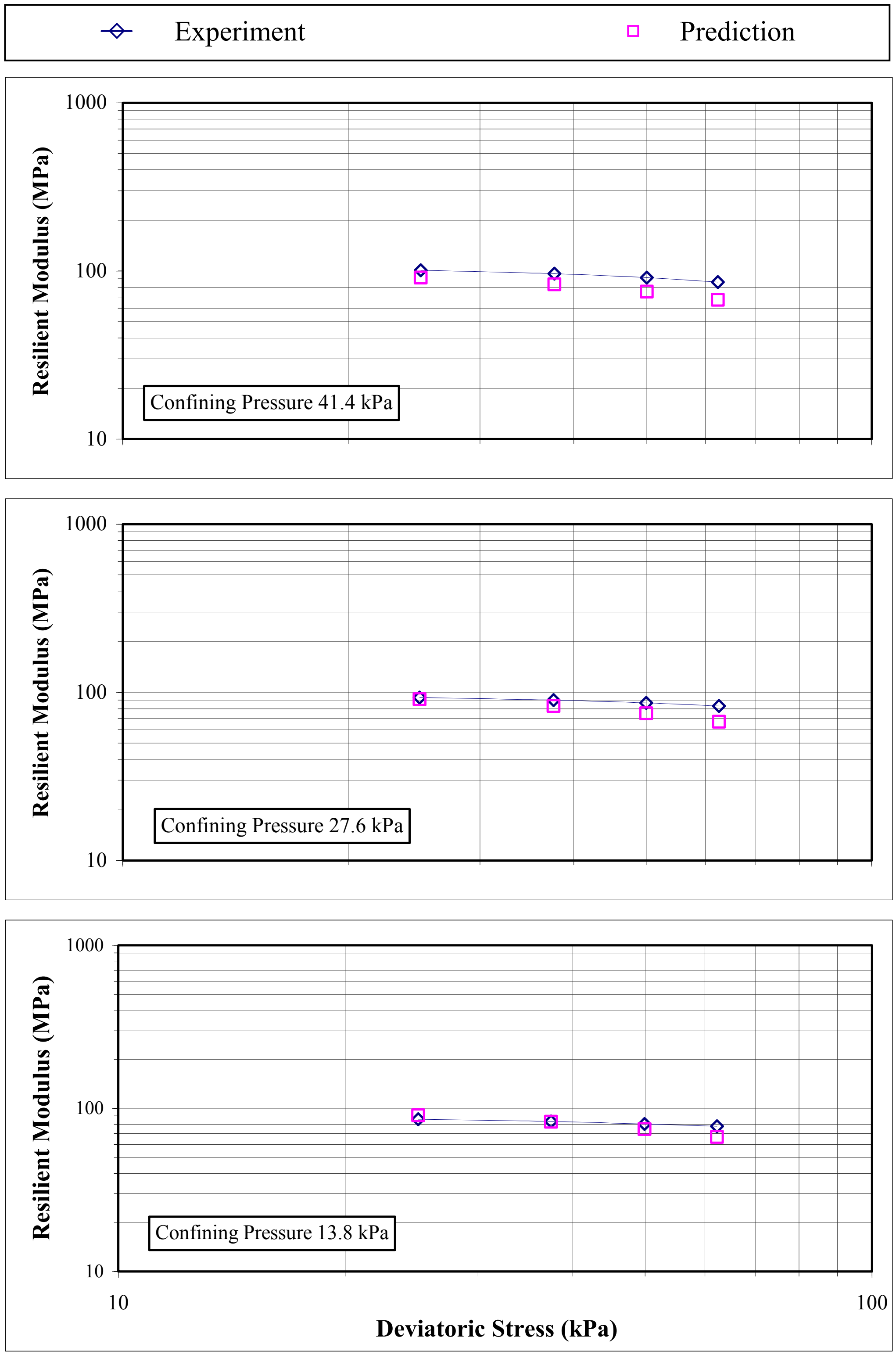

Figure 6-3 Resilient Modulus from Experiment and Linear Network (LN) Model: Specimen NO-7A

1 kPa = 0.145 psi

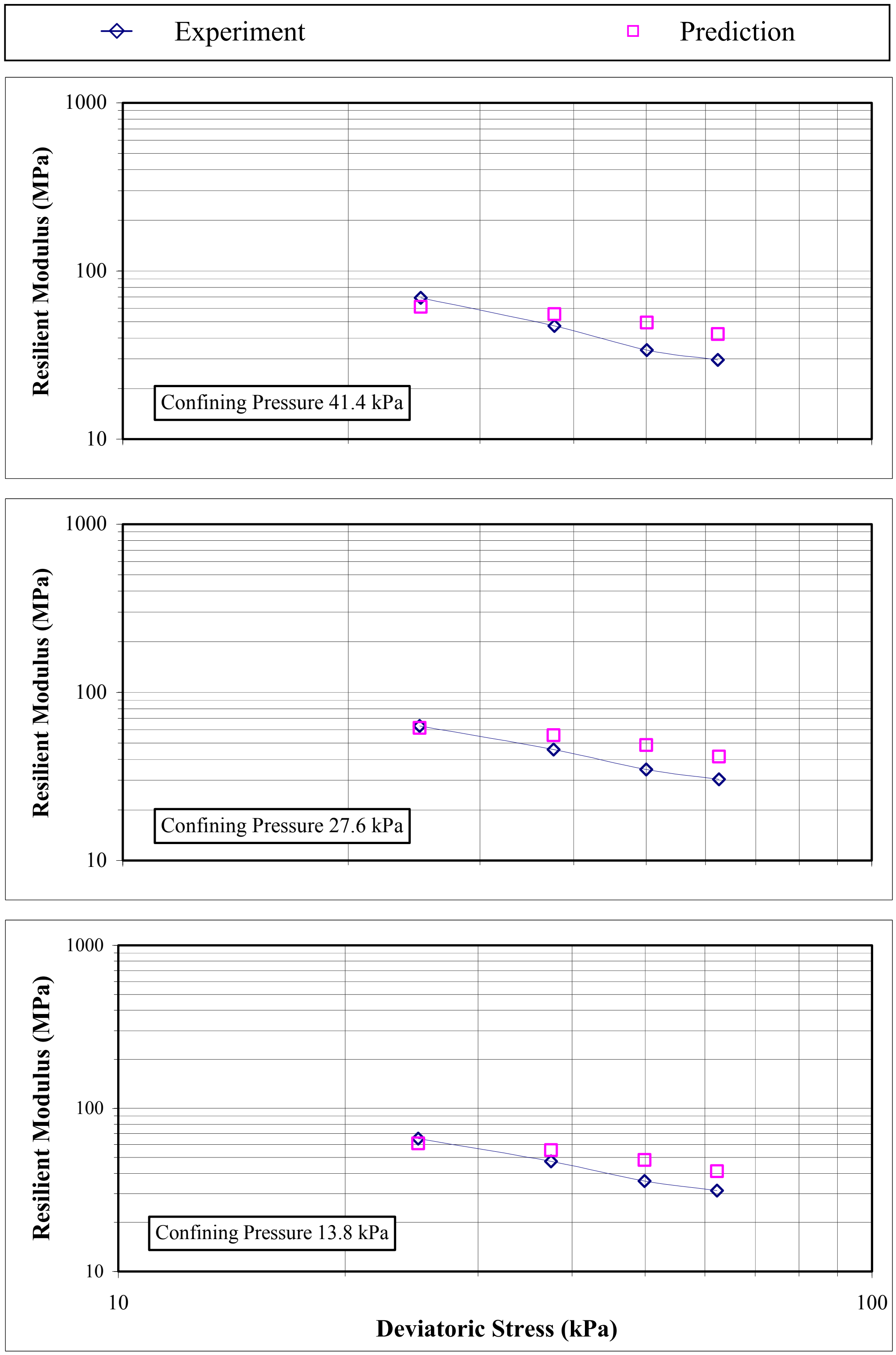

Figure 6-4 Resilient Modulus from Experiment and Linear Network (LN) Model: Specimen OS-1B

1 kPa = 0.145 psi

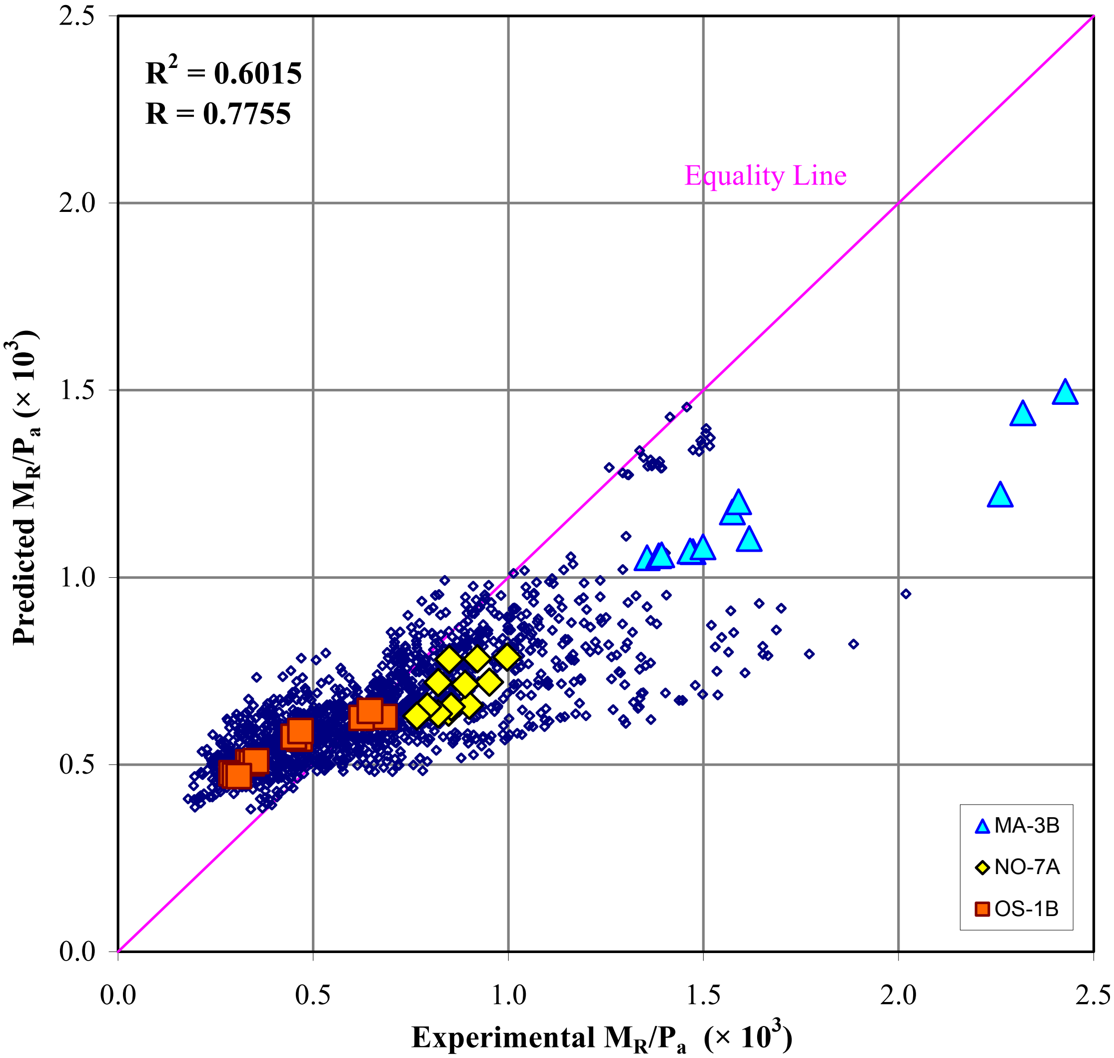

Figure 6-5 Comparison of Experimental and Predicted M_R/P_a for Development Dataset: Generalized Regression Neural Network (GRNN) Model

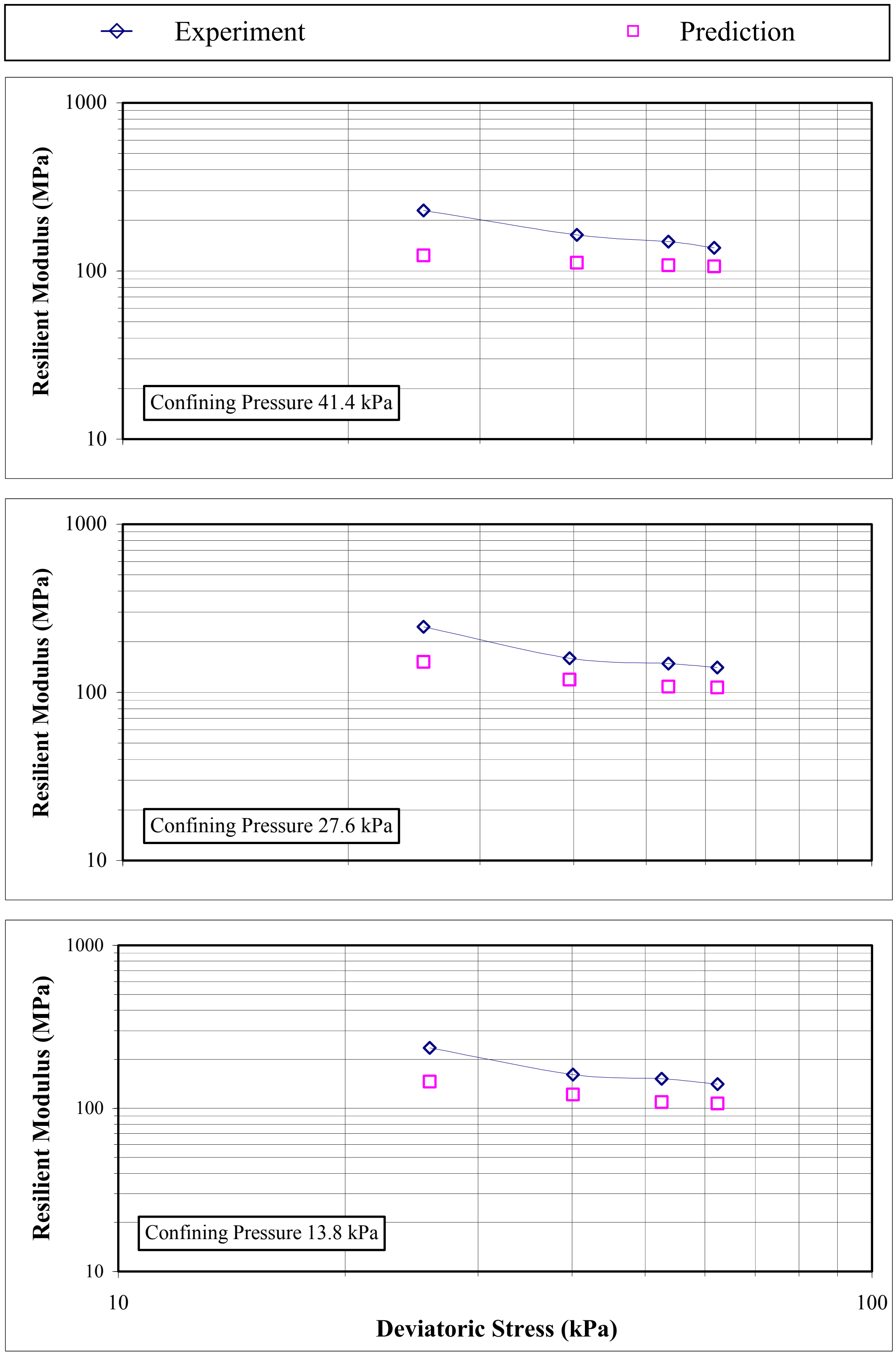

Figure 6-6 Resilient Modulus from Experiment and Generalized Regression Neural Network (GRNN) Model: Specimen MA-3B

1 kPa = 0.145 psi

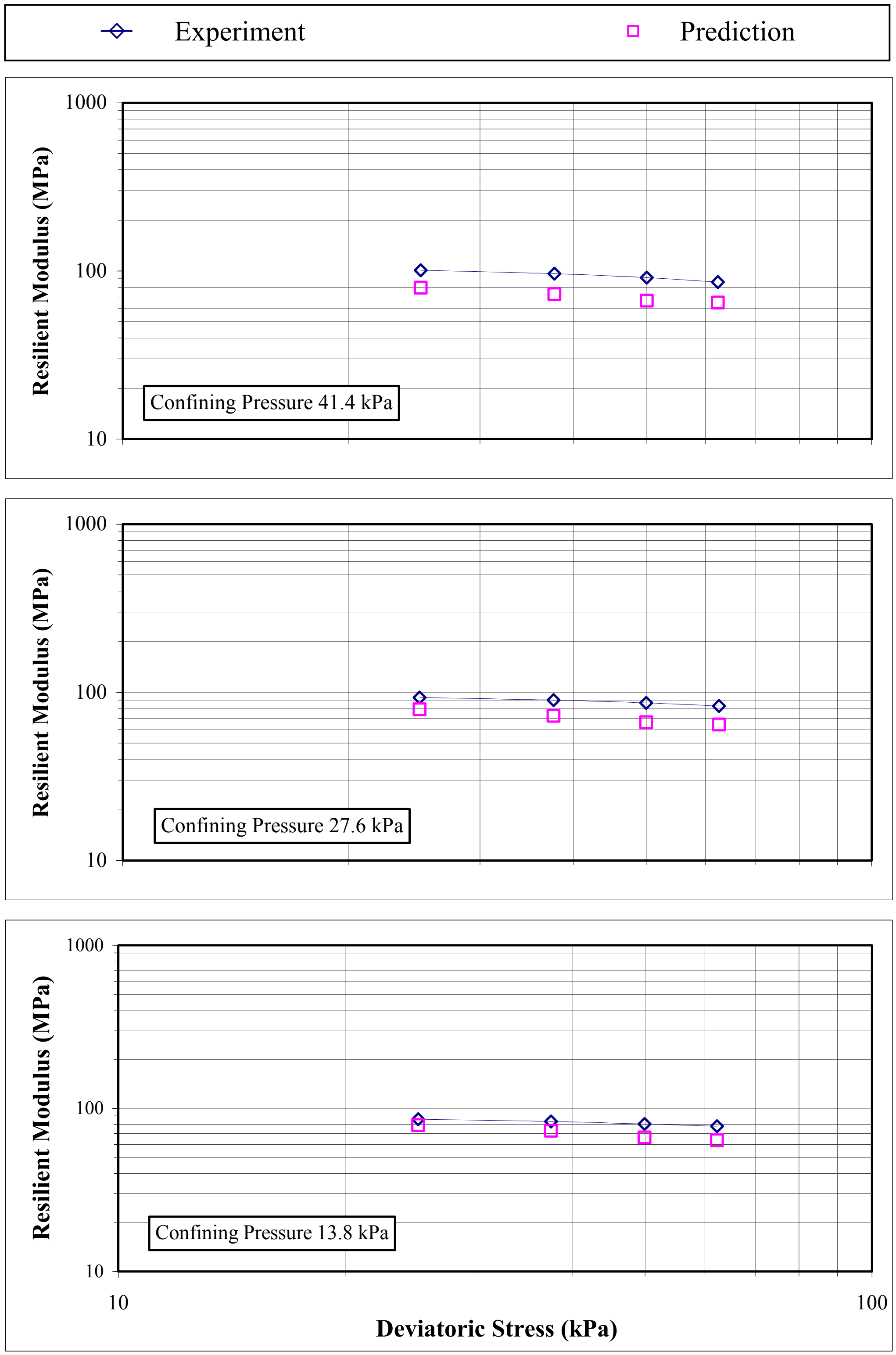

Figure 6-7 Resilient Modulus from Experiment and Generalized Regression Neural Network (GRNN) Model: Specimen NO-7A

1 kPa = 0.145 psi

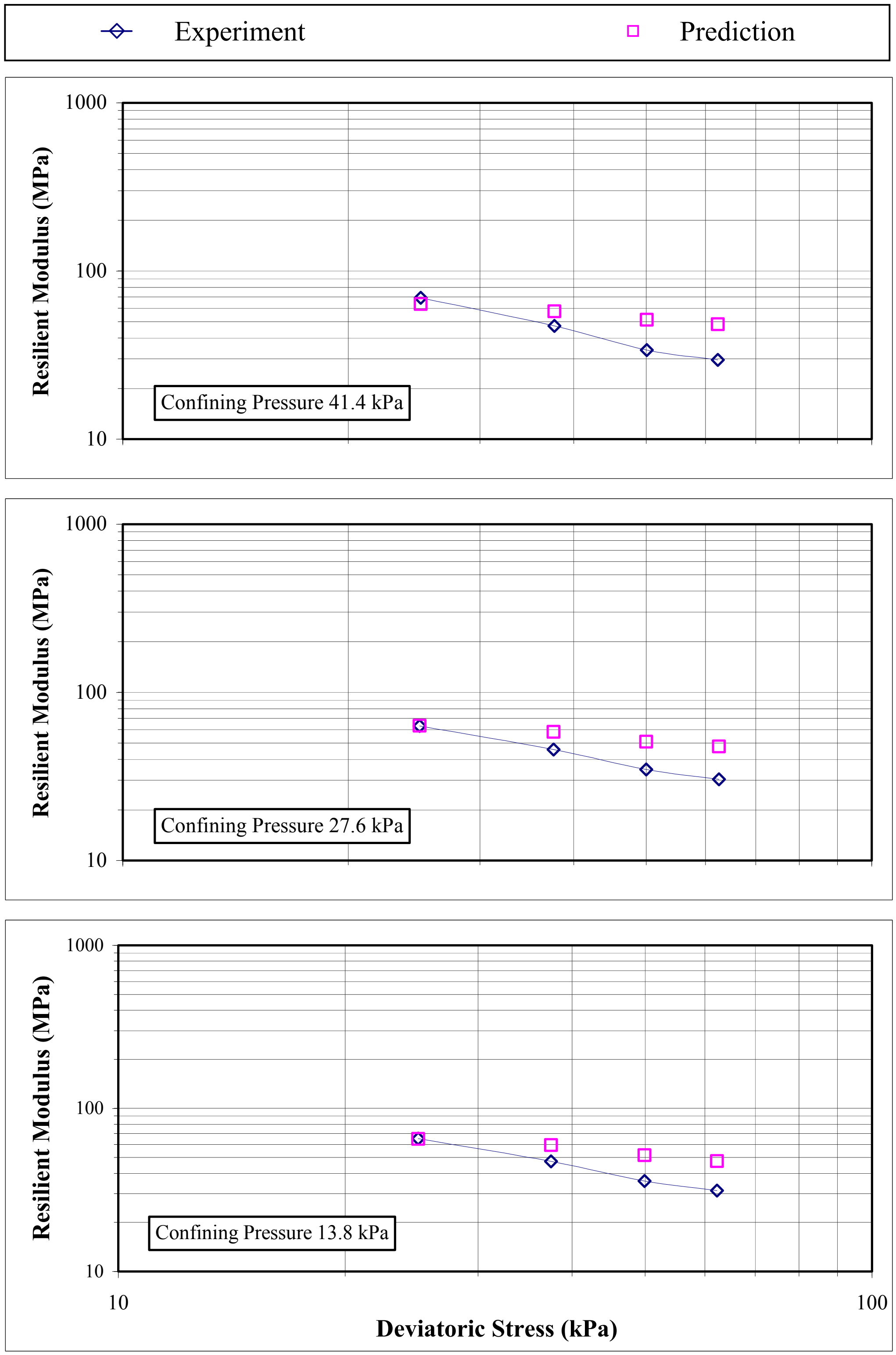

Figure 6-8 Resilient Modulus from Experiment and Generalized Regression Neural Network (GRNN) Model: Specimen OS-1B

1 kPa = 0.145 psi

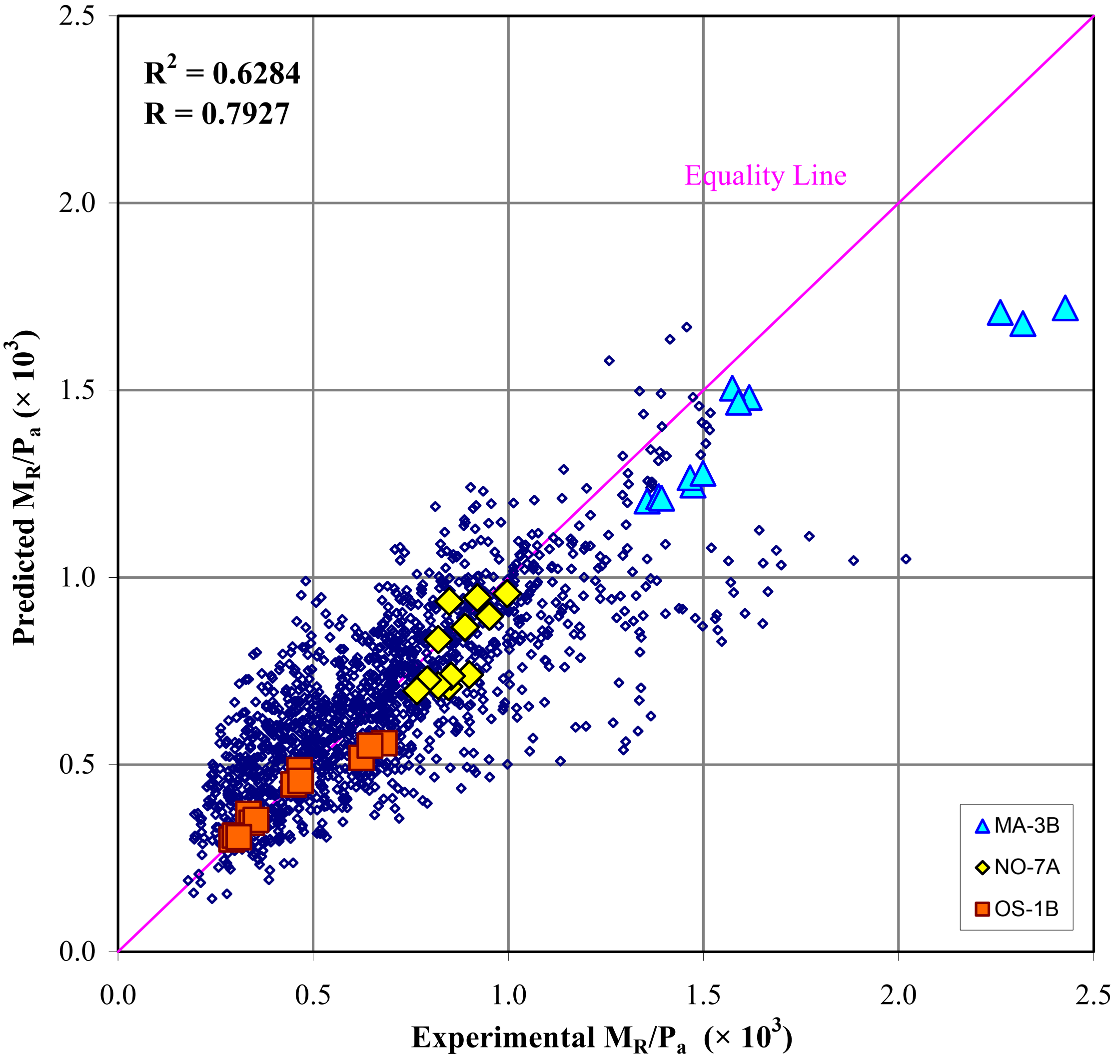

Figure 6-9 Comparison of Experimental and Predicted M_R/P_a for Development Dataset: Radial Basis Function Network (RBFN) Model

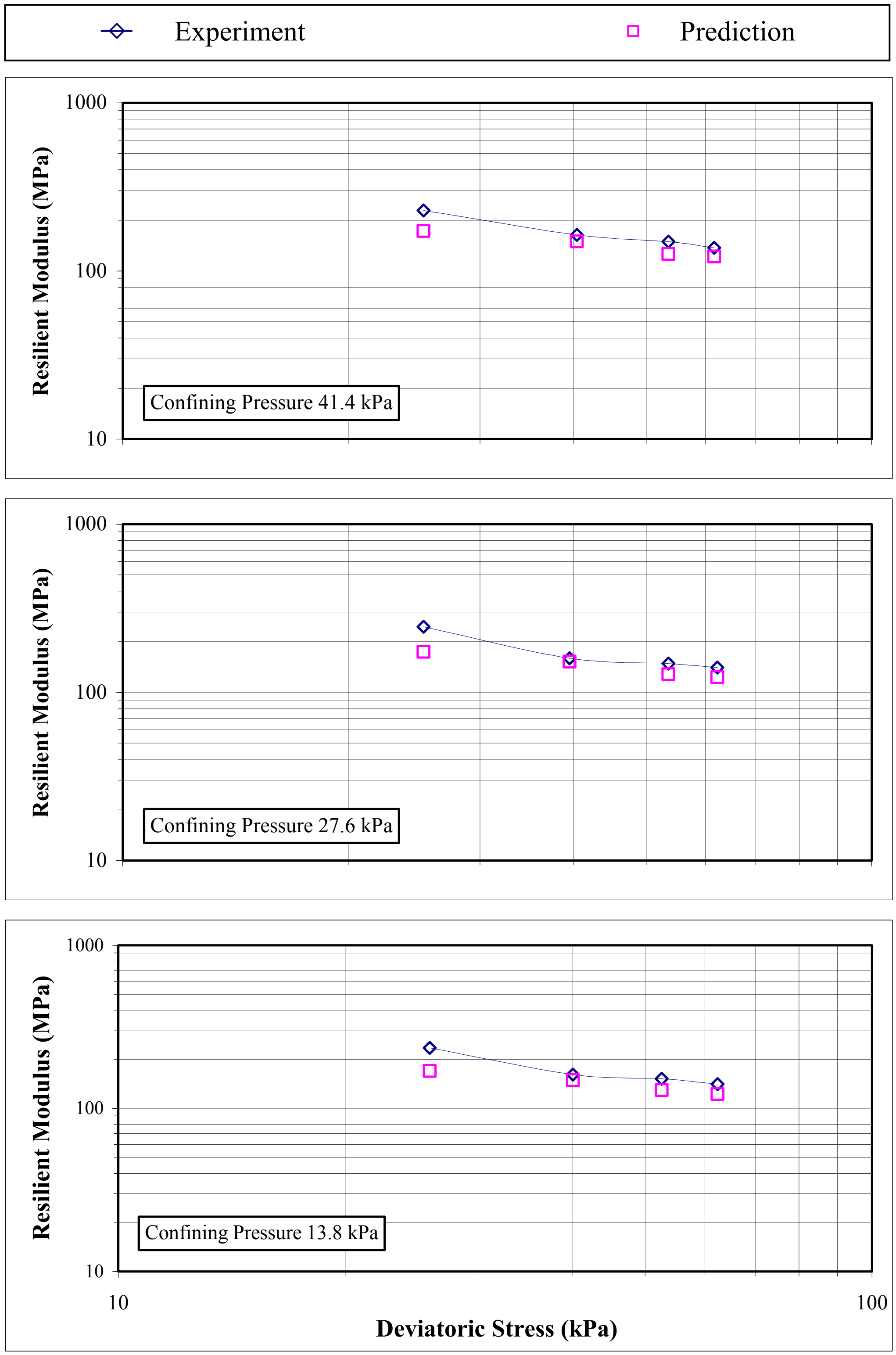

Figure 6-10 Resilient Modulus from Experiment and Radial Basis Function Network (RBFN) Model: Specimen MA-3B

1 kPa = 0.145 psi

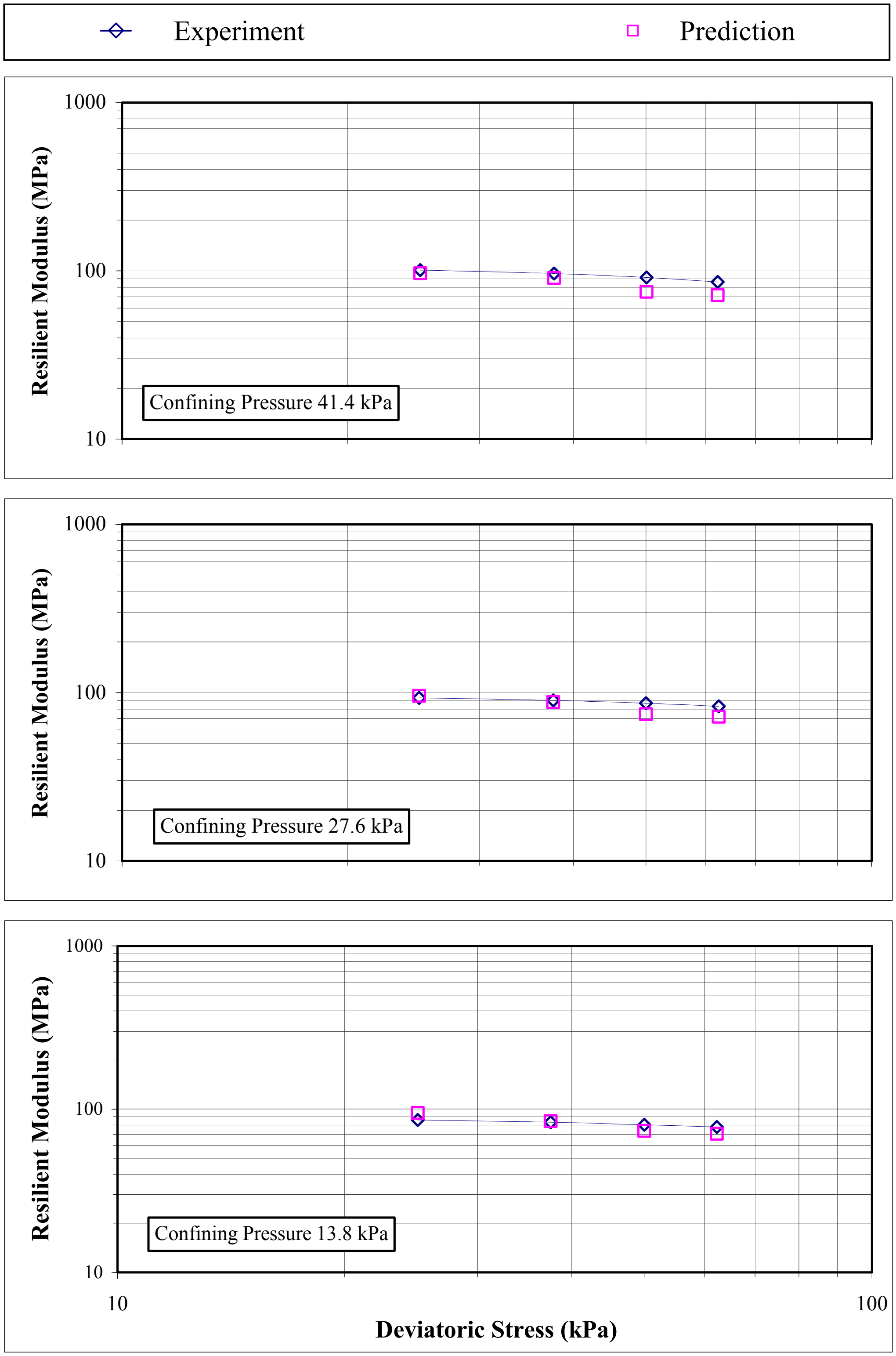

Figure 6-11 Resilient Modulus from Experiment and Radial Basis Function Network (RBFN) Model: Specimen NO-7A

1 kPa = 0.145 psi

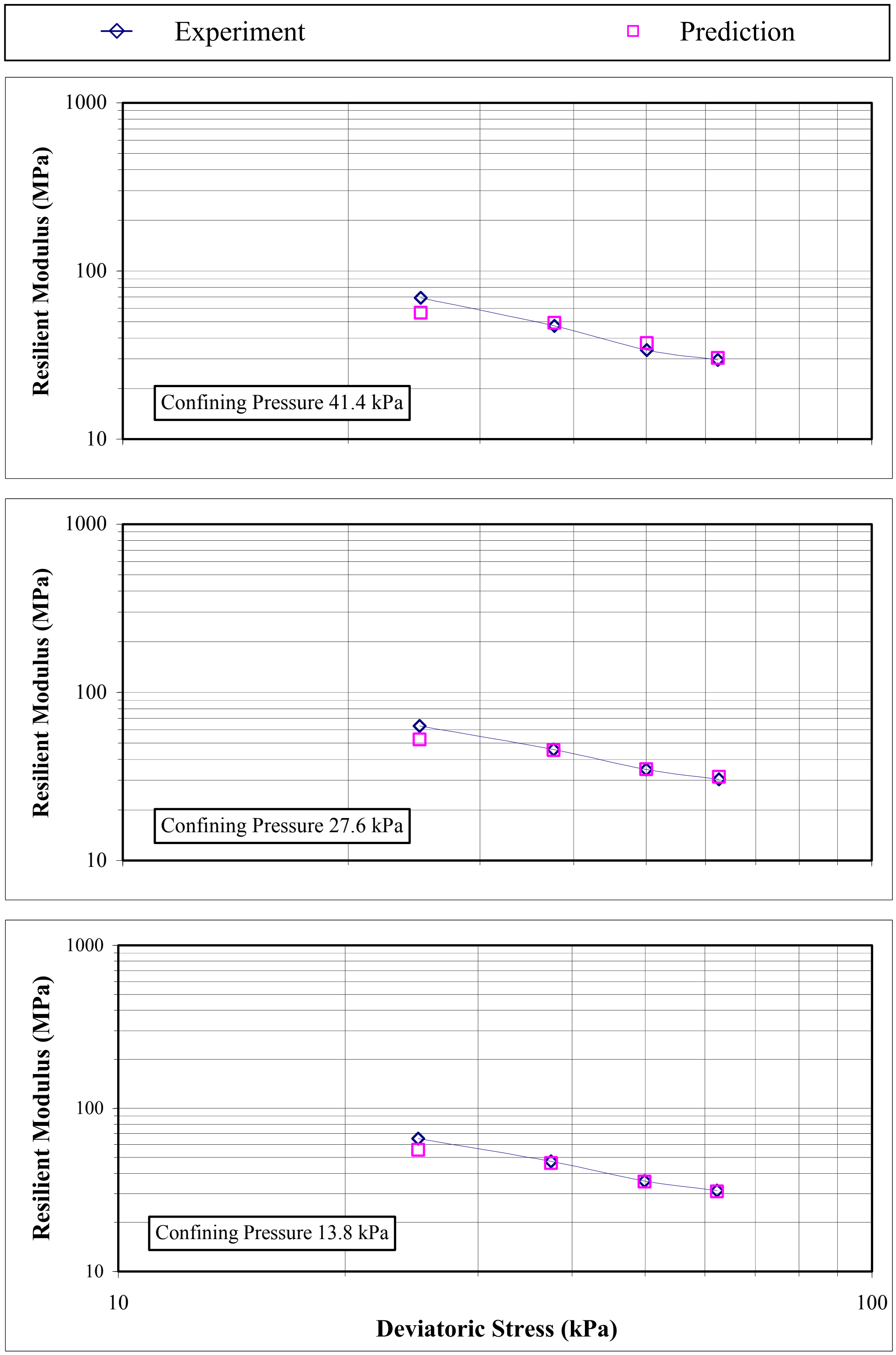

Figure 6-12 Resilient Modulus from Experiment and Radial Basis Function Network (RBFN) Model: Specimen OS-1B

1 kPa = 0.145 psi

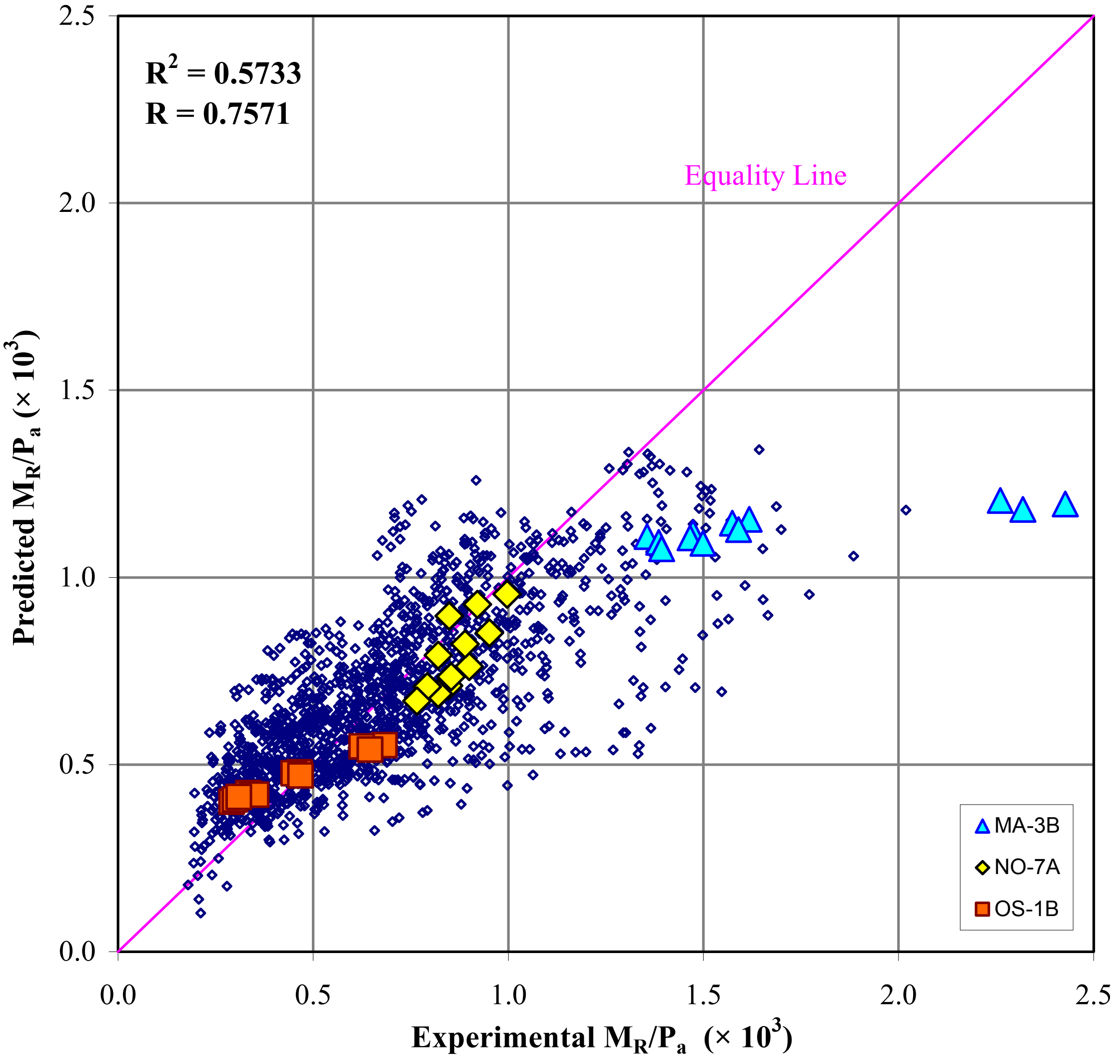

Figure 6-13 Comparison of Experimental and Predicted M_R/P_a for Development Dataset: Multilayer Perceptrons Network (MLPN-1) Model

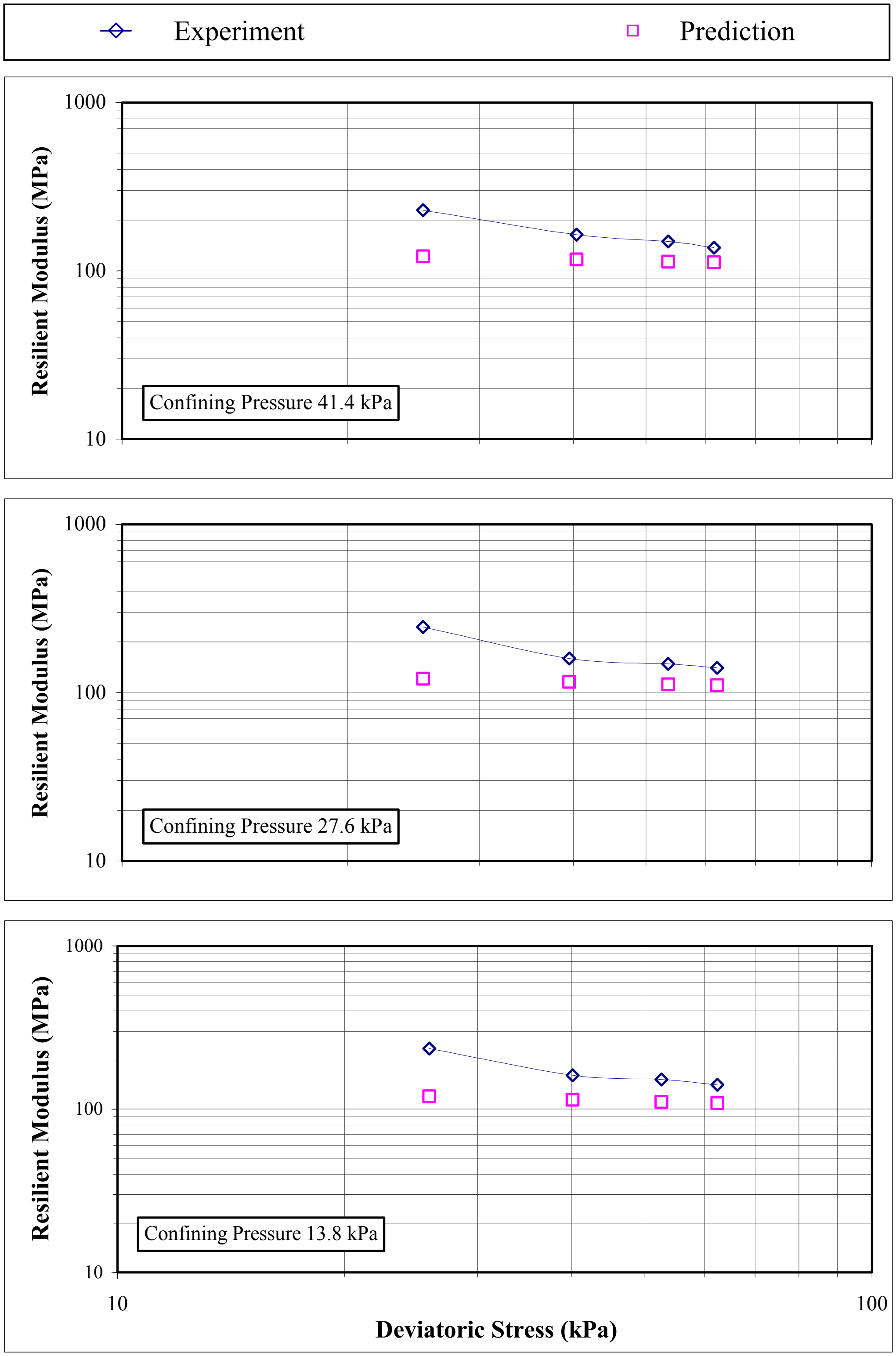

Figure 6-14 Resilient Modulus from Experiment and Multilayer Perceptrons Network (MLPN-1) Model: Specimen MA-3B

1 kPa = 0.145 psi

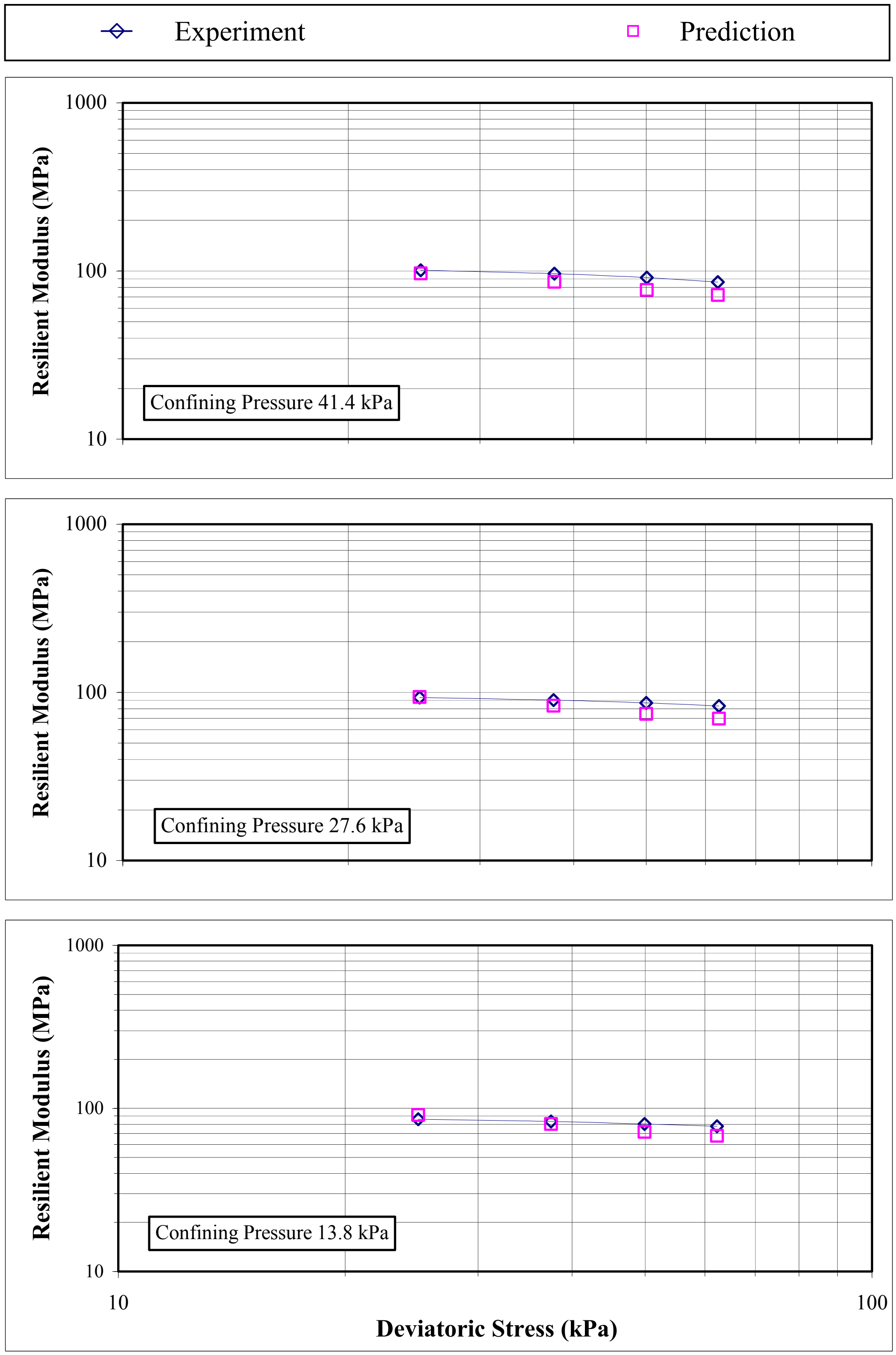

Figure 6-15 Resilient Modulus from Experiment and Multilayer Perceptrons Network (MLPN-1) Model: Specimen NO-7A

1 kPa = 0.145 psi

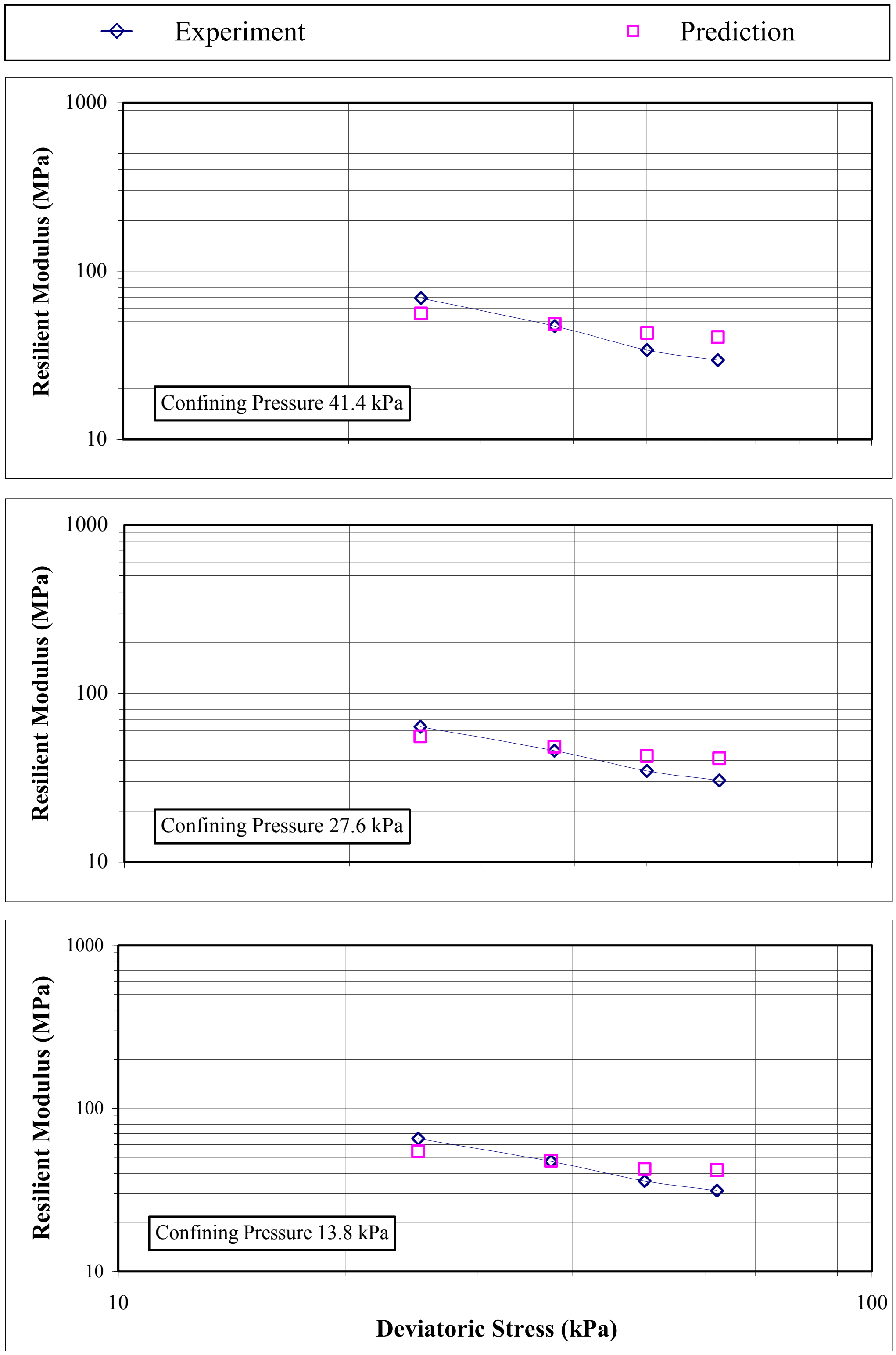

Figure 6-16 Resilient Modulus from Experiment and Multilayer Perceptrons Network (MLPN-1) Model: Specimen OS-1B

1 kPa = 0.145 psi

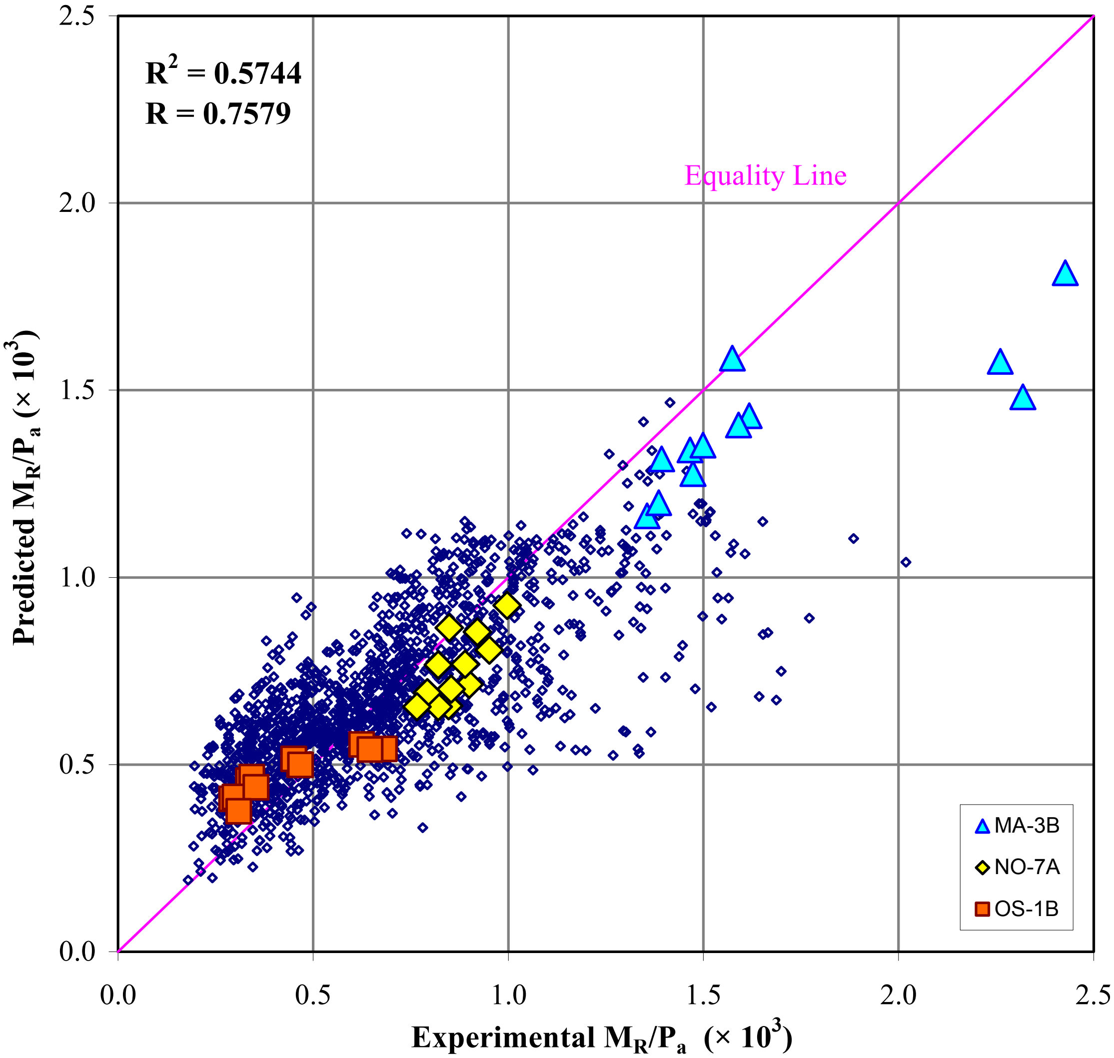

Figure 6-17 Comparison of Experimental and Predicted M_R/P_a for Development Dataset: Multilayer Perceptrons Network (MLPN-2) Model

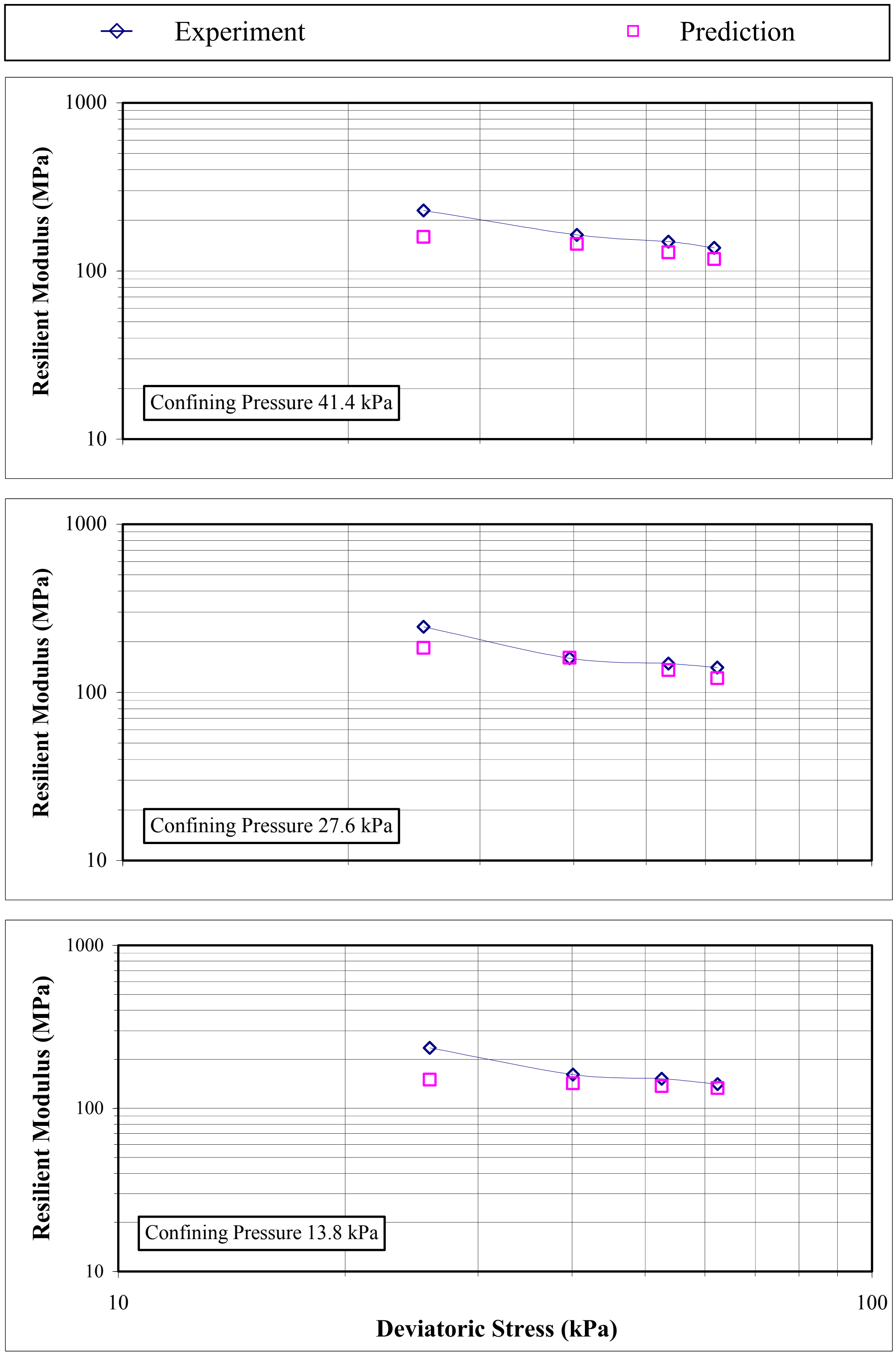

Figure 6-18 Resilient Modulus from Experiment and Multilayer Perceptrons Network (MLPN-2) Model: Specimen MA-3B

1 kPa = 0.145 psi

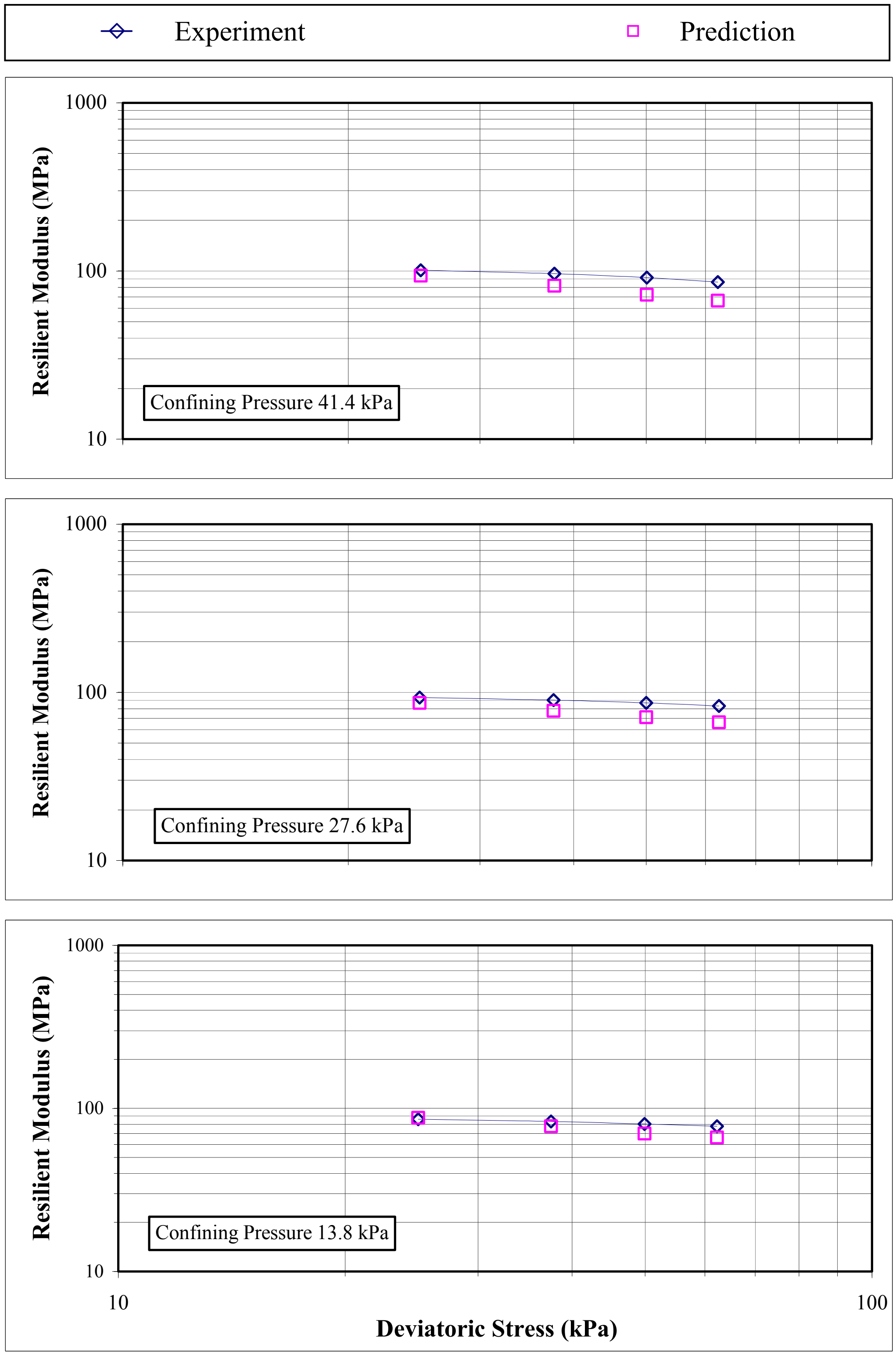

Figure 6-19 Resilient Modulus from Experiment and Multilayer Perceptrons Network (MLPN-2) Model: Specimen NO-7A

1 kPa = 0.145 psi

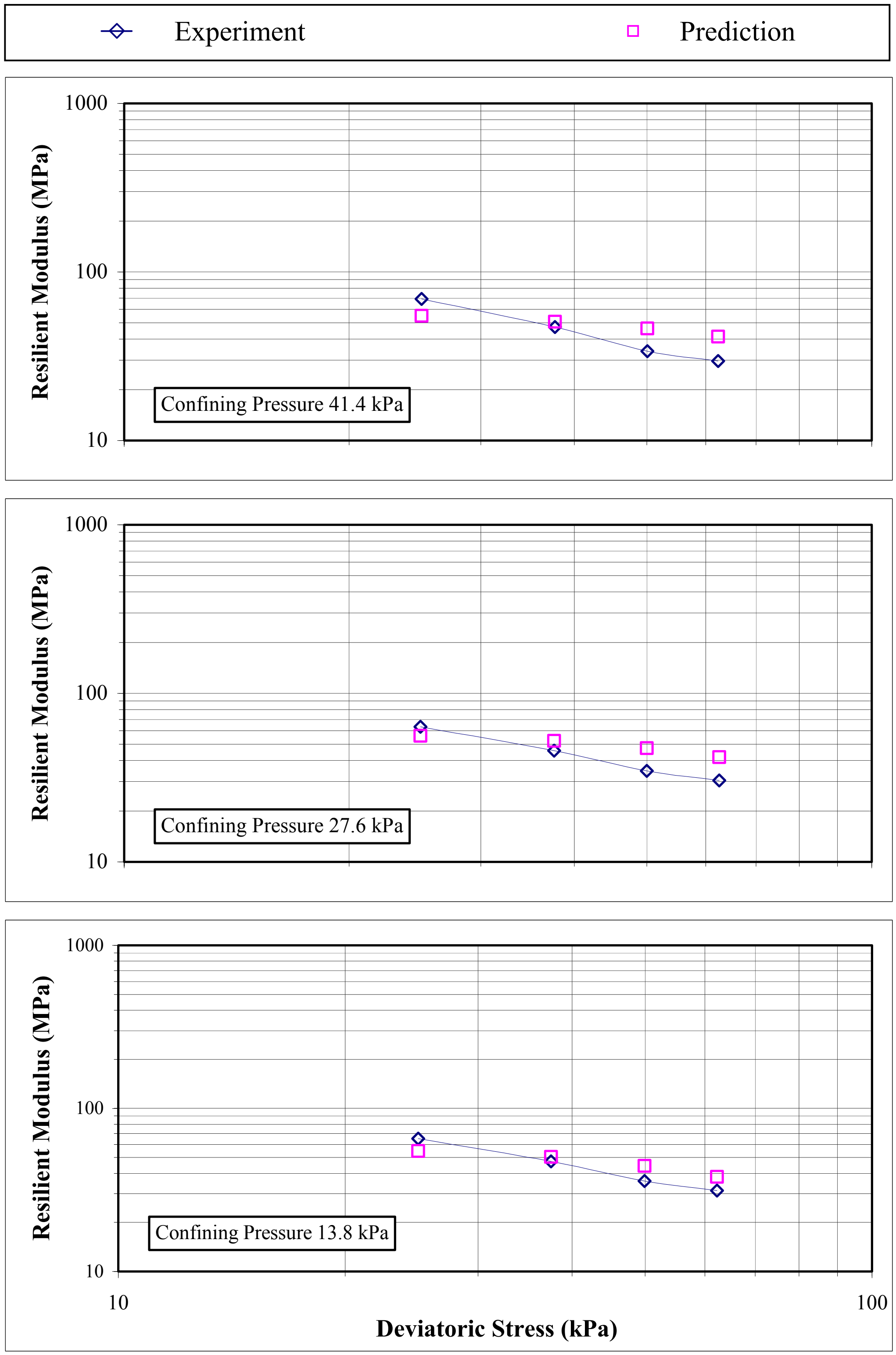

Figure 6-20 Resilient Modulus from Experiment and Multilayer Perceptrons Network (MLPN-2) Model: Specimen OS-1B

1 kPa = 0.145 psi

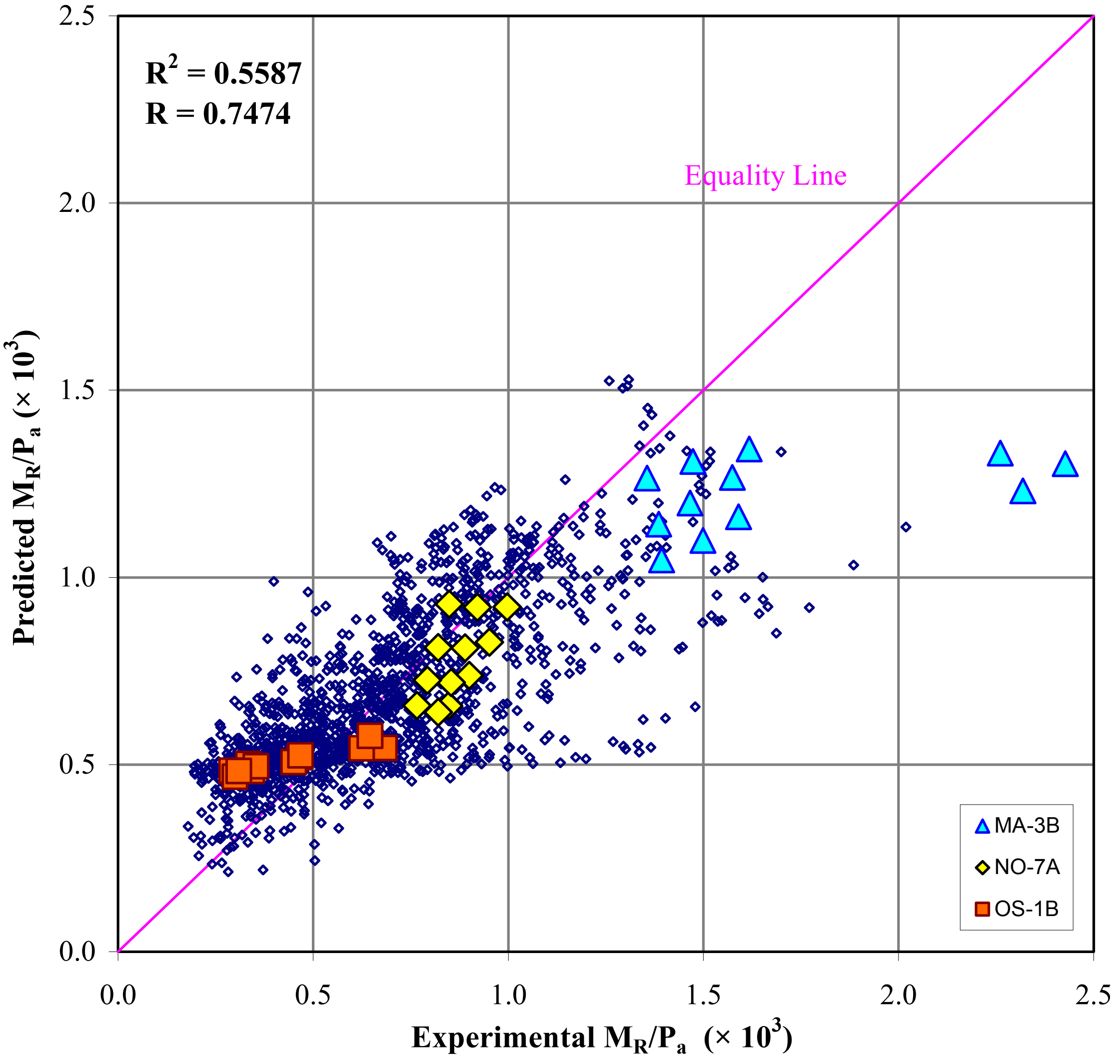

Figure 6-21 Comparison of Experimental and Predicted M_R/P_a for Development Dataset: Multilayer Perceptrons Network (MLPN-3) Model

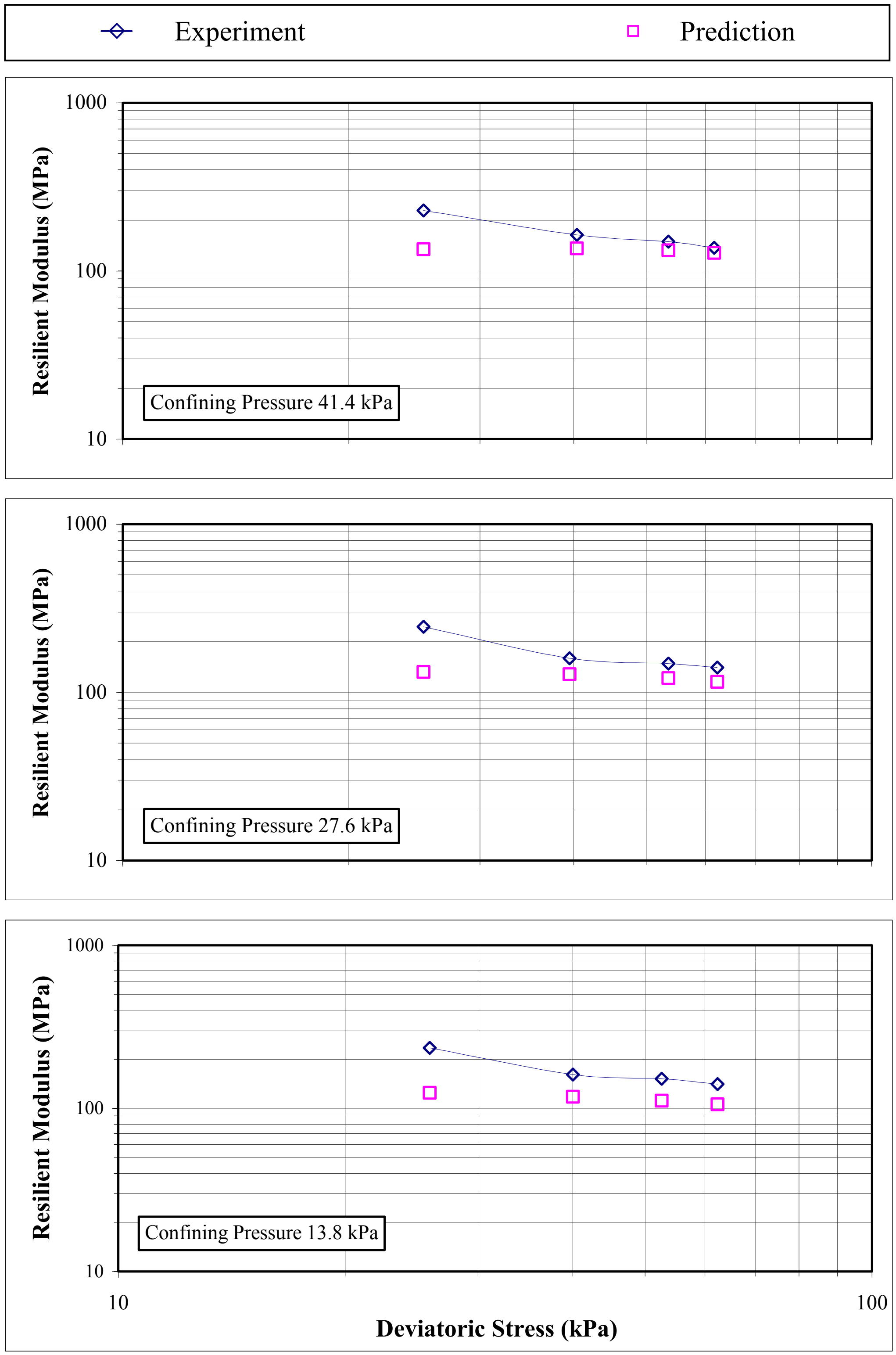

Figure 6-22 Resilient Modulus from Experiment and Multilayer Perceptrons Network (MLPN-3) Model: Specimen MA-3B

1 kPa = 0.145 psi

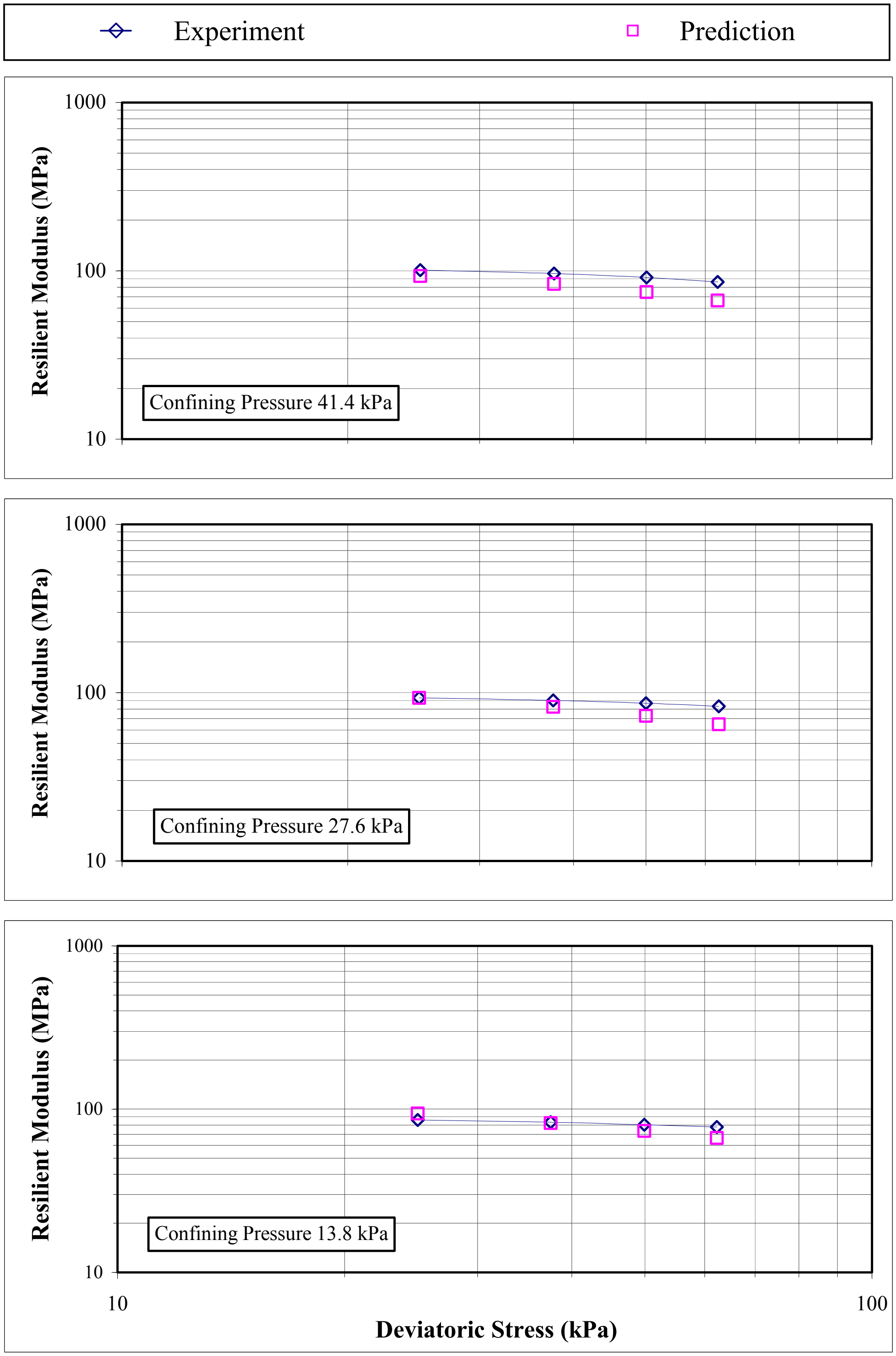

Figure 6-23 Resilient Modulus from Experiment and Multilayer Perceptrons Network (MLPN-3) Model: Specimen NO-7A

1 kPa = 0.145 psi

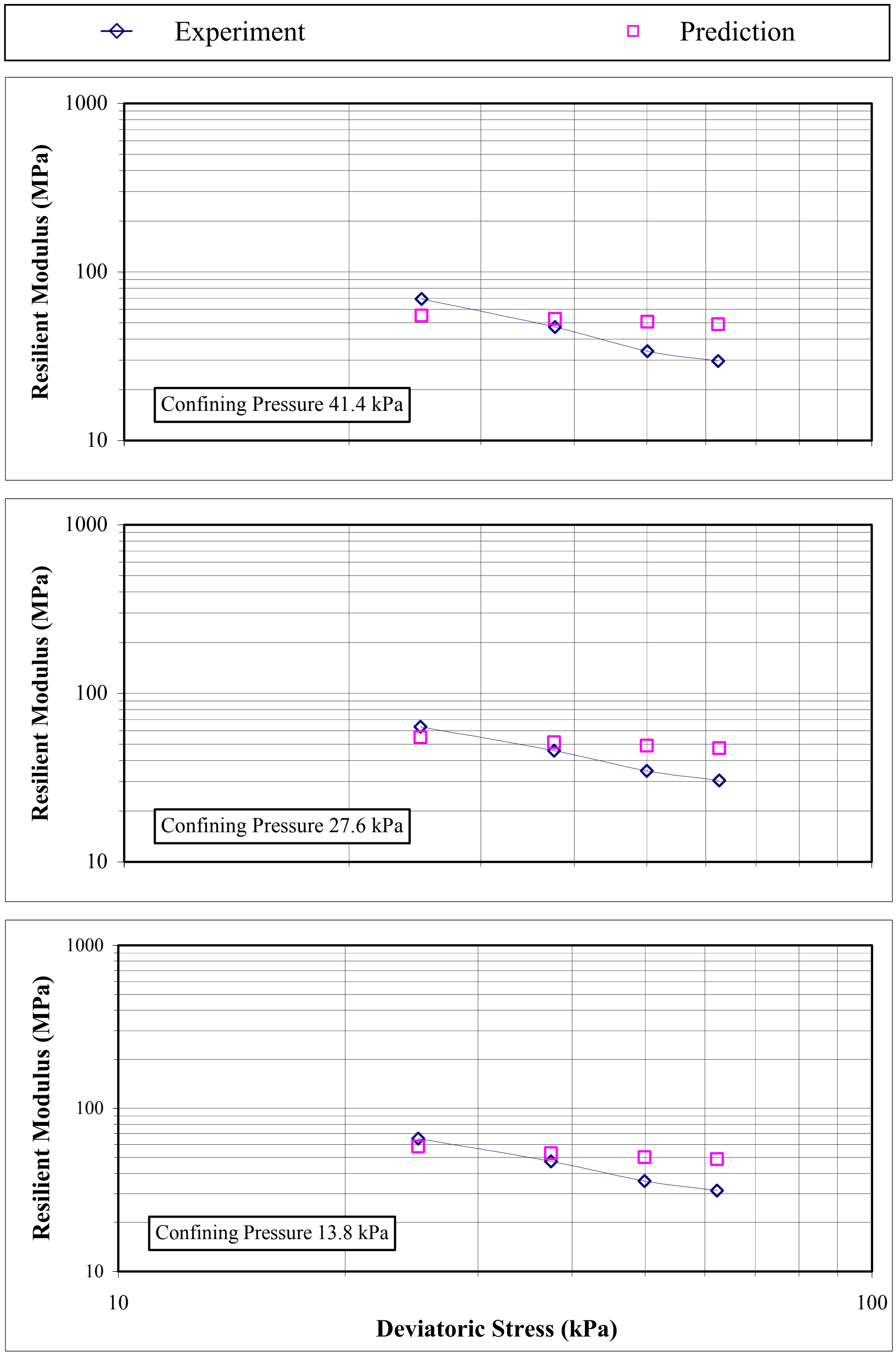

Figure 6-24 Resilient Modulus from Experiment and Multilayer Perceptrons Network (MLPN-3) Model: Specimen OS-1B

1 kPa = 0.145 psi

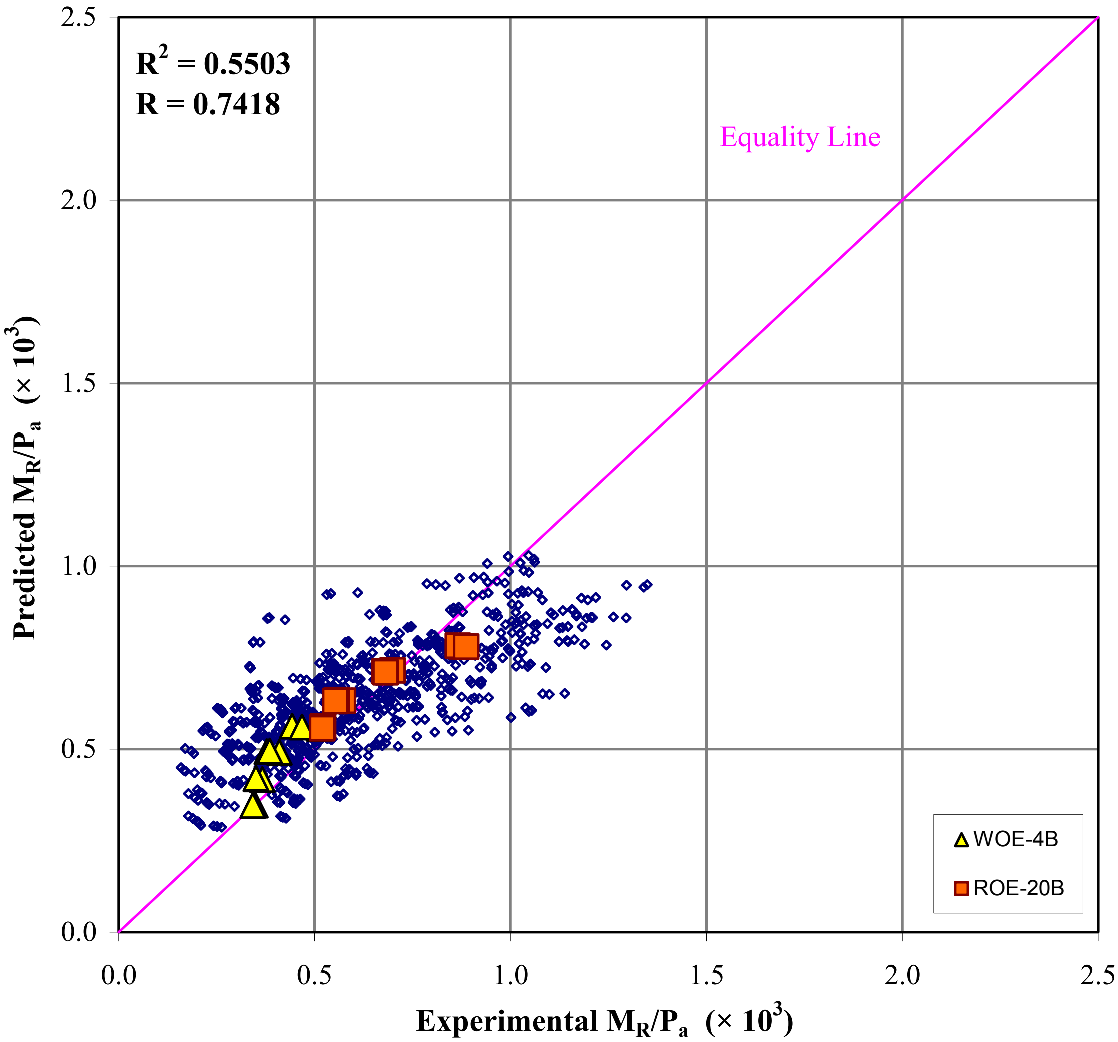

Figure 6-25 Comparison of Experimental and Predicted M_R/P_a for Combined Evaluation Dataset: Linear Network (LN) Model

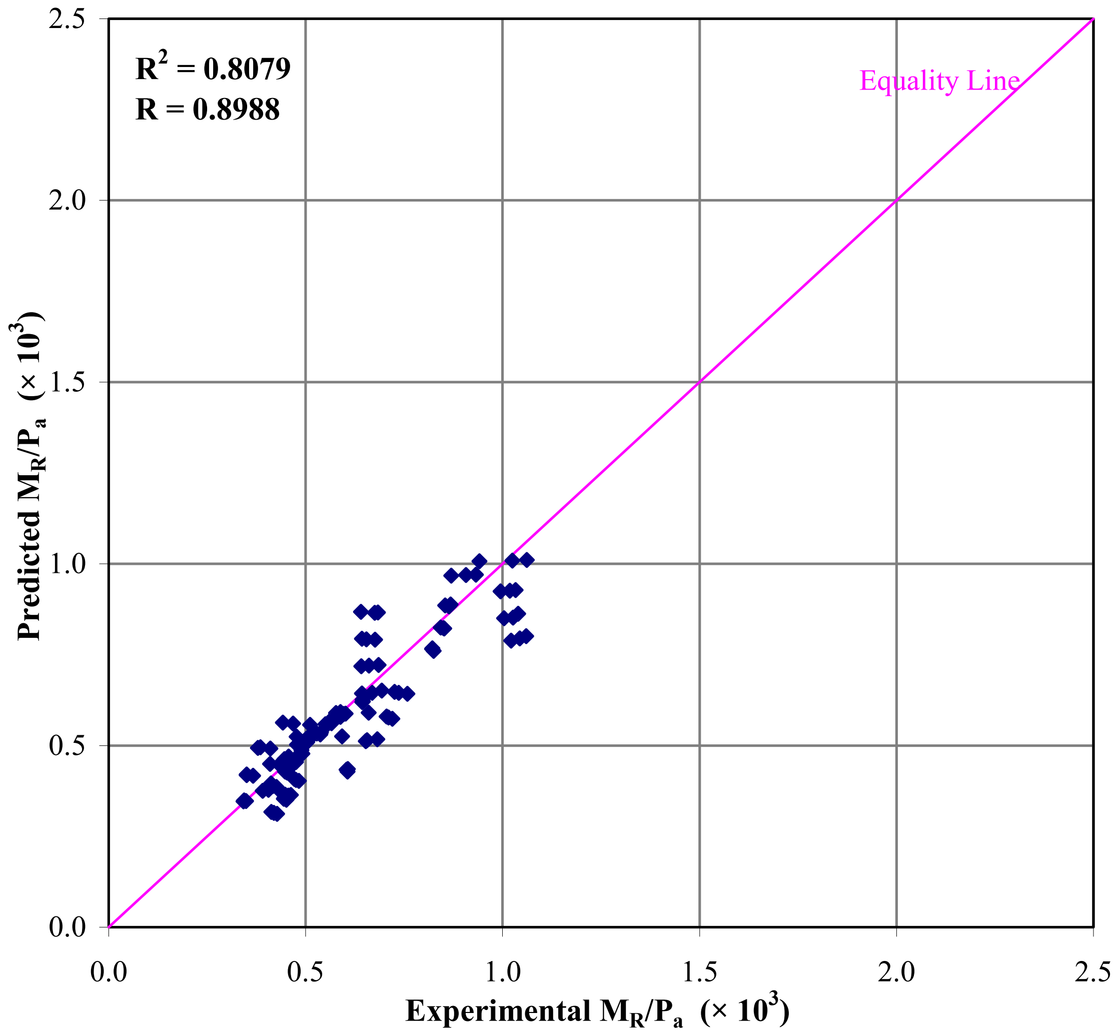

Figure 6-26 Comparison of Experimental and Predicted M_R/P_a for Evaluation Dataset from Woodward County: Linear Network (LN) Model

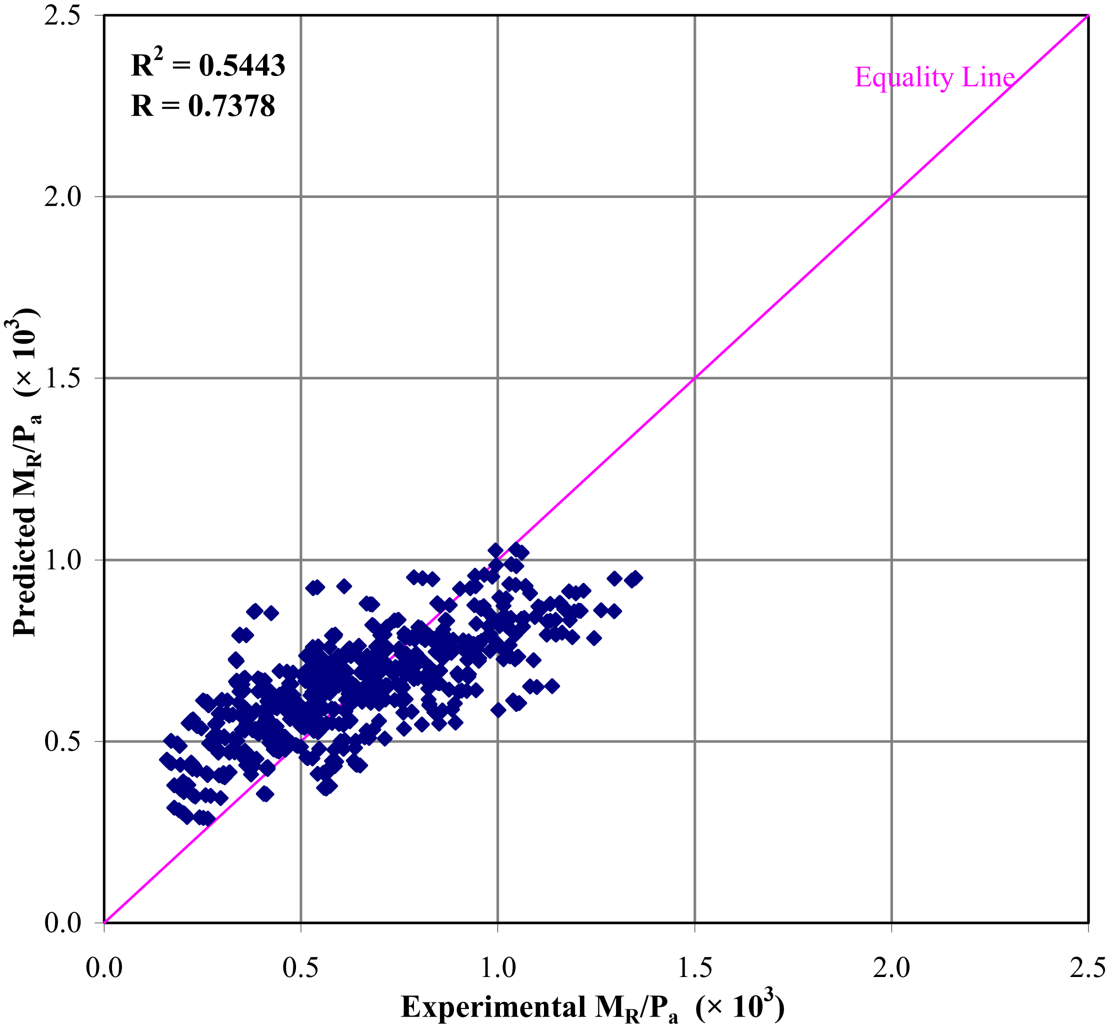

Figure 6-27 Comparison of Experimental and Predicted M_R/P_a for Evaluation Dataset from Roger County: Linear Network (LN) Model

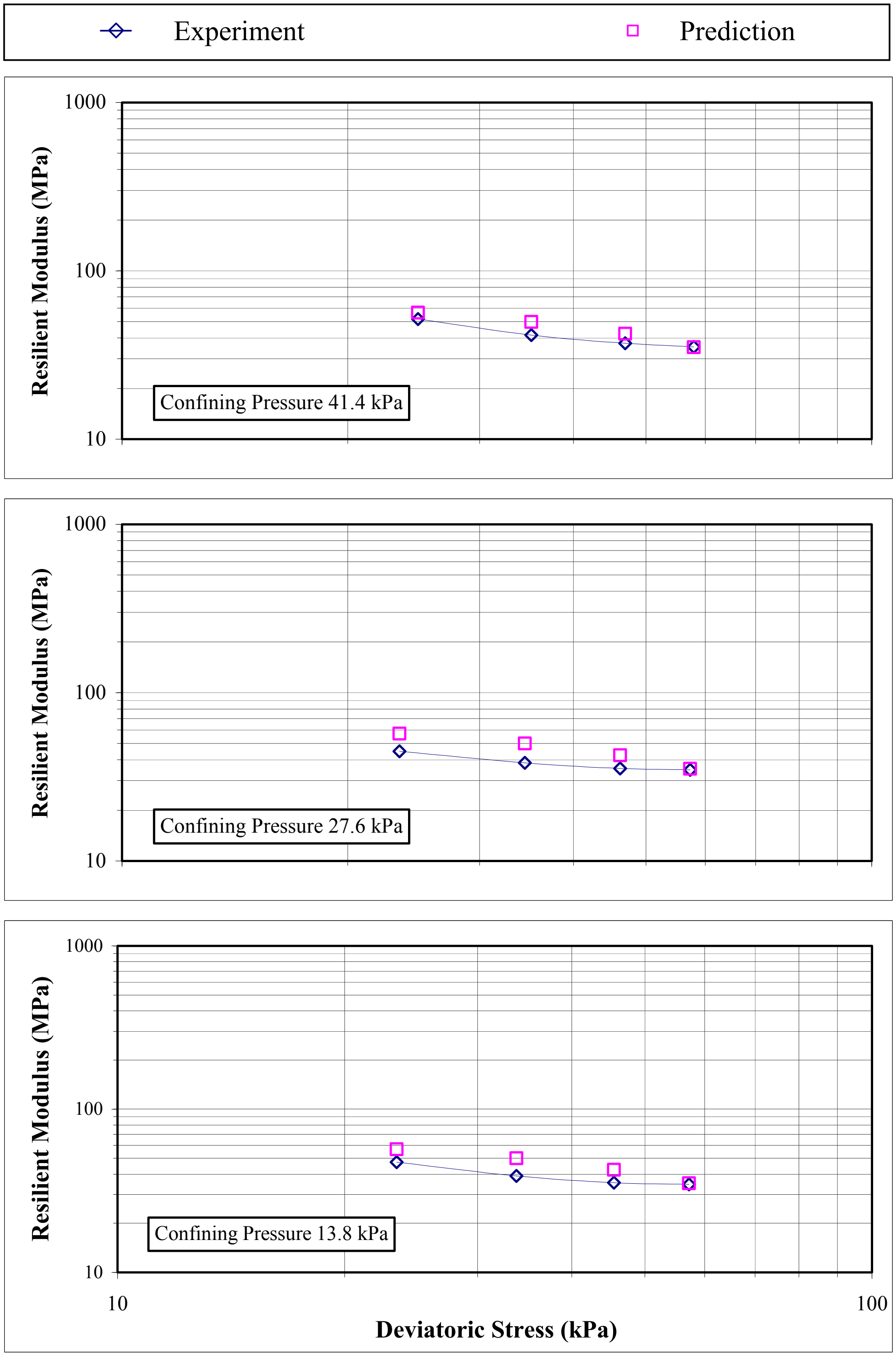

Figure 6-28 Resilient Modulus from Experiment and Linear Network (LN) Model: Specimen WOE-4B

1 kPa = 0.145 psi

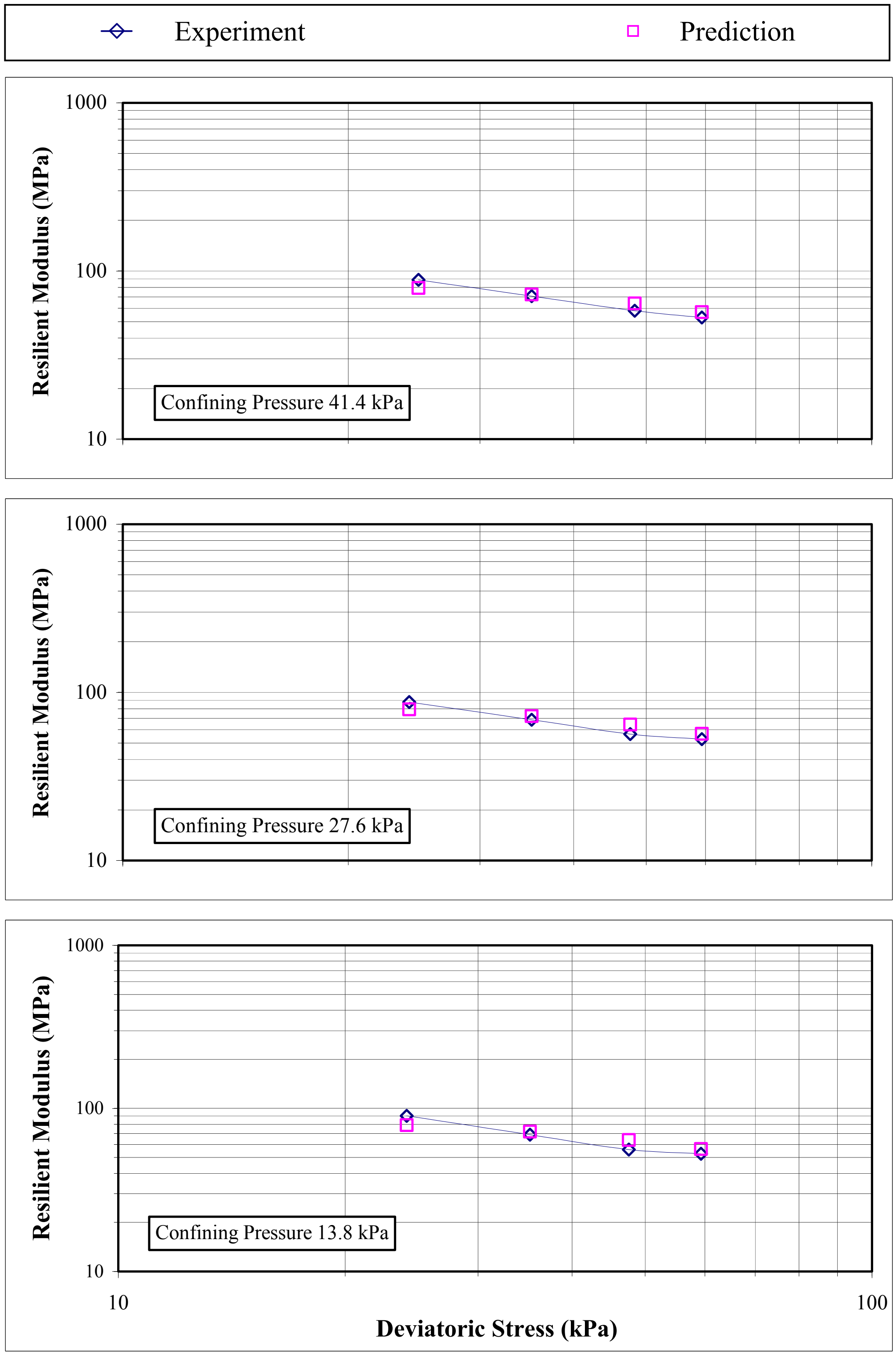

Figure 6-29 Resilient Modulus from Experiment and Linear Network (LN) Model: Specimen ROE-20B

1 kPa = 0.145 psi

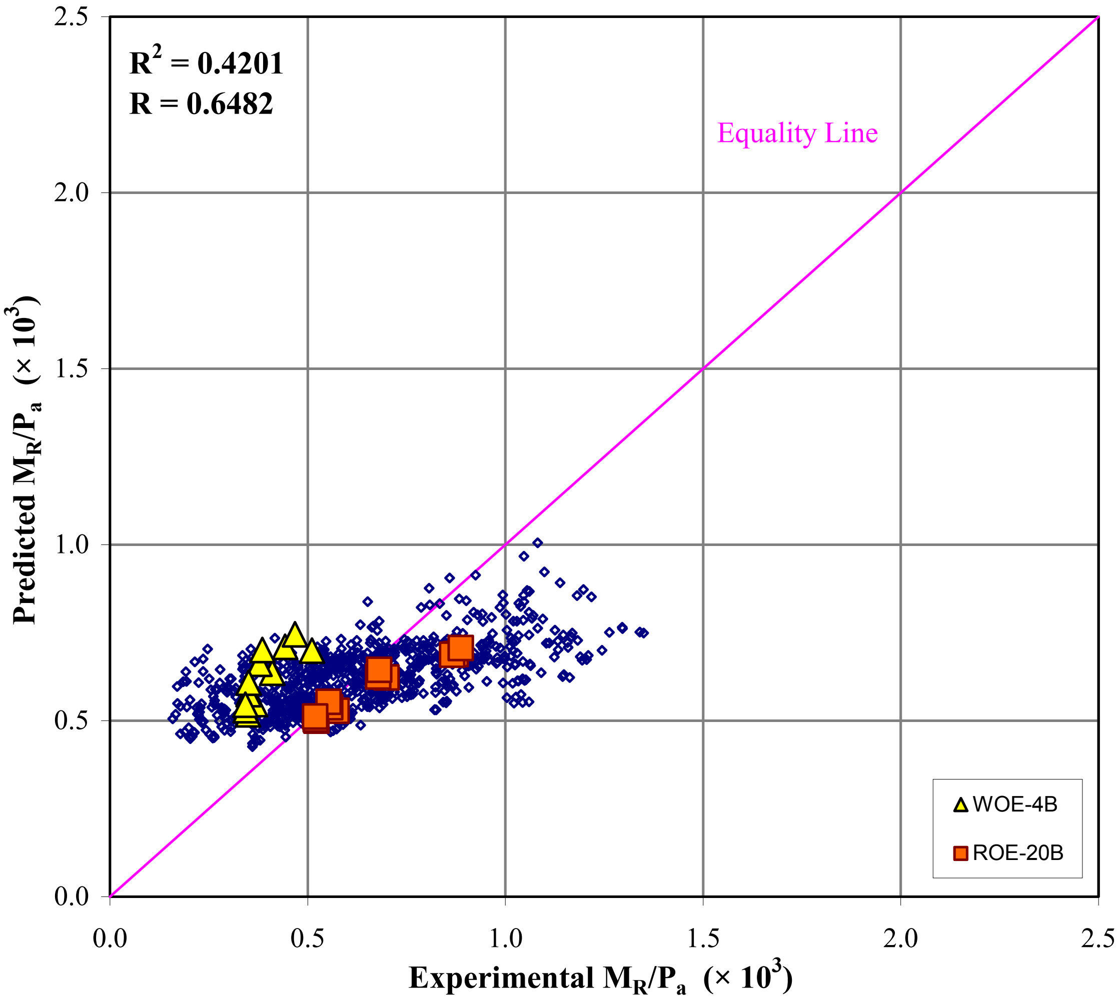

Figure 6-30 Comparison of Experimental and Predicted M_R/P_a for Combined Evaluation Dataset: Generalized Regression Neural Network (GRNN) Model

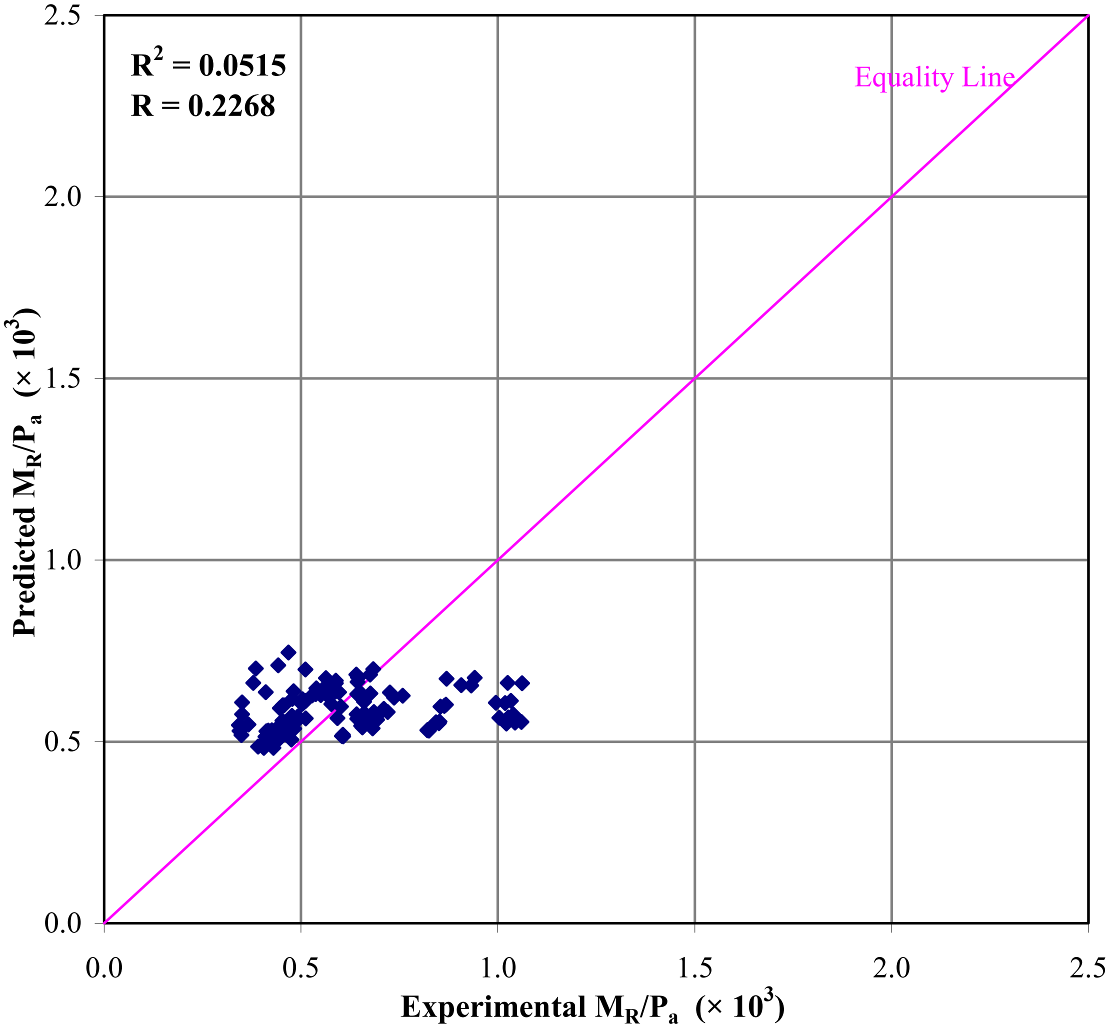

Figure 6-31 Comparison of Experimental and Predicted M_R/P_a for Evaluation Dataset from Woodward County: Generalized Regression Neural Network (GRNN) Model

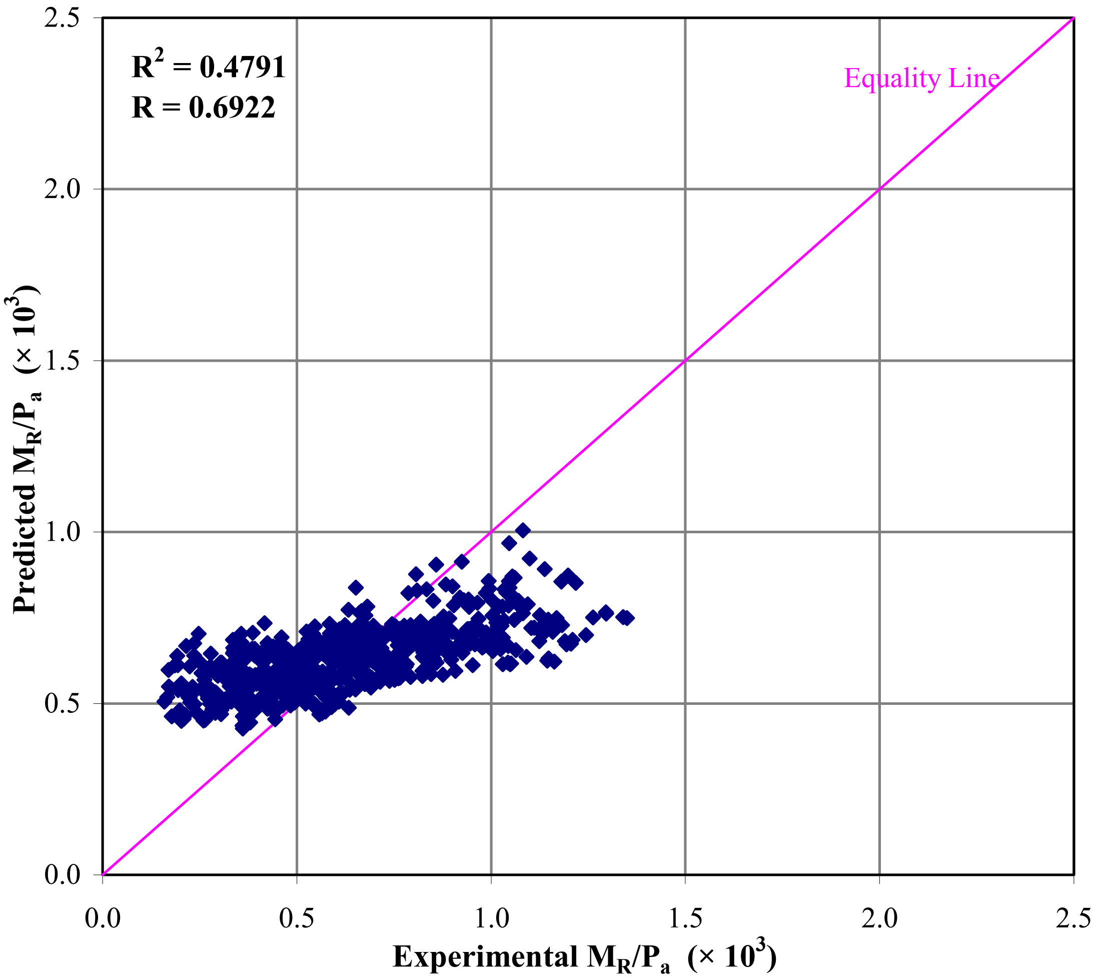

Figure 6-32 Comparison of Experimental and Predicted M_R/P_a for Evaluation Dataset from Roger County: Generalized Regression Neural Network (GRNN) Model

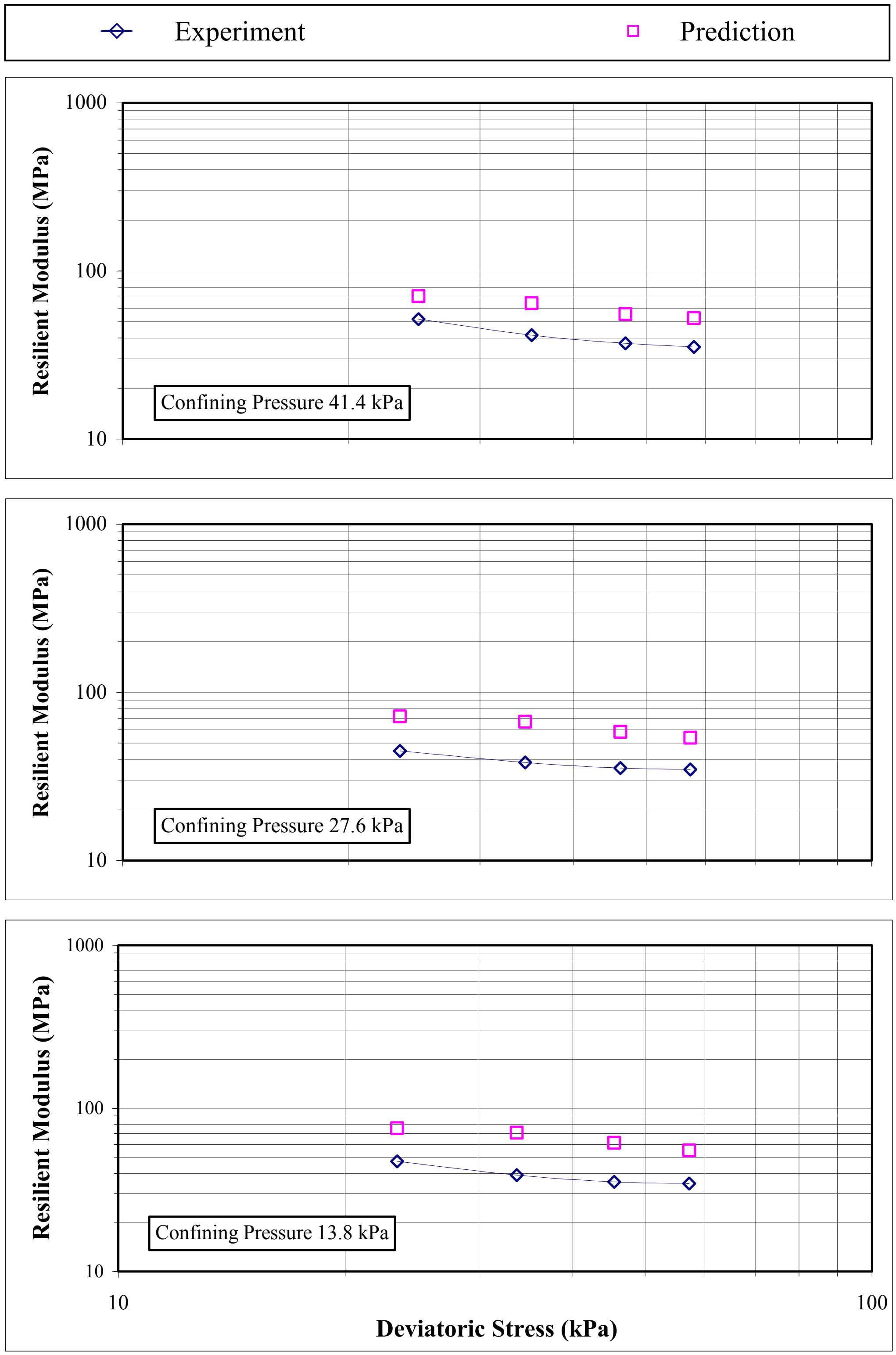

Figure 6-33 Resilient Modulus from Experiment and Generalized Regression Neural Network (GRNN) Model: Specimen WOE-4B

1 kPa = 0.145 psi

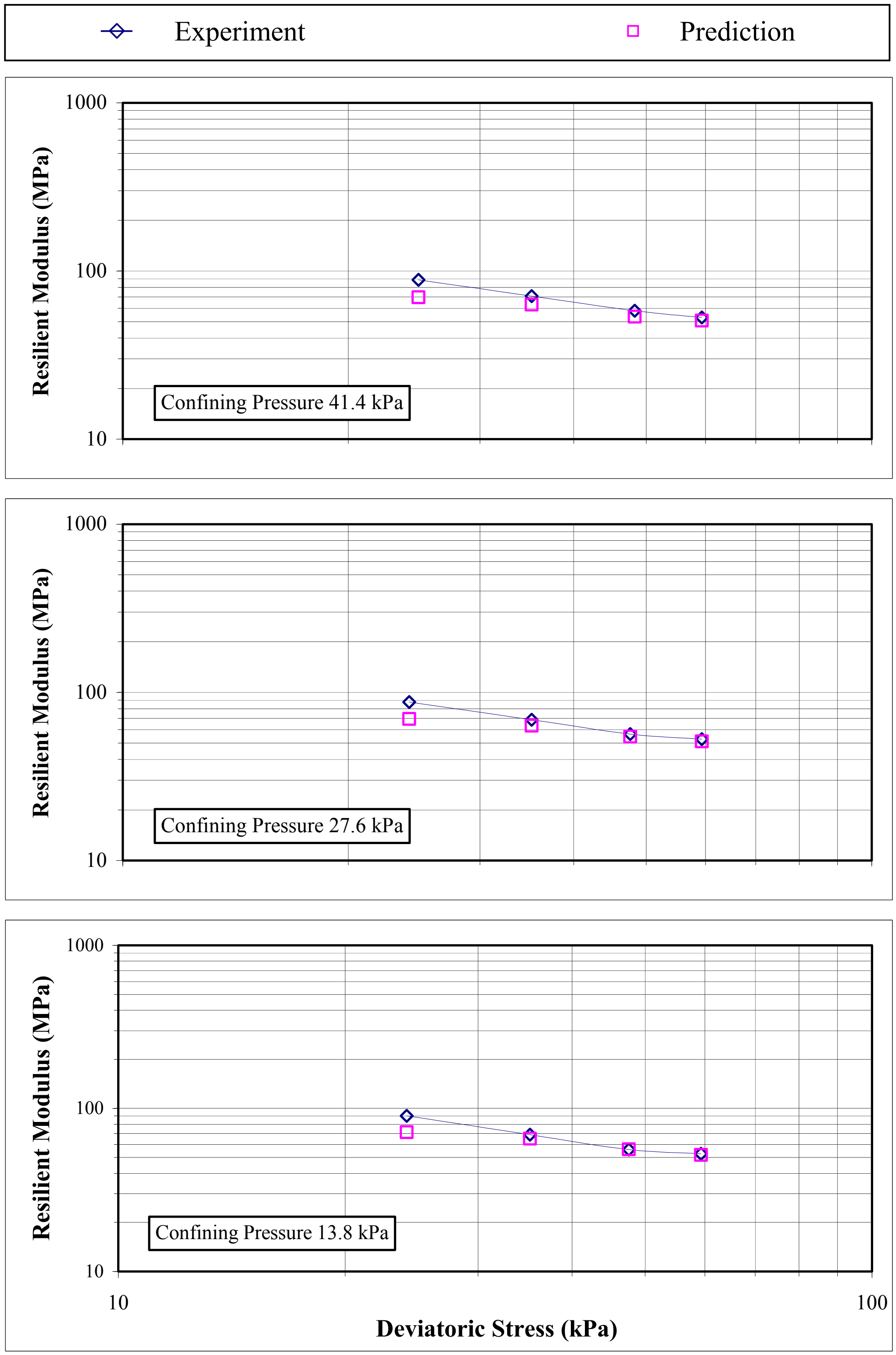

Figure 6-34 Resilient Modulus from Experiment and Generalized Regression Neural Network (GRNN) Model: Specimen ROE-20B

1 kPa = 0.145 psi

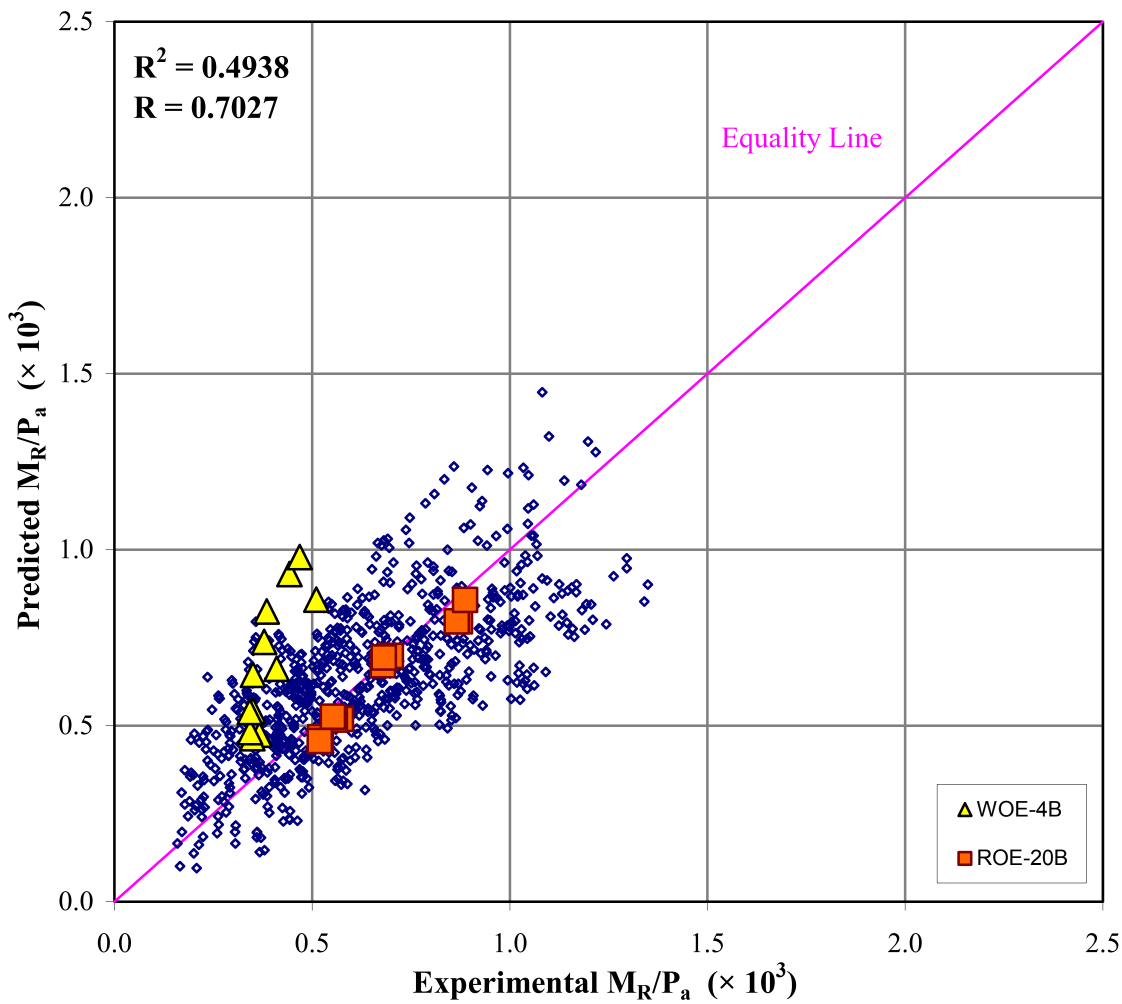

Figure 6-35 Comparison of Experimental and Predicted M_R/P_a for Combined Evaluation Dataset: Radial Basis Function Network (RBFN) Model

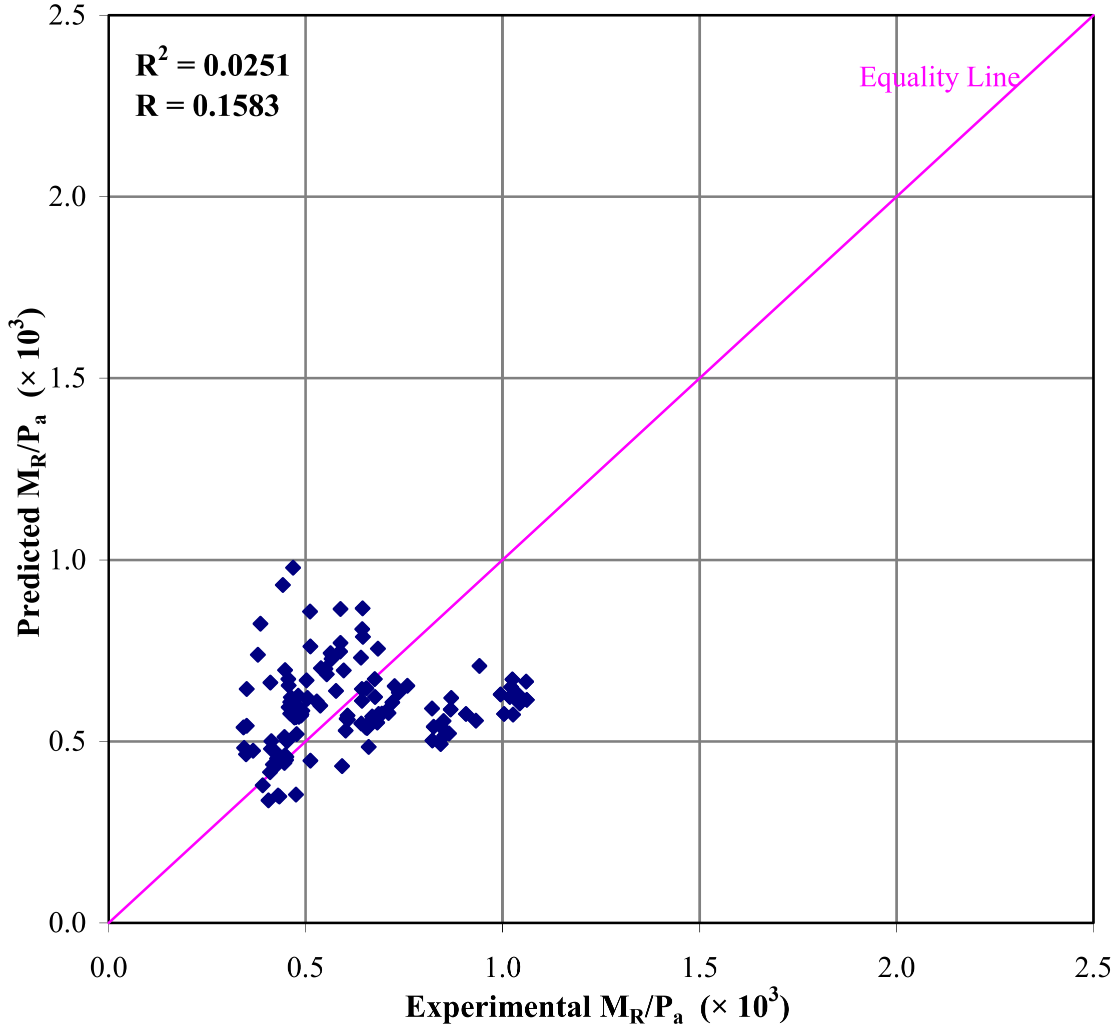

Figure 6-36 Comparison of Experimental and Predicted M_R/P_a for Evaluation Dataset from Woodward County: Radial Basis Function Network (RBFN) Model

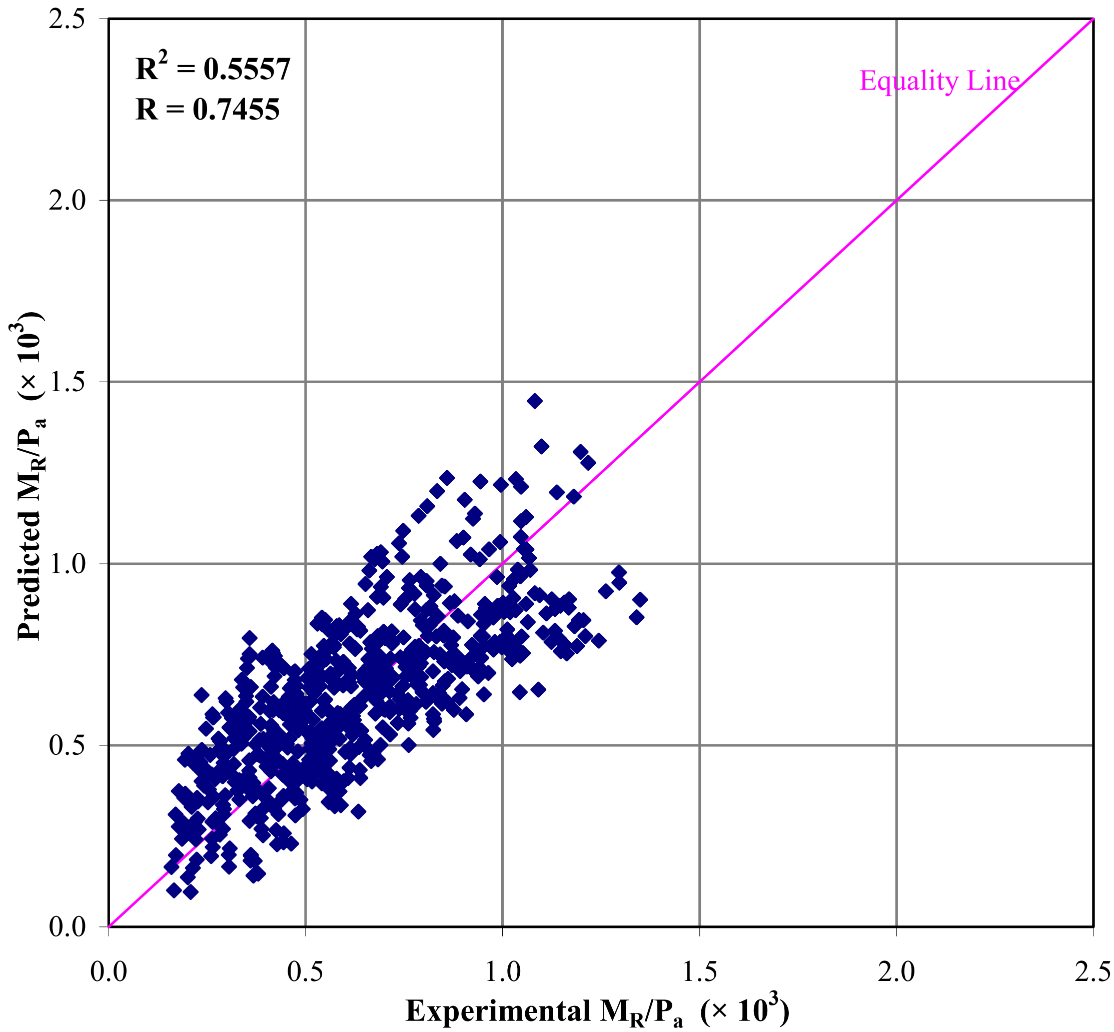

Figure 6-37 Comparison of Experimental and Predicted M_R/P_a for Evaluation Dataset from Roger County: Radial Basis Function Network (RBFN) Model

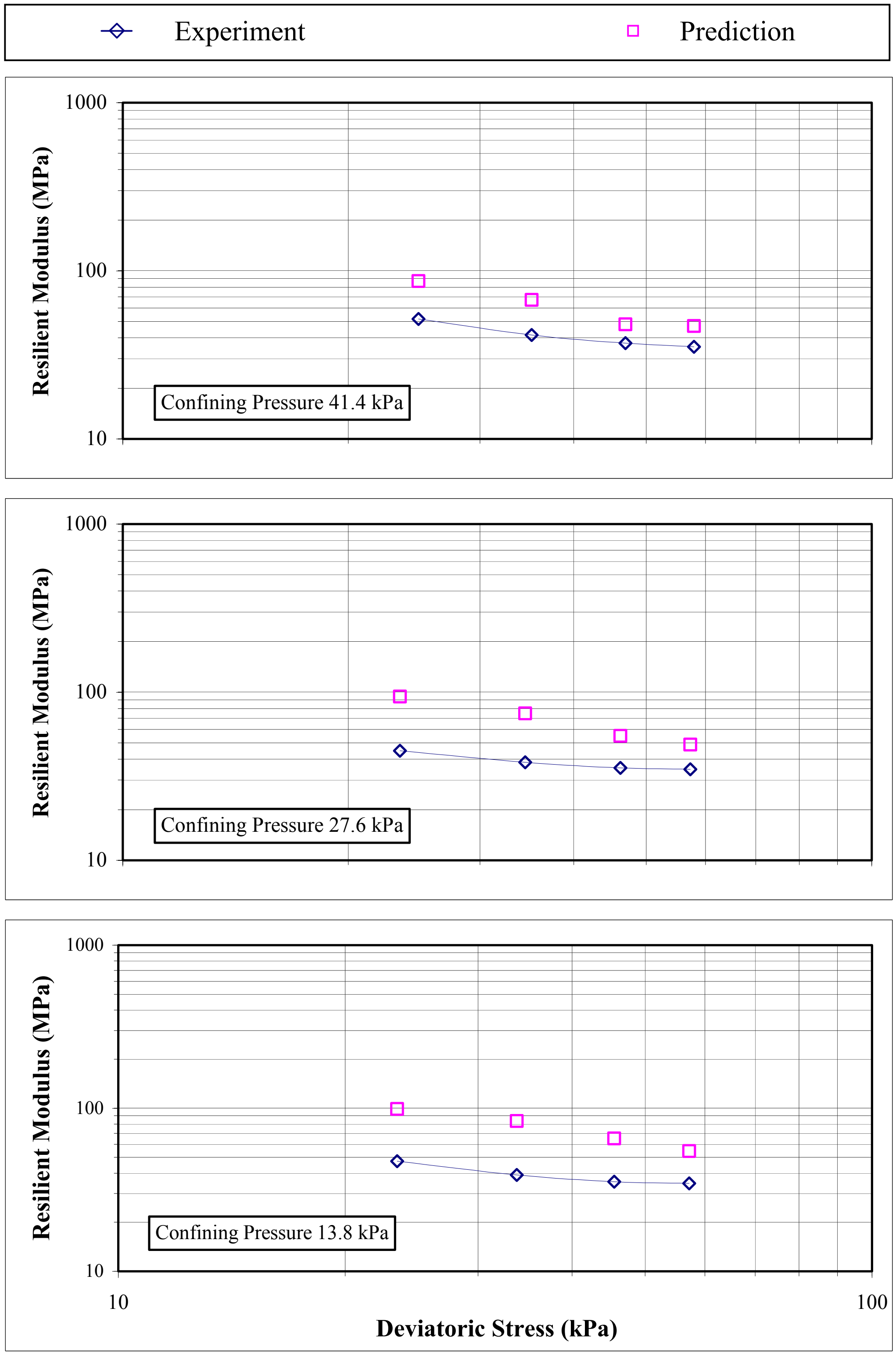

Figure 6-38 Resilient Modulus from Experiment and Radial Basis Function Network (RBFN) Model: Specimen WOE-4B

1 kPa = 0.145 psi

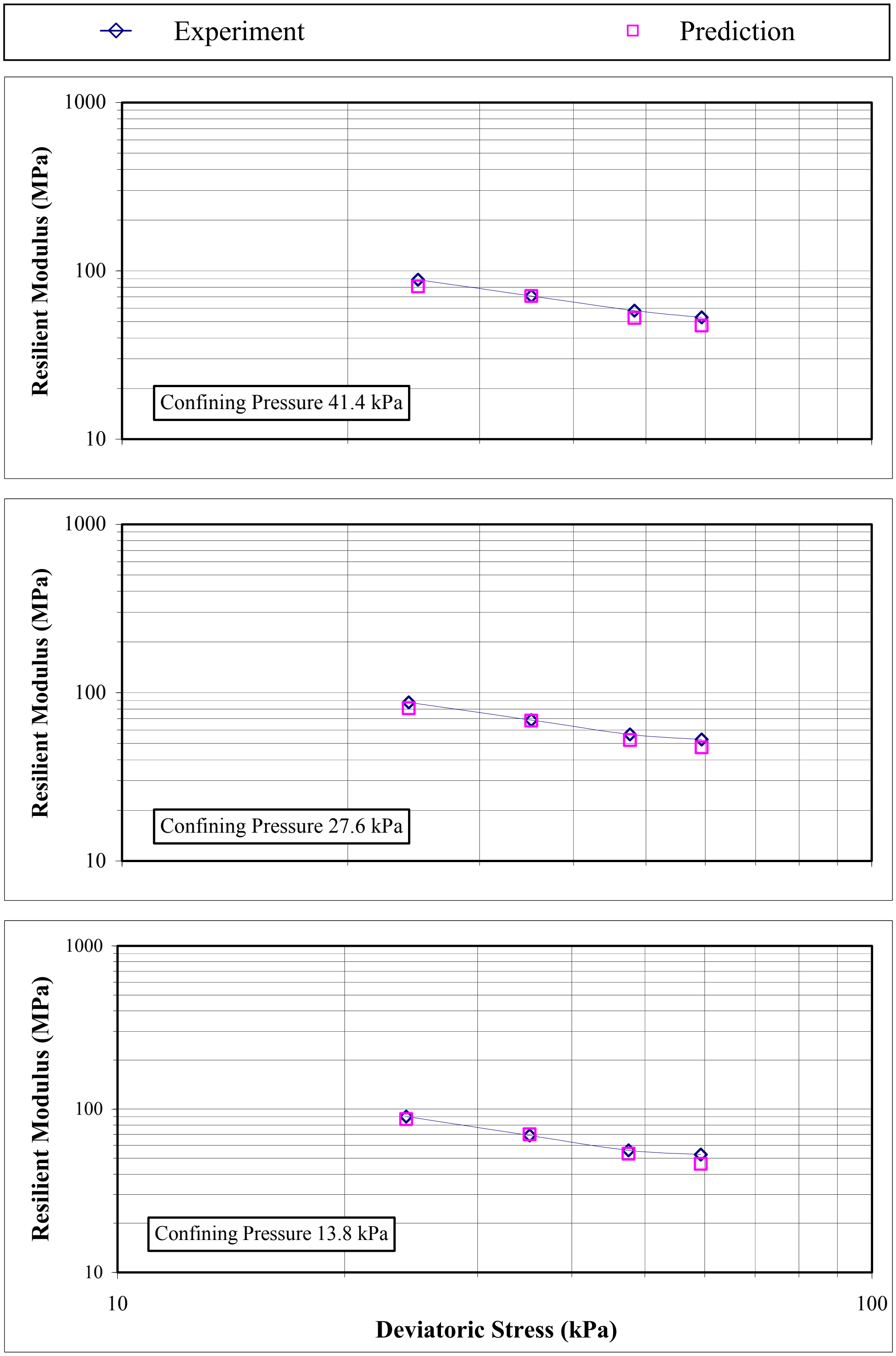

Figure 6-39 Resilient Modulus from Experiment and Radial Basis Function Network (RBFN) Model: Specimen ROE-20B

1 kPa = 0.145 psi

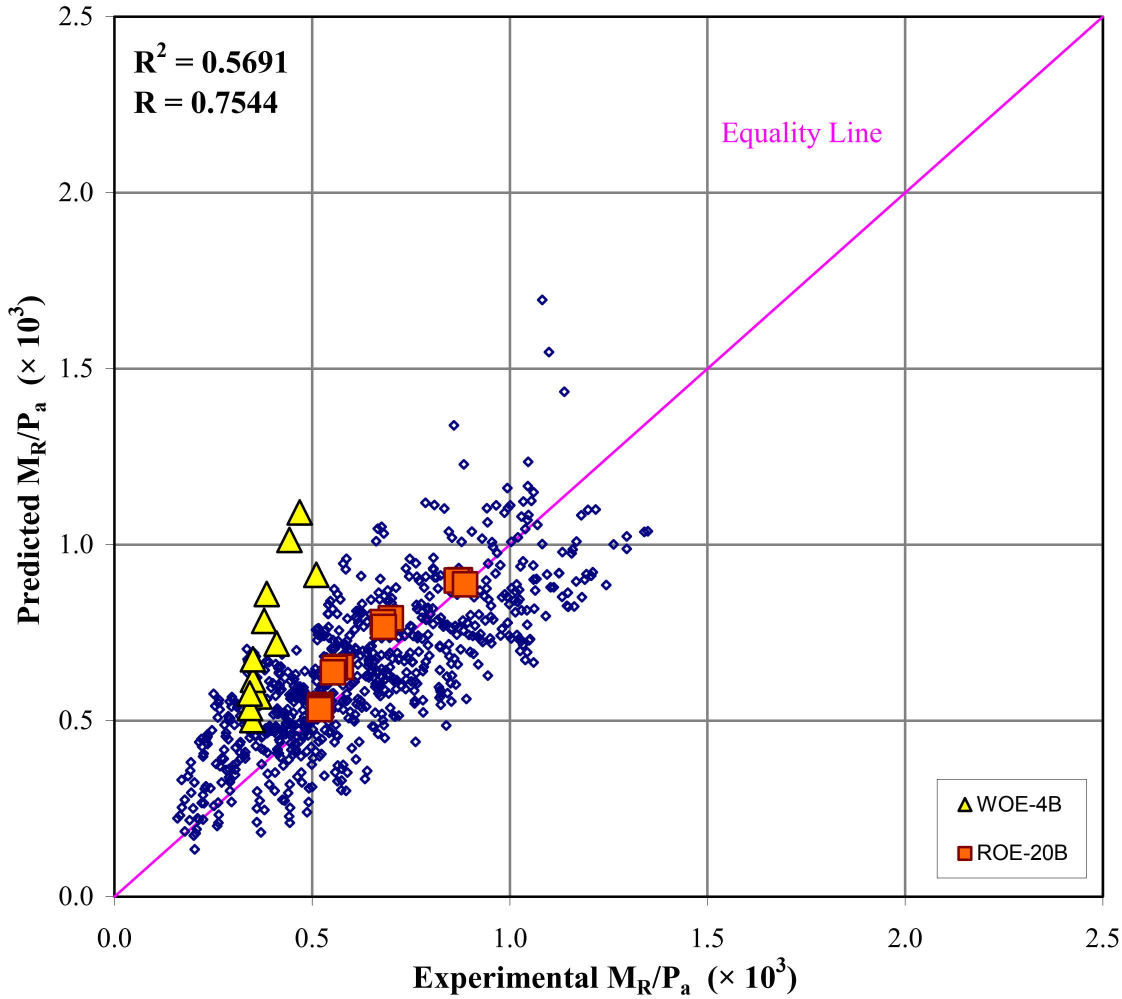

Figure 6-40 Comparison of Experimental and Predicted M_R/P_a for Combined Evaluation Dataset: Multilayer Perceptrons Network (MLPN-1) Model

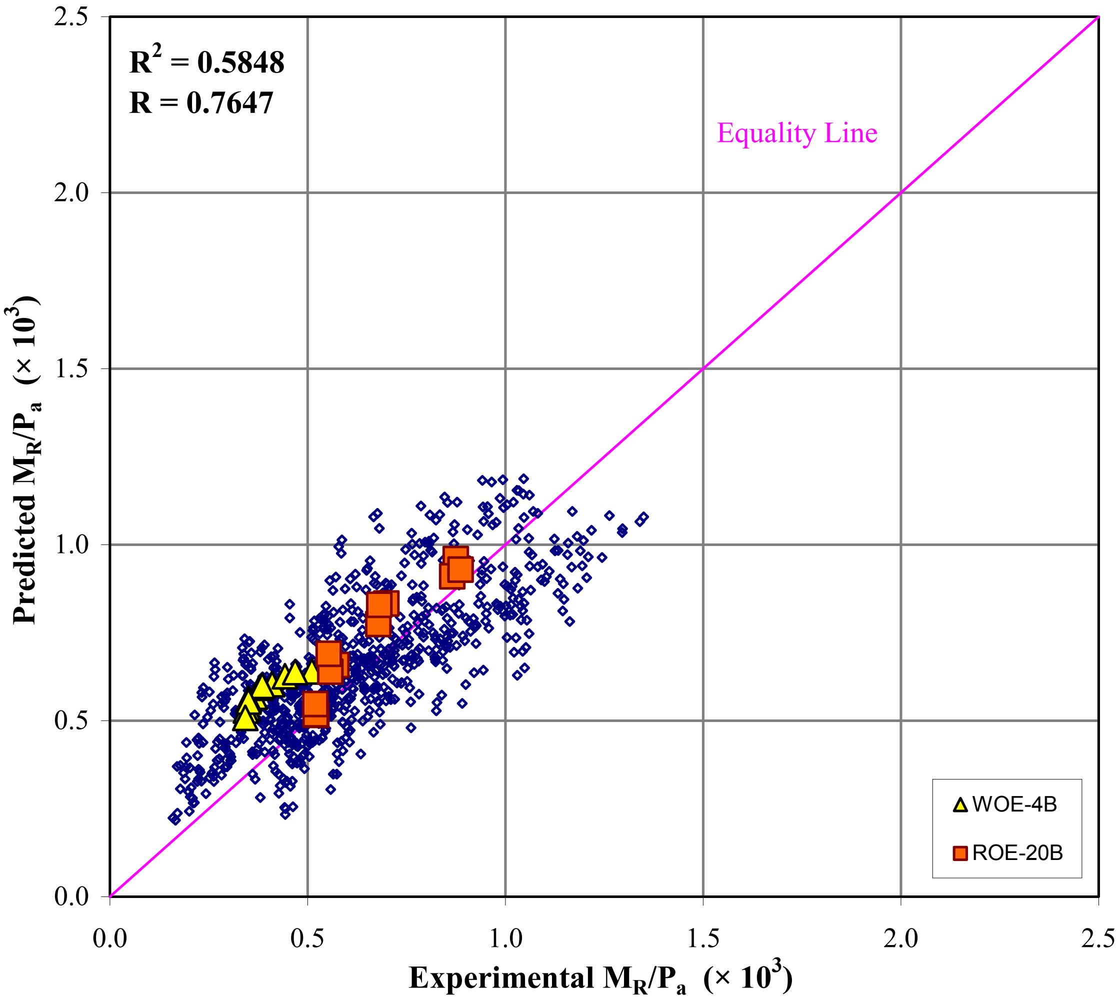

Figure 6-41 Comparison of Experimental and Predicted M_R/P_a for Combined Evaluation Dataset: Multilayer Perceptrons Network (MLPN-2) Model

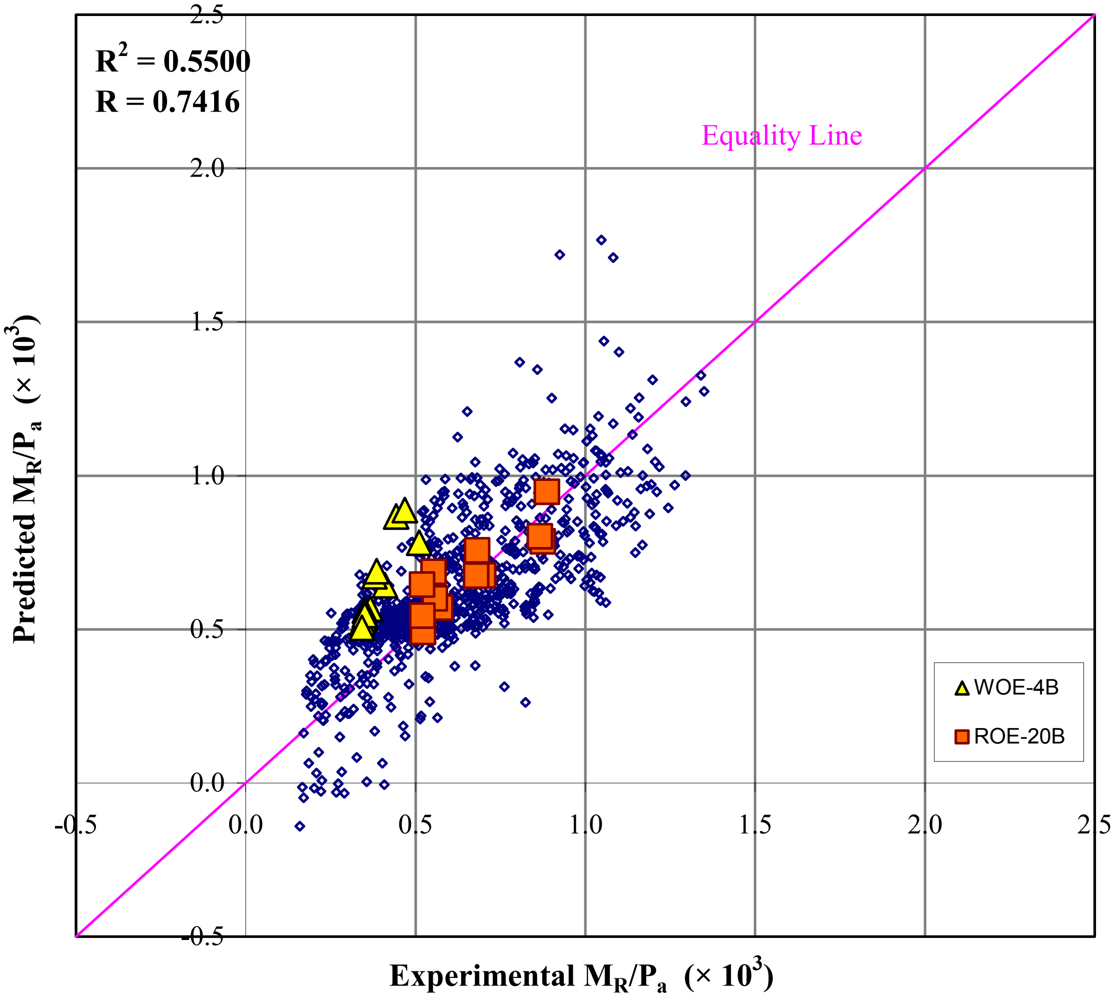

Figure 6-42 Comparison of Experimental and Predicted M_R/P_a for Combined Evaluation Dataset: Multilayer Perceptrons Network (MLPN-3) Model

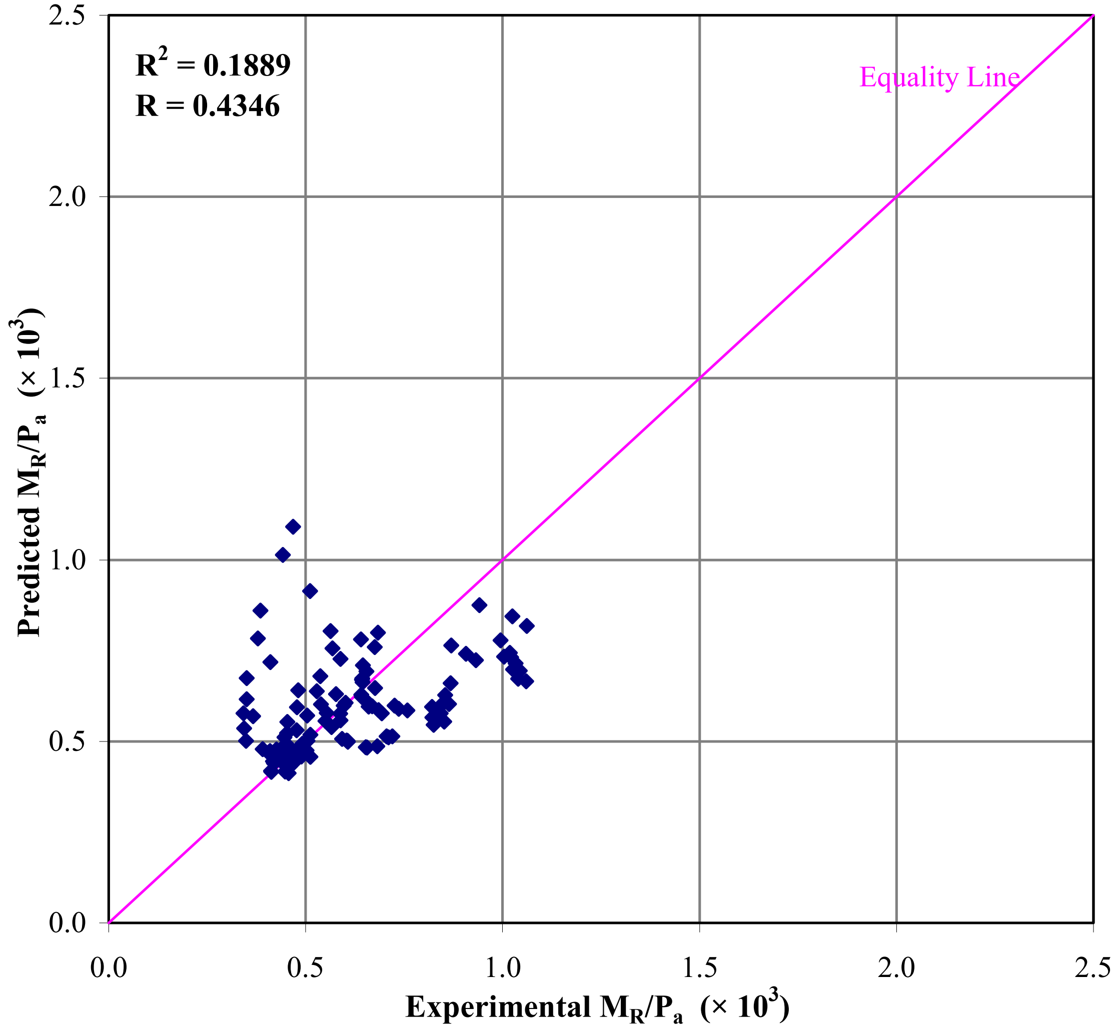

Figure 6-43 Comparison of Experimental and Predicted M_R/P_a for Evaluation Dataset from Woodward County: Multilayer Perceptrons Network (MLPN-1) Model

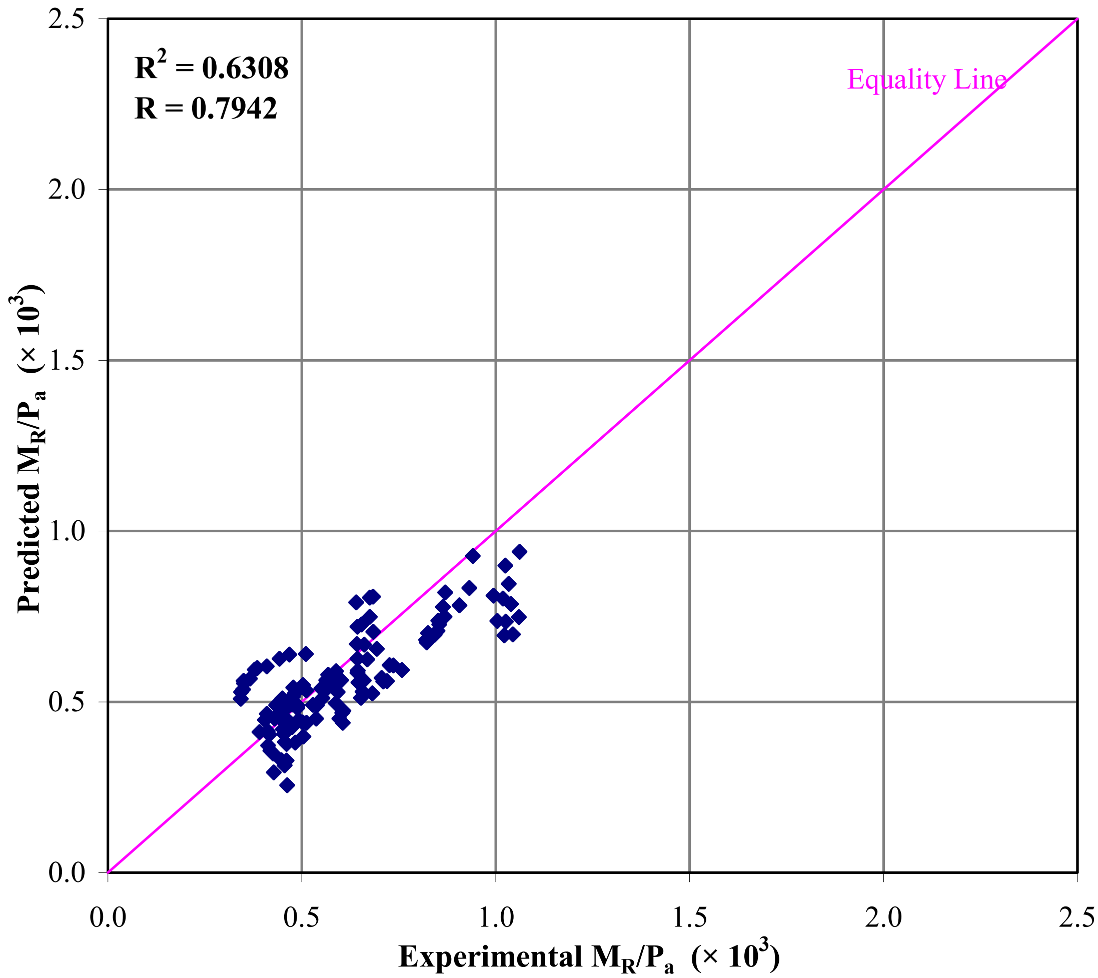

Figure 6-44 Comparison of Experimental and Predicted M_R/P_a for Evaluation Dataset from Woodward County: Multilayer Perceptrons Network (MLPN-2) Model

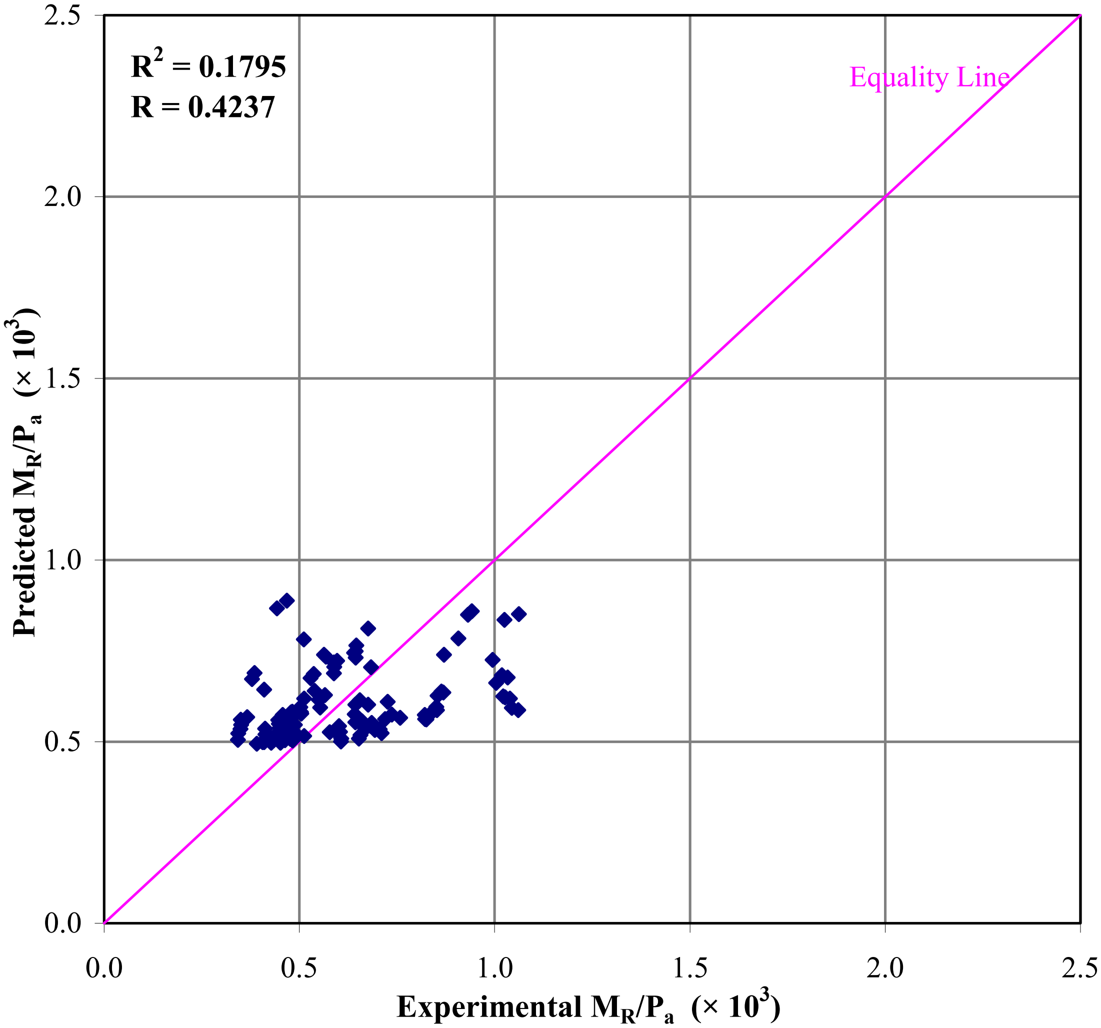

Figure 6-45 Comparison of Experimental and Predicted M_R/P_a for Evaluation Dataset from Woodward County: Multilayer Perceptrons Network (MLPN-3) Model

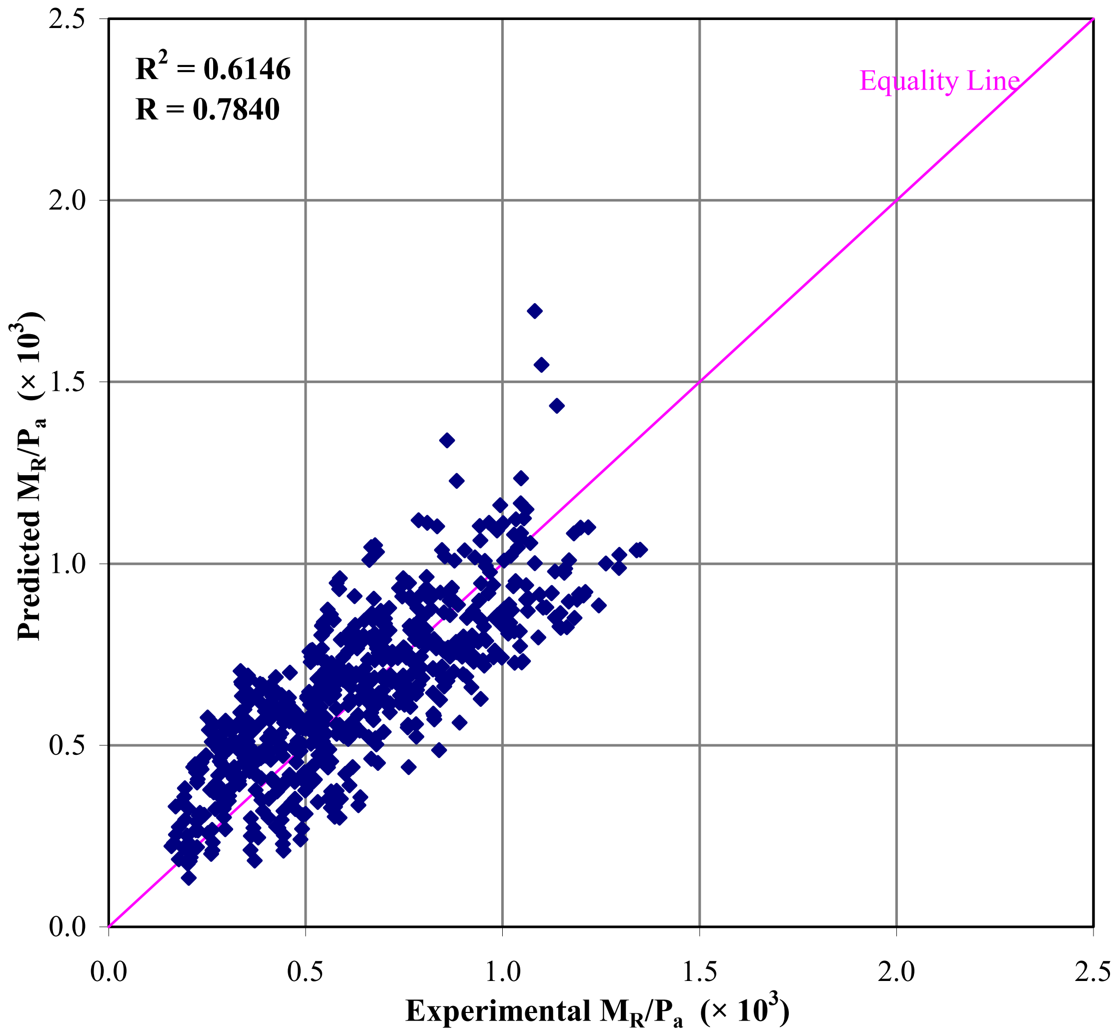

Figure 6-46 Comparison of Experimental and Predicted M_R/P_a for Evaluation Dataset from Roger County: Multilayer Perceptrons Network (MLPN-1) Model

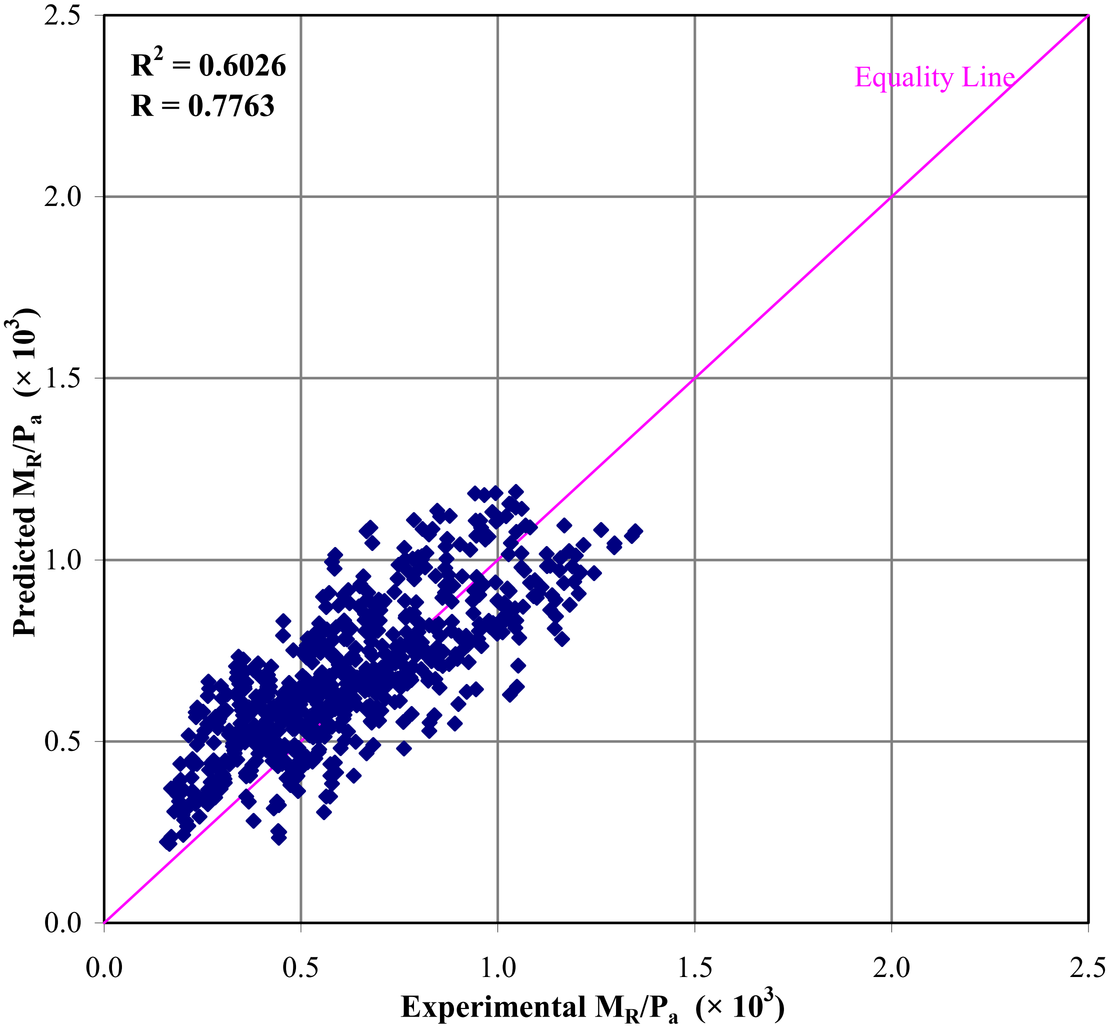

Figure 6-47 Comparison of Experimental and Predicted M_R/P_a for Evaluation Dataset from Roger County: Multilayer Perceptrons Network (MLPN-2) Model

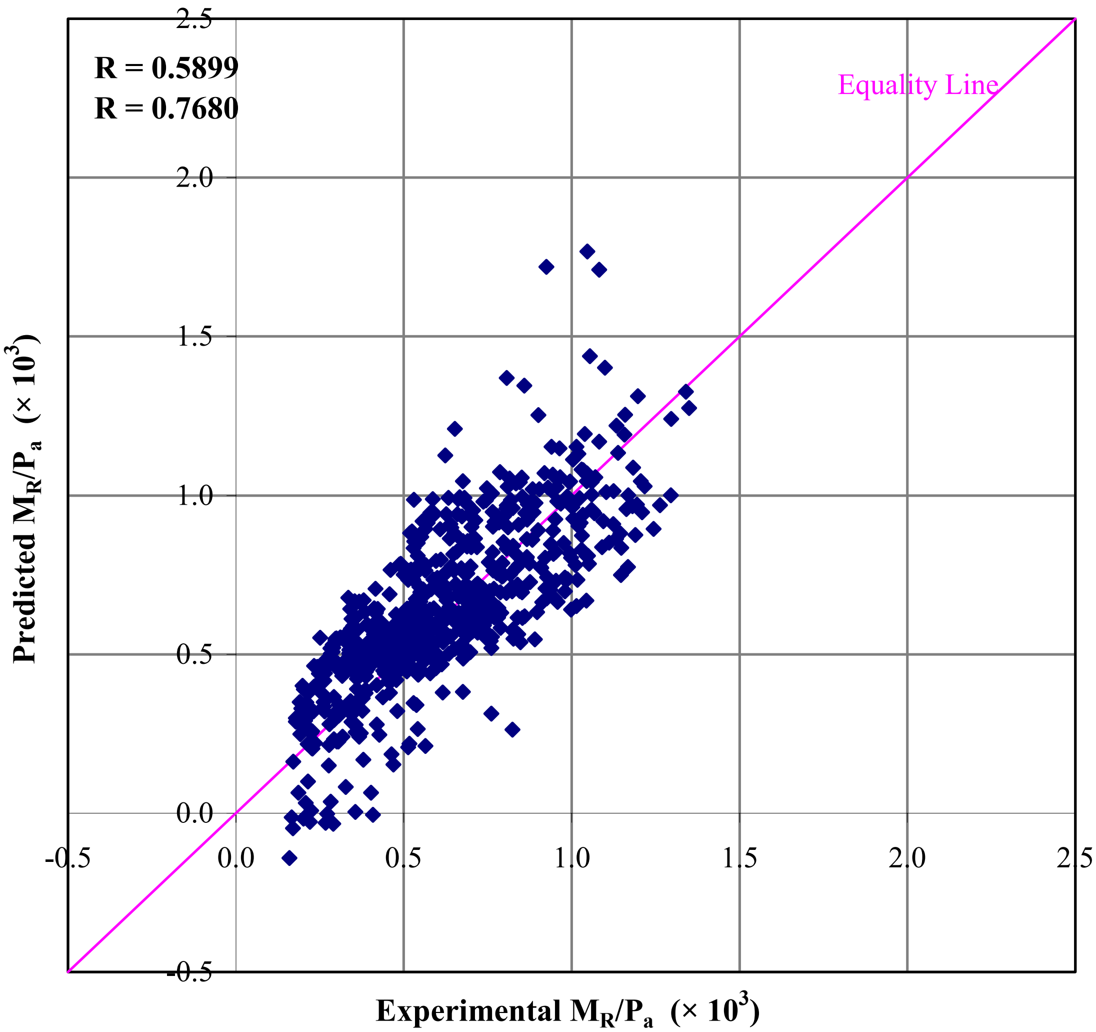

Figure 6-48 Comparison of Experimental and Predicted M_R/P_a for Evaluation Dataset from Roger County: Multilayer Perceptrons Network (MLPN-3) Model

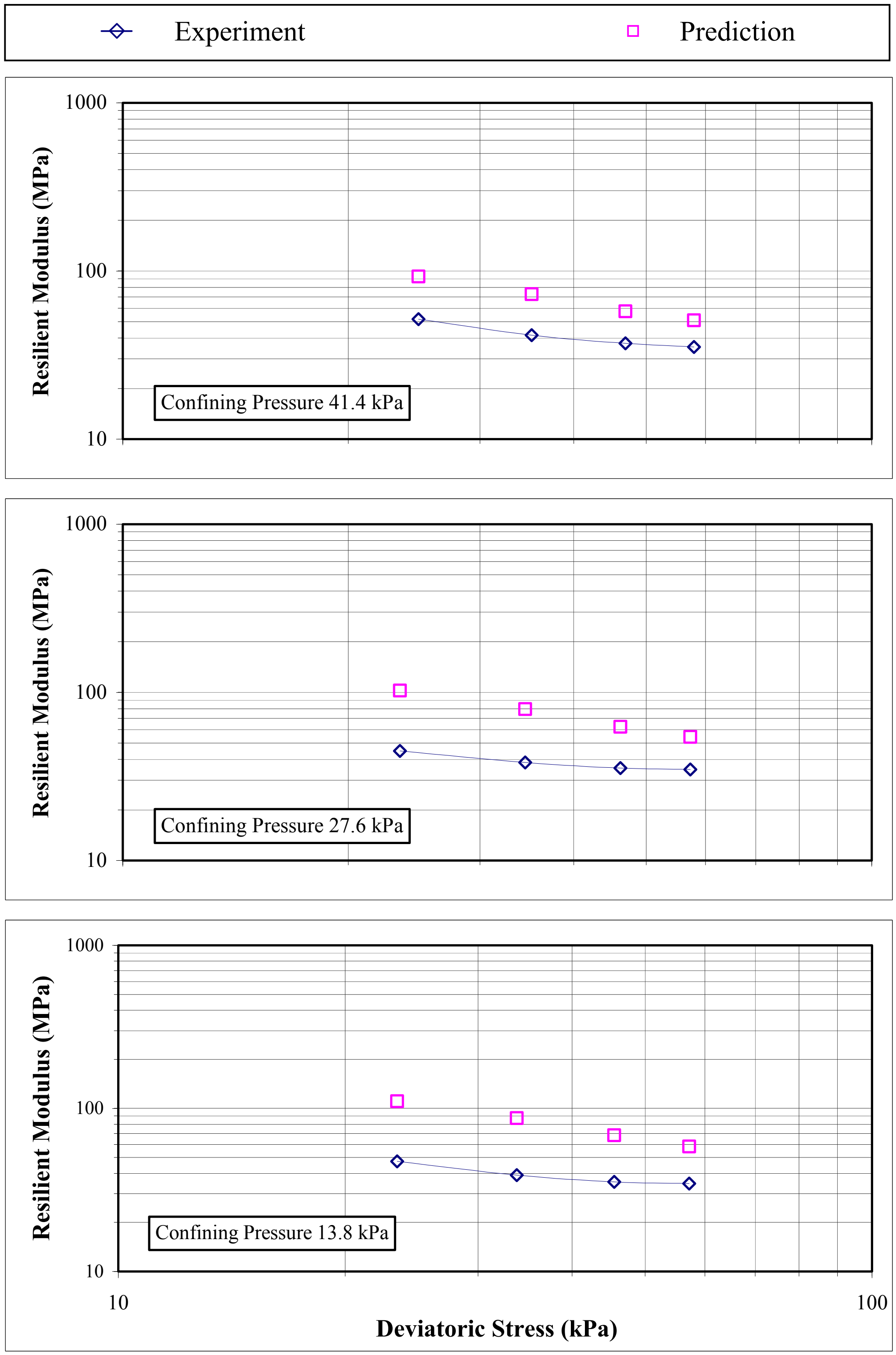

Figure 6-49 Resilient Modulus from Experiment and Multilayer Perceptrons Network (MLPN-1) Model: Specimen WOE-4B

1 kPa = 0.145 psi

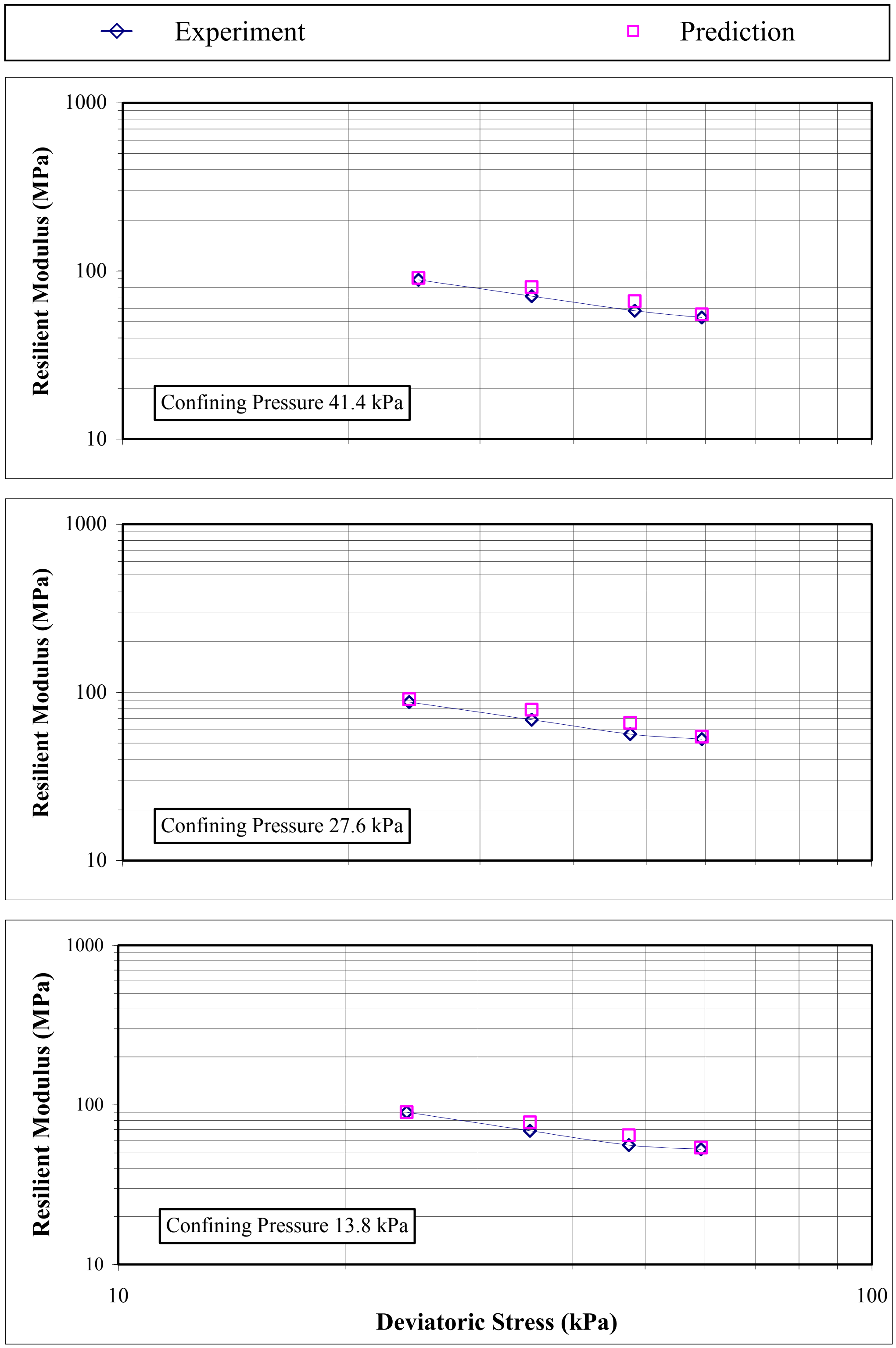

Figure 6-50 Resilient Modulus from Experiment and Multilayer Perceptrons Network (MLPN-1) Model: Specimen ROE-20B
1 kPa = 0.145 psi

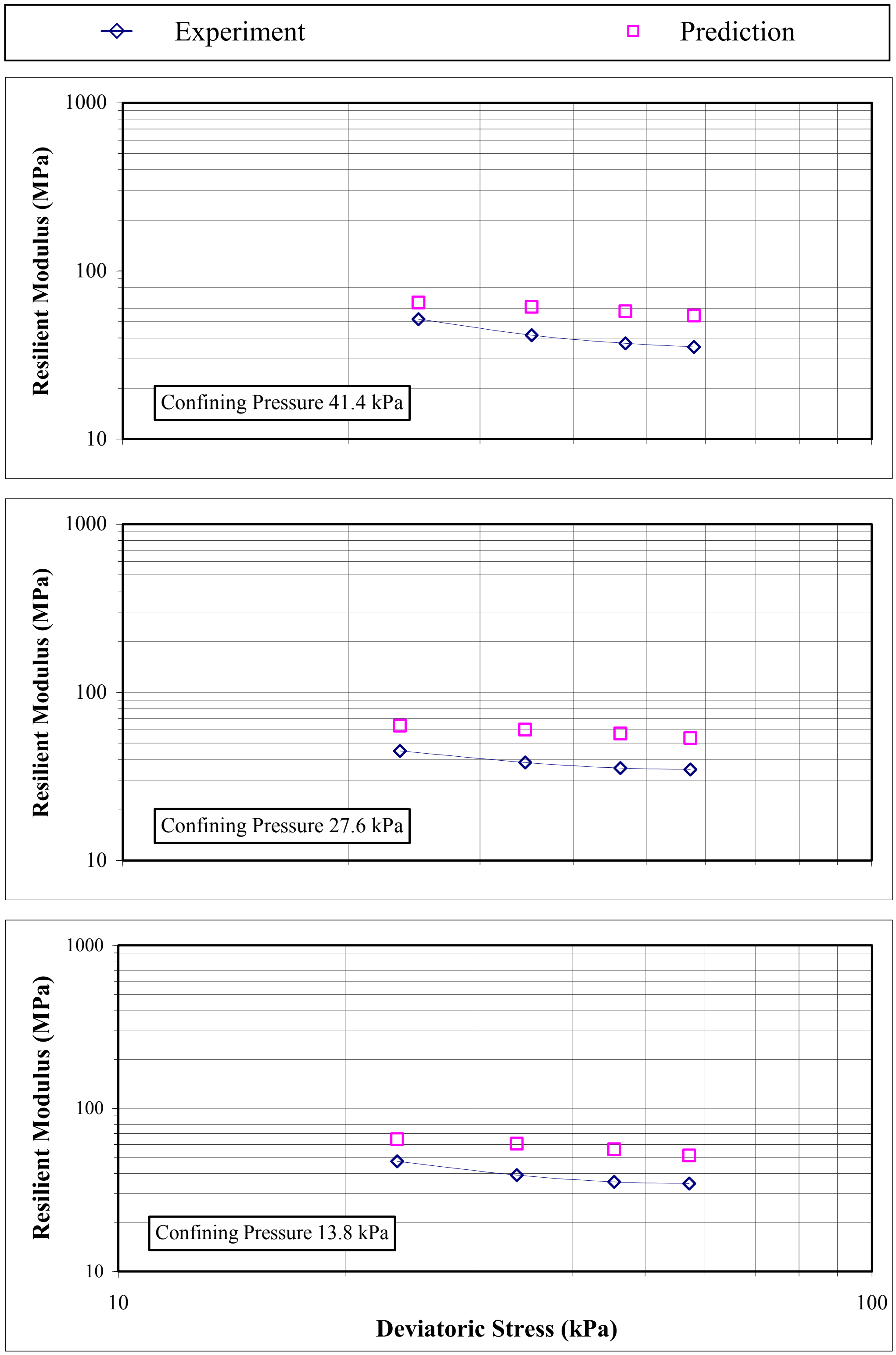

Figure 6-51 Resilient Modulus from Experiment and Multilayer Perceptrons Network (MLPN-2) Model: Specimen WOE-4B

1 kPa = 0.145 psi

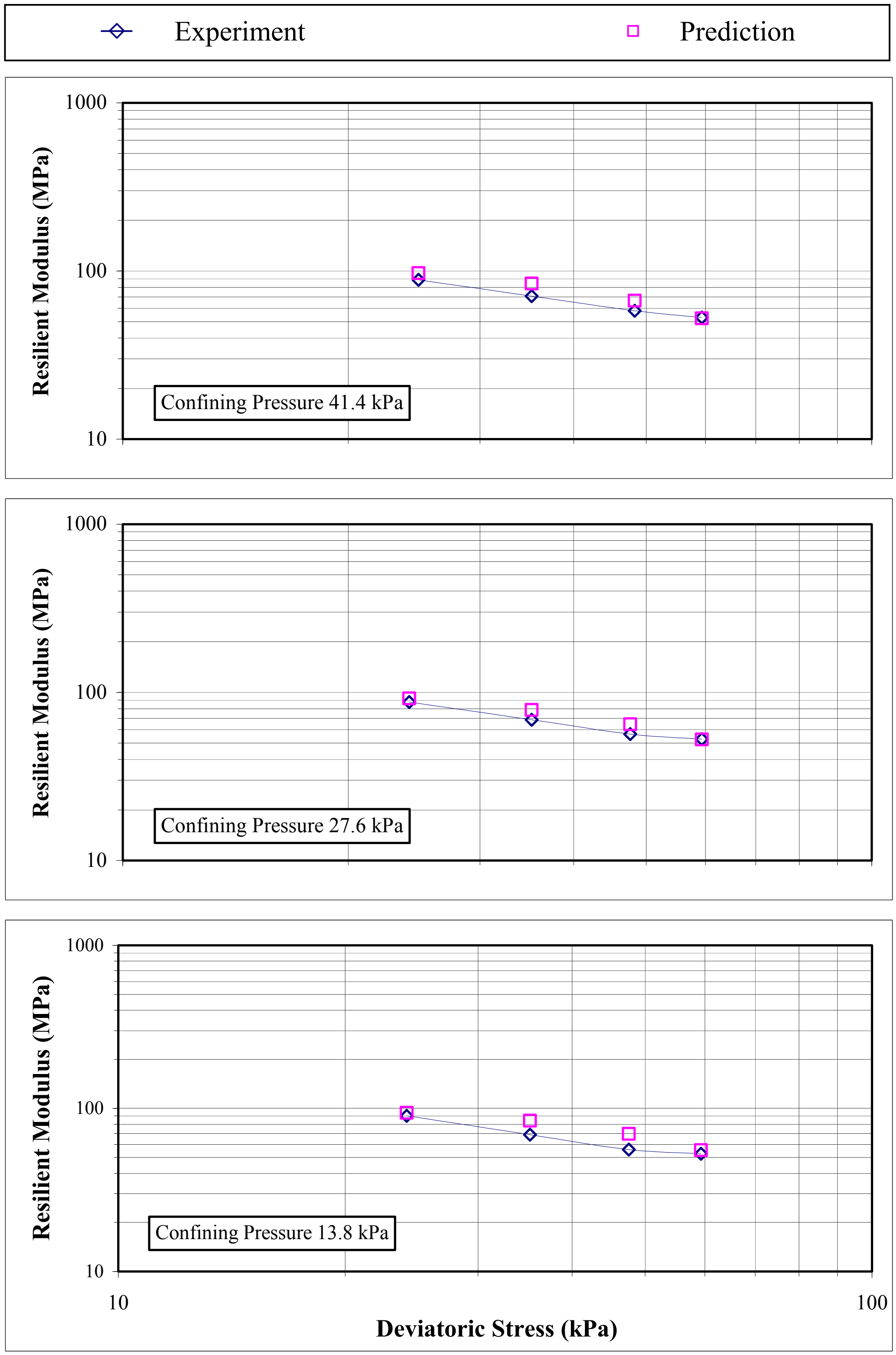

Figure 6-52 Resilient Modulus from Experiment and Multilayer Perceptrons Network (MLPN-2) Model: Specimen ROE-20B

1 kPa = 0.145 psi

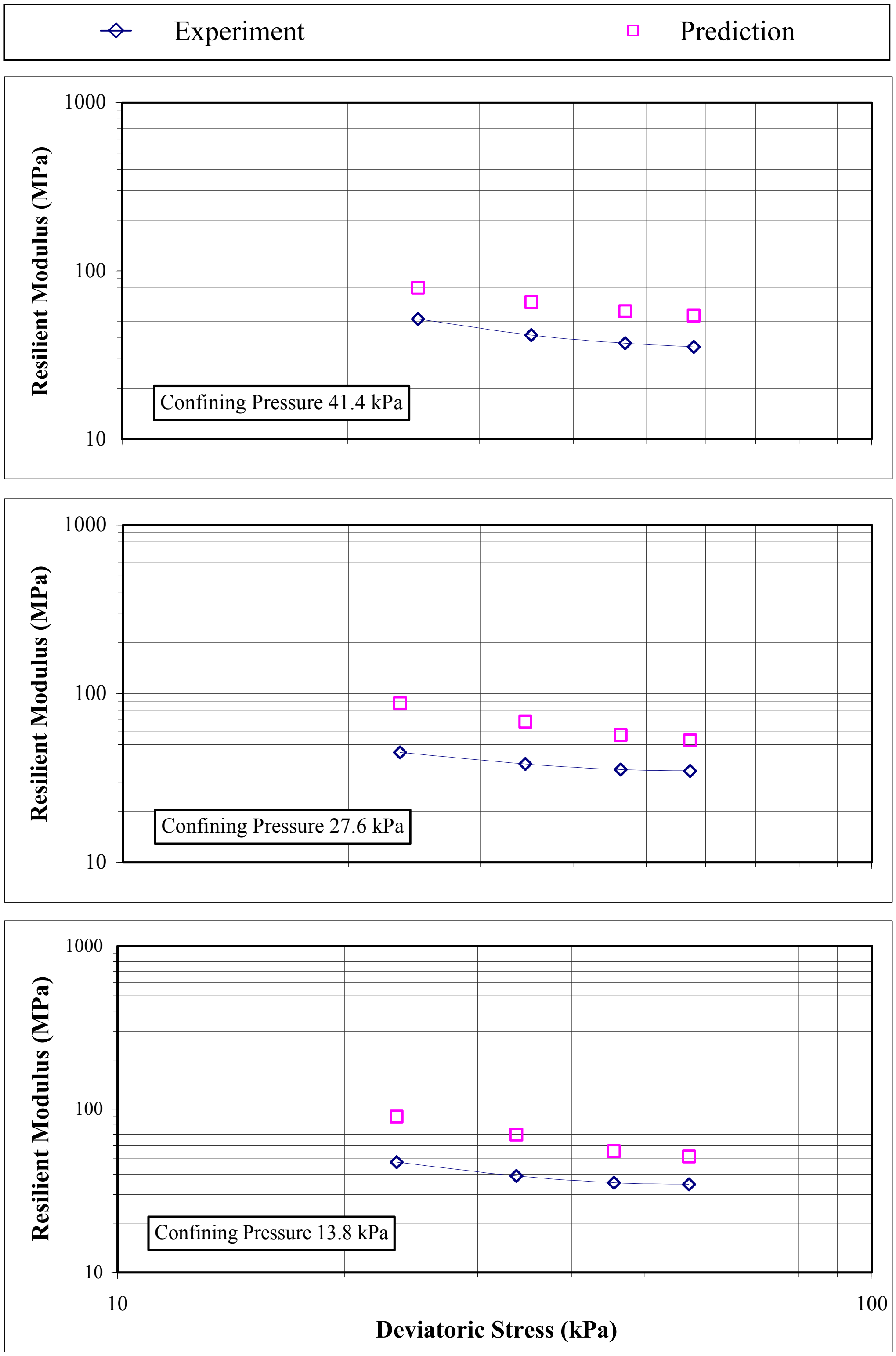

Figure 6-53 Resilient Modulus from Experiment and Multilayer Perceptrons Network (MLPN-3) Model: Specimen WOE-4B
1 kPa = 0.145 psi

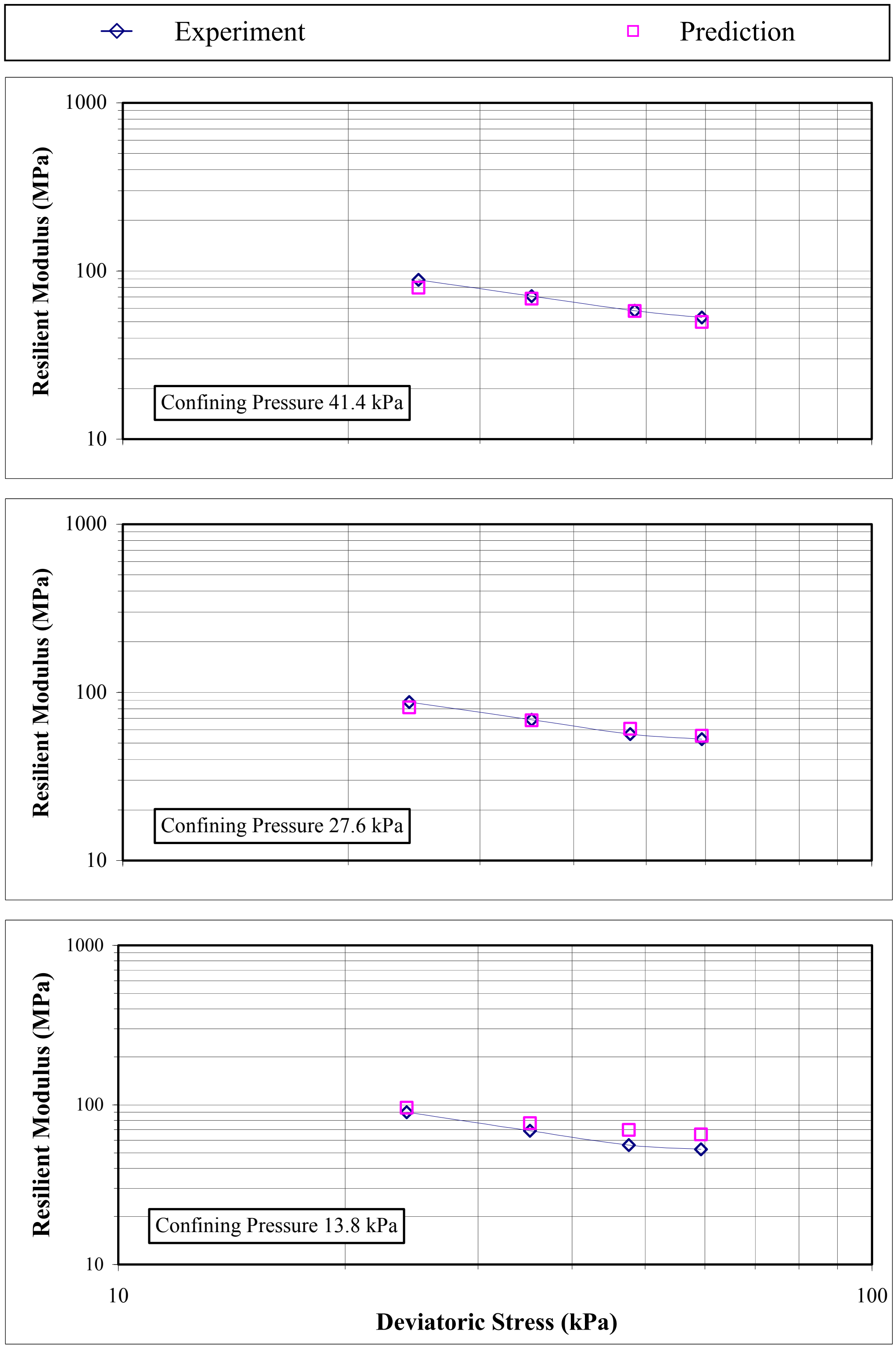

Figure 6-54 Resilient Modulus from Experiment and Multilayer Perceptrons Network (MLPN-3) Model: Specimen ROE-20B

1 kPa = 0.145 psi

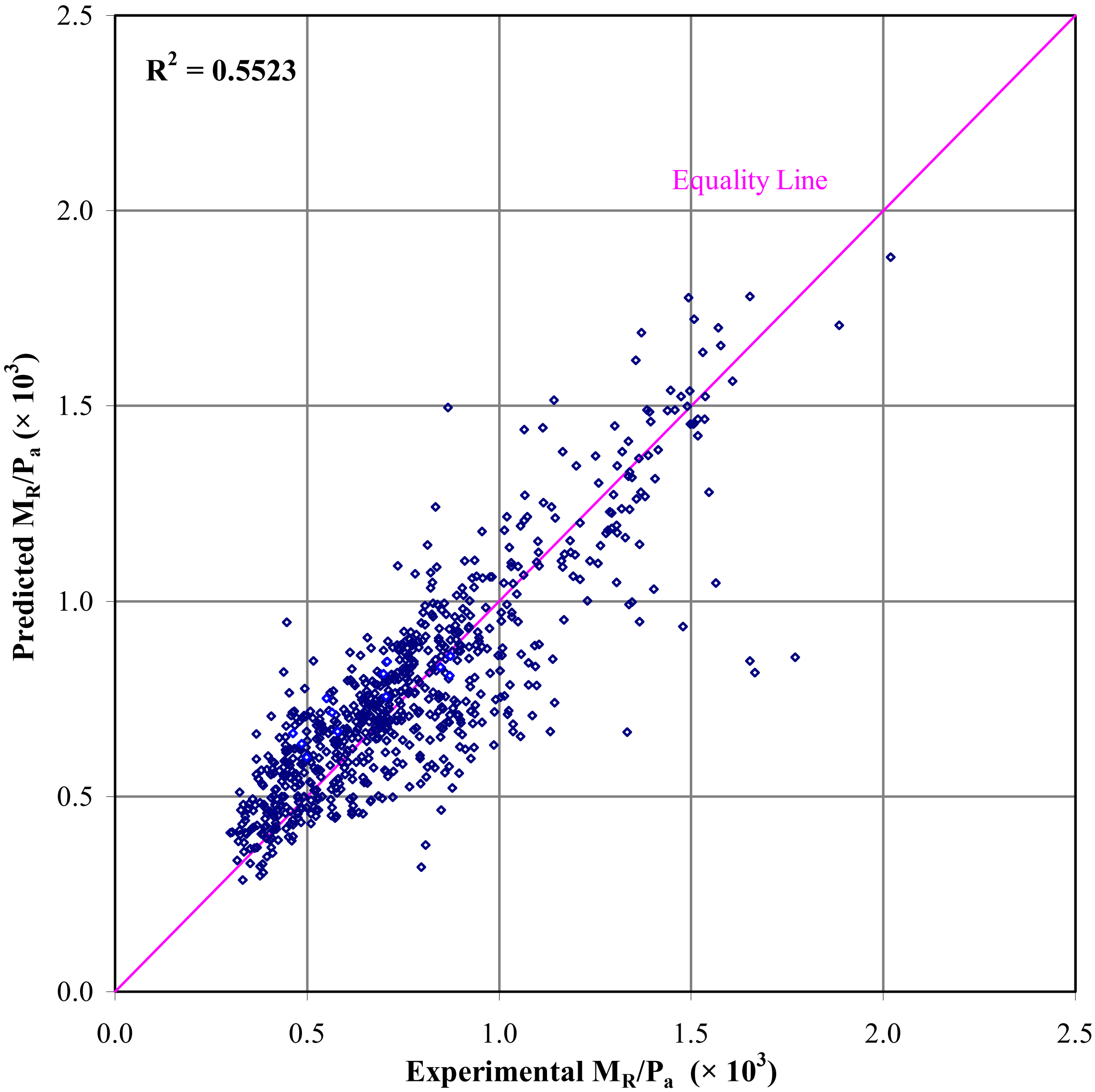

Figure 6-55 Comparison of Experimental and Back Predicted M_R/P_a for Development Dataset (Dry Specimens): Multilayer Perceptron Network (MLPN-2) Model

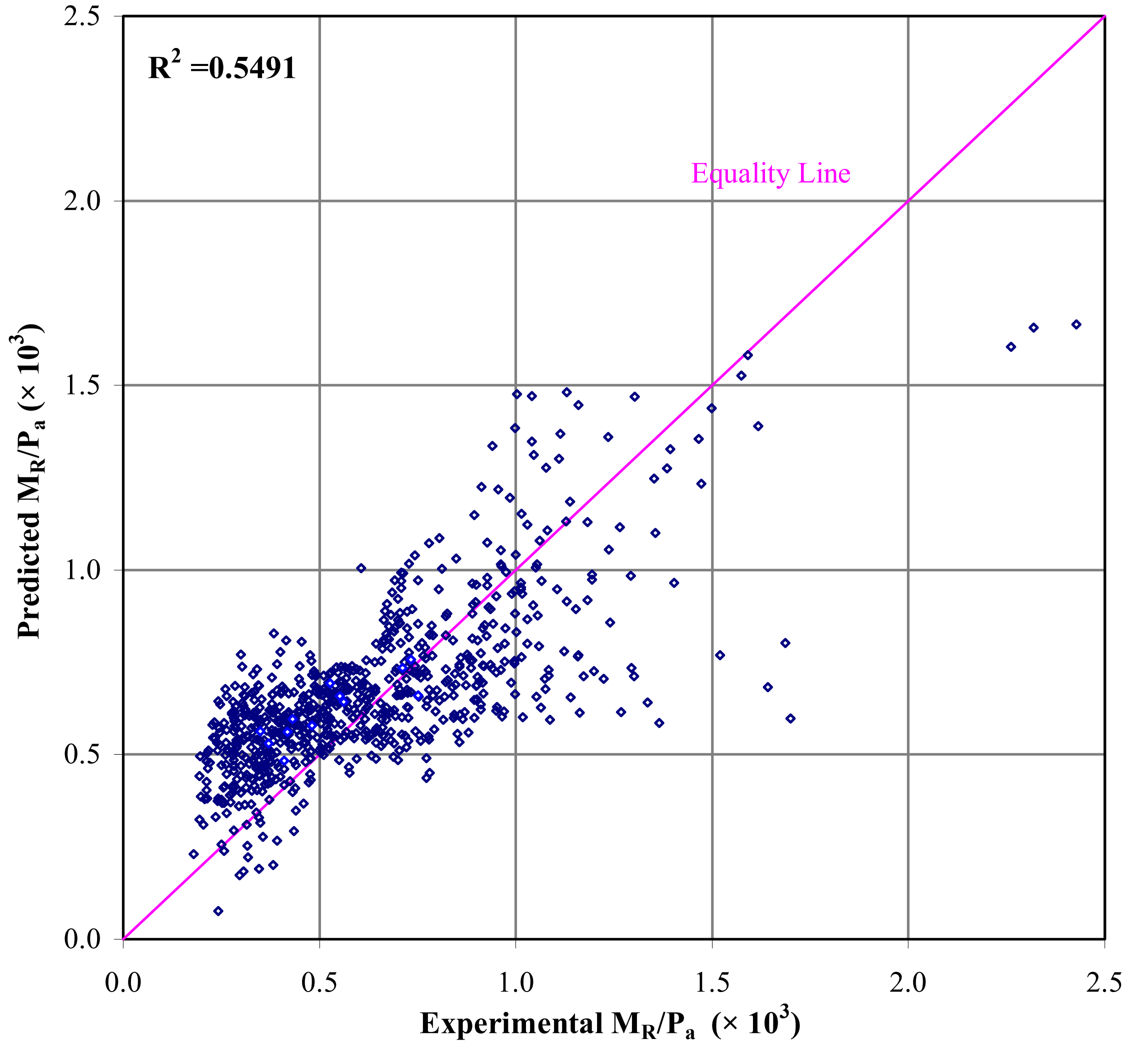

Figure 6-56 Comparison of Experimental and Back Predicted M_R/P_a for Development Dataset (wet Specimens): Multilayer Perceptron Network (MLPN-2) Model

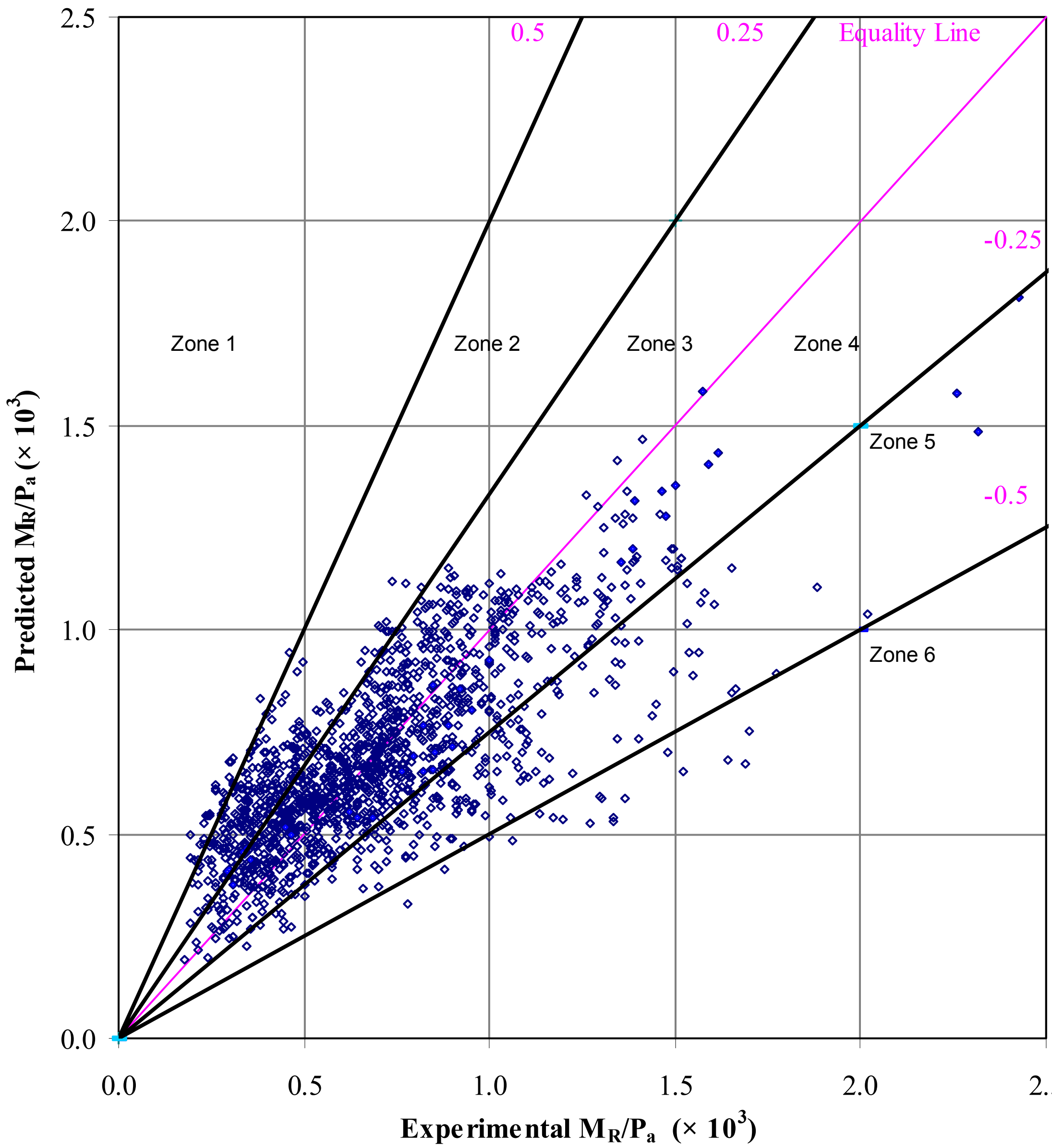

Figure 6-57 Design Chart for the MLPN-2 Model

CHAPTER 7

PAVEMENT DESIGN APPLICATION

7.1 Introduction

This chapter presents the application of a selected artificial neural network (ANN) model developed in Chapter 6 to pavement design. To demonstrate this application, typical pavement sections are designed based on the resilient modulus (M_R) values obtained experimentally as well as the (M_R) values predicted by the ANN model. The designed sections are then compared and evaluated. The ANN model used in this chapter is the Multilayer preceptrons network with two hidden layers (MLPN-2), which was determined to be the best prediction model in the present study. In this demonstration exercise, three different subgrade soils are selected – one (WOE-4B, SH 3) from Woodward County and two (ROE-3A, SH 20 and ROE-20B, SH 88) from Rogers County. A design M_R value is predicted using the MLPN-2 model based on the commonly used properties for each selected soil. , DARWin 3.1, pavement design software is utilized to determine the design thicknesses. DARWin 3.1 is one of the AASHTO software recommended for pavement design. This software implements the pavement design models presented in the 1993 AASHTO Design Guide. In this software, the structural design (structural number and thickness of each layer) of an asphalt pavement is based on the predicted subgrade M_R values. Finally, the structural numbers and the asphalt pavement thicknesses are calculated based on the experimental M_R values. A comparison of these results is presented in this chapter.

7.2 Resilient Modulus for Pavement Design

The predicted and experimental resilient modulus values for the three selected soils are presented in Table 7-1. It is seen that the experimental M_R values for soils WOE-4B and ROE-20B are lower than the corresponding predicted values. An opposite trend is seen for the third soil, ROE-3A. The maximum difference between the experimental and predicted M_R values for soil WOE-4B is 19.94 MPa (2,892 psi). The maximum differences for soils ROE-3A and ROE-20B, however, are much lower - 9.86 MPa (1,430 psi) and 7.28 MPa (1,056 psi), respectively.

7.3 Design Parameters

Before one can proceed with the design, there are several design parameters that need to be determined or assumed (Huang, 2004; AASHTO, 2002). These include design period, traffic data, reliability, and serviceability. The design period for the selected pavements is assumed to be 20 years. The initial two-way traffic for this design is assumed to as 11,378 with 3% of the traffic being heavy trucks (FHWA Class 5 or greater) (Yoder and Witczak, 1975; AASHTO, 1986; Huang, 2004). The equivalent single axle load (ESAL) is calculated from the information presented in Table 7-2. The ESAL for the present application is found to be 2,664,208. The Program determines the ESAL load based on the vehicle type, design period and growth factor. Table 7-3 presents the reliability (80% with a standard deviation of 0.49) and serviceability values used in this design application. These values are based on the recommendations by the AASHTO Design Guide (AASHTO, 1986). The initial and final serviceability values of the pavement are assumed as 4.2 and 3, respectively. These are typical values obtained from the AASHO Road Test (Yoder and Witczak, 1975; Huang, 2003). These design parameters were kept constant for all three soils. Only the subgrade M_R values are changed and their influence on the structural numbers and the design thickness is examined.

7.4 Pavement Design Results

Based on the design parameters selected in the preceding section, structural numbers and pavement thicknesses are calculated using DARWin 3.1 for each resilient modulus. The design results are summarized in Table 7-4. As expected, the design structural numbers of soils WOE-4B and ROE-20B from experimental M_R values are higher than the design structural numbers from the predicted M_R values. For the experimental M_R values, the design Structural Numbers (SN) are 4.72, 3.44, and 3.82 for soils WOE-4B, ROE-3A, ROE-20B, respectively. For the predicted M_R values, the corresponding design Structural Numbers (SN) are 3.98, 3.64, and 3.65.

In order to convert the design structural number to actual pavement thickness, a flexible pavement section (Asphalt Concrete (AC) is considered. In an AC pavement, the entire SN is converted to AC. Based on a typical value of 0.44 for the asphalt layer coefficient (AASHTO, 1986), the required asphalt thickness can be determined by dividing the structural number by the asphalt layer coefficient. Table 7-4 presents the required AC thickness for the calculated structural numbers pertaining to experimental M_R and predicted M_R.

It is evident that for soil WOE-4B the required AC thickness is under-predicted by 4.07 cm (1.6 in.), (approximately 15%). It should be noted that the WOE-4B soil was from western Oklahoma and the MLPN-2 model was developed with no soil from that part of the state. So, this level of difference in pavement thickness may be justifiable.

On the other hand, for soils ROE-3A and ROE-20B the differences in the required AC thickness are 1.27 cm (0.5 in.), (approximately (-6%) and 1.02 cm (0.4 in), (approximately (+5%), respectively. Both of these soils are from eastern Oklahoma, and the predicted M_R values and the corresponding pavement design thicknesses are closer to the values obtained from the experimental M_R. Overall, the design thicknesses are fairly comparable, indicating that the MLPN-2 model is capable of predicting the design M_R values based on routine soil properties, for pavement design applications.

Increasing the reliability factor in the design may compensate the lack of accuracy in the pavement design thickness for the predicted M_R from western Oklahoma. One soil (WOE-4B) is used to illustrate this argument. The results of increased reliability, for this selected soil (WOE-4B) and predicted M_R is presented in Table 7-5. Based on this table, increasing the reliability from 80% to 90%, the difference between pavement thickness (when using experimental M_R and predicted M_R) reduces from 15% to less than 7%. As mentioned previously, these results are very encouraging, indicating that it would be possible to use the MLPN-2 model to predict design M_R values based on routine soil properties and use them to design pavement sections.

Table 7-1 Subgrade Resilient Moduli for Pavement Design

Specimen ID and Location	Resilient Modulus	
	Experiment	Predicted (MLPN-2)
WOE-4B SH 3, Woodward County	38.34 MPa (5,560 psi)	58.29 MPa (8,452 psi)
ROE-3A SH 20, Rogers County	81.72 MPa (11,850 psi)	71.86 MPa (10,420 psi)
ROE-20B SH 88, Rogers County	64.18 MPa (9,306 psi)	71.46 MPa (10,362 psi)

Table 7-2 Equivalent Single Axle Load (ESAL) Calculation

Design Period (years)	20
Two-Way Traffic (ADT)	11,378
Number of Lanes in Design Direction	2
Percent of All Trucks in Design Lane	80%
Percent Trucks in Design Direction	50%
Percent Heavy Trucks (of ADT) FHWA Class 5 or Greater	3%
Average Initial Truck Factor (ESALs/truck)	2.338
Annual Truck Volume Growth Rate	1.5%
Total Calculated Cumulative ESALs	2,664,208

Table 7-3 Reliability and Serviceability

Reliability Level	80%
Overall Standard Deviation	0.49
Initial Serviceability	4.2
Terminal Serviceability	3.0

Table 7-4 Pavement Design Results

Specimen ID	Design Structural Number (SN)	Required Asphalt Thickness
WOE-4B (Experiment)	4.72	27.18 cm (10.7 in.)
WOE-4B (MLPN-2)	3.98	23.11 cm (9.1 in.)
ROE-3A (Experiment)	3.44	19.81 cm (7.8 in.)
ROE-3A (MLPN-2)	3.64	21.08 cm (8.3 in.)
ROE-20B (Experiment)	3.82	22.10 cm (8.7 in.)
ROE-20B (MLPN-2)	3.65	21.08 cm (8.3 in.)

Table 7-5 Comparison of the Effect of Reliability in SN and Pavement Design

WOE-4B	Reliability of Design	Design Structural Number (SN)	Required Asphalt Thickness
Experiment	80	4.72	27.18 cm (10.7 in.)
(MLPN-2)	80	3.98	23.11 cm (9.1 in.)
(MLPN-2)	85	4.15	23.95 cm (9.43 in.)
(MLPN-2)	90	4.35	25.12 cm (9.9 in.)
(MLPN-2)	95	4.67	26.95 cm (10.6 in.)

CHAPTER 8

SUMMARY, CONCLUSIONS, AND RECOMMENDATIONS

8.1 Summary

The objective of this study was to determine relationships or models between M_R and routinely determined material parameters. To this end, soils from seventeen highway project sites throughout Oklahoma were collected in accordance with the Oklahoma Department of Transportation (ODOT) specifications for Pedagogical Soil Survey. It was decided to use the results from fourteen sites from fourteen counties to develop the relationships or models. Data from these sites are collectively referred to as the Development Dataset. Test data from the remaining three sites, representing two different counties (Rogers County and Woodward County) are used to evaluate the developed models. These test data are collectively referred to as the Evaluation Dataset. Consequently, the development dataset contained test data from 63 soil samples, while the evaluation dataset contained test data from 34 soil samples.

The routine material parameters selected in the development of the models include moisture content (w), dry density (γ_d), plasticity index (PI), percent passing No. 200 sieve (P_{200}), and unconfined compressive strength (U_c). Bulk stress (θ) and deviatoric stress (σ_d) were used to identify the state of stress. The choice for the selection of these parameters was partly based on the ODOT requirements for conducting pedagogical soil survey. The influence of these parameters in the Mechanistic-Empirical pavement design also played a role in this selection. Of the seven independent variables used here, only two (θ and σ_d) are stress-related. The five remaining parameters (w, γ_d, PI, P_{200}, and U_c) are determined from routine soil testing.

Furthermore, the moisture content (w) and dry density (γ_d) represent the state of the specimens.

The laboratory testing program pursued in this study includes Atterberg Limits, sieve analysis and standard proctor tests. Based on the ODOT specifications, two specimens were prepared and tested for resilient modulus (M_R) for each soil. One of the M_R specimens was prepared at the Optimum Moisture Content (OMC) and 95% of the maximum dry density, while the other specimen was prepared at maximum dry density and 2% wet of the OMC. This yielded one hundred twenty six M_R specimens tests for the development dataset. The M_R test results were evaluated for quality assurance. Based on the high standard deviation of M_R (in excess of 340 Mpa) and high measurement error (in excess of 30%) for loading sequences 1, 6 and 11, the M_R values corresponding to these sequences were not included in the model development. Consequently, the development dataset consisted of 1512 M_R values. A similar approach was followed in the test program for the evaluation dataset. At the conclusion of each M_R test, an unconfined compression test was performed on the same Specimen. Although this test is not required by the ODOT specifications, it was included in the present study because a number of previous studies have indicated a strong correlation between M_R and unconfined compression.

Several statistical models were developed in this study. These models include: stress-based, multiple regression, polynomial, and factorial. Each model was ranked based on its R^2 (goodness of fit) and F values (significance of the model) for the development dataset. Based on the R^2 and F values, the second order polynomial and factorial models were further considered for the evaluation dataset. An evaluation of the two models indicated that for the combined development and evaluation datasets neither a second order polynomial nor a factorial model is a good statistical model for evaluating M_R from the selected routinely determined properties.

As a result, a more complex modeling technique, Artificial Neural Network (ANN), was employed in this study. Six different models were considered in this phase, namely, Linear Network (LN), Generalized Regression Neural Networks (GRNN), Radial Basic Function Networks (RBFN), and Multi-Layer Perceptrons Networks (MLPN) with one, two and three hidden layers (MLPN-1, MLPN-2, and MLPN-3). The degree of complexity of the models increases from LN being the simplest model with no hidden layers to MLPN models. The models were ranked based on their R^2 (goodness of fit) values. Based on the R^2 values, the MLPN-2 was determined to be the best model. The back-predictions of the development dataset for the ANN models were better than their statistical counterparts. A sensitivity study of the ANN models was performed. It was determined that the unconfined compression was a major contributor to the relationship between R_M and routinely determined material parameters, as reported in some previous studies. The MLPN-2 model was further evaluated to examine the effect of different moisture and density condition on the model. At this stage two additional MLPN-2 models were developed and evaluated by separating the development and evaluation datasets according to the specimens moisture content and dry density (OMC and 95% of the maximum dry density, and OMC+ 2% moisture content and maximum dry density). A careful evaluation of these two new MLPN-2 models indicated that even though these models did a reasonably good job for their respective datasets, they were incapable of extrapolation (i.e., the MLPN-2 model developed on the basis of OMC and

95% maximum dry density is unable to back predict the M_R values from the OMC+2% and maximum dry density dataset, and vice versa). Furthermore, during the sensitivity analysis it was evident that the effect of moisture content, dry density, and plasticity index were masked by the unconfined compression. However, since the thrust of this study was to develop models to be used for Level 2 and Level 3 pavement designs for Oklahoma subgrade, the MLPN-2 model that includes both moisture contents and dry densities was considered the best.

In order to illustrate the application of the developed model, the AASHTO flexible pavement design methodology was used to design asphalt concrete pavement sections. The design M_R values from three soil specimens from the evaluation dataset were calculated from the MLPN-2 model. The pavement sections determined from the experimental M_R values were compared with the pavement sections determined from the M_R values predicted by the MLPN-2 model.

8.2 Conclusions

The following conclusions were drawn from the present study summarized above:

(1) The stress-based model was found to have a low R^2 value (0.3226), with significant scatters in the back-prediction of the development dataset. The F value for this model was found to be 253.37, indicating that a more complex model may be needed in correlating M_R with the selected model parameters.

(2) The R^2 and F values for the multiple linear regression model were found to be 0.4357 and 165.88, respectively, indicating a significant improvement over the stress-based model. The back-predicted values correlated reasonably well with

the experimental values in the low range (up to 1,000) of the M_R/P_a values, beyond which larger deviations were observed. The model exhibited erratic prediction for the evolution dataset. Also, the multiple linear regression model and the linear network (LN) model, without any hidden layer, behaved alike, as expected.

(3) A second order polynomial multiple regression model was developed for the development dataset. The R^2 and F values for this model were found to be 0.4858 and 101.02, respectively. These values indicate a slight improvement over the multiple linear regression model. Although the effect of this improvement was not visually noticeable for the overall development dataset, the improvement was evident through the improvement in the R^2 values for the evolution dataset. Overall, the second order polynomial multiple regression model was a better model than the multiple linear regression model.

(4) One of the most complicated models considered in this study was a full factorial model. This model had 126 terms, and the R^2 and F values for the development dataset was found to be 0.6595 and 23.74, respectively. Based on these values and not considering the evaluation dataset, this model appeared to be the best statistical model. However, the R^2 values for the evaluation dataset (Roger County (0.4021), Woodward County (0.0962), and combined dataset (0.3634)) were relatively low, indicating that even this model was not a good model for the combined datasets (development and evaluation). A high R^2 value (0.4021) for the Rogers County soils is an indicator that these soils are similar to those in the evaluation dataset.

(5) The linear network (LN) model without having any hidden layer was found to have the lowest R^2 (0.4323), as expected, with significant scatters in data. For the GRNN model, having two hidden layers, the R^2 value (0.6284) improved significantly. The back-predicted values correlated with the experimental values well in the low range of the M_R/P_a values, up to approximately 1,000, beyond which larger deviations were observed. The fact that the GRNN model treats data points as a cluster than individual training case was clearly evident from the back-predicted response.

(6) For the RBFN model, with one hidden layer, the R^2 value for the development dataset improved further (0.6015). Also, the back predicted response (M_R as a function of deviatoric stress) for three selected specimens (MA-3B, NO-7A, and OS-1B) showed significant improvements. A better R^2 and improvements in back-prediction may be attributed to the use of hyperspheres in the RBFN model in the form of Gaussian (bell-shaped) function-type response surface in this model.

(7) The number of hidden layers in the MLPN models in STATISTICA can range from one to three. In the present study, three separate MLPN models (MLPN-1, MPLN-2, and MLPN-3) were developed with different number of hidden layers in each model. The R^2 values of the MLPN models were found to be 0.5733, 0.5744, and 0.5587 for one, two and three hidden layers, respectively, indicating that the MLPN-3 might have reached over-learning or over-fitting. Overall, the MLPN-2 model performed well.

(8) Although the RBFN model had higher R^2 than the MLPN-2 model for the development dataset, its predictive capability for the Woodward County soils was poor (R^2 of 0.0251). A lower R^2 value for the Woodward County soils partly results from the differences in the characteristics of these soils, as noted previously. The MLPN-2 model did a much better job in predicting the resilient modulus of subgrade soils in the evaluation dataset (overall R^2 = 0.5848), including the Woodward County soils (R^2 = 0.6308).

(9) For both selected specimens (WOE-4B and ROE-20B) from the evaluation dataset, the MLPN-2 model under-predicted the M_R values. This may be a potential concern in pavement design applications where lower thicknesses may result from using the predicted M_R values in design.

(10) Overall, the MLPN-2 model was found to be the best model for the present development and evaluation datasets. This model as well as the other models could be refined using an enriched database.

(11) ANN models are found to be a useful resource for correlating resilient modulus with routine soil properties. The input parameters used in ANN modeling here were motivated by the routine soil properties evaluated by the Oklahoma Department of Transportation for roadway projects. Other pertinent properties may be used in future developments.

(12) The MLPN-2 model was used to present the application of developed model in pavement design. Based on a reliability of 80%, the differences in the percent calculated Structural Number for three cases were found to be 15% for Woodward County and 6% and 4% for Rogers county. It is, therefore, possible

to predict the M_R for pavement design with a reasonable degree of certainty. It is, however, recommended that when using the MLPN-2 model the degree of reliability should be increased to as much as 90 percent for counties that were not included in the development of the model to insure that the model does not under predict the M_R values significantly.

8.3 Recommendations

The following recommendations are made for further studies.

(1) The development dataset and the evaluation dataset in this study consisted of 63 and 34 soils, respectively. It is recommended that these datasets be enriched by adding additional sites from throughout Oklahoma. It is suggested that different geological features be considered in selecting additional sites. Traning the ANN models using an enriched dataset is likely to improve the predictive capabilities of these models. Also, as the datasets include more soils from different locations, the models will become more representative of diversity in Oklahoma soils.

(2) This study combined the effect of silt and clay in percent passing # 200 sieve (P200). It is recommended that the effect of silt and clay be separated in a future study. This may improve the predictive capability of the models.

(3) The R^2 values for the ANN models were found to be around 0.6 indicating that the developed models are not fully capable of capturing the relationship between M_R and the selected material parameters. It is, therefore, recommended that other material parameters such as friction angle, cohesion, swelling potential, percent clay and percent silt, group index (GI), and geological features such as mineralogy be included in the future model development efforts.

(4) Since it is determined that more complex modeling techniques are required to capture the relationship between M_R and other material parameters, it is recommended that more complex modeling tools such as Recurrent Neural Network (RNN) or Data Mining be employed in future model development efforts.

(5) The accuracy of measuring devices for M_R should be improved. This may be achieved using a lower capacity load cell, more precise LVDTs, and larger diameter samples. A future study may address some of these issues. .

(6) Field studies may be conducted to correlate the laboratory measured M_R with in-situ measured M_R by using FWD or other in-situ testing methods. Significant studies have been done in other states in this area which may be a basis for similar studies in Oklahoma.

REFERENCES

Ali, H.E. and Najjar, Y.M. (2000). "Simulating the CD Behavior of Nevada Sand Via Feed-back Network Approach," *Proceedings, 14th Engineering Mechanics Conference*, The University of Texas, Austin, Texas, May 21-24.

American Association of State Highway and Transportation Officials (AASHTO) (1986). *Standard Specifications for Transportation Materials and Methods of Sampling and Testing,* Washington, D. C.

American Association of State Highway and Transportation Officials (AASHTO) (2004). *Standard Specifications for Transportation Materials and Methods of Sampling and Testing,* Washington, D. C.

American Society of Standard and Materials (ASTM) (2005). 2005 Annual Book of ASTM Standards, Vol. 4.08, Philadelphia, Pennsylvania.

Annamalai, M., Laguros, J.G., and Kumar, S. (1975). "Predictability of Volume Changes of Shales," *Proc. Istanbul Conference 1975*, Vol. 1, Istanbul Teknik Universitesi, Istanbul, Turkey, pp. 197-203.

Ashraf, R. and George, K.P. (2003). "Falling Weight Deflectometer for Estimating Subgrade Elastic Moduli," *Journal of Transportation Engineering*, Vol. 129, No. 1, American Society of Civil Engineering, Reston, Virginia, pp. 100-107.

Bishop, C. (1995). *Neural Networks for Pattern Recognition*, University Press, Oxford, United Kingdom.

Bors, A.G. (2001). "Introduction of the Radial Basis Function (RBF) Networks," Online *Symposium for Electronics Engineers*, Issue 1, Vol. 1, DSP Algorithms: Multimedia, pp. 1-7.

BP Corporation and EPA. (2002). *Monitoring Well Comparison Study: An Evaluation of Direct-Push Versus Conventional Monitoring Wells*, U.S. Environmental Protection Agency, Washington, D.C.

Carling, A. (1992). *Introducing Neural Networks*, Sigma Press, Wilmslow, United Kingdom.

Carmichael, R.F. III, and Stuart, E. (1978). "Predicting resilient modulus: A study to determine the mechanical properties of subgrade soils," *Transportation Research Record 1043*, Transportation Research Board, National Research Council, Washington, D.C., pp. 20-28.

Chen, D.H., Wang, J.N., and Bilyeu, J. (2001). "Application of the DCP in Evaluation of Base and Subgrade Layers," *80th Annual Meeting of the Transportation Research Board*, January 2001, Transportation Research Board, National Research Council, Washington, D.C.

Chen, D.H., Zaman, M.M., and Laguros, J.G. (1995). "Resilient Moduli of Aggregate Materials: Variability Due to Testing Procedure and Aggregate Type," *Transportation Research Record 1462*, Transportation Research Board, National Research Council, Washington, D.C., pp. 57-64.

Croney, D. and Croney, P. (1991). *The Design and Performance of Road Pavements*, McGraw-Hill Book Co., New York.

Dai, S. and Zollars, J. (2002). "Resilient Modulus of Minnesota Road Research Project Subgrade Soil," *Transportation Research Record 1786*, Transportation Research Board, National Research Council, Washington, D.C., pp. 20-28.

Drumm, E.C., Boateng-Poku, Y., and Pierce, T.J. (1990). "Estimation of subgrade resilient modulus from standard tests," *Journal of Geotechnical Engineering,* Vol. 116, No. 5, pp. 774-789.

Drumm, E.C., Reeves, J.S., Madgett, M.R., and Trolinger, W.D. (1997). "Subgrade Resilient Modulus Correction for Saturation Effects," *Journal of Geotechnical and Geoenvironmental Engineering*, Vol. 123, No. 7, American Society of Civil Engineering, New York, New York, pp. 663-670.

Dobson, A.J. (1990). *An Introduction to Generalized Linear Models*, Chapman & Hall, New York.

Dunlap, W.S. (1963). "A Report on a Mathematical Model Describing the Deformation Characteristics of Granular Materials," *Technical Report 1, Project 2-8-62-27*, TTI, Texas A&M University, Texas.

Elliott, R.P. and Thornton, S.I. (1988). "Simplification of Subgrade Resilient Modulus Testing," *Transportation Research Record 1192*, Transportation Research Board, National Research Council, Washington, D.C., pp. 1-7.

Farrar, M.J. and Turner, J.P. (1991). "Resilient Modulus of Wyoming Subgrade Soils," *Mountain Planins Consortium Report No. 91-1*, The University of Wyoming, Luramie, Wyoming.

Fausett, L.V. (1994). *Fundamentals Neural Networks: Architecture, Algorithms, and Applications*, Prentice-Hall, Inc., Englewood Cliffs, New Jersey.

Fernandez-Juricic, E., Sallent, A., Sanz, R., and Rodriguez-Prieto, I. (2003). "Testing the Risk-disturbance Hypothesis in a Fragmented Landscape: Non-linear Responses of House Sparrows to Humans", *The Condor*, Vol. 105, The Cooper Ornithological Society, Oregon, pp. 316-326.

FHWA (2000). *Our Nation's Highways – 2000*, Publication No. FHWA-PL-01-1012, Office of Highway Policy Information, FHWA, Washington, D.C.

FHWA (2002). *Study of LTPP Laboratory Resilient Modulus Test Data and Response Characteristics*, Final Report, October 2002, Publication No. FHWA-RD-02-051, Office of Engineering Research and Development, McLean, Virginia.

Fredlund, D.G., Vanapalli, S.K., Xing, A., and Pufahl, D.E. (1995). " Predicting the Shear Strength Functions for Unsaturated Soils using Soil-Water Characteristic Curves." 1st International Conference on Unsaturated Soils, ed. Alonso, E.E., and Delage, P., Paris September 6-8, 1995, A. A. Balkema, pp. 63-69

Gardner, M.W. and Dorling, S.R. (1998). "Artificial Neural Networks (The Multilayer Perceptron) – A Review of Applications in the Atmospheric Sciences," *Atmospheric Environment*, Vol. 32, Issues 14-15, Elsevier B.V., Philadelphia, Pennsylvania, pp. 2627-2636.

George, K.P. (1992). "Resilient Testing of Soils Using Gyratory Testing Machine," *Transportation Research Record 1369*, Transportation Research Board, National Research Council, Washington, D.C., pp. 63-72.

George, K.P. (2004). "Prediction of Resilient Modulus from Soil Index Properties," *Final Report November 2004*, FHWA/MS-DOT-RD-04-172, Mississippi Department of Transportation, Jackson, Mississippi.

George, K.P., Bajracharya, M., and Stubstad, R. (2004). "Subgrade Characterization Employing the Falling Weight Deflectometer," *Transportation Research Record 1869*, Transportation Research Board, National Research Council, Washington, D.C., pp. 73-79.

George, K.P. and Uddin, W. (1996). "Verifying Kneading Resilient Modulus of Soils with Backcalculated Values," *Transportation Research Record 1406*, Transportation Research Board, National Research Council, Washington, D.C., pp. 116-123.

Gurp, C., Groenendijk, J., and Beuving, E. (2000). "Experience with Various Types of Foundation Tests," *Proceedings of the Fifth International Conference on Unbound Aggregate in Roads*, Nottingham, United Kingdom.

Hassoun, M.H. (1995). *Fundamentals of Artificial Neural Network*, MIT Press, Cambridge, Massachusetts.

Haykin, W.L. (1994). *Neural Networks: A Comprehensive Foundation*, Macmillan College Publishing, New York.

Hays, W.L. (1988). *Statistics*, 4th Edition, CBS College Publishing, New York.

Hill, T. and Lewicki, P. (2006). *STATISTICS Methods and Applications*, StatSoft, Tulsa, Oklahoma.

Houston, W.N., Houston, S.L., and Anderson, T.W. (1994). "Stress State Consideration for Resilient Modulus Testing of Pavement Subgrade," *Transportation Research Record 1406*, Transportation Research Board, National Research Council, Washington, D.C., pp. 124-132.

Hopkins, T.C. and Beckham, T.L. (2000). "Influence of Clay Fraction and Moisture on the Behavior of Soil-Aggregate Mixtures," *Proceedings of the Fifth International Symposium on Unbound Aggregates in Roads*, UNBAR 5, University of Nottingham, United Kingdom, A. Balkema/Rotterdam/Brookfield.

Hopkins, T.C., Beckham, T.L., Sun, L., and Pfalzer, B. (2004). "Kentucky Geotechnical Database," *Research Report KTC-03-06/SPR-177-98-1F*, University of Kentucky Transportation Center, College of Engineering, Lexington, Kentucky.

Hopkins, T.C., Slepak, M.E., and Sun, L. (2002). "Limitting Equilibrium Methods in Bearing Capacity Analysis of Flexible Pavements Reinforced With Geosynthetics," *Proceedings*, Sixth International Conference on the Bearing Capacity of Roads, Railways, and Airfields (BCRA'02), Lisbon, Portugal.

Huang, Y.H. (2003). *Pavement Analysis and Design*, 2nd Edition, Prentice Hall, Upper Saddle River, New Jersey.

Kachigan, S.K. (1986). *Statistical Analysis: An interdisciplinary Introduction to Univariate and Multivariate Methods*, Redius Press, New York.

Kamal, M.A., Dawson, A.R., Farouki, D.A., Hughes, D.A.B., and Sha'at, A.A. (1996). "Field and Laboratory Evaluation of the Mechanical Behavior of Unbound Granular Materials in Pavements," *Transportation Research Record 1406*, Transportation Research Board, National Research Council, Washington, D.C., pp. 88-97.

Kariuki, P.C. and Van Der Meer, F. (2004). "A Unified Swelling Potential Index for Expansive Soils," *Engineering Geology*, No. 72, Elsevier B.V., Amsterdam, Netherlands, pp. 1-8.

Khazanovich, L., Celauro, C., Chadbourn, B., Zollars, J., and Dai, S. (2006). "Evaluation of Subgrade Resilient Modulus Predictive Model for Use in Mechanistic-Empirical Pavement Design Guide," *Transportation Research Record 1947*, Transportation Research Board, National Research Council, Washington, D.C., pp. 155-166.

Khedr, S. (1985). "Deformation Characteristics of Granular Base Course in Flexible Pavements," *Transportation Research Record 1043*, Transportation Research Board, National Research Council, Washington, D.C., pp. 131-138.

Kim, D., Kweon, G., and Lee, K. (1997). "Alternative Method of Determining Resilient Modulus of Compacted Subgrade Soils Using Free-Free Resonant Column Test," *Transportation Research Record 1577*, Transportation Research Board, National Research Council, Washington, D.C., pp. 62-69.

Kim, D. and Stokoe II, K.H. (1992). "Characterization of Resilient Modulus of Compacted Subgrade Soils Using Resonant Column and Torsional Shear Tests," *Transportation Research Record 1369*, Transportation Research Board, National Research Council, Washington, D.C., pp. 83-91.

Kohonen, T. (1989). *Self-Organization and Associative Memory*, 3rd Edition, Springer-Verlag, Berlin, Germany.

Lee, W., Bohra, N.C., Altschaeffl, A.G., and White, T.D. (1997). "Resilient Modulus of Cohesive Soils," *Journal of Geotechnical and Geoenvironmental Engineering*, Vol. 123, No. 2, American Society of Civil Engineering, New York, New York, pp. 131-136.

Li, D., and Selig, E.T. (1994). "Resilient Modulus for Fine-Grained Subgrade Soils," *Journal of Geotechnical Engineering*, Vol. 120, No. 6, American Society of Civil Engineering, New York, New York, pp. 939-957.

Long, B., Hossain, M., and Gisi, A.J. (1996). "Seasonal Variation of Backcalculated Subgrade Moduli," *Transportation Research Record 1577*, Transportation Research Board, National Research Council, Washington, D.C., pp. 70-80.

Lobbezoo, J.P. and Vanapalli, S.K., (2002). "A Simple Technique for Estimating the Coeficent of Permeability of Unsaturated Soils." 55th Canadian Geotechnical Conference

Marteau, P.F. (2004). "Conditional Prediction of Markov Processes Using Non-Parametric Viterbi Algorithm – Comparison with MLP and GRNN Models," *Proc. 4th WSEAS Neural Networks and Application Conference*, WSEAS, Udine, Italy, March 2004.

May, R.W. and Witczah, M.W. (1981). "Effective Granular Modulus to Model Pavement Response," *Transportation Research Record 810*, Transportation Research Board, National Research Council, Washington, D.C., pp. 1-9.

McCullagh, P. and Nelder, J.A. (1989). *Generalized Linear Models*, 2nd Edition, Chapman & Hall, New York.

Mehrotra, K., Mohan, C.K., and Ranka, S. (1996). *Elements of Artificial Neural Networks*. MIT Press, Cambridge, Massachusetts.

Meyerhof, G.G. (1965). "Shallow Foundations," *Journal of Soil Mechanics and Foundations Division*, Vol. 91, No. SM2, American Society of Civil Engineering, New York, New York, pp. 21-31.

Mohammad, L.N., Huang, B., Puppala, A.J., and Allen, A. (1999). "Regression Model for Resilient Modulus of Subgrade Soils," *Transportation Research Record 1687*, Transportation Research Board, National Research Council, Washington, D.C., pp. 47-54.

Mohammad, L.N., Puppala, A.J., and Alavilli, P. (1994). "Influence of Testing Procedure and LVDT Location on Resilient Modulus of Soils," *Transportation Research Record 1462*, Transportation Research Board, National Research Council, Washington, D.C., pp. 91-101.

Montgomery, D.C., Peck, E.A., and Vining, G.G. (2006). *Introduction to Linear Regression Analysis (Wiley Series in Probability and Statistics)*, John Wiley & Sons Inc., New Jersey.

Moossazadeh, J.M., and Witczak, M.W. (1981). "Prediction of Subgrade Moduli for Soil that Exhibits Nonlinear Behavior," *Transportation Research Record 810*, Transportation Research Board, National Research Council, Washington, D.C., pp. 9-17.

Motulsky, H.J. (2005). *Prism 4 Statistics Guide – Statistical Analyses for Laboratory and Clinical Researchers*, GraphPad Software Inc., San Diego, CA.

Myers, R.H., Montgomery, D.C., and Vining, G.G. (2001). *Generalized Linear Models: With Applications in Engineering and the Sciences*, John Wiley & Sons Inc., New Jersey.

Najjar, Y.M., Basheer, I.A., Ali, H.E., McReynolds, R.L. (2000). "Swelling Potential of Kansas Soils: Modeling and Validation Using Artificial Neural Network Reliability Approach," *Transportation Research Record 1736*, Transportation Research Board, National Research Council, Washington, D.C., pp. 141-147.

Narayan, S. (2002). "Using Genetic Algorithms to Adapt Neuron Functional Forms," *Proc. Artificial Intelligence and Soft Computing, July 2002*, Banff, Canada.

Nazzal, M.D. (2003). "Field Evaluation of In-Situ Test Technology for $Q_c \backslash Q_A$ During Construction of Pavement Layers and Embankments," *Master Thesis*, Department of Civil and Environmental Engineering, Louisiana State University, Baton Rouge, Louisiana.

NCHRP (1997). "Laboratory Determination of Resilient Modulus for Flexible Pavement Design," Final report, *Project 1-28*, NCHRP, Transportation Research Board, Washington D.C.

NCHRP (2003). "Procedure for Resilient Modulus of Unstabilized Aggregate Base and Subgrade Materials," *Project 1-28A*, NCHRP, Transportation Research Board, Washington D.C.

NCHRP (2004). "Guide for Mechanistic-Empirical Design of New and Rehabilitated Pavement Structures," *Final Report March 2004, Project 1-37A*, NCHRP, Transportation Research Board, Washington, D.C.

Pandey, K.K. (1996). "Evaluation of Resilient Moduli and Layer Coefficients of a Coal Ash Stabilized Marginal Aggregate Base for AASHTO Flexible Pavement Design," *Ph.D. Dissertation*, School of Civil Engineering and Environmental Science, University of Oklahoma, Norman, Oklahoma.

Park, H.I., Kweon, G.C., and Lee, S.R. (2006). "Prediction of Resilient Modulus of Subgrade Soils and Subbase Materials Based on Artificial Neural Network."

Patterson, D. (1996). *Artificial Neural Networks*, Prentice Hall, Singapore.

Ping, W.V., Yang, Z., and Ho, R. (1998). "Effect of Moisture on Resilient Characteristics of Compacted Granular Subgrades," Paper presented at the 77the Transportation Research Board Meeting, January 1998.

Ping, W.V. and Ge, L. (1996). "Field Verification of Laboratory Resilient Modulus Measurement on Subgrade Soils," *Transportation Research Record 1577*, Transportation Research Board, National Research Council, Washington, D.C., pp. 53-61.

Quintus, H.V. and Killingsworth, B. (1998). *Analyses Relating to Pavement Material Characterizations and Their Effects on Pavement Performance*, Publication FHWA-RD-97-085, FHWA, Washington, D.C.

Rada, G. and Witczak, M. (1981). "Comprehensive Evaluation of Laboratory Moduli Results for Granular Material," *Transportation Research Record 810*, Transportation Research Board, National Research Council, Washington, D.C., pp. 23-33.

Rahim, A.M. and George, J.P. (2004). "Subgrade Soil Index Properties to Estimate Resilient Modulus," *Paper Presented at 83rd Annual Meeting of Transportation Research Board*, Transportation Research Board, Washington D.C.

Rankine, R.M. and Sivakugan, N. (2005). " Prediction of Paste Backfill Performance Using Artificial Neural Networks," *Proc. the 16th ISSMGE*, Vol. 2, Osaka, pp. 1107-1110.

Ripley, B.D. (1996). *Pattern Recognition and Neural Networks*, Cambridge University Press, Cambridge, UK.

Rumelhart, D.E. and McClelland, J. (1986). *Parallel Distributed Processing, Vol. 1*, MIT Press, Cambridge, Massachusetts.

Runyon, R.P. and Haber, A. (1976). *Fundamentals of Behavioral Statistics*, Addison-Wesley, Reading, Massachusetts.

Russell, H.S. and Hossain, M. (2000). "Estimation of Design Resilient Modulus of Fine-Grained Subgrade Soil from Falling Weight Deflectometer Tests." *Geotechnical Special Publications No. 98: Pavement Subgrade, Unbound Materials, and Nondestructive Testing*, American Society of Civil Engineering, New York, New York, pp. 87-103.

Santha, B.L. (1994). "Resilient Modulus of Subgrade Soils: Comparison of Two Constitutive Equations," *Transportation Research Record 1462*, Transportation Research Board, National Research Council, Washington, D.C., pp. 79-90.

Schioler, H. and Hartmann, U. (1992). "Mapping Neural Network Derived from the Parzen Window Estimator," *Neural Networks*, Vol. 5, No. 6, pp. 903-909.

Schmertmann, J.H., Hartman, J.P., and Brown, P.B. (1978). "Improved Strain Influence Factor Diagrams," *Journal of Geotechnical and Geoenvironmental Engineering*, Vol. 104, No. 8, American Society of Civil Engineering, New York, New York, pp. 1131-1135.

Schultze, E. and Sherif, G. (1973). "Prediction of Settlements from Evaluated Settlement Observations for Sand," *Proceedings 8th International Conference Soil Mechanics and Foundation Engineering*, Vol. 1, No. 3, pp. 225-230.

Seed, H.B., Mitry, F.G., Monosmith, C.L., and Chan, C.K. (1967). "Prediction of Pavement Deflection from Laboratory Repeated Load Tests," *NCHRP Report 35*, NCHRP Transportation Research Board, Washington D.C.

Shahin, M.A., Jaksa, M.B., and Maier, H.R. (2001). "Artificial Neural Network Applications in Geotechnical Engineer," *Australian Geomechanics*, Vol. 36, No. 1, Australian Geomechanics Society, St. Ives, New South Wales, Australia, pp. 49-62.

Shahin, M.A., Maier, H.R., and Jaksa, M.B. (2002). "Predicting Settlement of Shallow Foundations using Neural Networks," *Journal of Geotechnical and Geoenvironmental Engineering*, Vol. 128, No. 9, American Society of Civil Engineering, New York, New York, pp. 785-793.

Shahin, M.A., Maier, H.R., and Jaksa, M.B. (2004). "Data Division for Developing Neural Networks Applied to Geotechnical Engineering," *Journal of Computing in Civil Engineering*, Vol. 18, No. 2, American Society of Civil Engineering, New York, New York, pp. 105-114.

Siekmeier, J, and Robertson, R., (2002), "Exterminating Material Moisture Characteristic for Pavement Drainage and Mechanistic Empirical Design", Minnesota Department of Transportation, Research Bulletin, 2002 M & RR 09

Skapura, D.M. (1996). *Building Neural Networks*, ACM Press, New York.

Soil Conservation Services (1952). *Soil Survey of Okfuskee County, Oklahoma*, U.S. Department of Agriculture, Washington, D.C.

Soil Conservation Services (1956). *Soil Survey of Noble County, Oklahoma*, U.S. Department of Agriculture, Washington, D.C.

Soil Conservation Services (1962). *Soil Survey of Kingfsiher County, Oklahoma*, U.S. Department of Agriculture, Washington, D.C.

Soil Conservation Services (1963). *Soil Survey of Woodward County, Oklahoma*, U.S. Department of Agriculture, Washington, D.C.

Soil Conservation Services (1965). *Soil Survey of Adair County, Oklahoma*, U.S. Department of Agriculture, Washington, D.C.

Soil Conservation Services (1966). *Soil Survey of Rogers County, Oklahoma*, U.S. Department of Agriculture, Washington, D.C.

Soil Conservation Services (1967). *Soil Survey of Greer County, Oklahoma*, U.S. Department of Agriculture, Washington, D.C.

Soil Conservation Services (1968). *Soil Survey of Major County, Oklahoma*, U.S. Department of Agriculture, Washington, D.C.

Soil Conservation Services (1970). *Soil Survey of Cherokee and Delaware Counties, Oklahoma*, U.S. Department of Agriculture, Washington, D.C.

Soil Conservation Services (1973). *Soil Survey of Jefferson County, Oklahoma*, U.S. Department of Agriculture, Washington, D.C.

Soil Conservation Services (1975). *Soil Survey of Alfalfa County, Oklahoma*, U.S. Department of Agriculture, Washington, D.C.

Soil Conservation Services (1978). *Soil Survey of Lincoln County, Oklahoma*, U.S. Department of Agriculture, Washington, D.C.

Soil Conservation Services (1979). *Soil Survey of Choctaw County, Oklahoma*, U.S. Department of Agriculture, Washington, D.C.

Soil Conservation Services (1979). *Soil Survey of McClain County, Oklahoma*, U.S. Department of Agriculture, Washington, D.C.

Soil Conservation Services (1979). *Soil Survey of Osage County, Oklahoma*, U.S. Department of Agriculture, Washington, D.C.

Sokal, R.R. and Rohlf, F.J. (1995). *Biometry: The Principles and Practice of Statistics in Biological Research*, 3rd Edition, W.H. Freeman and Co., New York.

Speckt, D.F. (1991). "A Generalized Regression Neural Network," *IEEE Transactions on Neural Networks*, Vol. 2, No. 6, IEEE, New York, pp. 568-576.

StatSoft, Inc. (2006). *Electronic Statistics Textbook*, Tulsa, Oklahoma.

Steil, J.J. (1999). "Input-output Stability of Recurrent Neural Networks with delays using circle criteria", *Ph.D. Dissertation*, University of Bielefeld, Bielefeld, Germany.

Stubstad, R.N. (2002). "NCHRP Web Document #52: LTPP Data Analysis: Feasibility of using FWD deflection data to characterize pavement construction quality," *Project 20-59(9)*, Washington, D.C.

Swenson, J., Guzina, B., Labuz, J., and Drescher, A, (2006) "Mistue Effect on PVD and DCP", University of Minnesota Department of Civil Engineering , Report No. MN/RC-2006-26

Tarefder, R.A., White, L., and Zaman, M. (2005). " Neural Network Model for Asphalt Concrete Permeability," *Journal of Materials in Civil Engineering*, Vol. 17, No. 1, American Society of Civil Engineering, New York, New York, pp. 19-27.

Thompson, M.R., and Robnett, Q.L. (1976). "Resilient Properties of Subgrade Soils," *Final Report*, FHWA-IL-UI-160, University of Illinois, Urbana, Illinois.

Thompson, M.R. and Smith, K.L. (1990). "Repeated Triaxial Characterization of Granular Bases," *Transportation Research Record 1278*, Transportation Research Board, National Research Council, Washington, D.C., pp. 7-17.

Tian, P., Zaman, M.M., and Laguros, J.G. (1998). "Variation of Resilient Modulus of Aggregate Base and Its Influence on Pavement Performance," *Journal of Testing and Evaluation*, JTEVA, Vol. 26, No. 4, pp. 329-335.

TRB (1999). "Use of Artificial Neural Networks in Geomechanical and Pavement Systems," *Transportation Research Circular Number E-C012*, December 1999, Transportation Research Board, National Research Council, Washington, D.C.

Uzan, J. (1985). "Characterization of Granular Material," *Transportation Research Record 1022*, Transportation Research Board, National Research Council, Washington, D.C., pp. 52-59.

Vanapalli, S.K., Pufahl, D.E., and Fredlund, D.G. (1998). "The Effect of Stress State on the Soil Water Characteristic Curve Behavior of a Compacted Sandy-Clay Till." 51st Canadian Geotechnical Conference, 1998, Edmonton, pp. 87-94.

Vanapalli, S.K., (2000). "A Simple Experimental Procedure for Exterminating the Fitting Parameter, Κ for Predicting the Shear Strength of an Unsaturated Soil." 54th Canadian Geotechnical Conferrence, Calgary, pp. 622-629.

Wersing, H., Beyn, W., and Ritter, H. (2001). "Dynamical Stability Conditions for Recurrent Neural Networks with Unsaturating Piecewise Linear Transfer Functions," *Neural Computation*, 13 (8), The MIT Press, Cambridge, Massachusetts, pp. 1811-1825.

Yau, A. and Von Quintus, H.L. (2002). "Study of LTPP Laboratory Resilient Modulus Test Data and Response Characteristics," *Final Report October 2002*, FHWA-RD-02-051, USDOT, FHWA.

Yildirim, T. and Ozyilmaz, L. (2002). "Dimensionality Reduction in Conic Section Function Neural Network," *Sadhana*, Vol. 27, Part 6, India, pp. 675-683.

Yoder, E.J. and Witczak, M.W. (1975). *Principles of Pavement Design*, 2nd Edition, John Wiley & Son, Inc., New York, New York.

Zhu, J. (1997). "Characterization of Cement-Kiln-Dust Stabilized Base/Subbase Aggregate," *Ph.D. Dissertation*, School of Civil Engineering and Environmental Science, University of Oklahoma, Norman, Oklahoma.

Zurada, J.M. (1992). *Introduction to Artificial Neural Systems*, West, St. Paul, Minnesota.

APPENDIX A

Development and Evaluation Datasets

Appendix A1 Soil Properties and Classifications for Development Dataset

No.	County	Sample I.D.	LL	PI	Percent Passing (%)				Soil Classification		OMC (%)	$\gamma_{d\ max}$ (kg/m^3)
					4.75mm (#4)	2.00mm (#10)	0.425mm (#40)	0.075mm (#200)	USCS	AASHTO		
1	Adair	AD-1	32	20	98.1	98.0	94.0	83.0	Lean clay with sand (CL)	A-6 (14)	18.3	1650.6
2	Adair	AD-2	33	24	74.3	70.2	67.5	59.7	Gravelly lean clay (CL)	A-6 (10)	15.8	1830.1
3	Adair	AD-3	28	9	75.3	72.2	69.6	61.1	Gravelly lean clay (CL)	A-4 (3)	17.3	1701.9
4	Adair	AD-4	33	19	96.2	95.1	86.3	81.2	Lean clay with sand (CL)	A-6 (14)	17.8	1724.4
5	Adair	AD-5	43	26	99.8	99.7	91.6	77.2	Lean clay with sand (CL)	A-7-6 (19)	17.0	1794.9
6	Adair	AD-6	44	28	99.6	98.0	95.0	83.2	Lean clay with sand (CL)	A-7-6 (23)	21.1	1544.9
7	Adair	AD-7	45	21	100	97.3	91.4	69.3	Sandy lean clay (CL)	A-7-6 (14)	20.7	1516.0
8	Adair	AD-8	67	43	100	96.4	92.0	68.6	Sandy fat clay (CH)	A-7-6 (29)	23.0	1516.0
9	Alfalfa	AL-1	27	13	100	100	97.4	83.6	Lean clay with sand (CL)	A-6 (9)	13.0	1785.3
10	Alfalfa	AL-2	25	10	100	100	97.6	76.4	Lean clay with sand (CL)	A-4 (5)	13.9	1844.6
11	Alfalfa	AL-3	31	15	100	100	99.9	97.5	Lean clay (CL)	A-6 (14)	16.8	1726.0
12	Alfalfa	AL-4	29	16	100	100	99.3	94.5	Lean clay (CL)	A-6 (13)	15.2	1722.8
13	Alfalfa	AL-5	34	19	100	100	92.0	75.6	Lean clay with sand (CL)	A-6 (12)	17.5	1716.3
14	Alfalfa	AL-6	43	27	100	100	97.5	93.8	Lean clay (CL)	A-7-6 (26)	19.6	1601.0
15	Alfalfa	AL-7	26	9	100	100	99.8	94.8	Lean clay (CL)	A-4 (7)	14.8	1774.0
16	Alfalfa	AL-8	31	18	100	100	95.6	89.2	Lean clay (CL)	A-6 (14)	15.4	1652.2
17	Alfalfa	AL-9	62	40	100	100	95.5	83.5	Fat clay (CH)	A-7-6 (36)	14.4	1504.8
18	Alfalfa	AL-10	25	10	100	100	94.5	79.7	Lean clay with sand (CL)	A-4 (6)	13.0	1798.1
19	Choctaw	CH-1	22	7	97.3	93.7	90.7	52.0	Sandy silty clay (CL-ML)	A-4 (1)	13.4	1909.4
20	Choctaw	CH-2	49	34	99.6	97.9	96.4	85.8	Lean clay (CL)	A-7-6 (29)	21.9	1675.5

1 kg/m^3 = 0.06243 pcf

Appendix A1 Soil Properties and Classifications for Development Dataset (Continued)

No.	County	Sample I.D.	LL	PI	Percent Passing (%)				Soil Classification		OMC (%)	$\gamma_{d\ max}$ (kg/m^3)
					4.75mm (#4)	2.00mm (#10)	0.425mm (#40)	0.075mm (#200)	USCS	AASHTO		
21	Choctaw	CH-3	34	16	99.9	99.0	97.0	91.2	Lean clay (CL)	A-6 (14)	18.4	1749.2
22	Choctaw	CH-4	53	38	100	99.7	98.9	95.8	Fat clay (CH)	A-7-6 (39)	22.9	1649.9
23	Delaware	DE-1	56	32	73.4	47.3	39.6	36.5	Clayey sand with gravel (SC)	A-7-6 (5)	20.7	1653.1
24	Delaware	DE-2	37	10	73.5	66.9	58.6	40.2	Clayey sand with gravel (SC)	A-4 (1)	18.5	1605.1
25	Delaware	DE-3	35	18	99.8	94.8	90.4	84.3	Lean clay with sand (CL)	A-6 (14)	14.0	1718.8
26	Delaware	DE-4	49	24	100	85.3	84.7	82.3	Lean clay with sand (CL)	A-7-6 (21)	17.8	1581.0
27	Greer	GR-1	48	34	98.5	92.5	79.8	71.2	Lean clay with sand (CL)	A-7-6 (22)	16.6	1567.3
28	Greer	GR-2	41	25	99.9	98.7	89.9	71.0	Lean clay with sand (CL)	A-7-6 (16)	16.7	1721.2
29	Greer	GR-3	34	17	98.7	98.1	96.5	89.1	Lean clay (CL)	A-6 (14)	18.3	1709.9
30	Jefferson	JE-1	24	11	100	100	99.8	70.1	Sandy lean clay (CL)	A-6 (5)	12.8	1879.0
31	Jefferson	JE-2	25	13	100	99.9	98.7	52.6	Sandy lean clay (CL)	A-6 (3)	13.6	1859.7
32	Jefferson	JE-3	22	10	100	99.9	97.5	55.4	Sandy lean clay (CL)	A-4 (2)	12.5	1895.0
33	Jefferson	JE-4	44	29	100	100	98.8	93.2	Lean clay (CL)	A-7-6 (28)	17.0	1749.2
34	Kingfisher	KI-1	25	11	100	100	95.5	60.5	Sandy lean clay (CL)	A-6 (4)	13.2	1896.6
35	Lincoln	LI-1	25	14	100	100	99.9	76.7	Lean clay with sand (CL)	A-6 (8)	12.5	1868.6
36	Lincoln	LI-2	41	26	100	100	99.9	81.6	Lean clay with sand (CL)	A-7-6 (20)	14.6	1791.7
37	Lincoln	LI-3	33	19	100	100	98.8	93.1	Lean clay (CL)	A-6 (17)	15.4	1782.1
38	Lincoln	LI-4	26	14	100	100	99.6	83.9	Lean clay with sand (CL)	A-6 (9)	13.3	1839.7
39	Lincoln	LI-5	21	10	100	100	99.4	45.6	Clayey Sand (SC)	A-4 (1)	12.7	1915.1
40	Lincoln	LI-6	22	8	100	100	98.9	50.5	Sandy lean clay (CL)	A-4 (1)	10.4	1881.4

1 kg/m^3 = 0.06243 pcf

Appendix A1 Soil Properties and Classifications for Development Dataset (Continued)

No.	County	Sample I.D.	LL	PI	Percent Passing (%)				Soil Classification		OMC (%)	$\gamma_{d\,max}$ (kg/m^3)
					4.75mm (#4)	2.00mm (#10)	0.425mm (#40)	0.075mm (#200)	USCS	AASHTO		
41	Major	MA-1	30	15	100	100	97.6	90.5	Lean clay (CL)	A-6 (12)	13.9	1810.1
42	Major	MA-2	28	14	100	100	96.9	88.6	Lean clay (CL)	A-6 (10)	12.7	1786.1
43	Major	MA-3	40	20	100	100	99.7	98.0	Lean clay (CL)	A-6 (21)	14.9	1488.1
44	Major	MA-4	33	20	99.3	97.6	89.3	75.2	Lean clay with sand (CL)	A-6 (13)	17.8	1746.0
45	McClain	MC-1	31	17	91.6	86.6	82.6	54.8	Sandy lean clay (CL)	A-6 (6)	15.2	1734.8
46	Noble	NO-1	23	7	99.9	99.1	98.0	77.1	Silty clay with sand (CL-ML)	A-4 (3)	14.3	1775.0
47	Noble	NO-2	22	8	97.6	92.0	91.0	58.6	Sandy lean clay (CL)	A-4 (2)	13.7	1800.0
48	Noble	NO-3	32	17	99.8	96.2	94.6	83.3	Lean clay with sand (CL)	A-6 (13)	18.5	1667.0
49	Noble	NO-4	29	11	100	99.5	99.0	92.1	Lean clay (CL)	A-6 (9)	19.4	1615.0
50	Noble	NO-5	28	9	100	99.5	99.1	92.0	Lean clay (CL)	A-4 (7)	16.8	1690.0
51	Noble	NO-6	29	12	100	100	99.8	91.9	Lean clay (CL)	A-6 (10)	17.4	1697.0
52	Noble	NO-7	36	18	100	100	99.1	90.5	Lean clay (CL)	A-6 (16)	17.3	1688.0
53	Noble	NO-8	38	21	100	97.8	97.2	94.8	Lean clay (CL)	A-6 (20)	15.7	1665.0
54	Noble	NO-9	34	20	99.6	96.5	93.4	80.4	Lean clay with sand (CL)	A-6 (14)	14.0	1816.0
55	Okfuskee	OK-1	43	26	100	100	97.3	82.3	Lean clay with sand (CL)	A-7-6 (21)	18.1	1669.1
56	Okfuskee	OK-2	26	11	100	100	99.5	77.3	Lean clay with sand (CL)	A-6 (6)	13.1	1824.5
57	Okfuskee	OK-3	35	16	100	100	98.9	77.8	Lean clay with sand (CL)	A-6 (11)	16.7	1672.3
58	Okfuskee	OK-4	34	19	99.8	99.5	97.3	84.3	Lean clay with sand (CL)	A-6 (15)	16.4	1720.4
59	Okfuskee	OK-5	30	15	100	99.9	98.2	87.5	Lean clay (CL)	A-6 (12)	16.3	1673.9
60	Osage	OS-1	29	14	100	100	98.1	87.1	Lean clay (CL)	A-6 (10)	16.3	1745.2

1 kg/m^3 = 0.06243 pcf

Appendix A1 Soil Properties and Classifications for Development Dataset (Continued)

No.	County	Sample I.D.	LL	PI	Percent Passing (%)				Soil Classification		OMC (%)	$\gamma_{d\ max}$ (kg/m^3)
					4.75mm (#4)	2.00mm (#10)	0.425mm (#40)	0.075mm (#200)	USCS	AASHTO		
61	Osage	OS-2	45	26	100	100	99.4	90.9	Lean clay (CL)	A-7-6 (25)	18.7	1649.0
62	Osage	OS-3	29	14	100	100	98.8	89.9	Lean clay (CL)	A-6 (11)	17.2	1665.1
63	Rogers	RO-1	43	23	100	98.1	95.8	88.4	Lean clay (CL)	A-7-6 (21)	22.0	1595.0

1 kg/m^3 = 0.06243 pcf

Appendix A2 Soil Properties and Classifications for Evaluation Dataset

No.	County	Sample I.D.	LL	PI	Percent Passing (%)				Soil Classification		OMC (%)	$\gamma_{d\ max}$ (kg/m^3)
					4.75mm (#4)	2.00mm (#10)	0.425mm (#40)	0.075mm (#200)	USCS	AASHTO		
1	Rogers	ROE-1	44	28	94.2	90.1	79.9	63.6	Sandy Lean Clay (CL)	A-7-6 (15)	20.3	1656.3
2	Rogers	ROE-2	37	17	99.2	93.5	75.3	60.6	Sandy Lean Clay (CL)	A-6 (8)	16.5	1766.8
3	Rogers	ROE-3	29	15	99.3	97.9	91.9	77.5	Lean Clay with Sand (CL)	A-6 (9)	15.9	1702.7
4	Rogers	ROE-4	41	28	100	100	98.6	91.4	Lean Clay (CL)	A-7-6 (25)	20.1	1691.5
5	Rogers	ROE-5	34	15	83.7	77.2	70.1	60.6	Sandy Lean Clay with Gravel (CL)	A-6 (7)	17.6	1657.9
6	Rogers	ROE-6	43	28	100	99.0	89.2	64.4	Sandy Lean Clay (CL)	A-7-6 (15)	19.5	1683.5
7	Rogers	ROE-7	30	12	90.2	85.5	49.3	37.9	Clayey Sand (SC)	A-6 (1)	11.8	1883.7
8	Rogers	ROE-8	38	17	79.1	74.6	62.1	50.7	Sandy Lean Clay with Gravel (CL)	A-6 (5)	14.0	1811.6
9	Rogers	ROE-9	27	11	97.8	96.3	85.1	59.8	Sandy Lean Clay (CL)	A-6 (4)	15.2	1792.4
10	Rogers	ROE-10	40	27	97.5	93.3	89.2	81.4	Lean Clay with Sand (CL)	A-6 (21)	17.8	1747.6
11	Rogers	ROE-11	32	17	100	100	97.6	82.0	Lean Clay with Sand (CL)	A-6 (12)	15.4	1763.6
12	Rogers	ROE-12	48	29	99.2	97.0	94.7	87.8	Lean Clay (CL)	A-7-6 (27)	17.8	1688.3
13	Rogers	ROE-13	47	33	94.2	90.7	84.1	76.4	Lean Clay with Sand (CL)	A-7-6 (24)	18.6	1718.7
14	Rogers	ROE-14	48	35	100	100	99.6	89.0	Lean Clay (CL)	A-7-6 (31)	18.4	1709.1
15	Rogers	ROE-15	24	6	94.3	82.8	75.3	62.9	Sandy Silty Clay (CL-ML)	A-4 (1)	14.0	1746.0
16	Rogers	ROE-16	52	33	99.3	94.2	90.7	82.7	Fat Clay with Sand (CH)	A-7-6 (28)	19.9	1670.7
17	Rogers	ROE-17	49	36	99.9	99.2	91.9	75.2	Lean Clay with Sand (CL)	A-7-6 (26)	18.8	1717.1
18	Rogers	ROE-18	27	7	100	100	92.5	68.0	Sandy Silty Clay (CL-ML)	A-4 (3)	12.7	1835.7
19	Rogers	ROE-19	30	13	100	99.6	86.1	68.7	Sandy Lean Clay (CL)	A-6 (7)	12.1	1866.1
20	Rogers	ROE-20	44	30	100	99.7	94.2	84.7	Lean Clay with Sand (CL)	A-7-6 (25)	18.2	1696.3

1 kg/m^3 = 0.06243 pcf

Appendix A2 Soil Properties and Classifications for Evaluation Dataset (Continued)

No.	County	Sample I.D.	LL	PI	Percent Passing (%)				Soil Classification		OMC (%)	$\gamma_{d\ max}$ (kg/m^3)
					4.75mm (#4)	2.00mm (#10)	0.425mm (#40)	0.075mm (#200)	USCS	AASHTO		
21	Rogers	ROE-21	50	30	100	100	96.2	91.8	Fat Clay (CH)	A-7-6 (30)	19.7	1625.8
22	Rogers	ROE-22	35	23	100	100	90.4	74.4	Lean Clay with Sand (CL)	A-6 (15)	16.3	1789.2
23	Rogers	ROE-23	35	22	100	100	100	87.8	Lean Clay (CL)	A-6 (18)	17.6	1752.4
24	Rogers	ROE-24	43	30	98.9	94.9	93.1	85.5	Lean Clay (CL)	A-7-6 (25)	19.1	1678.7
25	Rogers	ROE-25	37	22	94.9	90.1	77.5	67.8	Sandy Lean Clay (CL)	A-6 (12)	17.5	1737.9
26	Rogers	ROE-26	44	30	100	99.4	98.7	94.2	Lean Clay (CL)	A-7-6 (29)	19.0	1670.7
27	Rogers	ROE-27	35	23	99.9	99.6	97.1	94.1	Lean Clay (CL)	A-6 (21)	16.9	1747.6
28	Rogers	ROE-28	32	20	99.6	95.6	90.9	67.2	Sandy Lean Clay (CL)	A-6 (10)	15.5	1760.4
29	Rogers	ROE-29	35	21	100	99.4	94.7	75.1	Lean Clay with Sand (CL)	A-6 (14)	17.3	1733.1
30	Woodward	WOE-1	24	10	100	100	95.8	68.0	Sandy Lean Clay (CL)	A-4 (4)	13.4	1843.7
31	Woodward	WOE-2	24	6	100	100	97.7	70.2	Sandy Silty Clay (CL-ML)	A-4 (2)	12.8	1797.2
32	Woodward	WOE-3	27	13	100	100	95.1	70.3	Sandy Lean Clay (CL)	A-6 (6)	11.7	1888.5
33	Woodward	WOE-4	27	13	100	100	96.5	65.4	Sandy Lean Clay (CL)	A-6 (6)	13.4	1878.9
34	Woodward	WOE-5	28	12	100	100	96.6	85.8	Lean Clay (CL)	A-6 (9)	12.9	1856.5

1 kg/m^3 = 0.06243 pcf

Appendix A3 Specimen Properties for Development Dataset

No.	Sample I.D.	w (%)	γ_d (kg/m^3)	U_c (kPa)
1	AD-1A	18.4	1565.0	128.10
2	AD-1B	20.4	1633.9	80.90
3	AD-2A	16.2	1730.0	251.20
4	AD-2B	17.6	1755.6	187.20
5	AD-3A	17.8	1611.5	128.30
6	AD-3B	19.8	1664.3	89.10
7	AD-4A	17.6	1640.3	229.40
8	AD-4B	19.5	1683.5	172.90
9	AD-5A	17.1	1701.2	304.50
10	AD-5B	18.5	1683.5	175.20
11	AD-6A	20.8	1465.7	237.30
12	AD-6B	22.9	1460.9	196.40
13	AD-7A	21.2	1430.4	226.90
14	AD-7B	23.0	1492.9	237.30
15	AD-8A	23.1	1510.5	311.70
16	AD-8B	24.9	1454.5	169.50
17	AL-1A	13.6	1693.2	259.39
18	AL-1B	14.8	1748.4	178.78
19	AL-2A	13.5	1764.3	245.13
20	AL-2B	15.9	1799.8	216.62
21	AL-3A	17.6	1658.7	229.23
22	AL-3B	19.1	1675.5	218.26
23	AL-4A	15.9	1624.3	285.17
24	AL-4B	17.9	1715.6	332.88
25	AL-5A	17.9	1637.1	180.97
26	AL-5B	19.1	1654.7	179.87
27	AL-6A	19.2	1526.6	156.29
28	AL-6B	20.9	1573.0	128.32
29	AL-7A	14.6	1689.9	123.39
30	AL-7B	17.3	1739.6	194.68
31	AL-8A	15.9	1573.0	236.91
32	AL-8B	17.1	1625.9	268.71
33	AL-9A	14.2	1442.5	250.07
34	AL-9B	15.9	1482.0	291.75
35	AL-10A	13.2	1717.2	187.00

No.	Sample I.D.	w (%)	γ_d (kg/m^3)	U_c (kPa)
36	AL-10B	15.6	1764.3	184.26
37	CH-1A	13.3	1827.7	234.71
38	CH-1B	15.7	1872.6	123.94
39	CH-2A	22.3	1605.1	158.49
40	CH-2B	24.8	1656.3	176.58
41	CH-3A	18.3	1665.9	144.23
42	CH-3B	20.8	1717.2	91.58
43	CH-4A	22.8	1563.4	113.52
44	CH-4B	25.3	1608.3	104.20
45	DE-1A	21.2	1565.3	109.52
46	DE-1B	23.2	1583.3	50.88
47	DE-2A	18.4	1514.5	238.08
48	DE-2B	20.9	1561.4	222.54
49	DE-3A	14.5	1640.1	177.88
50	DE-3B	16.8	1727.4	128.56
51	DE-4A	18.5	1498.2	200.41
52	DE-4B	19.4	1572.3	248.95
53	GR-1A	16.5	1475.3	276.94
54	GR-1B	18.5	1520.2	223.75
55	GR-2A	16.5	1638.7	244.04
56	GR-2B	18.9	1680.3	148.62
57	GR-3A	18.0	1629.1	247.33
58	GR-3B	20.5	1678.7	137.10
59	JE-1A	12.5	1778.9	322.35
60	JE-1B	15.1	1835.7	221.48
61	JE-2A	13.9	1771.1	183.11
62	JE-2B	15.5	1799.5	107.45
63	JE-3A	12.7	1807.2	195.17
64	JE-3B	14.3	1839.7	126.64
65	JE-4A	17.2	1657.2	367.86
66	JE-4B	18.8	1725.3	224.22
67	KI-1A	13.0	1801.5	291.20
68	KI-1B	15.4	1824.7	164.52
69	LI-1A	12.2	1779.7	195.17
70	LI-1B	14.6	1826.1	149.12

1 kg/m^3 = 0.06243 pcf
1 kPa = 0.145 psi

Appendix A3 Specimen Properties for Development Dataset (Continued)

No.	Sample I.D.	w (%)	γ_d (kg/m^3)	U_c (kPa)
71	LI-2A	14.8	1698.0	189.14
72	LI-2B	16.5	1762.0	150.76
73	LI-3A	15.1	1698.0	202.29
74	LI-3B	17.5	1746.0	154.05
75	LI-4A	13.0	1754.0	171.05
76	LI-4B	15.2	1794.1	188.59
77	LI-5A	12.6	1810.1	247.25
78	LI-5B	14.8	1835.7	143.09
79	LI-6A	10.5	1782.9	268.08
80	LI-6B	12.3	1854.9	254.38
81	MA-1A	14.2	1706.0	134.31
82	MA-1B	16.1	1761.3	115.67
83	MA-2A	12.5	1693.2	402.40
84	MA-2B	15.0	1758.8	185.30
85	MA-3A	14.8	1409.6	443.51
86	MA-3B	16.7	1438.5	310.29
87	MA-4A	17.2	1651.5	156.79
88	MA-4B	20.3	1698.0	123.35
89	MC-1A	15.4	1645.0	316.43
90	MC-1B	16.9	1404.2	263.23
91	NO-1A	14.0	1686.8	241.50
92	NO-1B	16.1	1744.4	197.10
93	NO-2A	13.8	1704.4	208.90
94	NO-2B	15.6	1763.7	179.90
95	NO-3A	19.0	1571.4	165.90
96	NO-3B	20.6	1638.7	142.80
97	NO-4A	19.2	1542.6	159.20
98	NO-4B	21.6	1590.7	120.10
99	NO-5A	17.0	1584.3	241.60
100	NO-5B	19.3	1653.1	241.50
101	NO-6A	16.9	1616.3	157.70
102	NO-6B	19.0	1638.7	129.50
103	NO-7A	17.1	1613.1	271.60
104	NO-7B	18.9	1666.0	228.40
105	NO-8A	15.3	1577.8	368.70

1 kg/m^3 = 0.06243 pcf
1 kPa = 0.145 psi

No.	Sample I.D.	w (%)	γ_d (kg/m^3)	U_c (kPa)
106	NO-8B	17.5	1661.1	341.70
107	NO-9A	14.6	1722.0	226.70
108	NO-9B	16.0	1790.9	192.60
109	OK-1A	18.3	1578.7	203.94
110	OK-1B	20.4	1601.8	122.80
111	OK-2A	13.1	1741.2	268.63
112	OK-2B	15.3	1790.7	176.53
113	OK-3A	16.8	1601.8	290.01
114	OK-3B	18.9	1643.5	167.76
115	OK-4A	16.4	1632.3	160.63
116	OK-4B	18.5	1694.8	137.60
117	OK-5A	16.1	1600.2	200.65
118	OK-5B	18.3	1629.1	234.09
119	OS-1A	16.1	1661.1	335.07
120	OS-1B	18.5	1683.5	160.13
121	OS-2A	18.6	1565.0	332.33
122	OS-2B	20.5	1568.2	166.16
123	OS-3A	17.3	1577.8	291.20
124	OS-3B	19.1	1640.3	164.52
125	RO-1A	22.1	1515.4	165.90
126	RO-1B	23.9	1581.1	151.20

Appendix A4 Specimen Properties for Evaluation Dataset

No.	Sample I.D.	w (%)	γ_d (kg/m^3)	U_c (kPa)
1	ROE-1A	20.4	1573.0	164.06
2	ROE-1B	22.4	1630.7	141.01
3	ROE-2A	16.4	1678.7	218.38
4	ROE-2B	16.4	1730.0	212.89
5	ROE-3A	15.4	1617.9	219.47
6	ROE-3B	17.4	1675.5	123.45
7	ROE-4A	19.8	1606.7	102.60
8	ROE-4B	21.8	1625.9	73.52
9	ROE-5A	17.4	1574.6	100.41
10	ROE-5B	19.4	1637.1	93.28
11	ROE-6A	19.2	1600.2	211.79
12	ROE-6B	21.2	1643.5	194.23
13	ROE-7A	11.4	1789.3	221.67
14	ROE-7B	13.4	1837.3	110.83
15	ROE-8A	13.7	1722.0	98.21
16	ROE-8B	15.7	1795.7	93.82
17	ROE-9A	15.5	1702.8	114.67
18	ROE-9B	17.5	1747.6	86.14
19	ROE-10A	17.2	1661.1	211.79
20	ROE-10B	19.2	1707.6	173.93
21	ROE-11A	15.5	1675.5	196.98
22	ROE-11B	17.5	1733.2	77.36
23	ROE-12A	18.3	1603.9	217.83
24	ROE-12B	20.3	1664.3	181.07
25	ROE-13A	18.2	1632.9	151.99
26	ROE-13B	20.2	1688.3	116.87
27	ROE-14A	18.7	1623.8	115.77
28	ROE-14B	20.7	1646.7	70.23
29	ROE-15A	13.6	1658.7	200.82
30	ROE-15B	15.6	1725.2	277.63
31	ROE-16A	19.6	1587.3	274.89
32	ROE-16B	21.6	1646.7	173.93
33	ROE-17A	19.0	1630.7	198.07
34	ROE-17B	21.0	1678.7	118.52
35	ROE-18A	13.2	1743.9	171.19

No.	Sample I.D.	w (%)	γ_d (kg/m^3)	U_c (kPa)
36	ROE-18B	15.2	1811.7	197.53
37	ROE-19A	12.4	1772.9	216.18
38	ROE-19B	14.4	1824.5	207.40
39	ROE-20A	18.6	1611.6	245.81
40	ROE-20B	20.6	1653.1	187.10
41	ROE-21A	19.4	1544.7	245.81
42	ROE-21B	21.4	1600.2	292.45
43	ROE-22A	16.1	1699.9	145.95
44	ROE-22B	18.1	1757.2	143.21
45	ROE-23A	17.2	1664.8	142.11
46	ROE-23B	19.2	1704.4	56.51
47	ROE-24A	19.3	1594.8	187.10
48	ROE-24B	21.3	1635.5	144.85
49	ROE-25A	18.1	1651.2	143.21
50	ROE-25B	20.1	1706.0	144.85
51	ROE-26A	19.2	1587.3	184.36
52	ROE-26B	21.2	1627.5	172.29
53	ROE-27A	16.5	1660.3	151.99
54	ROE-27B	18.5	1701.2	73.52
55	ROE-28A	15.4	1672.5	167.90
56	ROE-28B	17.4	1720.4	155.83
57	ROE-29A	17.3	1646.7	115.22
58	ROE-29B	19.3	1677.1	91.63
59	WOE-1A	13.1	1752.4	140.46
60	WOE-1B	15.1	1782.9	127.84
61	WOE-2A	12.9	1707.6	122.91
62	WOE-2B	14.9	1746.0	110.83
63	WOE-3A	11.5	1794.1	357.74
64	WOE-3B	13.5	1862.9	357.74
65	WOE-4A	13.0	1784.5	269.95
66	WOE-4B	15.0	1837.3	127.84
67	WOE-5A	13.1	1763.6	192.59
68	WOE-5B	15.1	1818.1	183.26

1 kg/m^3 = 0.06243 pcf
1 kPa = 0.145 psi

APPENDIX B

Resilient Modulus Test Results

Appendix B1 Resilient Modulus Test Results for Development Dataset

Sequence Number		1	2	3	4	5	6	7	8	9	10	11	12	13	14	15
No.	**Sample I.D.**	**Resillient Modulus (MPa)**														
1	AD-1A	78.0	70.8	59.7	51.7	46.9	69.4	61.3	53.0	47.0	42.9	61.3	52.2	44.6	39.8	36.8
2	AD-1B	61.3	52.8	39.4	28.3	21.5	49.3	37.6	28.6	24.4	20.9	40.3	28.5	21.8	19.6	18.2
3	AD-2A	144.7	139.8	129.5	120.0	111.5	138.1	133.5	128.0	120.1	111.7	120.6	116.1	118.5	111.2	104.5
4	AD-2B	114.0	106.9	92.7	78.6	68.5	99.0	90.9	80.0	70.2	62.6	88.7	79.1	68.6	60.2	53.7
5	AD-3A	86.6	79.7	67.0	58.4	53.6	76.5	67.7	58.6	51.7	46.5	63.5	54.1	46.3	41.6	38.3
6	AD-3B	63.3	52.6	36.9	26.1	20.7	41.9	28.7	23.2	22.3	21.5	36.1	23.7	19.8	19.8	20.0
7	AD-4A	120.9	118.3	111.1	103.6	96.9	111.4	109.1	104.9	99.9	94.7	95.4	95.0	93.8	90.7	87.0
8	AD-4B	103.0	98.5	87.7	76.7	69.0	93.9	88.7	81.0	72.7	65.3	80.6	76.7	70.6	64.3	58.4
9	AD-5A	164.1	167.4	162.8	155.7	146.6	151.1	155.0	155.4	151.7	145.7	128.6	131.7	135.4	135.8	133.8
10	AD-5B	120.5	117.2	106.6	92.3	78.5	110.5	107.3	100.0	96.3	78.3	99.7	96.6	91.0	82.6	73.6
11	AD-6A	139.5	142.3	138.2	132.2	124.6	131.4	132.4	130.9	127.3	122.6	120.9	121.6	122.6	121.3	118.1
12	AD-6B	116.9	115.2	107.5	98.8	90.0	110.6	109.0	104.3	97.5	90.1	106.9	105.4	102.7	97.6	91.2
13	AD-7A	117.5	118.1	113.0	107.9	103.3	109.6	108.7	106.2	102.6	98.9	96.6	95.3	93.4	90.7	88.5
14	AD-7B	123.5	125.2	119.7	114.4	108.8	115.6	114.5	112.5	109.4	105.8	102.5	101.6	101.1	99.8	97.5
15	AD-8A	147.8	152.7	153.7	153.6	152.6	148.6	151.3	151.6	150.9	149.2	137.6	138.8	140.3	141.2	140.9
16	AD-8B	104.9	102.7	93.9	82.2	70.9	98.7	96.2	90.2	81.4	71.7	92.8	90.2	85.1	77.9	69.9
17	AL-1A	110.1	76.3	77.7	78.5	76.5	98.8	76.7	76.8	77.7	77.3	111.1	81.7	80.0	79.4	78.8
18	AL-1B	117.1	59.0	54.3	47.6	44.1	88.0	56.6	49.4	45.1	43.4	97.4	57.6	48.9	44.4	42.9
19	AL-2A	137.4	74.1	71.1	66.6	62.6	111.2	71.6	65.4	62.7	61.9	115.3	72.8	65.7	62.8	62.4
20	AL-2B	119.9	61.6	54.5	47.2	43.9	84.1	53.1	45.4	42.3	42.2	86.6	52.3	43.7	41.0	41.4
21	AL-3A	124.8	73.6	68.7	63.5	58.9	107.0	70.2	63.5	60.5	59.2	122.2	72.8	64.1	60.7	59.5
22	AL-3B	105.5	58.2	47.6	39.5	35.7	81.4	49.6	39.6	35.5	34.2	83.0	49.2	38.5	34.3	33.5
23	AL-4A	125.7	73.1	73.7	72.2	68.9	119.9	74.1	71.1	70.1	69.6	121.0	76.1	72.1	70.3	69.9
24	AL-4B	123.4	73.6	73.3	70.3	67.6	110.4	74.1	70.8	68.9	66.9	118.1	75.8	71.1	68.8	67.2
25	AL-5A	68.1	45.3	37.3	33.2	30.9	66.7	44.4	37.3	34.1	32.2	75.4	49.3	40.1	35.7	33.6
26	AL-5B	62.6	42.0	31.4	26.7	24.2	60.8	38.9	30.3	26.7	24.8	66.7	40.5	30.7	26.4	24.7

1 kPa = 0.145 psi

Appendix B1 Resilient Modulus Test Results for Development Dataset (Continued)

Sequence Number		1	2	3	4	5	6	7	8	9	10	11	12	13	14	15
No.	Sample I.D.	Resillient Modulus (MPa)														
27	AL-6A	61.9	50.2	41.8	36.4	33.5	59.6	46.4	38.5	35.3	34.4	63.6	48.8	40.1	36.2	35.1
28	AL-6B	54.6	45.2	35.0	30.3	26.9	52.0	38.4	31.5	28.5	26.6	55.1	39.8	31.8	28.4	26.7
29	AL-7A	175.0	63.0	53.2	47.4	44.9	131.2	59.9	49.0	45.0	44.6	127.5	59.6	48.5	45.0	44.9
30	AL-7B	81.5	49.8	40.6	37.5	38.0	76.8	47.0	38.7	36.5	37.4	77.2	46.7	38.4	36.3	37.7
31	AL-8A	133.1	73.2	70.0	66.2	61.3	103.5	71.9	67.8	64.2	61.8	107.6	74.4	68.5	64.8	62.4
32	AL-8B	128.4	70.1	69.1	66.4	62.4	113.8	72.3	67.5	64.8	62.8	112.2	73.8	68.1	65.2	63.3
33	AL-9A	124.9	96.0	82.4	81.9	80.7	240.8	108.0	102.0	89.0	86.1	312.1	115.7	107.8	93.8	90.6
34	AL-9B	330.9	71.8	73.2	68.6	67.3	94.2	75.2	71.8	71.4	70.8	95.6	78.9	76.1	74.6	73.2
35	AL-10A	176.0	58.6	49.7	44.7	41.1	87.9	51.6	44.4	42.1	41.3	98.9	53.8	45.5	42.7	42.0
36	AL-10B	95.5	51.3	41.5	34.5	30.7	79.1	42.6	33.7	30.5	29.4	82.4	41.5	32.3	29.2	28.5
37	CH-1A	305.2	110.1	86.6	73.4	68.1	209.8	104.2	85.9	75.8	69.3	228.4	107.1	85.8	75.3	69.5
38	CH-1B	1623.4	170.9	113.7	87.7	80.6	1176.4	154.0	117.4	101.0	85.8	1333.4	166.4	123.9	109.8	92.0
39	CH-2A	149.9	74.5	61.0	49.1	40.8	120.4	79.1	65.5	51.6	42.5	144.4	83.3	67.3	52.5	43.0
40	CH-2B	101.9	85.3	73.5	62.5	54.5	104.2	87.0	76.4	67.0	58.1	109.6	90.6	78.9	69.8	60.2
41	CH-3A	501.7	106.9	71.2	53.4	41.9	439.8	114.8	74.4	52.5	42.4	640.7	135.0	82.1	53.0	41.8
42	CH-3B	496.3	65.3	34.3	24.5	21.7	225.6	65.0	37.3	28.0	23.8	275.0	70.9	40.6	29.9	25.3
43	CH-4A	872.7	130.0	76.1	47.7	36.7	819.2	135.7	89.8	54.1	39.4	1143.5	156.7	103.4	58.4	41.4
44	CH-4B	228.0	78.2	43.7	31.7	26.6	207.3	78.2	44.4	33.0	27.7	262.0	86.7	47.9	34.4	28.5
45	DE-1A	52.3	45.7	41.8	39.9	37.5	56.3	47.0	43.9	41.3	38.9	63.7	53.4	46.3	41.2	38.2
46	DE-1B	511.7	71.6	42.6	36.9	34.5	323.6	83.2	59.2	45.5	39.2	327.1	85.3	62.5	48.2	43.1
47	DE-2A	316.2	81.8	76.8	74.7	71.9	109.0	83.3	78.3	77.4	75.1	115.5	84.8	80.8	79.5	77.5
48	DE-2B	705.4	121.0	102.6	94.8	86.8	669.6	131.0	108.0	101.0	93.2	874.9	142.1	112.0	102.9	94.3
49	DE-3A	1177.0	142.1	111.9	94.8	80.3	1189.2	136.3	110.8	101.7	86.9	1392.6	149.8	115.9	104.9	90.9
50	DE-3B	776.4	118.8	90.6	73.0	66.6	505.3	121.5	101.1	80.3	71.2	643.9	135.3	107.7	89.1	79.1
51	DE-4A	549.2	103.9	86.2	74.7	69.1	222.2	104.4	89.6	78.1	71.4	227.2	117.7	106.2	87.0	76.6
52	DE-4B	612.4	106.5	95.5	89.1	88.4	483.6	114.2	102.6	98.6	94.7	837.9	137.0	128.1	119.8	109.8

1 kPa = 0.145 psi

Appendix B1 Resilient Modulus Test Results for Development Dataset (Continued)

Sequence Number		1	2	3	4	5	6	7	8	9	10	11	12	13	14	15
No.	**Sample I.D.**	**Resillient Modulus (MPa)**														
53	GR-1A	974.1	126.6	107.0	102.7	84.6	791.4	137.3	112.7	107.8	87.9	803.7	204.5	159.0	159.8	190.9
54	GR-1B	865.1	125.6	102.8	89.6	72.5	720.9	121.0	101.4	92.3	77.4	830.1	125.2	116.7	104.3	85.6
55	GR-2A	106.9	74.9	71.5	66.4	58.5	143.5	78.7	75.9	70.4	61.6	186.1	82.6	77.5	72.2	63.5
56	GR-2B	526.5	86.7	60.6	45.7	38.5	210.6	76.2	55.9	45.5	39.9	209.3	78.1	60.3	52.9	43.5
57	GR-3A	100.8	66.4	57.4	48.4	42.1	123.3	67.7	58.0	49.2	43.3	134.0	67.1	58.1	49.9	44.0
58	GR-3B	325.0	73.5	51.4	36.9	31.7	312.3	76.2	54.5	39.7	33.2	601.8	128.5	86.2	58.2	44.5
59	JE-1A	59.7	56.7	51.6	48.9	47.2	61.7	54.3	49.7	48.4	48.3	68.5	57.1	50.5	48.2	48.1
60	JE-1B	75.7	52.9	38.6	31.0	28.7	70.3	40.7	31.4	29.0	28.7	70.8	40.0	30.4	28.7	29.0
61	JE-2A	478.6	98.9	76.0	56.9	50.5	547.7	95.2	75.2	60.3	54.1	859.0	101.8	77.6	63.2	57.5
62	JE-2B	831.1	98.2	60.0	48.5	48.2	567.6	115.4	85.4	63.2	52.9	760.6	172.1	110.1	78.8	65.2
63	JE-3A	74.0	47.6	36.0	34.0	35.7	81.1	51.4	42.8	39.3	38.5	84.2	53.9	44.9	40.8	40.0
64	JE-3B	373.1	85.0	57.8	53.0	50.0	372.1	109.0	79.9	62.3	56.2	414.1	117.7	88.1	66.7	62.7
65	JE-4A	789.3	120.8	104.6	96.0	84.5	473.0	125.2	106.0	101.9	89.7	434.7	134.5	111.9	104.9	93.5
66	JE-4B	77.2	61.6	49.1	40.3	35.1	71.5	58.1	47.9	40.5	36.5	81.0	61.8	51.4	42.7	37.9
67	KI-1A	463.3	95.6	69.2	47.3	43.4	717.2	93.6	65.5	49.0	41.5	707.2	91.5	65.6	48.6	42.2
68	KI-1B	216.2	54.8	33.9	31.4	33.1	289.0	74.3	47.7	38.7	35.4	419.3	103.1	59.4	44.0	40.2
69	LI-1A	310.6	89.0	78.9	69.2	68.0	283.9	90.3	79.1	72.2	70.0	349.5	98.0	101.5	100.4	94.4
70	LI-1B	485.8	87.1	72.0	63.6	62.2	447.8	93.1	78.1	70.0	66.4	516.9	97.7	81.5	73.3	69.8
71	LI-2A	1111.1	115.4	78.9	56.8	49.8	1013.9	138.3	90.4	64.6	53.7	1289.6	158.4	96.7	68.1	56.2
72	LI-2B	223.7	51.7	35.7	28.0	25.0	192.5	48.7	33.2	28.0	26.1	249.1	52.7	35.2	28.7	26.5
73	LI-3A	242.1	88.5	71.7	55.8	47.0	228.2	85.8	70.9	57.3	49.2	252.4	88.3	71.5	58.7	50.5
74	LI-3B	201.1	74.2	55.9	42.4	35.4	153.0	72.1	53.4	43.7	37.5	173.7	76.0	56.9	48.7	41.5
75	LI-4A	127.9	70.8	57.2	42.4	34.3	99.0	59.0	45.0	37.5	33.0	95.3	57.7	43.5	36.2	32.5
76	LI-4B	1168.9	131.2	96.5	71.9	55.1	1162.5	131.8	92.8	67.6	54.2	1297.8	138.4	92.3	66.7	53.6
77	LI-5A	497.2	93.6	92.5	85.3	75.6	243.2	86.0	87.1	84.7	78.2	302.7	93.2	91.3	86.3	79.9
78	LI-5B	238.3	90.0	74.8	57.8	48.3	264.9	89.7	72.2	57.6	49.8	290.7	93.0	73.2	58.2	50.3

1 kPa = 0.145 psi

Appendix B1 Resilient Modulus Test Results for Development Dataset (Continued)

Sequence Number		1	2	3	4	5	6	7	8	9	10	11	12	13	14	15
No.	Sample I.D.	Resillient Modulus (MPa)														
79	LI-6A	124.7	77.6	74.1	68.6	65.2	122.2	78.8	72.4	66.9	65.1	137.2	81.9	72.9	68.5	66.0
80	LI-6B	392.3	101.0	83.6	71.2	66.9	365.4	93.8	79.6	71.5	67.9	379.0	95.3	79.7	71.6	68.3
81	MA-1A	720.4	75.3	46.8	35.1	30.4	783.9	72.1	46.1	37.0	32.9	1146.2	80.5	51.3	39.5	34.6
82	MA-1B	67.4	34.5	24.6	24.3	25.3	70.4	41.1	31.0	28.5	28.7	74.9	46.7	34.4	31.0	30.3
83	MA-2A	217.7	104.7	93.7	87.3	81.2	219.2	98.8	90.3	85.5	81.7	248.8	102.2	91.1	85.7	81.1
84	MA-2B	82.6	48.2	34.9	30.0	29.2	85.1	45.3	33.6	30.7	30.0	86.6	46.5	34.4	31.2	30.9
85	MA-3A	156.9	127.5	131.0	132.2	132.5	292.8	143.3	136.4	138.6	137.5	451.5	147.6	135.4	140.6	138.2
86	MA-3B	2042.3	229.0	163.8	149.2	137.3	2160.8	245.9	159.5	148.5	140.3	1892.2	234.9	161.1	151.8	141.1
87	MA-4A	387.1	85.3	66.1	49.8	40.7	351.8	83.4	62.6	47.0	40.1	405.6	85.3	62.5	45.7	39.1
88	MA-4B	1138.4	83.8	49.1	33.0	27.7	1026.6	83.3	47.9	34.5	28.4	1578.9	91.3	51.3	35.4	29.3
89	MC-1A	100.1	90.0	84.3	82.7	80.3	105.4	90.5	88.2	86.2	83.8	107.9	94.8	91.0	89.1	87.1
90	MC-1B	485.0	105.9	90.6	85.9	73.8	417.9	105.5	95.2	92.5	81.6	1053.8	131.9	117.5	112.7	96.8
91	NO-1A	99.2	100.0	92.4	88.1	84.4	89.5	88.3	83.5	80.6	77.7	80.2	75.5	71.9	69.5	67.5
92	NO-1B	78.9	73.1	64.9	59.5	56.9	68.7	61.8	56.0	52.4	50.0	60.7	53.4	47.9	44.8	42.0
93	NO-2A	89.8	85.0	77.7	72.6	69.7	85.6	80.1	74.9	70.3	66.8	72.0	65.7	61.3	58.7	56.9
94	NO-2B	73.7	66.6	62.1	60.3	68.1	61.1	56.2	53.6	51.8	54.1	46.4	42.7	41.5	40.9	72.5
95	NO-3A	72.5	68.6	61.5	54.6	49.4	67.7	63.6	58.1	52.9	48.3	62.3	58.1	53.5	49.1	45.1
96	NO-3B	61.1	56.3	48.3	41.5	36.6	55.5	49.7	43.5	38.3	34.5	51.5	45.9	40.0	35.2	31.8
97	NO-4A	69.9	65.3	58.5	53.2	48.9	64.0	58.2	52.3	48.2	45.0	57.6	51.5	46.1	42.3	39.5
98	NO-4B	57.3	51.7	44.0	38.7	35.0	49.0	41.5	35.8	32.2	30.0	41.1	33.8	28.6	26.1	24.5
99	NO-5A	77.7	74.4	68.5	63.9	60.3	69.6	65.3	61.3	58.3	55.8	60.8	56.4	53.2	50.9	49.1
100	NO-5B	74.3	71.3	64.9	59.5	55.7	69.1	63.0	57.7	53.6	50.6	61.3	55.4	50.6	47.0	44.5
101	NO-6A	75.0	68.9	60.1	52.4	47.4	68.4	61.2	53.9	48.2	43.9	61.2	53.9	47.4	42.5	39.3
102	NO-6B	63.7	56.1	46.6	39.7	36.1	56.0	47.4	40.1	35.4	32.1	56.3	48.9	41.5	35.0	31.1
103	NO-7A	100.4	101.0	96.4	91.2	85.8	94.4	93.3	90.1	86.5	83.1	88.0	86.0	83.1	80.3	77.6
104	NO-7B	96.1	91.4	82.9	75.4	69.1	89.0	83.2	77.4	71.9	67.1	82.0	77.1	72.2	67.9	64.1

1 kPa = 0.145 psi

Appendix B1 Resilient Modulus Test Results for Development Dataset (Continued)

Sequence Number		1	2	3	4	5	6	7	8	9	10	11	12	13	14	15
No.	**Sample I.D.**	**Resillient Modulus (MPa)**														
105	NO-8A	98.5	99.4	97.8	95.7	93.3	92.1	92.2	91.9	91.4	90.7	81.9	82.4	83.7	83.8	83.5
106	NO-8B	105.5	106.7	104.3	101.0	97.4	101.1	101.2	100.3	98.4	96.2	94.4	94.0	93.9	92.7	91.5
107	NO-9A	96.6	91.8	82.9	75.3	68.3	90.0	83.9	76.5	70.1	65.2	82.2	76.3	70.2	65.0	61.0
108	NO-9B	89.4	83.2	74.1	65.0	57.6	83.9	76.0	67.3	60.1	54.7	78.6	70.6	62.7	56.6	51.6
109	OK-1A	411.7	131.5	96.9	76.2	64.7	343.2	115.1	94.6	78.0	67.5	402.9	130.4	135.5	110.7	87.5
110	OK-1B	214.1	61.3	48.3	35.7	29.2	173.3	60.6	44.9	33.7	28.3	178.9	59.4	43.1	32.5	27.5
111	OK-2A	75.7	65.7	54.4	45.2	41.2	70.4	54.7	45.1	41.6	40.4	65.6	50.7	41.2	39.0	38.8
112	OK-2B	223.8	57.5	38.3	34.1	34.6	195.2	55.1	38.7	35.8	35.5	186.1	52.5	38.9	36.4	36.5
113	OK-3A	365.7	91.2	76.0	62.4	52.3	338.6	87.9	70.1	57.5	50.1	334.1	85.3	67.7	55.0	47.9
114	OK-3B	341.2	78.9	52.1	36.6	33.2	316.8	75.4	46.5	35.5	31.8	489.9	91.3	55.7	38.4	33.5
115	OK-4A	161.2	66.5	45.9	37.3	32.9	168.8	62.0	46.7	37.7	33.8	198.7	62.2	47.2	38.2	34.4
116	OK-4B	255.7	53.2	33.7	24.9	22.0	220.7	45.5	28.9	23.5	21.7	202.8	44.1	28.3	23.1	21.6
117	OK-5A	268.8	72.8	63.0	53.8	46.1	229.7	69.9	57.9	50.3	45.2	241.5	70.2	57.7	49.4	44.5
118	OK-5B	99.3	48.6	41.9	38.4	38.2	82.7	46.0	38.3	37.1	37.5	154.6	70.1	57.2	52.7	47.1
119	OS-1A	95.7	77.1	74.4	71.3	65.5	104.6	77.6	73.9	70.4	66.6	107.5	79.0	74.5	71.1	67.4
120	OS-1B	258.4	69.2	47.1	33.9	29.6	243.1	63.2	45.6	34.7	30.4	252.4	65.4	47.4	35.8	31.4
121	OS-2A	365.3	91.5	90.0	87.1	84.0	434.1	94.8	92.7	88.2	85.3	462.4	96.9	94.2	90.0	86.9
122	OS-2B	169.2	65.1	51.0	40.6	34.0	222.3	67.2	53.0	42.8	36.3	223.7	69.4	55.0	44.2	37.7
123	OS-3A	1339.0	179.4	109.1	89.4	71.8	1770.9	167.5	102.7	86.5	71.6	1880.2	168.7	103.8	87.6	71.7
124	OS-3B	209.3	52.5	33.6	25.9	25.5	255.7	49.9	31.6	26.4	25.3	266.1	50.8	32.5	27.0	26.0
125	RO-1A	82.4	80.5	73.3	65.4	58.1	78.2	75.9	70.5	64.3	58.4	73.9	71.4	67.4	62.4	57.0
126	RO-1B	78.5	75.2	67.9	59.0	51.0	72.5	69.0	63.8	57.3	51.1	63.6	61.4	58.0	53.3	48.4

1 kPa = 0.145 psi

Appendix B2 Resilient Modulus Test Results for Evaluation Dataset

Sequence Number		1	2	3	4	5	6	7	8	9	10	11	12	13	14	15
No.	**Sample I.D.**	**Resillient Modulus (MPa)**														
1	ROE-1A	393.8	102.7	87.3	65.0	54.3	308.1	95.2	80.9	63.0	55.2	455.5	97.6	81.6	63.6	55.7
2	ROE-1B	229.9	77.5	55.7	41.3	34.6	218.1	71.1	52.0	40.2	34.9	248.8	72.2	53.7	40.6	35.1
3	ROE-2A	278.5	118.3	105.8	87.1	67.5	206.1	112.6	99.3	79.3	67.6	283.3	111.8	99.0	79.0	68.1
4	ROE-2B	373.6	116.2	101.1	74.9	63.0	479.5	114.7	96.2	71.4	62.9	817.0	119.8	96.6	71.5	63.4
5	ROE-3A	219.0	103.0	97.0	78.0	69.5	190.6	100.0	92.4	75.0	70.1	198.3	102.5	93.8	76.3	71.3
6	ROE-3B	128.7	90.2	77.1	64.2	58.1	113.1	83.7	69.3	59.7	57.2	120.2	83.6	67.5	58.7	56.5
7	ROE-4A	237.4	83.5	57.2	46.9	38.5	242.6	77.1	54.8	43.3	37.2	278.3	77.3	55.1	42.5	36.6
8	ROE-4B	75.5	41.3	27.0	22.4	20.4	77.7	40.7	27.5	22.7	21.1	83.0	44.3	28.1	23.1	21.6
9	ROE-5A	146.1	79.1	62.7	49.9	44.9	129.8	72.3	56.9	48.0	44.8	133.8	72.4	56.7	47.9	45.0
10	ROE-5B	201.1	76.9	53.0	43.0	37.6	163.7	68.0	48.3	39.7	36.5	200.0	67.1	47.4	39.2	36.5
11	ROE-6A	409.1	131.3	122.1	117.8	104.4	494.2	136.7	121.0	115.9	106.2	826.4	135.7	122.6	116.3	106.5
12	ROE-6B	339.1	117.2	107.8	80.3	68.4	356.1	114.8	101.8	76.6	68.5	461.2	117.4	103.7	77.8	69.4
13	ROE-7A	353.1	119.6	110.8	95.0	80.4	340.5	123.3	108.1	89.4	80.7	361.4	121.3	107.4	87.7	79.7
14	ROE-7B	351.5	115.3	101.5	72.2	65.9	344.2	111.3	89.5	68.2	65.0	404.4	109.6	87.0	67.1	64.7
15	ROE-8A	320.7	93.1	66.8	53.8	49.3	298.4	91.3	64.1	52.5	49.7	396.2	93.7	66.0	53.1	50.7
16	ROE-8B	357.6	105.2	90.4	64.6	57.2	358.9	106.8	86.2	61.6	56.4	368.6	106.0	81.7	59.2	54.9
17	ROE-9A	235.5	95.6	85.0	64.7	59.4	200.0	93.3	79.1	61.9	58.2	191.6	91.1	77.0	60.8	58.2
18	ROE-9B	133.7	70.7	48.3	42.1	41.1	117.9	63.4	46.4	41.6	41.1	125.4	63.2	46.6	42.0	41.7
19	ROE-10A	225.5	104.7	100.7	85.7	74.8	221.1	107.3	101.2	83.4	76.1	255.8	114.0	104.3	85.0	77.6
20	ROE-10B	245.8	102.7	85.8	62.1	55.0	218.3	93.4	75.5	59.4	55.3	261.3	96.4	76.4	58.5	53.9
21	ROE-11A	126.8	75.8	54.8	46.1	41.8	118.0	73.0	51.5	45.4	41.8	117.8	72.9	51.1	45.1	41.6
22	ROE-11B	88.1	55.4	37.8	30.0	26.7	85.0	46.6	32.3	27.5	25.5	88.4	44.5	30.7	26.1	24.6
23	ROE-12A	316.5	118.4	113.8	96.5	83.4	265.0	127.9	120.5	105.7	88.7	339.3	131.2	126.0	110.5	91.9
24	ROE-12B	244.0	94.8	86.4	65.9	58.6	230.8	99.3	90.9	69.9	60.4	268.2	103.3	93.8	72.4	61.6
25	ROE-13A	159.2	80.3	61.8	52.5	48.4	152.8	80.8	60.3	51.8	48.5	159.6	82.9	61.6	52.1	48.6
26	ROE-13B	130.1	68.4	47.5	36.1	29.4	108.6	62.5	42.5	33.1	28.6	113.6	62.0	41.3	32.2	28.0

1 kPa = 0.145 psi

Appendix B2 Resilient Modulus Test Results for Evaluation Dataset (Continued)

Sequence Number		1	2	3	4	5	6	7	8	9	10	11	12	13	14	15
No.	Sample I.D.	Resillient Modulus (MPa)														
27	ROE-14A	130.4	68.3	48.7	37.7	30.9	130.1	65.9	46.0	36.2	31.0	125.9	66.7	46.1	36.1	31.1
28	ROE-14B	85.6	36.1	21.8	17.2	16.1	86.7	39.1	23.8	18.8	16.8	96.8	42.2	25.0	19.4	17.3
29	ROE-15A	120.7	69.0	53.7	45.1	42.4	114.0	69.4	55.1	47.0	44.9	127.3	72.7	57.9	48.6	46.4
30	ROE-15B	113.5	61.8	43.0	36.6	33.9	89.9	54.9	39.0	34.9	33.9	94.8	53.7	38.5	34.7	34.1
31	ROE-16A	167.3	105.9	97.8	85.7	77.3	142.9	100.7	95.4	86.5	81.7	173.2	107.4	99.9	88.9	83.5
32	ROE-16B	127.5	82.1	67.1	53.6	49.0	123.0	79.8	67.2	54.7	50.0	142.9	82.5	69.8	55.8	51.0
33	ROE-17A	178.1	109.6	88.1	65.6	59.6	171.7	101.7	87.8	63.2	58.9	188.5	103.4	88.3	62.8	58.9
34	ROE-17B	102.3	54.1	34.2	26.5	22.9	100.4	54.8	34.1	25.8	22.5	103.4	55.3	34.0	25.4	22.3
35	ROE-18A	122.4	60.8	42.8	35.3	33.2	122.1	60.3	41.8	34.9	33.6	141.8	61.9	42.3	35.3	34.2
36	ROE-18B	125.8	57.0	39.6	31.5	29.7	105.4	52.8	35.9	30.0	29.4	110.0	52.0	34.8	29.5	29.2
37	ROE-19A	177.4	82.8	70.1	54.3	50.2	168.2	84.6	67.3	53.2	50.4	177.7	84.2	66.8	53.0	50.7
38	ROE-19B	191.1	81.6	62.3	48.8	43.8	176.8	78.8	58.5	46.6	43.2	187.9	78.8	57.6	46.0	43.0
39	ROE-20A	183.2	104.3	96.7	77.5	68.4	176.1	105.9	97.0	78.1	69.7	193.1	108.4	98.0	79.3	70.7
40	ROE-20B	143.0	88.6	70.8	58.0	52.9	156.8	87.7	68.7	56.5	52.7	185.9	89.8	69.0	56.0	52.6
41	ROE-21A	135.1	79.7	68.5	59.4	56.3	128.5	81.9	67.5	58.6	57.1	136.7	84.5	69.0	59.3	57.9
42	ROE-21B	183.2	104.7	95.6	75.7	70.0	162.3	100.8	91.6	74.7	70.4	185.3	106.1	94.2	75.5	71.5
43	ROE-22A	131.9	78.8	58.6	49.3	44.7	118.4	75.1	56.7	49.1	45.8	127.5	76.3	58.0	49.7	46.5
44	ROE-22B	104.5	63.9	42.6	36.2	32.4	106.2	62.3	42.1	35.7	32.2	110.8	62.3	42.1	35.4	32.1
45	ROE-23A	142.7	72.9	50.5	40.3	33.5	125.8	71.3	48.8	38.8	33.4	132.0	72.8	48.2	38.8	33.6
46	ROE-23B	143.6	52.3	29.6	22.7	20.5	110.6	52.0	30.5	23.0	20.8	112.9	53.6	31.0	23.4	21.3
47	ROE-24A	199.2	95.7	87.8	70.5	62.2	160.8	98.9	92.1	74.3	64.4	183.2	104.0	95.8	77.7	66.4
48	ROE-24B	148.8	79.9	60.3	46.5	38.2	137.7	80.0	61.5	46.3	39.1	168.9	83.6	64.7	47.3	39.7
49	ROE-25A	217.9	86.1	67.5	53.1	47.8	156.9	85.3	70.6	54.1	49.3	191.7	89.3	74.3	55.9	50.4
50	ROE-25B	140.0	59.7	35.6	27.0	23.6	115.2	54.7	34.3	26.7	23.6	112.9	55.9	34.5	26.8	24.0
51	ROE-26A	160.7	81.7	65.7	55.0	51.0	139.9	81.7	68.0	56.0	52.3	157.2	85.3	71.0	57.3	53.5
52	ROE-26B	114.6	67.7	52.3	42.6	36.6	123.8	69.2	51.7	42.0	37.0	126.5	70.0	52.1	42.1	37.2

1 kPa = 0.145 psi

Appendix B2 Resilient Modulus Test Results for Evaluation Dataset (Continued)

Sequence Number		1	2	3	4	5	6	7	8	9	10	11	12	13	14	15
No.	**Sample I.D.**	**Resillient Modulus (MPa)**														
53	ROE-27A	134.6	75.7	54.8	44.8	39.2	124.7	72.5	50.0	41.5	37.6	126.6	70.6	47.9	39.8	36.3
54	ROE-27B	79.0	28.2	19.6	18.0	18.1	80.2	33.9	22.7	19.7	19.2	87.4	36.2	23.9	20.5	20.1
55	ROE-28A	173.5	80.3	58.5	48.1	44.0	161.9	77.4	55.7	47.6	43.9	195.3	78.6	56.5	48.0	44.5
56	ROE-28B	134.9	63.5	39.6	31.7	29.2	107.9	54.8	36.2	30.3	28.5	121.1	54.9	35.8	30.1	28.6
57	ROE-29A	235.7	85.2	68.8	50.6	43.6	164.5	83.4	68.6	50.9	44.5	218.7	86.3	70.7	51.6	44.9
58	ROE-29B	135.9	62.4	38.3	29.6	26.3	99.4	54.5	36.1	29.6	26.8	102.9	56.6	36.2	29.4	26.6
59	WOE-1A	68.3	65.3	57.3	49.6	47.7	68.2	65.2	55.7	49.4	48.2	66.2	65.4	56.1	49.8	48.9
60	WOE-1B	62.5	59.6	51.0	45.6	45.2	71.8	57.6	48.4	45.3	45.1	71.9	57.0	48.8	45.9	45.7
61	WOE-2A	62.1	59.6	51.9	46.3	45.4	64.9	59.6	50.9	46.7	46.2	64.1	60.4	51.1	46.7	46.9
62	WOE-2B	64.6	54.6	46.3	41.8	41.8	64.9	53.5	45.2	42.2	42.5	68.7	54.4	46.0	43.2	43.3
63	WOE-3A	104.1	95.3	100.8	101.7	103.5	122.2	103.8	103.2	104.0	105.7	124.9	107.6	104.7	105.3	107.4
64	WOE-3B	91.4	88.1	88.0	86.1	83.2	102.9	91.8	86.5	85.4	83.3	102.4	94.4	87.5	86.3	83.6
65	WOE-4A	76.4	69.2	66.3	65.0	65.2	74.5	64.9	65.1	66.9	67.8	80.5	68.4	68.5	69.4	70.2
66	WOE-4B	58.1	51.8	41.5	37.1	35.3	57.1	44.8	38.3	35.5	34.8	54.1	47.4	39.0	35.5	34.7
67	WOE-5A	83.9	73.5	72.9	69.1	61.2	78.0	74.6	71.5	66.5	61.5	79.6	76.8	71.9	66.1	61.4
68	WOE-5B	72.8	66.8	60.0	48.2	43.6	73.0	60.9	51.8	43.9	41.1	60.5	58.5	48.3	41.5	39.6

1 kPa = 0.145 psi

APPENDIX C

Equation for Factorial Model

Appendix C Equation of Factorial Model

$$
\begin{aligned}
M_R/P_a = {} & 13.2514795 - 438.31923*w - 13.311426*\gamma_d + 2.41669221*PI + 27.2918109*P_{200} - \\
& 35.722370*U_c - 11.240229*\sigma_d + 85.5626222*\theta + 278.441637*w*\gamma_d - 16.168513*w*PI - \\
& 1.0992907*\gamma_d*PI + 14.4631546*w*P_{200} - 9.7399663*\gamma_d*P_{200} - 1.7766282*PI*P_{200} + \\
& 332.908859*w*U_c + 23.0157253*\gamma_d*U_c - .01410921*PI*U_c + 38.7543639*P_{200}*U_c + \\
& 799.099567*w*\sigma_d + 31.3535709*\gamma_d*\sigma_d - 3.3563515*PI*\sigma_d - 69.037455*P_{200}*\sigma_d - \\
& 47.303113*U_c*\sigma_d - 279.93578*w*\theta - 38.643251*\gamma_d*\theta - 1.0518368*PI*\theta - \\
& 84.485170*P_{200}*\theta - 29.795776*U_c*\theta - 106.57364*\sigma_d*\theta + 9.15134484*w*\gamma_d*PI - \\
& 28.679440*w*\gamma_d*P_{200} + 21.1200089*w*PI*P_{200} + .662040611*\gamma_d*PI*P_{200} - \\
& 200.60637*w*\gamma_d*U_c + 2.75148494*w*PI*U_c - .02351306*\gamma_d*PI*U_c - \\
& 244.11931*w*P_{200}*U_c - 25.359274*\gamma_d*P_{200}*U_c - 1.2799791*PI*P_{200}*U_c - \\
& 588.87015*w*\gamma_d*\sigma_d + 15.1565883*w*PI*\sigma_d + .481801078*\gamma_d*PI*\sigma_d - \\
& 218.18881*w*P_{200}*\sigma_d + 10.1638379*\gamma_d*P_{200}*\sigma_d + 2.36460454*PI*P_{200}*\sigma_d - \\
& 45.492450*w*U_c*\sigma_d + 12.7119527*\gamma_d*U_c*\sigma_d + 3.45466718*PI*U_c*\sigma_d + \\
& 73.1347282*P_{200}*U_c*\sigma_d + 115.117756*w*\gamma_d*\theta + 7.15819491*w*PI*\theta - .16922596*\gamma_d*PI*\theta \\
& + 319.715817*w*P_{200}*\theta + 37.2140312*\gamma_d*P_{200}*\theta + .456277589*PI*P_{200}*\theta + \\
& 87.1036047*w*U_c*\theta + 12.8403258*\gamma_d*U_c*\theta + .470678587*PI*U_c*\theta + \\
& 17.7135930*P_{200}*U_c*\theta + 117.516534*w*\sigma_d*\theta + 45.1075781*\gamma_d*\sigma_d*\theta + \\
& 4.48108267*PI*\sigma_d*\theta + 123.422308*P_{200}*\sigma_d*\theta + 69.9906302*U_c*\sigma_d*\theta - \\
& 11.825725*w*\gamma_d*PI*P_{200} - 2.1155135*w*\gamma_d*PI*U_c + 149.381038*w*\gamma_d*P_{200}*U_c + \\
& .461733179*w*PI*P_{200}*U_c + .843999848*\gamma_d*PI*P_{200}*U_c - 3.1294192*w*\gamma_d*PI*\sigma_d + \\
& 277.350974*w*\gamma_d*P_{200}*\sigma_d - 14.172917*w*PI*P_{200}*\sigma_d + .525633666*\gamma_d*PI*P_{200}*\sigma_d + \\
& 98.7215822*w*\gamma_d*U_c*\sigma_d - 15.964519*w*PI*U_c*\sigma_d - 1.1448209*\gamma_d*PI*U_c*\sigma_d - \\
& 169.47515*w*P_{200}*U_c*\sigma_d - 22.778234*\gamma_d*P_{200}*U_c*\sigma_d - 2.0574402*PI*P_{200}*U_c*\sigma_d - \\
& 1.1780048*w*\gamma_d*PI*\theta - 136.19640*w*\gamma_d*P_{200}*\theta - 5.5904934*w*PI*P_{200}*\theta + \\
& .582825521*\gamma_d*PI*P_{200}*\theta - 32.417984*w*\gamma_d*U_c*\theta - 4.4154766*w*PI*U_c*\theta - \\
& .03434428*\gamma_d*PI*U_c*\theta - 35.024894*w*P_{200}*U_c*\theta - 5.1994910*\gamma_d*P_{200}*U_c*\theta + \\
& .197336556*PI*P_{200}*U_c*\theta + 12.9337904*w*\gamma_d*\sigma_d*\theta - 14.637167*w*PI*\sigma_d*\theta - \\
& 1.4228429*\gamma_d*PI*\sigma_d*\theta - 175.26170*w*P_{200}*\sigma_d*\theta - 51.332213*\gamma_d*P_{200}*\sigma_d*\theta - \\
& 4.4923407*PI*P_{200}*\sigma_d*\theta - 150.22381*w*U_c*\sigma_d*\theta - 29.716170*\gamma_d*U_c*\sigma_d*\theta - \\
& 2.2982062*PI*U_c*\sigma_d*\theta - 70.820468*P_{200}*U_c*\sigma_d*\theta + 0.00000000*w*\gamma_d*PI*P_{200}*U_c + \\
& 0.00000000*w*\gamma_d*PI*P_{200}*\sigma_d + 5.73119283*w*\gamma_d*PI*U_c*\sigma_d + \\
& 0.00000000*w*\gamma_d*P_{200}*U_c*\sigma_d + 9.80008993*w*PI*P_{200}*U_c*\sigma_d - \\
& .05009087*\gamma_d*PI*P_{200}*U_c*\sigma_d + 0.00000000*w*\gamma_d*PI*P_{200}*\theta + 1.92867824*w*\gamma_d*PI*U_c*\theta \\
& + 0.00000000*w*\gamma_d*P_{200}*U_c*\theta + 1.30268945*w*PI*P_{200}*U_c*\theta - \\
& .38745801*\gamma_d*PI*P_{200}*U_c*\theta + 3.36590974*w*\gamma_d*PI*\sigma_d*\theta + 0.00000000*w*\gamma_d*P_{200}*\sigma_d*\theta + \\
& 11.4488598*w*PI*P_{200}*\sigma_d*\theta + 1.17782173*\gamma_d*PI*P_{200}*\sigma_d*\theta + 31.7684321*w*\gamma_d*U_c*\sigma_d*\theta \\
& + 5.85679607*w*PI*U_c*\sigma_d*\theta + .607338016*\gamma_d*PI*U_c*\sigma_d*BS + \\
& 128.506165*w*P_{200}*U_c*\sigma_d*\theta + 26.8574361*\gamma_d*P_{200}*U_c*\sigma_d*\theta + \\
& 1.63623868*PI*P_{200}*U_c*\sigma_d*\theta + 0.00000000*w*\gamma_d*PI*P_{200}*U_c*\sigma_d + \\
& 0.00000000*w*\gamma_d*PI*P_{200}*U_c*\theta + 0.00000000*w*\gamma_d*PI*P_{200}*\sigma_d*\theta + \\
& 0.00000000*w*\gamma_d*PI*U_c*\sigma_d*\theta + 0.00000000*w*\gamma_d*P_{200}*U_c*\sigma_d*\theta + \\
& 0.00000000*w*PI*P_{200}*U_c*\sigma_d*\theta + 0.00000000*\gamma_d*PI*P_{200}*U_c*\sigma_d*\theta - \\
& 4.6975464*w*\gamma_d*PI*P_{200}*U_c*\sigma_d*\theta
\end{aligned}
$$

APPENDIX D

Predictions of Resilient Modulus from Statistical and Artificial Neural Network Models

Appendix D1 Predictions of Resilient Modulus from Statistical Models for Development Dataset

Sample I.D.	Seq. No.	Experiment M_R/P_a (10^3)	Predicted M_R/P_a (10^3)			
			Stress-Based	Mult. Reg.	Polynomial	Factorial
AD-1A	2	0.6993	0.8042	0.6697	0.6928	0.5980
AD-1A	3	0.5898	0.6226	0.5912	0.5669	0.5225
AD-1A	4	0.5099	0.5197	0.5126	0.4900	0.4471
AD-1A	5	0.4632	0.4517	0.4337	0.4622	0.3712
AD-1A	7	0.6051	0.7899	0.6710	0.6944	0.5768
AD-1A	8	0.5227	0.6105	0.5916	0.5663	0.5004
AD-1A	9	0.4639	0.5109	0.5135	0.4893	0.4254
AD-1A	10	0.4238	0.4452	0.4354	0.4607	0.3503
AD-1A	12	0.5152	0.7636	0.6709	0.6951	0.5544
AD-1A	13	0.4400	0.5937	0.5919	0.5674	0.4784
AD-1A	14	0.3932	0.4984	0.5138	0.4898	0.4033
AD-1A	15	0.3633	0.4351	0.4353	0.4608	0.3278
AD-1B	2	0.5210	0.7451	0.5209	0.5284	0.4247
AD-1B	3	0.3891	0.5630	0.4449	0.4043	0.3168
AD-1B	4	0.2792	0.4602	0.3677	0.3251	0.2168
AD-1B	5	0.2120	0.3946	0.2914	0.2934	0.1274
AD-1B	7	0.3715	0.7273	0.5221	0.5301	0.4473
AD-1B	8	0.2821	0.5487	0.4453	0.4038	0.3218
AD-1B	9	0.2407	0.4495	0.3681	0.3241	0.2053
AD-1B	10	0.2068	0.3864	0.2922	0.2920	0.1002
AD-1B	12	0.2816	0.6973	0.5225	0.5316	0.4687
AD-1B	13	0.2156	0.5289	0.4457	0.4049	0.3268
AD-1B	14	0.1938	0.4355	0.3689	0.3250	0.1946
AD-1B	15	0.1795	0.3747	0.2917	0.2921	0.0712
AD-2A	2	1.3802	1.0370	1.0023	1.0179	1.2975
AD-2A	3	1.2780	0.8729	0.9220	0.8906	1.2252
AD-2A	4	1.1846	0.7721	0.8426	0.8151	1.1413
AD-2A	5	1.1007	0.7005	0.7623	0.7897	1.0437
AD-2A	7	1.3183	1.0734	1.0031	1.0187	1.2024
AD-2A	8	1.2641	0.9004	0.9228	0.8906	1.1509
AD-2A	9	1.1857	0.7939	0.8430	0.8140	1.0871
AD-2A	10	1.1031	0.7254	0.7710	0.7885	1.0188
AD-2A	12	1.1460	1.1267	1.0031	1.0193	1.1068
AD-2A	13	1.1696	0.9402	0.9232	0.8916	1.0762
AD-2A	14	1.0979	0.8327	0.8499	0.8190	1.0370
AD-2A	15	1.0318	0.7510	0.7714	0.7886	0.9832
AD-2B	2	1.0557	1.0179	0.8419	0.9047	0.9874
AD-2B	3	0.9149	0.8258	0.7625	0.7787	0.8674
AD-2B	4	0.7758	0.7150	0.6865	0.7052	0.7713
AD-2B	5	0.6765	0.6344	0.6062	0.6773	0.6894
AD-2B	7	0.8974	1.0461	0.8427	0.9054	0.9959
AD-2B	8	0.7897	0.8471	0.7637	0.7793	0.8440
AD-2B	9	0.6930	0.7323	0.6882	0.7051	0.7171
AD-2B	10	0.6182	0.6507	0.6106	0.6760	0.6053
AD-2B	12	0.7805	1.0888	0.8435	0.9078	1.0048
AD-2B	13	0.6771	0.8796	0.7658	0.7826	0.8232
AD-2B	14	0.5943	0.7545	0.6886	0.7056	0.6614
AD-2B	15	0.5299	0.6664	0.6088	0.6760	0.5138

Appendix D1 Predictions of Resilient Modulus from Statistical Models for Development Dataset (Continued)

Sample I.D.	Seq. No.	Experiment M_R/P_a (10^3)	Predicted M_R/P_a (10^3) Stress-Based	Mult. Reg.	Polynomial	Factorial
AD-3A	2	0.7868	0.8400	0.6684	0.5863	0.6508
AD-3A	3	0.6617	0.6741	0.5920	0.4640	0.6360
AD-3A	4	0.5764	0.5744	0.5126	0.3860	0.6008
AD-3A	5	0.5293	0.5119	0.4380	0.3584	0.5493
AD-3A	7	0.6688	0.7957	0.6701	0.5887	0.4876
AD-3A	8	0.5785	0.6383	0.5920	0.4629	0.5056
AD-3A	9	0.5105	0.5461	0.5121	0.3844	0.5036
AD-3A	10	0.4593	0.4874	0.4358	0.3568	0.4826
AD-3A	12	0.5340	0.7343	0.6726	0.5945	0.3227
AD-3A	13	0.4572	0.5964	0.5963	0.4691	0.3732
AD-3A	14	0.4104	0.5157	0.5190	0.3895	0.4051
AD-3A	15	0.3780	0.4624	0.4427	0.3574	0.4178
AD-3B	2	0.5188	0.8182	0.5469	0.4808	0.5442
AD-3B	3	0.3645	0.6401	0.4710	0.3569	0.4538
AD-3B	4	0.2579	0.5376	0.3937	0.2780	0.3519
AD-3B	5	0.2046	0.4716	0.3178	0.2466	0.2420
AD-3B	7	0.2831	0.7687	0.5486	0.4833	0.4886
AD-3B	8	0.2292	0.6017	0.4714	0.3564	0.4137
AD-3B	9	0.2200	0.5076	0.3937	0.2767	0.3283
AD-3B	10	0.2121	0.4472	0.3178	0.2451	0.2350
AD-3B	12	0.2341	0.6947	0.5490	0.4848	0.4315
AD-3B	13	0.1959	0.5509	0.4717	0.3575	0.3736
AD-3B	14	0.1951	0.4701	0.3949	0.2779	0.3061
AD-3B	15	0.1973	0.4168	0.3182	0.2453	0.2286
AD-4A	2	1.1683	0.9642	0.8489	0.8474	0.8728
AD-4A	3	1.0968	0.7943	0.7690	0.7209	0.7969
AD-4A	4	1.0224	0.6931	0.6896	0.6453	0.7223
AD-4A	5	0.9561	0.6234	0.6097	0.6200	0.6483
AD-4A	7	1.0769	0.9569	0.8501	0.8489	0.8535
AD-4A	8	1.0359	0.7883	0.7703	0.7214	0.7759
AD-4A	9	0.9861	0.6877	0.6904	0.6446	0.6993
AD-4A	10	0.9346	0.6182	0.6097	0.6184	0.6229
AD-4A	12	0.9378	0.9411	0.8501	0.8496	0.8330
AD-4A	13	0.9263	0.7766	0.7698	0.7213	0.7533
AD-4A	14	0.8957	0.6792	0.6904	0.6448	0.6756
AD-4A	15	0.8588	0.6123	0.6109	0.6185	0.5988
AD-4B	2	0.9721	0.9340	0.6929	0.7217	0.6895
AD-4B	3	0.8653	0.7444	0.6135	0.5955	0.5987
AD-4B	4	0.7569	0.6376	0.5372	0.5214	0.5172
AD-4B	5	0.6810	0.5650	0.4604	0.4937	0.4412
AD-4B	7	0.8758	0.9176	0.6937	0.7225	0.6859
AD-4B	8	0.7993	0.7314	0.6139	0.5949	0.5842
AD-4B	9	0.7172	0.6270	0.5371	0.5201	0.4924
AD-4B	10	0.6446	0.5563	0.4603	0.4922	0.4064
AD-4B	12	0.7570	0.8916	0.6941	0.7240	0.6819
AD-4B	13	0.6970	0.7162	0.6160	0.5982	0.5722
AD-4B	14	0.6345	0.6146	0.5388	0.5216	0.4697
AD-4B	15	0.5768	0.5459	0.4616	0.4923	0.3731

Appendix D1 Predictions of Resilient Modulus from Statistical Models for Development Dataset (Continued)

Sample I.D.	Seq. No.	Experiment M_R/P_a (10^3)	Predicted M_R/P_a (10^3)			
			Stress-Based	Mult. Reg.	Polynomial	Factorial
AD-5A	2	1.6523	1.0491	1.0563	1.0644	1.3635
AD-5A	3	1.6068	0.8989	0.9755	0.9365	1.3325
AD-5A	4	1.5367	0.8061	0.8966	0.8615	1.2838
AD-5A	5	1.4468	0.7386	0.8158	0.8361	1.2149
AD-5A	7	1.5303	1.0827	1.0566	1.0643	1.2181
AD-5A	8	1.5342	0.9263	0.9768	0.9370	1.2184
AD-5A	9	1.4977	0.8276	0.8969	0.8605	1.1998
AD-5A	10	1.4378	0.7571	0.8167	0.8346	1.1624
AD-5A	12	1.3005	1.1335	1.0566	1.0649	1.0730
AD-5A	13	1.3368	0.9642	0.9767	0.9375	1.1038
AD-5A	14	1.3403	0.8581	0.8973	0.8610	1.1159
AD-5A	15	1.3207	0.7820	0.8170	0.8346	1.1093
AD-5B	2	1.1571	0.9679	0.7799	0.7949	0.8258
AD-5B	3	1.0523	0.7664	0.6996	0.6675	0.7126
AD-5B	4	0.9113	0.6531	0.6228	0.5937	0.6156
AD-5B	5	0.7746	0.5775	0.5477	0.5669	0.5316
AD-5B	7	1.0591	0.9862	0.7803	0.7948	0.8473
AD-5B	8	0.9875	0.7796	0.7000	0.6670	0.7141
AD-5B	9	0.9510	0.6629	0.6227	0.5924	0.5975
AD-5B	10	0.7731	0.5844	0.5464	0.5653	0.4932
AD-5B	12	0.9537	1.0140	0.7806	0.7963	0.8687
AD-5B	13	0.8986	0.8004	0.7012	0.6691	0.7172
AD-5B	14	0.8155	0.6784	0.6240	0.5935	0.5814
AD-5B	15	0.7265	0.5966	0.5476	0.5654	0.4581
AD-6A	2	1.4050	1.1438	1.0131	1.1650	1.2851
AD-6A	3	1.3646	0.9470	0.9332	1.0385	1.1710
AD-6A	4	1.3054	0.8301	0.8543	0.9633	1.0638
AD-6A	5	1.2302	0.7482	0.7735	0.9376	0.9601
AD-6A	7	1.3067	1.1254	1.0139	1.1658	1.3265
AD-6A	8	1.2925	0.9320	0.9336	1.0380	1.2024
AD-6A	9	1.2571	0.8181	0.8547	0.9622	1.0860
AD-6A	10	1.2100	0.7386	0.7744	0.9361	0.9733
AD-6A	12	1.2004	1.0964	1.0143	1.1673	1.3673
AD-6A	13	1.2104	0.9119	0.9344	1.0395	1.2345
AD-6A	14	1.1979	0.8013	0.8546	0.9625	1.1074
AD-6A	15	1.1657	0.7251	0.7743	0.9361	0.9854
AD-6B	2	1.1374	1.1863	0.9197	1.0883	1.1051
AD-6B	3	1.0610	0.9554	0.8386	0.9585	1.0310
AD-6B	4	0.9754	0.8248	0.7596	0.8824	0.9592
AD-6B	5	0.8888	0.7367	0.6806	0.8560	0.8879
AD-6B	7	1.0763	1.1416	0.9188	1.0858	1.0999
AD-6B	8	1.0293	0.9288	0.8403	0.9596	1.0274
AD-6B	9	0.9622	0.8011	0.7595	0.8811	0.9534
AD-6B	10	0.8892	0.7157	0.6788	0.8544	0.8798
AD-6B	12	1.0408	1.0865	0.9196	1.0881	1.0963
AD-6B	13	1.0139	0.8870	0.8398	0.9595	1.0219
AD-6B	14	0.9638	0.7714	0.7608	0.8822	0.9488
AD-6B	15	0.8999	0.6917	0.6801	0.8545	0.8745

Appendix D1 Predictions of Resilient Modulus from Statistical Models for Development Dataset (Continued)

Sample I.D.	Seq. No.	Experiment M_R/P_a (10^3)	Predicted M_R/P_a (10^3)			
			Stress-Based	Mult. Reg.	Polynomial	Factorial
AD-7A	2	1.1656	1.1869	1.0240	1.2399	1.2023
AD-7A	3	1.1155	0.9961	0.9432	1.1121	1.1100
AD-7A	4	1.0652	0.8862	0.8656	1.0379	1.0104
AD-7A	5	1.0201	0.8094	0.7866	1.0117	0.8984
AD-7A	7	1.0727	1.1230	1.0243	1.2399	1.1956
AD-7A	8	1.0487	0.9480	0.9441	1.1120	1.1221
AD-7A	9	1.0125	0.8458	0.8655	1.0366	1.0394
AD-7A	10	0.9764	0.7749	0.7861	1.0102	0.9448
AD-7A	12	0.9410	1.0342	1.0247	1.2413	1.1889
AD-7A	13	0.9216	0.8831	0.9449	1.1136	1.1341
AD-7A	14	0.8956	0.7949	0.8672	1.0380	1.0701
AD-7A	15	0.8737	0.7332	0.7882	1.0103	0.9943
AD-7B	2	1.2358	1.2560	1.0035	1.1123	1.3674
AD-7B	3	1.1820	1.0603	0.9223	0.9828	1.2944
AD-7B	4	1.1294	0.9452	0.8420	0.9061	1.2123
AD-7B	5	1.0744	0.8671	0.7622	0.8808	1.1210
AD-7B	7	1.1298	1.1774	1.0025	1.1097	1.2727
AD-7B	8	1.1104	1.0015	0.9218	0.9811	1.2162
AD-7B	9	1.0797	0.8992	0.8433	0.9057	1.1515
AD-7B	10	1.0440	0.8272	0.7626	0.8792	1.0753
AD-7B	12	1.0031	1.0737	1.0025	1.1104	1.1789
AD-7B	13	0.9983	0.9259	0.9226	0.9827	1.1389
AD-7B	14	0.9853	0.8374	0.8428	0.9056	1.0892
AD-7B	15	0.9622	0.7774	0.7638	0.8793	1.0304
AD-8A	2	1.5072	1.3189	1.3347	1.2705	1.4582
AD-8A	3	1.5175	1.1443	1.2553	1.1434	1.4970
AD-8A	4	1.5165	1.0313	1.1746	1.0657	1.5273
AD-8A	5	1.5062	0.9550	1.0991	1.0399	1.5475
AD-8A	7	1.4932	1.3708	1.3364	1.2729	1.3451
AD-8A	8	1.4964	1.1798	1.2544	1.1412	1.4002
AD-8A	9	1.4892	1.0619	1.1745	1.0644	1.4448
AD-8A	10	1.4733	0.9781	1.0956	1.0382	1.4802
AD-8A	12	1.3697	1.4387	1.3346	1.2702	1.2346
AD-8A	13	1.3849	1.2364	1.2552	1.1428	1.3025
AD-8A	14	1.3939	1.1062	1.1749	1.0649	1.3621
AD-8A	15	1.3909	1.0147	1.0960	1.0383	1.4120
AD-8B	2	1.0135	1.3637	1.0497	1.0800	1.0117
AD-8B	3	0.9274	1.0871	0.9703	0.9535	0.9053
AD-8B	4	0.8111	0.9299	0.8939	0.8792	0.7928
AD-8B	5	0.6998	0.8237	0.8185	0.8512	0.6719
AD-8B	7	0.9497	1.3821	1.0497	1.0791	0.9574
AD-8B	8	0.8908	1.1008	0.9702	0.9524	0.8687
AD-8B	9	0.8037	0.9394	0.8930	0.8773	0.7722
AD-8B	10	0.7077	0.8317	0.8175	0.8497	0.6680
AD-8B	12	0.8900	1.4132	1.0500	1.0806	0.9036
AD-8B	13	0.8396	1.1235	0.9711	0.9540	0.8332
AD-8B	14	0.7689	0.9565	0.8938	0.8781	0.7540
AD-8B	15	0.6897	0.8441	0.8175	0.8497	0.6657

Appendix D1 Predictions of Resilient Modulus from Statistical Models for Development Dataset (Continued)

Sample I.D.	Seq. No.	Experiment M_R/P_a (10^3)	Predicted M_R/P_a (10^3)			
			Stress-Based	Mult. Reg.	Polynomial	Factorial
AL-1A	2	0.7533	0.8554	0.8535	0.8175	0.7744
AL-1A	3	0.7673	0.7147	0.7793	0.6917	0.7150
AL-1A	4	0.7745	0.6333	0.7095	0.6131	0.6565
AL-1A	5	0.7557	0.5699	0.6310	0.5712	0.5876
AL-1A	7	0.7575	0.8561	0.8539	0.8175	0.7599
AL-1A	8	0.7585	0.7153	0.7797	0.6912	0.7057
AL-1A	9	0.7669	0.6380	0.7143	0.6161	0.6555
AL-1A	10	0.7631	0.5733	0.6357	0.5709	0.5923
AL-1A	12	0.8065	0.8571	0.8543	0.8191	0.7455
AL-1A	13	0.7893	0.7160	0.7801	0.6923	0.6965
AL-1A	14	0.7840	0.6386	0.7146	0.6168	0.6508
AL-1A	15	0.7784	0.5738	0.6361	0.5711	0.5930
AL-1B	2	0.5824	0.7819	0.6546	0.7075	0.6495
AL-1B	3	0.5365	0.6098	0.5804	0.5739	0.5906
AL-1B	4	0.4701	0.5179	0.5106	0.4881	0.5374
AL-1B	5	0.4349	0.4530	0.4364	0.4395	0.4831
AL-1B	7	0.5582	0.7808	0.6550	0.7076	0.6536
AL-1B	8	0.4879	0.6164	0.5852	0.5802	0.5942
AL-1B	9	0.4448	0.5219	0.5154	0.4916	0.5370
AL-1B	10	0.4285	0.4557	0.4412	0.4399	0.4784
AL-1B	12	0.5685	0.7791	0.6554	0.7092	0.6577
AL-1B	13	0.4826	0.6152	0.5856	0.5814	0.5945
AL-1B	14	0.4379	0.5210	0.5157	0.4924	0.5333
AL-1B	15	0.4239	0.4550	0.4416	0.4402	0.4705
AL-2A	2	0.7311	0.8530	0.7993	0.8183	0.6213
AL-2A	3	0.7016	0.6901	0.7120	0.6717	0.5864
AL-2A	4	0.6570	0.6094	0.6378	0.5947	0.5511
AL-2A	5	0.6177	0.5531	0.5637	0.5615	0.5103
AL-2A	7	0.7072	0.8395	0.7953	0.8095	0.5727
AL-2A	8	0.6460	0.6944	0.7168	0.6771	0.5512
AL-2A	9	0.6192	0.6121	0.6426	0.5971	0.5255
AL-2A	10	0.6114	0.5520	0.5641	0.5601	0.4925
AL-2A	12	0.7187	0.8476	0.8001	0.8199	0.5261
AL-2A	13	0.6484	0.6981	0.7215	0.6843	0.5149
AL-2A	14	0.6200	0.6142	0.6473	0.6013	0.4988
AL-2A	15	0.6161	0.5505	0.5644	0.5602	0.4746
AL-2B	2	0.6083	0.9121	0.7141	0.8356	0.5327
AL-2B	3	0.5381	0.7307	0.6356	0.6955	0.4890
AL-2B	4	0.4662	0.6377	0.5658	0.6122	0.4499
AL-2B	5	0.4339	0.5705	0.4916	0.5661	0.4080
AL-2B	7	0.5238	0.8969	0.7145	0.8357	0.5061
AL-2B	8	0.4481	0.7341	0.6447	0.7083	0.4679
AL-2B	9	0.4181	0.6334	0.5705	0.6154	0.4269
AL-2B	10	0.4167	0.5631	0.4920	0.5648	0.3832
AL-2B	12	0.5165	0.8882	0.7193	0.8466	0.4819
AL-2B	13	0.4317	0.7252	0.6494	0.7164	0.4442
AL-2B	14	0.4045	0.6256	0.5753	0.6205	0.4039
AL-2B	15	0.4089	0.5596	0.5011	0.5683	0.3632

Appendix D1 Predictions of Resilient Modulus from Statistical Models for Development Dataset (Continued)

Sample I.D.	Seq. No.	Experiment M_R/P_a (10^3)	Predicted M_R/P_a (10^3)			
			Stress-Based	Mult. Reg.	Polynomial	Factorial
AL-3A	2	0.7262	0.8985	0.7378	0.7640	0.6906
AL-3A	3	0.6781	0.7068	0.6505	0.6174	0.6241
AL-3A	4	0.6271	0.6147	0.5763	0.5405	0.5698
AL-3A	5	0.5815	0.5517	0.5022	0.5072	0.5177
AL-3A	7	0.6931	0.8625	0.7338	0.7552	0.6763
AL-3A	8	0.6271	0.7039	0.6596	0.6289	0.6159
AL-3A	9	0.5974	0.6060	0.5811	0.5428	0.5543
AL-3A	10	0.5844	0.5408	0.5025	0.5058	0.4950
AL-3A	12	0.7186	0.8423	0.7385	0.7656	0.6693
AL-3A	13	0.6329	0.6872	0.6644	0.6363	0.6050
AL-3A	14	0.5994	0.5924	0.5858	0.5470	0.5392
AL-3A	15	0.5875	0.5295	0.5073	0.5068	0.4758
AL-3B	2	0.5747	0.9463	0.7014	0.7516	0.5619
AL-3B	3	0.4698	0.7666	0.6316	0.6270	0.5164
AL-3B	4	0.3900	0.6667	0.5661	0.5455	0.4767
AL-3B	5	0.3522	0.5942	0.4963	0.4961	0.4373
AL-3B	7	0.4896	0.9284	0.7061	0.7607	0.5679
AL-3B	8	0.3913	0.7583	0.6407	0.6402	0.5194
AL-3B	9	0.3500	0.6574	0.5752	0.5537	0.4737
AL-3B	10	0.3380	0.5814	0.5011	0.4968	0.4253
AL-3B	12	0.4862	0.8943	0.7109	0.7716	0.5747
AL-3B	13	0.3797	0.7389	0.6498	0.6556	0.5240
AL-3B	14	0.3386	0.6349	0.5800	0.5592	0.4690
AL-3B	15	0.3309	0.5630	0.5058	0.4994	0.4141
AL-4A	2	0.7220	0.9246	0.9016	0.8913	0.9499
AL-4A	3	0.7276	0.7709	0.8187	0.7563	0.8618
AL-4A	4	0.7128	0.6918	0.7489	0.6851	0.7884
AL-4A	5	0.6805	0.6291	0.6703	0.6513	0.7066
AL-4A	7	0.7315	0.9243	0.9063	0.8999	0.9480
AL-4A	8	0.7017	0.7743	0.8278	0.7675	0.8631
AL-4A	9	0.6917	0.6887	0.7536	0.6875	0.7836
AL-4A	10	0.6866	0.6260	0.6751	0.6505	0.7003
AL-4A	12	0.7510	0.8963	0.9024	0.8928	0.9366
AL-4A	13	0.7113	0.7618	0.8282	0.7686	0.8551
AL-4A	14	0.6945	0.6788	0.7540	0.6881	0.7743
AL-4A	15	0.6904	0.6179	0.6755	0.6506	0.6896
AL-4B	2	0.7267	1.0386	0.9512	1.0034	0.5470
AL-4B	3	0.7240	0.8831	0.8640	0.8569	0.5563
AL-4B	4	0.6937	0.8035	0.7898	0.7799	0.5615
AL-4B	5	0.6676	0.7497	0.7200	0.7474	0.5640
AL-4B	7	0.7312	1.0114	0.9472	0.9946	0.5075
AL-4B	8	0.6990	0.8757	0.8687	0.8623	0.5206
AL-4B	9	0.6799	0.7965	0.7945	0.7823	0.5304
AL-4B	10	0.6599	0.7402	0.7204	0.7460	0.5376
AL-4B	12	0.7487	0.9870	0.9476	0.9962	0.4675
AL-4B	13	0.7019	0.8573	0.8691	0.8633	0.4853
AL-4B	14	0.6790	0.7853	0.7993	0.7864	0.4988
AL-4B	15	0.6634	0.7277	0.7207	0.7462	0.5112

Appendix D1 Predictions of Resilient Modulus from Statistical Models for Development Dataset (Continued)

Sample I.D.	Seq. No.	Experiment M_R/P_a (10^3)	Predicted M_R/P_a (10^3)			
			Stress-Based	**Mult. Reg.**	**Polynomial**	**Factorial**
AL-5A	2	0.4475	1.0159	0.7976	0.8150	0.7988
AL-5A	3	0.3684	0.8112	0.7278	0.6880	0.7225
AL-5A	4	0.3280	0.6929	0.6580	0.5998	0.6490
AL-5A	5	0.3052	0.6221	0.5969	0.5545	0.5869
AL-5A	7	0.4385	1.0025	0.7980	0.8150	0.7934
AL-5A	8	0.3686	0.8107	0.7325	0.6945	0.7170
AL-5A	9	0.3363	0.6851	0.6584	0.5990	0.6334
AL-5A	10	0.3178	0.6114	0.5929	0.5512	0.5621
AL-5A	12	0.4870	0.9825	0.7984	0.8167	0.7879
AL-5A	13	0.3955	0.7963	0.7329	0.6957	0.7068
AL-5A	14	0.3526	0.6800	0.6631	0.6043	0.6229
AL-5A	15	0.3322	0.6026	0.5933	0.5516	0.5417
AL-5B	2	0.4146	1.0404	0.7749	0.8003	0.7858
AL-5B	3	0.3102	0.8557	0.7138	0.6892	0.7223
AL-5B	4	0.2634	0.7422	0.6527	0.6078	0.6611
AL-5B	5	0.2393	0.6637	0.5916	0.5560	0.6021
AL-5B	7	0.3837	1.0370	0.7796	0.8094	0.7688
AL-5B	8	0.2991	0.8496	0.7185	0.6958	0.7004
AL-5B	9	0.2636	0.7293	0.6531	0.6070	0.6296
AL-5B	10	0.2450	0.6529	0.5920	0.5549	0.5658
AL-5B	12	0.3994	1.0054	0.7800	0.8110	0.7473
AL-5B	13	0.3035	0.8264	0.7189	0.6971	0.6740
AL-5B	14	0.2606	0.7176	0.6578	0.6128	0.6030
AL-5B	15	0.2433	0.6383	0.5924	0.5554	0.5294
AL-6A	2	0.4953	0.8358	0.7335	0.7927	0.8557
AL-6A	3	0.4124	0.6770	0.6637	0.6876	0.7292
AL-6A	4	0.3594	0.5687	0.5852	0.6156	0.5913
AL-6A	5	0.3312	0.4997	0.5110	0.5927	0.4653
AL-6A	7	0.4583	0.8613	0.7426	0.8085	0.8903
AL-6A	8	0.3801	0.6834	0.6685	0.6924	0.7482
AL-6A	9	0.3488	0.5726	0.5899	0.6173	0.6023
AL-6A	10	0.3396	0.4989	0.5114	0.5912	0.4610
AL-6A	12	0.4814	0.8588	0.7430	0.8099	0.9088
AL-6A	13	0.3960	0.6816	0.6689	0.6935	0.7594
AL-6A	14	0.3576	0.5712	0.5903	0.6178	0.6057
AL-6A	15	0.3464	0.4979	0.5118	0.5912	0.4567
AL-6B	2	0.4463	0.8262	0.6380	0.6634	0.6547
AL-6B	3	0.3455	0.6605	0.5682	0.5583	0.5422
AL-6B	4	0.2990	0.5539	0.4940	0.4890	0.4281
AL-6B	5	0.2658	0.4857	0.4242	0.4638	0.3257
AL-6B	7	0.3791	0.8473	0.6471	0.6792	0.6845
AL-6B	8	0.3109	0.6629	0.5730	0.5631	0.5547
AL-6B	9	0.2813	0.5547	0.4988	0.4909	0.4305
AL-6B	10	0.2627	0.4823	0.4246	0.4624	0.3117
AL-6B	12	0.3927	0.8360	0.6475	0.6806	0.6998
AL-6B	13	0.3141	0.6631	0.5777	0.5698	0.5683
AL-6B	14	0.2808	0.5540	0.5035	0.4945	0.4340
AL-6B	15	0.2639	0.4813	0.4293	0.4630	0.3052

Appendix D1 Predictions of Resilient Modulus from Statistical Models for Development Dataset (Continued)

Sample I.D.	Seq. No.	Experiment M_R/P_a (10^3)	Predicted M_R/P_a (10^3)			
			Stress-Based	**Mult. Reg.**	**Polynomial**	**Factorial**
AL-7A	2	0.6214	0.4685	0.4797	0.4501	0.5647
AL-7A	3	0.5249	0.3499	0.4055	0.3165	0.5076
AL-7A	4	0.4678	0.2861	0.3313	0.2267	0.4495
AL-7A	5	0.4434	0.2455	0.2572	0.1806	0.3903
AL-7A	7	0.5915	0.4568	0.4801	0.4502	0.5765
AL-7A	8	0.4835	0.3467	0.4103	0.3228	0.5245
AL-7A	9	0.4438	0.2830	0.3361	0.2299	0.4682
AL-7A	10	0.4407	0.2407	0.2575	0.1793	0.4076
AL-7A	12	0.5888	0.4492	0.4848	0.4611	0.5914
AL-7A	13	0.4788	0.3399	0.4150	0.3309	0.5412
AL-7A	14	0.4444	0.2746	0.3365	0.2307	0.4835
AL-7A	15	0.4431	0.2344	0.2579	0.1796	0.4248
AL-7B	2	0.4913	0.7627	0.5790	0.6218	0.4296
AL-7B	3	0.4008	0.6245	0.5136	0.5085	0.4054
AL-7B	4	0.3698	0.5316	0.4394	0.4212	0.3790
AL-7B	5	0.3749	0.4644	0.3565	0.3754	0.3507
AL-7B	7	0.4636	0.7452	0.5837	0.6306	0.4335
AL-7B	8	0.3818	0.6088	0.5183	0.5146	0.4075
AL-7B	9	0.3601	0.5141	0.4398	0.4203	0.3773
AL-7B	10	0.3687	0.4503	0.3569	0.3741	0.3469
AL-7B	12	0.4610	0.7136	0.5885	0.6411	0.4376
AL-7B	13	0.3786	0.5775	0.5187	0.5158	0.4079
AL-7B	14	0.3586	0.4907	0.4401	0.4210	0.3757
AL-7B	15	0.3720	0.4321	0.3572	0.3743	0.3431
AL-8A	2	0.7228	0.9561	0.8875	0.9150	0.9840
AL-8A	3	0.6909	0.7372	0.7915	0.7504	0.8549
AL-8A	4	0.6533	0.6491	0.7217	0.6768	0.7636
AL-8A	5	0.6049	0.5838	0.6475	0.6410	0.6691
AL-8A	7	0.7099	0.9049	0.8748	0.8882	0.9761
AL-8A	8	0.6693	0.7372	0.7962	0.7558	0.8661
AL-8A	9	0.6339	0.6481	0.7264	0.6793	0.7705
AL-8A	10	0.6096	0.5792	0.6479	0.6396	0.6657
AL-8A	12	0.7345	0.8911	0.8751	0.8898	0.9861
AL-8A	13	0.6764	0.7274	0.7966	0.7569	0.8714
AL-8A	14	0.6395	0.6404	0.7268	0.6800	0.7718
AL-8A	15	0.6162	0.5762	0.6526	0.6407	0.6683
AL-8B	2	0.6919	1.0298	0.9200	0.9420	0.9539
AL-8B	3	0.6819	0.8229	0.8284	0.7833	0.8620
AL-8B	4	0.6552	0.7285	0.7542	0.7038	0.7896
AL-8B	5	0.6163	0.6628	0.6800	0.6680	0.7187
AL-8B	7	0.7134	0.9894	0.9116	0.9240	0.9324
AL-8B	8	0.6667	0.8203	0.8331	0.7889	0.8506
AL-8B	9	0.6399	0.7253	0.7589	0.7063	0.7751
AL-8B	10	0.6197	0.6563	0.6804	0.6666	0.6969
AL-8B	12	0.7287	0.9705	0.9120	0.9256	0.9197
AL-8B	13	0.6724	0.8066	0.8335	0.7900	0.8348
AL-8B	14	0.6436	0.7145	0.7593	0.7070	0.7564
AL-8B	15	0.6252	0.6507	0.6851	0.6677	0.6796

Appendix D1 Predictions of Resilient Modulus from Statistical Models for Development Dataset (Continued)

Sample I.D.	Seq. No.	Experiment M_R/P_a (10^3)	Predicted M_R/P_a (10^3) Stress-Based	Mult. Reg.	Polynomial	Factorial
AL-9A	2	0.9481	1.0226	1.1932	1.2495	0.8018
AL-9A	3	0.8129	0.8785	1.1409	1.1561	0.7180
AL-9A	4	0.8087	0.7598	1.0754	1.0700	0.6129
AL-9A	5	0.7969	0.6674	1.0012	1.0136	0.4937
AL-9A	7	1.0662	1.2263	1.2198	1.3045	0.9465
AL-9A	8	1.0067	1.0085	1.1631	1.1921	0.8561
AL-9A	9	0.8785	0.8166	1.0758	1.0692	0.7166
AL-9A	10	0.8495	0.7084	0.9973	1.0104	0.5908
AL-9A	12	1.1421	1.4255	1.2245	1.3159	1.0563
AL-9A	13	1.0641	1.1343	1.1634	1.1935	0.9592
AL-9A	14	0.9260	0.9038	1.0762	1.0701	0.8203
AL-9A	15	0.8942	0.7755	0.9976	1.0108	0.6949
AL-9B	2	0.7083	1.0528	1.2392	1.2286	0.9594
AL-9B	3	0.7226	0.8712	1.1519	1.0942	0.8947
AL-9B	4	0.6772	0.7743	1.0778	1.0275	0.8408
AL-9B	5	0.6642	0.7036	1.0036	1.0046	0.7883
AL-9B	7	0.7426	1.1198	1.2352	1.2204	1.0149
AL-9B	8	0.7085	0.9387	1.1567	1.0989	0.9543
AL-9B	9	0.7045	0.8286	1.0825	1.0292	0.8983
AL-9B	10	0.6993	0.7448	1.0040	1.0030	0.8403
AL-9B	12	0.7788	1.2484	1.2356	1.2218	1.0736
AL-9B	13	0.7517	1.0321	1.1571	1.0998	1.0108
AL-9B	14	0.7363	0.9018	1.0829	1.0297	0.9527
AL-9B	15	0.7227	0.8084	1.0087	1.0033	0.8958
AL-10A	2	0.5781	0.7469	0.6939	0.6635	0.7012
AL-10A	3	0.4905	0.5822	0.6154	0.5234	0.6580
AL-10A	4	0.4417	0.4953	0.5412	0.4361	0.6135
AL-10A	5	0.4059	0.4375	0.4670	0.3926	0.5654
AL-10A	7	0.5093	0.7295	0.6899	0.6545	0.6707
AL-10A	8	0.4387	0.5854	0.6201	0.5295	0.6384
AL-10A	9	0.4157	0.4968	0.5460	0.4392	0.6005
AL-10A	10	0.4075	0.4382	0.4718	0.3927	0.5590
AL-10A	12	0.5307	0.7351	0.6947	0.6652	0.6440
AL-10A	13	0.4489	0.5872	0.6249	0.5374	0.6179
AL-10A	14	0.4211	0.4972	0.5507	0.4441	0.5867
AL-10A	15	0.4151	0.4353	0.4722	0.3930	0.5497
AL-10B	2	0.5063	0.8544	0.6579	0.7287	0.6199
AL-10B	3	0.4099	0.6733	0.5881	0.5969	0.5677
AL-10B	4	0.3402	0.5818	0.5270	0.5134	0.5223
AL-10B	5	0.3035	0.5190	0.4659	0.4595	0.4774
AL-10B	7	0.4209	0.8541	0.6626	0.7384	0.6185
AL-10B	8	0.3331	0.6954	0.6059	0.6260	0.5752
AL-10B	9	0.3011	0.5829	0.5361	0.5229	0.5224
AL-10B	10	0.2904	0.5148	0.4706	0.4614	0.4733
AL-10B	12	0.4102	0.8454	0.6674	0.7498	0.6173
AL-10B	13	0.3192	0.6860	0.6107	0.6351	0.5731
AL-10B	14	0.2882	0.5746	0.5408	0.5292	0.5193
AL-10B	15	0.2811	0.5076	0.4754	0.4650	0.4693

Appendix D1 Predictions of Resilient Modulus from Statistical Models for Development Dataset (Continued)

Sample I.D.	Seq. No.	Experiment M_R/P_a (10^3)	Predicted M_R/P_a (10^3)			
			Stress-Based	Mult. Reg.	Polynomial	Factorial
CH-1A	2	1.0869	0.8361	0.8031	0.8464	0.7711
CH-1A	3	0.8549	0.7410	0.7398	0.7536	0.7246
CH-1A	4	0.7246	0.6710	0.6715	0.6892	0.6760
CH-1A	5	0.6723	0.6073	0.5835	0.6610	0.6158
CH-1A	7	1.0286	0.8254	0.8003	0.8407	0.7471
CH-1A	8	0.8480	0.7355	0.7390	0.7515	0.6993
CH-1A	9	0.7483	0.6676	0.6719	0.6882	0.6485
CH-1A	10	0.6841	0.6041	0.5833	0.6595	0.5839
CH-1A	12	1.0573	0.8206	0.8020	0.8442	0.7265
CH-1A	13	0.8470	0.7336	0.7425	0.7563	0.6774
CH-1A	14	0.7433	0.6640	0.6735	0.6896	0.6220
CH-1A	15	0.6861	0.6004	0.5837	0.6595	0.5523
CH-1B	2	1.6871	0.6946	0.5196	0.6935	1.1691
CH-1B	3	1.1224	0.6074	0.4697	0.6201	1.0510
CH-1B	4	0.8657	0.5128	0.3867	0.5422	0.8760
CH-1B	5	0.7957	0.4505	0.3038	0.5189	0.7269
CH-1B	7	1.5202	0.6611	0.5093	0.6757	1.2287
CH-1B	8	1.1589	0.5712	0.4504	0.5960	1.0639
CH-1B	9	0.9970	0.5118	0.3947	0.5460	0.9201
CH-1B	10	0.8470	0.4414	0.2998	0.5176	0.7019
CH-1B	12	1.6426	0.6465	0.5109	0.6789	1.3189
CH-1B	13	1.2231	0.5535	0.4470	0.5927	1.1086
CH-1B	14	1.0839	0.5060	0.4008	0.5506	0.9662
CH-1B	15	0.9082	0.4321	0.2983	0.5178	0.6790
CH-2A	2	0.7354	1.0572	0.7817	0.7600	0.8625
CH-2A	3	0.6022	0.8702	0.7190	0.6607	0.7534
CH-2A	4	0.4847	0.7339	0.6456	0.5842	0.6292
CH-2A	5	0.4028	0.6420	0.5722	0.5505	0.5089
CH-2A	7	0.7808	1.0507	0.7764	0.7495	0.8852
CH-2A	8	0.6466	0.8850	0.7207	0.6619	0.7832
CH-2A	9	0.5094	0.7440	0.6467	0.5837	0.6509
CH-2A	10	0.4195	0.6494	0.5726	0.5490	0.5226
CH-2A	12	0.8223	1.0806	0.7787	0.7543	0.9217
CH-2A	13	0.6644	0.9053	0.7223	0.6647	0.8132
CH-2A	14	0.5183	0.7609	0.6496	0.5863	0.6763
CH-2A	15	0.4245	0.6609	0.5743	0.5495	0.5386
CH-2B	2	0.8421	1.0874	0.7564	0.7219	0.7619
CH-2B	3	0.7256	0.9149	0.6899	0.6297	0.6769
CH-2B	4	0.6170	0.8093	0.6292	0.5761	0.5921
CH-2B	5	0.5380	0.7077	0.5463	0.5504	0.4655
CH-2B	7	0.8588	1.0692	0.7504	0.7113	0.7641
CH-2B	8	0.7542	0.9038	0.6840	0.6220	0.6943
CH-2B	9	0.6614	0.8202	0.6359	0.5793	0.6387
CH-2B	10	0.5735	0.7075	0.5454	0.5488	0.5226
CH-2B	12	0.8944	1.0864	0.7552	0.7198	0.7773
CH-2B	13	0.7789	0.9137	0.6882	0.6270	0.7235
CH-2B	14	0.6890	0.8339	0.6439	0.5854	0.6834
CH-2B	15	0.5943	0.7090	0.5458	0.5488	0.5819

Appendix D1 Predictions of Resilient Modulus from Statistical Models for Development Dataset (Continued)

Sample I.D.	Seq. No.	Experiment M_R/P_a (10^3)	Predicted M_R/P_a (10^3) Stress-Based	Mult. Reg.	Polynomial	Factorial
CH-3A	2	1.0553	0.6999	0.5598	0.5621	0.5612
CH-3A	3	0.7029	0.5797	0.4997	0.4675	0.4978
CH-3A	4	0.5271	0.4885	0.4263	0.3909	0.4244
CH-3A	5	0.4136	0.4329	0.3605	0.3587	0.3622
CH-3A	7	1.1333	0.6749	0.5571	0.5562	0.5634
CH-3A	8	0.7345	0.5722	0.5039	0.4721	0.5017
CH-3A	9	0.5183	0.4812	0.4299	0.3924	0.4195
CH-3A	10	0.4186	0.4265	0.3641	0.3581	0.3502
CH-3A	12	1.3327	0.6608	0.5619	0.5657	0.5747
CH-3A	13	0.8105	0.5524	0.5037	0.4723	0.5008
CH-3A	14	0.5232	0.4700	0.4334	0.3956	0.4153
CH-3A	15	0.4126	0.4172	0.3676	0.3593	0.3389
CH-3B	2	0.6446	0.6923	0.4264	0.4901	0.5717
CH-3B	3	0.3386	0.5526	0.3701	0.3907	0.4525
CH-3B	4	0.2419	0.4643	0.3119	0.3145	0.3366
CH-3B	5	0.2142	0.4033	0.2524	0.2644	0.2259
CH-3B	7	0.6417	0.6622	0.4255	0.4876	0.6509
CH-3B	8	0.3682	0.5231	0.3648	0.3817	0.5054
CH-3B	9	0.2764	0.4403	0.3046	0.3057	0.3694
CH-3B	10	0.2349	0.3847	0.2452	0.2589	0.2426
CH-3B	12	0.6999	0.6234	0.4253	0.4879	0.7311
CH-3B	13	0.4008	0.4939	0.3632	0.3800	0.5650
CH-3B	14	0.2952	0.4170	0.3019	0.3033	0.4089
CH-3B	15	0.2498	0.3658	0.2417	0.2573	0.2640
CH-4A	2	1.2833	0.9305	0.6801	0.6429	0.9051
CH-4A	3	0.7512	0.7843	0.6326	0.5675	0.7560
CH-4A	4	0.4709	0.6485	0.5649	0.4909	0.5534
CH-4A	5	0.3623	0.5643	0.5029	0.4528	0.3782
CH-4A	7	1.3396	0.9492	0.6799	0.6416	0.9884
CH-4A	8	0.8865	0.8045	0.6343	0.5688	0.8299
CH-4A	9	0.5341	0.6573	0.5628	0.4879	0.5919
CH-4A	10	0.3889	0.5710	0.5001	0.4504	0.3943
CH-4A	12	1.5469	0.9660	0.6764	0.6363	1.0591
CH-4A	13	1.0207	0.8260	0.6334	0.5681	0.8952
CH-4A	14	0.5765	0.6755	0.5632	0.4886	0.6378
CH-4A	15	0.4087	0.5839	0.4992	0.4502	0.4147
CH-4B	2	0.7720	1.1014	0.6434	0.6013	0.6516
CH-4B	3	0.4314	0.8743	0.5852	0.5013	0.4762
CH-4B	4	0.3129	0.7304	0.5251	0.4263	0.3118
CH-4B	5	0.2626	0.6377	0.4687	0.3822	0.1732
CH-4B	7	0.7720	1.1220	0.6457	0.6049	0.7324
CH-4B	8	0.4383	0.8746	0.5830	0.4971	0.5053
CH-4B	9	0.3258	0.7280	0.5210	0.4211	0.2987
CH-4B	10	0.2734	0.6382	0.4659	0.3793	0.1303
CH-4B	12	0.8559	1.1181	0.6423	0.5990	0.7906
CH-4B	13	0.4729	0.8822	0.5821	0.4964	0.5365
CH-4B	14	0.3396	0.7365	0.5214	0.4219	0.2969
CH-4B	15	0.2813	0.6398	0.4625	0.3778	0.0814

Appendix D1 Predictions of Resilient Modulus from Statistical Models for Development Dataset (Continued)

Sample I.D.	Seq. No.	Experiment M_R/P_a (10^3)	Predicted M_R/P_a (10^3)			
			Stress-Based	**Mult. Reg.**	**Polynomial**	**Factorial**
DE-1A	2	0.4511	1.1783	0.9354	0.8662	0.5339
DE-1A	3	0.4126	0.9711	0.8664	0.7614	0.5064
DE-1A	4	0.3939	0.8293	0.7905	0.6898	0.4878
DE-1A	5	0.3702	0.7318	0.7139	0.6641	0.4813
DE-1A	7	0.4640	1.1917	0.9364	0.8671	0.5454
DE-1A	8	0.4334	0.9853	0.8693	0.7640	0.4999
DE-1A	9	0.4077	0.8387	0.7928	0.6900	0.4596
DE-1A	10	0.3840	0.7370	0.7143	0.6626	0.4311
DE-1A	12	0.5271	1.1927	0.9330	0.8617	0.5527
DE-1A	13	0.4571	1.0050	0.8729	0.7691	0.4953
DE-1A	14	0.4067	0.8507	0.7951	0.6919	0.4324
DE-1A	15	0.3771	0.7470	0.7172	0.6628	0.3823
DE-1B	2	0.7068	1.4214	0.8334	0.7859	0.6195
DE-1B	3	0.4205	1.1025	0.7732	0.6710	0.4895
DE-1B	4	0.3643	0.9136	0.7112	0.5826	0.3540
DE-1B	5	0.3406	0.7852	0.6467	0.5231	0.2116
DE-1B	7	0.8213	1.3190	0.8192	0.7554	0.6636
DE-1B	8	0.5844	1.0503	0.7603	0.6491	0.5386
DE-1B	9	0.4492	0.8691	0.6932	0.5615	0.3947
DE-1B	10	0.3870	0.7706	0.6395	0.5172	0.2783
DE-1B	12	0.8421	1.3272	0.8221	0.7622	0.7443
DE-1B	13	0.6170	1.0472	0.7613	0.6514	0.6180
DE-1B	14	0.4758	0.8625	0.6924	0.5611	0.4731
DE-1B	15	0.4255	0.7694	0.6411	0.5185	0.3644
DE-2A	2	0.8075	1.0930	1.0438	0.9960	0.8653
DE-2A	3	0.7581	0.9677	0.9590	0.8833	0.8423
DE-2A	4	0.7374	0.9076	0.8976	0.8373	0.8280
DE-2A	5	0.7098	0.8543	0.8248	0.8217	0.8135
DE-2A	7	0.8223	1.0141	1.0404	0.9895	0.8389
DE-2A	8	0.7730	0.9049	0.9549	0.8781	0.8102
DE-2A	9	0.7641	0.8543	0.8954	0.8349	0.7925
DE-2A	10	0.7414	0.8131	0.8321	0.8198	0.7755
DE-2A	12	0.8371	0.9170	1.0401	0.9897	0.8133
DE-2A	13	0.7976	0.8293	0.9547	0.8783	0.7790
DE-2A	14	0.7848	0.7887	0.8952	0.8350	0.7573
DE-2A	15	0.7651	0.7603	0.8420	0.8201	0.7394
DE-2B	2	1.1945	1.1588	0.9735	0.8974	0.9519
DE-2B	3	1.0128	1.0482	0.9108	0.8073	0.9037
DE-2B	4	0.9358	0.9831	0.8583	0.7558	0.8521
DE-2B	5	0.8569	0.8982	0.7608	0.7184	0.7289
DE-2B	7	1.2932	1.0518	0.9650	0.8824	0.9205
DE-2B	8	1.0661	0.9663	0.9068	0.8014	0.9027
DE-2B	9	0.9970	0.9094	0.8523	0.7501	0.8746
DE-2B	10	0.9200	0.8410	0.7600	0.7169	0.8017
DE-2B	12	1.4028	0.9396	0.9685	0.8889	0.8941
DE-2B	13	1.1056	0.8633	0.9015	0.7958	0.9060
DE-2B	14	1.0158	0.8218	0.8489	0.7480	0.9036
DE-2B	15	0.9309	0.7731	0.7641	0.7170	0.8780

Appendix D1 Predictions of Resilient Modulus from Statistical Models for Development Dataset (Continued)

Sample I.D.	Seq. No.	Experiment M_R/P_a (10^3)	Predicted M_R/P_a (10^3) Stress-Based	Mult. Reg.	Polynomial	Factorial
DE-3A	2	1.4028	0.6636	0.6942	0.6328	0.7397
DE-3A	3	1.1046	0.5536	0.6227	0.5368	0.6489
DE-3A	4	0.9358	0.5051	0.5771	0.4969	0.5933
DE-3A	5	0.7927	0.4312	0.4797	0.4668	0.4802
DE-3A	7	1.3455	0.6823	0.7009	0.6430	0.7628
DE-3A	8	1.0938	0.5587	0.6237	0.5368	0.6559
DE-3A	9	1.0039	0.5089	0.5775	0.4959	0.5942
DE-3A	10	0.8578	0.4345	0.4807	0.4652	0.4711
DE-3A	12	1.4788	0.7107	0.7101	0.6596	0.7913
DE-3A	13	1.1441	0.5658	0.6247	0.5383	0.6630
DE-3A	14	1.0355	0.5076	0.5709	0.4917	0.5854
DE-3A	15	0.8973	0.4401	0.4836	0.4651	0.4647
DE-3B	2	1.1728	0.6493	0.5438	0.5709	0.5752
DE-3B	3	0.8944	0.5384	0.4849	0.4807	0.4910
DE-3B	4	0.7206	0.4555	0.4159	0.4099	0.4022
DE-3B	5	0.6575	0.3901	0.3343	0.3751	0.3108
DE-3B	7	1.1994	0.6361	0.5378	0.5597	0.6174
DE-3B	8	0.9980	0.5331	0.4809	0.4744	0.5198
DE-3B	9	0.7927	0.4595	0.4195	0.4114	0.4228
DE-3B	10	0.7029	0.3892	0.3322	0.3734	0.2993
DE-3B	12	1.3356	0.6427	0.5401	0.5643	0.6728
DE-3B	13	1.0632	0.5501	0.4914	0.4887	0.5744
DE-3B	14	0.8796	0.4596	0.4186	0.4110	0.4373
DE-3B	15	0.7808	0.3927	0.3363	0.3739	0.2966
DE-4A	2	1.0257	0.9352	0.8781	0.9588	0.9516
DE-4A	3	0.8509	0.7964	0.8136	0.8629	0.8662
DE-4A	4	0.7374	0.7024	0.7471	0.7987	0.7784
DE-4A	5	0.6821	0.6146	0.6560	0.7679	0.6581
DE-4A	7	1.0306	0.9019	0.8703	0.9444	0.9528
DE-4A	8	0.8845	0.7745	0.8064	0.8531	0.8681
DE-4A	9	0.7710	0.6969	0.7494	0.7991	0.7927
DE-4A	10	0.7048	0.6093	0.6577	0.7663	0.6714
DE-4A	12	1.1619	0.9556	0.8966	0.9923	0.9994
DE-4A	13	1.0484	0.7726	0.8137	0.8624	0.8893
DE-4A	14	0.8588	0.6855	0.7492	0.7992	0.8037
DE-4A	15	0.7562	0.6006	0.6574	0.7664	0.6821
DE-4B	2	1.0513	1.0240	0.9374	0.9503	1.0866
DE-4B	3	0.9427	0.8966	0.8760	0.8577	1.0234
DE-4B	4	0.8796	0.8052	0.8108	0.7922	0.9553
DE-4B	5	0.8727	0.7146	0.7172	0.7572	0.8555
DE-4B	7	1.1273	1.0021	0.9334	0.9424	1.0682
DE-4B	8	1.0128	0.8776	0.8701	0.8492	1.0050
DE-4B	9	0.9733	0.8015	0.8144	0.7936	0.9486
DE-4B	10	0.9348	0.7067	0.7150	0.7556	0.8460
DE-4B	12	1.3524	0.9868	0.9337	0.9437	1.0543
DE-4B	13	1.2646	0.8956	0.8888	0.8740	1.0110
DE-4B	14	1.1826	0.7914	0.8148	0.7942	0.9386
DE-4B	15	1.0839	0.6974	0.7135	0.7557	0.8372

Appendix D1 Predictions of Resilient Modulus from Statistical Models for Development Dataset (Continued)

Sample I.D.	Seq. No.	Experiment M_R/P_a (10^3)	Predicted M_R/P_a (10^3)			
			Stress-Based	Mult. Reg.	Polynomial	Factorial
GR-1A	2	1.2500	1.0121	1.1921	1.2186	1.1202
GR-1A	3	1.0558	0.8895	1.1223	1.1231	0.9832
GR-1A	4	1.0134	0.8236	1.0699	1.0769	0.8674
GR-1A	5	0.8349	0.7523	0.9957	1.0489	0.6845
GR-1A	7	1.3556	1.0542	1.1925	1.2183	1.3335
GR-1A	8	1.1130	0.9171	1.1183	1.1177	1.2265
GR-1A	9	1.0644	0.8483	1.0659	1.0730	1.1376
GR-1A	10	0.8673	0.7737	0.9917	1.0471	0.9927
GR-1A	12	2.0185	1.1543	1.2059	1.2419	1.5564
GR-1A	13	1.5700	1.0213	1.1492	1.1548	1.5097
GR-1A	14	1.5773	0.8963	1.0707	1.0765	1.4235
GR-1A	15	1.8848	0.8043	0.9878	1.0470	1.3054
GR-1B	2	1.2399	1.0422	1.0502	1.0420	1.1056
GR-1B	3	1.0144	0.8890	0.9804	0.9417	0.9969
GR-1B	4	0.8842	0.8155	0.9324	0.8952	0.9187
GR-1B	5	0.7161	0.7219	0.8495	0.8581	0.7772
GR-1B	7	1.1941	1.0759	1.0506	1.0418	1.2023
GR-1B	8	1.0010	0.9077	0.9764	0.9360	1.0982
GR-1B	9	0.9112	0.8325	0.9284	0.8909	1.0273
GR-1B	10	0.7638	0.7364	0.8455	0.8562	0.8983
GR-1B	12	1.2362	1.1275	1.0509	1.0431	1.2990
GR-1B	13	1.1523	0.9544	0.9811	0.9420	1.2121
GR-1B	14	1.0292	0.8651	0.9288	0.8915	1.1431
GR-1B	15	0.8449	0.7620	0.8459	0.8563	1.0272
GR-2A	2	0.7393	0.9346	0.9553	0.9042	1.0784
GR-2A	3	0.7061	0.7996	0.8767	0.7995	0.9828
GR-2A	4	0.6553	0.7466	0.8331	0.7626	0.9276
GR-2A	5	0.5777	0.6702	0.7502	0.7341	0.8187
GR-2A	7	0.7765	0.9563	0.9557	0.9039	1.0839
GR-2A	8	0.7496	0.8105	0.8728	0.7944	0.9911
GR-2A	9	0.6949	0.7521	0.8248	0.7559	0.9350
GR-2A	10	0.6081	0.6827	0.7506	0.7326	0.8448
GR-2A	12	0.8151	0.9890	0.9561	0.9052	1.0893
GR-2A	13	0.7648	0.8346	0.8732	0.7952	1.0049
GR-2A	14	0.7125	0.7679	0.8208	0.7538	0.9489
GR-2A	15	0.6271	0.7034	0.7553	0.7328	0.8759
GR-2B	2	0.8561	0.9291	0.7350	0.7331	0.7580
GR-2B	3	0.5980	0.7572	0.6652	0.6255	0.6402
GR-2B	4	0.4515	0.6558	0.5998	0.5599	0.5435
GR-2B	5	0.3805	0.5839	0.5343	0.5283	0.4601
GR-2B	7	0.7522	0.9538	0.7398	0.7410	0.8118
GR-2B	8	0.5520	0.7732	0.6700	0.6306	0.6647
GR-2B	9	0.4493	0.6618	0.6002	0.5589	0.5327
GR-2B	10	0.3936	0.5889	0.5347	0.5270	0.4226
GR-2B	12	0.7706	0.9542	0.7358	0.7344	0.8463
GR-2B	13	0.5957	0.7843	0.6703	0.6316	0.6822
GR-2B	14	0.5224	0.6703	0.6005	0.5595	0.5219
GR-2B	15	0.4291	0.5958	0.5351	0.5272	0.3852

Appendix D1 Predictions of Resilient Modulus from Statistical Models for Development Dataset (Continued)

Sample I.D.	Seq. No.	Experiment M_R/P_a (10^3)	Predicted M_R/P_a (10^3) Stress-Based	Mult. Reg.	Polynomial	Factorial
GR-3A	2	0.6558	0.8968	0.8119	0.7976	0.8296
GR-3A	3	0.5664	0.7796	0.7465	0.7025	0.7710
GR-3A	4	0.4777	0.7194	0.6985	0.6543	0.7287
GR-3A	5	0.4153	0.6435	0.6156	0.6143	0.6572
GR-3A	7	0.6678	0.8767	0.8123	0.7974	0.8075
GR-3A	8	0.5723	0.7695	0.7512	0.7071	0.7505
GR-3A	9	0.4853	0.7052	0.6988	0.6534	0.7024
GR-3A	10	0.4278	0.6318	0.6159	0.6129	0.6279
GR-3A	12	0.6625	0.8480	0.8127	0.7987	0.7853
GR-3A	13	0.5739	0.7468	0.7516	0.7081	0.7261
GR-3A	14	0.4928	0.6860	0.6992	0.6541	0.6762
GR-3A	15	0.4339	0.6165	0.6163	0.6130	0.5987
GR-3B	2	0.7258	0.8009	0.5502	0.5764	0.5164
GR-3B	3	0.5076	0.6832	0.5022	0.4967	0.4553
GR-3B	4	0.3647	0.5789	0.4367	0.4174	0.3765
GR-3B	5	0.3125	0.5046	0.3669	0.3704	0.2982
GR-3B	7	0.7526	0.7856	0.5549	0.5845	0.5437
GR-3B	8	0.5383	0.6523	0.4982	0.4899	0.4626
GR-3B	9	0.3916	0.5610	0.4371	0.4166	0.3797
GR-3B	10	0.3277	0.4864	0.3629	0.3675	0.2849
GR-3B	12	1.2688	0.7570	0.5597	0.5943	0.5725
GR-3B	13	0.8513	0.6141	0.4942	0.4848	0.4686
GR-3B	14	0.5749	0.5319	0.4331	0.4132	0.3764
GR-3B	15	0.4396	0.4710	0.3677	0.3695	0.2825
JE-1A	2	0.5597	0.8564	0.9630	0.9424	0.7386
JE-1A	3	0.5094	0.7758	0.8965	0.8465	0.6801
JE-1A	4	0.4827	0.7132	0.8219	0.7806	0.6057
JE-1A	5	0.4659	0.6626	0.7390	0.7595	0.5127
JE-1A	7	0.5360	0.8707	0.9665	0.9476	0.6791
JE-1A	8	0.4906	0.7902	0.9032	0.8535	0.6372
JE-1A	9	0.4778	0.7194	0.8216	0.7792	0.5736
JE-1A	10	0.4768	0.6703	0.7431	0.7577	0.5024
JE-1A	12	0.5637	0.8828	0.9656	0.9467	0.6164
JE-1A	13	0.4985	0.8031	0.9049	0.8560	0.5891
JE-1A	14	0.4758	0.7315	0.8258	0.7819	0.5446
JE-1A	15	0.4748	0.6792	0.7454	0.7576	0.4890
JE-1B	2	0.5222	0.8387	0.7165	0.8718	0.5963
JE-1B	3	0.3810	0.7201	0.6526	0.7702	0.5490
JE-1B	4	0.3060	0.6374	0.5842	0.6976	0.4977
JE-1B	5	0.2833	0.5758	0.5121	0.6612	0.4427
JE-1B	7	0.4018	0.8692	0.7296	0.8957	0.5810
JE-1B	8	0.3100	0.7375	0.6650	0.7864	0.5347
JE-1B	9	0.2863	0.6411	0.5891	0.7002	0.4795
JE-1B	10	0.2833	0.5747	0.5119	0.6597	0.4223
JE-1B	12	0.3949	0.8708	0.7312	0.8997	0.5573
JE-1B	13	0.3001	0.7422	0.6692	0.7931	0.5142
JE-1B	14	0.2833	0.6427	0.5920	0.7031	0.4597
JE-1B	15	0.2863	0.5743	0.5129	0.6600	0.4028

Appendix D1 Predictions of Resilient Modulus from Statistical Models for Development Dataset (Continued)

Sample I.D.	Seq. No.	Experiment M_R/P_a (10^3)	Predicted M_R/P_a (10^3)			
			Stress-Based	Mult. Reg.	Polynomial	Factorial
JE-2A	2	0.9763	0.8225	0.7722	0.7672	0.7082
JE-2A	3	0.7502	0.7159	0.7153	0.6797	0.6269
JE-2A	4	0.5617	0.6423	0.6583	0.6180	0.5510
JE-2A	5	0.4985	0.5695	0.5792	0.5752	0.4546
JE-2A	7	0.9398	0.8413	0.7777	0.7761	0.7984
JE-2A	8	0.7423	0.7273	0.7194	0.6842	0.7020
JE-2A	9	0.5953	0.6476	0.6593	0.6177	0.6085
JE-2A	10	0.5341	0.5723	0.5783	0.5735	0.4920
JE-2A	12	1.0049	0.8546	0.7793	0.7798	0.8835
JE-2A	13	0.7660	0.7343	0.7192	0.6845	0.7708
JE-2A	14	0.6239	0.6526	0.6584	0.6173	0.6630
JE-2A	15	0.5676	0.5764	0.5774	0.5734	0.5290
JE-2B	2	0.9694	0.7385	0.5908	0.6510	0.7142
JE-2B	3	0.5923	0.6358	0.5433	0.5739	0.5938
JE-2B	4	0.4788	0.5412	0.4775	0.4967	0.4468
JE-2B	5	0.4758	0.4668	0.3996	0.4498	0.3028
JE-2B	7	1.1392	0.7143	0.5816	0.6339	0.8799
JE-2B	8	0.8430	0.6161	0.5323	0.5576	0.7229
JE-2B	9	0.6239	0.5346	0.4722	0.4907	0.5493
JE-2B	10	0.5222	0.4628	0.3950	0.4470	0.3546
JE-2B	12	1.6989	0.7678	0.6023	0.6724	1.1531
JE-2B	13	1.0869	0.6211	0.5358	0.5630	0.8910
JE-2B	14	0.7779	0.5316	0.4700	0.4892	0.6547
JE-2B	15	0.6436	0.4602	0.3922	0.4465	0.4051
JE-3A	2	0.4699	0.8102	0.7619	0.8017	0.7955
JE-3A	3	0.3554	0.7010	0.7062	0.7083	0.7489
JE-3A	4	0.3356	0.6079	0.6328	0.6228	0.6909
JE-3A	5	0.3524	0.5375	0.5499	0.5779	0.6298
JE-3A	7	0.5074	0.8097	0.7592	0.7956	0.8304
JE-3A	8	0.4225	0.7009	0.7028	0.7023	0.7783
JE-3A	9	0.3880	0.6042	0.6250	0.6150	0.7099
JE-3A	10	0.3801	0.5378	0.5453	0.5755	0.6442
JE-3A	12	0.5321	0.8128	0.7564	0.7911	0.8647
JE-3A	13	0.4432	0.7043	0.7001	0.6990	0.8076
JE-3A	14	0.4028	0.6100	0.6247	0.6152	0.7346
JE-3A	15	0.3949	0.5420	0.5444	0.5755	0.6611
JE-3B	2	0.8391	0.7264	0.5878	0.7150	0.8457
JE-3B	3	0.5706	0.6199	0.5385	0.6308	0.7669
JE-3B	4	0.5232	0.5227	0.4682	0.5442	0.6683
JE-3B	5	0.4936	0.4495	0.3866	0.4930	0.5736
JE-3B	7	1.0760	0.7058	0.5800	0.6995	0.9647
JE-3B	8	0.7887	0.6139	0.5351	0.6247	0.8748
JE-3B	9	0.6150	0.5149	0.4610	0.5364	0.7409
JE-3B	10	0.5548	0.4452	0.3806	0.4899	0.6156
JE-3B	12	1.1619	0.6990	0.5772	0.6951	1.0895
JE-3B	13	0.8697	0.6093	0.5323	0.6212	0.9811
JE-3B	14	0.6584	0.5148	0.4608	0.5365	0.8219
JE-3B	15	0.6190	0.4470	0.3829	0.4907	0.6674

Appendix D1 Predictions of Resilient Modulus from Statistical Models for Development Dataset (Continued)

Sample I.D.	Seq. No.	Experiment M_R/P_a (10^3)	Predicted M_R/P_a (10^3)			
			Stress-Based	Mult. Reg.	Polynomial	Factorial
JE-4A	2	1.1925	0.9893	1.1304	1.0839	1.1251
JE-4A	3	1.0326	0.8935	1.0595	0.9857	1.0526
JE-4A	4	0.9477	0.8355	1.0000	0.9341	0.9925
JE-4A	5	0.8342	0.7713	0.9127	0.9094	0.9057
JE-4A	7	1.2359	1.0102	1.1213	1.0681	1.1412
JE-4A	8	1.0464	0.9207	1.0567	0.9815	1.0734
JE-4A	9	1.0059	0.8603	0.9979	0.9315	1.0124
JE-4A	10	0.8855	0.7937	0.9124	0.9079	0.9251
JE-4A	12	1.3277	1.0584	1.1179	1.0633	1.1630
JE-4A	13	1.1046	0.9649	1.0565	0.9817	1.0969
JE-4A	14	1.0355	0.8943	0.9938	0.9293	1.0302
JE-4A	15	0.9230	0.8271	0.9153	0.9077	0.9478
JE-4B	2	0.6081	0.9101	0.7797	0.8248	0.6432
JE-4B	3	0.4847	0.7877	0.7240	0.7412	0.5657
JE-4B	4	0.3978	0.6823	0.6525	0.6701	0.4624
JE-4B	5	0.3465	0.6072	0.5797	0.6394	0.3530
JE-4B	7	0.5735	0.9504	0.7833	0.8301	0.7147
JE-4B	8	0.4729	0.8190	0.7276	0.7448	0.6431
JE-4B	9	0.3998	0.7065	0.6561	0.6714	0.5475
JE-4B	10	0.3603	0.6250	0.5814	0.6382	0.4434
JE-4B	12	0.6101	0.9969	0.7830	0.8304	0.7811
JE-4B	13	0.5074	0.8542	0.7267	0.7442	0.7146
JE-4B	14	0.4215	0.7392	0.6590	0.6739	0.6313
JE-4B	15	0.3741	0.6489	0.5824	0.6384	0.5326
KI-1A	2	0.9437	0.8914	0.9407	0.9709	0.7797
KI-1A	3	0.6831	0.8036	0.8806	0.8772	0.7156
KI-1A	4	0.4669	0.7384	0.8167	0.8091	0.6425
KI-1A	5	0.4284	0.6826	0.7420	0.7706	0.5506
KI-1A	7	0.9240	0.9098	0.9462	0.9799	0.7457
KI-1A	8	0.6466	0.8159	0.8848	0.8817	0.6906
KI-1A	9	0.4837	0.7433	0.8152	0.8066	0.6224
KI-1A	10	0.4097	0.6882	0.7424	0.7693	0.5447
KI-1A	12	0.9033	0.9200	0.9447	0.9779	0.7052
KI-1A	13	0.6476	0.8278	0.8858	0.8837	0.6619
KI-1A	14	0.4798	0.7530	0.8162	0.8078	0.6052
KI-1A	15	0.4166	0.6937	0.7396	0.7688	0.5357
KI-1B	2	0.5410	0.8300	0.6575	0.7863	0.7735
KI-1B	3	0.3346	0.7008	0.5993	0.6878	0.6752
KI-1B	4	0.3100	0.6016	0.5284	0.6043	0.5652
KI-1B	5	0.3268	0.5285	0.4499	0.5584	0.4559
KI-1B	7	0.7335	0.7986	0.6477	0.7671	0.8273
KI-1B	8	0.4709	0.6696	0.5825	0.6635	0.7009
KI-1B	9	0.3820	0.5814	0.5123	0.5896	0.5748
KI-1B	10	0.3495	0.5206	0.4427	0.5551	0.4602
KI-1B	12	1.0178	0.7727	0.6399	0.7536	0.8800
KI-1B	13	0.5864	0.6594	0.5791	0.6595	0.7460
KI-1B	14	0.4344	0.5735	0.5083	0.5869	0.5996
KI-1B	15	0.3968	0.5141	0.4380	0.5543	0.4650

Appendix D1 Predictions of Resilient Modulus from Statistical Models for Development Dataset (Continued)

Sample I.D.	Seq. No.	Experiment M_R/P_a (10^3)	Predicted M_R/P_a (10^3)			
			Stress-Based	Mult. Reg.	Polynomial	Factorial
LI-1A	2	0.8786	0.7024	0.7021	0.7348	0.6781
LI-1A	3	0.7787	0.5837	0.6367	0.6283	0.6267
LI-1A	4	0.6834	0.4998	0.5625	0.5487	0.5710
LI-1A	5	0.6713	0.4342	0.4752	0.5112	0.5087
LI-1A	7	0.8913	0.7213	0.7025	0.7347	0.7002
LI-1A	8	0.7810	0.5982	0.6370	0.6278	0.6449
LI-1A	9	0.7127	0.5113	0.5629	0.5478	0.5846
LI-1A	10	0.6914	0.4433	0.4756	0.5097	0.5169
LI-1A	12	0.9677	0.7620	0.7072	0.7445	0.7264
LI-1A	13	1.0022	0.6265	0.6418	0.6350	0.6669
LI-1A	14	0.9911	0.5232	0.5589	0.5450	0.5944
LI-1A	15	0.9316	0.4529	0.4716	0.5095	0.5215
LI-1B	2	0.8597	0.6978	0.5728	0.7357	0.5639
LI-1B	3	0.7104	0.5687	0.5117	0.6310	0.4921
LI-1B	4	0.6280	0.4698	0.4331	0.5399	0.4121
LI-1B	5	0.6139	0.3974	0.3415	0.4957	0.3366
LI-1B	7	0.9188	0.6959	0.5688	0.7271	0.6521
LI-1B	8	0.7714	0.5692	0.5077	0.6242	0.5628
LI-1B	9	0.6908	0.4712	0.4292	0.5354	0.4603
LI-1B	10	0.6555	0.4019	0.3419	0.4943	0.3629
LI-1B	12	0.9647	0.7108	0.5692	0.7287	0.7458
LI-1B	13	0.8050	0.5802	0.5081	0.6253	0.6383
LI-1B	14	0.7238	0.4792	0.4295	0.5360	0.5125
LI-1B	15	0.6893	0.4079	0.3423	0.4944	0.3892
LI-2A	2	1.1396	0.9033	0.8170	0.8301	0.8692
LI-2A	3	0.7784	0.7154	0.7472	0.7056	0.7476
LI-2A	4	0.5606	0.5940	0.6686	0.6118	0.6269
LI-2A	5	0.4916	0.5149	0.5901	0.5671	0.5230
LI-2A	7	1.3651	0.9495	0.8173	0.8301	0.9446
LI-2A	8	0.8924	0.7489	0.7475	0.7052	0.7979
LI-2A	9	0.6375	0.6194	0.6690	0.6109	0.6488
LI-2A	10	0.5297	0.5313	0.5861	0.5647	0.5099
LI-2A	12	1.5639	1.0433	0.8221	0.8409	1.0311
LI-2A	13	0.9549	0.8001	0.7479	0.7064	0.8481
LI-2A	14	0.6727	0.6504	0.6650	0.6078	0.6615
LI-2A	15	0.5544	0.5596	0.5865	0.5649	0.5020
LI-2B	2	0.5101	0.8224	0.6714	0.7566	0.6133
LI-2B	3	0.3526	0.6677	0.6103	0.6540	0.5102
LI-2B	4	0.2763	0.5700	0.5492	0.5811	0.4229
LI-2B	5	0.2471	0.4974	0.4837	0.5359	0.3467
LI-2B	7	0.4808	0.8912	0.6805	0.7737	0.7307
LI-2B	8	0.3281	0.7141	0.6194	0.6665	0.5917
LI-2B	9	0.2767	0.5921	0.5496	0.5803	0.4521
LI-2B	10	0.2577	0.5154	0.4841	0.5347	0.3399
LI-2B	12	0.5205	0.9345	0.6765	0.7666	0.8192
LI-2B	13	0.3472	0.7579	0.6198	0.6676	0.6595
LI-2B	14	0.2835	0.6311	0.5543	0.5853	0.4920
LI-2B	15	0.2614	0.5457	0.4889	0.5370	0.3425

Appendix D1 Predictions of Resilient Modulus from Statistical Models for Development Dataset (Continued)

Sample I.D.	Seq. No.	Experiment M_R/P_a (10^3)	Predicted M_R/P_a (10^3)			
			Stress-Based	Mult. Reg.	Polynomial	Factorial
LI-3A	2	0.8732	0.7348	0.6979	0.7032	0.7699
LI-3A	3	0.7082	0.6248	0.6412	0.6128	0.7123
LI-3A	4	0.5510	0.5414	0.5757	0.5404	0.6505
LI-3A	5	0.4637	0.4698	0.4928	0.4975	0.5794
LI-3A	7	0.8472	0.7575	0.7027	0.7111	0.7575
LI-3A	8	0.6995	0.6341	0.6416	0.6123	0.6862
LI-3A	9	0.5653	0.5488	0.5761	0.5395	0.6145
LI-3A	10	0.4856	0.4726	0.4889	0.4953	0.5266
LI-3A	12	0.8721	0.7756	0.7030	0.7125	0.7405
LI-3A	13	0.7061	0.6406	0.6376	0.6075	0.6543
LI-3A	14	0.5794	0.5594	0.5765	0.5402	0.5784
LI-3A	15	0.4983	0.4806	0.4892	0.4955	0.4773
LI-3B	2	0.7324	0.7641	0.5760	0.6740	0.5827
LI-3B	3	0.5514	0.6066	0.5106	0.5606	0.5059
LI-3B	4	0.4187	0.5025	0.4364	0.4733	0.4266
LI-3B	5	0.3491	0.4347	0.3622	0.4298	0.3557
LI-3B	7	0.7115	0.7670	0.5764	0.6739	0.6158
LI-3B	8	0.5272	0.6167	0.5153	0.5667	0.5318
LI-3B	9	0.4310	0.5041	0.4368	0.4725	0.4321
LI-3B	10	0.3701	0.4360	0.3626	0.4285	0.3465
LI-3B	12	0.7507	0.7862	0.5811	0.6843	0.6559
LI-3B	13	0.5617	0.6199	0.5157	0.5679	0.5528
LI-3B	14	0.4804	0.5064	0.4371	0.4732	0.4376
LI-3B	15	0.4094	0.4345	0.3586	0.4275	0.3317
LI-4A	2	0.6986	0.6042	0.6108	0.6139	0.6397
LI-4A	3	0.5645	0.5057	0.5497	0.5197	0.5984
LI-4A	4	0.4183	0.4371	0.4842	0.4518	0.5563
LI-4A	5	0.3383	0.3858	0.4144	0.4169	0.5140
LI-4A	7	0.5826	0.6239	0.6155	0.6216	0.6483
LI-4A	8	0.4447	0.5317	0.5631	0.5369	0.6089
LI-4A	9	0.3699	0.4475	0.4890	0.4544	0.5557
LI-4A	10	0.3260	0.3912	0.4148	0.4156	0.5054
LI-4A	12	0.5691	0.6500	0.6203	0.6311	0.6574
LI-4A	13	0.4291	0.5441	0.5635	0.5380	0.6107
LI-4A	14	0.3575	0.4567	0.4894	0.4550	0.5523
LI-4A	15	0.3206	0.4014	0.4195	0.4169	0.5000
LI-4B	2	1.2951	0.7212	0.6193	0.7225	0.5826
LI-4B	3	0.9525	0.6015	0.5538	0.6205	0.5348
LI-4B	4	0.7098	0.5288	0.4927	0.5560	0.4931
LI-4B	5	0.5438	0.4637	0.4142	0.5168	0.4439
LI-4B	7	1.3010	0.7252	0.6196	0.7223	0.5858
LI-4B	8	0.9163	0.6109	0.5586	0.6257	0.5348
LI-4B	9	0.6677	0.5313	0.4931	0.5551	0.4834
LI-4B	10	0.5349	0.4657	0.4146	0.5154	0.4261
LI-4B	12	1.3658	0.7420	0.6244	0.7318	0.5931
LI-4B	13	0.9107	0.6221	0.5633	0.6327	0.5357
LI-4B	14	0.6586	0.5394	0.4979	0.5595	0.4774
LI-4B	15	0.5294	0.4685	0.4150	0.5156	0.4084

Appendix D1 Predictions of Resilient Modulus from Statistical Models for Development Dataset (Continued)

Sample I.D.	Seq. No.	Experiment M_R/P_a (10^3)	Predicted M_R/P_a (10^3)			
			Stress-Based	Mult. Reg.	Polynomial	Factorial
LI-5A	2	0.9238	0.8690	0.9005	0.9115	0.8381
LI-5A	3	0.9131	0.7395	0.8045	0.7836	0.7095
LI-5A	4	0.8420	0.6887	0.7477	0.7425	0.6366
LI-5A	5	0.7464	0.6457	0.6867	0.7268	0.5608
LI-5A	7	0.8494	0.8620	0.8921	0.8966	0.8714
LI-5A	8	0.8602	0.7372	0.7961	0.7748	0.7342
LI-5A	9	0.8363	0.6910	0.7438	0.7392	0.6622
LI-5A	10	0.7722	0.6564	0.6958	0.7257	0.5979
LI-5A	12	0.9201	0.8743	0.8925	0.8979	0.9167
LI-5A	13	0.9008	0.7462	0.7965	0.7755	0.7702
LI-5A	14	0.8521	0.7023	0.7485	0.7417	0.6996
LI-5A	15	0.7889	0.6663	0.7005	0.7263	0.6306
LI-5B	2	0.8886	0.8006	0.6584	0.7599	0.9354
LI-5B	3	0.7387	0.6747	0.5929	0.6602	0.8061
LI-5B	4	0.5704	0.6021	0.5362	0.6013	0.7064
LI-5B	5	0.4768	0.5342	0.4620	0.5630	0.5933
LI-5B	7	0.8858	0.7980	0.6588	0.7597	1.0526
LI-5B	8	0.7123	0.6861	0.6021	0.6710	0.9134
LI-5B	9	0.5685	0.6003	0.5366	0.6004	0.7669
LI-5B	10	0.4913	0.5327	0.4624	0.5616	0.6193
LI-5B	12	0.9178	0.8048	0.6635	0.7690	1.1831
LI-5B	13	0.7229	0.6830	0.6024	0.6721	1.0043
LI-5B	14	0.5743	0.6027	0.5414	0.6047	0.8387
LI-5B	15	0.4969	0.5308	0.4628	0.5618	0.6453
LI-6A	2	0.7656	0.8336	0.9433	0.8646	0.7507
LI-6A	3	0.7315	0.7358	0.8735	0.7570	0.7125
LI-6A	4	0.6775	0.6809	0.8167	0.6981	0.6935
LI-6A	5	0.6441	0.6168	0.7251	0.6571	0.6855
LI-6A	7	0.7779	0.8299	0.9349	0.8488	0.7647
LI-6A	8	0.7147	0.7402	0.8695	0.7509	0.7017
LI-6A	9	0.6604	0.6890	0.8171	0.6972	0.6615
LI-6A	10	0.6431	0.6235	0.7255	0.6556	0.6134
LI-6A	12	0.8080	0.8545	0.9397	0.8579	0.7911
LI-6A	13	0.7198	0.7587	0.8742	0.7574	0.6983
LI-6A	14	0.6762	0.7005	0.8175	0.6979	0.6296
LI-6A	15	0.6519	0.6327	0.7259	0.6557	0.5412
LI-6B	2	0.9975	0.8607	0.8634	0.9703	0.9119
LI-6B	3	0.8248	0.7656	0.8023	0.8741	0.8503
LI-6B	4	0.7031	0.6959	0.7369	0.8039	0.7826
LI-6B	5	0.6605	0.6274	0.6452	0.7628	0.6848
LI-6B	7	0.9262	0.8773	0.8681	0.9782	0.9225
LI-6B	8	0.7858	0.7721	0.8027	0.8735	0.8601
LI-6B	9	0.7055	0.7014	0.7372	0.8029	0.7959
LI-6B	10	0.6699	0.6320	0.6456	0.7614	0.7031
LI-6B	12	0.9406	0.8894	0.8685	0.9796	0.9287
LI-6B	13	0.7872	0.7817	0.8031	0.8746	0.8699
LI-6B	14	0.7068	0.7092	0.7376	0.8036	0.8092
LI-6B	15	0.6739	0.6382	0.6460	0.7615	0.7214

Appendix D1 Predictions of Resilient Modulus from Statistical Models for Development Dataset (Continued)

Sample I.D.	Seq. No.	Experiment M_R/P_a (10^3)	Predicted M_R/P_a (10^3)			
			Stress-Based	Mult. Reg.	Polynomial	Factorial
MA-1A	2	0.7433	0.5423	0.5430	0.5312	0.6434
MA-1A	3	0.4620	0.4399	0.4835	0.4317	0.5886
MA-1A	4	0.3465	0.3736	0.4221	0.3586	0.5346
MA-1A	5	0.3001	0.3257	0.3576	0.3140	0.4810
MA-1A	7	0.7117	0.5562	0.5478	0.5396	0.6564
MA-1A	8	0.4551	0.4477	0.4877	0.4368	0.5950
MA-1A	9	0.3653	0.3729	0.4193	0.3548	0.5284
MA-1A	10	0.3248	0.3239	0.3523	0.3104	0.4664
MA-1A	12	0.7947	0.5556	0.5457	0.5362	0.6623
MA-1A	13	0.5064	0.4473	0.4849	0.4333	0.5946
MA-1A	14	0.3899	0.3753	0.4191	0.3549	0.5242
MA-1A	15	0.3416	0.3247	0.3501	0.3098	0.4539
MA-1B	2	0.3406	0.5884	0.4774	0.5663	0.5956
MA-1B	3	0.2428	0.4710	0.4223	0.4664	0.5267
MA-1B	4	0.2399	0.3822	0.3515	0.3732	0.4451
MA-1B	5	0.2498	0.3213	0.2736	0.3169	0.3644
MA-1B	7	0.4057	0.5774	0.4740	0.5586	0.6485
MA-1B	8	0.3060	0.4511	0.4101	0.4464	0.5563
MA-1B	9	0.2813	0.3673	0.3360	0.3570	0.4574
MA-1B	10	0.2833	0.3156	0.2652	0.3122	0.3709
MA-1B	12	0.4610	0.5649	0.4699	0.5513	0.6988
MA-1B	13	0.3396	0.4487	0.4092	0.4457	0.5990
MA-1B	14	0.3060	0.3641	0.3333	0.3548	0.4823
MA-1B	15	0.2991	0.3126	0.2611	0.3110	0.3798
MA-2A	2	1.0336	0.8693	1.1085	0.9971	1.0053
MA-2A	3	0.9250	0.7917	1.0174	0.8792	0.9034
MA-2A	4	0.8618	0.7604	0.9661	0.8418	0.8395
MA-2A	5	0.8016	0.7359	0.9180	0.8258	0.7751
MA-2A	7	0.9753	0.8821	1.1101	0.9990	0.9707
MA-2A	8	0.8914	0.8069	1.0260	0.8863	0.8974
MA-2A	9	0.8440	0.7711	0.9703	0.8428	0.8418
MA-2A	10	0.8065	0.7441	0.9190	0.8245	0.7856
MA-2A	12	1.0089	0.9043	1.1149	1.0078	0.9373
MA-2A	13	0.8993	0.8247	1.0320	0.8930	0.8856
MA-2A	14	0.8460	0.7868	0.9770	0.8470	0.8443
MA-2A	15	0.8006	0.7535	0.9169	0.8242	0.7929
MA-2B	2	0.4758	0.7260	0.6270	0.6912	0.6139
MA-2B	3	0.3445	0.6045	0.5694	0.5916	0.5743
MA-2B	4	0.2962	0.5112	0.4979	0.5046	0.5274
MA-2B	5	0.2883	0.4459	0.4219	0.4567	0.4803
MA-2B	7	0.4472	0.7495	0.6350	0.7063	0.6141
MA-2B	8	0.3317	0.6081	0.5710	0.5931	0.5660
MA-2B	9	0.3031	0.5091	0.4951	0.5008	0.5115
MA-2B	10	0.2962	0.4446	0.4192	0.4544	0.4597
MA-2B	12	0.4590	0.7434	0.6322	0.7015	0.6064
MA-2B	13	0.3396	0.6104	0.5714	0.5943	0.5569
MA-2B	14	0.3080	0.5089	0.4936	0.4998	0.4961
MA-2B	15	0.3050	0.4441	0.4170	0.4539	0.4392

Appendix D1 Predictions of Resilient Modulus from Statistical Models for Development Dataset (Continued)

Sample I.D.	Seq. No.	Experiment M_R/P_a (10^3)	Predicted M_R/P_a (10^3)			
			Stress-Based	Mult. Reg.	Polynomial	Factorial
MA-3A	2	1.2586	0.9720	1.3469	1.5113	1.4126
MA-3A	3	1.2932	0.9071	1.2545	1.3940	1.3734
MA-3A	4	1.3050	0.8741	1.1868	1.3512	1.3572
MA-3A	5	1.3080	0.8487	1.1210	1.3445	1.3518
MA-3A	7	1.4146	0.9588	1.3467	1.5100	1.4988
MA-3A	8	1.3465	0.9053	1.2707	1.4085	1.4419
MA-3A	9	1.3682	0.8662	1.1910	1.3514	1.3967
MA-3A	10	1.3574	0.8392	1.1189	1.3432	1.3686
MA-3A	12	1.4571	0.9450	1.3521	1.5197	1.5911
MA-3A	13	1.3366	0.8889	1.2686	1.4068	1.5027
MA-3A	14	1.3880	0.8453	1.1705	1.3450	1.4198
MA-3A	15	1.3643	0.8269	1.1161	1.3437	1.3835
MA-3B	2	2.2606	0.9894	1.0664	1.2602	1.4918
MA-3B	3	1.6170	0.8270	0.9702	1.1139	1.3185
MA-3B	4	1.4729	0.7444	0.8873	1.0468	1.1863
MA-3B	5	1.3554	0.7064	0.8361	1.0327	1.1124
MA-3B	7	2.4274	0.9656	1.0668	1.2601	1.4979
MA-3B	8	1.5745	0.8160	0.9763	1.1199	1.3070
MA-3B	9	1.4659	0.7297	0.8877	1.0457	1.1384
MA-3B	10	1.3850	0.6907	0.8327	1.0310	1.0427
MA-3B	12	2.3189	0.9218	1.0628	1.2532	1.4930
MA-3B	13	1.5903	0.7868	0.9729	1.1163	1.2771
MA-3B	14	1.4985	0.7144	0.8938	1.0490	1.1025
MA-3B	15	1.3929	0.6727	0.8318	1.0310	0.9757
MA-4A	2	0.8421	0.8413	0.7188	0.7010	0.6956
MA-4A	3	0.6525	0.6997	0.6568	0.6020	0.6126
MA-4A	4	0.4916	0.6061	0.5929	0.5319	0.5327
MA-4A	5	0.4018	0.5320	0.5194	0.4916	0.4482
MA-4A	7	0.8233	0.8457	0.7211	0.7044	0.7287
MA-4A	8	0.6180	0.7174	0.6673	0.6156	0.6463
MA-4A	9	0.4640	0.6069	0.5945	0.5321	0.5413
MA-4A	10	0.3959	0.5308	0.5192	0.4901	0.4405
MA-4A	12	0.8421	0.8515	0.7240	0.7106	0.7636
MA-4A	13	0.6170	0.7209	0.6702	0.6204	0.6710
MA-4A	14	0.4511	0.6081	0.5968	0.5345	0.5513
MA-4A	15	0.3860	0.5316	0.5215	0.4908	0.4364
MA-4B	2	0.8272	0.9157	0.6159	0.6502	0.7088
MA-4B	3	0.4847	0.7533	0.5590	0.5529	0.5936
MA-4B	4	0.3258	0.6441	0.4982	0.4776	0.4810
MA-4B	5	0.2734	0.5647	0.4337	0.4298	0.3728
MA-4B	7	0.8223	0.9121	0.6201	0.6575	0.7609
MA-4B	8	0.4729	0.7510	0.5644	0.5601	0.6267
MA-4B	9	0.3406	0.6316	0.4973	0.4756	0.4768
MA-4B	10	0.2804	0.5546	0.4328	0.4280	0.3447
MA-4B	12	0.9013	0.8815	0.6192	0.6566	0.8013
MA-4B	13	0.5064	0.7288	0.5635	0.5594	0.6465
MA-4B	14	0.3495	0.6160	0.4971	0.4758	0.4733
MA-4B	15	0.2892	0.5411	0.4313	0.4275	0.3142

Appendix D1 Predictions of Resilient Modulus from Statistical Models for Development Dataset (Continued)

Sample I.D.	Seq. No.	Experiment M_R/P_a (10^3)	Predicted M_R/P_a (10^3)			
			Stress-Based	**Mult. Reg.**	**Polynomial**	**Factorial**
MC-1A	2	0.8885	0.9728	1.1126	1.0027	0.9992
MC-1A	3	0.8322	0.8841	1.0290	0.9059	0.9130
MC-1A	4	0.8164	0.8357	0.9651	0.8694	0.8411
MC-1A	5	0.7927	0.8087	0.9214	0.8630	0.7889
MC-1A	7	0.8934	0.9851	1.1231	1.0179	1.0217
MC-1A	8	0.8707	0.8797	1.0256	0.9019	0.9380
MC-1A	9	0.8509	0.8301	0.9585	0.8660	0.8733
MC-1A	10	0.8272	0.8013	0.9104	0.8623	0.8234
MC-1A	12	0.9358	0.9701	1.1140	1.0045	1.0284
MC-1A	13	0.8983	0.8754	1.0228	0.9001	0.9647
MC-1A	14	0.8796	0.8258	0.9545	0.8651	0.9099
MC-1A	15	0.8598	0.7975	0.9064	0.8628	0.8678
MC-1B	2	1.0454	1.0428	1.1469	1.3391	0.9137
MC-1B	3	0.8944	0.9378	1.0766	1.2437	0.8158
MC-1B	4	0.8480	0.8822	1.0241	1.1980	0.7467
MC-1B	5	0.7285	0.8251	0.9532	1.1712	0.6590
MC-1B	7	1.0415	1.0037	1.1492	1.3419	1.1094
MC-1B	8	0.9398	0.9019	1.0764	1.2423	0.9957
MC-1B	9	0.9131	0.8503	1.0239	1.1966	0.9178
MC-1B	10	0.8055	0.7994	0.9562	1.1700	0.8226
MC-1B	12	1.3021	0.9495	1.1527	1.3485	1.3079
MC-1B	13	1.1599	0.8629	1.0850	1.2523	1.1903
MC-1B	14	1.1125	0.8149	1.0319	1.2024	1.1020
MC-1B	15	0.9556	0.7618	0.9527	1.1697	0.9774
NO-1A	2	0.9872	0.8147	0.7902	0.6929	0.5774
NO-1A	3	0.9121	0.6813	0.7098	0.5656	0.5463
NO-1A	4	0.8697	0.6043	0.6332	0.4921	0.5136
NO-1A	5	0.8332	0.5496	0.5548	0.4652	0.4770
NO-1A	7	0.8717	0.7914	0.7906	0.6929	0.5498
NO-1A	8	0.8243	0.6650	0.7115	0.5667	0.5245
NO-1A	9	0.7957	0.5903	0.6342	0.4915	0.4967
NO-1A	10	0.7670	0.5378	0.5558	0.4637	0.4654
NO-1A	12	0.7453	0.7604	0.7922	0.6968	0.5225
NO-1A	13	0.7098	0.6426	0.7137	0.5702	0.5027
NO-1A	14	0.6861	0.5723	0.6365	0.4934	0.4801
NO-1A	15	0.6663	0.5225	0.5574	0.4639	0.4539
NO-1B	2	0.7216	0.8009	0.6526	0.6407	0.5627
NO-1B	3	0.6407	0.6563	0.5761	0.5171	0.5164
NO-1B	4	0.5874	0.5698	0.4989	0.4397	0.4680
NO-1B	5	0.5617	0.5107	0.4210	0.4097	0.4172
NO-1B	7	0.6101	0.7727	0.6537	0.6419	0.5331
NO-1B	8	0.5528	0.6357	0.5777	0.5182	0.4904
NO-1B	9	0.5173	0.5531	0.5005	0.4396	0.4451
NO-1B	10	0.4936	0.4968	0.4227	0.4083	0.3976
NO-1B	12	0.5271	0.7332	0.6553	0.6458	0.5038
NO-1B	13	0.4729	0.6028	0.5762	0.5168	0.4625
NO-1B	14	0.4423	0.5304	0.5022	0.4411	0.4221
NO-1B	15	0.4146	0.4748	0.4180	0.4080	0.3741

Appendix D1 Predictions of Resilient Modulus from Statistical Models for Development Dataset (Continued)

Sample I.D.	Seq. No.	Experiment M_R/P_a (10^3)	Predicted M_R/P_a (10^3)			
			Stress-Based	Mult. Reg.	Polynomial	Factorial
NO-2A	2	0.8391	0.8560	0.8140	0.7141	0.7417
NO-2A	3	0.7670	0.7146	0.7362	0.5896	0.7054
NO-2A	4	0.7167	0.6296	0.6590	0.5137	0.6745
NO-2A	5	0.6881	0.5704	0.5811	0.4852	0.6484
NO-2A	7	0.7907	0.8384	0.8144	0.7140	0.6719
NO-2A	8	0.7394	0.7004	0.7359	0.5882	0.6267
NO-2A	9	0.6940	0.6187	0.6594	0.5127	0.5876
NO-2A	10	0.6594	0.5609	0.5809	0.4837	0.5527
NO-2A	12	0.6486	0.8138	0.8154	0.7167	0.6015
NO-2A	13	0.6051	0.6846	0.7389	0.5925	0.5487
NO-2A	14	0.5795	0.6048	0.6610	0.5141	0.5002
NO-2A	15	0.5617	0.5495	0.5825	0.4839	0.4564
NO-2B	2	0.7275	0.8615	0.7090	0.7022	0.8102
NO-2B	3	0.6575	0.7078	0.6318	0.5782	0.7238
NO-2B	4	0.6130	0.6161	0.5546	0.5015	0.6398
NO-2B	5	0.5953	0.5531	0.4768	0.4723	0.5574
NO-2B	7	0.6032	0.8420	0.7107	0.7046	0.7777
NO-2B	8	0.5548	0.6925	0.6335	0.5793	0.6873
NO-2B	9	0.5291	0.6041	0.5569	0.5019	0.6000
NO-2B	10	0.5114	0.5400	0.4746	0.4706	0.5089
NO-2B	12	0.4580	0.8070	0.7104	0.7049	0.7425
NO-2B	13	0.4215	0.6650	0.6313	0.5770	0.6459
NO-2B	14	0.4097	0.5821	0.5535	0.4998	0.5532
NO-2B	15	0.4038	0.5251	0.4750	0.4707	0.4622
NO-3A	2	0.6772	0.8939	0.7194	0.7418	0.6787
NO-3A	3	0.6071	0.7156	0.6435	0.6191	0.6254
NO-3A	4	0.5390	0.6115	0.5676	0.5421	0.5706
NO-3A	5	0.4877	0.5402	0.4897	0.5109	0.5129
NO-3A	7	0.6278	0.8627	0.7205	0.7430	0.6327
NO-3A	8	0.5735	0.6924	0.6445	0.6194	0.5820
NO-3A	9	0.5222	0.5931	0.5686	0.5416	0.5298
NO-3A	10	0.4768	0.5255	0.4914	0.5096	0.4752
NO-3A	12	0.5735	0.8163	0.7215	0.7457	0.5857
NO-3A	13	0.5281	0.6594	0.6455	0.6213	0.5376
NO-3A	14	0.4847	0.5671	0.5690	0.5422	0.4876
NO-3A	15	0.4452	0.5048	0.4918	0.5097	0.4356
NO-3B	2	0.5558	0.9002	0.6249	0.6398	0.5546
NO-3B	3	0.4768	0.7071	0.5477	0.5142	0.4818
NO-3B	4	0.4097	0.5990	0.4723	0.4374	0.4140
NO-3B	5	0.3613	0.5256	0.3951	0.4054	0.3475
NO-3B	7	0.4906	0.8675	0.6265	0.6422	0.5389
NO-3B	8	0.4294	0.6828	0.5493	0.5154	0.4608
NO-3B	9	0.3781	0.5790	0.4734	0.4369	0.3870
NO-3B	10	0.3406	0.5087	0.3955	0.4040	0.3146
NO-3B	12	0.4531	0.8107	0.6256	0.6413	0.5204
NO-3B	13	0.3949	0.6462	0.5497	0.5164	0.4384
NO-3B	14	0.3475	0.5508	0.4731	0.4370	0.3587
NO-3B	15	0.3139	0.4873	0.3965	0.4042	0.2822

Appendix D1 Predictions of Resilient Modulus from Statistical Models for Development Dataset (Continued)

Sample I.D.	Seq. No.	Experiment M_R/P_a (10^3)	Predicted M_R/P_a (10^3)			
			Stress-Based	**Mult. Reg.**	**Polynomial**	**Factorial**
NO-4A	2	0.6446	0.7738	0.6263	0.6514	0.5423
NO-4A	3	0.5775	0.6182	0.5510	0.5298	0.5398
NO-4A	4	0.5252	0.5267	0.4744	0.4524	0.5348
NO-4A	5	0.4827	0.4632	0.3934	0.4214	0.5266
NO-4A	7	0.5745	0.7269	0.6286	0.6549	0.4371
NO-4A	8	0.5163	0.5767	0.5489	0.5259	0.4391
NO-4A	9	0.4758	0.4985	0.4767	0.4528	0.4384
NO-4A	10	0.4442	0.4379	0.3919	0.4198	0.4348
NO-4A	12	0.5084	0.6580	0.6302	0.6589	0.3318
NO-4A	13	0.4551	0.5262	0.5486	0.5262	0.3385
NO-4A	14	0.4176	0.4547	0.4701	0.4485	0.3422
NO-4A	15	0.3899	0.4075	0.3923	0.4199	0.3431
NO-4B	2	0.5104	0.7565	0.5055	0.5078	0.1934
NO-4B	3	0.4344	0.5803	0.4245	0.3768	0.2268
NO-4B	4	0.3820	0.4863	0.3460	0.2997	0.2561
NO-4B	5	0.3455	0.4256	0.2682	0.2716	0.2823
NO-4B	7	0.4097	0.6917	0.5040	0.5041	0.1158
NO-4B	8	0.3534	0.5404	0.4261	0.3779	0.1529
NO-4B	9	0.3179	0.4542	0.3464	0.2987	0.1879
NO-4B	10	0.2962	0.3999	0.2692	0.2702	0.2187
NO-4B	12	0.3337	0.6137	0.5050	0.5068	0.0371
NO-4B	13	0.2823	0.4851	0.4259	0.3781	0.0799
NO-4B	14	0.2577	0.4143	0.3481	0.3001	0.1190
NO-4B	15	0.2419	0.3681	0.2708	0.2704	0.1548
NO-5A	2	0.7345	0.8617	0.7757	0.7411	0.8969
NO-5A	3	0.6762	0.7173	0.6972	0.6154	0.8188
NO-5A	4	0.6308	0.6326	0.6200	0.5395	0.7395
NO-5A	5	0.5953	0.5744	0.5422	0.5110	0.6569
NO-5A	7	0.6446	0.8165	0.7767	0.7422	0.8680
NO-5A	8	0.6051	0.6843	0.6995	0.6173	0.7954
NO-5A	9	0.5755	0.6044	0.6210	0.5389	0.7191
NO-5A	10	0.5508	0.5501	0.5425	0.5095	0.6402
NO-5A	12	0.5568	0.7531	0.7784	0.7461	0.8390
NO-5A	13	0.5252	0.6364	0.7005	0.6192	0.7703
NO-5A	14	0.5025	0.5662	0.6214	0.5395	0.6978
NO-5A	15	0.4847	0.5188	0.5429	0.5096	0.6233
NO-5B	2	0.7038	0.9310	0.7240	0.7017	0.6343
NO-5B	3	0.6407	0.7781	0.6462	0.5772	0.6073
NO-5B	4	0.5874	0.6864	0.5677	0.5005	0.5866
NO-5B	5	0.5499	0.6276	0.4943	0.4731	0.5731
NO-5B	7	0.6219	0.8774	0.7263	0.7053	0.5688
NO-5B	8	0.5696	0.7379	0.6497	0.5808	0.5315
NO-5B	9	0.5291	0.6508	0.5687	0.4999	0.4988
NO-5B	10	0.4995	0.5941	0.4903	0.4713	0.4738
NO-5B	12	0.5469	0.7922	0.7248	0.7031	0.5007
NO-5B	13	0.4995	0.6793	0.6514	0.5835	0.4549
NO-5B	14	0.4640	0.6025	0.5672	0.4992	0.4093
NO-5B	15	0.4393	0.5548	0.4894	0.4713	0.3739

Appendix D1 Predictions of Resilient Modulus from Statistical Models for Development Dataset (Continued)

Sample I.D.	Seq. No.	Experiment M_R/P_a (10^3)	Predicted M_R/P_a (10^3)			
			Stress-Based	Mult. Reg.	Polynomial	Factorial
NO-6A	2	0.6802	0.6831	0.6011	0.5762	0.6239
NO-6A	3	0.5933	0.5404	0.5252	0.4538	0.5670
NO-6A	4	0.5173	0.4545	0.4454	0.3746	0.5068
NO-6A	5	0.4679	0.3986	0.3663	0.3461	0.4465
NO-6A	7	0.6041	0.6589	0.6021	0.5773	0.5965
NO-6A	8	0.5321	0.5235	0.5268	0.4549	0.5408
NO-6A	9	0.4758	0.4443	0.4509	0.3772	0.4842
NO-6A	10	0.4334	0.3866	0.3661	0.3446	0.4205
NO-6A	12	0.5321	0.6270	0.6044	0.5825	0.5703
NO-6A	13	0.4679	0.4996	0.5284	0.4576	0.5148
NO-6A	14	0.4195	0.4256	0.4519	0.3782	0.4585
NO-6A	15	0.3880	0.3760	0.3747	0.3453	0.4012
NO-6B	2	0.5538	0.6750	0.5163	0.5047	0.4675
NO-6B	3	0.4600	0.5260	0.4397	0.3819	0.4186
NO-6B	4	0.3919	0.4390	0.3606	0.3040	0.3694
NO-6B	5	0.3564	0.3805	0.2784	0.2757	0.3197
NO-6B	7	0.4679	0.6411	0.5167	0.5046	0.4494
NO-6B	8	0.3959	0.5070	0.4439	0.3863	0.4008
NO-6B	9	0.3495	0.4257	0.3673	0.3074	0.3510
NO-6B	10	0.3169	0.3685	0.2838	0.2744	0.2980
NO-6B	12	0.4827	0.5942	0.5171	0.5061	0.4315
NO-6B	13	0.4097	0.4742	0.4443	0.3874	0.3808
NO-6B	14	0.3455	0.4012	0.3677	0.3079	0.3287
NO-6B	15	0.3070	0.3531	0.2911	0.2751	0.2780
NO-7A	2	0.9970	0.9614	0.9040	0.9051	0.9608
NO-7A	3	0.9516	0.8057	0.8236	0.7770	0.8748
NO-7A	4	0.9003	0.7134	0.7451	0.7014	0.7934
NO-7A	5	0.8470	0.6502	0.6679	0.6749	0.7156
NO-7A	7	0.9210	0.9496	0.9050	0.9062	0.9522
NO-7A	8	0.8894	0.7963	0.8246	0.7772	0.8619
NO-7A	9	0.8539	0.7056	0.7461	0.7008	0.7763
NO-7A	10	0.8203	0.6423	0.6670	0.6734	0.6925
NO-7A	12	0.8490	0.9281	0.9047	0.9065	0.9421
NO-7A	13	0.8203	0.7826	0.8256	0.7791	0.8490
NO-7A	14	0.7927	0.6948	0.7471	0.7018	0.7592
NO-7A	15	0.7660	0.6338	0.6687	0.6735	0.6719
NO-7B	2	0.9023	0.9523	0.7700	0.7961	0.6977
NO-7B	3	0.8184	0.7826	0.6922	0.6720	0.6360
NO-7B	4	0.7443	0.6824	0.6156	0.5970	0.5768
NO-7B	5	0.6821	0.6136	0.5390	0.5686	0.5190
NO-7B	7	0.8213	0.9342	0.7710	0.7972	0.6890
NO-7B	8	0.7641	0.7656	0.6913	0.6698	0.6233
NO-7B	9	0.7098	0.6697	0.6154	0.5955	0.5621
NO-7B	10	0.6624	0.6031	0.5388	0.5670	0.5019
NO-7B	12	0.7611	0.9034	0.7708	0.7975	0.6793
NO-7B	13	0.7127	0.7477	0.6936	0.6733	0.6132
NO-7B	14	0.6703	0.6542	0.6164	0.5965	0.5486
NO-7B	15	0.6328	0.5856	0.5329	0.5668	0.4803

Appendix D1 Predictions of Resilient Modulus from Statistical Models for Development Dataset (Continued)

Sample I.D.	Seq. No.	Experiment M_R/P_a (10^3)	Predicted M_R/P_a (10^3)			
			Stress-Based	Mult. Reg.	Polynomial	Factorial
NO-8A	2	0.9812	0.9823	1.1440	1.1245	1.1756
NO-8A	3	0.9654	0.8693	1.0643	0.9980	1.0934
NO-8A	4	0.9447	0.7973	0.9852	0.9225	1.0254
NO-8A	5	0.9210	0.7445	0.9048	0.8967	0.9700
NO-8A	7	0.9102	0.9903	1.1444	1.1244	1.1779
NO-8A	8	0.9072	0.8764	1.0653	0.9982	1.0741
NO-8A	9	0.9023	0.8022	0.9849	0.9210	0.9824
NO-8A	10	0.8954	0.7488	0.9046	0.8952	0.9046
NO-8A	12	0.8134	1.0035	1.1454	1.1271	1.1813
NO-8A	13	0.8263	0.8850	1.0651	0.9984	1.0531
NO-8A	14	0.8272	0.8102	0.9860	0.9219	0.9405
NO-8A	15	0.8243	0.7562	0.9068	0.8952	0.8412
NO-8B	2	1.0533	1.0188	1.0270	1.0328	0.9222
NO-8B	3	1.0296	0.8869	0.9466	0.9055	0.8589
NO-8B	4	0.9970	0.8049	0.8675	0.8303	0.7971
NO-8B	5	0.9615	0.7464	0.7884	0.8049	0.7358
NO-8B	7	0.9990	1.0206	1.0274	1.0327	0.9270
NO-8B	8	0.9901	0.8883	0.9470	0.9049	0.8629
NO-8B	9	0.9714	0.8061	0.8679	0.8293	0.8003
NO-8B	10	0.9497	0.7466	0.7875	0.8034	0.7372
NO-8B	12	0.9279	1.0247	1.0284	1.0354	0.9324
NO-8B	13	0.9269	0.8912	0.9480	0.9067	0.8675
NO-8B	14	0.9151	0.8089	0.8695	0.8306	0.8046
NO-8B	15	0.9033	0.7492	0.7898	0.8035	0.7412
NO-9A	2	0.9062	0.8652	0.8251	0.8423	0.8798
NO-9A	3	0.8184	0.7051	0.7460	0.7154	0.7826
NO-9A	4	0.7433	0.6114	0.6694	0.6400	0.6946
NO-9A	5	0.6742	0.5448	0.5903	0.6110	0.6101
NO-9A	7	0.8282	0.8853	0.8242	0.8398	0.8819
NO-9A	8	0.7552	0.7226	0.7463	0.7148	0.7759
NO-9A	9	0.6920	0.6241	0.6685	0.6381	0.6761
NO-9A	10	0.6436	0.5572	0.5919	0.6096	0.5841
NO-9A	12	0.7532	0.9256	0.8258	0.8437	0.8876
NO-9A	13	0.6930	0.7506	0.7480	0.7175	0.7711
NO-9A	14	0.6417	0.6467	0.6714	0.6404	0.6624
NO-9A	15	0.6022	0.5741	0.5936	0.6098	0.5582
NO-9B	2	0.8213	0.8461	0.7042	0.8361	0.7008
NO-9B	3	0.7315	0.6795	0.6276	0.7128	0.6128
NO-9B	4	0.6417	0.5782	0.5492	0.6349	0.5347
NO-9B	5	0.5686	0.5092	0.4701	0.6060	0.4683
NO-9B	7	0.7502	0.8696	0.7052	0.8372	0.7255
NO-9B	8	0.6644	0.6922	0.6261	0.7098	0.6142
NO-9B	9	0.5933	0.5885	0.5477	0.6326	0.5160
NO-9B	10	0.5400	0.5178	0.4686	0.6044	0.4294
NO-9B	12	0.6969	0.9027	0.7056	0.8387	0.7492
NO-9B	13	0.6190	0.7183	0.6284	0.7133	0.6206
NO-9B	14	0.5587	0.6049	0.5474	0.6327	0.4983
NO-9B	15	0.5094	0.5333	0.4715	0.6046	0.3954

Appendix D1 Predictions of Resilient Modulus from Statistical Models for Development Dataset (Continued)

Sample I.D.	Seq. No.	Experiment M_R/P_a (10^3)	Predicted M_R/P_a (10^3)			
			Stress-Based	Mult. Reg.	Polynomial	Factorial
OK-1A	2	1.2981	0.8940	0.8421	0.8306	0.8969
OK-1A	3	0.9566	0.7809	0.7858	0.7516	0.8214
OK-1A	4	0.7522	0.6875	0.7181	0.6900	0.7324
OK-1A	5	0.6387	0.6113	0.6396	0.6642	0.6317
OK-1A	7	1.1362	0.9194	0.8501	0.8429	0.9251
OK-1A	8	0.9339	0.7890	0.7881	0.7532	0.8384
OK-1A	9	0.7700	0.6901	0.7172	0.6881	0.7414
OK-1A	10	0.6663	0.6146	0.6400	0.6627	0.6380
OK-1A	12	1.2873	1.0018	0.8752	0.8886	0.9795
OK-1A	13	1.3376	0.8095	0.7960	0.7635	0.8640
OK-1A	14	1.0928	0.6913	0.7138	0.6863	0.7466
OK-1A	15	0.8638	0.6128	0.6328	0.6628	0.6339
OK-1B	2	0.6051	0.8665	0.6639	0.6634	0.6159
OK-1B	3	0.4768	0.7229	0.6083	0.5759	0.5329
OK-1B	4	0.3524	0.6188	0.5462	0.5075	0.4458
OK-1B	5	0.2883	0.5440	0.4823	0.4690	0.3618
OK-1B	7	0.5982	0.8802	0.6700	0.6736	0.6392
OK-1B	8	0.4432	0.7335	0.6156	0.5850	0.5472
OK-1B	9	0.3327	0.6191	0.5491	0.5088	0.4407
OK-1B	10	0.2794	0.5433	0.4846	0.4684	0.3435
OK-1B	12	0.5864	0.8789	0.6723	0.6786	0.6574
OK-1B	13	0.4255	0.7330	0.6185	0.5898	0.5561
OK-1B	14	0.3208	0.6199	0.5533	0.5129	0.4389
OK-1B	15	0.2715	0.5416	0.4869	0.4694	0.3258
OK-2A	2	0.6486	0.7749	0.8198	0.7661	0.6552
OK-2A	3	0.5370	0.7005	0.7666	0.6904	0.6237
OK-2A	4	0.4462	0.6264	0.6907	0.6211	0.5742
OK-2A	5	0.4067	0.5733	0.6141	0.5977	0.5187
OK-2A	7	0.5400	0.8045	0.8360	0.7928	0.6293
OK-2A	8	0.4452	0.7109	0.7746	0.6992	0.6012
OK-2A	9	0.4107	0.6285	0.6923	0.6208	0.5580
OK-2A	10	0.3988	0.5749	0.6157	0.5962	0.5121
OK-2A	12	0.5005	0.8141	0.8401	0.8010	0.5958
OK-2A	13	0.4067	0.7096	0.7724	0.6970	0.5732
OK-2A	14	0.3850	0.6314	0.6946	0.6225	0.5419
OK-2A	15	0.3830	0.5772	0.6180	0.5963	0.5056
OK-2B	2	0.5676	0.7266	0.6073	0.6812	0.6078
OK-2B	3	0.3781	0.6028	0.5402	0.5755	0.5480
OK-2B	4	0.3366	0.5163	0.4643	0.4989	0.4835
OK-2B	5	0.3416	0.4560	0.3858	0.4680	0.4203
OK-2B	7	0.5439	0.7312	0.6121	0.6893	0.6269
OK-2B	8	0.3820	0.5955	0.5387	0.5724	0.5558
OK-2B	9	0.3534	0.5080	0.4596	0.4944	0.4827
OK-2B	10	0.3504	0.4514	0.3836	0.4664	0.4160
OK-2B	12	0.5183	0.7205	0.6118	0.6896	0.6413
OK-2B	13	0.3840	0.5889	0.5391	0.5735	0.5653
OK-2B	14	0.3593	0.5047	0.4619	0.4963	0.4880
OK-2B	15	0.3603	0.4478	0.3847	0.4665	0.4142

Appendix D1 Predictions of Resilient Modulus from Statistical Models for Development Dataset (Continued)

Sample I.D.	Seq. No.	Experiment M_R/P_a (10^3)	Predicted M_R/P_a (10^3)			
			Stress-Based	Mult. Reg.	Polynomial	Factorial
OK-3A	2	0.9003	0.9580	0.9734	0.9270	0.9972
OK-3A	3	0.7502	0.8469	0.8994	0.8232	0.9198
OK-3A	4	0.6160	0.7985	0.8538	0.7809	0.8728
OK-3A	5	0.5163	0.7330	0.7722	0.7465	0.7898
OK-3A	7	0.8677	0.9485	0.9795	0.9366	1.0009
OK-3A	8	0.6920	0.8425	0.9099	0.8342	0.9260
OK-3A	9	0.5676	0.7861	0.8567	0.7819	0.8695
OK-3A	10	0.4946	0.7210	0.7732	0.7451	0.7820
OK-3A	12	0.8421	0.9225	0.9818	0.9413	1.0008
OK-3A	13	0.6683	0.8221	0.9128	0.8382	0.9244
OK-3A	14	0.5429	0.7666	0.8577	0.7830	0.8642
OK-3A	15	0.4729	0.7054	0.7748	0.7454	0.7749
OK-3B	2	0.7789	0.8951	0.6969	0.6887	0.6735
OK-3B	3	0.5143	0.7621	0.6418	0.5976	0.6219
OK-3B	4	0.3613	0.6643	0.5798	0.5238	0.5651
OK-3B	5	0.3277	0.5870	0.5083	0.4768	0.5011
OK-3B	7	0.7443	0.8796	0.7017	0.6969	0.6519
OK-3B	8	0.4590	0.7487	0.6473	0.6045	0.5986
OK-3B	9	0.3504	0.6457	0.5802	0.5230	0.5342
OK-3B	10	0.3139	0.5706	0.5074	0.4751	0.4660
OK-3B	12	0.9013	0.8505	0.7065	0.7070	0.6307
OK-3B	13	0.5499	0.7129	0.6458	0.6029	0.5686
OK-3B	14	0.3791	0.6205	0.5806	0.5238	0.5033
OK-3B	15	0.3307	0.5511	0.5085	0.4756	0.4326
OK-4A	2	0.6565	0.7468	0.6829	0.6605	0.7087
OK-4A	3	0.4531	0.6219	0.6215	0.5645	0.6313
OK-4A	4	0.3682	0.5374	0.5570	0.4959	0.5535
OK-4A	5	0.3248	0.4730	0.4861	0.4587	0.4724
OK-4A	7	0.6120	0.7553	0.6871	0.6673	0.7246
OK-4A	8	0.4610	0.6321	0.6289	0.5734	0.6440
OK-4A	9	0.3722	0.5364	0.5574	0.4950	0.5493
OK-4A	10	0.3337	0.4702	0.4840	0.4568	0.4567
OK-4A	12	0.6140	0.7546	0.6881	0.6699	0.7366
OK-4A	13	0.4659	0.6282	0.6280	0.5728	0.6463
OK-4A	14	0.3771	0.5350	0.5577	0.4956	0.5450
OK-4A	15	0.3396	0.4692	0.4843	0.4570	0.4438
OK-4B	2	0.5252	0.7886	0.5970	0.6249	0.6142
OK-4B	3	0.3327	0.6462	0.5369	0.5258	0.5258
OK-4B	4	0.2458	0.5662	0.4850	0.4633	0.4549
OK-4B	5	0.2172	0.4975	0.4224	0.4164	0.3756
OK-4B	7	0.4492	0.8088	0.6063	0.6419	0.6646
OK-4B	8	0.2853	0.6666	0.5512	0.5458	0.5695
OK-4B	9	0.2320	0.5636	0.4873	0.4644	0.4660
OK-4B	10	0.2142	0.4939	0.4234	0.4155	0.3698
OK-4B	12	0.4353	0.8026	0.6085	0.6472	0.7053
OK-4B	13	0.2794	0.6611	0.5535	0.5499	0.5969
OK-4B	14	0.2280	0.5606	0.4908	0.4685	0.4803
OK-4B	15	0.2132	0.4883	0.4238	0.4160	0.3633

Appendix D1 Predictions of Resilient Modulus from Statistical Models for Development Dataset (Continued)

Sample I.D.	Seq. No.	Experiment M_R/P_a (10^3)	Predicted M_R/P_a (10^3)			
			Stress-Based	Mult. Reg.	Polynomial	Factorial
OK-5A	2	0.7187	0.7490	0.7267	0.6880	0.7767
OK-5A	3	0.6219	0.6344	0.6584	0.5905	0.7038
OK-5A	4	0.5311	0.5696	0.6008	0.5373	0.6426
OK-5A	5	0.4551	0.5098	0.5274	0.5077	0.5650
OK-5A	7	0.6900	0.7378	0.7290	0.6910	0.7671
OK-5A	8	0.5716	0.6324	0.6664	0.5989	0.6995
OK-5A	9	0.4965	0.5637	0.6056	0.5395	0.6343
OK-5A	10	0.4462	0.5011	0.5271	0.5061	0.5505
OK-5A	12	0.6930	0.7249	0.7338	0.7000	0.7602
OK-5A	13	0.5696	0.6187	0.6693	0.6030	0.6899
OK-5A	14	0.4877	0.5511	0.6073	0.5410	0.6226
OK-5A	15	0.4393	0.4905	0.5282	0.5063	0.5373
OK-5B	2	0.4798	0.9324	0.7932	0.7879	0.7973
OK-5B	3	0.4136	0.7855	0.7210	0.6738	0.7388
OK-5B	4	0.3791	0.6902	0.6451	0.5984	0.6786
OK-5B	5	0.3771	0.6218	0.5654	0.5686	0.6172
OK-5B	7	0.4541	0.9161	0.7993	0.7986	0.7697
OK-5B	8	0.3781	0.7708	0.7277	0.6816	0.7089
OK-5B	9	0.3662	0.6730	0.6480	0.5992	0.6429
OK-5B	10	0.3702	0.6081	0.5695	0.5674	0.5796
OK-5B	12	0.6920	0.8967	0.8098	0.8200	0.7464
OK-5B	13	0.5647	0.7460	0.7345	0.6914	0.6796
OK-5B	14	0.5202	0.6537	0.6560	0.6055	0.6116
OK-5B	15	0.4650	0.5900	0.5750	0.5681	0.5432
OS-1A	2	0.7616	0.9498	0.9873	0.9387	0.8695
OS-1A	3	0.7347	0.8479	0.9131	0.8283	0.8228
OS-1A	4	0.7034	0.7740	0.8302	0.7566	0.7682
OS-1A	5	0.6464	0.7264	0.7560	0.7389	0.7172
OS-1A	7	0.7663	0.9332	0.9877	0.9385	0.8383
OS-1A	8	0.7291	0.8390	0.9179	0.8330	0.7978
OS-1A	9	0.6949	0.7658	0.8350	0.7579	0.7475
OS-1A	10	0.6576	0.7190	0.7608	0.7371	0.7002
OS-1A	12	0.7794	0.9093	0.9881	0.9399	0.8070
OS-1A	13	0.7351	0.8245	0.9226	0.8394	0.7724
OS-1A	14	0.7017	0.7505	0.8354	0.7584	0.7238
OS-1A	15	0.6650	0.7082	0.7655	0.7372	0.6828
OS-1B	2	0.6827	0.7622	0.5887	0.5904	0.5743
OS-1B	3	0.4650	0.6440	0.5319	0.5000	0.5183
OS-1B	4	0.3348	0.5607	0.4709	0.4313	0.4605
OS-1B	5	0.2919	0.4948	0.4010	0.3891	0.3977
OS-1B	7	0.6241	0.7488	0.5934	0.5983	0.5808
OS-1B	8	0.4504	0.6315	0.5367	0.5056	0.5193
OS-1B	9	0.3429	0.5402	0.4669	0.4267	0.4469
OS-1B	10	0.3000	0.4784	0.3971	0.3865	0.3778
OS-1B	12	0.6456	0.7129	0.5938	0.5997	0.5828
OS-1B	13	0.4680	0.6041	0.5371	0.5067	0.5162
OS-1B	14	0.3535	0.5191	0.4673	0.4273	0.4373
OS-1B	15	0.3095	0.4615	0.3974	0.3868	0.3618

Appendix D1 Predictions of Resilient Modulus from Statistical Models for Development Dataset (Continued)

Sample I.D.	Seq. No.	Experiment M_R/P_a (10^3)	Predicted M_R/P_a (10^3)			
			Stress-Based	Mult. Reg.	Polynomial	Factorial
OS-2A	2	0.9033	1.0277	1.0888	1.0877	1.2192
OS-2A	3	0.8880	0.8953	0.9972	0.9672	1.1323
OS-2A	4	0.8595	0.8286	0.9273	0.9201	1.0702
OS-2A	5	0.8288	0.7953	0.8837	0.9104	1.0331
OS-2A	7	0.9355	1.0307	1.0892	1.0874	1.2460
OS-2A	8	0.9149	0.8881	0.9888	0.9583	1.1415
OS-2A	9	0.8706	0.8270	0.9234	0.9172	1.0773
OS-2A	10	0.8420	0.7911	0.8754	0.9088	1.0322
OS-2A	12	0.9561	1.0352	1.0896	1.0887	1.2728
OS-2A	13	0.9297	0.8961	0.9936	0.9630	1.1635
OS-2A	14	0.8885	0.8262	0.9194	0.9160	1.0836
OS-2A	15	0.8576	0.7906	0.8714	0.9089	1.0341
OS-2B	2	0.6423	0.9108	0.7313	0.7621	0.7652
OS-2B	3	0.5037	0.7697	0.6746	0.6737	0.6870
OS-2B	4	0.4012	0.6633	0.6092	0.6035	0.5990
OS-2B	5	0.3361	0.5849	0.5394	0.5662	0.5079
OS-2B	7	0.6631	0.9148	0.7361	0.7698	0.7861
OS-2B	8	0.5229	0.7619	0.6750	0.6732	0.6972
OS-2B	9	0.4226	0.6571	0.6096	0.6026	0.6043
OS-2B	10	0.3585	0.5757	0.5354	0.5638	0.5020
OS-2B	12	0.6853	0.9002	0.7365	0.7712	0.8009
OS-2B	13	0.5431	0.7428	0.6710	0.6685	0.7008
OS-2B	14	0.4359	0.6486	0.6099	0.6033	0.6096
OS-2B	15	0.3722	0.5690	0.5358	0.5640	0.5018
OS-3A	2	1.7709	0.9348	0.9157	0.8946	1.0782
OS-3A	3	1.0771	0.8134	0.8372	0.7817	0.9761
OS-3A	4	0.8822	0.7547	0.7804	0.7308	0.9037
OS-3A	5	0.7090	0.7005	0.7106	0.7031	0.8163
OS-3A	7	1.6532	0.9275	0.9292	0.9180	1.0859
OS-3A	8	1.0141	0.7867	0.8375	0.7811	0.9619
OS-3A	9	0.8543	0.7351	0.7852	0.7328	0.8925
OS-3A	10	0.7065	0.6803	0.7110	0.7017	0.7960
OS-3A	12	1.6654	0.8616	0.9208	0.9035	1.0638
OS-3A	13	1.0252	0.7505	0.8379	0.7820	0.9477
OS-3A	14	0.8647	0.7038	0.7856	0.7334	0.8758
OS-3A	15	0.7078	0.6541	0.7114	0.7018	0.7756
OS-3B	2	0.5180	0.8317	0.6232	0.6316	0.5820
OS-3B	3	0.3318	0.7007	0.5708	0.5400	0.5416
OS-3B	4	0.2556	0.5976	0.5054	0.4562	0.4926
OS-3B	5	0.2518	0.5245	0.4356	0.4043	0.4424
OS-3B	7	0.4928	0.8095	0.6279	0.6402	0.5646
OS-3B	8	0.3119	0.6809	0.5756	0.5464	0.5212
OS-3B	9	0.2603	0.5753	0.5057	0.4554	0.4652
OS-3B	10	0.2501	0.5027	0.4316	0.4011	0.4078
OS-3B	12	0.5018	0.7579	0.6283	0.6417	0.5437
OS-3B	13	0.3208	0.6338	0.5716	0.5408	0.4937
OS-3B	14	0.2666	0.5407	0.5018	0.4518	0.4340
OS-3B	15	0.2567	0.4760	0.4276	0.3997	0.3728

Appendix D1 Predictions of Resilient Modulus from Statistical Models for Development Dataset (Continued)

Sample I.D.	Seq. No.	Experiment M_R/P_a (10^3)	Predicted M_R/P_a (10^3)			
			Stress-Based	**Mult. Reg.**	**Polynomial**	**Factorial**
RO-1A	2	0.7947	0.9868	0.7455	0.8346	0.7444
RO-1A	3	0.7236	0.7824	0.6601	0.7087	0.6951
RO-1A	4	0.6456	0.6659	0.5753	0.6412	0.6451
RO-1A	5	0.5735	0.5894	0.4917	0.6306	0.5948
RO-1A	7	0.7493	0.9581	0.7497	0.8414	0.6977
RO-1A	8	0.6960	0.7594	0.6642	0.7124	0.6501
RO-1A	9	0.6347	0.6470	0.5794	0.6418	0.6017
RO-1A	10	0.5765	0.5726	0.4946	0.6284	0.5523
RO-1A	12	0.7048	0.9092	0.7532	0.8488	0.6505
RO-1A	13	0.6654	0.7231	0.6672	0.7164	0.6042
RO-1A	14	0.6160	0.6199	0.5830	0.6439	0.5578
RO-1A	15	0.5627	0.5508	0.4982	0.6278	0.5101
RO-1B	2	0.7423	1.0103	0.6652	0.6969	0.5543
RO-1B	3	0.6703	0.7954	0.5792	0.5716	0.5021
RO-1B	4	0.5824	0.6759	0.4956	0.5063	0.4519
RO-1B	5	0.5035	0.5952	0.4108	0.4969	0.4012
RO-1B	7	0.6811	0.9761	0.6694	0.7036	0.5222
RO-1B	8	0.6298	0.7685	0.5833	0.5752	0.4694
RO-1B	9	0.5656	0.6533	0.4992	0.5066	0.4181
RO-1B	10	0.5044	0.5764	0.4144	0.4945	0.3669
RO-1B	12	0.6061	0.9180	0.6723	0.7097	0.4896
RO-1B	13	0.5726	0.7274	0.5863	0.5791	0.4361
RO-1B	14	0.5262	0.6231	0.5034	0.5089	0.3851
RO-1B	15	0.4778	0.5518	0.4179	0.4938	0.3328

Appendix D2 Predictions of Resilient Modulus from Statistical Models for Evaluation Dataset

Sample I.D.	Seq. No.	Experiment M_R/P_a (10^3)	Predicted M_R/P_a (10^3)			
			Stress-Based	Mult. Reg.	Polynomial	Factorial
ROE-1A	2	1.0139	1.1117	0.8936	0.8907	0.8769
ROE-1A	3	0.8616	0.9230	0.8282	0.7841	0.8239
ROE-1A	4	0.6413	0.7972	0.7584	0.7081	0.7680
ROE-1A	5	0.5363	0.7149	0.6929	0.6719	0.7162
ROE-1A	7	0.9401	1.1274	0.8984	0.8989	0.8482
ROE-1A	8	0.7985	0.9422	0.8373	0.7959	0.7975
ROE-1A	9	0.6222	0.8096	0.7675	0.7146	0.7402
ROE-1A	10	0.5447	0.7144	0.6933	0.6706	0.6801
ROE-1A	12	0.9638	1.1257	0.8988	0.9004	0.8159
ROE-1A	13	0.8052	0.9409	0.8377	0.7971	0.7640
ROE-1A	14	0.6282	0.8087	0.7679	0.7153	0.7054
ROE-1A	15	0.5499	0.7184	0.6981	0.6723	0.6475
ROE-1B	2	0.7654	1.2033	0.8139	0.8117	1.0623
ROE-1B	3	0.5494	0.9978	0.7572	0.7115	0.9970
ROE-1B	4	0.4079	0.8505	0.6918	0.6276	0.9285
ROE-1B	5	0.3420	0.7564	0.6307	0.5802	0.8711
ROE-1B	7	0.7016	1.2132	0.8187	0.8204	0.9569
ROE-1B	8	0.5129	1.0018	0.7620	0.7179	0.8786
ROE-1B	9	0.3966	0.8517	0.6965	0.6314	0.7950
ROE-1B	10	0.3444	0.7509	0.6311	0.5790	0.7187
ROE-1B	12	0.7123	1.2179	0.8234	0.8310	0.8535
ROE-1B	13	0.5296	0.9894	0.7623	0.7192	0.7553
ROE-1B	14	0.4009	0.8423	0.6969	0.6323	0.6572
ROE-1B	15	0.3462	0.7433	0.6314	0.5795	0.5663
ROE-2A	2	1.1676	0.9514	0.8833	0.8405	0.8598
ROE-2A	3	1.0440	0.8107	0.8092	0.7301	0.7818
ROE-2A	4	0.8597	0.7296	0.7437	0.6690	0.7140
ROE-2A	5	0.6666	0.6533	0.6564	0.6405	0.6250
ROE-2A	7	1.1112	0.9468	0.8837	0.8404	0.8470
ROE-2A	8	0.9804	0.8135	0.8139	0.7348	0.7715
ROE-2A	9	0.7829	0.7221	0.7397	0.6651	0.6925
ROE-2A	10	0.6675	0.6509	0.6568	0.6390	0.6056
ROE-2A	12	1.1033	0.9619	0.8928	0.8577	0.8440
ROE-2A	13	0.9772	0.8084	0.8143	0.7358	0.7567
ROE-2A	14	0.7803	0.7224	0.7445	0.6685	0.6803
ROE-2A	15	0.6724	0.6507	0.6616	0.6390	0.5909
ROE-2B	2	1.1467	0.9715	0.8551	0.8672	0.8598
ROE-2B	3	0.9982	0.8294	0.7896	0.7606	0.7824
ROE-2B	4	0.7393	0.7372	0.7242	0.6882	0.7077
ROE-2B	5	0.6224	0.6673	0.6544	0.6484	0.6311
ROE-2B	7	1.1326	0.9729	0.8555	0.8671	0.8470
ROE-2B	8	0.9500	0.8381	0.7944	0.7662	0.7695
ROE-2B	9	0.7046	0.7381	0.7246	0.6873	0.6839
ROE-2B	10	0.6210	0.6681	0.6548	0.6471	0.6014
ROE-2B	12	1.1828	0.9876	0.8602	0.8769	0.8401
ROE-2B	13	0.9536	0.8397	0.7948	0.7673	0.7515
ROE-2B	14	0.7060	0.7446	0.7293	0.6918	0.6657
ROE-2B	15	0.6260	0.6730	0.6595	0.6488	0.5771

Appendix D2 Predictions of Resilient Modulus from Statistical Models for Evaluation Dataset (Continued)

Sample I.D.	Seq. No.	Experiment M_R/P_a (10^3)	Predicted M_R/P_a (10^3)			
			Stress-Based	Mult. Reg.	Polynomial	Factorial
ROE-3A	2	1.0171	0.8829	0.8403	0.8005	0.8221
ROE-3A	3	0.9580	0.7391	0.7705	0.6856	0.7495
ROE-3A	4	0.7696	0.6451	0.6963	0.6061	0.6735
ROE-3A	5	0.6861	0.5805	0.6221	0.5703	0.5986
ROE-3A	7	0.9873	0.8594	0.8363	0.7921	0.8187
ROE-3A	8	0.9119	0.7367	0.7752	0.6912	0.7535
ROE-3A	9	0.7405	0.6421	0.7011	0.6086	0.6753
ROE-3A	10	0.6924	0.5775	0.6269	0.5698	0.5983
ROE-3A	12	1.0118	0.8532	0.8411	0.8019	0.8247
ROE-3A	13	0.9258	0.7234	0.7756	0.6923	0.7529
ROE-3A	14	0.7534	0.6362	0.7058	0.6130	0.6774
ROE-3A	15	0.7037	0.5691	0.6273	0.5700	0.5937
ROE-3B	2	0.8904	0.7402	0.5897	0.5764	0.6275
ROE-3B	3	0.7612	0.5873	0.5199	0.4615	0.5377
ROE-3B	4	0.6341	0.4792	0.4326	0.3725	0.4326
ROE-3B	5	0.5735	0.4230	0.3628	0.3449	0.3543
ROE-3B	7	0.8267	0.7243	0.5901	0.5763	0.6440
ROE-3B	8	0.6836	0.5757	0.5203	0.4610	0.5447
ROE-3B	9	0.5891	0.4706	0.4330	0.3715	0.4277
ROE-3B	10	0.5644	0.4130	0.3588	0.3430	0.3345
ROE-3B	12	0.8254	0.7012	0.5905	0.5778	0.6605
ROE-3B	13	0.6665	0.5595	0.5206	0.4621	0.5517
ROE-3B	14	0.5790	0.4629	0.4377	0.3751	0.4290
ROE-3B	15	0.5580	0.4066	0.3636	0.3436	0.3253
ROE-4A	2	0.8239	0.8266	0.6150	0.6337	0.6679
ROE-4A	3	0.5647	0.6376	0.5496	0.5204	0.5353
ROE-4A	4	0.4633	0.5331	0.4885	0.4453	0.4192
ROE-4A	5	0.3799	0.4664	0.4318	0.4022	0.3180
ROE-4A	7	0.7610	0.8511	0.6198	0.6425	0.7063
ROE-4A	8	0.5415	0.6718	0.5630	0.5400	0.5759
ROE-4A	9	0.4275	0.5493	0.4976	0.4535	0.4332
ROE-4A	10	0.3672	0.4739	0.4365	0.4035	0.3076
ROE-4A	12	0.7629	0.8805	0.6245	0.6531	0.7470
ROE-4A	13	0.5439	0.6791	0.5634	0.5412	0.5906
ROE-4A	14	0.4199	0.5613	0.5023	0.4591	0.4414
ROE-4A	15	0.3609	0.4827	0.4412	0.4066	0.2996
ROE-4B	2	0.4081	0.8783	0.5443	0.5755	0.5678
ROE-4B	3	0.2667	0.6874	0.4920	0.4767	0.4522
ROE-4B	4	0.2209	0.5717	0.4396	0.3996	0.3463
ROE-4B	5	0.2010	0.4932	0.3873	0.3444	0.2500
ROE-4B	7	0.4021	0.8955	0.5491	0.5848	0.5963
ROE-4B	8	0.2718	0.6840	0.4924	0.4764	0.4444
ROE-4B	9	0.2239	0.5691	0.4400	0.3991	0.3143
ROE-4B	10	0.2084	0.4857	0.3833	0.3398	0.1843
ROE-4B	12	0.4378	0.8670	0.5451	0.5772	0.6006
ROE-4B	13	0.2776	0.6792	0.4928	0.4777	0.4366
ROE-4B	14	0.2283	0.5579	0.4360	0.3946	0.2699
ROE-4B	15	0.2135	0.4829	0.3837	0.3405	0.1261

Appendix D2 Predictions of Resilient Modulus from Statistical Models for Evaluation Dataset (Continued)

Sample I.D.	Seq. No.	Experiment M_R/P_a (10^3)	Predicted M_R/P_a (10^3)			
			Stress-Based	Mult. Reg.	Polynomial	Factorial
ROE-5A	2	0.7805	0.8475	0.6931	0.6627	0.5324
ROE-5A	3	0.6190	0.6931	0.6364	0.5625	0.5244
ROE-5A	4	0.4922	0.5787	0.5666	0.4743	0.5037
ROE-5A	5	0.4436	0.5080	0.5012	0.4269	0.4736
ROE-5A	7	0.7132	0.8337	0.6979	0.6715	0.4110
ROE-5A	8	0.5619	0.6710	0.6368	0.5622	0.4221
ROE-5A	9	0.4739	0.5616	0.5670	0.4736	0.4236
ROE-5A	10	0.4421	0.4939	0.5016	0.4257	0.4142
ROE-5A	12	0.7145	0.7910	0.6983	0.6731	0.2894
ROE-5A	13	0.5600	0.6484	0.6416	0.5702	0.3179
ROE-5A	14	0.4727	0.5436	0.5717	0.4788	0.3423
ROE-5A	15	0.4443	0.4754	0.5019	0.4261	0.3549
ROE-5B	2	0.7589	0.9037	0.6320	0.6014	0.4946
ROE-5B	3	0.5233	0.7278	0.5709	0.4946	0.4248
ROE-5B	4	0.4247	0.6147	0.5055	0.4130	0.3492
ROE-5B	5	0.3707	0.5432	0.4444	0.3677	0.2781
ROE-5B	7	0.6718	0.8997	0.6411	0.6192	0.4872
ROE-5B	8	0.4763	0.7184	0.5800	0.5077	0.4187
ROE-5B	9	0.3921	0.6044	0.5146	0.4212	0.3446
ROE-5B	10	0.3603	0.5250	0.4448	0.3665	0.2649
ROE-5B	12	0.6623	0.8436	0.6415	0.6208	0.4698
ROE-5B	13	0.4682	0.6871	0.5848	0.5159	0.4074
ROE-5B	14	0.3874	0.5740	0.5150	0.4221	0.3299
ROE-5B	15	0.3605	0.5049	0.4495	0.3692	0.2566
ROE-6A	2	1.2960	1.0995	0.9786	0.9568	1.1491
ROE-6A	3	1.2056	0.8970	0.8914	0.8253	1.0850
ROE-6A	4	1.1628	0.8080	0.8303	0.7694	1.0372
ROE-6A	5	1.0302	0.7371	0.7648	0.7423	0.9835
ROE-6A	7	1.3494	1.1266	0.9834	0.9649	1.0977
ROE-6A	8	1.1941	0.9064	0.8918	0.8247	1.0381
ROE-6A	9	1.1445	0.8159	0.8307	0.7684	0.9955
ROE-6A	10	1.0488	0.7439	0.7652	0.7409	0.9471
ROE-6A	12	1.3400	1.1313	0.9794	0.9581	1.0409
ROE-6A	13	1.2098	0.9276	0.8965	0.8308	0.9939
ROE-6A	14	1.1479	0.8268	0.8311	0.7689	0.9537
ROE-6A	15	1.0515	0.7573	0.7700	0.7419	0.9137
ROE-6B	2	1.1569	1.1758	0.9147	0.9083	1.2453
ROE-6B	3	1.0640	0.9869	0.8493	0.7995	1.2292
ROE-6B	4	0.7928	0.8540	0.7751	0.7174	1.2130
ROE-6B	5	0.6752	0.7678	0.7053	0.6801	1.1995
ROE-6B	7	1.1333	1.1779	0.9151	0.9082	1.0649
ROE-6B	8	1.0046	0.9985	0.8540	0.8053	1.0470
ROE-6B	9	0.7559	0.8553	0.7755	0.7165	1.0259
ROE-6B	10	0.6764	0.7689	0.7057	0.6787	1.0091
ROE-6B	12	1.1587	1.1979	0.9199	0.9182	0.8861
ROE-6B	13	1.0241	1.0009	0.8544	0.8064	0.8637
ROE-6B	14	0.7682	0.8635	0.7802	0.7208	0.8401
ROE-6B	15	0.6854	0.7704	0.7061	0.6790	0.8186

Appendix D2 Predictions of Resilient Modulus from Statistical Models for Evaluation Dataset (Continued)

Sample I.D.	Seq. No.	Experiment M_R/P_a (10^3)	Predicted M_R/P_a (10^3)			
			Stress-Based	Mult. Reg.	Polynomial	Factorial
ROE-7A	2	1.1808	0.8917	0.9404	0.9137	0.7961
ROE-7A	3	1.0942	0.7684	0.8706	0.8013	0.6751
ROE-7A	4	0.9378	0.6839	0.7964	0.7243	0.5554
ROE-7A	5	0.7932	0.6150	0.7092	0.6898	0.4264
ROE-7A	7	1.2175	0.9249	0.9452	0.9220	0.9904
ROE-7A	8	1.0673	0.7864	0.8710	0.8008	0.8455
ROE-7A	9	0.8826	0.6944	0.7925	0.7202	0.7019
ROE-7A	10	0.7962	0.6241	0.7052	0.6881	0.5545
ROE-7A	12	1.1977	0.9494	0.9412	0.9151	1.1672
ROE-7A	13	1.0599	0.8129	0.8714	0.8018	1.0158
ROE-7A	14	0.8661	0.7151	0.7928	0.7207	0.8552
ROE-7A	15	0.7871	0.6406	0.7056	0.6882	0.6888
ROE-7B	2	1.1382	0.7939	0.6677	0.7661	0.5688
ROE-7B	3	1.0015	0.6482	0.6022	0.6573	0.4400
ROE-7B	4	0.7127	0.5431	0.5237	0.5717	0.3223
ROE-7B	5	0.6501	0.4772	0.4495	0.5359	0.2481
ROE-7B	7	1.0989	0.8068	0.6680	0.7661	0.9065
ROE-7B	8	0.8834	0.6656	0.6069	0.6631	0.7331
ROE-7B	9	0.6729	0.5554	0.5284	0.5743	0.5461
ROE-7B	10	0.6422	0.4867	0.4542	0.5355	0.4064
ROE-7B	12	1.0819	0.8404	0.6728	0.7761	1.2612
ROE-7B	13	0.8588	0.6801	0.6073	0.6642	1.0186
ROE-7B	14	0.6619	0.5711	0.5332	0.5786	0.7774
ROE-7B	15	0.6385	0.4986	0.4590	0.5368	0.5722
ROE-8A	2	0.9194	0.7701	0.6887	0.6444	0.3013
ROE-8A	3	0.6597	0.6110	0.6233	0.5311	0.1707
ROE-8A	4	0.5307	0.5104	0.5535	0.4477	0.0586
ROE-8A	5	0.4872	0.4542	0.4968	0.4086	-0.0118
ROE-8A	7	0.9008	0.7867	0.6891	0.6444	0.5894
ROE-8A	8	0.6331	0.6314	0.6280	0.5372	0.4207
ROE-8A	9	0.5188	0.5303	0.5626	0.4553	0.2637
ROE-8A	10	0.4910	0.4620	0.4971	0.4074	0.1315
ROE-8A	12	0.9246	0.8122	0.6895	0.6460	0.8775
ROE-8A	13	0.6517	0.6586	0.6328	0.5451	0.6773
ROE-8A	14	0.5245	0.5441	0.5630	0.4561	0.4564
ROE-8A	15	0.5001	0.4729	0.4975	0.4078	0.2748
ROE-8B	2	1.0389	0.8267	0.6271	0.7148	0.4108
ROE-8B	3	0.8925	0.6637	0.5660	0.6080	0.1901
ROE-8B	4	0.6373	0.5522	0.4962	0.5222	-0.0199
ROE-8B	5	0.5647	0.4786	0.4264	0.4752	-0.1850
ROE-8B	7	1.0545	0.8240	0.6231	0.7062	0.7993
ROE-8B	8	0.8509	0.6732	0.5664	0.6076	0.5271
ROE-8B	9	0.6079	0.5595	0.4966	0.5214	0.2327
ROE-8B	10	0.5571	0.4884	0.4311	0.4758	-0.0024
ROE-8B	12	1.0468	0.8429	0.6235	0.7077	1.2047
ROE-8B	13	0.8070	0.6871	0.5668	0.6088	0.8640
ROE-8B	14	0.5842	0.5698	0.4970	0.5222	0.4854
ROE-8B	15	0.5422	0.4966	0.4315	0.4762	0.1713

Appendix D2 Predictions of Resilient Modulus from Statistical Models for Evaluation Dataset (Continued)

Sample I.D.	Seq. No.	Experiment M_R/P_a (10^3)	Predicted M_R/P_a (10^3)			
			Stress-Based	Mult. Reg.	Polynomial	Factorial
ROE-9A	2	0.9441	0.7516	0.6271	0.5696	0.8768
ROE-9A	3	0.8391	0.6134	0.5660	0.4648	0.8058
ROE-9A	4	0.6390	0.5084	0.4875	0.3738	0.7152
ROE-9A	5	0.5859	0.4474	0.4176	0.3340	0.6353
ROE-9A	7	0.9205	0.7358	0.6275	0.5695	0.8373
ROE-9A	8	0.7813	0.6089	0.5707	0.4709	0.7704
ROE-9A	9	0.6109	0.5038	0.4922	0.3767	0.6784
ROE-9A	10	0.5749	0.4399	0.4180	0.3327	0.5922
ROE-9A	12	0.8997	0.7128	0.6278	0.5710	0.7978
ROE-9A	13	0.7601	0.5916	0.5711	0.4721	0.7299
ROE-9A	14	0.6006	0.4912	0.4926	0.3774	0.6366
ROE-9A	15	0.5742	0.4300	0.4184	0.3330	0.5492
ROE-9B	2	0.6984	0.7890	0.5429	0.5616	0.9871
ROE-9B	3	0.4764	0.6246	0.4818	0.4505	0.8288
ROE-9B	4	0.4157	0.5215	0.4163	0.3644	0.6699
ROE-9B	5	0.4055	0.4461	0.3422	0.3080	0.5036
ROE-9B	7	0.6262	0.7803	0.5476	0.5707	1.0774
ROE-9B	8	0.4579	0.6151	0.4865	0.4571	0.8973
ROE-9B	9	0.4109	0.5075	0.4167	0.3637	0.7035
ROE-9B	10	0.4061	0.4386	0.3469	0.3090	0.5225
ROE-9B	12	0.6239	0.7438	0.5480	0.5723	1.1560
ROE-9B	13	0.4602	0.5894	0.4869	0.4584	0.9549
ROE-9B	14	0.4150	0.4886	0.4171	0.3645	0.7371
ROE-9B	15	0.4119	0.4238	0.3473	0.3094	0.5320
ROE-10A	2	1.0333	0.9711	0.8670	0.8655	0.9462
ROE-10A	3	0.9939	0.8073	0.8016	0.7567	0.8569
ROE-10A	4	0.8458	0.6762	0.7143	0.6646	0.7439
ROE-10A	5	0.7381	0.6021	0.6401	0.6340	0.6533
ROE-10A	7	1.0594	1.0008	0.8674	0.8654	0.9630
ROE-10A	8	0.9985	0.8215	0.7976	0.7502	0.8594
ROE-10A	9	0.8231	0.6990	0.7191	0.6668	0.7482
ROE-10A	10	0.7512	0.6203	0.6449	0.6331	0.6484
ROE-10A	12	1.1252	1.0313	0.8634	0.8586	0.9726
ROE-10A	13	1.0298	0.8548	0.7980	0.7512	0.8677
ROE-10A	14	0.8393	0.7299	0.7238	0.6708	0.7536
ROE-10A	15	0.7658	0.6445	0.6496	0.6341	0.6446
ROE-10B	2	1.0143	0.9944	0.7530	0.7996	0.7961
ROE-10B	3	0.8473	0.8074	0.6876	0.6885	0.7017
ROE-10B	4	0.6128	0.6740	0.6090	0.6002	0.5984
ROE-10B	5	0.5430	0.6079	0.5523	0.5670	0.5308
ROE-10B	7	0.9221	1.0153	0.7534	0.7996	0.8133
ROE-10B	8	0.7449	0.8232	0.6879	0.6881	0.7035
ROE-10B	9	0.5864	0.6983	0.6181	0.6068	0.5948
ROE-10B	10	0.5455	0.6227	0.5570	0.5674	0.5068
ROE-10B	12	0.9514	1.0476	0.7538	0.8011	0.8305
ROE-10B	13	0.7546	0.8463	0.6883	0.6892	0.7053
ROE-10B	14	0.5779	0.7225	0.6229	0.6114	0.5877
ROE-10B	15	0.5322	0.6419	0.5618	0.5696	0.4850

Appendix D2 Predictions of Resilient Modulus from Statistical Models for Evaluation Dataset (Continued)

Sample I.D.	Seq. No.	Experiment M_R/P_a (10^3)	Predicted M_R/P_a (10^3)			
			Stress-Based	Mult. Reg.	Polynomial	Factorial
ROE-11A	2	0.7483	0.8396	0.7555	0.7472	0.7666
ROE-11A	3	0.5406	0.6930	0.6900	0.6361	0.6948
ROE-11A	4	0.4552	0.6068	0.6290	0.5632	0.6306
ROE-11A	5	0.4122	0.5455	0.5679	0.5199	0.5689
ROE-11A	7	0.7203	0.8540	0.7602	0.7558	0.7785
ROE-11A	8	0.5086	0.6940	0.6904	0.6357	0.6954
ROE-11A	9	0.4482	0.6076	0.6293	0.5624	0.6255
ROE-11A	10	0.4131	0.5462	0.5683	0.5187	0.5582
ROE-11A	12	0.7196	0.8559	0.7606	0.7573	0.7855
ROE-11A	13	0.5042	0.6953	0.6908	0.6368	0.6960
ROE-11A	14	0.4454	0.6139	0.6341	0.5674	0.6258
ROE-11A	15	0.4112	0.5471	0.5686	0.5191	0.5475
ROE-11B	2	0.5465	0.6238	0.4669	0.5241	0.6254
ROE-11B	3	0.3727	0.4657	0.3971	0.3995	0.4743
ROE-11B	4	0.2961	0.3829	0.3317	0.3180	0.3476
ROE-11B	5	0.2633	0.3346	0.2750	0.2749	0.2495
ROE-11B	7	0.4601	0.6197	0.4673	0.5241	0.7465
ROE-11B	8	0.3186	0.4772	0.4062	0.4126	0.5863
ROE-11B	9	0.2710	0.3897	0.3408	0.3262	0.4287
ROE-11B	10	0.2518	0.3360	0.2797	0.2762	0.2946
ROE-11B	12	0.4390	0.6135	0.4677	0.5257	0.8675
ROE-11B	13	0.3032	0.4730	0.4066	0.4139	0.6803
ROE-11B	14	0.2574	0.3911	0.3455	0.3317	0.5057
ROE-11B	15	0.2425	0.3367	0.2845	0.2793	0.3437
ROE-12A	2	1.1688	0.9899	0.8866	0.8869	0.9567
ROE-12A	3	1.1238	0.8178	0.8167	0.7745	0.8545
ROE-12A	4	0.9525	0.7157	0.7513	0.7043	0.7614
ROE-12A	5	0.8232	0.6267	0.6684	0.6643	0.6474
ROE-12A	7	1.2626	1.0131	0.8869	0.8868	0.9893
ROE-12A	8	1.1894	0.8270	0.8128	0.7682	0.8746
ROE-12A	9	1.0434	0.7300	0.7517	0.7034	0.7828
ROE-12A	10	0.8758	0.6382	0.6688	0.6629	0.6620
ROE-12A	12	1.2955	1.0486	0.8873	0.8883	1.0219
ROE-12A	13	1.2443	0.8524	0.8132	0.7692	0.9011
ROE-12A	14	1.0907	0.7504	0.7521	0.7041	0.8043
ROE-12A	15	0.9077	0.6540	0.6692	0.6631	0.6766
ROE-12B	2	0.9363	1.0299	0.7713	0.7968	0.7572
ROE-12B	3	0.8530	0.8671	0.7189	0.7052	0.6804
ROE-12B	4	0.6507	0.7235	0.6447	0.6128	0.5737
ROE-12B	5	0.5785	0.6345	0.5749	0.5658	0.4755
ROE-12B	7	0.9799	1.0641	0.7760	0.8054	0.7987
ROE-12B	8	0.8970	0.8691	0.7149	0.6981	0.7056
ROE-12B	9	0.6904	0.7334	0.6451	0.6120	0.6011
ROE-12B	10	0.5963	0.6425	0.5753	0.5645	0.4988
ROE-12B	12	1.0195	1.0896	0.7764	0.8069	0.8338
ROE-12B	13	0.9264	0.8877	0.7153	0.6993	0.7371
ROE-12B	14	0.7142	0.7474	0.6455	0.6127	0.6286
ROE-12B	15	0.6083	0.6536	0.5757	0.5649	0.5222

Appendix D2 Predictions of Resilient Modulus from Statistical Models for Evaluation Dataset (Continued)

Sample I.D.	Seq. No.	Experiment M_R/P_a (10^3)	Predicted M_R/P_a (10^3)			
			Stress-Based	Mult. Reg.	Polynomial	Factorial
ROE-13A	2	0.7928	0.9970	0.8275	0.7922	0.8211
ROE-13A	3	0.6096	0.7989	0.7620	0.6811	0.6839
ROE-13A	4	0.5187	0.6775	0.6966	0.6041	0.5611
ROE-13A	5	0.4779	0.6035	0.6398	0.5649	0.4665
ROE-13A	7	0.7972	1.0624	0.8322	0.8008	0.9448
ROE-13A	8	0.5949	0.8550	0.7711	0.6935	0.7883
ROE-13A	9	0.5112	0.7114	0.7013	0.6073	0.6249
ROE-13A	10	0.4788	0.6261	0.6402	0.5637	0.4954
ROE-13A	12	0.8185	1.1375	0.8326	0.8023	1.0588
ROE-13A	13	0.6079	0.9089	0.7715	0.6947	0.8753
ROE-13A	14	0.5142	0.7593	0.7060	0.6124	0.6926
ROE-13A	15	0.4797	0.6582	0.6406	0.5641	0.5244
ROE-13B	2	0.6757	1.0633	0.7229	0.7292	0.8387
ROE-13B	3	0.4694	0.8462	0.6662	0.6251	0.6830
ROE-13B	4	0.3560	0.7048	0.6051	0.5415	0.5368
ROE-13B	5	0.2899	0.6155	0.5484	0.4905	0.4209
ROE-13B	7	0.6169	1.1279	0.7277	0.7383	0.9565
ROE-13B	8	0.4199	0.8899	0.6710	0.6319	0.7554
ROE-13B	9	0.3269	0.7368	0.6099	0.5459	0.5602
ROE-13B	10	0.2823	0.6347	0.5488	0.4895	0.3871
ROE-13B	12	0.6122	1.1944	0.7281	0.7400	1.0616
ROE-13B	13	0.4081	0.9370	0.6713	0.6332	0.8164
ROE-13B	14	0.3178	0.7719	0.6103	0.5468	0.5737
ROE-13B	15	0.2767	0.6688	0.5535	0.4931	0.3682
ROE-14A	2	0.6746	0.9361	0.7166	0.6933	0.8340
ROE-14A	3	0.4804	0.7134	0.6512	0.5754	0.6570
ROE-14A	4	0.3723	0.5992	0.5945	0.5008	0.5149
ROE-14A	5	0.3049	0.5202	0.5377	0.4517	0.3833
ROE-14A	7	0.6509	0.9839	0.7170	0.6933	0.9197
ROE-14A	8	0.4543	0.7708	0.6603	0.5888	0.7412
ROE-14A	9	0.3573	0.6333	0.5992	0.5049	0.5608
ROE-14A	10	0.3059	0.5418	0.5381	0.4507	0.3925
ROE-14A	12	0.6579	1.0609	0.7174	0.6949	1.0053
ROE-14A	13	0.4549	0.8248	0.6607	0.5901	0.8027
ROE-14A	14	0.3563	0.6733	0.5996	0.5058	0.5961
ROE-14A	15	0.3070	0.5729	0.5385	0.4512	0.4018
ROE-14B	2	0.3566	0.9907	0.6126	0.6117	0.7740
ROE-14B	3	0.2147	0.7834	0.5690	0.5233	0.6309
ROE-14B	4	0.1701	0.6436	0.5210	0.4435	0.4867
ROE-14B	5	0.1590	0.5428	0.4686	0.3774	0.3453
ROE-14B	7	0.3861	1.0017	0.6086	0.6023	0.8239
ROE-14B	8	0.2353	0.7959	0.5650	0.5151	0.6475
ROE-14B	9	0.1858	0.6554	0.5170	0.4367	0.4667
ROE-14B	10	0.1661	0.5533	0.4647	0.3721	0.2853
ROE-14B	12	0.4167	1.0611	0.6090	0.6040	0.8886
ROE-14B	13	0.2471	0.8225	0.5610	0.5086	0.6573
ROE-14B	14	0.1917	0.6773	0.5130	0.4316	0.4399
ROE-14B	15	0.1705	0.5787	0.4650	0.3729	0.2364

Appendix D2 Predictions of Resilient Modulus from Statistical Models for Evaluation Dataset (Continued)

Sample I.D.	Seq. No.	Experiment M_R/P_a (10^3)	Predicted M_R/P_a (10^3)			
			Stress-Based	Mult. Reg.	Polynomial	Factorial
ROE-15A	2	0.6809	0.8448	0.8004	0.6709	0.7701
ROE-15A	3	0.5301	0.7157	0.7394	0.5619	0.7608
ROE-15A	4	0.4450	0.6294	0.6739	0.4781	0.7522
ROE-15A	5	0.4190	0.5698	0.6085	0.4283	0.7452
ROE-15A	7	0.6849	0.8162	0.8008	0.6709	0.6383
ROE-15A	8	0.5439	0.7000	0.7441	0.5684	0.6270
ROE-15A	9	0.4638	0.6110	0.6743	0.4773	0.6146
ROE-15A	10	0.4430	0.5511	0.6045	0.4251	0.6039
ROE-15A	12	0.7175	0.7749	0.8012	0.6725	0.5065
ROE-15A	13	0.5721	0.6680	0.7445	0.5696	0.4926
ROE-15A	14	0.4797	0.5860	0.6747	0.4782	0.4770
ROE-15A	15	0.4583	0.5307	0.6049	0.4255	0.4631
ROE-15B	2	0.6099	1.0230	0.9273	0.8769	0.3519
ROE-15B	3	0.4245	0.8797	0.8531	0.7433	0.3113
ROE-15B	4	0.3612	0.8068	0.7920	0.6661	0.2842
ROE-15B	5	0.3343	0.7507	0.7266	0.6163	0.2616
ROE-15B	7	0.5417	0.9809	0.9277	0.8769	0.3397
ROE-15B	8	0.3847	0.8587	0.8622	0.7564	0.2901
ROE-15B	9	0.3449	0.7826	0.7968	0.6699	0.2471
ROE-15B	10	0.3345	0.7261	0.7270	0.6152	0.2086
ROE-15B	12	0.5305	0.9205	0.9281	0.8786	0.3275
ROE-15B	13	0.3802	0.8117	0.8626	0.7576	0.2646
ROE-15B	14	0.3428	0.7440	0.7972	0.6707	0.2083
ROE-15B	15	0.3367	0.6937	0.7273	0.6156	0.1555
ROE-16A	2	1.0459	1.1246	1.0716	1.0531	1.2326
ROE-16A	3	0.9653	0.9623	1.0018	0.9407	1.1820
ROE-16A	4	0.8460	0.8464	0.9233	0.8606	1.1146
ROE-16A	5	0.7626	0.7620	0.8404	0.8292	1.0315
ROE-16A	7	0.9937	1.1571	1.0720	1.0530	1.2398
ROE-16A	8	0.9418	0.9878	1.0022	0.9402	1.2056
ROE-16A	9	0.8535	0.8616	0.9193	0.8565	1.1537
ROE-16A	10	0.8067	0.7790	0.8408	0.8277	1.0930
ROE-16A	12	1.0604	1.1928	1.0680	1.0463	1.2462
ROE-16A	13	0.9862	1.0256	1.0026	0.9412	1.2292
ROE-16A	14	0.8779	0.8963	0.9240	0.8602	1.1988
ROE-16A	15	0.8247	0.8024	0.8411	0.8278	1.1546
ROE-16B	2	0.8104	1.1219	0.8181	0.8133	0.9164
ROE-16B	3	0.6625	0.9101	0.7526	0.7022	0.8245
ROE-16B	4	0.5288	0.7524	0.6697	0.6105	0.7109
ROE-16B	5	0.4839	0.6743	0.6086	0.5778	0.6293
ROE-16B	7	0.7875	1.1457	0.8184	0.8133	0.9153
ROE-16B	8	0.6635	0.9279	0.7530	0.7018	0.8192
ROE-16B	9	0.5396	0.7659	0.6701	0.6095	0.7005
ROE-16B	10	0.4935	0.6856	0.6090	0.5765	0.6151
ROE-16B	12	0.8148	1.1823	0.8188	0.8148	0.9141
ROE-16B	13	0.6889	0.9541	0.7534	0.7029	0.8140
ROE-16B	14	0.5512	0.7919	0.6748	0.6137	0.6965
ROE-16B	15	0.5037	0.7064	0.6137	0.5782	0.6071

Appendix D2 Predictions of Resilient Modulus from Statistical Models for Evaluation Dataset (Continued)

Sample I.D.	Seq. No.	Experiment M_R/P_a (10^3)	Predicted M_R/P_a (10^3)			
			Stress-Based	Mult. Reg.	Polynomial	Factorial
ROE-17A	2	1.0817	1.1080	0.9549	0.9036	1.1319
ROE-17A	3	0.8697	0.8911	0.8807	0.7803	1.0318
ROE-17A	4	0.6473	0.7669	0.8109	0.7042	0.9419
ROE-17A	5	0.5880	0.6946	0.7542	0.6709	0.8718
ROE-17A	7	1.0037	1.1316	0.9465	0.8867	1.1339
ROE-17A	8	0.8671	0.9448	0.8855	0.7858	1.0448
ROE-17A	9	0.6235	0.7947	0.8069	0.6998	0.9350
ROE-17A	10	0.5809	0.7188	0.7502	0.6681	0.8589
ROE-17A	12	1.0204	1.2217	0.9469	0.8882	1.1479
ROE-17A	13	0.8712	1.0120	0.8858	0.7869	1.0521
ROE-17A	14	0.6202	0.8444	0.8073	0.7004	0.9335
ROE-17A	15	0.5818	0.7603	0.7506	0.6684	0.8512
ROE-17B	2	0.5343	1.1318	0.7585	0.7374	0.9928
ROE-17B	3	0.3378	0.9151	0.7061	0.6404	0.8444
ROE-17B	4	0.2617	0.7688	0.6494	0.5599	0.7025
ROE-17B	5	0.2261	0.6820	0.6014	0.5117	0.5978
ROE-17B	7	0.5414	1.2075	0.7632	0.7465	1.0770
ROE-17B	8	0.3363	0.9682	0.7109	0.6474	0.8855
ROE-17B	9	0.2547	0.8084	0.6542	0.5646	0.6969
ROE-17B	10	0.2218	0.7072	0.6018	0.5108	0.5403
ROE-17B	12	0.5462	1.2901	0.7636	0.7482	1.1481
ROE-17B	13	0.3352	1.0280	0.7113	0.6487	0.9149
ROE-17B	14	0.2512	0.8646	0.6589	0.5710	0.6984
ROE-17B	15	0.2197	0.7436	0.6022	0.5115	0.4827
ROE-18A	2	0.5998	0.7617	0.6800	0.6387	0.8315
ROE-18A	3	0.4222	0.6310	0.6233	0.5326	0.8181
ROE-18A	4	0.3489	0.5393	0.5579	0.4419	0.7993
ROE-18A	5	0.3278	0.4780	0.4924	0.3854	0.7766
ROE-18A	7	0.5957	0.7627	0.6848	0.6480	0.7465
ROE-18A	8	0.4124	0.6292	0.6281	0.5396	0.7398
ROE-18A	9	0.3447	0.5366	0.5626	0.4463	0.7286
ROE-18A	10	0.3313	0.4718	0.4928	0.3843	0.7126
ROE-18A	12	0.6107	0.7440	0.6852	0.6497	0.6606
ROE-18A	13	0.4178	0.6153	0.6284	0.5409	0.6604
ROE-18A	14	0.3486	0.5260	0.5630	0.4472	0.6566
ROE-18A	15	0.3378	0.4634	0.4932	0.3848	0.6485
ROE-18B	2	0.5630	0.8946	0.6926	0.7975	0.6497
ROE-18B	3	0.3913	0.7491	0.6359	0.6895	0.6067
ROE-18B	4	0.3108	0.6525	0.5748	0.6017	0.5597
ROE-18B	5	0.2928	0.5825	0.5094	0.5406	0.5088
ROE-18B	7	0.5217	0.8886	0.6974	0.8070	0.6322
ROE-18B	8	0.3549	0.7414	0.6406	0.6966	0.5905
ROE-18B	9	0.2965	0.6395	0.5752	0.6011	0.5416
ROE-18B	10	0.2898	0.5716	0.5097	0.5396	0.4920
ROE-18B	12	0.5132	0.8574	0.6977	0.8087	0.6115
ROE-18B	13	0.3439	0.7180	0.6410	0.6980	0.5709
ROE-18B	14	0.2913	0.6266	0.5799	0.6074	0.5267
ROE-18B	15	0.2882	0.5569	0.5101	0.5401	0.4753

Appendix D2 Predictions of Resilient Modulus from Statistical Models for Evaluation Dataset (Continued)

Sample I.D.	Seq. No.	Experiment M_R/P_a (10^3)	Predicted M_R/P_a (10^3)			
			Stress-Based	Mult. Reg.	Polynomial	Factorial
ROE-19A	2	0.8171	0.8173	0.7964	0.8183	0.7393
ROE-19A	3	0.6922	0.6979	0.7397	0.7181	0.6840
ROE-19A	4	0.5363	0.6091	0.6743	0.6343	0.6209
ROE-19A	5	0.4960	0.5509	0.6132	0.5868	0.5627
ROE-19A	7	0.8352	0.8340	0.7968	0.8183	0.7679
ROE-19A	8	0.6639	0.7188	0.7444	0.7246	0.7157
ROE-19A	9	0.5250	0.6249	0.6790	0.6381	0.6511
ROE-19A	10	0.4978	0.5563	0.6092	0.5834	0.5829
ROE-19A	12	0.8317	0.8597	0.7972	0.8199	0.7965
ROE-19A	13	0.6591	0.7388	0.7448	0.7258	0.7431
ROE-19A	14	0.5236	0.6406	0.6794	0.6389	0.6770
ROE-19A	15	0.5001	0.5689	0.6096	0.5838	0.6073
ROE-19B	2	0.8058	0.8755	0.7423	0.8960	0.6922
ROE-19B	3	0.6155	0.7423	0.6856	0.7938	0.6336
ROE-19B	4	0.4815	0.6502	0.6245	0.7124	0.5725
ROE-19B	5	0.4323	0.5816	0.5591	0.6581	0.5092
ROE-19B	7	0.7778	0.8992	0.7471	0.9050	0.7157
ROE-19B	8	0.5774	0.7585	0.6904	0.8005	0.6531
ROE-19B	9	0.4599	0.6623	0.6293	0.7166	0.5875
ROE-19B	10	0.4262	0.5870	0.5595	0.6570	0.5151
ROE-19B	12	0.7775	0.9149	0.7475	0.9066	0.7345
ROE-19B	13	0.5688	0.7705	0.6908	0.8017	0.6680
ROE-19B	14	0.4541	0.6717	0.6297	0.7175	0.5983
ROE-19B	15	0.4242	0.5945	0.5599	0.6575	0.5210
ROE-20A	2	1.0291	1.0488	0.9652	0.9564	1.0692
ROE-20A	3	0.9551	0.8900	0.8997	0.8499	0.9940
ROE-20A	4	0.7648	0.7701	0.8212	0.7670	0.9017
ROE-20A	5	0.6755	0.6883	0.7426	0.7332	0.8069
ROE-20A	7	1.0450	1.0766	0.9655	0.9563	1.0831
ROE-20A	8	0.9574	0.9118	0.9001	0.8494	1.0113
ROE-20A	9	0.7705	0.7930	0.8259	0.7694	0.9278
ROE-20A	10	0.6882	0.6986	0.7386	0.7313	0.8269
ROE-20A	12	1.0702	1.1193	0.9659	0.9578	1.0971
ROE-20A	13	0.9677	0.9440	0.9005	0.8505	1.0285
ROE-20A	14	0.7833	0.8179	0.8263	0.7700	0.9488
ROE-20A	15	0.6975	0.7179	0.7390	0.7314	0.8522
ROE-20B	2	0.8743	1.0574	0.8089	0.8194	0.8443
ROE-20B	3	0.6994	0.8676	0.7434	0.7106	0.7583
ROE-20B	4	0.5729	0.7241	0.6605	0.6217	0.6505
ROE-20B	5	0.5222	0.6434	0.5907	0.5892	0.5607
ROE-20B	7	0.8657	1.0922	0.8136	0.8278	0.8642
ROE-20B	8	0.6787	0.8807	0.7438	0.7101	0.7706
ROE-20B	9	0.5573	0.7402	0.6653	0.6240	0.6665
ROE-20B	10	0.5202	0.6517	0.5911	0.5878	0.5692
ROE-20B	12	0.8870	1.1192	0.8140	0.8293	0.8783
ROE-20B	13	0.6810	0.8999	0.7442	0.7112	0.7829
ROE-20B	14	0.5531	0.7544	0.6657	0.6247	0.6768
ROE-20B	15	0.5193	0.6630	0.5915	0.5880	0.5776

Appendix D2 Predictions of Resilient Modulus from Statistical Models for Evaluation Dataset (Continued)

Sample I.D.	Seq. No.	Experiment M_R/P_a (10^3)	Predicted M_R/P_a (10^3)			
			Stress-Based	Mult. Reg.	Polynomial	Factorial
ROE-21A	2	0.7867	1.0855	0.9721	1.0207	1.0850
ROE-21A	3	0.6761	0.8943	0.8979	0.8974	0.9817
ROE-21A	4	0.5867	0.7673	0.8150	0.8113	0.8724
ROE-21A	5	0.5557	0.6902	0.7408	0.7807	0.7805
ROE-21A	7	0.8090	1.0984	0.9724	1.0206	1.1480
ROE-21A	8	0.6664	0.9127	0.9026	0.9029	1.0416
ROE-21A	9	0.5789	0.7750	0.8154	0.8103	0.9153
ROE-21A	10	0.5641	0.6966	0.7412	0.7792	0.8138
ROE-21A	12	0.8343	1.1180	0.9728	1.0221	1.2110
ROE-21A	13	0.6810	0.9271	0.9030	0.9040	1.0957
ROE-21A	14	0.5852	0.7856	0.8158	0.8109	0.9582
ROE-21A	15	0.5712	0.7052	0.7416	0.7794	0.8472
ROE-21B	2	1.0341	1.1517	1.0225	1.0342	0.9930
ROE-21B	3	0.9433	1.0093	0.9614	0.9337	0.9383
ROE-21B	4	0.7474	0.8756	0.8697	0.8386	0.8353
ROE-21B	5	0.6909	0.8023	0.7956	0.8106	0.7337
ROE-21B	7	0.9954	1.1558	1.0228	1.0341	1.1198
ROE-21B	8	0.9039	1.0045	0.9574	0.9272	1.0862
ROE-21B	9	0.7374	0.8782	0.8701	0.8376	1.0216
ROE-21B	10	0.6951	0.8045	0.7959	0.8091	0.9489
ROE-21B	12	1.0469	1.1618	1.0232	1.0356	1.2464
ROE-21B	13	0.9295	1.0173	0.9621	0.9344	1.2393
ROE-21B	14	0.7450	0.8869	0.8749	0.8412	1.2099
ROE-21B	15	0.7060	0.8112	0.8007	0.8097	1.1670
ROE-22A	2	0.7782	0.8440	0.7156	0.7244	0.6219
ROE-22A	3	0.5782	0.6863	0.6545	0.6197	0.5109
ROE-22A	4	0.4872	0.5874	0.5935	0.5446	0.4128
ROE-22A	5	0.4415	0.5185	0.5324	0.4992	0.3278
ROE-22A	7	0.7411	0.8821	0.7204	0.7330	0.7550
ROE-22A	8	0.5598	0.7217	0.6637	0.6324	0.6247
ROE-22A	9	0.4846	0.6009	0.5938	0.5438	0.4798
ROE-22A	10	0.4518	0.5296	0.5328	0.4981	0.3669
ROE-22A	12	0.7528	0.9176	0.7208	0.7345	0.8796
ROE-22A	13	0.5726	0.7478	0.6640	0.6337	0.7235
ROE-22A	14	0.4904	0.6203	0.5942	0.5446	0.5467
ROE-22A	15	0.4589	0.5453	0.5331	0.4985	0.4060
ROE-22B	2	0.6303	0.9561	0.6800	0.7849	0.7378
ROE-22B	3	0.4206	0.7551	0.6146	0.6670	0.5970
ROE-22B	4	0.3575	0.6495	0.5579	0.5924	0.4902
ROE-22B	5	0.3198	0.5657	0.4924	0.5381	0.3846
ROE-22B	7	0.6146	0.9739	0.6804	0.7850	0.8442
ROE-22B	8	0.4156	0.7783	0.6193	0.6735	0.6768
ROE-22B	9	0.3524	0.6599	0.5582	0.5917	0.5259
ROE-22B	10	0.3177	0.5741	0.4928	0.5370	0.3825
ROE-22B	12	0.6150	1.0013	0.6808	0.7866	0.9505
ROE-22B	13	0.4152	0.7979	0.6197	0.6747	0.7479
ROE-22B	14	0.3498	0.6749	0.5586	0.5926	0.5617
ROE-22B	15	0.3166	0.5910	0.4975	0.5401	0.3919

Appendix D2 Predictions of Resilient Modulus from Statistical Models for Evaluation Dataset (Continued)

Sample I.D.	Seq. No.	Experiment M_R/P_a (10^3)	Predicted M_R/P_a (10^3)			
			Stress-Based	Mult. Reg.	Polynomial	Factorial
ROE-23A	2	0.7199	0.8113	0.6541	0.6779	0.6905
ROE-23A	3	0.4981	0.6468	0.5930	0.5690	0.5992
ROE-23A	4	0.3980	0.5529	0.5363	0.4944	0.5202
ROE-23A	5	0.3312	0.4831	0.4752	0.4426	0.4412
ROE-23A	7	0.7035	0.8187	0.6545	0.6779	0.7241
ROE-23A	8	0.4820	0.6613	0.5977	0.5754	0.6265
ROE-23A	9	0.3835	0.5572	0.5367	0.4936	0.5275
ROE-23A	10	0.3296	0.4866	0.4756	0.4415	0.4349
ROE-23A	12	0.7188	0.8299	0.6549	0.6795	0.7578
ROE-23A	13	0.4762	0.6695	0.5981	0.5767	0.6475
ROE-23A	14	0.3828	0.5634	0.5370	0.4945	0.5349
ROE-23A	15	0.3314	0.4916	0.4760	0.4420	0.4286
ROE-23B	2	0.5167	0.6392	0.4451	0.4999	0.5753
ROE-23B	3	0.2921	0.5059	0.3972	0.4084	0.4574
ROE-23B	4	0.2243	0.4170	0.3448	0.3296	0.3400
ROE-23B	5	0.2029	0.3573	0.2924	0.2725	0.2346
ROE-23B	7	0.5133	0.6546	0.4499	0.5092	0.6832
ROE-23B	8	0.3006	0.5053	0.3975	0.4082	0.5243
ROE-23B	9	0.2269	0.4165	0.3452	0.3290	0.3773
ROE-23B	10	0.2057	0.3569	0.2928	0.2717	0.2422
ROE-23B	12	0.5291	0.6532	0.4503	0.5109	0.7798
ROE-23B	13	0.3065	0.5043	0.3979	0.4096	0.5913
ROE-23B	14	0.2313	0.4157	0.3456	0.3301	0.4146
ROE-23B	15	0.2103	0.3522	0.2888	0.2685	0.2366
ROE-24A	2	0.9450	1.0147	0.8447	0.8506	0.9133
ROE-24A	3	0.8664	0.8410	0.7836	0.7479	0.8169
ROE-24A	4	0.6957	0.7048	0.7051	0.6596	0.6971
ROE-24A	5	0.6142	0.6239	0.6352	0.6223	0.5943
ROE-24A	7	0.9763	1.0178	0.8407	0.8421	0.9446
ROE-24A	8	0.9096	0.8461	0.7796	0.7413	0.8426
ROE-24A	9	0.7337	0.7224	0.7098	0.6624	0.7293
ROE-24A	10	0.6359	0.6332	0.6356	0.6210	0.6129
ROE-24A	12	1.0270	1.0466	0.8411	0.8436	0.9829
ROE-24A	13	0.9459	0.8676	0.7800	0.7424	0.8750
ROE-24A	14	0.7667	0.7388	0.7102	0.6630	0.7551
ROE-24A	15	0.6553	0.6461	0.6360	0.6212	0.6315
ROE-24B	2	0.7886	1.0482	0.7288	0.7440	0.7665
ROE-24B	3	0.5958	0.8543	0.6721	0.6438	0.6661
ROE-24B	4	0.4590	0.7244	0.6110	0.5645	0.5639
ROE-24B	5	0.3766	0.6355	0.5500	0.5149	0.4676
ROE-24B	7	0.7899	1.0574	0.7292	0.7440	0.7939
ROE-24B	8	0.6074	0.8732	0.6769	0.6502	0.6900
ROE-24B	9	0.4574	0.7300	0.6114	0.5638	0.5664
ROE-24B	10	0.3860	0.6401	0.5503	0.5138	0.4573
ROE-24B	12	0.8258	1.0715	0.7296	0.7455	0.8213
ROE-24B	13	0.6382	0.8838	0.6773	0.6515	0.7064
ROE-24B	14	0.4670	0.7457	0.6162	0.5693	0.5779
ROE-24B	15	0.3916	0.6464	0.5507	0.5143	0.4469

Appendix D2 Predictions of Resilient Modulus from Statistical Models for Evaluation Dataset (Continued)

Sample I.D.	Seq. No.	Experiment M_R/P_a (10^3)	Predicted M_R/P_a (10^3)			
			Stress-Based	Mult. Reg.	Polynomial	Factorial
ROE-25A	2	0.8502	0.9701	0.7580	0.7552	0.7112
ROE-25A	3	0.6659	0.8015	0.7012	0.6550	0.6218
ROE-25A	4	0.5240	0.6808	0.6358	0.5711	0.5276
ROE-25A	5	0.4721	0.5991	0.5703	0.5214	0.4432
ROE-25A	7	0.8421	0.9704	0.7584	0.7551	0.7690
ROE-25A	8	0.6966	0.8018	0.7016	0.6546	0.6627
ROE-25A	9	0.5341	0.6810	0.6362	0.5704	0.5491
ROE-25A	10	0.4866	0.5993	0.5707	0.5202	0.4453
ROE-25A	12	0.8815	0.9709	0.7587	0.7567	0.8267
ROE-25A	13	0.7330	0.8123	0.7064	0.6627	0.7129
ROE-25A	14	0.5517	0.6812	0.6366	0.5712	0.5706
ROE-25A	15	0.4974	0.5995	0.5711	0.5207	0.4474
ROE-25B	2	0.5893	1.1006	0.7333	0.7890	0.9200
ROE-25B	3	0.3514	0.8859	0.6722	0.6758	0.8003
ROE-25B	4	0.2664	0.7644	0.6155	0.5973	0.6998
ROE-25B	5	0.2326	0.6854	0.5632	0.5475	0.6163
ROE-25B	7	0.5399	1.0916	0.7337	0.7891	0.9389
ROE-25B	8	0.3382	0.8906	0.6770	0.6826	0.8035
ROE-25B	9	0.2633	0.7666	0.6203	0.6018	0.6784
ROE-25B	10	0.2333	0.6807	0.5635	0.5465	0.5636
ROE-25B	12	0.5517	1.0780	0.7341	0.7907	0.9577
ROE-25B	13	0.3410	0.8807	0.6774	0.6839	0.7985
ROE-25B	14	0.2650	0.7588	0.6206	0.6027	0.6495
ROE-25B	15	0.2365	0.6744	0.5639	0.5471	0.5109
ROE-26A	2	0.8062	0.9755	0.8034	0.8263	0.8829
ROE-26A	3	0.6491	0.7985	0.7423	0.7216	0.7696
ROE-26A	4	0.5429	0.6744	0.6725	0.6382	0.6444
ROE-26A	5	0.5036	0.5953	0.6070	0.5953	0.5313
ROE-26A	7	0.8070	0.9940	0.8037	0.8263	0.9385
ROE-26A	8	0.6709	0.8227	0.7470	0.7277	0.8261
ROE-26A	9	0.5527	0.6853	0.6728	0.6374	0.6837
ROE-26A	10	0.5165	0.6043	0.6074	0.5941	0.5625
ROE-26A	12	0.8422	1.0223	0.8041	0.8278	0.9941
ROE-26A	13	0.7012	0.8438	0.7474	0.7289	0.8747
ROE-26A	14	0.5658	0.7076	0.6776	0.6423	0.7319
ROE-26A	15	0.5283	0.6168	0.6078	0.5944	0.5938
ROE-26B	2	0.6684	1.0615	0.7531	0.7856	0.7057
ROE-26B	3	0.5167	0.8562	0.6920	0.6766	0.5982
ROE-26B	4	0.4207	0.7232	0.6265	0.5928	0.4840
ROE-26B	5	0.3616	0.6387	0.5654	0.5453	0.3781
ROE-26B	7	0.6826	1.0707	0.7534	0.7856	0.7852
ROE-26B	8	0.5100	0.8744	0.6967	0.6831	0.6839
ROE-26B	9	0.4146	0.7359	0.6313	0.5966	0.5679
ROE-26B	10	0.3653	0.6432	0.5658	0.5442	0.4527
ROE-26B	12	0.6905	1.0846	0.7538	0.7872	0.8647
ROE-26B	13	0.5146	0.8847	0.6971	0.6843	0.7619
ROE-26B	14	0.4159	0.7436	0.6317	0.5975	0.6442
ROE-26B	15	0.3676	0.6493	0.5662	0.5447	0.5273

Appendix D2 Predictions of Resilient Modulus from Statistical Models for Evaluation Dataset (Continued)

Sample I.D.	Seq. No.	Experiment M_R/P_a (10^3)	Predicted M_R/P_a (10^3)			
			Stress-Based	Mult. Reg.	Polynomial	Factorial
ROE-27A	2	0.7478	0.7576	0.6529	0.6725	0.7507
ROE-27A	3	0.5415	0.5832	0.5787	0.5466	0.6434
ROE-27A	4	0.4420	0.4934	0.5133	0.4718	0.5552
ROE-27A	5	0.3872	0.4354	0.4522	0.4328	0.4785
ROE-27A	7	0.7155	0.7865	0.6576	0.6812	0.7665
ROE-27A	8	0.4940	0.6007	0.5835	0.5523	0.6448
ROE-27A	9	0.4100	0.5113	0.5224	0.4790	0.5505
ROE-27A	10	0.3711	0.4454	0.4569	0.4334	0.4554
ROE-27A	12	0.6970	0.8250	0.6624	0.6918	0.7840
ROE-27A	13	0.4726	0.6236	0.5882	0.5599	0.6479
ROE-27A	14	0.3928	0.5281	0.5271	0.4841	0.5417
ROE-27A	15	0.3579	0.4543	0.4573	0.4338	0.4269
ROE-27B	2	0.2784	0.6738	0.4761	0.5510	0.6041
ROE-27B	3	0.1934	0.5235	0.4281	0.4545	0.5145
ROE-27B	4	0.1781	0.4204	0.3714	0.3642	0.4172
ROE-27B	5	0.1784	0.3504	0.3103	0.2955	0.3231
ROE-27B	7	0.3350	0.6615	0.4721	0.5415	0.6337
ROE-27B	8	0.2241	0.5078	0.4198	0.4387	0.5169
ROE-27B	9	0.1944	0.4114	0.3630	0.3520	0.3994
ROE-27B	10	0.1898	0.3487	0.3063	0.2908	0.2913
ROE-27B	12	0.3575	0.6698	0.4725	0.5432	0.6717
ROE-27B	13	0.2354	0.5136	0.4202	0.4401	0.5348
ROE-27B	14	0.2025	0.4098	0.3591	0.3474	0.3853
ROE-27B	15	0.1988	0.3480	0.3023	0.2878	0.2562
ROE-28A	2	0.7927	0.8880	0.7949	0.7698	0.7065
ROE-28A	3	0.5779	0.7278	0.7295	0.6587	0.6042
ROE-28A	4	0.4752	0.6338	0.6684	0.5858	0.5165
ROE-28A	5	0.4346	0.5671	0.6073	0.5425	0.4362
ROE-28A	7	0.7644	0.9162	0.7997	0.7784	0.8079
ROE-28A	8	0.5496	0.7551	0.7386	0.6712	0.6957
ROE-28A	9	0.4697	0.6478	0.6731	0.5892	0.5837
ROE-28A	10	0.4335	0.5740	0.6077	0.5413	0.4803
ROE-28A	12	0.7759	0.9371	0.8000	0.7799	0.9022
ROE-28A	13	0.5578	0.7705	0.7390	0.6723	0.7740
ROE-28A	14	0.4733	0.6597	0.6735	0.5900	0.6449
ROE-28A	15	0.4392	0.5836	0.6081	0.5417	0.5244
ROE-28B	2	0.6269	0.9986	0.7489	0.7985	0.7726
ROE-28B	3	0.3911	0.8071	0.6878	0.6853	0.6602
ROE-28B	4	0.3130	0.6913	0.6268	0.6018	0.5591
ROE-28B	5	0.2880	0.6119	0.5657	0.5479	0.4692
ROE-28B	7	0.5411	1.0234	0.7537	0.8078	0.8633
ROE-28B	8	0.3578	0.8220	0.6926	0.6921	0.7260
ROE-28B	9	0.2994	0.7016	0.6315	0.6061	0.6000
ROE-28B	10	0.2817	0.6148	0.5660	0.5469	0.4775
ROE-28B	12	0.5418	1.0133	0.7497	0.8002	0.9337
ROE-28B	13	0.3538	0.8286	0.6930	0.6934	0.7842
ROE-28B	14	0.2968	0.7067	0.6319	0.6070	0.6341
ROE-28B	15	0.2825	0.6188	0.5664	0.5474	0.4857

Appendix D2 Predictions of Resilient Modulus from Statistical Models for Evaluation Dataset (Continued)

Sample I.D.	Seq. No.	Experiment M_R/P_a (10^3)	Predicted M_R/P_a (10^3)			
			Stress-Based	Mult. Reg.	Polynomial	Factorial
ROE-29A	2	0.8413	0.8337	0.6628	0.6608	0.6049
ROE-29A	3	0.6794	0.6717	0.6061	0.5586	0.5106
ROE-29A	4	0.4994	0.5590	0.5407	0.4725	0.4113
ROE-29A	5	0.4306	0.4845	0.4752	0.4205	0.3223
ROE-29A	7	0.8234	0.8350	0.6632	0.6608	0.6789
ROE-29A	8	0.6768	0.6727	0.6065	0.5583	0.5668
ROE-29A	9	0.5025	0.5598	0.5410	0.4718	0.4469
ROE-29A	10	0.4391	0.4851	0.4756	0.4194	0.3374
ROE-29A	12	0.8520	0.8369	0.6636	0.6624	0.7529
ROE-29A	13	0.6980	0.6741	0.6069	0.5595	0.6230
ROE-29A	14	0.5092	0.5608	0.5414	0.4727	0.4826
ROE-29A	15	0.4434	0.4859	0.4760	0.4198	0.3525
ROE-29B	2	0.6158	0.8655	0.5889	0.6137	0.6103
ROE-29B	3	0.3779	0.6759	0.5278	0.5026	0.4739
ROE-29B	4	0.2924	0.5707	0.4711	0.4260	0.3592
ROE-29B	5	0.2598	0.4939	0.4100	0.3722	0.2484
ROE-29B	7	0.5380	0.8755	0.5936	0.6228	0.7190
ROE-29B	8	0.3568	0.6797	0.5325	0.5092	0.5531
ROE-29B	9	0.2919	0.5657	0.4714	0.4253	0.4005
ROE-29B	10	0.2642	0.4899	0.4104	0.3711	0.2612
ROE-29B	12	0.5590	0.8621	0.5940	0.6244	0.8175
ROE-29B	13	0.3572	0.6704	0.5329	0.5105	0.6230
ROE-29B	14	0.2899	0.5587	0.4718	0.4262	0.4418
ROE-29B	15	0.2623	0.4844	0.4107	0.3716	0.2740
WOE-1A	2	0.6444	0.6578	0.6160	0.5885	0.7883
WOE-1A	3	0.5655	0.5323	0.5505	0.4774	0.7499
WOE-1A	4	0.4892	0.4474	0.4764	0.3927	0.7070
WOE-1A	5	0.4713	0.3885	0.3978	0.3508	0.6624
WOE-1A	7	0.6437	0.6462	0.6120	0.5800	0.7737
WOE-1A	8	0.5500	0.5318	0.5509	0.4770	0.7367
WOE-1A	9	0.4882	0.4432	0.4724	0.3882	0.6899
WOE-1A	10	0.4753	0.3882	0.3982	0.3494	0.6465
WOE-1A	12	0.6457	0.6562	0.6168	0.5900	0.7643
WOE-1A	13	0.5535	0.5311	0.5513	0.4781	0.7235
WOE-1A	14	0.4916	0.4426	0.4728	0.3889	0.6753
WOE-1A	15	0.4824	0.3878	0.3986	0.3496	0.6306
WOE-1B	2	0.5885	0.7190	0.5701	0.6244	0.8125
WOE-1B	3	0.5036	0.5656	0.5003	0.5023	0.7176
WOE-1B	4	0.4499	0.4681	0.4218	0.4112	0.6187
WOE-1B	5	0.4459	0.4085	0.3476	0.3703	0.5329
WOE-1B	7	0.5682	0.6972	0.5661	0.6156	0.8540
WOE-1B	8	0.4782	0.5523	0.4963	0.4955	0.7472
WOE-1B	9	0.4475	0.4632	0.4222	0.4103	0.6410
WOE-1B	10	0.4448	0.4045	0.3480	0.3690	0.5421
WOE-1B	12	0.5632	0.6843	0.5665	0.6172	0.9015
WOE-1B	13	0.4814	0.5498	0.5011	0.5030	0.7898
WOE-1B	14	0.4526	0.4564	0.4225	0.4110	0.6632
WOE-1B	15	0.4514	0.3992	0.3484	0.3692	0.5513

Appendix D2 Predictions of Resilient Modulus from Statistical Models for Evaluation Dataset (Continued)

Sample I.D.	Seq. No.	Experiment M_R/P_a (10^3)	Predicted M_R/P_a (10^3)			
			Stress-Based	Mult. Reg.	Polynomial	Factorial
WOE-2A	2	0.5888	0.5499	0.5612	0.4444	1.0733
WOE-2A	3	0.5122	0.4365	0.4914	0.3272	1.0673
WOE-2A	4	0.4569	0.3631	0.4128	0.2416	1.0459
WOE-2A	5	0.4477	0.3155	0.3343	0.2050	1.0090
WOE-2A	7	0.5880	0.5376	0.5616	0.4444	0.8953
WOE-2A	8	0.5021	0.4275	0.4917	0.3267	0.9124
WOE-2A	9	0.4609	0.3562	0.4132	0.2406	0.9170
WOE-2A	10	0.4560	0.3100	0.3347	0.2036	0.9060
WOE-2A	12	0.5964	0.5197	0.5619	0.4459	0.7174
WOE-2A	13	0.5043	0.4199	0.4965	0.3341	0.7554
WOE-2A	14	0.4610	0.3499	0.4180	0.2448	0.7868
WOE-2A	15	0.4627	0.3048	0.3394	0.2046	0.8025
WOE-2B	2	0.5390	0.5937	0.5075	0.4636	1.0038
WOE-2B	3	0.4569	0.4721	0.4421	0.3503	0.9522
WOE-2B	4	0.4123	0.3924	0.3679	0.2630	0.8870
WOE-2B	5	0.4131	0.3382	0.2894	0.2183	0.8100
WOE-2B	7	0.5283	0.5742	0.5079	0.4636	0.9225
WOE-2B	8	0.4461	0.4522	0.4381	0.3435	0.8793
WOE-2B	9	0.4166	0.3780	0.3639	0.2583	0.8264
WOE-2B	10	0.4193	0.3295	0.2897	0.2170	0.7663
WOE-2B	12	0.5369	0.5463	0.5083	0.4652	0.8412
WOE-2B	13	0.4539	0.4380	0.4428	0.3510	0.8122
WOE-2B	14	0.4262	0.3635	0.3643	0.2590	0.7700
WOE-2B	15	0.4275	0.3181	0.2901	0.2172	0.7226
WOE-3A	2	0.9412	0.8494	1.0430	1.0300	1.1547
WOE-3A	3	0.9946	0.7685	0.9601	0.9210	0.9919
WOE-3A	4	1.0037	0.7180	0.8859	0.8697	0.8286
WOE-3A	5	1.0220	0.6855	0.8248	0.8604	0.6818
WOE-3A	7	1.0247	0.8794	1.0478	1.0370	1.0702
WOE-3A	8	1.0185	0.7921	0.9649	0.9246	0.9409
WOE-3A	9	1.0266	0.7381	0.8907	0.8703	0.8078
WOE-3A	10	1.0439	0.7055	0.8340	0.8584	0.6949
WOE-3A	12	1.0618	0.9232	1.0525	1.0458	0.9821
WOE-3A	13	1.0333	0.8255	0.9696	0.9300	0.8865
WOE-3A	14	1.0394	0.7717	0.9042	0.8772	0.7965
WOE-3A	15	1.0601	0.7321	0.8431	0.8586	0.7008
WOE-3B	2	0.8698	0.9135	1.0111	1.1956	1.0836
WOE-3B	3	0.8683	0.8253	0.9325	1.0800	1.0272
WOE-3B	4	0.8503	0.7744	0.8671	1.0212	0.9540
WOE-3B	5	0.8208	0.7397	0.8104	0.9978	0.8714
WOE-3B	7	0.9067	0.9408	1.0158	1.2033	0.8118
WOE-3B	8	0.8542	0.8424	0.9329	1.0794	0.8135
WOE-3B	9	0.8425	0.7924	0.8718	1.0230	0.7904
WOE-3B	10	0.8219	0.7556	0.8151	0.9973	0.7504
WOE-3B	12	0.9319	0.9800	1.0206	1.2128	0.5335
WOE-3B	13	0.8636	0.8672	0.9333	1.0803	0.5999
WOE-3B	14	0.8519	0.8136	0.8722	1.0236	0.6212
WOE-3B	15	0.8253	0.7716	0.8111	0.9966	0.6217

Appendix D2 Predictions of Resilient Modulus from Statistical Models for Evaluation Dataset (Continued)

Sample I.D.	Seq. No.	Experiment M_R/P_a (10^3)	Predicted M_R/P_a (10^3)			
			Stress-Based	Mult. Reg.	Polynomial	Factorial
WOE-4A	2	0.6835	0.8499	0.8895	0.9058	0.8174
WOE-4A	3	0.6543	0.7408	0.8153	0.7980	0.7321
WOE-4A	4	0.6416	0.6686	0.7412	0.7339	0.6414
WOE-4A	5	0.6432	0.6159	0.6670	0.7135	0.5453
WOE-4A	7	0.6403	0.8725	0.8943	0.9134	0.8030
WOE-4A	8	0.6430	0.7573	0.8201	0.8025	0.7274
WOE-4A	9	0.6608	0.6817	0.7459	0.7354	0.6465
WOE-4A	10	0.6690	0.6267	0.6717	0.7120	0.5602
WOE-4A	12	0.6757	0.8940	0.8946	0.9148	0.7837
WOE-4A	13	0.6758	0.7737	0.8205	0.8034	0.7176
WOE-4A	14	0.6848	0.6988	0.7507	0.7386	0.6504
WOE-4A	15	0.6935	0.6436	0.6808	0.7126	0.5785
WOE-4B	2	0.5109	0.7163	0.5638	0.7300	0.6269
WOE-4B	3	0.4101	0.5786	0.4983	0.6212	0.5005
WOE-4B	4	0.3663	0.4849	0.4242	0.5390	0.3784
WOE-4B	5	0.3487	0.4258	0.3544	0.5017	0.2838
WOE-4B	7	0.4424	0.7481	0.5729	0.7470	0.8301
WOE-4B	8	0.3784	0.5902	0.5031	0.6269	0.6564
WOE-4B	9	0.3502	0.4928	0.4289	0.5418	0.4935
WOE-4B	10	0.3435	0.4317	0.3591	0.5016	0.3606
WOE-4B	12	0.4682	0.7575	0.5733	0.7486	1.0151
WOE-4B	13	0.3855	0.6043	0.5078	0.6344	0.8169
WOE-4B	14	0.3504	0.5024	0.4337	0.5463	0.6133
WOE-4B	15	0.3423	0.4356	0.3595	0.5019	0.4320
WOE-5A	2	0.7260	0.6689	0.6429	0.6687	0.6363
WOE-5A	3	0.7197	0.5391	0.5687	0.5480	0.6015
WOE-5A	4	0.6816	0.4768	0.5120	0.4852	0.5732
WOE-5A	5	0.6041	0.4138	0.4291	0.4394	0.5291
WOE-5A	7	0.7364	0.6750	0.6433	0.6687	0.6109
WOE-5A	8	0.7055	0.5554	0.5778	0.5595	0.5842
WOE-5A	9	0.6562	0.4806	0.5124	0.4843	0.5556
WOE-5A	10	0.6072	0.4195	0.4338	0.4391	0.5186
WOE-5A	12	0.7579	0.6843	0.6437	0.6702	0.5854
WOE-5A	13	0.7102	0.5622	0.5782	0.5606	0.5627
WOE-5A	14	0.6523	0.4859	0.5128	0.4851	0.5380
WOE-5A	15	0.6061	0.4208	0.4299	0.4383	0.5039
WOE-5B	2	0.6597	0.7329	0.5903	0.7501	0.5281
WOE-5B	3	0.5923	0.5956	0.5249	0.6368	0.4908
WOE-5B	4	0.4755	0.5074	0.4551	0.5534	0.4529
WOE-5B	5	0.4300	0.4447	0.3809	0.5073	0.4145
WOE-5B	7	0.6014	0.7335	0.5907	0.7501	0.5321
WOE-5B	8	0.5118	0.6031	0.5296	0.6429	0.4942
WOE-5B	9	0.4333	0.5033	0.4511	0.5487	0.4476
WOE-5B	10	0.4053	0.4450	0.3813	0.5061	0.4081
WOE-5B	12	0.5773	0.7469	0.5955	0.7605	0.5391
WOE-5B	13	0.4768	0.6037	0.5300	0.6441	0.4952
WOE-5B	14	0.4098	0.5082	0.4558	0.5533	0.4473
WOE-5B	15	0.3912	0.4453	0.3817	0.5064	0.4016

Appendix D3 Predictions of Resilient Modulus from Artificial Neural Network Models for Development Dataset

Sample I.D.	Seq. No.	Experiment M_R/P_a (10^3)	Predicted M_R/P_a (10^3)					
			LN	GRNN	RBFN	MLPN-1	MLPN-2	MLPN-3
AD-1A	2	0.6993	0.6873	0.6548	0.7201	0.6684	0.7052	0.6241
AD-1A	3	0.5898	0.6086	0.5789	0.5521	0.5264	0.5481	0.5337
AD-1A	4	0.5099	0.5299	0.5022	0.3786	0.4002	0.4026	0.4766
AD-1A	5	0.4632	0.4508	0.4856	0.4072	0.3150	0.2706	0.4339
AD-1A	7	0.6051	0.6855	0.6413	0.6555	0.6766	0.7124	0.5793
AD-1A	8	0.5227	0.6060	0.5735	0.5029	0.5341	0.5682	0.4667
AD-1A	9	0.4639	0.5278	0.5007	0.3816	0.4139	0.4365	0.4146
AD-1A	10	0.4238	0.4495	0.4795	0.4343	0.3381	0.3075	0.3857
AD-1A	12	0.5152	0.6825	0.6512	0.6936	0.6789	0.6570	0.6724
AD-1A	13	0.4400	0.6034	0.5806	0.5117	0.5393	0.5539	0.5159
AD-1A	14	0.3932	0.5251	0.5016	0.3818	0.4260	0.4367	0.4611
AD-1A	15	0.3633	0.4465	0.4752	0.4005	0.3604	0.2966	0.4398
AD-1B	2	0.5210	0.5376	0.6073	0.4409	0.4416	0.4651	0.3445
AD-1B	3	0.3891	0.4616	0.5221	0.3010	0.2933	0.3710	0.3239
AD-1B	4	0.2792	0.3842	0.4387	0.1549	0.1753	0.2882	0.3165
AD-1B	5	0.2120	0.3077	0.4173	0.1842	0.1036	0.2145	0.3093
AD-1B	7	0.3715	0.5359	0.5976	0.3486	0.4669	0.4778	0.2183
AD-1B	8	0.2821	0.4589	0.5209	0.2279	0.3185	0.3947	0.2138
AD-1B	9	0.2407	0.3816	0.4392	0.1415	0.2051	0.3144	0.2343
AD-1B	10	0.2068	0.3055	0.4128	0.2079	0.1405	0.2365	0.2562
AD-1B	12	0.2816	0.5332	0.6165	0.4187	0.4907	0.4657	0.3497
AD-1B	13	0.2156	0.4563	0.5349	0.2586	0.3444	0.3751	0.2874
AD-1B	14	0.1938	0.3794	0.4432	0.1570	0.2366	0.2816	0.3049
AD-1B	15	0.1795	0.3020	0.4084	0.1908	0.1788	0.1913	0.3353
AD-2A	2	1.3802	0.9575	0.8757	0.9915	1.0479	1.0755	1.0837
AD-2A	3	1.2780	0.8771	0.7930	0.8917	0.9191	0.9751	0.8728
AD-2A	4	1.1846	0.7976	0.7299	0.7850	0.7958	0.8528	0.7541
AD-2A	5	1.1007	0.7172	0.7228	0.8464	0.6904	0.7199	0.6761
AD-2A	7	1.3183	0.9554	0.8533	1.0152	1.0369	1.0697	1.2082
AD-2A	8	1.2641	0.8749	0.7876	0.9412	0.9002	0.9636	0.9165
AD-2A	9	1.1857	0.7950	0.7251	0.8457	0.7722	0.8430	0.7701
AD-2A	10	1.1031	0.7228	0.7116	0.8576	0.6767	0.7298	0.6881
AD-2A	12	1.1460	0.9523	0.8345	0.9695	1.0242	1.0722	1.2609
AD-2A	13	1.1696	0.8723	0.7781	0.9161	0.8806	1.0174	1.0049
AD-2A	14	1.0979	0.7989	0.7157	0.8512	0.7597	0.9345	0.8041
AD-2A	15	1.0318	0.7202	0.6855	0.8333	0.6562	0.8174	0.6888
AD-2B	2	1.0557	0.8042	0.8051	0.9785	0.9237	0.9462	0.8061
AD-2B	3	0.9149	0.7247	0.7145	0.7906	0.7401	0.8323	0.6625
AD-2B	4	0.7758	0.6486	0.6417	0.6263	0.5916	0.7181	0.5949
AD-2B	5	0.6765	0.5682	0.6375	0.6622	0.4724	0.6014	0.5545
AD-2B	7	0.8974	0.8020	0.7773	0.9996	0.9341	0.9091	0.9444
AD-2B	8	0.7897	0.7229	0.7052	0.8435	0.7435	0.7985	0.6870
AD-2B	9	0.6930	0.6473	0.6400	0.6890	0.5932	0.6962	0.5838
AD-2B	10	0.6182	0.5695	0.6290	0.6790	0.4785	0.5940	0.5382
AD-2B	12	0.7805	0.7998	0.7728	0.9806	0.9464	0.9641	0.8998
AD-2B	13	0.6771	0.7220	0.7028	0.8521	0.7507	0.8772	0.7023
AD-2B	14	0.5943	0.6447	0.6319	0.7094	0.5945	0.7723	0.5165
AD-2B	15	0.5299	0.5647	0.6236	0.6578	0.4803	0.6504	0.4767

Appendix D3 Predictions of Resilient Modulus from Artificial Neural Network Models for Development Dataset (Continued)

Sample I.D.	Seq. No.	Experiment M_R/P_a (10^3)	Predicted M_R/P_a (10^3)					
			LN	GRNN	RBFN	MLPN-1	MLPN-2	MLPN-3
AD-3A	2	0.7868	0.6976	0.6390	0.6683	0.6053	0.6273	0.5911
AD-3A	3	0.6617	0.6211	0.5702	0.5050	0.4674	0.5293	0.5492
AD-3A	4	0.5764	0.5416	0.5011	0.3467	0.3641	0.4486	0.5305
AD-3A	5	0.5293	0.4668	0.4846	0.3875	0.3216	0.3853	0.5203
AD-3A	7	0.6688	0.6963	0.5940	0.5320	0.6142	0.6178	0.6135
AD-3A	8	0.5785	0.6180	0.5454	0.4233	0.4752	0.5299	0.5464
AD-3A	9	0.5105	0.5381	0.4823	0.3157	0.3784	0.4506	0.5225
AD-3A	10	0.4593	0.4616	0.4633	0.3555	0.3435	0.3795	0.5110
AD-3A	12	0.5340	0.6958	0.5733	0.5000	0.6244	0.5675	0.6690
AD-3A	13	0.4572	0.6194	0.5271	0.4121	0.4897	0.4968	0.5545
AD-3A	14	0.4104	0.5420	0.4620	0.3224	0.3995	0.4243	0.5197
AD-3A	15	0.3780	0.4655	0.4299	0.2991	0.3680	0.3463	0.5062
AD-3B	2	0.5188	0.5760	0.5869	0.6378	0.5097	0.5838	0.5586
AD-3B	3	0.3645	0.5000	0.5116	0.4811	0.3562	0.5256	0.5219
AD-3B	4	0.2579	0.4226	0.4332	0.3323	0.2494	0.4784	0.5082
AD-3B	5	0.2046	0.3465	0.4063	0.3696	0.2031	0.4353	0.5011
AD-3B	7	0.2831	0.5747	0.5354	0.4829	0.5474	0.5787	0.5441
AD-3B	8	0.2292	0.4973	0.4859	0.3892	0.3888	0.5256	0.5038
AD-3B	9	0.2200	0.4195	0.4219	0.3041	0.2830	0.4767	0.4899
AD-3B	10	0.2121	0.3435	0.3970	0.3523	0.2407	0.4268	0.4832
AD-3B	12	0.2341	0.5721	0.5191	0.4465	0.5849	0.5455	0.5572
AD-3B	13	0.1959	0.4947	0.4680	0.3672	0.4237	0.4967	0.4965
AD-3B	14	0.1951	0.4178	0.4065	0.3005	0.3203	0.4420	0.4805
AD-3B	15	0.1973	0.3409	0.3858	0.3094	0.2810	0.3814	0.4740
AD-4A	2	1.1683	0.8428	0.7214	0.8481	0.8928	0.8758	0.8079
AD-4A	3	1.0968	0.7628	0.6497	0.7775	0.7753	0.7493	0.7140
AD-4A	4	1.0224	0.6832	0.5839	0.6260	0.6715	0.6519	0.6440
AD-4A	5	0.9561	0.6033	0.5767	0.6224	0.6068	0.5747	0.5884
AD-4A	7	1.0769	0.8410	0.7126	0.8212	0.8696	0.8391	0.8371
AD-4A	8	1.0359	0.7610	0.6459	0.7594	0.7508	0.7308	0.7158
AD-4A	9	0.9861	0.6810	0.5812	0.6457	0.6498	0.6481	0.6349
AD-4A	10	0.9346	0.6002	0.5702	0.6470	0.5926	0.5784	0.5766
AD-4A	12	0.9378	0.8379	0.7188	0.7930	0.8435	0.8101	0.8899
AD-4A	13	0.9263	0.7575	0.6519	0.7165	0.7236	0.7204	0.7356
AD-4A	14	0.8957	0.6780	0.5824	0.6277	0.6279	0.6593	0.6452
AD-4A	15	0.8588	0.5984	0.5659	0.6169	0.5803	0.5894	0.5890
AD-4B	2	0.9721	0.6906	0.6524	0.6949	0.6912	0.6628	0.6286
AD-4B	3	0.8653	0.6111	0.5689	0.5875	0.5621	0.5852	0.5500
AD-4B	4	0.7569	0.5346	0.4988	0.4235	0.4655	0.5241	0.5066
AD-4B	5	0.6810	0.4577	0.4925	0.4081	0.4110	0.4662	0.4752
AD-4B	7	0.8758	0.6884	0.6456	0.6600	0.6786	0.6436	0.6467
AD-4B	8	0.7993	0.6085	0.5684	0.5635	0.5508	0.5816	0.5268
AD-4B	9	0.7172	0.5315	0.4976	0.4364	0.4594	0.5281	0.4781
AD-4B	10	0.6446	0.4546	0.4857	0.4302	0.4139	0.4711	0.4525
AD-4B	12	0.7570	0.6858	0.6636	0.6693	0.6661	0.6449	0.7562
AD-4B	13	0.6970	0.6076	0.5844	0.5572	0.5428	0.5865	0.5693
AD-4B	14	0.6345	0.5302	0.5024	0.4385	0.4558	0.5199	0.5050
AD-4B	15	0.5768	0.4529	0.4822	0.4059	0.4180	0.4476	0.4806

Appendix D3 Predictions of Resilient Modulus from Artificial Neural Network Models for Development Dataset (Continued)

Sample I.D.	Seq. No.	Experiment M_R/P_a (10^3)	Predicted M_R/P_a (10^3)					
			LN	GRNN	RBFN	MLPN-1	MLPN-2	MLPN-3
AD-5A	2	1.6523	1.0104	0.8161	0.8766	1.0762	1.1492	1.0006
AD-5A	3	1.6068	0.9296	0.7451	0.9042	0.9785	1.0629	0.9455
AD-5A	4	1.5367	0.8505	0.6861	0.8596	0.8767	0.9451	0.8826
AD-5A	5	1.4468	0.7696	0.6719	0.9151	0.7830	0.8181	0.8142
AD-5A	7	1.5303	1.0078	0.8142	0.8898	1.0544	1.1115	1.0175
AD-5A	8	1.5342	0.9278	0.7489	0.9001	0.9517	1.0130	0.9530
AD-5A	9	1.4977	0.8478	0.6875	0.8695	0.8454	0.8966	0.8789
AD-5A	10	1.4378	0.7674	0.6716	0.9174	0.7533	0.7888	0.8080
AD-5A	12	1.3005	1.0047	0.8120	0.8698	1.0308	1.0829	1.0899
AD-5A	13	1.3368	0.9248	0.7544	0.8532	0.9225	1.0311	0.9882
AD-5A	14	1.3403	0.8452	0.6902	0.8396	0.8144	0.9744	0.8923
AD-5A	15	1.3207	0.7648	0.6667	0.8834	0.7248	0.8811	0.8171
AD-5B	2	1.1571	0.7568	0.6923	0.8022	0.8295	0.8750	0.7430
AD-5B	3	1.0523	0.6764	0.6036	0.6556	0.6799	0.7169	0.6016
AD-5B	4	0.9113	0.5995	0.5260	0.4868	0.5489	0.5709	0.5303
AD-5B	5	0.7746	0.5243	0.5167	0.4852	0.4463	0.4419	0.4854
AD-5B	7	1.0591	0.7542	0.6849	0.7948	0.8259	0.8295	0.7811
AD-5B	8	0.9875	0.6738	0.6039	0.6555	0.6744	0.6838	0.5903
AD-5B	9	0.9510	0.5964	0.5301	0.5134	0.5454	0.5615	0.5190
AD-5B	10	0.7731	0.5199	0.5168	0.5165	0.4484	0.4463	0.4839
AD-5B	12	0.9537	0.7516	0.7022	0.8116	0.8204	0.8566	0.9545
AD-5B	13	0.8986	0.6720	0.6190	0.6558	0.6689	0.7364	0.6337
AD-5B	14	0.8155	0.5947	0.5382	0.5150	0.5428	0.6004	0.5428
AD-5B	15	0.7265	0.5182	0.5202	0.4872	0.4530	0.4593	0.5079
AD-6A	2	1.4050	1.0048	0.9523	1.3243	1.1299	1.1120	1.0796
AD-6A	3	1.3646	0.9248	0.8855	1.2397	1.0681	1.1109	1.0781
AD-6A	4	1.3054	0.8457	0.8252	1.0778	0.9936	1.0592	1.0603
AD-6A	5	1.2302	0.7649	0.8065	1.0241	0.9104	0.9363	1.0180
AD-6A	7	1.3067	1.0026	0.9332	1.2785	1.1360	1.0744	1.0187
AD-6A	8	1.2925	0.9222	0.8760	1.2199	1.0717	1.0890	0.9978
AD-6A	9	1.2571	0.8431	0.8199	1.1135	0.9950	1.0721	0.9777
AD-6A	10	1.2100	0.7627	0.8013	1.0842	0.9119	0.9557	0.9427
AD-6A	12	1.2004	1.0000	0.9144	1.2380	1.1373	1.1011	1.0022
AD-6A	13	1.2104	0.9200	0.8675	1.1659	1.0706	1.0742	0.9699
AD-6A	14	1.1979	0.8400	0.8148	1.0842	0.9908	1.0255	0.9547
AD-6A	15	1.1657	0.7596	0.7950	1.0631	0.9077	0.9519	0.9325
AD-6B	2	1.1374	0.9186	0.9204	1.2118	1.0368	1.1171	1.0399
AD-6B	3	1.0610	0.8373	0.8505	1.1153	0.9527	1.0365	1.0048
AD-6B	4	0.9754	0.7582	0.7867	0.9481	0.8550	0.8820	0.9681
AD-6B	5	0.8888	0.6791	0.7642	0.8856	0.7484	0.6575	0.9113
AD-6B	7	1.0763	0.9147	0.8893	1.1182	1.0467	1.0852	1.0009
AD-6B	8	1.0293	0.8360	0.8394	1.0611	0.9630	1.0494	0.9117
AD-6B	9	0.9622	0.7552	0.7802	0.9618	0.8610	0.9012	0.8654
AD-6B	10	0.8892	0.6743	0.7579	0.9404	0.7521	0.6777	0.8195
AD-6B	12	1.0408	0.9125	0.8695	1.0809	1.0528	1.0657	0.9841
AD-6B	13	1.0139	0.8325	0.8247	1.0085	0.9648	0.9949	0.8644
AD-6B	14	0.9638	0.7534	0.7712	0.9382	0.8632	0.8922	0.8371
AD-6B	15	0.8999	0.6726	0.7484	0.9280	0.7551	0.7224	0.8205

Appendix D3 Predictions of Resilient Modulus from Artificial Neural Network Models for Development Dataset (Continued)

Sample I.D.	Seq. No.	Experiment M_R/P_a (10^3)	Predicted M_R/P_a (10^3)					
			LN	GRNN	RBFN	MLPN-1	MLPN-2	MLPN-3
AD-7A	2	1.1656	1.0327	1.0354	1.0965	1.1049	1.1417	1.1374
AD-7A	3	1.1155	0.9519	0.9832	1.1064	1.0386	1.1026	1.1206
AD-7A	4	1.0652	0.8741	0.9339	1.0349	0.9624	0.9877	1.0944
AD-7A	5	1.0201	0.7950	0.9159	1.0360	0.8814	0.7880	1.0522
AD-7A	7	1.0727	1.0301	0.9868	0.9815	1.1139	1.1010	1.1365
AD-7A	8	1.0487	0.9497	0.9537	1.0370	1.0459	1.0662	1.1018
AD-7A	9	1.0125	0.8710	0.9127	1.0278	0.9671	0.9930	1.0653
AD-7A	10	0.9764	0.7915	0.8977	1.0486	0.8859	0.8194	1.0077
AD-7A	12	0.9410	1.0275	0.9444	0.9404	1.1180	1.0987	1.1143
AD-7A	13	0.9216	0.9475	0.9195	0.9801	1.0480	1.0405	1.0336
AD-7A	14	0.8956	0.8697	0.8832	0.9855	0.9683	0.9526	0.9921
AD-7A	15	0.8737	0.7906	0.8660	0.9878	0.8880	0.8155	0.9413
AD-7B	2	1.2358	1.0031	0.9919	1.0562	1.1070	1.1257	1.1410
AD-7B	3	1.1820	0.9218	0.9377	1.1378	1.0276	1.0195	1.1143
AD-7B	4	1.1294	0.8413	0.8904	1.0932	0.9341	0.8607	1.0768
AD-7B	5	1.0744	0.7614	0.8813	1.0853	0.8356	0.6747	1.0216
AD-7B	7	1.1298	0.9991	0.9413	0.8960	1.0994	1.0833	1.1361
AD-7B	8	1.1104	0.9183	0.9071	1.0251	1.0162	1.0120	1.0772
AD-7B	9	1.0797	0.8396	0.8691	1.0596	0.9219	0.8690	1.0267
AD-7B	10	1.0440	0.7587	0.8623	1.0867	0.8225	0.6922	0.9563
AD-7B	12	1.0031	0.9961	0.8928	0.8077	1.0889	1.0420	1.1303
AD-7B	13	0.9983	0.9161	0.8697	0.9135	1.0024	0.9588	1.0060
AD-7B	14	0.9853	0.8361	0.8373	0.9733	0.9037	0.8581	0.9500
AD-7B	15	0.9622	0.7570	0.8299	1.0010	0.8072	0.7286	0.8919
AD-8A	2	1.5072	1.2626	1.3980	1.4060	1.2315	1.1537	1.2989
AD-8A	3	1.5175	1.1830	1.3729	1.4399	1.2053	1.1756	1.3357
AD-8A	4	1.5165	1.1022	1.3512	1.3937	1.1717	1.1731	1.3106
AD-8A	5	1.5062	1.0266	1.3852	1.3573	1.1324	1.1480	1.2228
AD-8A	7	1.4932	1.2612	1.3654	1.3277	1.2440	1.1498	1.2312
AD-8A	8	1.4964	1.1791	1.3555	1.4140	1.2172	1.1966	1.2714
AD-8A	9	1.4892	1.0991	1.3361	1.4572	1.1839	1.1973	1.2466
AD-8A	10	1.4733	1.0200	1.3401	1.4817	1.1420	1.1694	1.1486
AD-8A	12	1.3697	1.2564	1.3044	1.2468	1.2523	1.1460	1.1592
AD-8A	13	1.3849	1.1769	1.3003	1.3119	1.2262	1.1658	1.1984
AD-8A	14	1.3939	1.0965	1.2930	1.4034	1.1922	1.1814	1.1490
AD-8A	15	1.3909	1.0174	1.2917	1.4910	1.1493	1.1703	1.0294
AD-8B	2	1.0135	1.0071	1.0107	1.1990	0.7976	0.9849	1.0622
AD-8B	3	0.9274	0.9275	0.9201	0.9724	0.7415	0.8981	1.0989
AD-8B	4	0.8111	0.8510	0.8395	0.7287	0.6820	0.7837	1.1119
AD-8B	5	0.6998	0.7754	0.8538	0.5986	0.6155	0.6648	1.1102
AD-8B	7	0.9497	1.0040	0.9787	1.1452	0.8375	0.9944	0.9031
AD-8B	8	0.8908	0.9245	0.9283	0.9955	0.7762	0.9241	0.9248
AD-8B	9	0.8037	0.8471	0.8512	0.8358	0.7096	0.8218	0.9305
AD-8B	10	0.7077	0.7715	0.8165	0.7485	0.6359	0.7048	0.9351
AD-8B	12	0.8900	1.0014	0.9472	1.1467	0.8789	1.0511	0.8320
AD-8B	13	0.8396	0.9223	0.9066	1.0250	0.8132	0.9775	0.8829
AD-8B	14	0.7689	0.8449	0.8431	0.9279	0.7409	0.8597	0.9156
AD-8B	15	0.6897	0.7684	0.7998	0.8891	0.6595	0.7204	0.9487

Appendix D3 Predictions of Resilient Modulus from Artificial Neural Network Models for Development Dataset (Continued)

Sample I.D.	Seq. No.	Experiment M_R/P_a (10^3)	Predicted M_R/P_a (10^3)					
			LN	GRNN	RBFN	MLPN-1	MLPN-2	MLPN-3
AL-1A	2	0.7533	0.8529	0.7093	0.7879	0.8139	0.7995	0.7316
AL-1A	3	0.7673	0.7786	0.6659	0.7685	0.7148	0.7111	0.6496
AL-1A	4	0.7745	0.7087	0.6142	0.6746	0.6507	0.6562	0.6057
AL-1A	5	0.7557	0.6300	0.5885	0.6246	0.6293	0.6115	0.5730
AL-1A	7	0.7575	0.8503	0.6886	0.7443	0.7839	0.7595	0.7057
AL-1A	8	0.7585	0.7760	0.6536	0.7237	0.6858	0.7006	0.6203
AL-1A	9	0.7669	0.7104	0.6118	0.6735	0.6290	0.6580	0.5827
AL-1A	10	0.7631	0.6317	0.5839	0.6448	0.6108	0.6161	0.5549
AL-1A	12	0.8065	0.8476	0.6852	0.6920	0.7552	0.7494	0.7270
AL-1A	13	0.7893	0.7733	0.6514	0.6560	0.6592	0.6771	0.6204
AL-1A	14	0.7840	0.7078	0.6097	0.6418	0.6078	0.6382	0.5774
AL-1A	15	0.7784	0.6291	0.5802	0.6543	0.5957	0.6114	0.5490
AL-1B	2	0.5824	0.6601	0.6457	0.6174	0.6356	0.6087	0.5848
AL-1B	3	0.5365	0.5858	0.5998	0.5607	0.5275	0.5570	0.5421
AL-1B	4	0.4701	0.5159	0.5365	0.4616	0.4669	0.5120	0.5249
AL-1B	5	0.4349	0.4416	0.5061	0.4179	0.4571	0.4629	0.5142
AL-1B	7	0.5582	0.6575	0.6311	0.6206	0.6298	0.6053	0.5771
AL-1B	8	0.4879	0.5876	0.5978	0.5439	0.5270	0.5628	0.5304
AL-1B	9	0.4448	0.5176	0.5422	0.4610	0.4668	0.5193	0.5144
AL-1B	10	0.4285	0.4433	0.5065	0.4254	0.4583	0.4679	0.5059
AL-1B	12	0.5685	0.6549	0.6369	0.6635	0.6281	0.5915	0.5843
AL-1B	13	0.4826	0.5849	0.6050	0.5531	0.5252	0.5518	0.5289
AL-1B	14	0.4379	0.5150	0.5465	0.4722	0.4680	0.4994	0.5106
AL-1B	15	0.4239	0.4407	0.5087	0.4375	0.4638	0.4355	0.5020
AL-2A	2	0.7311	0.7963	0.6622	0.6348	0.6991	0.6877	0.6728
AL-2A	3	0.7016	0.7089	0.6074	0.5856	0.5878	0.6267	0.5866
AL-2A	4	0.6570	0.6346	0.5565	0.5013	0.5456	0.5883	0.5577
AL-2A	5	0.6177	0.5603	0.5430	0.5153	0.5580	0.5520	0.5408
AL-2A	7	0.7072	0.7894	0.6344	0.5680	0.6712	0.6726	0.6582
AL-2A	8	0.6460	0.7107	0.5981	0.5224	0.5717	0.6258	0.5623
AL-2A	9	0.6192	0.6364	0.5541	0.4662	0.5300	0.5886	0.5347
AL-2A	10	0.6114	0.5577	0.5377	0.4833	0.5433	0.5482	0.5208
AL-2A	12	0.7187	0.7911	0.6297	0.5235	0.6616	0.6553	0.6888
AL-2A	13	0.6484	0.7124	0.5966	0.4684	0.5605	0.6218	0.5568
AL-2A	14	0.6200	0.6381	0.5527	0.4493	0.5199	0.5862	0.5273
AL-2A	15	0.6161	0.5551	0.5347	0.4844	0.5344	0.5326	0.5144
AL-2B	2	0.6083	0.7115	0.6307	0.5514	0.6472	0.6311	0.5989
AL-2B	3	0.5381	0.6329	0.5832	0.4957	0.5348	0.5929	0.5441
AL-2B	4	0.4662	0.5629	0.5259	0.4052	0.4793	0.5645	0.5269
AL-2B	5	0.4339	0.4886	0.5036	0.3778	0.4761	0.5347	0.5170
AL-2B	7	0.5238	0.7089	0.6054	0.5297	0.6445	0.6198	0.6129
AL-2B	8	0.4481	0.6390	0.5774	0.4594	0.5392	0.5913	0.5391
AL-2B	9	0.4181	0.5647	0.5261	0.3717	0.4756	0.5621	0.5178
AL-2B	10	0.4167	0.4860	0.4987	0.3353	0.4718	0.5284	0.5087
AL-2B	12	0.5165	0.7106	0.6020	0.5496	0.6563	0.6252	0.6194
AL-2B	13	0.4317	0.6407	0.5783	0.4563	0.5450	0.5910	0.5380
AL-2B	14	0.4045	0.5664	0.5261	0.3831	0.4779	0.5518	0.5143
AL-2B	15	0.4089	0.4921	0.4960	0.3426	0.4708	0.5106	0.5059

Appendix D3 Predictions of Resilient Modulus from Artificial Neural Network Models for Development Dataset (Continued)

Sample I.D.	Seq. No.	Experiment M_R/P_a (10^3)	Predicted M_R/P_a (10^3)					
			LN	GRNN	RBFN	MLPN-1	MLPN-2	MLPN-3
AL-3A	2	0.7262	0.7483	0.7081	0.6828	0.7116	0.6988	0.6621
AL-3A	3	0.6781	0.6609	0.6401	0.6146	0.5993	0.6397	0.5766
AL-3A	4	0.6271	0.5866	0.5779	0.4786	0.5384	0.6014	0.5257
AL-3A	5	0.5815	0.5123	0.5579	0.4438	0.5266	0.5621	0.4852
AL-3A	7	0.6931	0.7413	0.6988	0.6926	0.6767	0.6774	0.6569
AL-3A	8	0.6271	0.6670	0.6431	0.5848	0.5840	0.6399	0.5684
AL-3A	9	0.5974	0.5884	0.5755	0.4460	0.5234	0.6079	0.5132
AL-3A	10	0.5844	0.5097	0.5495	0.4117	0.5177	0.5707	0.4776
AL-3A	12	0.7186	0.7431	0.7047	0.7820	0.6553	0.6522	0.7129
AL-3A	13	0.6329	0.6688	0.6546	0.6198	0.5652	0.6309	0.6016
AL-3A	14	0.5994	0.5901	0.5797	0.4680	0.5099	0.6145	0.5424
AL-3A	15	0.5875	0.5114	0.5435	0.4077	0.5097	0.5746	0.5105
AL-3B	2	0.5747	0.7117	0.6827	0.6473	0.6505	0.6480	0.6191
AL-3B	3	0.4698	0.6418	0.6294	0.6100	0.5604	0.6049	0.5493
AL-3B	4	0.3900	0.5763	0.5661	0.4973	0.4982	0.5678	0.5020
AL-3B	5	0.3522	0.5063	0.5297	0.3908	0.4686	0.5257	0.4613
AL-3B	7	0.4896	0.7135	0.6784	0.6766	0.6307	0.6406	0.6301
AL-3B	8	0.3913	0.6479	0.6340	0.5858	0.5476	0.6108	0.5358
AL-3B	9	0.3500	0.5824	0.5700	0.4671	0.4871	0.5809	0.4807
AL-3B	10	0.3380	0.5081	0.5225	0.3531	0.4596	0.5399	0.4415
AL-3B	12	0.4862	0.7152	0.6893	0.7941	0.6125	0.6303	0.7195
AL-3B	13	0.3797	0.6540	0.6544	0.6540	0.5362	0.6163	0.5995
AL-3B	14	0.3386	0.5841	0.5820	0.5030	0.4744	0.5843	0.5291
AL-3B	15	0.3309	0.5098	0.5226	0.3721	0.4521	0.5353	0.4919
AL-4A	2	0.7220	0.9032	0.7989	0.9415	0.9262	0.8968	0.9159
AL-4A	3	0.7276	0.8202	0.7385	0.8820	0.8211	0.7838	0.8094
AL-4A	4	0.7128	0.7503	0.6840	0.7439	0.7501	0.7134	0.7292
AL-4A	5	0.6805	0.6716	0.6566	0.6828	0.7114	0.6646	0.6501
AL-4A	7	0.7315	0.9050	0.7952	0.9378	0.9012	0.8311	0.8892
AL-4A	8	0.7017	0.8263	0.7375	0.8606	0.7999	0.7498	0.7850
AL-4A	9	0.6917	0.7520	0.6808	0.7375	0.7255	0.7024	0.7029
AL-4A	10	0.6866	0.6733	0.6524	0.6772	0.6906	0.6648	0.6314
AL-4A	12	0.7510	0.8980	0.7874	0.9357	0.8640	0.8620	0.8841
AL-4A	13	0.7113	0.8237	0.7388	0.8319	0.7686	0.7730	0.7787
AL-4A	14	0.6945	0.7494	0.6792	0.7313	0.6989	0.7040	0.6995
AL-4A	15	0.6904	0.6707	0.6456	0.6872	0.6706	0.6614	0.6363
AL-4B	2	0.7267	0.9342	0.7914	0.7623	0.8235	0.8233	0.8692
AL-4B	3	0.7240	0.8468	0.7436	0.8021	0.7046	0.7238	0.7801
AL-4B	4	0.6937	0.7725	0.7007	0.7133	0.6246	0.6740	0.7087
AL-4B	5	0.6676	0.7026	0.6844	0.6632	0.5869	0.6447	0.6471
AL-4B	7	0.7312	0.9272	0.7795	0.7637	0.7836	0.7528	0.8671
AL-4B	8	0.6990	0.8486	0.7369	0.7371	0.6774	0.6952	0.7760
AL-4B	9	0.6799	0.7743	0.6918	0.6466	0.6003	0.6628	0.7009
AL-4B	10	0.6599	0.7000	0.6721	0.5864	0.5665	0.6403	0.6372
AL-4B	12	0.7487	0.9246	0.7686	0.7997	0.7507	0.7478	0.8863
AL-4B	13	0.7019	0.8460	0.7338	0.7245	0.6464	0.6977	0.7866
AL-4B	14	0.6790	0.7760	0.6898	0.6495	0.5781	0.6797	0.7129
AL-4B	15	0.6634	0.6974	0.6620	0.5937	0.5494	0.6528	0.6498

Appendix D3 Predictions of Resilient Modulus from Artificial Neural Network Models for Development Dataset (Continued)

Sample I.D.	Seq. No.	Experiment M_R/P_a (10^3)	Predicted M_R/P_a (10^3)					
			LN	GRNN	RBFN	MLPN-1	MLPN-2	MLPN-3
AL-5A	2	0.4475	0.7968	0.6927	0.8153	0.8492	0.8412	0.7733
AL-5A	3	0.3684	0.7268	0.6417	0.7430	0.7294	0.7178	0.6682
AL-5A	4	0.3280	0.6569	0.5655	0.5913	0.6174	0.6088	0.6066
AL-5A	5	0.3052	0.5957	0.5261	0.4791	0.5357	0.5268	0.5697
AL-5A	7	0.4385	0.7941	0.6796	0.7686	0.8378	0.8205	0.8377
AL-5A	8	0.3686	0.7286	0.6381	0.7077	0.7240	0.7129	0.6836
AL-5A	9	0.3363	0.6543	0.5639	0.5958	0.6069	0.6105	0.5944
AL-5A	10	0.3178	0.5887	0.5229	0.5120	0.5258	0.5303	0.5497
AL-5A	12	0.4870	0.7915	0.6904	0.7513	0.8246	0.7748	0.9615
AL-5A	13	0.3955	0.7259	0.6485	0.6680	0.7097	0.6985	0.7316
AL-5A	14	0.3526	0.6560	0.5735	0.5786	0.6015	0.6226	0.6111
AL-5A	15	0.3322	0.5861	0.5222	0.4990	0.5206	0.5349	0.5546
AL-5B	2	0.4146	0.7721	0.6740	0.7645	0.8106	0.7803	0.7540
AL-5B	3	0.3102	0.7109	0.6262	0.7156	0.7033	0.6884	0.6580
AL-5B	4	0.2634	0.6497	0.5575	0.5972	0.6044	0.6099	0.5998
AL-5B	5	0.2393	0.5885	0.5112	0.4726	0.5203	0.5434	0.5598
AL-5B	7	0.3837	0.7738	0.6629	0.7095	0.8052	0.7588	0.8363
AL-5B	8	0.2991	0.7127	0.6227	0.6664	0.6966	0.6766	0.6695
AL-5B	9	0.2636	0.6471	0.5551	0.5815	0.5922	0.6050	0.5789
AL-5B	10	0.2450	0.5859	0.5091	0.4930	0.5126	0.5458	0.5312
AL-5B	12	0.3994	0.7712	0.6752	0.6937	0.7912	0.7349	0.9898
AL-5B	13	0.3035	0.7100	0.6349	0.6257	0.6819	0.6773	0.7335
AL-5B	14	0.2606	0.6488	0.5672	0.5569	0.5859	0.6198	0.6075
AL-5B	15	0.2433	0.5833	0.5096	0.4770	0.5050	0.5500	0.5439
AL-6A	2	0.4953	0.7386	0.6723	0.8445	0.8243	0.9211	0.7752
AL-6A	3	0.4124	0.6687	0.6016	0.6487	0.7156	0.8062	0.6671
AL-6A	4	0.3594	0.5900	0.5295	0.4595	0.5906	0.6606	0.5490
AL-6A	5	0.3312	0.5157	0.5126	0.4860	0.4895	0.5188	0.4446
AL-6A	7	0.4583	0.7448	0.6735	0.8827	0.8443	0.9460	0.7492
AL-6A	8	0.3801	0.6705	0.6066	0.6598	0.7282	0.8307	0.6585
AL-6A	9	0.3488	0.5918	0.5346	0.4763	0.6042	0.6873	0.5732
AL-6A	10	0.3396	0.5131	0.5123	0.5012	0.5026	0.5519	0.4945
AL-6A	12	0.4814	0.7421	0.6815	0.9899	0.8460	0.8995	0.8249
AL-6A	13	0.3960	0.6678	0.6171	0.7304	0.7290	0.7940	0.7410
AL-6A	14	0.3576	0.5892	0.5418	0.5204	0.6078	0.6983	0.6770
AL-6A	15	0.3464	0.5105	0.5159	0.5004	0.5139	0.5869	0.6225
AL-6B	2	0.4463	0.6420	0.6306	0.6046	0.6716	0.7124	0.4847
AL-6B	3	0.3455	0.5720	0.5521	0.4306	0.5456	0.5841	0.3890
AL-6B	4	0.2990	0.4978	0.4774	0.2703	0.4188	0.4490	0.3043
AL-6B	5	0.2658	0.4278	0.4571	0.2876	0.3210	0.3243	0.2378
AL-6B	7	0.3791	0.6481	0.6311	0.6107	0.6918	0.7229	0.4915
AL-6B	8	0.3109	0.5738	0.5594	0.4124	0.5587	0.5997	0.4107
AL-6B	9	0.2813	0.4995	0.4835	0.2634	0.4354	0.4875	0.3510
AL-6B	10	0.2627	0.4252	0.4566	0.2870	0.3386	0.3701	0.3017
AL-6B	12	0.3927	0.6455	0.6434	0.7370	0.6922	0.6997	0.6466
AL-6B	13	0.3141	0.5755	0.5777	0.5072	0.5685	0.6192	0.5649
AL-6B	14	0.2808	0.5012	0.4943	0.3219	0.4494	0.5109	0.5131
AL-6B	15	0.2639	0.4269	0.4581	0.2898	0.3593	0.3786	0.4745

Appendix D3 Predictions of Resilient Modulus from Artificial Neural Network Models for Development Dataset (Continued)

Sample I.D.	Seq. No.	Experiment M_R/P_a (10^3)	Predicted M_R/P_a (10^3)					
			LN	GRNN	RBFN	MLPN-1	MLPN-2	MLPN-3
AL-7A	2	0.6214	0.5174	0.6132	0.5784	0.4789	0.4973	0.5716
AL-7A	3	0.5249	0.4431	0.5643	0.5608	0.4072	0.4214	0.5362
AL-7A	4	0.4678	0.3688	0.4959	0.5270	0.3890	0.3525	0.5174
AL-7A	5	0.4434	0.2945	0.4657	0.5640	0.4091	0.2883	0.5040
AL-7A	7	0.5915	0.5147	0.6032	0.5557	0.4831	0.5149	0.5395
AL-7A	8	0.4835	0.4448	0.5650	0.4986	0.4182	0.4497	0.5119
AL-7A	9	0.4438	0.3705	0.5014	0.4839	0.4030	0.3795	0.4991
AL-7A	10	0.4407	0.2918	0.4637	0.5640	0.4248	0.3049	0.4912
AL-7A	12	0.5888	0.5165	0.6146	0.6670	0.4949	0.5081	0.5288
AL-7A	13	0.4788	0.4466	0.5796	0.5370	0.4306	0.4421	0.5044
AL-7A	14	0.4444	0.3679	0.5064	0.4815	0.4184	0.3553	0.4938
AL-7A	15	0.4431	0.2892	0.4639	0.5398	0.4405	0.2679	0.4887
AL-7B	2	0.4913	0.5994	0.6110	0.4008	0.4913	0.5171	0.5404
AL-7B	3	0.4008	0.5339	0.5646	0.3730	0.4361	0.4741	0.5198
AL-7B	4	0.3698	0.4596	0.5027	0.2933	0.4158	0.4242	0.5047
AL-7B	5	0.3749	0.3765	0.4814	0.2908	0.4501	0.3661	0.4911
AL-7B	7	0.4636	0.6012	0.6000	0.4031	0.4870	0.5349	0.5364
AL-7B	8	0.3818	0.5356	0.5626	0.3298	0.4322	0.4937	0.5127
AL-7B	9	0.3601	0.4569	0.4996	0.2460	0.4143	0.4376	0.4970
AL-7B	10	0.3687	0.3739	0.4717	0.2549	0.4515	0.3727	0.4862
AL-7B	12	0.4610	0.6029	0.6075	0.5182	0.4863	0.5289	0.5432
AL-7B	13	0.3786	0.5330	0.5695	0.3845	0.4289	0.4753	0.5158
AL-7B	14	0.3586	0.4543	0.5008	0.2815	0.4161	0.4084	0.5003
AL-7B	15	0.3720	0.3713	0.4668	0.2704	0.4553	0.3350	0.4918
AL-8A	2	0.7228	0.8951	0.7893	1.0809	1.0000	0.9973	0.9350
AL-8A	3	0.6909	0.7989	0.7166	0.9763	0.8798	0.8571	0.8060
AL-8A	4	0.6533	0.7290	0.6522	0.8151	0.7992	0.7562	0.7248
AL-8A	5	0.6049	0.6547	0.6211	0.7363	0.7428	0.6773	0.6492
AL-8A	7	0.7099	0.8793	0.7843	1.0750	0.9625	0.9471	0.9038
AL-8A	8	0.6693	0.8007	0.7170	0.9727	0.8614	0.8165	0.7877
AL-8A	9	0.6339	0.7307	0.6531	0.8436	0.7815	0.7473	0.7046
AL-8A	10	0.6096	0.6521	0.6183	0.7764	0.7265	0.6845	0.6285
AL-8A	12	0.7345	0.8767	0.7836	1.0665	0.9387	0.9244	0.9153
AL-8A	13	0.6764	0.7980	0.7234	0.9391	0.8359	0.8201	0.7867
AL-8A	14	0.6395	0.7281	0.6561	0.8286	0.7587	0.7401	0.7053
AL-8A	15	0.6162	0.6538	0.6167	0.7691	0.7119	0.6756	0.6412
AL-8B	2	0.6919	0.9162	0.7855	0.9006	0.9669	0.9452	0.9131
AL-8B	3	0.6819	0.8244	0.7196	0.8749	0.8454	0.8061	0.8077
AL-8B	4	0.6552	0.7501	0.6562	0.7380	0.7551	0.7172	0.7286
AL-8B	5	0.6163	0.6758	0.6298	0.6651	0.6960	0.6585	0.6566
AL-8B	7	0.7134	0.9048	0.7765	0.9047	0.9272	0.8592	0.9098
AL-8B	8	0.6667	0.8261	0.7173	0.8490	0.8204	0.7728	0.8032
AL-8B	9	0.6399	0.7518	0.6545	0.7370	0.7309	0.7053	0.7178
AL-8B	10	0.6197	0.6732	0.6249	0.6692	0.6736	0.6549	0.6422
AL-8B	12	0.7287	0.9022	0.7731	0.9064	0.8979	0.8666	0.9296
AL-8B	13	0.6724	0.8235	0.7214	0.8133	0.7895	0.7659	0.8103
AL-8B	14	0.6436	0.7492	0.6555	0.7190	0.7029	0.6942	0.7236
AL-8B	15	0.6252	0.6749	0.6210	0.6619	0.6544	0.6571	0.6585

Appendix D3 Predictions of Resilient Modulus from Artificial Neural Network Models for Development Dataset (Continued)

Sample I.D.	Seq. No.	Experiment M_R/P_a (10^3)	Predicted M_R/P_a (10^3)					
			LN	GRNN	RBFN	MLPN-1	MLPN-2	MLPN-3
AL-9A	2	0.9481	1.1542	0.8586	1.0956	1.0031	0.9888	1.0552
AL-9A	3	0.8129	1.1018	0.8232	0.9280	0.9744	0.8959	1.0460
AL-9A	4	0.8087	1.0362	0.7885	0.7638	0.9365	0.8362	1.0626
AL-9A	5	0.7969	0.9619	0.7604	0.7178	0.8922	0.8106	1.0914
AL-9A	7	1.0662	1.1778	0.9561	1.2067	1.0569	0.9349	1.1122
AL-9A	8	1.0067	1.1210	0.8940	0.9871	1.0271	0.8360	1.0508
AL-9A	9	0.8785	1.0336	0.8198	0.7388	0.9768	0.7814	1.0335
AL-9A	10	0.8495	0.9549	0.7883	0.6997	0.9290	0.8011	1.0461
AL-9A	12	1.1421	1.1796	1.0199	1.2882	1.0956	0.7926	1.1586
AL-9A	13	1.0641	1.1184	0.9541	1.0216	1.0643	0.8030	1.0250
AL-9A	14	0.9260	1.0310	0.8566	0.7468	1.0144	0.8451	0.9622
AL-9A	15	0.8942	0.9523	0.8146	0.6922	0.9666	0.8835	0.9720
AL-9B	2	0.7083	1.1888	0.8406	0.9706	1.1727	0.8107	1.0479
AL-9B	3	0.7226	1.1014	0.7938	0.7936	1.1356	0.8542	1.0484
AL-9B	4	0.6772	1.0271	0.7638	0.7331	1.0984	0.8989	1.0733
AL-9B	5	0.6642	0.9528	0.7410	0.8534	1.0587	0.9478	1.0932
AL-9B	7	0.7426	1.1818	0.8987	0.9465	1.1916	0.7884	1.0532
AL-9B	8	0.7085	1.1031	0.8269	0.7666	1.1592	0.8463	1.0350
AL-9B	9	0.7045	1.0288	0.7895	0.7072	1.1231	0.9277	1.0478
AL-9B	10	0.6993	0.9502	0.7647	0.8380	1.0820	1.0120	1.0592
AL-9B	12	0.7788	1.1792	0.9364	0.9674	1.2080	0.9154	1.0369
AL-9B	13	0.7517	1.1005	0.8665	0.7543	1.1763	0.9652	0.9803
AL-9B	14	0.7363	1.0262	0.8172	0.6869	1.1406	0.9974	0.9903
AL-9B	15	0.7227	0.9519	0.7908	0.7969	1.1025	1.0200	1.0078
AL-10A	2	0.5781	0.7077	0.6572	0.7796	0.6642	0.6341	0.6623
AL-10A	3	0.4905	0.6290	0.6138	0.7290	0.5579	0.5715	0.5862
AL-10A	4	0.4417	0.5547	0.5551	0.6318	0.5086	0.5191	0.5558
AL-10A	5	0.4059	0.4804	0.5333	0.6035	0.5124	0.4659	0.5383
AL-10A	7	0.5093	0.7007	0.6338	0.7084	0.6441	0.6303	0.6295
AL-10A	8	0.4387	0.6308	0.6052	0.6615	0.5513	0.5808	0.5540
AL-10A	9	0.4157	0.5565	0.5559	0.6064	0.5038	0.5276	0.5277
AL-10A	10	0.4075	0.4822	0.5300	0.6034	0.5084	0.4695	0.5156
AL-10A	12	0.5307	0.7024	0.6338	0.6733	0.6416	0.5915	0.6365
AL-10A	13	0.4489	0.6325	0.6082	0.6006	0.5481	0.5539	0.5417
AL-10A	14	0.4211	0.5582	0.5576	0.5671	0.5024	0.5060	0.5162
AL-10A	15	0.4151	0.4795	0.5290	0.5845	0.5089	0.4367	0.5061
AL-10B	2	0.5063	0.6665	0.6305	0.5586	0.6312	0.5892	0.5902
AL-10B	3	0.4099	0.5965	0.5951	0.5103	0.5284	0.5487	0.5429
AL-10B	4	0.3402	0.5354	0.5411	0.4296	0.4719	0.5166	0.5265
AL-10B	5	0.3035	0.4742	0.5044	0.3591	0.4533	0.4846	0.5172
AL-10B	7	0.4209	0.6682	0.6088	0.5413	0.6379	0.5892	0.5994
AL-10B	8	0.3331	0.6114	0.5929	0.4792	0.5478	0.5589	0.5397
AL-10B	9	0.3011	0.5415	0.5453	0.4023	0.4756	0.5221	0.5167
AL-10B	10	0.2904	0.4759	0.5046	0.3403	0.4535	0.4852	0.5080
AL-10B	12	0.4102	0.6700	0.6081	0.5807	0.6506	0.5786	0.5934
AL-10B	13	0.3192	0.6131	0.5965	0.4835	0.5561	0.5474	0.5364
AL-10B	14	0.2882	0.5432	0.5488	0.4042	0.4811	0.5019	0.5121
AL-10B	15	0.2811	0.4777	0.5050	0.3511	0.4583	0.4552	0.5038

Appendix D3 Predictions of Resilient Modulus from Artificial Neural Network Models for Development Dataset (Continued)

Sample I.D.	Seq. No.	Experiment M_R/P_a (10^3)	Predicted M_R/P_a (10^3)					
			LN	GRNN	RBFN	MLPN-1	MLPN-2	MLPN-3
CH-1A	2	1.0869	0.7893	0.8004	0.9306	0.7903	0.7553	0.7896
CH-1A	3	0.8549	0.7259	0.7277	0.7980	0.6853	0.7098	0.6750
CH-1A	4	0.7246	0.6574	0.6527	0.6898	0.6263	0.6734	0.6143
CH-1A	5	0.6723	0.5693	0.6215	0.7571	0.6391	0.6379	0.5775
CH-1A	7	1.0286	0.7835	0.7903	0.8767	0.7797	0.7456	0.8602
CH-1A	8	0.8480	0.7220	0.7321	0.7573	0.6716	0.7061	0.7057
CH-1A	9	0.7483	0.6548	0.6641	0.6385	0.6086	0.6710	0.6109
CH-1A	10	0.6841	0.5660	0.6278	0.6433	0.6138	0.6335	0.5601
CH-1A	12	1.0573	0.7821	0.8056	0.8400	0.7896	0.7715	0.8983
CH-1A	13	0.8470	0.7225	0.7481	0.7581	0.6758	0.7414	0.7290
CH-1A	14	0.7433	0.6534	0.6736	0.6590	0.6038	0.7079	0.5855
CH-1A	15	0.6861	0.5634	0.6253	0.6165	0.6002	0.6591	0.5287
CH-1B	2	1.6871	0.5180	0.8596	1.0726	1.1896	0.6725	0.8511
CH-1B	3	1.1224	0.4679	0.7773	0.9328	1.0094	0.6513	0.7410
CH-1B	4	0.8657	0.3849	0.6346	0.7961	0.8023	0.6229	0.6196
CH-1B	5	0.7957	0.3018	0.6104	0.9210	0.7170	0.5977	0.5645
CH-1B	7	1.5202	0.5046	0.8725	1.0793	1.2354	0.6537	0.8979
CH-1B	8	1.1589	0.4456	0.7854	0.9283	1.0201	0.6337	0.7784
CH-1B	9	0.9970	0.3899	0.6891	0.8231	0.8708	0.6165	0.6628
CH-1B	10	0.8470	0.2948	0.6269	0.8827	0.7443	0.5874	0.5631
CH-1B	12	1.6426	0.5032	0.9306	1.1258	1.3413	0.6815	0.9029
CH-1B	13	1.2231	0.4392	0.8283	0.9911	1.0915	0.6505	0.8118
CH-1B	14	1.0839	0.3929	0.7427	0.9000	0.9542	0.6287	0.6899
CH-1B	15	0.9082	0.2903	0.6417	0.8604	0.7856	0.5824	0.5440
CH-2A	2	0.7354	0.7546	0.7120	0.7646	0.8501	0.9514	0.9034
CH-2A	3	0.6022	0.6919	0.6290	0.6143	0.7462	0.8044	0.7128
CH-2A	4	0.4847	0.6184	0.5294	0.4245	0.6176	0.5952	0.5683
CH-2A	5	0.4028	0.5448	0.4936	0.3589	0.4889	0.3827	0.4798
CH-2A	7	0.7808	0.7463	0.7151	0.7119	0.8497	0.9192	0.8731
CH-2A	8	0.6466	0.6905	0.6494	0.5767	0.7550	0.7784	0.6975
CH-2A	9	0.5094	0.6164	0.5451	0.4120	0.6246	0.5796	0.5744
CH-2A	10	0.4195	0.5422	0.4997	0.3649	0.4969	0.3881	0.5295
CH-2A	12	0.8223	0.7456	0.7417	0.7789	0.8569	0.9518	0.9441
CH-2A	13	0.6644	0.6892	0.6782	0.6209	0.7593	0.8344	0.7456
CH-2A	14	0.5183	0.6163	0.5681	0.4508	0.6311	0.6456	0.6562
CH-2A	15	0.4245	0.5408	0.5074	0.3862	0.5044	0.4327	0.6464
CH-2B	2	0.8421	0.7203	0.6973	0.8959	0.8330	0.8544	0.8553
CH-2B	3	0.7256	0.6537	0.6009	0.7678	0.7185	0.7242	0.6724
CH-2B	4	0.6170	0.5929	0.5287	0.6372	0.6147	0.6045	0.5637
CH-2B	5	0.5380	0.5098	0.5025	0.5953	0.4828	0.4525	0.4650
CH-2B	7	0.8588	0.7113	0.7098	0.8236	0.8127	0.7639	0.8240
CH-2B	8	0.7542	0.6448	0.6198	0.7071	0.6974	0.6572	0.6427
CH-2B	9	0.6614	0.5966	0.5581	0.6234	0.6165	0.5851	0.5714
CH-2B	10	0.5735	0.5059	0.5127	0.5912	0.4782	0.4517	0.5143
CH-2B	12	0.8944	0.7131	0.7436	0.8528	0.8081	0.8151	0.9089
CH-2B	13	0.7789	0.6459	0.6535	0.7255	0.6911	0.7023	0.7100
CH-2B	14	0.6890	0.6016	0.5894	0.6501	0.6176	0.6271	0.6644
CH-2B	15	0.5943	0.5033	0.5206	0.6006	0.4736	0.4582	0.6505

Appendix D3 Predictions of Resilient Modulus from Artificial Neural Network Models for Development Dataset (Continued)

Sample I.D.	Seq. No.	Experiment M_R/P_a (10^3)	Predicted M_R/P_a (10^3)					
			LN	GRNN	RBFN	MLPN-1	MLPN-2	MLPN-3
CH-3A	2	1.0553	0.5772	0.6302	0.5358	0.5405	0.5400	0.5190
CH-3A	3	0.7029	0.5170	0.5657	0.4500	0.4596	0.4884	0.4895
CH-3A	4	0.5271	0.4434	0.4912	0.3152	0.3928	0.4270	0.4638
CH-3A	5	0.4136	0.3775	0.4701	0.2957	0.3739	0.3718	0.4448
CH-3A	7	1.1333	0.5714	0.6252	0.5093	0.5288	0.5498	0.5051
CH-3A	8	0.7345	0.5181	0.5724	0.4267	0.4606	0.5094	0.4729
CH-3A	9	0.5183	0.4440	0.4949	0.3157	0.3987	0.4498	0.4497
CH-3A	10	0.4186	0.3780	0.4657	0.3076	0.3858	0.3918	0.4382
CH-3A	12	1.3327	0.5732	0.6502	0.5896	0.5288	0.5417	0.5545
CH-3A	13	0.8105	0.5149	0.5895	0.4666	0.4571	0.4961	0.5033
CH-3A	14	0.5232	0.4445	0.5054	0.3436	0.4045	0.4287	0.4784
CH-3A	15	0.4126	0.3786	0.4659	0.3055	0.3971	0.3599	0.4697
CH-3B	2	0.6446	0.4460	0.6025	0.5924	0.4716	0.4150	0.4290
CH-3B	3	0.3386	0.3896	0.5396	0.5433	0.3841	0.3788	0.4046
CH-3B	4	0.2419	0.3313	0.4614	0.4478	0.3162	0.3439	0.3871
CH-3B	5	0.2142	0.2717	0.4132	0.3559	0.2727	0.3093	0.3720
CH-3B	7	0.6417	0.4421	0.6072	0.5804	0.4932	0.4375	0.3945
CH-3B	8	0.3682	0.3812	0.5422	0.5205	0.3996	0.3990	0.3650
CH-3B	9	0.2764	0.3210	0.4632	0.4472	0.3334	0.3594	0.3552
CH-3B	10	0.2349	0.2614	0.4132	0.3939	0.2968	0.3188	0.3532
CH-3B	12	0.6999	0.4388	0.6454	0.6776	0.5183	0.4115	0.4776
CH-3B	13	0.4008	0.3767	0.5736	0.5779	0.4215	0.3638	0.4321
CH-3B	14	0.2952	0.3152	0.4809	0.4878	0.3556	0.3170	0.4192
CH-3B	15	0.2498	0.2550	0.4204	0.4243	0.3234	0.2719	0.4199
CH-4A	2	1.2833	0.6600	0.7485	0.7190	0.6625	0.8460	0.7854
CH-4A	3	0.7512	0.6125	0.6450	0.5509	0.5817	0.7248	0.6673
CH-4A	4	0.4709	0.5446	0.4991	0.3320	0.4613	0.5059	0.4998
CH-4A	5	0.3623	0.4825	0.4419	0.2329	0.3498	0.2970	0.3915
CH-4A	7	1.3396	0.6568	0.7865	0.7050	0.6827	0.8643	0.8031
CH-4A	8	0.8865	0.6111	0.6963	0.5330	0.6019	0.7351	0.7043
CH-4A	9	0.5341	0.5395	0.5278	0.3061	0.4708	0.5053	0.5584
CH-4A	10	0.3889	0.4767	0.4537	0.2175	0.3567	0.3090	0.4927
CH-4A	12	1.5469	0.6503	0.8402	0.8284	0.6948	0.8883	0.8853
CH-4A	13	1.0207	0.6072	0.7546	0.6511	0.6160	0.7792	0.7688
CH-4A	14	0.5765	0.5369	0.5691	0.4103	0.4849	0.5620	0.6500
CH-4A	15	0.4087	0.4728	0.4690	0.3000	0.3685	0.3507	0.6277
CH-4B	2	0.7720	0.6195	0.7476	0.8699	0.6610	0.7242	0.7115
CH-4B	3	0.4314	0.5612	0.6303	0.7005	0.5471	0.5593	0.5921
CH-4B	4	0.3129	0.5009	0.4942	0.5192	0.4298	0.3884	0.4402
CH-4B	5	0.2626	0.4445	0.4268	0.3930	0.3233	0.2443	0.3095
CH-4B	7	0.7720	0.6187	0.7872	0.8332	0.6822	0.6860	0.7261
CH-4B	8	0.4383	0.5560	0.6735	0.6383	0.5570	0.5283	0.6435
CH-4B	9	0.3258	0.4939	0.5291	0.4627	0.4356	0.3827	0.5190
CH-4B	10	0.2734	0.4387	0.4495	0.3577	0.3330	0.2632	0.4180
CH-4B	12	0.8559	0.6123	0.8417	0.9343	0.6890	0.7091	0.9019
CH-4B	13	0.4729	0.5521	0.7319	0.7270	0.5674	0.5591	0.7911
CH-4B	14	0.3396	0.4912	0.5759	0.5463	0.4491	0.4076	0.6488
CH-4B	15	0.2813	0.4323	0.4697	0.4301	0.3420	0.2670	0.5685

Appendix D3 Predictions of Resilient Modulus from Artificial Neural Network Models for Development Dataset (Continued)

Sample I.D.	Seq. No.	Experiment M_R/P_a (10^3)	Predicted M_R/P_a (10^3)					
			LN	GRNN	RBFN	MLPN-1	MLPN-2	MLPN-3
DE-1A	2	0.4511	0.9007	0.4834	0.7463	0.6507	0.5477	0.5072
DE-1A	3	0.4126	0.8316	0.4214	0.5409	0.5557	0.5237	0.5363
DE-1A	4	0.3939	0.7555	0.3923	0.4310	0.4515	0.4980	0.5038
DE-1A	5	0.3702	0.6788	0.3834	0.5483	0.3442	0.4687	0.4245
DE-1A	7	0.4640	0.8987	0.5408	0.6993	0.6792	0.5574	0.4639
DE-1A	8	0.4334	0.8315	0.4587	0.5097	0.5741	0.5377	0.5380
DE-1A	9	0.4077	0.7548	0.4132	0.3891	0.4561	0.5125	0.5115
DE-1A	10	0.3840	0.6762	0.3959	0.4747	0.3346	0.4806	0.4221
DE-1A	12	0.5271	0.8922	0.5777	0.7784	0.7060	0.5835	0.5237
DE-1A	13	0.4571	0.8320	0.4978	0.5947	0.5998	0.5521	0.5474
DE-1A	14	0.4067	0.7541	0.4291	0.4213	0.4660	0.5131	0.5342
DE-1A	15	0.3771	0.6761	0.4122	0.4123	0.3342	0.4754	0.4361
DE-1B	2	0.7068	0.8059	0.5736	0.7452	0.7148	0.5420	0.8425
DE-1B	3	0.4205	0.7457	0.4776	0.5278	0.5774	0.5217	0.6534
DE-1B	4	0.3643	0.6836	0.4084	0.3481	0.4474	0.5002	0.5393
DE-1B	5	0.3406	0.6189	0.3808	0.2709	0.3207	0.4756	0.4367
DE-1B	7	0.8213	0.7887	0.6247	0.6103	0.7141	0.5433	0.7922
DE-1B	8	0.5844	0.7298	0.5332	0.4060	0.5663	0.5277	0.5728
DE-1B	9	0.4492	0.6626	0.4378	0.2378	0.4128	0.5057	0.4105
DE-1B	10	0.3870	0.6087	0.4077	0.1926	0.2986	0.4835	0.3031
DE-1B	12	0.8421	0.7886	0.6740	0.7515	0.7631	0.5618	0.9992
DE-1B	13	0.6170	0.7278	0.5857	0.5248	0.5922	0.5340	0.7222
DE-1B	14	0.4758	0.6587	0.4760	0.3202	0.4177	0.5022	0.4559
DE-1B	15	0.4255	0.6073	0.4339	0.2354	0.2993	0.4785	0.3220
DE-2A	2	0.8075	1.0540	0.9197	0.9399	1.0561	1.0445	0.9053
DE-2A	3	0.7581	0.9690	0.8501	0.7961	0.9632	0.9544	0.7926
DE-2A	4	0.7374	0.9076	0.8129	0.7097	0.8937	0.8660	0.7383
DE-2A	5	0.7098	0.8347	0.7761	0.7562	0.8245	0.7376	0.6897
DE-2A	7	0.8223	1.0476	0.9544	1.0018	1.0479	1.0118	0.9878
DE-2A	8	0.7730	0.9620	0.8778	0.8677	0.9495	0.9468	0.8513
DE-2A	9	0.7641	0.9024	0.8302	0.7354	0.8809	0.8767	0.7872
DE-2A	10	0.7414	0.8390	0.8012	0.6648	0.8209	0.7801	0.7340
DE-2A	12	0.8371	1.0443	0.9924	1.1209	1.0393	0.9939	1.0820
DE-2A	13	0.7976	0.9587	0.9123	1.0126	0.9369	0.9188	0.8937
DE-2A	14	0.7848	0.8991	0.8529	0.8425	0.8677	0.8536	0.8198
DE-2A	15	0.7651	0.8459	0.8210	0.6859	0.8176	0.7839	0.7669
DE-2B	2	1.1945	0.9806	0.9853	1.0748	0.9755	1.0426	0.8859
DE-2B	3	1.0128	0.9178	0.9177	1.0170	0.8867	0.9760	0.7844
DE-2B	4	0.9358	0.8652	0.8743	0.9445	0.8107	0.9085	0.7289
DE-2B	5	0.8569	0.7676	0.8118	0.9306	0.6854	0.7675	0.6612
DE-2B	7	1.2932	0.9691	1.0207	1.0587	0.9497	1.0134	0.9953
DE-2B	8	1.0661	0.9107	0.9577	1.0295	0.8637	0.9722	0.8701
DE-2B	9	0.9970	0.8562	0.8942	0.9505	0.7839	0.9182	0.7893
DE-2B	10	0.9200	0.7637	0.8333	0.8505	0.6693	0.8047	0.6996
DE-2B	12	1.4028	0.9696	1.0652	1.0887	0.9385	0.9713	1.1116
DE-2B	13	1.1056	0.9024	0.9889	1.0760	0.8364	0.9286	0.9459
DE-2B	14	1.0158	0.8498	0.9187	0.9907	0.7593	0.8921	0.8440
DE-2B	15	0.9309	0.7649	0.8473	0.7976	0.6582	0.8227	0.7315

Appendix D3 Predictions of Resilient Modulus from Artificial Neural Network Models for Development Dataset (Continued)

Sample I.D.	Seq. No.	Experiment M_R/P_a (10^3)	Predicted M_R/P_a (10^3)					
			LN	GRNN	RBFN	MLPN-1	MLPN-2	MLPN-3
DE-3A	2	1.4028	0.7003	0.6913	0.9030	0.7078	0.7327	0.6240
DE-3A	3	1.1046	0.6287	0.6160	0.7622	0.6032	0.6380	0.5778
DE-3A	4	0.9358	0.5830	0.5749	0.6729	0.5527	0.5854	0.5579
DE-3A	5	0.7927	0.4854	0.5598	0.7120	0.5026	0.4748	0.5279
DE-3A	7	1.3455	0.7040	0.6922	0.8976	0.7054	0.7327	0.6201
DE-3A	8	1.0938	0.6267	0.6196	0.7792	0.5954	0.6456	0.5654
DE-3A	9	1.0039	0.5804	0.5799	0.7144	0.5489	0.5978	0.5463
DE-3A	10	0.8578	0.4834	0.5573	0.7704	0.5088	0.4913	0.5206
DE-3A	12	1.4788	0.7102	0.7114	0.8908	0.7056	0.7025	0.6541
DE-3A	13	1.1441	0.6247	0.6278	0.7606	0.5870	0.6247	0.5649
DE-3A	14	1.0355	0.5708	0.5802	0.6995	0.5406	0.5828	0.5398
DE-3A	15	0.8973	0.4833	0.5573	0.7390	0.5149	0.4882	0.5176
DE-3B	2	1.1728	0.5472	0.6358	0.5998	0.5333	0.5392	0.5192
DE-3B	3	0.8944	0.4883	0.5703	0.4926	0.4369	0.4890	0.5016
DE-3B	4	0.7206	0.4192	0.4982	0.3559	0.3578	0.4329	0.4899
DE-3B	5	0.6575	0.3374	0.4813	0.3654	0.3235	0.3656	0.4804
DE-3B	7	1.1994	0.5382	0.6306	0.6023	0.5338	0.5374	0.5151
DE-3B	8	0.9980	0.4812	0.5717	0.5003	0.4439	0.4947	0.4956
DE-3B	9	0.7927	0.4197	0.5084	0.3961	0.3773	0.4460	0.4862
DE-3B	10	0.7029	0.3322	0.4808	0.4101	0.3474	0.3701	0.4802
DE-3B	12	1.3356	0.5375	0.6541	0.6716	0.5513	0.5294	0.5328
DE-3B	13	1.0632	0.4887	0.6019	0.5711	0.4724	0.4854	0.5020
DE-3B	14	0.8796	0.4158	0.5174	0.4364	0.3943	0.4145	0.4851
DE-3B	15	0.7808	0.3334	0.4833	0.4045	0.3716	0.3312	0.4809
DE-4A	2	1.0257	0.8816	0.7748	1.0969	0.9878	1.0716	1.0685
DE-4A	3	0.8509	0.8169	0.7135	0.9643	0.9117	1.0116	0.9921
DE-4A	4	0.7374	0.7503	0.6555	0.8048	0.8265	0.8975	0.9046
DE-4A	5	0.6821	0.6591	0.6390	0.7807	0.7188	0.6784	0.7735
DE-4A	7	1.0306	0.8707	0.7616	1.0568	0.9837	1.0377	0.9953
DE-4A	8	0.8845	0.8067	0.7025	0.9449	0.9054	0.9935	0.9157
DE-4A	9	0.7710	0.7496	0.6555	0.8415	0.8316	0.9153	0.8447
DE-4A	10	0.7048	0.6577	0.6352	0.8298	0.7259	0.7130	0.7286
DE-4A	12	1.1619	0.8940	0.7800	1.0881	1.0137	1.0359	1.0238
DE-4A	13	1.0484	0.8110	0.7152	0.9399	0.9122	0.9517	0.9112
DE-4A	14	0.8588	0.7464	0.6604	0.8322	0.8285	0.8694	0.8436
DE-4A	15	0.7562	0.6544	0.6360	0.8033	0.7276	0.7288	0.7586
DE-4B	2	1.0513	0.9241	0.7688	1.0610	1.0482	1.0919	1.0895
DE-4B	3	0.9427	0.8626	0.7104	1.0107	0.9773	1.0074	1.0294
DE-4B	4	0.8796	0.7973	0.6545	0.8926	0.8956	0.8912	0.9557
DE-4B	5	0.8727	0.7035	0.6396	0.8434	0.7855	0.7185	0.8344
DE-4B	7	1.1273	0.9170	0.7600	1.0228	1.0268	1.0437	1.0567
DE-4B	8	1.0128	0.8536	0.7023	0.9795	0.9497	0.9677	0.9803
DE-4B	9	0.9733	0.7979	0.6558	0.9075	0.8782	0.8716	0.9142
DE-4B	10	0.9348	0.6983	0.6365	0.8772	0.7643	0.7066	0.7948
DE-4B	12	1.3524	0.9144	0.7649	0.9757	1.0073	1.0104	1.0548
DE-4B	13	1.2646	0.8694	0.7286	0.9412	0.9509	0.9602	0.9905
DE-4B	14	1.1826	0.7952	0.6635	0.8678	0.8544	0.8720	0.9057
DE-4B	15	1.0839	0.6938	0.6381	0.8385	0.7429	0.7547	0.8111

Appendix D3 Predictions of Resilient Modulus from Artificial Neural Network Models for Development Dataset (Continued)

Sample I.D.	Seq. No.	Experiment M_R/P_a (10^3)	Predicted M_R/P_a (10^3)					
			LN	GRNN	RBFN	MLPN-1	MLPN-2	MLPN-3
GR-1A	2	1.2500	1.1541	0.8927	1.0460	1.1330	0.9099	1.1183
GR-1A	3	1.0558	1.0842	0.8432	0.9630	1.0966	0.9801	1.1078
GR-1A	4	1.0134	1.0318	0.8144	0.9228	1.0659	1.0222	1.1160
GR-1A	5	0.8349	0.9575	0.7933	0.9835	1.0199	1.0643	1.1275
GR-1A	7	1.3556	1.1515	0.9218	1.0490	1.1557	0.9160	1.1255
GR-1A	8	1.1130	1.0772	0.8588	0.9879	1.1173	0.9938	1.0938
GR-1A	9	1.0644	1.0248	0.8277	0.9735	1.0866	1.0489	1.0926
GR-1A	10	0.8673	0.9505	0.8054	1.0544	1.0409	1.1058	1.0911
GR-1A	12	2.0185	1.1620	0.9560	1.0493	1.1799	1.0407	1.1349
GR-1A	13	1.5700	1.1052	0.9110	0.9869	1.1522	1.0662	1.0557
GR-1A	14	1.5773	1.0265	0.8528	0.9591	1.1076	1.0892	1.0342
GR-1A	15	1.8848	0.9435	0.8218	1.0451	1.0572	1.1037	1.0333
GR-1B	2	1.2399	1.0153	0.8805	1.0304	1.0236	1.0679	1.2240
GR-1B	3	1.0144	0.9454	0.8110	0.9090	0.9642	1.0738	1.1017
GR-1B	4	0.8842	0.8973	0.7686	0.8264	0.9181	1.0491	1.0432
GR-1B	5	0.7161	0.8143	0.7442	0.8078	0.8296	0.9474	0.9849
GR-1B	7	1.1941	1.0127	0.8779	1.0006	1.0508	1.0901	1.1899
GR-1B	8	1.0010	0.9384	0.8135	0.9071	0.9857	1.1119	1.0252
GR-1B	9	0.9112	0.8903	0.7733	0.8575	0.9377	1.0874	0.9612
GR-1B	10	0.7638	0.8073	0.7476	0.8791	0.8460	0.9820	0.9124
GR-1B	12	1.2362	1.0101	0.8891	0.9695	1.0730	1.1170	1.1704
GR-1B	13	1.1523	0.9402	0.8342	0.8759	1.0104	1.1171	0.9769
GR-1B	14	1.0292	0.8877	0.7901	0.8307	0.9568	1.0945	0.9042
GR-1B	15	0.8449	0.8047	0.7586	0.8543	0.8631	0.9946	0.8747
GR-2A	2	0.7393	0.9260	0.7560	0.9651	1.0226	1.1177	1.0019
GR-2A	3	0.7061	0.8473	0.6753	0.8547	0.9211	1.0067	0.8967
GR-2A	4	0.6553	0.8036	0.6421	0.7886	0.8624	0.9217	0.8450
GR-2A	5	0.5777	0.7206	0.6303	0.8081	0.7602	0.7303	0.7577
GR-2A	7	0.7765	0.9234	0.7544	0.9698	1.0108	1.1161	1.0236
GR-2A	8	0.7496	0.8403	0.6746	0.8910	0.8990	0.9963	0.8939
GR-2A	9	0.6949	0.7923	0.6413	0.8412	0.8336	0.9016	0.8323
GR-2A	10	0.6081	0.7180	0.6294	0.8649	0.7449	0.7366	0.7518
GR-2A	12	0.8151	0.9208	0.7622	0.9149	0.9960	1.0699	1.0791
GR-2A	13	0.7648	0.8377	0.6830	0.8565	0.8802	1.0076	0.9033
GR-2A	14	0.7125	0.7853	0.6434	0.8198	0.8085	0.9442	0.8280
GR-2A	15	0.6271	0.7197	0.6273	0.8296	0.7328	0.8249	0.7563
GR-2B	2	0.8561	0.7160	0.6677	0.7579	0.7401	0.7955	0.5826
GR-2B	3	0.5980	0.6461	0.5844	0.5933	0.5945	0.6524	0.4902
GR-2B	4	0.4515	0.5805	0.5139	0.4302	0.4707	0.5229	0.4577
GR-2B	5	0.3805	0.5149	0.4945	0.3862	0.3668	0.4054	0.4408
GR-2B	7	0.7522	0.7177	0.6587	0.7300	0.7600	0.7736	0.6214
GR-2B	8	0.5520	0.6478	0.5871	0.5978	0.6113	0.6379	0.4476
GR-2B	9	0.4493	0.5779	0.5174	0.4604	0.4802	0.5151	0.4107
GR-2B	10	0.3936	0.5123	0.4964	0.4257	0.3806	0.4084	0.4062
GR-2B	12	0.7706	0.7107	0.6703	0.7203	0.7589	0.7978	0.8087
GR-2B	13	0.5957	0.6452	0.5988	0.5946	0.6183	0.6841	0.4780
GR-2B	14	0.5224	0.5753	0.5225	0.4657	0.4892	0.5519	0.4116
GR-2B	15	0.4291	0.5097	0.4988	0.4126	0.3946	0.4259	0.4077

Appendix D3 Predictions of Resilient Modulus from Artificial Neural Network Models for Development Dataset (Continued)

Sample I.D.	Seq. No.	Experiment M_R/P_a (10^3)	Predicted M_R/P_a (10^3)					
			LN	GRNN	RBFN	MLPN-1	MLPN-2	MLPN-3
GR-3A	2	0.6558	0.8136	0.7181	0.8546	0.8258	0.7748	0.7745
GR-3A	3	0.5664	0.7481	0.6568	0.7779	0.7361	0.7008	0.7016
GR-3A	4	0.4777	0.7000	0.6166	0.6796	0.6793	0.6607	0.6548
GR-3A	5	0.4153	0.6169	0.5900	0.5977	0.6189	0.6069	0.5845
GR-3A	7	0.6678	0.8110	0.7100	0.8110	0.7957	0.7426	0.7799
GR-3A	8	0.5723	0.7498	0.6548	0.7417	0.7125	0.6896	0.6951
GR-3A	9	0.4853	0.6974	0.6111	0.6548	0.6530	0.6544	0.6373
GR-3A	10	0.4278	0.6143	0.5827	0.5896	0.6012	0.6093	0.5648
GR-3A	12	0.6625	0.8084	0.7157	0.7873	0.7655	0.7185	0.8087
GR-3A	13	0.5739	0.7472	0.6601	0.7071	0.6839	0.6678	0.7132
GR-3A	14	0.4928	0.6947	0.6125	0.6320	0.6281	0.6435	0.6550
GR-3A	15	0.4339	0.6117	0.5774	0.5699	0.5854	0.6132	0.5895
GR-3B	2	0.7258	0.5635	0.6128	0.5760	0.5316	0.5169	0.4920
GR-3B	3	0.5076	0.5154	0.5598	0.5167	0.4624	0.4804	0.4595
GR-3B	4	0.3647	0.4499	0.4824	0.3855	0.3881	0.4338	0.4283
GR-3B	5	0.3125	0.3799	0.4443	0.2885	0.3417	0.3853	0.4020
GR-3B	7	0.7526	0.5652	0.6154	0.5435	0.5347	0.5308	0.4551
GR-3B	8	0.5383	0.5084	0.5578	0.4692	0.4555	0.4932	0.4029
GR-3B	9	0.3916	0.4472	0.4859	0.3716	0.3913	0.4511	0.3765
GR-3B	10	0.3277	0.3729	0.4402	0.3044	0.3509	0.3958	0.3613
GR-3B	12	1.2688	0.5670	0.6468	0.6116	0.5389	0.5243	0.5612
GR-3B	13	0.8513	0.5014	0.5758	0.4912	0.4500	0.4721	0.4637
GR-3B	14	0.5749	0.4402	0.4945	0.3853	0.3916	0.4197	0.4323
GR-3B	15	0.4396	0.3747	0.4432	0.3123	0.3624	0.3619	0.4225
JE-1A	2	0.5597	0.9400	0.6785	0.6712	0.8022	0.8212	0.7512
JE-1A	3	0.5094	0.8735	0.6235	0.6206	0.7201	0.7444	0.6641
JE-1A	4	0.4827	0.7987	0.5727	0.5457	0.6678	0.6864	0.6142
JE-1A	5	0.4659	0.7156	0.5534	0.6134	0.6698	0.6433	0.5807
JE-1A	7	0.5360	0.9406	0.6596	0.6075	0.7727	0.8016	0.7513
JE-1A	8	0.4906	0.8772	0.6192	0.5801	0.6924	0.7396	0.6409
JE-1A	9	0.4778	0.7954	0.5699	0.5209	0.6363	0.6822	0.5835
JE-1A	10	0.4768	0.7168	0.5525	0.5575	0.6383	0.6427	0.5555
JE-1A	12	0.5637	0.9367	0.6541	0.5334	0.7409	0.8166	0.7713
JE-1A	13	0.4985	0.8758	0.6176	0.5348	0.6644	0.7577	0.6386
JE-1A	14	0.4758	0.7966	0.5701	0.5403	0.6127	0.7083	0.5765
JE-1A	15	0.4748	0.7161	0.5498	0.5895	0.6150	0.6671	0.5491
JE-1B	2	0.5222	0.7028	0.6437	0.6448	0.6793	0.6613	0.6128
JE-1B	3	0.3810	0.6388	0.5898	0.5548	0.5797	0.6305	0.5578
JE-1B	4	0.3060	0.5703	0.5302	0.4564	0.5184	0.6045	0.5345
JE-1B	5	0.2833	0.4981	0.5113	0.4674	0.5123	0.5796	0.5221
JE-1B	7	0.4018	0.7128	0.6311	0.6459	0.7084	0.6497	0.6608
JE-1B	8	0.3100	0.6482	0.5958	0.5516	0.5944	0.6246	0.5560
JE-1B	9	0.2863	0.5721	0.5366	0.4359	0.5161	0.5986	0.5218
JE-1B	10	0.2833	0.4948	0.5112	0.4161	0.5059	0.5720	0.5100
JE-1B	12	0.3949	0.7115	0.6337	0.6464	0.7244	0.6689	0.6644
JE-1B	13	0.3001	0.6494	0.6035	0.5597	0.6072	0.6382	0.5505
JE-1B	14	0.2833	0.5720	0.5417	0.4631	0.5210	0.6005	0.5131
JE-1B	15	0.2863	0.4928	0.5112	0.4255	0.5073	0.5625	0.5035

Appendix D3 Predictions of Resilient Modulus from Artificial Neural Network Models for Development Dataset (Continued)

Sample I.D.	Seq. No.	Experiment M_R/P_a (10^3)	Predicted M_R/P_a (10^3)					
			LN	GRNN	RBFN	MLPN-1	MLPN-2	MLPN-3
JE-2A	2	0.9763	0.7581	0.7749	0.9193	0.8234	0.8242	0.8392
JE-2A	3	0.7502	0.7011	0.7080	0.7367	0.6968	0.7526	0.7226
JE-2A	4	0.5617	0.6440	0.6370	0.5788	0.6008	0.6905	0.6476
JE-2A	5	0.4985	0.5648	0.5926	0.5353	0.5286	0.6185	0.5887
JE-2A	7	0.9398	0.7606	0.7839	0.9596	0.8454	0.8204	0.9291
JE-2A	8	0.7423	0.7023	0.7270	0.8014	0.7071	0.7533	0.7690
JE-2A	9	0.5953	0.6421	0.6541	0.6370	0.6007	0.6914	0.6505
JE-2A	10	0.5341	0.5609	0.5978	0.5413	0.5260	0.6170	0.5722
JE-2A	12	1.0049	0.7592	0.8134	0.9567	0.8650	0.8328	1.0363
JE-2A	13	0.7660	0.6990	0.7499	0.8394	0.7153	0.7867	0.7844
JE-2A	14	0.6239	0.6382	0.6693	0.7061	0.6051	0.7355	0.6210
JE-2A	15	0.5676	0.5570	0.6014	0.5831	0.5312	0.6556	0.5395
JE-2B	2	0.9694	0.5853	0.7948	0.8950	0.9091	0.7309	0.9397
JE-2B	3	0.5923	0.5378	0.7316	0.7087	0.7396	0.6841	0.8458
JE-2B	4	0.4788	0.4719	0.6213	0.4929	0.5574	0.6293	0.7283
JE-2B	5	0.4758	0.3939	0.5584	0.4459	0.4246	0.5741	0.6284
JE-2B	7	1.1392	0.5732	0.8220	0.9176	0.9515	0.6992	0.9882
JE-2B	8	0.8430	0.5238	0.7567	0.7488	0.7717	0.6584	0.8827
JE-2B	9	0.6239	0.4635	0.6561	0.5642	0.6010	0.6144	0.7575
JE-2B	10	0.5222	0.3862	0.5748	0.4854	0.4643	0.5619	0.6320
JE-2B	12	1.6989	0.5909	0.9177	1.0330	1.1280	0.7497	1.3351
JE-2B	13	1.0869	0.5243	0.8218	0.8582	0.8604	0.6982	0.9538
JE-2B	14	0.7779	0.4584	0.6982	0.6775	0.6609	0.6416	0.7609
JE-2B	15	0.6436	0.3804	0.5990	0.5533	0.5158	0.5703	0.6080
JE-3A	2	0.4699	0.7508	0.7846	0.9524	0.8493	0.7588	0.8665
JE-3A	3	0.3554	0.6950	0.7335	0.7997	0.7267	0.7059	0.7540
JE-3A	4	0.3356	0.6215	0.6436	0.6172	0.6205	0.6524	0.6562
JE-3A	5	0.3524	0.5384	0.5959	0.5890	0.5865	0.6056	0.5992
JE-3A	7	0.5074	0.7450	0.7790	0.9328	0.8516	0.7442	0.9100
JE-3A	8	0.4225	0.6886	0.7351	0.7954	0.7218	0.6973	0.7801
JE-3A	9	0.3880	0.6106	0.6496	0.6109	0.6082	0.6441	0.6359
JE-3A	10	0.3801	0.5307	0.6020	0.5567	0.5775	0.5978	0.5703
JE-3A	12	0.5321	0.7392	0.7983	0.9030	0.8628	0.7511	0.9232
JE-3A	13	0.4432	0.6828	0.7512	0.7999	0.7273	0.7157	0.7827
JE-3A	14	0.4028	0.6073	0.6628	0.6598	0.6132	0.6684	0.5989
JE-3A	15	0.3949	0.5268	0.6047	0.5816	0.5782	0.6115	0.5323
JE-3B	2	0.8391	0.5837	0.8086	0.9751	1.0558	0.6875	0.9042
JE-3B	3	0.5706	0.5342	0.7580	0.8082	0.8818	0.6551	0.8135
JE-3B	4	0.5232	0.4639	0.6444	0.6048	0.6989	0.6180	0.6903
JE-3B	5	0.4936	0.3821	0.5744	0.5656	0.5879	0.5814	0.6050
JE-3B	7	1.0760	0.5728	0.8247	0.9873	1.1006	0.6636	0.9290
JE-3B	8	0.7887	0.5278	0.7827	0.8492	0.9350	0.6395	0.8639
JE-3B	9	0.6150	0.4536	0.6725	0.6400	0.7319	0.6048	0.7053
JE-3B	10	0.5548	0.3731	0.5908	0.5719	0.6170	0.5692	0.5945
JE-3B	12	1.1619	0.5670	0.8790	1.0231	1.1747	0.6849	0.9555
JE-3B	13	0.8697	0.5220	0.8286	0.9129	1.0003	0.6592	0.8860
JE-3B	14	0.6584	0.4504	0.7117	0.7361	0.7904	0.6156	0.7047
JE-3B	15	0.6190	0.3724	0.6124	0.6247	0.6637	0.5666	0.5695

Appendix D3 Predictions of Resilient Modulus from Artificial Neural Network Models for Development Dataset (Continued)

Sample I.D.	Seq. No.	Experiment M_R/P_a (10^3)	Predicted M_R/P_a (10^3)					
			LN	GRNN	RBFN	MLPN-1	MLPN-2	MLPN-3
JE-4A	2	1.1925	1.0802	0.9462	0.9511	1.1437	1.1617	1.1613
JE-4A	3	1.0326	1.0092	0.8956	0.9346	1.0818	1.1392	1.1510
JE-4A	4	0.9477	0.9497	0.8498	0.8989	1.0234	1.0915	1.1284
JE-4A	5	0.8342	0.8622	0.8075	0.9787	0.9412	0.9828	1.0746
JE-4A	7	1.2359	1.0681	0.9480	0.9431	1.1155	1.1024	1.1232
JE-4A	8	1.0464	1.0035	0.9033	0.8947	1.0539	1.0758	1.0945
JE-4A	9	1.0059	0.9445	0.8592	0.8535	0.9927	1.0261	1.0635
JE-4A	10	0.8855	0.8589	0.8186	0.9218	0.9113	0.9249	1.0124
JE-4A	12	1.3277	1.0617	0.9511	0.9512	1.0898	1.1049	1.1009
JE-4A	13	1.1046	1.0002	0.9154	0.8861	1.0269	1.0727	1.0604
JE-4A	14	1.0355	0.9374	0.8675	0.8460	0.9589	1.0286	1.0247
JE-4A	15	0.9230	0.8588	0.8303	0.8996	0.8840	0.9659	0.9843
JE-4B	2	0.6081	0.7442	0.6825	0.6880	0.8102	0.8478	0.7493
JE-4B	3	0.4847	0.6884	0.6210	0.6218	0.7212	0.7647	0.6642
JE-4B	4	0.3978	0.6168	0.5489	0.5129	0.6171	0.6777	0.5783
JE-4B	5	0.3465	0.5439	0.5261	0.5115	0.5340	0.6055	0.5094
JE-4B	7	0.5735	0.7447	0.6881	0.7297	0.7918	0.7700	0.7960
JE-4B	8	0.4729	0.6889	0.6297	0.6182	0.7021	0.7118	0.7081
JE-4B	9	0.3998	0.6173	0.5576	0.4782	0.5998	0.6553	0.6319
JE-4B	10	0.3603	0.5425	0.5301	0.4495	0.5196	0.6022	0.5754
JE-4B	12	0.6101	0.7415	0.7049	0.8418	0.7672	0.8034	0.8878
JE-4B	13	0.5074	0.6850	0.6453	0.6856	0.6766	0.7476	0.7772
JE-4B	14	0.4215	0.6172	0.5724	0.5161	0.5823	0.6829	0.6982
JE-4B	15	0.3741	0.5405	0.5366	0.4366	0.5060	0.6129	0.6416
KI-1A	2	0.9437	0.9150	0.7367	0.7600	0.8204	0.8324	0.7491
KI-1A	3	0.6831	0.8548	0.6790	0.6798	0.7300	0.7674	0.6467
KI-1A	4	0.4669	0.7908	0.6143	0.5851	0.6626	0.7148	0.5990
KI-1A	5	0.4284	0.7160	0.5781	0.5693	0.6370	0.6699	0.5702
KI-1A	7	0.9240	0.9175	0.7223	0.7208	0.8019	0.8187	0.8477
KI-1A	8	0.6466	0.8560	0.6771	0.6530	0.7044	0.7606	0.6524
KI-1A	9	0.4837	0.7863	0.6157	0.5584	0.6298	0.7086	0.5793
KI-1A	10	0.4097	0.7134	0.5806	0.5173	0.6066	0.6666	0.5489
KI-1A	12	0.9033	0.9129	0.7228	0.6607	0.7772	0.8388	0.9821
KI-1A	13	0.6476	0.8540	0.6810	0.6218	0.6815	0.7946	0.6716
KI-1A	14	0.4798	0.7843	0.6186	0.5733	0.6070	0.7525	0.5706
KI-1A	15	0.4166	0.7076	0.5784	0.5433	0.5857	0.7057	0.5376
KI-1B	2	0.5410	0.6492	0.7273	0.8759	0.8458	0.6916	0.7627
KI-1B	3	0.3346	0.5909	0.6752	0.7280	0.6997	0.6550	0.6399
KI-1B	4	0.3100	0.5199	0.5841	0.5566	0.5779	0.6205	0.5709
KI-1B	5	0.3268	0.4413	0.5409	0.5223	0.5200	0.5886	0.5383
KI-1B	7	0.7335	0.6365	0.7254	0.8589	0.8527	0.6643	0.8154
KI-1B	8	0.4709	0.5712	0.6706	0.7067	0.6888	0.6331	0.6396
KI-1B	9	0.3820	0.5008	0.5883	0.5525	0.5743	0.6045	0.5551
KI-1B	10	0.3495	0.4311	0.5477	0.5176	0.5286	0.5771	0.5242
KI-1B	12	1.0178	0.6256	0.7514	0.8455	0.8726	0.6839	0.8149
KI-1B	13	0.5864	0.5647	0.6933	0.7323	0.7140	0.6506	0.6323
KI-1B	14	0.4344	0.4937	0.6032	0.5983	0.5938	0.6105	0.5333
KI-1B	15	0.3968	0.4234	0.5536	0.5380	0.5464	0.5708	0.5064

Appendix D3 Predictions of Resilient Modulus from Artificial Neural Network Models for Development Dataset (Continued)

Sample I.D.	Seq. No.	Experiment M_R/P_a (10^3)	Predicted M_R/P_a (10^3)					
			LN	GRNN	RBFN	MLPN-1	MLPN-2	MLPN-3
LI-1A	2	0.8786	0.6948	0.6632	0.8485	0.6908	0.6639	0.6722
LI-1A	3	0.7787	0.6293	0.6127	0.7580	0.5900	0.6110	0.5990
LI-1A	4	0.6834	0.5550	0.5525	0.6411	0.5267	0.5606	0.5606
LI-1A	5	0.6713	0.4676	0.5366	0.6646	0.5276	0.5016	0.5368
LI-1A	7	0.8913	0.6922	0.6502	0.8389	0.6846	0.6519	0.6415
LI-1A	8	0.7810	0.6266	0.6104	0.7547	0.5826	0.6065	0.5586
LI-1A	9	0.7127	0.5523	0.5581	0.6596	0.5213	0.5589	0.5272
LI-1A	10	0.6914	0.4649	0.5387	0.6801	0.5228	0.4981	0.5122
LI-1A	12	0.9677	0.6940	0.6594	0.8209	0.6923	0.6446	0.6462
LI-1A	13	1.0022	0.6284	0.6233	0.7395	0.5860	0.6074	0.5442
LI-1A	14	0.9911	0.5454	0.5658	0.6652	0.5202	0.5470	0.5121
LI-1A	15	0.9316	0.4579	0.5490	0.6943	0.5242	0.4689	0.5019
LI-1B	2	0.8597	0.5673	0.6366	0.7157	0.7281	0.5914	0.6153
LI-1B	3	0.7104	0.5061	0.5891	0.5997	0.5978	0.5583	0.5530
LI-1B	4	0.6280	0.4274	0.5157	0.4478	0.4936	0.5185	0.5227
LI-1B	5	0.6139	0.3356	0.4977	0.4737	0.4689	0.4693	0.5082
LI-1B	7	0.9188	0.5603	0.6278	0.7587	0.7512	0.5805	0.6091
LI-1B	8	0.7714	0.4991	0.5877	0.6332	0.6160	0.5514	0.5347
LI-1B	9	0.6908	0.4204	0.5230	0.4802	0.5099	0.5116	0.5071
LI-1B	10	0.6555	0.3330	0.5004	0.4799	0.4844	0.4613	0.4977
LI-1B	12	0.9647	0.5577	0.6419	0.8268	0.7932	0.5751	0.5810
LI-1B	13	0.8050	0.4965	0.6036	0.7004	0.6492	0.5368	0.5190
LI-1B	14	0.7238	0.4178	0.5348	0.5503	0.5364	0.4856	0.4959
LI-1B	15	0.6893	0.3304	0.5083	0.5048	0.5059	0.4253	0.4899
LI-2A	2	1.1396	0.7920	0.7617	0.9512	0.8914	0.9938	0.8160
LI-2A	3	0.7784	0.7221	0.6921	0.8439	0.7660	0.8694	0.6862
LI-2A	4	0.5606	0.6434	0.5991	0.6767	0.6339	0.7100	0.6081
LI-2A	5	0.4916	0.5648	0.5576	0.6183	0.5290	0.5556	0.5627
LI-2A	7	1.3651	0.7894	0.7715	0.9967	0.8867	0.9660	0.8600
LI-2A	8	0.8924	0.7195	0.7021	0.8670	0.7581	0.8318	0.6845
LI-2A	9	0.6375	0.6408	0.6103	0.7103	0.6269	0.6896	0.5953
LI-2A	10	0.5297	0.5578	0.5640	0.6599	0.5242	0.5517	0.5499
LI-2A	12	1.5639	0.7911	0.8009	1.0437	0.8885	0.9450	1.0254
LI-2A	13	0.9549	0.7168	0.7218	0.8732	0.7485	0.8588	0.7075
LI-2A	14	0.6727	0.6338	0.6188	0.7060	0.6127	0.7371	0.5805
LI-2A	15	0.5544	0.5551	0.5711	0.6482	0.5239	0.5887	0.5366
LI-2B	2	0.5101	0.6447	0.6915	0.7893	0.7267	0.7285	0.5599
LI-2B	3	0.3526	0.5836	0.6239	0.6675	0.5911	0.6356	0.5098
LI-2B	4	0.2763	0.5224	0.5452	0.5228	0.4779	0.5520	0.4896
LI-2B	5	0.2471	0.4568	0.5016	0.4363	0.3851	0.4686	0.4802
LI-2B	7	0.4808	0.6509	0.6973	0.8660	0.7610	0.6904	0.5956
LI-2B	8	0.3281	0.5897	0.6379	0.7271	0.6195	0.6195	0.4991
LI-2B	9	0.2767	0.5197	0.5543	0.5562	0.4887	0.5452	0.4694
LI-2B	10	0.2577	0.4542	0.5088	0.4605	0.3993	0.4732	0.4659
LI-2B	12	0.5205	0.6439	0.7181	0.9465	0.7648	0.7197	0.6947
LI-2B	13	0.3472	0.5870	0.6576	0.7938	0.6314	0.6462	0.4952
LI-2B	14	0.2835	0.5215	0.5720	0.6177	0.5078	0.5599	0.4385
LI-2B	15	0.2614	0.4559	0.5181	0.4894	0.4192	0.4712	0.4364

Appendix D3 Predictions of Resilient Modulus from Artificial Neural Network Models for Development Dataset (Continued)

Sample I.D.	Seq. No.	Experiment M_R/P_a (10^3)	Predicted M_R/P_a (10^3)					
			LN	GRNN	RBFN	MLPN-1	MLPN-2	MLPN-3
LI-3A	2	0.8732	0.6951	0.6948	0.6681	0.6940	0.7078	0.6148
LI-3A	3	0.7082	0.6382	0.6424	0.6126	0.6135	0.6585	0.5750
LI-3A	4	0.5510	0.5727	0.5763	0.5133	0.5438	0.6133	0.5445
LI-3A	5	0.4637	0.4896	0.5432	0.4936	0.5099	0.5586	0.5179
LI-3A	7	0.8472	0.6968	0.6962	0.7070	0.6790	0.6897	0.6166
LI-3A	8	0.6995	0.6356	0.6441	0.6203	0.5943	0.6492	0.5676
LI-3A	9	0.5653	0.5701	0.5810	0.5239	0.5302	0.6143	0.5381
LI-3A	10	0.4856	0.4827	0.5437	0.5166	0.5056	0.5639	0.5149
LI-3A	12	0.8721	0.6942	0.7083	0.7858	0.6585	0.6675	0.6516
LI-3A	13	0.7061	0.6286	0.6509	0.6555	0.5715	0.6411	0.5751
LI-3A	14	0.5794	0.5674	0.5884	0.5554	0.5184	0.6198	0.5405
LI-3A	15	0.4983	0.4800	0.5453	0.5266	0.5031	0.5640	0.5161
LI-3B	2	0.7324	0.5751	0.6516	0.5334	0.5796	0.5782	0.5231
LI-3B	3	0.5514	0.5096	0.5919	0.4711	0.4819	0.5306	0.4932
LI-3B	4	0.4187	0.4353	0.5077	0.3505	0.4058	0.4776	0.4742
LI-3B	5	0.3491	0.3610	0.4740	0.3085	0.3765	0.4220	0.4611
LI-3B	7	0.7115	0.5725	0.6531	0.6141	0.5786	0.5794	0.5372
LI-3B	8	0.5272	0.5113	0.6024	0.5147	0.4874	0.5433	0.5000
LI-3B	9	0.4310	0.4326	0.5151	0.3751	0.4094	0.4905	0.4807
LI-3B	10	0.3701	0.3583	0.4748	0.3261	0.3864	0.4327	0.4732
LI-3B	12	0.7507	0.5742	0.6789	0.7843	0.5881	0.5824	0.5932
LI-3B	13	0.5617	0.5087	0.6250	0.6279	0.4896	0.5356	0.5216
LI-3B	14	0.4804	0.4300	0.5286	0.4528	0.4150	0.4713	0.4922
LI-3B	15	0.4094	0.3513	0.4790	0.3635	0.3984	0.3994	0.4838
LI-4A	2	0.6986	0.6142	0.6370	0.7542	0.5895	0.5976	0.5895
LI-4A	3	0.5645	0.5530	0.5849	0.6877	0.5114	0.5525	0.5545
LI-4A	4	0.4183	0.4875	0.5315	0.6049	0.4692	0.5048	0.5349
LI-4A	5	0.3383	0.4175	0.5155	0.6128	0.4722	0.4507	0.5222
LI-4A	7	0.5826	0.6159	0.6309	0.7503	0.5933	0.5996	0.5627
LI-4A	8	0.4447	0.5635	0.5965	0.6955	0.5233	0.5650	0.5320
LI-4A	9	0.3699	0.4892	0.5403	0.6226	0.4726	0.5127	0.5142
LI-4A	10	0.3260	0.4149	0.5177	0.6399	0.4767	0.4530	0.5057
LI-4A	12	0.5691	0.6177	0.6432	0.7675	0.6013	0.5881	0.5603
LI-4A	13	0.4291	0.5609	0.6066	0.6941	0.5251	0.5540	0.5222
LI-4A	14	0.3575	0.4866	0.5487	0.6293	0.4784	0.4930	0.5052
LI-4A	15	0.3206	0.4166	0.5251	0.6384	0.4834	0.4244	0.4986
LI-4B	2	1.2951	0.6152	0.6204	0.5393	0.5856	0.5900	0.5498
LI-4B	3	0.9525	0.5496	0.5649	0.4661	0.5017	0.5540	0.5272
LI-4B	4	0.7098	0.4884	0.5151	0.3827	0.4585	0.5213	0.5165
LI-4B	5	0.5438	0.4097	0.4993	0.3936	0.4609	0.4767	0.5079
LI-4B	7	1.3010	0.6125	0.6104	0.5618	0.5851	0.5868	0.5408
LI-4B	8	0.9163	0.5513	0.5682	0.4785	0.5047	0.5569	0.5185
LI-4B	9	0.6677	0.4858	0.5187	0.3895	0.4584	0.5219	0.5084
LI-4B	10	0.5349	0.4071	0.4976	0.3896	0.4629	0.4741	0.5017
LI-4B	12	1.3658	0.6143	0.6200	0.6299	0.5972	0.5870	0.5458
LI-4B	13	0.9107	0.5531	0.5791	0.5307	0.5128	0.5489	0.5181
LI-4B	14	0.6586	0.4875	0.5263	0.4398	0.4646	0.5044	0.5057
LI-4B	15	0.5294	0.4045	0.5004	0.4122	0.4693	0.4433	0.4984

Appendix D3 Predictions of Resilient Modulus from Artificial Neural Network Models for Development Dataset (Continued)

Sample I.D.	Seq. No.	Experiment M_R/P_a (10^3)	Predicted M_R/P_a (10^3)					
			LN	GRNN	RBFN	MLPN-1	MLPN-2	MLPN-3
LI-5A	2	0.9238	0.8756	0.8242	1.0041	0.9072	0.8974	0.8825
LI-5A	3	0.9131	0.7794	0.7175	0.7494	0.7414	0.7984	0.7083
LI-5A	4	0.8420	0.7226	0.6701	0.6694	0.6897	0.7510	0.6528
LI-5A	5	0.7464	0.6614	0.6484	0.7206	0.6801	0.7081	0.6159
LI-5A	7	0.8494	0.8642	0.8105	0.9979	0.8737	0.8920	0.9362
LI-5A	8	0.8602	0.7680	0.7176	0.7498	0.7044	0.8032	0.7156
LI-5A	9	0.8363	0.7156	0.6780	0.6500	0.6576	0.7600	0.6437
LI-5A	10	0.7722	0.6675	0.6573	0.6332	0.6464	0.7236	0.6039
LI-5A	12	0.9201	0.8616	0.8267	1.0020	0.8686	0.9152	1.0101
LI-5A	13	0.9008	0.7654	0.7279	0.8169	0.6891	0.8618	0.7110
LI-5A	14	0.8521	0.7173	0.6888	0.7229	0.6426	0.8336	0.6157
LI-5A	15	0.7889	0.6693	0.6634	0.6651	0.6266	0.8011	0.5673
LI-5B	2	0.8886	0.6470	0.8532	1.0809	1.0885	0.7896	0.9497
LI-5B	3	0.7387	0.5815	0.7569	0.8538	0.8635	0.7345	0.8544
LI-5B	4	0.5704	0.5247	0.6621	0.7112	0.7216	0.6957	0.7636
LI-5B	5	0.4768	0.4504	0.6057	0.7096	0.6152	0.6539	0.6694
LI-5B	7	0.8858	0.6444	0.8756	1.1379	1.1584	0.7730	0.9876
LI-5B	8	0.7123	0.5876	0.8064	0.9583	0.9449	0.7304	0.9182
LI-5B	9	0.5685	0.5220	0.7014	0.7718	0.7613	0.6888	0.8169
LI-5B	10	0.4913	0.4477	0.6264	0.7023	0.6407	0.6481	0.6934
LI-5B	12	0.9178	0.6462	0.9395	1.1919	1.2598	0.8241	1.1677
LI-5B	13	0.7229	0.5850	0.8541	1.0459	1.0126	0.7894	0.9618
LI-5B	14	0.5743	0.5238	0.7465	0.8880	0.8249	0.7496	0.8495
LI-5B	15	0.4969	0.4451	0.6454	0.7544	0.6792	0.6922	0.6767
LI-6A	2	0.7656	0.9261	0.8112	1.0090	0.9021	0.8981	0.9148
LI-6A	3	0.7315	0.8561	0.7464	0.8299	0.7981	0.8061	0.7901
LI-6A	4	0.6775	0.7993	0.6924	0.6938	0.7466	0.7449	0.7254
LI-6A	5	0.6441	0.7075	0.6444	0.6485	0.7393	0.6706	0.6649
LI-6A	7	0.7779	0.9147	0.7940	0.9575	0.8585	0.8878	0.9436
LI-6A	8	0.7147	0.8491	0.7405	0.8095	0.7583	0.8192	0.7808
LI-6A	9	0.6604	0.7967	0.6963	0.6843	0.7097	0.7669	0.6928
LI-6A	10	0.6431	0.7049	0.6486	0.5772	0.6977	0.6874	0.6156
LI-6A	12	0.8080	0.9164	0.8061	0.9238	0.8462	0.8851	1.0320
LI-6A	13	0.7198	0.8509	0.7519	0.8289	0.7386	0.8304	0.7961
LI-6A	14	0.6762	0.7941	0.7023	0.7347	0.6834	0.7861	0.6471
LI-6A	15	0.6519	0.7023	0.6518	0.6221	0.6678	0.7201	0.5590
LI-6B	2	0.9975	0.8396	0.8282	0.9947	0.8789	0.8035	0.8798
LI-6B	3	0.8248	0.7785	0.7647	0.8528	0.7615	0.7537	0.7576
LI-6B	4	0.7031	0.7129	0.6889	0.7237	0.6860	0.7128	0.6736
LI-6B	5	0.6605	0.6211	0.6379	0.7320	0.6779	0.6703	0.6155
LI-6B	7	0.9262	0.8414	0.8200	0.9695	0.8863	0.7970	0.9351
LI-6B	8	0.7858	0.7758	0.7653	0.8247	0.7477	0.7493	0.7976
LI-6B	9	0.7055	0.7103	0.6991	0.6832	0.6642	0.7105	0.6694
LI-6B	10	0.6699	0.6185	0.6464	0.6254	0.6471	0.6675	0.5882
LI-6B	12	0.9406	0.8388	0.8345	0.9360	0.8961	0.8330	0.9411
LI-6B	13	0.7872	0.7732	0.7779	0.8272	0.7468	0.7978	0.8233
LI-6B	14	0.7068	0.7076	0.7095	0.7161	0.6561	0.7648	0.6421
LI-6B	15	0.6739	0.6159	0.6501	0.6311	0.6300	0.7124	0.5451

Appendix D3 Predictions of Resilient Modulus from Artificial Neural Network Models for Development Dataset (Continued)

Sample I.D.	Seq. No.	Experiment M_R/P_a (10^3)	Predicted M_R/P_a (10^3)					
			LN	GRNN	RBFN	MLPN-1	MLPN-2	MLPN-3
MA-1A	2	0.7433	0.5590	0.6437	0.6984	0.5312	0.5683	0.5534
MA-1A	3	0.4620	0.4994	0.5939	0.6469	0.4484	0.5140	0.5292
MA-1A	4	0.3465	0.4380	0.5297	0.5714	0.3954	0.4580	0.5150
MA-1A	5	0.3001	0.3733	0.4921	0.5420	0.3808	0.3974	0.5050
MA-1A	7	0.7117	0.5608	0.6426	0.7100	0.5419	0.5785	0.5384
MA-1A	8	0.4551	0.5006	0.6006	0.6415	0.4593	0.5303	0.5147
MA-1A	9	0.3653	0.4322	0.5352	0.5757	0.4061	0.4714	0.5025
MA-1A	10	0.3248	0.3650	0.4958	0.5777	0.3992	0.4070	0.4959
MA-1A	12	0.7947	0.5557	0.6588	0.7820	0.5431	0.5589	0.5389
MA-1A	13	0.5064	0.4948	0.6133	0.6744	0.4638	0.5156	0.5100
MA-1A	14	0.3899	0.4289	0.5449	0.5938	0.4196	0.4516	0.4975
MA-1A	15	0.3416	0.3598	0.5013	0.5820	0.4182	0.3730	0.4919
MA-1B	2	0.3406	0.4898	0.6207	0.5492	0.5450	0.4807	0.5189
MA-1B	3	0.2428	0.4346	0.5803	0.5019	0.4543	0.4387	0.5028
MA-1B	4	0.2399	0.3636	0.5025	0.4090	0.3774	0.3866	0.4918
MA-1B	5	0.2498	0.2857	0.4570	0.3662	0.3525	0.3301	0.4839
MA-1B	7	0.4057	0.4833	0.6200	0.6051	0.5615	0.4911	0.5112
MA-1B	8	0.3060	0.4193	0.5742	0.5172	0.4587	0.4451	0.4949
MA-1B	9	0.2813	0.3452	0.4986	0.4229	0.3896	0.3881	0.4870
MA-1B	10	0.2833	0.2742	0.4602	0.4123	0.3788	0.3309	0.4832
MA-1B	12	0.4610	0.4763	0.6400	0.7390	0.5804	0.4673	0.5062
MA-1B	13	0.3396	0.4154	0.5944	0.6162	0.4815	0.4135	0.4936
MA-1B	14	0.3060	0.3394	0.5092	0.4905	0.4130	0.3449	0.4857
MA-1B	15	0.2991	0.2671	0.4664	0.4504	0.4064	0.2811	0.4831
MA-2A	2	1.0336	1.0850	0.8396	0.8889	1.0022	1.0027	1.1064
MA-2A	3	0.9250	0.9937	0.7936	0.8062	0.9153	0.8942	1.0019
MA-2A	4	0.8618	0.9424	0.7705	0.7398	0.8836	0.8275	0.9490
MA-2A	5	0.8016	0.8942	0.7501	0.7304	0.8667	0.7738	0.8992
MA-2A	7	0.9753	1.0836	0.8191	0.8716	0.9724	0.9399	0.9441
MA-2A	8	0.8914	0.9993	0.7911	0.8388	0.8892	0.8370	0.8861
MA-2A	9	0.8440	0.9435	0.7657	0.7888	0.8540	0.7909	0.8466
MA-2A	10	0.8065	0.8922	0.7465	0.7746	0.8359	0.7558	0.8072
MA-2A	12	1.0089	1.0854	0.7965	0.8243	0.9462	1.0061	0.9324
MA-2A	13	0.8993	1.0024	0.8024	0.8481	0.8623	0.9226	0.8762
MA-2A	14	0.8460	0.9473	0.7782	0.8590	0.8275	0.8604	0.8336
MA-2A	15	0.8006	0.8870	0.7441	0.8851	0.8066	0.7930	0.7854
MA-2B	2	0.4758	0.6301	0.6367	0.5384	0.5878	0.5970	0.5604
MA-2B	3	0.3445	0.5725	0.5955	0.5027	0.5128	0.5601	0.5363
MA-2B	4	0.2962	0.5008	0.5300	0.4175	0.4574	0.5150	0.5204
MA-2B	5	0.2883	0.4248	0.5001	0.3915	0.4547	0.4638	0.5099
MA-2B	7	0.4472	0.6351	0.6297	0.5716	0.5919	0.6002	0.5564
MA-2B	8	0.3317	0.5711	0.5938	0.5000	0.5075	0.5655	0.5262
MA-2B	9	0.3031	0.4950	0.5312	0.4127	0.4534	0.5197	0.5112
MA-2B	10	0.2962	0.4190	0.4996	0.4001	0.4573	0.4660	0.5030
MA-2B	12	0.4590	0.6293	0.6374	0.6490	0.5836	0.5946	0.5635
MA-2B	13	0.3396	0.5685	0.6031	0.5454	0.5046	0.5587	0.5271
MA-2B	14	0.3080	0.4905	0.5355	0.4460	0.4539	0.5004	0.5083
MA-2B	15	0.3050	0.4138	0.5020	0.4240	0.4631	0.4344	0.5000

Appendix D3 Predictions of Resilient Modulus from Artificial Neural Network Models for Development Dataset (Continued)

Sample I.D.	Seq. No.	Experiment M_R/P_a (10^3)	Predicted M_R/P_a (10^3)					
			LN	GRNN	RBFN	MLPN-1	MLPN-2	MLPN-3
MA-3A	2	1.2586	1.3409	1.2939	1.5788	1.2907	1.3297	1.5254
MA-3A	3	1.2932	1.2483	1.2789	1.3246	1.2869	1.2996	1.5058
MA-3A	4	1.3050	1.1805	1.2744	1.1998	1.3034	1.2521	1.5116
MA-3A	5	1.3080	1.1146	1.2738	1.2490	1.3349	1.1898	1.5289
MA-3A	7	1.4146	1.3376	1.4287	1.6365	1.2862	1.4674	1.3781
MA-3A	8	1.3465	1.2615	1.3198	1.4361	1.2814	1.4154	1.4056
MA-3A	9	1.3682	1.1817	1.2981	1.2547	1.2982	1.3388	1.4342
MA-3A	10	1.3574	1.1094	1.2971	1.2580	1.3299	1.2571	1.4528
MA-3A	12	1.4571	1.3401	1.4553	1.6685	1.2819	1.2839	1.3379
MA-3A	13	1.3366	1.2564	1.3385	1.4980	1.2763	1.2740	1.3514
MA-3A	14	1.3880	1.1581	1.3094	1.3359	1.3027	1.2756	1.3451
MA-3A	15	1.3643	1.1036	1.3143	1.3413	1.3229	1.2851	1.3322
MA-3B	2	2.2606	1.0782	1.2225	1.7083	1.2056	1.5773	1.3323
MA-3B	3	1.6170	0.9818	1.1038	1.4803	1.1549	1.4322	1.3433
MA-3B	4	1.4729	0.8988	1.0686	1.2465	1.1192	1.2773	1.3095
MA-3B	5	1.3554	0.8474	1.0529	1.2041	1.1087	1.1643	1.2656
MA-3B	7	2.4274	1.0755	1.4965	1.7201	1.1960	1.8137	1.3035
MA-3B	8	1.5745	0.9849	1.1749	1.5056	1.1451	1.5856	1.2670
MA-3B	9	1.4659	0.8961	1.0702	1.2660	1.1054	1.3409	1.1991
MA-3B	10	1.3850	0.8410	1.0579	1.2157	1.0935	1.1999	1.1421
MA-3B	12	2.3189	1.0685	1.4395	1.6777	1.1820	1.4826	1.2312
MA-3B	13	1.5903	0.9785	1.2018	1.4679	1.1279	1.4071	1.1617
MA-3B	14	1.4985	0.8992	1.0814	1.2778	1.0913	1.3536	1.0989
MA-3B	15	1.3929	0.8371	1.0601	1.2115	1.0763	1.3170	1.0470
MA-4A	2	0.8421	0.7171	0.6755	0.7820	0.7231	0.7381	0.6547
MA-4A	3	0.6525	0.6550	0.6115	0.6542	0.6084	0.6255	0.5904
MA-4A	4	0.4916	0.5910	0.5417	0.4922	0.5032	0.5216	0.5524
MA-4A	5	0.4018	0.5174	0.5120	0.4170	0.4130	0.4157	0.5244
MA-4A	7	0.8233	0.7164	0.6669	0.7477	0.7253	0.7292	0.6850
MA-4A	8	0.6180	0.6625	0.6198	0.6610	0.6251	0.6392	0.5956
MA-4A	9	0.4640	0.5896	0.5448	0.5230	0.5072	0.5320	0.5386
MA-4A	10	0.3959	0.5142	0.5109	0.4669	0.4223	0.4277	0.5101
MA-4A	12	0.8421	0.7163	0.6827	0.7385	0.7271	0.7118	0.7854
MA-4A	13	0.6170	0.6624	0.6343	0.6477	0.6267	0.6450	0.6270
MA-4A	14	0.4511	0.5889	0.5518	0.5241	0.5111	0.5429	0.5396
MA-4A	15	0.3860	0.5135	0.5106	0.4558	0.4335	0.4242	0.5077
MA-4B	2	0.8272	0.6141	0.6313	0.6650	0.6194	0.6318	0.4986
MA-4B	3	0.4847	0.5570	0.5687	0.5676	0.5015	0.5712	0.4562
MA-4B	4	0.3258	0.4962	0.4916	0.4184	0.3962	0.5158	0.4369
MA-4B	5	0.2734	0.4315	0.4479	0.2998	0.3098	0.4626	0.4257
MA-4B	7	0.8223	0.6153	0.6246	0.6065	0.6423	0.6137	0.4811
MA-4B	8	0.4729	0.5595	0.5722	0.5333	0.5251	0.5663	0.3953
MA-4B	9	0.3406	0.4923	0.4928	0.4175	0.4100	0.5152	0.3729
MA-4B	10	0.2804	0.4276	0.4487	0.3345	0.3283	0.4660	0.3739
MA-4B	12	0.9013	0.6114	0.6447	0.6145	0.6551	0.6210	0.6638
MA-4B	13	0.5064	0.5556	0.5890	0.5290	0.5373	0.5699	0.4570
MA-4B	14	0.3495	0.4890	0.5012	0.4238	0.4254	0.5070	0.4009
MA-4B	15	0.2892	0.4231	0.4487	0.3407	0.3468	0.4432	0.3991

Appendix D3 Predictions of Resilient Modulus from Artificial Neural Network Models for Development Dataset (Continued)

Sample I.D.	Seq. No.	Experiment M_R/P_a (10^3)	Predicted M_R/P_a (10^3)					
			LN	GRNN	RBFN	MLPN-1	MLPN-2	MLPN-3
MC-1A	2	0.8885	1.0834	0.8220	0.8451	1.1026	1.1499	0.8828
MC-1A	3	0.8322	0.9998	0.7668	0.7778	1.0186	1.0582	0.8165
MC-1A	4	0.8164	0.9357	0.7475	0.7605	0.9568	0.9640	0.7739
MC-1A	5	0.7927	0.8920	0.7427	0.8218	0.9234	0.8928	0.7467
MC-1A	7	0.8934	1.0910	0.8242	0.9052	1.0912	1.1287	0.9014
MC-1A	8	0.8707	0.9933	0.7697	0.8610	0.9862	1.0672	0.8140
MC-1A	9	0.8509	0.9261	0.7544	0.8174	0.9197	0.9830	0.7711
MC-1A	10	0.8272	0.8780	0.7487	0.8504	0.8852	0.9112	0.7421
MC-1A	12	0.9358	1.0788	0.8161	0.9131	1.0587	1.0917	0.9112
MC-1A	13	0.8983	0.9875	0.7666	0.9168	0.9543	1.0426	0.8216
MC-1A	14	0.8796	0.9191	0.7490	0.8674	0.8863	0.9969	0.7756
MC-1A	15	0.8598	0.8709	0.7493	0.8602	0.8540	0.9543	0.7453
MC-1B	2	1.0454	1.1558	0.9738	0.9491	1.1326	1.0453	1.0318
MC-1B	3	0.8944	1.0854	0.9047	0.8730	1.0928	1.0634	0.9974
MC-1B	4	0.8480	1.0328	0.8558	0.8220	1.0620	1.0604	0.9723
MC-1B	5	0.7285	0.9618	0.8038	0.8528	1.0279	0.9975	0.9410
MC-1B	7	1.0415	1.1550	1.0186	1.0211	1.1495	1.0831	1.0549
MC-1B	8	0.9398	1.0821	0.9534	0.9620	1.1081	1.0792	1.0344
MC-1B	9	0.9131	1.0295	0.9032	0.8983	1.0775	1.0643	1.0161
MC-1B	10	0.8055	0.9617	0.8502	0.8630	1.0457	1.0219	0.9907
MC-1B	12	1.3021	1.1556	1.1099	1.1410	1.1627	1.1259	1.0583
MC-1B	13	1.1599	1.0878	1.0552	1.1029	1.1239	1.1104	1.0514
MC-1B	14	1.1125	1.0345	0.9974	1.0307	1.0928	1.0884	1.0366
MC-1B	15	0.9556	0.9553	0.9157	0.9090	1.0569	1.0272	1.0052
NO-1A	2	0.9872	0.8055	0.6759	0.7295	0.7039	0.6770	0.6614
NO-1A	3	0.9121	0.7250	0.6250	0.6890	0.6157	0.6144	0.5986
NO-1A	4	0.8697	0.6483	0.5804	0.5938	0.5846	0.5681	0.5692
NO-1A	5	0.8332	0.5697	0.5741	0.6167	0.5954	0.5217	0.5498
NO-1A	7	0.8717	0.8029	0.6446	0.5995	0.6765	0.6698	0.6394
NO-1A	8	0.8243	0.7236	0.6083	0.5849	0.5933	0.6200	0.5696
NO-1A	9	0.7957	0.6463	0.5693	0.5427	0.5676	0.5732	0.5431
NO-1A	10	0.7670	0.5677	0.5609	0.5832	0.5789	0.5207	0.5281
NO-1A	12	0.7453	0.8015	0.6332	0.4981	0.6536	0.6292	0.6469
NO-1A	13	0.7098	0.7229	0.5972	0.4872	0.5749	0.5836	0.5597
NO-1A	14	0.6861	0.6456	0.5575	0.4960	0.5545	0.5471	0.5334
NO-1A	15	0.6663	0.5663	0.5471	0.5547	0.5666	0.4946	0.5203
NO-1B	2	0.7216	0.6681	0.6225	0.5375	0.5679	0.5671	0.5685
NO-1B	3	0.6407	0.5914	0.5665	0.4758	0.4872	0.5273	0.5369
NO-1B	4	0.5874	0.5141	0.5158	0.3848	0.4615	0.4896	0.5231
NO-1B	5	0.5617	0.4361	0.5134	0.4338	0.4912	0.4494	0.5145
NO-1B	7	0.6101	0.6661	0.5969	0.4398	0.5604	0.5688	0.5644
NO-1B	8	0.5528	0.5901	0.5564	0.3840	0.4809	0.5288	0.5257
NO-1B	9	0.5173	0.5127	0.5094	0.3251	0.4578	0.4872	0.5127
NO-1B	10	0.4936	0.4347	0.5011	0.3787	0.4871	0.4417	0.5057
NO-1B	12	0.5271	0.6648	0.5908	0.4050	0.5587	0.5502	0.5631
NO-1B	13	0.4729	0.5855	0.5479	0.3377	0.4771	0.5035	0.5189
NO-1B	14	0.4423	0.5114	0.5013	0.3028	0.4587	0.4531	0.5076
NO-1B	15	0.4146	0.4271	0.4913	0.3552	0.4902	0.3928	0.5014

Appendix D3 Predictions of Resilient Modulus from Artificial Neural Network Models for Development Dataset (Continued)

Sample I.D.	Seq. No.	Experiment M_R/P_a (10^3)	Predicted M_R/P_a (10^3)					
			LN	GRNN	RBFN	MLPN-1	MLPN-2	MLPN-3
NO-2A	2	0.8391	0.8202	0.7381	0.8758	0.7797	0.7696	0.7088
NO-2A	3	0.7670	0.7422	0.6748	0.7316	0.6598	0.6738	0.6080
NO-2A	4	0.7167	0.6649	0.6101	0.5820	0.5895	0.6053	0.5698
NO-2A	5	0.6881	0.5869	0.5938	0.5972	0.5800	0.5519	0.5497
NO-2A	7	0.7907	0.8176	0.7139	0.7979	0.7622	0.7560	0.7765
NO-2A	8	0.7394	0.7390	0.6656	0.6951	0.6402	0.6761	0.6057
NO-2A	9	0.6940	0.6623	0.6058	0.5713	0.5738	0.6107	0.5550
NO-2A	10	0.6594	0.5837	0.5855	0.5551	0.5662	0.5514	0.5334
NO-2A	12	0.6486	0.8156	0.7049	0.7220	0.7492	0.7191	0.8872
NO-2A	13	0.6051	0.7389	0.6605	0.6631	0.6287	0.6528	0.6086
NO-2A	14	0.5795	0.6609	0.5952	0.5824	0.5638	0.5952	0.5396
NO-2A	15	0.5617	0.5823	0.5674	0.5405	0.5577	0.5354	0.5192
NO-2B	2	0.7275	0.7126	0.7248	0.8367	0.7205	0.6922	0.6824
NO-2B	3	0.6575	0.6353	0.6539	0.6844	0.5839	0.6383	0.5805
NO-2B	4	0.6130	0.5580	0.5754	0.5449	0.5080	0.5993	0.5454
NO-2B	5	0.5953	0.4800	0.5589	0.5864	0.5025	0.5660	0.5292
NO-2B	7	0.6032	0.7113	0.7126	0.7717	0.7298	0.6823	0.7744
NO-2B	8	0.5548	0.6340	0.6595	0.6531	0.5865	0.6346	0.5943
NO-2B	9	0.5291	0.5573	0.5827	0.5288	0.5083	0.5954	0.5394
NO-2B	10	0.5114	0.4749	0.5550	0.5386	0.5013	0.5569	0.5190
NO-2B	12	0.4580	0.7081	0.7221	0.7163	0.7421	0.6739	0.8361
NO-2B	13	0.4215	0.6288	0.6657	0.6295	0.5905	0.6344	0.5969
NO-2B	14	0.4097	0.5508	0.5813	0.5333	0.5124	0.5932	0.5252
NO-2B	15	0.4038	0.4722	0.5447	0.5068	0.5062	0.5459	0.5073
NO-3A	2	0.6772	0.7382	0.6639	0.7780	0.7749	0.7229	0.7037
NO-3A	3	0.6071	0.6622	0.5941	0.6621	0.6529	0.6115	0.6169
NO-3A	4	0.5390	0.5861	0.5243	0.4964	0.5463	0.5154	0.5551
NO-3A	5	0.4877	0.5081	0.5075	0.4753	0.4772	0.4242	0.5046
NO-3A	7	0.6278	0.7363	0.6509	0.6916	0.7632	0.7125	0.6967
NO-3A	8	0.5735	0.6602	0.5883	0.5912	0.6429	0.6193	0.5689
NO-3A	9	0.5222	0.5841	0.5203	0.4779	0.5423	0.5349	0.4931
NO-3A	10	0.4768	0.5068	0.4991	0.4842	0.4833	0.4469	0.4410
NO-3A	12	0.5735	0.7343	0.6607	0.6847	0.7485	0.6609	0.7675
NO-3A	13	0.5281	0.6582	0.5959	0.5584	0.6305	0.5884	0.5980
NO-3A	14	0.4847	0.5815	0.5202	0.4502	0.5360	0.5204	0.5175
NO-3A	15	0.4452	0.5042	0.4926	0.4388	0.4878	0.4298	0.4743
NO-3B	2	0.5558	0.6392	0.6258	0.6141	0.6202	0.5759	0.5761
NO-3B	3	0.4768	0.5618	0.5448	0.5086	0.4965	0.5032	0.5081
NO-3B	4	0.4097	0.4864	0.4715	0.3519	0.4028	0.4414	0.4667
NO-3B	5	0.3613	0.4091	0.4566	0.3308	0.3501	0.3810	0.4332
NO-3B	7	0.4906	0.6378	0.6182	0.5267	0.6143	0.5781	0.5363
NO-3B	8	0.4294	0.5605	0.5450	0.4387	0.4940	0.5159	0.4312
NO-3B	9	0.3781	0.4844	0.4700	0.3348	0.4061	0.4561	0.3865
NO-3B	10	0.3406	0.4065	0.4489	0.3438	0.3626	0.3920	0.3617
NO-3B	12	0.4531	0.6339	0.6370	0.5350	0.6038	0.5612	0.6352
NO-3B	13	0.3949	0.5579	0.5597	0.4203	0.4894	0.5015	0.4746
NO-3B	14	0.3475	0.4812	0.4733	0.3201	0.4079	0.4299	0.4238
NO-3B	15	0.3139	0.4045	0.4437	0.3100	0.3749	0.3533	0.4085

Appendix D3 Predictions of Resilient Modulus from Artificial Neural Network Models for Development Dataset (Continued)

Sample I.D.	Seq. No.	Experiment M_R/P_a (10^3)	Predicted M_R/P_a (10^3)					
			LN	GRNN	RBFN	MLPN-1	MLPN-2	MLPN-3
NO-4A	2	0.6446	0.6699	0.6430	0.7850	0.6677	0.6324	0.6025
NO-4A	3	0.5775	0.5945	0.5760	0.6716	0.5662	0.5540	0.5511
NO-4A	4	0.5252	0.5178	0.5118	0.5283	0.4993	0.4798	0.5106
NO-4A	5	0.4827	0.4366	0.4930	0.5450	0.4806	0.4026	0.4729
NO-4A	7	0.5745	0.6692	0.6285	0.6564	0.6512	0.6377	0.5601
NO-4A	8	0.5163	0.5893	0.5647	0.5308	0.5502	0.5714	0.4718
NO-4A	9	0.4758	0.5171	0.5041	0.4396	0.4967	0.5082	0.4198
NO-4A	10	0.4442	0.4321	0.4804	0.5032	0.4865	0.4253	0.3747
NO-4A	12	0.5084	0.6678	0.6373	0.6568	0.6327	0.6013	0.5812
NO-4A	13	0.4551	0.5861	0.5682	0.4812	0.5361	0.5452	0.4656
NO-4A	14	0.4176	0.5075	0.4950	0.3761	0.4913	0.4882	0.4154
NO-4A	15	0.3899	0.4295	0.4685	0.4195	0.4913	0.4092	0.3898
NO-4B	2	0.5104	0.5496	0.5969	0.5685	0.4915	0.4060	0.5221
NO-4B	3	0.4344	0.4684	0.5131	0.4674	0.3956	0.3354	0.4792
NO-4B	4	0.3820	0.3898	0.4462	0.3543	0.3429	0.2775	0.4453
NO-4B	5	0.3455	0.3119	0.4342	0.4076	0.3429	0.2268	0.4126
NO-4B	7	0.4097	0.5450	0.5865	0.4215	0.4819	0.4340	0.4230
NO-4B	8	0.3534	0.4671	0.5131	0.3288	0.3967	0.3701	0.3537
NO-4B	9	0.3179	0.3872	0.4403	0.2731	0.3525	0.3053	0.3117
NO-4B	10	0.2962	0.3099	0.4221	0.3726	0.3613	0.2454	0.2820
NO-4B	12	0.3337	0.5431	0.6082	0.4388	0.4757	0.4165	0.4208
NO-4B	13	0.2823	0.4638	0.5268	0.2950	0.3958	0.3422	0.3334
NO-4B	14	0.2577	0.3858	0.4428	0.2259	0.3617	0.2669	0.3050
NO-4B	15	0.2419	0.3085	0.4132	0.2972	0.3780	0.1977	0.2964
NO-5A	2	0.7345	0.8062	0.7217	0.9507	0.7771	0.7400	0.7056
NO-5A	3	0.6762	0.7276	0.6625	0.8755	0.6844	0.6684	0.6388
NO-5A	4	0.6308	0.6502	0.6023	0.7185	0.6341	0.6202	0.5910
NO-5A	5	0.5953	0.5723	0.5799	0.6820	0.6246	0.5779	0.5528
NO-5A	7	0.6446	0.8042	0.6996	0.8325	0.7472	0.7097	0.6979
NO-5A	8	0.6051	0.7268	0.6471	0.7547	0.6595	0.6704	0.6155
NO-5A	9	0.5755	0.6482	0.5910	0.6420	0.6156	0.6311	0.5593
NO-5A	10	0.5508	0.5696	0.5677	0.6359	0.6105	0.5884	0.5177
NO-5A	12	0.5568	0.8028	0.7025	0.7721	0.7182	0.7098	0.7122
NO-5A	13	0.5252	0.7248	0.6469	0.6667	0.6344	0.6497	0.6130
NO-5A	14	0.5025	0.6456	0.5826	0.5785	0.5987	0.6114	0.5557
NO-5A	15	0.4847	0.5670	0.5538	0.5810	0.5977	0.5835	0.5199
NO-5B	2	0.7038	0.7462	0.6690	0.7209	0.6202	0.6165	0.6241
NO-5B	3	0.6407	0.6682	0.6080	0.6668	0.5360	0.5708	0.5765
NO-5B	4	0.5874	0.5896	0.5532	0.5235	0.4944	0.5253	0.5421
NO-5B	5	0.5499	0.5161	0.5416	0.4953	0.5049	0.4785	0.5152
NO-5B	7	0.6219	0.7455	0.6511	0.6168	0.5956	0.6188	0.6285
NO-5B	8	0.5696	0.6688	0.5980	0.5446	0.5169	0.5800	0.5544
NO-5B	9	0.5291	0.5877	0.5405	0.4281	0.4813	0.5349	0.5055
NO-5B	10	0.4995	0.5091	0.5254	0.4236	0.4995	0.4822	0.4707
NO-5B	12	0.5469	0.7410	0.6557	0.5907	0.5682	0.5991	0.6582
NO-5B	13	0.4995	0.6674	0.6016	0.4895	0.4984	0.5739	0.5631
NO-5B	14	0.4640	0.5831	0.5331	0.3841	0.4709	0.5207	0.5084
NO-5B	15	0.4393	0.5052	0.5121	0.3779	0.4952	0.4567	0.4805

Appendix D3 Predictions of Resilient Modulus from Artificial Neural Network Models for Development Dataset (Continued)

Sample I.D.	Seq. No.	Experiment M_R/P_a (10^3)	Predicted M_R/P_a (10^3)					
			LN	GRNN	RBFN	MLPN-1	MLPN-2	MLPN-3
NO-6A	2	0.6802	0.6331	0.6519	0.6700	0.5991	0.6041	0.5643
NO-6A	3	0.5933	0.5570	0.5844	0.5758	0.5054	0.5359	0.5281
NO-6A	4	0.5173	0.4772	0.5143	0.4474	0.4550	0.4661	0.5019
NO-6A	5	0.4679	0.3979	0.4984	0.4886	0.4550	0.3944	0.4800
NO-6A	7	0.6041	0.6311	0.6407	0.6039	0.5847	0.6140	0.5519
NO-6A	8	0.5321	0.5557	0.5808	0.5018	0.4977	0.5561	0.5073
NO-6A	9	0.4758	0.4796	0.5135	0.4180	0.4572	0.4923	0.4822
NO-6A	10	0.4334	0.3947	0.4893	0.4926	0.4629	0.4114	0.4635
NO-6A	12	0.5321	0.6304	0.6526	0.6392	0.5723	0.5789	0.5750
NO-6A	13	0.4679	0.5543	0.5897	0.4914	0.4905	0.5374	0.5181
NO-6A	14	0.4195	0.4776	0.5134	0.3973	0.4585	0.4792	0.4940
NO-6A	15	0.3880	0.4003	0.4820	0.4313	0.4688	0.3972	0.4821
NO-6B	2	0.5538	0.5502	0.6149	0.5112	0.4949	0.4620	0.5174
NO-6B	3	0.4600	0.4735	0.5361	0.4136	0.4065	0.3947	0.4870
NO-6B	4	0.3919	0.3942	0.4647	0.2934	0.3610	0.3313	0.4627
NO-6B	5	0.3564	0.3118	0.4526	0.3595	0.3705	0.2696	0.4387
NO-6B	7	0.4679	0.5475	0.6084	0.4384	0.4899	0.4863	0.4890
NO-6B	8	0.3959	0.4746	0.5409	0.3414	0.4107	0.4254	0.4472
NO-6B	9	0.3495	0.3979	0.4659	0.2639	0.3718	0.3601	0.4230
NO-6B	10	0.3169	0.3143	0.4420	0.3469	0.3861	0.2886	0.4054
NO-6B	12	0.4827	0.5449	0.6291	0.4940	0.4856	0.4689	0.5227
NO-6B	13	0.4097	0.4720	0.5563	0.3516	0.4118	0.4022	0.4712
NO-6B	14	0.3455	0.3953	0.4698	0.2571	0.3813	0.3246	0.4514
NO-6B	15	0.3070	0.3186	0.4362	0.2929	0.3995	0.2488	0.4446
NO-7A	2	0.9970	0.9019	0.7865	0.9572	0.9555	0.9255	0.9208
NO-7A	3	0.9516	0.8214	0.7199	0.8962	0.8515	0.8057	0.8269
NO-7A	4	0.9003	0.7428	0.6584	0.7403	0.7617	0.7144	0.7383
NO-7A	5	0.8470	0.6654	0.6396	0.7083	0.7108	0.6570	0.6571
NO-7A	7	0.9210	0.8999	0.7830	0.9457	0.9280	0.8542	0.9205
NO-7A	8	0.8894	0.8194	0.7146	0.8676	0.8220	0.7681	0.8117
NO-7A	9	0.8539	0.7408	0.6542	0.7368	0.7347	0.7017	0.7195
NO-7A	10	0.8203	0.6615	0.6353	0.7105	0.6892	0.6543	0.6398
NO-7A	12	0.8490	0.8966	0.7805	0.9354	0.8975	0.8659	0.9286
NO-7A	13	0.8203	0.8174	0.7192	0.8339	0.7920	0.7663	0.8126
NO-7A	14	0.7927	0.7388	0.6542	0.7259	0.7084	0.6917	0.7253
NO-7A	15	0.7660	0.6602	0.6298	0.6969	0.6699	0.6542	0.6578
NO-7B	2	0.9023	0.7685	0.6985	0.7408	0.7578	0.7191	0.7158
NO-7B	3	0.8184	0.6905	0.6274	0.6768	0.6468	0.6493	0.6242
NO-7B	4	0.7443	0.6138	0.5645	0.5283	0.5616	0.5981	0.5570
NO-7B	5	0.6821	0.5371	0.5536	0.4994	0.5211	0.5504	0.5030
NO-7B	7	0.8213	0.7665	0.6930	0.7317	0.7306	0.6908	0.7312
NO-7B	8	0.7641	0.6866	0.6229	0.6378	0.6192	0.6383	0.6095
NO-7B	9	0.7098	0.6105	0.5593	0.5062	0.5409	0.5991	0.5378
NO-7B	10	0.6624	0.5338	0.5451	0.4822	0.5099	0.5561	0.4885
NO-7B	12	0.7611	0.7632	0.7015	0.7648	0.7022	0.6712	0.7957
NO-7B	13	0.7127	0.6859	0.6342	0.6384	0.5968	0.6422	0.6520
NO-7B	14	0.6703	0.6085	0.5617	0.5069	0.5233	0.6045	0.5755
NO-7B	15	0.6328	0.5249	0.5408	0.4693	0.5014	0.5458	0.5281

Appendix D3 Predictions of Resilient Modulus from Artificial Neural Network Models for Development Dataset (Continued)

Sample I.D.	Seq. No.	Experiment M_R/P_a (10^3)	Predicted M_R/P_a (10^3)					
			LN	GRNN	RBFN	MLPN-1	MLPN-2	MLPN-3
NO-8A	2	0.9812	1.1251	0.9516	1.1477	1.1731	1.0848	1.2338
NO-8A	3	0.9654	1.0453	0.9039	1.0680	1.1159	1.0525	1.2409
NO-8A	4	0.9447	0.9660	0.8589	0.9167	1.0586	0.9879	1.2175
NO-8A	5	0.9210	0.8855	0.8333	0.9036	1.0206	0.8870	1.1597
NO-8A	7	0.9102	1.1225	0.9764	1.1838	1.1557	1.0957	1.1540
NO-8A	8	0.9072	1.0433	0.9036	1.0891	1.0944	1.0183	1.1479
NO-8A	9	0.9023	0.9628	0.8515	0.9473	1.0336	0.9207	1.1111
NO-8A	10	0.8954	0.8823	0.8301	0.9192	0.9954	0.8415	1.0514
NO-8A	12	0.8134	1.1205	0.9516	1.1894	1.1372	1.1033	1.1157
NO-8A	13	0.8263	1.0400	0.9000	1.0890	1.0704	1.0549	1.0870
NO-8A	14	0.8272	0.9608	0.8464	0.9906	1.0086	0.9943	1.0406
NO-8A	15	0.8243	0.8815	0.8247	0.9713	0.9706	0.9229	0.9871
NO-8B	2	1.0533	1.0023	0.8640	0.9545	1.0116	1.0178	1.0734
NO-8B	3	1.0296	0.9218	0.8127	0.9498	0.9137	0.9092	1.0172
NO-8B	4	0.9970	0.8425	0.7626	0.8385	0.8200	0.7977	0.9385
NO-8B	5	0.9615	0.7633	0.7378	0.8266	0.7553	0.7187	0.8448
NO-8B	7	0.9990	0.9997	0.8597	0.9642	0.9830	0.9221	1.0448
NO-8B	8	0.9901	0.9192	0.8079	0.9125	0.8814	0.8328	0.9769
NO-8B	9	0.9714	0.8400	0.7589	0.8005	0.7880	0.7542	0.8991
NO-8B	10	0.9497	0.7594	0.7386	0.7797	0.7277	0.6989	0.8162
NO-8B	12	0.9279	0.9977	0.8462	0.9862	0.9538	0.9572	1.0300
NO-8B	13	0.9269	0.9172	0.8065	0.8982	0.8493	0.8570	0.9535
NO-8B	14	0.9151	0.8386	0.7568	0.8029	0.7578	0.7677	0.8821
NO-8B	15	0.9033	0.7587	0.7340	0.7779	0.7032	0.7177	0.8165
NO-9A	2	0.9062	0.8062	0.7230	0.8179	0.8351	0.8517	0.7018
NO-9A	3	0.8184	0.7270	0.6535	0.7317	0.7098	0.7347	0.6223
NO-9A	4	0.7433	0.6503	0.5879	0.6043	0.6144	0.6490	0.5807
NO-9A	5	0.6742	0.5711	0.5748	0.6208	0.5660	0.5770	0.5532
NO-9A	7	0.8282	0.8024	0.7152	0.8367	0.8111	0.8073	0.7153
NO-9A	8	0.7552	0.7244	0.6534	0.7489	0.6870	0.7098	0.6192
NO-9A	9	0.6920	0.6464	0.5903	0.6407	0.5942	0.6399	0.5737
NO-9A	10	0.6436	0.5697	0.5728	0.6514	0.5543	0.5792	0.5476
NO-9A	12	0.7532	0.8010	0.7229	0.8308	0.7921	0.8019	0.7901
NO-9A	13	0.6930	0.7230	0.6609	0.7342	0.6674	0.7294	0.6390
NO-9A	14	0.6417	0.6463	0.5955	0.6495	0.5796	0.6690	0.5750
NO-9A	15	0.6022	0.5684	0.5726	0.6496	0.5453	0.5930	0.5435
NO-9B	2	0.8213	0.6825	0.6738	0.7063	0.7096	0.6897	0.5922
NO-9B	3	0.7315	0.6058	0.6021	0.5944	0.5754	0.6259	0.5455
NO-9B	4	0.6417	0.5272	0.5325	0.4557	0.4819	0.5739	0.5246
NO-9B	5	0.5686	0.4479	0.5257	0.4865	0.4460	0.5241	0.5123
NO-9B	7	0.7502	0.6805	0.6666	0.7651	0.7078	0.6590	0.6115
NO-9B	8	0.6644	0.6012	0.6014	0.6282	0.5672	0.6121	0.5429
NO-9B	9	0.5933	0.5226	0.5357	0.4845	0.4767	0.5690	0.5192
NO-9B	10	0.5400	0.4434	0.5235	0.4939	0.4470	0.5209	0.5078
NO-9B	12	0.6969	0.6779	0.6780	0.8253	0.7091	0.6817	0.6774
NO-9B	13	0.6190	0.6005	0.6133	0.6773	0.5688	0.6254	0.5544
NO-9B	14	0.5587	0.5194	0.5404	0.5269	0.4766	0.5661	0.5143
NO-9B	15	0.5094	0.4433	0.5245	0.4945	0.4516	0.5074	0.5018

Appendix D3 Predictions of Resilient Modulus from Artificial Neural Network Models for Development Dataset (Continued)

Sample I.D.	Seq. No.	Experiment M_R/P_a (10^3)	Predicted M_R/P_a (10^3)					
			LN	**GRNN**	**RBFN**	**MLPN-1**	**MLPN-2**	**MLPN-3**
OK-1A	2	1.2981	0.8299	0.7131	0.9103	0.9384	1.0379	0.9556
OK-1A	3	0.9566	0.7734	0.6520	0.7945	0.8599	0.9426	0.8716
OK-1A	4	0.7522	0.7056	0.5902	0.6462	0.7614	0.7948	0.7743
OK-1A	5	0.6387	0.6270	0.5777	0.6414	0.6576	0.6070	0.6666
OK-1A	7	1.1362	0.8348	0.7156	0.9079	0.9434	1.0403	0.9283
OK-1A	8	0.9339	0.7727	0.6549	0.8001	0.8554	0.9378	0.8355
OK-1A	9	0.7700	0.7017	0.5930	0.6778	0.7524	0.7859	0.7460
OK-1A	10	0.6663	0.6244	0.5775	0.6852	0.6549	0.6178	0.6599
OK-1A	12	1.2873	0.8569	0.7446	0.9503	0.9681	1.0119	1.0058
OK-1A	13	1.3376	0.7777	0.6764	0.8004	0.8551	0.9218	0.8613
OK-1A	14	1.0928	0.6953	0.6014	0.6662	0.7364	0.8107	0.7693
OK-1A	15	0.8638	0.6142	0.5853	0.6700	0.6428	0.6547	0.7008
OK-1B	2	0.6051	0.6619	0.6329	0.5776	0.6398	0.6788	0.4361
OK-1B	3	0.4768	0.6061	0.5717	0.4490	0.5318	0.5446	0.3678
OK-1B	4	0.3524	0.5440	0.4998	0.2941	0.4165	0.4033	0.3175
OK-1B	5	0.2883	0.4800	0.4632	0.2208	0.3107	0.2744	0.2791
OK-1B	7	0.5982	0.6650	0.6268	0.5269	0.6628	0.6867	0.4092
OK-1B	8	0.4432	0.6105	0.5765	0.4133	0.5563	0.5642	0.3327
OK-1B	9	0.3327	0.5439	0.5036	0.2840	0.4337	0.4282	0.2923
OK-1B	10	0.2794	0.4793	0.4643	0.2366	0.3302	0.3077	0.2708
OK-1B	12	0.5864	0.6643	0.6401	0.5902	0.6754	0.6925	0.5850
OK-1B	13	0.4255	0.6104	0.5907	0.4540	0.5700	0.5902	0.4598
OK-1B	14	0.3208	0.5451	0.5149	0.3151	0.4516	0.4547	0.4121
OK-1B	15	0.2715	0.4785	0.4667	0.2456	0.3496	0.3145	0.3927
OK-2A	2	0.6486	0.8137	0.6586	0.6921	0.7055	0.7100	0.6559
OK-2A	3	0.5370	0.7604	0.6191	0.6490	0.6457	0.6665	0.6130
OK-2A	4	0.4462	0.6844	0.5746	0.5620	0.6032	0.6215	0.5775
OK-2A	5	0.4067	0.6077	0.5652	0.6048	0.6109	0.5828	0.5549
OK-2A	7	0.5400	0.8269	0.6453	0.6252	0.6979	0.7115	0.6490
OK-2A	8	0.4452	0.7654	0.6125	0.6025	0.6257	0.6673	0.5870
OK-2A	9	0.4107	0.6830	0.5698	0.5478	0.5817	0.6214	0.5514
OK-2A	10	0.3988	0.6063	0.5591	0.5886	0.5904	0.5822	0.5338
OK-2A	12	0.5005	0.8281	0.6406	0.5481	0.6778	0.6962	0.6646
OK-2A	13	0.4067	0.7602	0.6059	0.5377	0.6007	0.6528	0.5795
OK-2A	14	0.3850	0.6823	0.5668	0.5398	0.5654	0.6215	0.5449
OK-2A	15	0.3830	0.6056	0.5554	0.5965	0.5752	0.5797	0.5285
OK-2B	2	0.5676	0.6099	0.6177	0.5801	0.6011	0.5784	0.5647
OK-2B	3	0.3781	0.5427	0.5621	0.4868	0.5098	0.5446	0.5329
OK-2B	4	0.3366	0.4667	0.5055	0.3788	0.4613	0.5080	0.5179
OK-2B	5	0.3416	0.3881	0.5002	0.4328	0.4765	0.4678	0.5094
OK-2B	7	0.5439	0.6117	0.6048	0.5686	0.6157	0.5767	0.5622
OK-2B	8	0.3820	0.5382	0.5583	0.4664	0.5117	0.5417	0.5195
OK-2B	9	0.3534	0.4590	0.5055	0.3693	0.4645	0.5016	0.5063
OK-2B	10	0.3504	0.3829	0.4968	0.4200	0.4806	0.4585	0.5006
OK-2B	12	0.5183	0.6085	0.6087	0.5860	0.6279	0.5678	0.5493
OK-2B	13	0.3840	0.5356	0.5623	0.4821	0.5214	0.5236	0.5109
OK-2B	14	0.3593	0.4583	0.5082	0.3968	0.4744	0.4731	0.5003
OK-2B	15	0.3603	0.3809	0.4972	0.4156	0.4882	0.4203	0.4960

Appendix D3 Predictions of Resilient Modulus from Artificial Neural Network Models for Development Dataset (Continued)

Sample I.D.	Seq. No.	Experiment M_R/P_a (10^3)	Predicted M_R/P_a (10^3)					
			LN	GRNN	RBFN	MLPN-1	MLPN-2	MLPN-3
OK-3A	2	0.9003	0.9684	0.7701	0.9733	1.0094	1.0146	0.8771
OK-3A	3	0.7502	0.8942	0.7028	0.9246	0.9222	0.8908	0.8242
OK-3A	4	0.6160	0.8486	0.6673	0.8515	0.8713	0.8147	0.7904
OK-3A	5	0.5163	0.7668	0.6407	0.8010	0.8050	0.7073	0.7296
OK-3A	7	0.8677	0.9715	0.7586	0.9255	0.9897	0.9534	0.8853
OK-3A	8	0.6920	0.9017	0.7020	0.9210	0.9048	0.8644	0.8345
OK-3A	9	0.5676	0.8485	0.6621	0.8698	0.8443	0.8030	0.7919
OK-3A	10	0.4946	0.7648	0.6346	0.8245	0.7794	0.7117	0.7250
OK-3A	12	0.8421	0.9707	0.7611	0.8468	0.9645	0.9554	0.8940
OK-3A	13	0.6683	0.9017	0.7049	0.8577	0.8779	0.8685	0.8389
OK-3A	14	0.5429	0.8465	0.6603	0.8402	0.8156	0.7994	0.7900
OK-3A	15	0.4729	0.7635	0.6275	0.8135	0.7555	0.7131	0.7223
OK-3B	2	0.7789	0.7064	0.6458	0.6897	0.6942	0.6512	0.6324
OK-3B	3	0.5143	0.6512	0.5930	0.6191	0.6036	0.5889	0.5859
OK-3B	4	0.3613	0.5891	0.5266	0.4861	0.5158	0.5293	0.5523
OK-3B	5	0.3277	0.5175	0.4911	0.3819	0.4454	0.4683	0.5245
OK-3B	7	0.7443	0.7082	0.6367	0.6094	0.6883	0.6472	0.6587
OK-3B	8	0.4590	0.6537	0.5923	0.5584	0.5993	0.5945	0.5793
OK-3B	9	0.3504	0.5865	0.5242	0.4639	0.5081	0.5368	0.5271
OK-3B	10	0.3139	0.5136	0.4855	0.3968	0.4449	0.4749	0.4946
OK-3B	12	0.9013	0.7100	0.6524	0.5868	0.6822	0.6237	0.7498
OK-3B	13	0.5499	0.6491	0.6014	0.5151	0.5842	0.5786	0.6060
OK-3B	14	0.3791	0.5838	0.5282	0.4368	0.5006	0.5243	0.5365
OK-3B	15	0.3307	0.5116	0.4818	0.3745	0.4461	0.4530	0.5020
OK-4A	2	0.6565	0.6902	0.6829	0.7833	0.6996	0.7061	0.6193
OK-4A	3	0.4531	0.6287	0.6207	0.6700	0.5974	0.6192	0.5700
OK-4A	4	0.3682	0.5641	0.5520	0.5232	0.5067	0.5370	0.5364
OK-4A	5	0.3248	0.4931	0.5213	0.4677	0.4431	0.4502	0.5100
OK-4A	7	0.6120	0.6914	0.6795	0.7678	0.6979	0.7054	0.6282
OK-4A	8	0.4610	0.6331	0.6276	0.6705	0.6019	0.6327	0.5657
OK-4A	9	0.3722	0.5615	0.5547	0.5441	0.5060	0.5520	0.5252
OK-4A	10	0.3337	0.4879	0.5202	0.5146	0.4505	0.4660	0.5015
OK-4A	12	0.6140	0.6894	0.6949	0.7863	0.6888	0.6657	0.6788
OK-4A	13	0.4659	0.6292	0.6384	0.6674	0.5921	0.6119	0.5819
OK-4A	14	0.3771	0.5588	0.5609	0.5454	0.5047	0.5473	0.5319
OK-4A	15	0.3396	0.4853	0.5209	0.5028	0.4589	0.4561	0.5084
OK-4B	2	0.5252	0.6005	0.6443	0.6043	0.5893	0.5785	0.5294
OK-4B	3	0.3327	0.5403	0.5804	0.5082	0.4866	0.5219	0.4943
OK-4B	4	0.2458	0.4883	0.5175	0.3915	0.4142	0.4772	0.4761
OK-4B	5	0.2172	0.4255	0.4735	0.2878	0.3522	0.4251	0.4603
OK-4B	7	0.4492	0.6067	0.6468	0.6063	0.6074	0.5829	0.5451
OK-4B	8	0.2853	0.5516	0.5987	0.5212	0.5113	0.5395	0.4895
OK-4B	9	0.2320	0.4876	0.5242	0.4040	0.4229	0.4901	0.4628
OK-4B	10	0.2142	0.4236	0.4751	0.3196	0.3649	0.4379	0.4517
OK-4B	12	0.4353	0.6060	0.6707	0.6748	0.6134	0.5803	0.6346
OK-4B	13	0.2794	0.5509	0.6218	0.5629	0.5176	0.5345	0.5295
OK-4B	14	0.2280	0.4881	0.5410	0.4401	0.4331	0.4759	0.4848
OK-4B	15	0.2132	0.4209	0.4795	0.3399	0.3776	0.4084	0.4702

Appendix D3 Predictions of Resilient Modulus from Artificial Neural Network Models for Development Dataset (Continued)

Sample I.D.	Seq. No.	Experiment M_R/P_a (10^3)	Predicted M_R/P_a (10^3)					
			LN	GRNN	RBFN	MLPN-1	MLPN-2	MLPN-3
OK-5A	2	0.7187	0.7437	0.6942	0.8782	0.7670	0.7374	0.6628
OK-5A	3	0.6219	0.6752	0.6282	0.7614	0.6751	0.6615	0.6088
OK-5A	4	0.5311	0.6175	0.5788	0.6409	0.6179	0.6112	0.5749
OK-5A	5	0.4551	0.5440	0.5577	0.6120	0.5842	0.5526	0.5406
OK-5A	7	0.6900	0.7430	0.6851	0.8272	0.7470	0.7166	0.6563
OK-5A	8	0.5716	0.6802	0.6301	0.7413	0.6643	0.6695	0.5978
OK-5A	9	0.4965	0.6193	0.5787	0.6488	0.6072	0.6253	0.5595
OK-5A	10	0.4462	0.5407	0.5519	0.6398	0.5782	0.5658	0.5246
OK-5A	12	0.6930	0.7448	0.6955	0.8027	0.7297	0.6909	0.6819
OK-5A	13	0.5696	0.6801	0.6370	0.7066	0.6469	0.6358	0.6060
OK-5A	14	0.4877	0.6180	0.5796	0.6262	0.5943	0.5986	0.5638
OK-5A	15	0.4393	0.5388	0.5467	0.6128	0.5727	0.5548	0.5310
OK-5B	2	0.4798	0.8014	0.7041	0.8125	0.7952	0.7350	0.7271
OK-5B	3	0.4136	0.7292	0.6412	0.7532	0.6948	0.6634	0.6562
OK-5B	4	0.3791	0.6531	0.5796	0.6030	0.6121	0.6087	0.5987
OK-5B	5	0.3771	0.5732	0.5649	0.5661	0.5747	0.5579	0.5495
OK-5B	7	0.4541	0.8045	0.6959	0.7545	0.7742	0.7177	0.7521
OK-5B	8	0.3781	0.7329	0.6394	0.6957	0.6749	0.6618	0.6521
OK-5B	9	0.3662	0.6530	0.5741	0.5759	0.5921	0.6127	0.5770
OK-5B	10	0.3702	0.5744	0.5547	0.5464	0.5619	0.5663	0.5240
OK-5B	12	0.6920	0.8120	0.7063	0.7460	0.7599	0.6924	0.8174
OK-5B	13	0.5647	0.7366	0.6518	0.6553	0.6556	0.6378	0.6804
OK-5B	14	0.5202	0.6580	0.5785	0.5552	0.5769	0.6079	0.5973
OK-5B	15	0.4650	0.5769	0.5475	0.5106	0.5504	0.5647	0.5454
OS-1A	2	0.7616	0.9779	0.7926	0.8621	0.9219	0.9059	0.8693
OS-1A	3	0.7347	0.9036	0.7406	0.8478	0.8298	0.7969	0.8095
OS-1A	4	0.7034	0.8205	0.6908	0.7310	0.7512	0.7105	0.7429
OS-1A	5	0.6464	0.7462	0.6735	0.7428	0.7228	0.6654	0.6868
OS-1A	7	0.7663	0.9752	0.7749	0.8073	0.8892	0.8299	0.8459
OS-1A	8	0.7291	0.9053	0.7313	0.7993	0.8012	0.7633	0.7919
OS-1A	9	0.6949	0.8223	0.6839	0.7157	0.7244	0.7009	0.7268
OS-1A	10	0.6576	0.7480	0.6674	0.7129	0.6988	0.6639	0.6727
OS-1A	12	0.7794	0.9726	0.7700	0.7494	0.8563	0.8643	0.8489
OS-1A	13	0.7351	0.9071	0.7318	0.7441	0.7735	0.7820	0.7936
OS-1A	14	0.7017	0.8197	0.6790	0.7140	0.6971	0.6973	0.7214
OS-1A	15	0.6650	0.7497	0.6584	0.7234	0.6773	0.6660	0.6716
OS-1B	2	0.6827	0.6044	0.6271	0.5574	0.5521	0.5418	0.5440
OS-1B	3	0.4650	0.5476	0.5693	0.4855	0.4791	0.5000	0.5197
OS-1B	4	0.3348	0.4864	0.5062	0.3678	0.4237	0.4571	0.5012
OS-1B	5	0.2919	0.4165	0.4764	0.3000	0.4006	0.4082	0.4838
OS-1B	7	0.6241	0.6062	0.6247	0.5178	0.5483	0.5536	0.5433
OS-1B	8	0.4504	0.5493	0.5739	0.4472	0.4767	0.5154	0.5071
OS-1B	9	0.3429	0.4794	0.5029	0.3447	0.4194	0.4666	0.4827
OS-1B	10	0.3000	0.4095	0.4705	0.3105	0.4066	0.4139	0.4677
OS-1B	12	0.6456	0.6035	0.6432	0.5503	0.5401	0.5402	0.5765
OS-1B	13	0.4680	0.5467	0.5893	0.4561	0.4711	0.4986	0.5242
OS-1B	14	0.3535	0.4768	0.5093	0.3517	0.4195	0.4389	0.4955
OS-1B	15	0.3095	0.4069	0.4687	0.3059	0.4137	0.3751	0.4830

Appendix D3 Predictions of Resilient Modulus from Artificial Neural Network Models for Development Dataset (Continued)

Sample I.D.	Seq. No.	Experiment M_R/P_a (10^3)	Predicted M_R/P_a (10^3)					
			LN	GRNN	RBFN	MLPN-1	MLPN-2	MLPN-3
OS-2A	2	0.9033	1.0623	0.9128	1.2409	1.1647	1.1346	1.1799
OS-2A	3	0.8880	0.9705	0.8409	1.1547	1.0921	1.1015	1.1667
OS-2A	4	0.8595	0.9006	0.8078	1.0610	1.0302	1.0280	1.1346
OS-2A	5	0.8288	0.8569	0.7973	1.0659	0.9944	0.9661	1.1049
OS-2A	7	0.9355	1.0597	0.9346	1.2302	1.1486	1.0952	1.1626
OS-2A	8	0.9149	0.9591	0.8405	1.1298	1.0623	1.0343	1.1142
OS-2A	9	0.8706	0.8936	0.8087	1.0572	1.0018	0.9744	1.0730
OS-2A	10	0.8420	0.8455	0.7992	1.0703	0.9631	0.9132	1.0386
OS-2A	12	0.9561	1.0570	0.9334	1.1970	1.1306	1.1001	1.1297
OS-2A	13	0.9297	0.9609	0.8534	1.0997	1.0427	1.0438	1.0672
OS-2A	14	0.8885	0.8866	0.8124	1.0362	0.9719	0.9804	1.0246
OS-2A	15	0.8576	0.8385	0.8025	1.0508	0.9345	0.9325	0.9978
OS-2B	2	0.6423	0.7310	0.6656	0.7799	0.8260	0.8468	0.7421
OS-2B	3	0.5037	0.6742	0.6078	0.6567	0.7345	0.7434	0.6500
OS-2B	4	0.4012	0.6086	0.5388	0.4916	0.6280	0.6262	0.5509
OS-2B	5	0.3361	0.5387	0.5066	0.4144	0.5246	0.5067	0.4528
OS-2B	7	0.6631	0.7327	0.6614	0.7674	0.8272	0.8383	0.7082
OS-2B	8	0.5229	0.6715	0.6066	0.6279	0.7284	0.7291	0.6232
OS-2B	9	0.4226	0.6060	0.5407	0.4821	0.6239	0.6271	0.5467
OS-2B	10	0.3585	0.5317	0.5057	0.4256	0.5210	0.5215	0.4696
OS-2B	12	0.6853	0.7301	0.6711	0.8358	0.8173	0.7936	0.8008
OS-2B	13	0.5431	0.6645	0.6127	0.6552	0.7114	0.7157	0.7105
OS-2B	14	0.4359	0.6034	0.5488	0.5078	0.6165	0.6472	0.6523
OS-2B	15	0.3722	0.5291	0.5082	0.4283	0.5208	0.5407	0.5959
OS-3A	2	1.7709	0.9249	0.7958	1.1095	0.9543	0.8909	0.9197
OS-3A	3	1.0771	0.8463	0.7252	1.0195	0.8612	0.7814	0.8427
OS-3A	4	0.8822	0.7894	0.6823	0.8936	0.8057	0.7198	0.7850
OS-3A	5	0.7090	0.7195	0.6575	0.8198	0.7663	0.6690	0.7145
OS-3A	7	1.6532	0.9354	0.7950	1.0380	0.9407	0.8473	0.9412
OS-3A	8	1.0141	0.8436	0.7146	0.9578	0.8303	0.7410	0.8321
OS-3A	9	0.8543	0.7912	0.6766	0.8678	0.7806	0.7103	0.7705
OS-3A	10	0.7065	0.7169	0.6505	0.8009	0.7426	0.6703	0.6876
OS-3A	12	1.6654	0.9240	0.7913	0.9620	0.8991	0.8529	0.9217
OS-3A	13	1.0252	0.8410	0.7158	0.8869	0.7995	0.7551	0.8168
OS-3A	14	0.8647	0.7886	0.6734	0.8244	0.7529	0.7051	0.7587
OS-3A	15	0.7078	0.7143	0.6420	0.7753	0.7203	0.6545	0.6867
OS-3B	2	0.5180	0.6450	0.6425	0.6107	0.6105	0.5755	0.5705
OS-3B	3	0.3318	0.5926	0.5970	0.5596	0.5373	0.5317	0.5351
OS-3B	4	0.2556	0.5270	0.5260	0.4380	0.4658	0.4798	0.5032
OS-3B	5	0.2518	0.4571	0.4830	0.3325	0.4260	0.4251	0.4757
OS-3B	7	0.4928	0.6468	0.6371	0.5595	0.6001	0.5869	0.5622
OS-3B	8	0.3119	0.5943	0.5976	0.4927	0.5288	0.5493	0.5048
OS-3B	9	0.2603	0.5244	0.5246	0.3875	0.4578	0.4972	0.4611
OS-3B	10	0.2501	0.4501	0.4757	0.3166	0.4260	0.4378	0.4330
OS-3B	12	0.5018	0.6441	0.6545	0.6015	0.5840	0.5632	0.6204
OS-3B	13	0.3208	0.5873	0.6095	0.4908	0.5105	0.5312	0.5337
OS-3B	14	0.2666	0.5174	0.5282	0.3734	0.4479	0.4758	0.4849
OS-3B	15	0.2567	0.4431	0.4724	0.3020	0.4282	0.4040	0.4626

Appendix D3 Predictions of Resilient Modulus from Artificial Neural Network Models for Development Dataset (Continued)

Sample I.D.	Seq. No.	Experiment M_R/P_a (10^3)	Predicted M_R/P_a (10^3)					
			LN	GRNN	RBFN	MLPN-1	MLPN-2	MLPN-3
RO-1A	2	0.7947	0.7583	0.7113	0.8998	0.8590	0.8299	0.8754
RO-1A	3	0.7236	0.6727	0.6304	0.7445	0.7264	0.6727	0.7388
RO-1A	4	0.6456	0.5878	0.5719	0.5858	0.5949	0.5267	0.6024
RO-1A	5	0.5735	0.5041	0.5716	0.6713	0.4939	0.3910	0.4719
RO-1A	7	0.7493	0.7594	0.6969	0.8087	0.8591	0.8259	0.7807
RO-1A	8	0.6960	0.6739	0.6284	0.6795	0.7263	0.6816	0.6532
RO-1A	9	0.6347	0.5889	0.5696	0.5708	0.5982	0.5548	0.5376
RO-1A	10	0.5765	0.5040	0.5657	0.6686	0.5036	0.4288	0.4278
RO-1A	12	0.7048	0.7600	0.6944	0.8187	0.8536	0.7704	0.8087
RO-1A	13	0.6654	0.6738	0.6296	0.6603	0.7199	0.6620	0.6935
RO-1A	14	0.6160	0.5895	0.5672	0.5498	0.5969	0.5665	0.6107
RO-1A	15	0.5627	0.5045	0.5590	0.6091	0.5111	0.4363	0.5350
RO-1B	2	0.7423	0.6724	0.6578	0.7617	0.7207	0.6424	0.6626
RO-1B	3	0.6703	0.5862	0.5694	0.6303	0.5780	0.5312	0.5148
RO-1B	4	0.5824	0.5025	0.5099	0.4898	0.4553	0.4374	0.3929
RO-1B	5	0.5035	0.4176	0.5121	0.5826	0.3684	0.3478	0.2875
RO-1B	7	0.6811	0.6736	0.6476	0.6477	0.7147	0.6340	0.5720
RO-1B	8	0.6298	0.5874	0.5713	0.5478	0.5747	0.5442	0.4330
RO-1B	9	0.5656	0.5031	0.5089	0.4618	0.4573	0.4632	0.3300
RO-1B	10	0.5044	0.4181	0.5059	0.5686	0.3800	0.3756	0.2438
RO-1B	12	0.6061	0.6735	0.6517	0.6533	0.7041	0.6314	0.6550
RO-1B	13	0.5726	0.5873	0.5774	0.5252	0.5671	0.5502	0.5198
RO-1B	14	0.5262	0.5043	0.5079	0.4412	0.4577	0.4569	0.4417
RO-1B	15	0.4778	0.4187	0.4981	0.5146	0.3894	0.3520	0.3772

Appendix D4 Predictions of Resilient Modulus from Artificial Neural Network Models for Evaluation Dataset

Sample I.D.	Seq. No.	Experiment M_R/P_a (10^3)	Predicted M_R/P_a (10^3)					
			LN	GRNN	RBFN	MLPN-1	MLPN-2	MLPN-3
ROE-1A	2	1.0139	0.8737	0.7358	0.7971	0.8677	0.8728	1.1526
ROE-1A	3	0.8616	0.8081	0.6721	0.6828	0.7689	0.7470	0.9441
ROE-1A	4	0.6413	0.7382	0.6006	0.5403	0.6554	0.5995	0.7767
ROE-1A	5	0.5363	0.6727	0.5798	0.4917	0.5450	0.4529	0.6743
ROE-1A	7	0.9401	0.8754	0.7172	0.7144	0.8984	0.9146	1.1530
ROE-1A	8	0.7985	0.8143	0.6717	0.6448	0.8025	0.8016	0.9353
ROE-1A	9	0.6222	0.7443	0.6064	0.5571	0.6856	0.6489	0.7033
ROE-1A	10	0.5447	0.6700	0.5795	0.5279	0.5578	0.4705	0.5754
ROE-1A	12	0.9638	0.8728	0.7190	0.6993	0.9186	0.9314	1.1479
ROE-1A	13	0.8052	0.8116	0.6748	0.6195	0.8187	0.8208	0.9590
ROE-1A	14	0.6282	0.7417	0.6091	0.5414	0.6984	0.6722	0.6884
ROE-1A	15	0.5499	0.6718	0.5785	0.5051	0.5768	0.5162	0.5799
ROE-1B	2	0.7654	0.7907	0.6886	0.7118	0.8173	0.8399	0.9013
ROE-1B	3	0.5494	0.7339	0.6333	0.6263	0.7026	0.7439	0.6951
ROE-1B	4	0.4079	0.6684	0.5536	0.4943	0.5709	0.6223	0.4729
ROE-1B	5	0.3420	0.6072	0.5087	0.4035	0.4516	0.5031	0.3523
ROE-1B	7	0.7016	0.7925	0.6721	0.5979	0.8485	0.8610	0.9011
ROE-1B	8	0.5129	0.7357	0.6288	0.5371	0.7289	0.7564	0.7501
ROE-1B	9	0.3966	0.6701	0.5580	0.4602	0.5938	0.6248	0.4747
ROE-1B	10	0.3444	0.6046	0.5124	0.4076	0.4650	0.4932	0.2872
ROE-1B	12	0.7123	0.7942	0.6792	0.5997	0.8778	0.8866	0.8649
ROE-1B	13	0.5296	0.7331	0.6350	0.5133	0.7439	0.7907	0.8342
ROE-1B	14	0.4009	0.6675	0.5630	0.4412	0.6063	0.6741	0.5446
ROE-1B	15	0.3462	0.6019	0.5123	0.3937	0.4779	0.5490	0.3405
ROE-2A	2	1.1676	0.8688	0.7384	0.8787	0.8955	0.9361	0.7750
ROE-2A	3	1.0440	0.7945	0.6682	0.7470	0.7730	0.8125	0.6694
ROE-2A	4	0.8597	0.7289	0.6194	0.6187	0.6767	0.7082	0.6198
ROE-2A	5	0.6666	0.6415	0.6177	0.6462	0.5897	0.5879	0.5795
ROE-2A	7	1.1112	0.8662	0.7206	0.8629	0.8794	0.9246	0.8512
ROE-2A	8	0.9804	0.7962	0.6661	0.7850	0.7608	0.8155	0.6978
ROE-2A	9	0.7829	0.7219	0.6145	0.6672	0.6527	0.7058	0.6230
ROE-2A	10	0.6675	0.6389	0.6083	0.6633	0.5775	0.5940	0.5787
ROE-2A	12	1.1033	0.8723	0.7203	0.8100	0.8791	0.9093	1.0102
ROE-2A	13	0.9772	0.7936	0.6630	0.7632	0.7420	0.8325	0.7381
ROE-2A	14	0.7803	0.7237	0.6077	0.6844	0.6412	0.7548	0.6367
ROE-2A	15	0.6724	0.6406	0.5925	0.6345	0.5698	0.6424	0.5804
ROE-2B	2	1.1467	0.8352	0.7439	0.8841	0.8641	0.8894	0.7492
ROE-2B	3	0.9982	0.7696	0.6832	0.7692	0.7415	0.7971	0.6409
ROE-2B	4	0.7393	0.7041	0.6197	0.6274	0.6374	0.7148	0.5913
ROE-2B	5	0.6224	0.6341	0.5955	0.5695	0.5572	0.6409	0.5620
ROE-2B	7	1.1326	0.8325	0.7268	0.8753	0.8517	0.8622	0.8636
ROE-2B	8	0.9500	0.7714	0.6821	0.7994	0.7332	0.7827	0.6763
ROE-2B	9	0.7046	0.7014	0.6195	0.6753	0.6209	0.7036	0.5960
ROE-2B	10	0.6210	0.6315	0.5920	0.6022	0.5438	0.6352	0.5600
ROE-2B	12	1.1828	0.8343	0.7285	0.8279	0.8511	0.8764	1.0869
ROE-2B	13	0.9536	0.7687	0.6835	0.7736	0.7197	0.8232	0.7310
ROE-2B	14	0.7060	0.7032	0.6204	0.6932	0.6135	0.7633	0.6125
ROE-2B	15	0.6260	0.6332	0.5832	0.6118	0.5375	0.6887	0.5617

Appendix D4 Predictions of Resilient Modulus from Artificial Neural Network Models for Evaluation Dataset (Continued)

Sample I.D.	Seq. No.	Experiment M_R/P_a (10^3)	Predicted M_R/P_a (10^3)					
			LN	GRNN	RBFN	MLPN-1	MLPN-2	MLPN-3
ROE-3A	2	1.0171	0.8469	0.7251	0.9387	0.8874	0.8814	0.7345
ROE-3A	3	0.9580	0.7770	0.6720	0.8648	0.7872	0.7626	0.6645
ROE-3A	4	0.7696	0.7027	0.6052	0.7119	0.6963	0.6596	0.6164
ROE-3A	5	0.6861	0.6284	0.5798	0.6481	0.6437	0.5789	0.5823
ROE-3A	7	0.9873	0.8399	0.7066	0.8842	0.8587	0.8259	0.7367
ROE-3A	8	0.9119	0.7788	0.6655	0.8408	0.7702	0.7534	0.6639
ROE-3A	9	0.7405	0.7045	0.6046	0.7419	0.6812	0.6706	0.6099
ROE-3A	10	0.6924	0.6302	0.5748	0.6911	0.6328	0.5954	0.5745
ROE-3A	12	1.0118	0.8417	0.7113	0.8192	0.8417	0.8004	0.7804
ROE-3A	13	0.9258	0.7761	0.6676	0.7728	0.7466	0.7187	0.6760
ROE-3A	14	0.7534	0.7062	0.6063	0.7159	0.6659	0.6489	0.6128
ROE-3A	15	0.7037	0.6275	0.5693	0.6783	0.6211	0.5840	0.5714
ROE-3B	2	0.8904	0.6046	0.6425	0.6305	0.5623	0.5488	0.5473
ROE-3B	3	0.7612	0.5347	0.5738	0.5008	0.4398	0.4803	0.5195
ROE-3B	4	0.6341	0.4473	0.4877	0.3176	0.3348	0.4054	0.5022
ROE-3B	5	0.5735	0.3774	0.4762	0.3326	0.3029	0.3480	0.4927
ROE-3B	7	0.8267	0.6020	0.6323	0.5660	0.5715	0.5518	0.5494
ROE-3B	8	0.6836	0.5321	0.5728	0.4607	0.4511	0.4903	0.5099
ROE-3B	9	0.5891	0.4447	0.4893	0.3349	0.3530	0.4143	0.4908
ROE-3B	10	0.5644	0.3704	0.4719	0.3753	0.3280	0.3479	0.4827
ROE-3B	12	0.8254	0.5994	0.6483	0.5732	0.5816	0.5285	0.5783
ROE-3B	13	0.6665	0.5295	0.5850	0.4566	0.4630	0.4672	0.5152
ROE-3B	14	0.5790	0.4464	0.4949	0.3432	0.3746	0.3834	0.4906
ROE-3B	15	0.5580	0.3721	0.4682	0.3441	0.3537	0.3048	0.4840
ROE-4A	2	0.8239	0.6151	0.6364	0.5424	0.5871	0.6765	0.2627
ROE-4A	3	0.5647	0.5495	0.5727	0.3837	0.4561	0.5324	0.2119
ROE-4A	4	0.4633	0.4883	0.4945	0.2296	0.3411	0.3984	0.1851
ROE-4A	5	0.3799	0.4315	0.4449	0.1460	0.2462	0.2815	0.1684
ROE-4A	7	0.7610	0.6168	0.6313	0.5595	0.6120	0.6842	0.3137
ROE-4A	8	0.5415	0.5600	0.5870	0.3948	0.4968	0.5689	0.2647
ROE-4A	9	0.4275	0.4944	0.5090	0.2278	0.3729	0.4458	0.2466
ROE-4A	10	0.3672	0.4333	0.4516	0.1413	0.2723	0.3340	0.2408
ROE-4A	12	0.7629	0.6186	0.6499	0.7450	0.6350	0.6869	0.5551
ROE-4A	13	0.5439	0.5574	0.6037	0.5190	0.5105	0.5882	0.4362
ROE-4A	14	0.4199	0.4962	0.5285	0.3254	0.3966	0.4731	0.4027
ROE-4A	15	0.3609	0.4350	0.4621	0.1984	0.2989	0.3478	0.3910
ROE-4B	2	0.4081	0.5468	0.6344	0.4628	0.4846	0.5221	-0.0053
ROE-4B	3	0.2667	0.4944	0.5889	0.3575	0.3707	0.4213	-0.0302
ROE-4B	4	0.2209	0.4419	0.5190	0.2408	0.2664	0.3273	-0.0270
ROE-4B	5	0.2010	0.3895	0.4532	0.1370	0.1735	0.2423	-0.0168
ROE-4B	7	0.4021	0.5486	0.6293	0.4434	0.5183	0.5296	0.0645
ROE-4B	8	0.2718	0.4917	0.5890	0.2992	0.3933	0.4396	-0.0021
ROE-4B	9	0.2239	0.4393	0.5250	0.1848	0.2895	0.3619	0.0080
ROE-4B	10	0.2084	0.3825	0.4551	0.0959	0.1915	0.2801	0.0325
ROE-4B	12	0.4378	0.5416	0.6435	0.6030	0.5324	0.5336	0.3644
ROE-4B	13	0.2776	0.4891	0.6077	0.4266	0.4169	0.4481	0.2149
ROE-4B	14	0.2283	0.4323	0.5369	0.2678	0.3064	0.3535	0.2033
ROE-4B	15	0.2135	0.3799	0.4661	0.1621	0.2189	0.2672	0.2172

Appendix D4 Predictions of Resilient Modulus from Artificial Neural Network Models for Evaluation Dataset (Continued)

Sample I.D.	Seq. No.	Experiment M_R/P_a (10^3)	Predicted M_R/P_a (10^3)					
			LN	GRNN	RBFN	MLPN-1	MLPN-2	MLPN-3
ROE-5A	2	0.7805	0.7154	0.6515	0.6895	0.5582	0.6688	0.6153
ROE-5A	3	0.6190	0.6586	0.6074	0.5287	0.4398	0.5271	0.5720
ROE-5A	4	0.4922	0.5886	0.5299	0.3244	0.3079	0.3635	0.5423
ROE-5A	5	0.4436	0.5231	0.4867	0.2323	0.2100	0.2341	0.5258
ROE-5A	7	0.7132	0.7171	0.6137	0.5913	0.5904	0.6760	0.6353
ROE-5A	8	0.5619	0.6559	0.5811	0.4572	0.4583	0.5349	0.5596
ROE-5A	9	0.4739	0.5860	0.5164	0.3070	0.3246	0.3800	0.5187
ROE-5A	10	0.4421	0.5204	0.4738	0.2357	0.2285	0.2533	0.5012
ROE-5A	12	0.7145	0.7145	0.6036	0.6077	0.6140	0.6180	0.7169
ROE-5A	13	0.5600	0.6577	0.5732	0.4892	0.4880	0.5129	0.5826
ROE-5A	14	0.4727	0.5878	0.5062	0.3538	0.3527	0.3800	0.5077
ROE-5A	15	0.4443	0.5178	0.4536	0.2570	0.2525	0.2504	0.4829
ROE-5B	2	0.7589	0.6479	0.6192	0.5922	0.5494	0.6673	0.5417
ROE-5B	3	0.5233	0.5867	0.5626	0.4410	0.4055	0.5693	0.5146
ROE-5B	4	0.4247	0.5211	0.4844	0.2665	0.2758	0.4782	0.5014
ROE-5B	5	0.3707	0.4599	0.4416	0.1816	0.1826	0.4054	0.4945
ROE-5B	7	0.6718	0.6540	0.5848	0.4760	0.6030	0.6726	0.5321
ROE-5B	8	0.4763	0.5928	0.5483	0.3698	0.4528	0.5804	0.4719
ROE-5B	9	0.3921	0.5272	0.4834	0.2525	0.3189	0.4945	0.4532
ROE-5B	10	0.3603	0.4573	0.4356	0.1828	0.2120	0.4121	0.4485
ROE-5B	12	0.6623	0.6513	0.5821	0.4733	0.6364	0.6390	0.6075
ROE-5B	13	0.4682	0.5945	0.5475	0.3761	0.4933	0.5739	0.4759
ROE-5B	14	0.3874	0.5246	0.4747	0.2701	0.3492	0.4888	0.4301
ROE-5B	15	0.3605	0.4590	0.4264	0.1960	0.2505	0.4039	0.4233
ROE-6A	2	1.2960	0.9481	0.7618	0.9473	1.0240	1.0455	1.2408
ROE-6A	3	1.2056	0.8607	0.6740	0.8442	0.9122	0.9067	1.0448
ROE-6A	4	1.1628	0.7995	0.6223	0.7527	0.8248	0.7820	0.9570
ROE-6A	5	1.0302	0.7340	0.6141	0.7465	0.7271	0.6288	0.8731
ROE-6A	7	1.3494	0.9499	0.7488	0.9008	1.0382	1.0788	1.2745
ROE-6A	8	1.1941	0.8581	0.6722	0.8454	0.9162	0.9398	0.9717
ROE-6A	9	1.1445	0.7969	0.6252	0.7929	0.8265	0.8114	0.8807
ROE-6A	10	1.0488	0.7314	0.6144	0.7993	0.7280	0.6504	0.8100
ROE-6A	12	1.3400	0.9429	0.7514	0.8525	1.0368	1.0658	1.3263
ROE-6A	13	1.2098	0.8599	0.6852	0.8007	0.9218	0.9652	0.9475
ROE-6A	14	1.1479	0.7943	0.6313	0.7587	0.8237	0.8441	0.8357
ROE-6A	15	1.0515	0.7331	0.6160	0.7537	0.7317	0.7083	0.7850
ROE-6B	2	1.1569	0.8819	0.7217	0.8927	0.9754	0.9717	1.1905
ROE-6B	3	1.0640	0.8163	0.6560	0.8395	0.8698	0.8713	0.9500
ROE-6B	4	0.7928	0.7420	0.5775	0.7251	0.7444	0.7371	0.7875
ROE-6B	5	0.6752	0.6721	0.5564	0.6784	0.6260	0.5992	0.6892
ROE-6B	7	1.1333	0.8792	0.7020	0.8156	0.9789	0.9835	1.2190
ROE-6B	8	1.0046	0.8180	0.6524	0.7940	0.8763	0.8818	0.9269
ROE-6B	9	0.7559	0.7394	0.5782	0.7318	0.7411	0.7311	0.6993
ROE-6B	10	0.6764	0.6695	0.5578	0.7124	0.6232	0.5923	0.6112
ROE-6B	12	1.1587	0.8810	0.7085	0.7753	0.9863	1.0048	1.2531
ROE-6B	13	1.0241	0.8154	0.6585	0.7373	0.8719	0.9216	0.9912
ROE-6B	14	0.7682	0.7411	0.5856	0.6926	0.7419	0.8004	0.7066
ROE-6B	15	0.6854	0.6668	0.5584	0.6703	0.6180	0.6594	0.6240

Appendix D4 Predictions of Resilient Modulus from Artificial Neural Network Models for Evaluation Dataset (Continued)

Sample I.D.	Seq. No.	Experiment M_R/P_a (10^3)	Predicted M_R/P_a (10^3)					
			LN	GRNN	RBFN	MLPN-1	MLPN-2	MLPN-3
ROE-7A	2	1.1808	0.9129	0.8551	1.1847	1.0835	1.0240	0.9666
ROE-7A	3	1.0942	0.8430	0.7892	0.9129	0.9151	0.9444	0.9189
ROE-7A	4	0.9378	0.7687	0.7149	0.6891	0.7847	0.8537	0.8460
ROE-7A	5	0.7932	0.6813	0.6678	0.6879	0.7144	0.7493	0.7559
ROE-7A	7	1.2175	0.9146	0.8521	1.2770	1.0997	1.0407	1.0291
ROE-7A	8	1.0673	0.8403	0.7914	1.0156	0.9032	0.9707	0.9436
ROE-7A	9	0.8826	0.7617	0.7224	0.7469	0.7560	0.8853	0.8607
ROE-7A	10	0.7962	0.6743	0.6763	0.6473	0.6846	0.7819	0.7465
ROE-7A	12	1.1977	0.9076	0.8728	1.3073	1.0990	1.0123	1.3121
ROE-7A	13	1.0599	0.8377	0.8083	1.1285	0.9012	0.9790	1.0025
ROE-7A	14	0.8661	0.7591	0.7335	0.8916	0.7444	0.9303	0.8628
ROE-7A	15	0.7871	0.6716	0.6852	0.7164	0.6676	0.8534	0.6955
ROE-7B	2	1.1382	0.6520	0.8919	1.1963	1.4345	0.9029	1.1340
ROE-7B	3	1.0015	0.5864	0.8022	0.8921	1.1119	0.8265	0.9629
ROE-7B	4	0.7127	0.5078	0.6652	0.6477	0.8161	0.7418	0.9220
ROE-7B	5	0.6501	0.4335	0.6083	0.6755	0.6408	0.6699	0.8805
ROE-7B	7	1.0989	0.6494	0.9227	1.3220	1.5471	0.8957	1.4020
ROE-7B	8	0.8834	0.5882	0.8468	1.0621	1.2283	0.8300	1.0193
ROE-7B	9	0.6729	0.5095	0.7156	0.7728	0.9032	0.7490	0.9337
ROE-7B	10	0.6422	0.4352	0.6365	0.6908	0.7008	0.6763	0.8989
ROE-7B	12	1.0819	0.6511	1.0052	1.4471	1.6954	0.9372	1.7101
ROE-7B	13	0.8588	0.5855	0.9053	1.2360	1.3391	0.8954	1.3453
ROE-7B	14	0.6619	0.5112	0.7653	0.9809	1.0098	0.8337	0.9880
ROE-7B	15	0.6385	0.4369	0.6642	0.8158	0.7813	0.7569	0.9097
ROE-8A	2	0.9194	0.6828	0.8085	1.0250	0.7382	0.7903	1.0698
ROE-8A	3	0.6597	0.6172	0.7300	0.7159	0.5230	0.6571	0.9406
ROE-8A	4	0.5307	0.5473	0.6218	0.4373	0.3435	0.5109	0.8553
ROE-8A	5	0.4872	0.4905	0.5714	0.3498	0.2404	0.3995	0.7828
ROE-8A	7	0.9008	0.6801	0.8411	1.0718	0.7996	0.7917	1.2527
ROE-8A	8	0.6331	0.6189	0.7731	0.8258	0.5836	0.6686	0.9921
ROE-8A	9	0.5188	0.5534	0.6692	0.5705	0.3995	0.5341	0.8818
ROE-8A	10	0.4910	0.4878	0.5902	0.4242	0.2695	0.4047	0.7844
ROE-8A	12	0.9246	0.6775	0.9135	1.1237	0.8704	0.7733	1.7187
ROE-8A	13	0.6517	0.6207	0.8378	0.9444	0.6564	0.6790	1.2093
ROE-8A	14	0.5245	0.5508	0.7098	0.7099	0.4476	0.5517	0.8871
ROE-8A	15	0.5001	0.4852	0.6163	0.5408	0.3115	0.4278	0.7501
ROE-8B	2	1.0389	0.6129	0.8241	0.9835	1.0443	0.8252	1.1930
ROE-8B	3	0.8925	0.5517	0.7480	0.7040	0.7785	0.7409	0.9763
ROE-8B	4	0.6373	0.4818	0.6264	0.4320	0.5401	0.6513	0.8646
ROE-8B	5	0.5647	0.4119	0.5593	0.3501	0.3730	0.5701	0.7635
ROE-8B	7	1.0545	0.6059	0.8702	1.0404	1.1246	0.7851	1.4380
ROE-8B	8	0.8509	0.5491	0.7991	0.8153	0.8654	0.7146	1.0559
ROE-8B	9	0.6079	0.4792	0.6760	0.5509	0.6106	0.6348	0.8942
ROE-8B	10	0.5571	0.4136	0.5886	0.4234	0.4386	0.5641	0.7864
ROE-8B	12	1.0468	0.6033	0.9675	1.1171	1.2351	0.8334	1.7670
ROE-8B	13	0.8070	0.5465	0.8768	0.9397	0.9632	0.7731	1.3689
ROE-8B	14	0.5842	0.4765	0.7321	0.7063	0.6930	0.6887	0.9335
ROE-8B	15	0.5422	0.4110	0.6283	0.5448	0.5088	0.6027	0.7786

Appendix D4 Predictions of Resilient Modulus from Artificial Neural Network Models for Evaluation Dataset (Continued)

Sample I.D.	Seq. No.	Experiment M_R/P_a (10^3)	Predicted M_R/P_a (10^3) LN	GRNN	RBFN	MLPN-1	MLPN-2	MLPN-3
ROE-9A	2	0.9441	0.6413	0.7037	0.8017	0.6278	0.6435	0.7209
ROE-9A	3	0.8391	0.5801	0.6499	0.6246	0.4866	0.5725	0.6158
ROE-9A	4	0.6390	0.5014	0.5578	0.4096	0.3570	0.4989	0.5564
ROE-9A	5	0.5859	0.4315	0.5251	0.3728	0.3009	0.4420	0.5320
ROE-9A	7	0.9205	0.6387	0.6925	0.7416	0.6598	0.6364	0.8044
ROE-9A	8	0.7813	0.5819	0.6561	0.6140	0.5239	0.5759	0.6462
ROE-9A	9	0.6109	0.5032	0.5700	0.4380	0.3900	0.5030	0.5535
ROE-9A	10	0.5749	0.4289	0.5224	0.3854	0.3301	0.4372	0.5220
ROE-9A	12	0.8997	0.6360	0.7091	0.7281	0.6958	0.6030	0.8904
ROE-9A	13	0.7601	0.5792	0.6697	0.6240	0.5562	0.5537	0.6665
ROE-9A	14	0.6006	0.5006	0.5754	0.4810	0.4216	0.4812	0.5414
ROE-9A	15	0.5742	0.4263	0.5172	0.4042	0.3641	0.4054	0.5088
ROE-9B	2	0.6984	0.5563	0.6988	0.8130	0.7439	0.6366	0.7771
ROE-9B	3	0.4764	0.4951	0.6511	0.6418	0.5574	0.5893	0.6253
ROE-9B	4	0.4157	0.4295	0.5595	0.4499	0.4072	0.5479	0.5554
ROE-9B	5	0.4055	0.3552	0.4950	0.3465	0.3007	0.5058	0.5220
ROE-9B	7	0.6262	0.5580	0.6936	0.7649	0.8314	0.6263	0.9412
ROE-9B	8	0.4579	0.4968	0.6631	0.6339	0.6314	0.5844	0.6890
ROE-9B	9	0.4109	0.4269	0.5804	0.4752	0.4606	0.5418	0.5633
ROE-9B	10	0.4061	0.3570	0.5091	0.3818	0.3530	0.5007	0.5186
ROE-9B	12	0.6239	0.5554	0.7283	0.7683	0.9106	0.6155	1.1259
ROE-9B	13	0.4602	0.4942	0.6931	0.6570	0.7001	0.5769	0.7661
ROE-9B	14	0.4150	0.4243	0.6013	0.5289	0.5201	0.5286	0.5747
ROE-9B	15	0.4119	0.3544	0.5221	0.4285	0.4072	0.4761	0.5139
ROE-10A	2	1.0333	0.8404	0.7422	0.8719	0.9523	1.0462	0.9394
ROE-10A	3	0.9939	0.7748	0.6768	0.7847	0.8520	0.9375	0.8182
ROE-10A	4	0.8458	0.6874	0.5855	0.6148	0.7170	0.7598	0.6990
ROE-10A	5	0.7381	0.6131	0.5659	0.5999	0.6172	0.6079	0.6211
ROE-10A	7	1.0594	0.8378	0.7433	0.8898	0.9408	1.0180	0.9553
ROE-10A	8	0.9985	0.7678	0.6756	0.7808	0.8305	0.8875	0.8043
ROE-10A	9	0.8231	0.6892	0.5952	0.6437	0.7088	0.7396	0.6983
ROE-10A	10	0.7512	0.6149	0.5684	0.6207	0.6121	0.6120	0.6287
ROE-10A	12	1.1252	0.8308	0.7570	0.9016	0.9195	0.9827	1.0138
ROE-10A	13	1.0298	0.7652	0.6915	0.7737	0.8133	0.9142	0.8293
ROE-10A	14	0.8393	0.6909	0.6108	0.6426	0.6987	0.8123	0.7194
ROE-10A	15	0.7658	0.6166	0.5753	0.5959	0.6055	0.6765	0.6535
ROE-10B	2	1.0143	0.7268	0.6834	0.7623	0.8078	0.8290	0.6514
ROE-10B	3	0.8473	0.6613	0.6151	0.6650	0.6826	0.7157	0.5382
ROE-10B	4	0.6128	0.5826	0.5228	0.4915	0.5475	0.5920	0.4679
ROE-10B	5	0.5430	0.5258	0.4944	0.4233	0.4656	0.5119	0.4359
ROE-10B	7	0.9221	0.7242	0.6777	0.7764	0.8019	0.7643	0.7072
ROE-10B	8	0.7449	0.6586	0.6148	0.6619	0.6753	0.6724	0.5518
ROE-10B	9	0.5864	0.5887	0.5353	0.5173	0.5560	0.5887	0.4850
ROE-10B	10	0.5455	0.5275	0.4987	0.4384	0.4702	0.5183	0.4566
ROE-10B	12	0.9514	0.7216	0.6979	0.8342	0.7954	0.8042	0.9249
ROE-10B	13	0.7546	0.6560	0.6325	0.6890	0.6673	0.7154	0.6384
ROE-10B	14	0.5779	0.5904	0.5517	0.5436	0.5568	0.6227	0.5439
ROE-10B	15	0.5322	0.5293	0.5063	0.4448	0.4738	0.5349	0.5069

Appendix D4 Predictions of Resilient Modulus from Artificial Neural Network Models for Evaluation Dataset (Continued)

Sample I.D.	Seq. No.	Experiment M_R/P_a (10^3)	Predicted M_R/P_a (10^3)					
			LN	GRNN	RBFN	MLPN-1	MLPN-2	MLPN-3
ROE-11A	2	0.7483	0.7558	0.7022	0.7967	0.7691	0.7487	0.6517
ROE-11A	3	0.5406	0.6902	0.6506	0.7270	0.6659	0.6670	0.5975
ROE-11A	4	0.4552	0.6290	0.5888	0.6077	0.5863	0.6056	0.5674
ROE-11A	5	0.4122	0.5678	0.5515	0.5181	0.5346	0.5512	0.5465
ROE-11A	7	0.7203	0.7575	0.6941	0.7864	0.7571	0.7350	0.6689
ROE-11A	8	0.5086	0.6876	0.6464	0.7115	0.6474	0.6614	0.5935
ROE-11A	9	0.4482	0.6264	0.5897	0.6206	0.5716	0.6083	0.5601
ROE-11A	10	0.4131	0.5652	0.5518	0.5548	0.5263	0.5577	0.5392
ROE-11A	12	0.7196	0.7549	0.7027	0.7799	0.7381	0.6999	0.7228
ROE-11A	13	0.5042	0.6850	0.6544	0.6845	0.6296	0.6430	0.6074
ROE-11A	14	0.4454	0.6281	0.5981	0.6127	0.5623	0.6066	0.5637
ROE-11A	15	0.4112	0.5626	0.5529	0.5535	0.5197	0.5543	0.5368
ROE-11B	2	0.5465	0.4793	0.6397	0.6217	0.5346	0.4778	0.4964
ROE-11B	3	0.3727	0.4094	0.5763	0.5025	0.3765	0.4198	0.4748
ROE-11B	4	0.2961	0.3438	0.4935	0.3620	0.2690	0.3695	0.4659
ROE-11B	5	0.2633	0.2870	0.4522	0.2890	0.2104	0.3269	0.4614
ROE-11B	7	0.4601	0.4767	0.6393	0.6216	0.5845	0.4831	0.4898
ROE-11B	8	0.3186	0.4155	0.5928	0.5195	0.4395	0.4375	0.4693
ROE-11B	9	0.2710	0.3499	0.5150	0.4071	0.3248	0.3874	0.4605
ROE-11B	10	0.2518	0.2887	0.4617	0.3427	0.2582	0.3385	0.4590
ROE-11B	12	0.4390	0.4741	0.6658	0.7193	0.6383	0.4615	0.4766
ROE-11B	13	0.3032	0.4129	0.6188	0.5901	0.4882	0.4058	0.4715
ROE-11B	14	0.2574	0.3517	0.5382	0.4737	0.3775	0.3490	0.4613
ROE-11B	15	0.2425	0.2905	0.4735	0.3886	0.3084	0.2929	0.4604
ROE-12A	2	1.1688	0.8641	0.7488	0.9020	1.0095	1.0948	1.0003
ROE-12A	3	1.1238	0.7942	0.6813	0.7841	0.9189	1.0164	0.9094
ROE-12A	4	0.9525	0.7286	0.6120	0.6398	0.8267	0.9034	0.8226
ROE-12A	5	0.8232	0.6456	0.5797	0.5853	0.7127	0.7316	0.7109
ROE-12A	7	1.2626	0.8615	0.7505	0.9243	1.0008	1.0824	0.9692
ROE-12A	8	1.1894	0.7872	0.6817	0.7727	0.9009	0.9823	0.8757
ROE-12A	9	1.0434	0.7260	0.6195	0.6458	0.8136	0.8668	0.8101
ROE-12A	10	0.8758	0.6429	0.5836	0.5980	0.7023	0.7136	0.7276
ROE-12A	12	1.2955	0.8588	0.7655	0.9758	0.9883	1.0350	1.0005
ROE-12A	13	1.2443	0.7845	0.6996	0.7880	0.8850	0.9639	0.8951
ROE-12A	14	1.0907	0.7233	0.6363	0.6529	0.7971	0.9001	0.8374
ROE-12A	15	0.9077	0.6403	0.5949	0.5852	0.6896	0.7818	0.7750
ROE-12B	2	0.9363	0.7474	0.6798	0.7496	0.8539	0.8876	0.7036
ROE-12B	3	0.8530	0.6949	0.6308	0.6760	0.7639	0.7909	0.6142
ROE-12B	4	0.6507	0.6206	0.5404	0.5151	0.6389	0.6566	0.5166
ROE-12B	5	0.5785	0.5507	0.4919	0.4082	0.5317	0.5408	0.4402
ROE-12B	7	0.9799	0.7491	0.6793	0.7734	0.8506	0.8282	0.7415
ROE-12B	8	0.8970	0.6879	0.6276	0.6538	0.7440	0.7271	0.6326
ROE-12B	9	0.6904	0.6180	0.5467	0.5005	0.6278	0.6314	0.5585
ROE-12B	10	0.5963	0.5481	0.4966	0.4012	0.5252	0.5431	0.5032
ROE-12B	12	1.0195	0.7465	0.6990	0.8669	0.8374	0.8480	0.9042
ROE-12B	13	0.9264	0.6853	0.6468	0.7054	0.7296	0.7699	0.7424
ROE-12B	14	0.7142	0.6154	0.5629	0.5294	0.6150	0.6690	0.6608
ROE-12B	15	0.6083	0.5455	0.5055	0.4101	0.5175	0.5624	0.6114

Appendix D4 Predictions of Resilient Modulus from Artificial Neural Network Models for Evaluation Dataset (Continued)

Sample I.D.	Seq. No.	Experiment M_R/P_a (10^3)	Predicted M_R/P_a (10^3)					
			LN	GRNN	RBFN	MLPN-1	MLPN-2	MLPN-3
ROE-13A	2	0.7928	0.7956	0.7135	0.8433	0.8206	0.9679	0.7871
ROE-13A	3	0.6096	0.7300	0.6446	0.6709	0.7064	0.8332	0.5728
ROE-13A	4	0.5187	0.6644	0.5579	0.4908	0.5881	0.6539	0.4658
ROE-13A	5	0.4779	0.6076	0.5111	0.4044	0.4854	0.4814	0.4187
ROE-13A	7	0.7972	0.7973	0.7132	0.8303	0.8532	1.0075	0.8535
ROE-13A	8	0.5949	0.7361	0.6576	0.6651	0.7418	0.8749	0.5961
ROE-13A	9	0.5112	0.6662	0.5724	0.4908	0.6115	0.6733	0.4719
ROE-13A	10	0.4788	0.6050	0.5223	0.4123	0.4989	0.4789	0.4402
ROE-13A	12	0.8185	0.7947	0.7384	0.8738	0.8751	1.0193	0.9855
ROE-13A	13	0.6079	0.7335	0.6790	0.6816	0.7590	0.9024	0.6979
ROE-13A	14	0.5142	0.6679	0.5969	0.5049	0.6337	0.7308	0.5190
ROE-13A	15	0.4797	0.6024	0.5378	0.4041	0.5121	0.5342	0.4804
ROE-13B	2	0.6757	0.6900	0.6792	0.7174	0.7346	0.7961	0.3817
ROE-13B	3	0.4694	0.6332	0.6247	0.5736	0.5971	0.6611	0.1526
ROE-13B	4	0.3560	0.5720	0.5377	0.3982	0.4579	0.5067	0.0042
ROE-13B	5	0.2899	0.5152	0.4728	0.2698	0.3390	0.3674	-0.0336
ROE-13B	7	0.6169	0.6917	0.6730	0.6948	0.7785	0.7807	0.5383
ROE-13B	8	0.4199	0.6349	0.6276	0.5391	0.6340	0.6383	0.2789
ROE-13B	9	0.3269	0.5737	0.5502	0.3754	0.4900	0.4864	0.0829
ROE-13B	10	0.2823	0.5125	0.4825	0.2539	0.3599	0.3459	0.0363
ROE-13B	12	0.6122	0.6891	0.6942	0.7801	0.8115	0.8148	0.7098
ROE-13B	13	0.4081	0.6323	0.6474	0.5947	0.6609	0.6818	0.5132
ROE-13B	14	0.3178	0.5711	0.5685	0.4138	0.5136	0.5302	0.2403
ROE-13B	15	0.2767	0.5143	0.4990	0.2849	0.3916	0.3914	0.1499
ROE-14A	2	0.6746	0.6930	0.6897	0.6829	0.6861	0.8861	0.5082
ROE-14A	3	0.4804	0.6274	0.6225	0.4831	0.5616	0.7506	0.3211
ROE-14A	4	0.3723	0.5706	0.5368	0.3124	0.4529	0.5789	0.2520
ROE-14A	5	0.3049	0.5138	0.4690	0.1986	0.3467	0.3873	0.2257
ROE-14A	7	0.6509	0.6903	0.6928	0.7053	0.7115	0.9326	0.6039
ROE-14A	8	0.4543	0.6335	0.6437	0.4934	0.5985	0.7915	0.4165
ROE-14A	9	0.3573	0.5723	0.5573	0.2916	0.4774	0.5982	0.3498
ROE-14A	10	0.3059	0.5111	0.4809	0.1654	0.3610	0.3970	0.3413
ROE-14A	12	0.6579	0.6877	0.7208	0.8716	0.7354	0.9544	0.8228
ROE-14A	13	0.4549	0.6309	0.6720	0.6185	0.6181	0.8312	0.5635
ROE-14A	14	0.3563	0.5697	0.5844	0.3785	0.4942	0.6509	0.4610
ROE-14A	15	0.3070	0.5085	0.4992	0.2160	0.3772	0.4466	0.4506
ROE-14B	2	0.3566	0.5935	0.7034	0.5773	0.5424	0.6456	0.2544
ROE-14B	3	0.2147	0.5498	0.6674	0.4517	0.4394	0.5162	0.1000
ROE-14B	4	0.1701	0.5017	0.5973	0.3097	0.3319	0.3704	-0.0479
ROE-14B	5	0.1590	0.4493	0.5050	0.1652	0.2224	0.2232	-0.1408
ROE-14B	7	0.3861	0.5865	0.7064	0.5589	0.5623	0.6244	0.3888
ROE-14B	8	0.2353	0.5428	0.6752	0.4010	0.4543	0.4907	0.2205
ROE-14B	9	0.1858	0.4947	0.6107	0.2426	0.3429	0.3518	0.0646
ROE-14B	10	0.1661	0.4423	0.5182	0.1007	0.2312	0.2176	-0.0137
ROE-14B	12	0.4167	0.5839	0.7342	0.7547	0.5962	0.6543	0.6295
ROE-14B	13	0.2471	0.5358	0.7034	0.5453	0.4723	0.5102	0.4394
ROE-14B	14	0.1917	0.4877	0.6388	0.3556	0.3580	0.3682	0.2491
ROE-14B	15	0.1705	0.4397	0.5490	0.1979	0.2541	0.2371	0.1619

Appendix D4 Predictions of Resilient Modulus from Artificial Neural Network Models for Evaluation Dataset (Continued)

Sample I.D.	Seq. No.	Experiment M_R/P_a (10^3)	Predicted M_R/P_a (10^3)					
			LN	GRNN	RBFN	MLPN-1	MLPN-2	MLPN-3
ROE-15A	2	0.6809	0.8209	0.7205	0.9090	0.7742	0.7362	0.7106
ROE-15A	3	0.5301	0.7597	0.6874	0.8345	0.6828	0.6542	0.6271
ROE-15A	4	0.4450	0.6942	0.6323	0.7121	0.6135	0.5853	0.5871
ROE-15A	5	0.4190	0.6286	0.5983	0.6186	0.5854	0.5304	0.5652
ROE-15A	7	0.6849	0.8183	0.6832	0.7862	0.7543	0.7018	0.7514
ROE-15A	8	0.5439	0.7615	0.6649	0.7431	0.6688	0.6497	0.6235
ROE-15A	9	0.4638	0.6916	0.6180	0.6621	0.5973	0.5881	0.5661
ROE-15A	10	0.4430	0.6216	0.5833	0.5883	0.5733	0.5286	0.5422
ROE-15A	12	0.7175	0.8157	0.6616	0.6922	0.7365	0.6574	0.8375
ROE-15A	13	0.5721	0.7589	0.6453	0.6586	0.6516	0.6037	0.6282
ROE-15A	14	0.4797	0.6889	0.5981	0.6217	0.5847	0.5459	0.5504
ROE-15A	15	0.4583	0.6190	0.5600	0.5759	0.5656	0.4904	0.5263
ROE-15B	2	0.6099	0.9276	0.7160	0.7127	0.7950	0.7820	0.7083
ROE-15B	3	0.4245	0.8533	0.6757	0.7142	0.6879	0.7059	0.6093
ROE-15B	4	0.3612	0.7921	0.6233	0.6600	0.6232	0.6625	0.5776
ROE-15B	5	0.3343	0.7265	0.5888	0.6002	0.5907	0.6290	0.5586
ROE-15B	7	0.5417	0.9249	0.6793	0.5952	0.7663	0.7623	0.8105
ROE-15B	8	0.3847	0.8594	0.6589	0.6040	0.6694	0.7076	0.6341
ROE-15B	9	0.3449	0.7938	0.6142	0.5796	0.5988	0.6654	0.5774
ROE-15B	10	0.3345	0.7239	0.5790	0.5273	0.5669	0.6290	0.5514
ROE-15B	12	0.5305	0.9223	0.6607	0.5071	0.7411	0.7470	0.9869
ROE-15B	13	0.3802	0.8568	0.6442	0.5102	0.6438	0.6957	0.6704
ROE-15B	14	0.3428	0.7912	0.5994	0.5221	0.5761	0.6589	0.5803
ROE-15B	15	0.3367	0.7213	0.5611	0.5042	0.5493	0.6284	0.5476
ROE-16A	2	1.0459	1.0291	0.8560	1.0736	1.1664	1.1871	1.0694
ROE-16A	3	0.9653	0.9592	0.7939	1.0389	1.1121	1.1784	1.0567
ROE-16A	4	0.8460	0.8805	0.7248	0.9400	1.0376	1.1351	1.0416
ROE-16A	5	0.7626	0.7975	0.7071	0.9323	0.9472	1.0327	1.0061
ROE-16A	7	0.9937	1.0265	0.8576	1.0592	1.1611	1.1841	1.0415
ROE-16A	8	0.9418	0.9566	0.8036	1.0120	1.1032	1.1831	1.0135
ROE-16A	9	0.8535	0.8735	0.7320	0.9369	1.0200	1.1199	0.9955
ROE-16A	10	0.8067	0.7949	0.7113	0.9517	0.9317	1.0100	0.9687
ROE-16A	12	1.0604	1.0195	0.8669	1.0397	1.1494	1.1409	1.0433
ROE-16A	13	0.9862	0.9539	0.8217	0.9637	1.0910	1.1320	0.9962
ROE-16A	14	0.8779	0.8753	0.7540	0.8965	1.0084	1.1212	0.9785
ROE-16A	15	0.8247	0.7922	0.7236	0.9130	0.9130	1.0703	0.9599
ROE-16B	2	0.8104	0.7844	0.7043	0.8015	0.9069	0.9843	0.9001
ROE-16B	3	0.6625	0.7189	0.6359	0.6866	0.7963	0.8512	0.6907
ROE-16B	4	0.5288	0.6358	0.5298	0.4968	0.6511	0.6459	0.5503
ROE-16B	5	0.4839	0.5747	0.4937	0.4287	0.5459	0.4902	0.4848
ROE-16B	7	0.7875	0.7818	0.7040	0.7739	0.9090	0.9468	0.9240
ROE-16B	8	0.6635	0.7163	0.6458	0.6449	0.7953	0.8038	0.6814
ROE-16B	9	0.5396	0.6332	0.5423	0.4791	0.6496	0.6163	0.5665
ROE-16B	10	0.4935	0.5720	0.5021	0.4270	0.5467	0.4822	0.5339
ROE-16B	12	0.8148	0.7792	0.7252	0.8313	0.9070	0.9791	1.0530
ROE-16B	13	0.6889	0.7136	0.6681	0.6679	0.7904	0.8617	0.7547
ROE-16B	14	0.5512	0.6350	0.5657	0.4983	0.6523	0.6856	0.6512
ROE-16B	15	0.5037	0.5738	0.5142	0.4298	0.5517	0.5358	0.6366

Appendix D4 Predictions of Resilient Modulus from Artificial Neural Network Models for Evaluation Dataset (Continued)

Sample I.D.	Seq. No.	Experiment M_R/P_a (10^3)	Predicted M_R/P_a (10^3)					
			LN	GRNN	RBFN	MLPN-1	MLPN-2	MLPN-3
ROE-17A	2	1.0817	0.9076	0.7628	0.9185	1.0014	1.0891	1.1688
ROE-17A	3	0.8697	0.8333	0.6855	0.7759	0.9042	1.0030	0.9727
ROE-17A	4	0.6473	0.7633	0.5998	0.6331	0.8023	0.8714	0.8155
ROE-17A	5	0.5880	0.7065	0.5638	0.5859	0.7132	0.7345	0.7358
ROE-17A	7	1.0037	0.8962	0.7568	0.8673	1.0083	1.1135	1.1123
ROE-17A	8	0.8671	0.8350	0.6997	0.7438	0.9245	1.0364	0.9237
ROE-17A	9	0.6235	0.7563	0.6093	0.6109	0.8059	0.8804	0.7555
ROE-17A	10	0.5809	0.6995	0.5745	0.5892	0.7147	0.7322	0.7048
ROE-17A	12	1.0204	0.8936	0.7824	0.8723	1.0213	1.1205	1.1304
ROE-17A	13	0.8712	0.8324	0.7237	0.7214	0.9337	1.0574	0.9482
ROE-17A	14	0.6202	0.7537	0.6319	0.5805	0.8116	0.9167	0.7509
ROE-17A	15	0.5818	0.6969	0.5924	0.5535	0.7193	0.7799	0.7048
ROE-17B	2	0.5343	0.7180	0.7016	0.7281	0.7568	0.7882	0.6113
ROE-17B	3	0.3378	0.6656	0.6519	0.5864	0.6358	0.6765	0.5034
ROE-17B	4	0.2617	0.6088	0.5687	0.4195	0.5091	0.5470	0.3492
ROE-17B	5	0.2261	0.5607	0.5035	0.2983	0.4064	0.4354	0.2047
ROE-17B	7	0.5414	0.7198	0.7012	0.6902	0.8033	0.7979	0.6580
ROE-17B	8	0.3363	0.6673	0.6621	0.5362	0.6747	0.6722	0.5658
ROE-17B	9	0.2547	0.6105	0.5886	0.3781	0.5418	0.5291	0.4139
ROE-17B	10	0.2218	0.5581	0.5178	0.2620	0.4260	0.4006	0.2614
ROE-17B	12	0.5462	0.7172	0.7250	0.7735	0.8396	0.8252	0.7126
ROE-17B	13	0.3352	0.6647	0.6857	0.5918	0.7040	0.7070	0.6778
ROE-17B	14	0.2512	0.6123	0.6195	0.4288	0.5764	0.5817	0.5525
ROE-17B	15	0.2197	0.5555	0.5375	0.2896	0.4478	0.4455	0.3828
ROE-18A	2	0.5998	0.6948	0.6816	0.8210	0.6841	0.6135	0.7403
ROE-18A	3	0.4222	0.6380	0.6544	0.7461	0.5891	0.5714	0.6426
ROE-18A	4	0.3489	0.5724	0.5948	0.6359	0.5201	0.5310	0.5894
ROE-18A	5	0.3278	0.5069	0.5521	0.5580	0.5013	0.4941	0.5624
ROE-18A	7	0.5957	0.6966	0.6564	0.7303	0.6948	0.6139	0.7937
ROE-18A	8	0.4124	0.6398	0.6414	0.6607	0.5950	0.5746	0.6444
ROE-18A	9	0.3447	0.5742	0.5956	0.5809	0.5228	0.5329	0.5677
ROE-18A	10	0.3313	0.5043	0.5505	0.5214	0.5020	0.4878	0.5361
ROE-18A	12	0.6107	0.6939	0.6521	0.6726	0.7030	0.5729	0.7982
ROE-18A	13	0.4178	0.6371	0.6402	0.5969	0.6004	0.5399	0.6346
ROE-18A	14	0.3486	0.5716	0.5940	0.5404	0.5283	0.4996	0.5417
ROE-18A	15	0.3378	0.5016	0.5467	0.5053	0.5086	0.4492	0.5134
ROE-18B	2	0.5630	0.6951	0.6649	0.6969	0.7155	0.6361	0.6877
ROE-18B	3	0.3913	0.6382	0.6397	0.6337	0.6121	0.6090	0.5941
ROE-18B	4	0.3108	0.5770	0.5814	0.5447	0.5379	0.5852	0.5535
ROE-18B	5	0.2928	0.5115	0.5303	0.4701	0.5060	0.5621	0.5344
ROE-18B	7	0.5217	0.6968	0.6401	0.6438	0.7383	0.6270	0.7669
ROE-18B	8	0.3549	0.6400	0.6278	0.5705	0.6259	0.6032	0.6139
ROE-18B	9	0.2965	0.5744	0.5813	0.4846	0.5399	0.5787	0.5439
ROE-18B	10	0.2898	0.5089	0.5326	0.4151	0.5055	0.5545	0.5208
ROE-18B	12	0.5132	0.6942	0.6378	0.6218	0.7606	0.6259	0.7345
ROE-18B	13	0.3439	0.6374	0.6299	0.5387	0.6411	0.6014	0.6120
ROE-18B	14	0.2913	0.5762	0.5874	0.4734	0.5544	0.5723	0.5323
ROE-18B	15	0.2882	0.5062	0.5323	0.4149	0.5131	0.5371	0.5074

Appendix D4 Predictions of Resilient Modulus from Artificial Neural Network Models for Evaluation Dataset (Continued)

Sample I.D.	Seq. No.	Experiment M_R/P_a (10^3)	Predicted M_R/P_a (10^3)					
			LN	GRNN	RBFN	MLPN-1	MLPN-2	MLPN-3
ROE-19A	2	0.8171	0.7852	0.6964	0.8820	0.7861	0.7500	0.7517
ROE-19A	3	0.6922	0.7283	0.6589	0.7936	0.6865	0.6871	0.6499
ROE-19A	4	0.5363	0.6628	0.5972	0.6632	0.6036	0.6313	0.5942
ROE-19A	5	0.4960	0.6016	0.5594	0.5804	0.5665	0.5892	0.5664
ROE-19A	7	0.8352	0.7825	0.6785	0.8551	0.7740	0.7327	0.7729
ROE-19A	8	0.6639	0.7301	0.6532	0.7839	0.6785	0.6822	0.6309
ROE-19A	9	0.5250	0.6645	0.6023	0.6789	0.5926	0.6308	0.5621
ROE-19A	10	0.4978	0.5946	0.5611	0.5944	0.5525	0.5832	0.5338
ROE-19A	12	0.8317	0.7799	0.6815	0.7994	0.7672	0.7209	0.8176
ROE-19A	13	0.6591	0.7275	0.6589	0.7369	0.6691	0.6815	0.6216
ROE-19A	14	0.5236	0.6619	0.6083	0.6690	0.5834	0.6382	0.5429
ROE-19A	15	0.5001	0.5920	0.5660	0.6148	0.5460	0.5861	0.5186
ROE-19B	2	0.8058	0.7263	0.6738	0.7559	0.7746	0.6992	0.6936
ROE-19B	3	0.6155	0.6695	0.6366	0.6622	0.6603	0.6593	0.5997
ROE-19B	4	0.4815	0.6083	0.5747	0.5414	0.5720	0.6262	0.5571
ROE-19B	5	0.4323	0.5427	0.5296	0.4571	0.5220	0.5968	0.5356
ROE-19B	7	0.7778	0.7280	0.6591	0.7709	0.7926	0.6764	0.7557
ROE-19B	8	0.5774	0.6712	0.6338	0.6740	0.6697	0.6456	0.6020
ROE-19B	9	0.4599	0.6100	0.5833	0.5575	0.5745	0.6182	0.5424
ROE-19B	10	0.4262	0.5401	0.5350	0.4549	0.5176	0.5895	0.5191
ROE-19B	12	0.7775	0.7254	0.6650	0.7700	0.8087	0.6972	0.7667
ROE-19B	13	0.5688	0.6686	0.6434	0.6766	0.6792	0.6661	0.5959
ROE-19B	14	0.4541	0.6074	0.5922	0.5820	0.5798	0.6309	0.5296
ROE-19B	15	0.4242	0.5375	0.5408	0.4915	0.5211	0.5902	0.5088
ROE-20A	2	1.0291	0.9331	0.7827	0.9570	1.0802	1.1549	1.0816
ROE-20A	3	0.9551	0.8675	0.7221	0.8894	1.0077	1.1083	1.0260
ROE-20A	4	0.7648	0.7889	0.6452	0.7536	0.9091	1.0016	0.9477
ROE-20A	5	0.6755	0.7102	0.6226	0.7258	0.8072	0.8454	0.8566
ROE-20A	7	1.0450	0.9305	0.7852	0.9654	1.0700	1.1438	1.0451
ROE-20A	8	0.9574	0.8649	0.7287	0.8780	0.9937	1.0886	0.9815
ROE-20A	9	0.7705	0.7906	0.6568	0.7632	0.8978	0.9709	0.9166
ROE-20A	10	0.6882	0.7032	0.6270	0.7446	0.7853	0.8054	0.8395
ROE-20A	12	1.0702	0.9278	0.7990	0.9829	1.0566	1.0949	1.0570
ROE-20A	13	0.9677	0.8623	0.7469	0.8624	0.9764	1.0564	0.9747
ROE-20A	14	0.7833	0.7880	0.6751	0.7443	0.8778	1.0035	0.9148
ROE-20A	15	0.6975	0.7006	0.6389	0.7153	0.7665	0.8905	0.8574
ROE-20B	2	0.8743	0.7812	0.6887	0.7965	0.8994	0.9593	0.7861
ROE-20B	3	0.6994	0.7157	0.6226	0.6983	0.7909	0.8327	0.6754
ROE-20B	4	0.5729	0.6326	0.5278	0.5192	0.6525	0.6579	0.5706
ROE-20B	5	0.5222	0.5627	0.5000	0.4663	0.5446	0.5168	0.4910
ROE-20B	7	0.8657	0.7830	0.6875	0.7965	0.8983	0.9098	0.8027
ROE-20B	8	0.6787	0.7130	0.6258	0.6719	0.7802	0.7748	0.6741
ROE-20B	9	0.5573	0.6344	0.5386	0.5172	0.6498	0.6387	0.6009
ROE-20B	10	0.5202	0.5601	0.5039	0.4670	0.5394	0.5185	0.5447
ROE-20B	12	0.8870	0.7803	0.7060	0.8573	0.8870	0.9288	0.9471
ROE-20B	13	0.6810	0.7104	0.6444	0.6933	0.7667	0.8292	0.7571
ROE-20B	14	0.5531	0.6317	0.5533	0.5255	0.6375	0.6899	0.6874
ROE-20B	15	0.5193	0.5574	0.5119	0.4565	0.5324	0.5470	0.6455

Appendix D4 Predictions of Resilient Modulus from Artificial Neural Network Models for Evaluation Dataset (Continued)

Sample I.D.	Seq. No.	Experiment M_R/P_a (10^3)	Predicted M_R/P_a (10^3)					
			LN	GRNN	RBFN	MLPN-1	MLPN-2	MLPN-3
ROE-21A	2	0.7867	0.9519	0.8216	1.1319	1.1191	1.1098	1.0733
ROE-21A	3	0.6761	0.8776	0.7566	1.0128	1.0507	1.0889	1.0446
ROE-21A	4	0.5867	0.7946	0.6848	0.8212	0.9596	1.0136	0.9889
ROE-21A	5	0.5557	0.7203	0.6670	0.7674	0.8735	0.8985	0.9193
ROE-21A	7	0.8090	0.9493	0.8291	1.1581	1.1128	1.0849	1.0272
ROE-21A	8	0.6664	0.8794	0.7692	1.0193	1.0454	1.0794	0.9943
ROE-21A	9	0.5789	0.7920	0.6906	0.8281	0.9467	0.9948	0.9453
ROE-21A	10	0.5641	0.7177	0.6685	0.7786	0.8604	0.8704	0.8946
ROE-21A	12	0.8343	0.9467	0.8327	1.2002	1.1030	1.0855	1.0382
ROE-21A	13	0.6810	0.8767	0.7825	1.0265	1.0318	1.0462	0.9927
ROE-21A	14	0.5852	0.7893	0.7045	0.8304	0.9298	0.9755	0.9493
ROE-21A	15	0.5712	0.7150	0.6768	0.7698	0.8441	0.9085	0.9140
ROE-21B	2	1.0341	0.9882	0.8332	1.2327	1.1223	1.1539	1.0792
ROE-21B	3	0.9433	0.9270	0.7821	1.2260	1.0636	1.1077	1.0648
ROE-21B	4	0.7474	0.8352	0.7099	1.0909	0.9599	0.9865	1.0228
ROE-21B	5	0.6909	0.7609	0.6962	1.0312	0.8701	0.8632	0.9703
ROE-21B	7	0.9954	0.9856	0.8345	1.2171	1.1044	1.1050	1.0437
ROE-21B	8	0.9039	0.9200	0.7862	1.1761	1.0368	1.0431	1.0192
ROE-21B	9	0.7374	0.8326	0.7163	1.0562	0.9331	0.9114	0.9805
ROE-21B	10	0.6951	0.7583	0.6982	1.0058	0.8421	0.8045	0.9398
ROE-21B	12	1.0469	0.9830	0.8377	1.2121	1.0844	1.0771	1.0634
ROE-21B	13	0.9295	0.9218	0.8009	1.1380	1.0176	1.0279	1.0249
ROE-21B	14	0.7450	0.8344	0.7308	1.0187	0.9101	0.9483	0.9842
ROE-21B	15	0.7060	0.7601	0.7047	0.9638	0.8182	0.8795	0.9536
ROE-22A	2	0.7782	0.7015	0.7090	0.8744	0.7327	0.7784	0.6404
ROE-22A	3	0.5782	0.6403	0.6480	0.7326	0.6008	0.6548	0.5705
ROE-22A	4	0.4872	0.5791	0.5719	0.5615	0.4842	0.5380	0.5355
ROE-22A	5	0.4415	0.5179	0.5266	0.4487	0.3892	0.4318	0.5161
ROE-22A	7	0.7411	0.7032	0.7062	0.8879	0.7546	0.7603	0.6827
ROE-22A	8	0.5598	0.6464	0.6580	0.7685	0.6285	0.6528	0.5726
ROE-22A	9	0.4846	0.5765	0.5786	0.6028	0.4947	0.5346	0.5178
ROE-22A	10	0.4518	0.5153	0.5331	0.5042	0.4033	0.4385	0.4998
ROE-22A	12	0.7528	0.7006	0.7254	0.9030	0.7661	0.7681	0.7898
ROE-22A	13	0.5726	0.6438	0.6743	0.7761	0.6379	0.6807	0.5773
ROE-22A	14	0.4904	0.5739	0.5887	0.6200	0.5054	0.5589	0.4870
ROE-22A	15	0.4589	0.5127	0.5386	0.5181	0.4184	0.4459	0.4695
ROE-22B	2	0.6303	0.6594	0.6899	0.8187	0.7674	0.7360	0.5597
ROE-22B	3	0.4206	0.5939	0.6288	0.6904	0.6088	0.6507	0.5029
ROE-22B	4	0.3575	0.5371	0.5550	0.5382	0.4952	0.5869	0.4830
ROE-22B	5	0.3198	0.4715	0.5006	0.3982	0.3924	0.5215	0.4734
ROE-22B	7	0.6146	0.6568	0.6792	0.8440	0.7878	0.6851	0.6047
ROE-22B	8	0.4156	0.5956	0.6297	0.7261	0.6347	0.6251	0.5000
ROE-22B	9	0.3524	0.5344	0.5587	0.5800	0.5103	0.5724	0.4640
ROE-22B	10	0.3177	0.4689	0.5059	0.4478	0.4089	0.5176	0.4566
ROE-22B	12	0.6150	0.6542	0.6985	0.8892	0.8113	0.7186	0.7234
ROE-22B	13	0.4152	0.5930	0.6468	0.7604	0.6534	0.6521	0.5247
ROE-22B	14	0.3498	0.5318	0.5697	0.6196	0.5273	0.5859	0.4441
ROE-22B	15	0.3166	0.4706	0.5126	0.4896	0.4326	0.5199	0.4319

Appendix D4 Predictions of Resilient Modulus from Artificial Neural Network Models for Evaluation Dataset (Continued)

Sample I.D.	Seq. No.	Experiment M_R/P_a (10^3)	Predicted M_R/P_a (10^3)					
			LN	GRNN	RBFN	MLPN-1	MLPN-2	MLPN-3
ROE-23A	2	0.7199	0.6544	0.6852	0.6837	0.6777	0.6862	0.5685
ROE-23A	3	0.4981	0.5933	0.6316	0.5885	0.5646	0.6022	0.5109
ROE-23A	4	0.3980	0.5364	0.5612	0.4628	0.4719	0.5301	0.4808
ROE-23A	5	0.3312	0.4752	0.5050	0.3510	0.3924	0.4550	0.4595
ROE-23A	7	0.7035	0.6518	0.6831	0.7114	0.6765	0.6722	0.5907
ROE-23A	8	0.4820	0.5950	0.6375	0.5997	0.5721	0.6057	0.5147
ROE-23A	9	0.3835	0.5338	0.5665	0.4720	0.4753	0.5410	0.4792
ROE-23A	10	0.3296	0.4726	0.5098	0.3772	0.4020	0.4747	0.4633
ROE-23A	12	0.7188	0.6492	0.7046	0.8132	0.6740	0.6542	0.6964
ROE-23A	13	0.4762	0.5924	0.6576	0.6635	0.5708	0.6067	0.5615
ROE-23A	14	0.3828	0.5312	0.5809	0.5150	0.4779	0.5440	0.5045
ROE-23A	15	0.3314	0.4700	0.5176	0.4037	0.4112	0.4670	0.4836
ROE-23B	2	0.5167	0.4544	0.6289	0.5189	0.4414	0.4428	0.2185
ROE-23B	3	0.2921	0.4063	0.5866	0.4511	0.3250	0.3891	0.2326
ROE-23B	4	0.2243	0.3539	0.5156	0.3557	0.2192	0.3348	0.2528
ROE-23B	5	0.2029	0.3014	0.4492	0.2598	0.1349	0.2841	0.2715
ROE-23B	7	0.5133	0.4561	0.6306	0.5246	0.5040	0.4584	0.2078
ROE-23B	8	0.3006	0.4037	0.5894	0.4318	0.3727	0.4095	0.2257
ROE-23B	9	0.2269	0.3512	0.5242	0.3451	0.2650	0.3604	0.2578
ROE-23B	10	0.2057	0.2988	0.4586	0.2727	0.1803	0.3102	0.2906
ROE-23B	12	0.5291	0.4535	0.6606	0.6846	0.5589	0.4445	0.3463
ROE-23B	13	0.3065	0.4011	0.6190	0.5493	0.4238	0.3865	0.3071
ROE-23B	14	0.2313	0.3486	0.5482	0.4324	0.3141	0.3282	0.3203
ROE-23B	15	0.2103	0.2918	0.4681	0.3304	0.2229	0.2661	0.3485
ROE-24A	2	0.9450	0.8245	0.7177	0.8592	0.9462	1.0668	0.8898
ROE-24A	3	0.8664	0.7633	0.6604	0.7408	0.8583	0.9780	0.8057
ROE-24A	4	0.6957	0.6846	0.5703	0.5490	0.7358	0.8053	0.7089
ROE-24A	5	0.6142	0.6147	0.5355	0.4763	0.6265	0.6188	0.6221
ROE-24A	7	0.9763	0.8175	0.7105	0.8516	0.9416	1.0640	0.8504
ROE-24A	8	0.9096	0.7563	0.6572	0.7167	0.8507	0.9550	0.7717
ROE-24A	9	0.7337	0.6864	0.5812	0.5618	0.7407	0.7949	0.7097
ROE-24A	10	0.6359	0.6121	0.5400	0.4956	0.6266	0.6175	0.6484
ROE-24A	12	1.0270	0.8148	0.7270	0.9051	0.9381	1.0157	0.9143
ROE-24A	13	0.9459	0.7537	0.6744	0.7406	0.8448	0.9530	0.8158
ROE-24A	14	0.7667	0.6837	0.5974	0.5752	0.7344	0.8464	0.7635
ROE-24A	15	0.6553	0.6094	0.5510	0.4935	0.6235	0.6810	0.7211
ROE-24B	2	0.7886	0.7105	0.6709	0.6893	0.7860	0.8388	0.5829
ROE-24B	3	0.5958	0.6537	0.6171	0.5814	0.6793	0.7113	0.4566
ROE-24B	4	0.4590	0.5925	0.5370	0.4293	0.5656	0.5694	0.3788
ROE-24B	5	0.3766	0.5313	0.4788	0.3043	0.4573	0.4348	0.3218
ROE-24B	7	0.7899	0.7079	0.6660	0.6667	0.7910	0.7956	0.6305
ROE-24B	8	0.6074	0.6554	0.6242	0.5516	0.6911	0.6840	0.4805
ROE-24B	9	0.4574	0.5899	0.5445	0.4028	0.5697	0.5571	0.4107
ROE-24B	10	0.3860	0.5287	0.4855	0.2996	0.4645	0.4465	0.3775
ROE-24B	12	0.8258	0.7052	0.6836	0.7562	0.7924	0.8195	0.8408
ROE-24B	13	0.6382	0.6528	0.6427	0.6085	0.6913	0.7248	0.6199
ROE-24B	14	0.4670	0.5916	0.5674	0.4509	0.5789	0.6028	0.5458
ROE-24B	15	0.3916	0.5261	0.4954	0.3256	0.4697	0.4667	0.5179

Appendix D4 Predictions of Resilient Modulus from Artificial Neural Network Models for Evaluation Dataset (Continued)

Sample I.D.	Seq. No.	Experiment M_R/P_a (10^3)	Predicted M_R/P_a (10^3)					
			LN	GRNN	RBFN	MLPN-1	MLPN-2	MLPN-3
ROE-25A	2	0.8502	0.7495	0.6827	0.8021	0.7598	0.8233	0.7040
ROE-25A	3	0.6659	0.6927	0.6313	0.6788	0.6410	0.7009	0.6060
ROE-25A	4	0.5240	0.6271	0.5518	0.4969	0.5123	0.5587	0.5505
ROE-25A	5	0.4721	0.5616	0.5047	0.3710	0.3994	0.4282	0.5202
ROE-25A	7	0.8421	0.7469	0.6661	0.7472	0.7730	0.8169	0.7812
ROE-25A	8	0.6966	0.6901	0.6219	0.6486	0.6515	0.6945	0.5929
ROE-25A	9	0.5341	0.6245	0.5513	0.5137	0.5225	0.5599	0.5110
ROE-25A	10	0.4866	0.5590	0.5067	0.4167	0.4124	0.4359	0.4813
ROE-25A	12	0.8815	0.7443	0.6784	0.7339	0.7843	0.8046	0.9732
ROE-25A	13	0.7330	0.6918	0.6371	0.6407	0.6695	0.7194	0.6609
ROE-25A	14	0.5517	0.6219	0.5566	0.5151	0.5319	0.5894	0.4972
ROE-25A	15	0.4974	0.5563	0.5067	0.4201	0.4258	0.4592	0.4605
ROE-25B	2	0.5893	0.7181	0.6736	0.8058	0.7904	0.8149	0.6449
ROE-25B	3	0.3514	0.6569	0.6189	0.7130	0.6484	0.7238	0.5219
ROE-25B	4	0.2664	0.6001	0.5457	0.5775	0.5322	0.6453	0.4803
ROE-25B	5	0.2326	0.5476	0.4946	0.4533	0.4393	0.5802	0.4634
ROE-25B	7	0.5399	0.7154	0.6552	0.7486	0.8035	0.7662	0.7680
ROE-25B	8	0.3382	0.6586	0.6126	0.6806	0.6678	0.6904	0.5008
ROE-25B	9	0.2633	0.6018	0.5484	0.5858	0.5497	0.6252	0.4169
ROE-25B	10	0.2333	0.5450	0.4964	0.4839	0.4501	0.5670	0.3980
ROE-25B	12	0.5517	0.7128	0.6702	0.7373	0.8175	0.7968	0.8699
ROE-25B	13	0.3410	0.6560	0.6264	0.6593	0.6781	0.7330	0.6429
ROE-25B	14	0.2650	0.5992	0.5569	0.5769	0.5594	0.6643	0.4404
ROE-25B	15	0.2365	0.5424	0.4979	0.4879	0.4614	0.5935	0.3970
ROE-26A	2	0.8062	0.7890	0.7016	0.8253	0.9325	1.0080	0.8433
ROE-26A	3	0.6491	0.7278	0.6454	0.6874	0.8436	0.9269	0.7633
ROE-26A	4	0.5429	0.6579	0.5637	0.5034	0.7353	0.8047	0.6723
ROE-26A	5	0.5036	0.5923	0.5194	0.4063	0.6348	0.6803	0.5866
ROE-26A	7	0.8070	0.7864	0.7011	0.8727	0.9288	1.0019	0.8324
ROE-26A	8	0.6709	0.7296	0.6541	0.7067	0.8446	0.9100	0.7703
ROE-26A	9	0.5527	0.6553	0.5712	0.4979	0.7293	0.7737	0.7015
ROE-26A	10	0.5165	0.5897	0.5247	0.4000	0.6316	0.6682	0.6441
ROE-26A	12	0.8422	0.7837	0.7169	0.9997	0.9204	0.9557	0.9078
ROE-26A	13	0.7012	0.7269	0.6718	0.7948	0.8344	0.8869	0.8377
ROE-26A	14	0.5658	0.6570	0.5927	0.5659	0.7260	0.8082	0.7809
ROE-26A	15	0.5283	0.5871	0.5357	0.4275	0.6251	0.7174	0.7358
ROE-26B	2	0.6684	0.7358	0.6816	0.7664	0.8633	0.8913	0.7020
ROE-26B	3	0.5167	0.6746	0.6251	0.6575	0.7625	0.7833	0.6117
ROE-26B	4	0.4207	0.6091	0.5410	0.4991	0.6535	0.6689	0.5278
ROE-26B	5	0.3616	0.5479	0.4865	0.3804	0.5566	0.5686	0.4536
ROE-26B	7	0.6826	0.7332	0.6800	0.8004	0.8532	0.8323	0.7176
ROE-26B	8	0.5100	0.6764	0.6356	0.6583	0.7585	0.7375	0.6437
ROE-26B	9	0.4146	0.6108	0.5558	0.4871	0.6504	0.6493	0.5850
ROE-26B	10	0.3653	0.5453	0.4933	0.3597	0.5501	0.5711	0.5329
ROE-26B	12	0.6905	0.7306	0.6987	0.9360	0.8398	0.8262	0.8563
ROE-26B	13	0.5146	0.6738	0.6561	0.7509	0.7441	0.7641	0.7631
ROE-26B	14	0.4159	0.6082	0.5752	0.5484	0.6376	0.6835	0.7065
ROE-26B	15	0.3676	0.5426	0.5044	0.3962	0.5416	0.5941	0.6654

Appendix D4 Predictions of Resilient Modulus from Artificial Neural Network Models for Evaluation Dataset (Continued)

Sample I.D.	Seq. No.	Experiment M_R/P_a (10^3)	Predicted M_R/P_a (10^3)					
			LN	GRNN	RBFN	MLPN-1	MLPN-2	MLPN-3
ROE-27A	2	0.7478	0.6528	0.6975	0.6640	0.6923	0.7243	0.5680
ROE-27A	3	0.5415	0.5785	0.6256	0.5467	0.5649	0.6357	0.5007
ROE-27A	4	0.4420	0.5130	0.5475	0.4183	0.4704	0.5662	0.4669
ROE-27A	5	0.3872	0.4518	0.5069	0.3673	0.4090	0.5002	0.4456
ROE-27A	7	0.7155	0.6546	0.7023	0.7388	0.6930	0.7100	0.6008
ROE-27A	8	0.4940	0.5803	0.6356	0.5735	0.5670	0.6352	0.5167
ROE-27A	9	0.4100	0.5191	0.5638	0.4458	0.4817	0.5836	0.4865
ROE-27A	10	0.3711	0.4535	0.5133	0.3825	0.4205	0.5245	0.4699
ROE-27A	12	0.6970	0.6563	0.7262	0.9065	0.6923	0.6865	0.7070
ROE-27A	13	0.4726	0.5820	0.6604	0.6797	0.5676	0.6377	0.5635
ROE-27A	14	0.3928	0.5208	0.5827	0.5175	0.4858	0.5960	0.5181
ROE-27A	15	0.3579	0.4509	0.5208	0.4105	0.4282	0.5263	0.4961
ROE-27B	2	0.2784	0.4837	0.6453	0.5183	0.4885	0.4959	0.2799
ROE-27B	3	0.1934	0.4356	0.6117	0.4604	0.3815	0.4383	0.2791
ROE-27B	4	0.1781	0.3788	0.5413	0.3738	0.2751	0.3731	0.2879
ROE-27B	5	0.1784	0.3176	0.4623	0.2761	0.1856	0.3068	0.2996
ROE-27B	7	0.3350	0.4767	0.6464	0.5763	0.5133	0.5019	0.3222
ROE-27B	8	0.2241	0.4242	0.6079	0.4703	0.3979	0.4513	0.3156
ROE-27B	9	0.1944	0.3674	0.5391	0.3667	0.2956	0.3943	0.3295
ROE-27B	10	0.1898	0.3106	0.4685	0.2853	0.2175	0.3348	0.3492
ROE-27B	12	0.3575	0.4740	0.6784	0.7952	0.5502	0.4971	0.4656
ROE-27B	13	0.2354	0.4216	0.6398	0.6380	0.4335	0.4385	0.3998
ROE-27B	14	0.2025	0.3604	0.5588	0.4773	0.3249	0.3661	0.3899
ROE-27B	15	0.1988	0.3036	0.4799	0.3601	0.2512	0.2980	0.4013
ROE-28A	2	0.7927	0.7847	0.7280	0.9637	0.8157	0.8832	0.7442
ROE-28A	3	0.5779	0.7191	0.6690	0.8096	0.6874	0.7445	0.6412
ROE-28A	4	0.4752	0.6579	0.6010	0.6361	0.5780	0.6137	0.5913
ROE-28A	5	0.4346	0.5968	0.5631	0.5268	0.4874	0.4929	0.5615
ROE-28A	7	0.7644	0.7864	0.7175	0.9549	0.8288	0.8866	0.8208
ROE-28A	8	0.5496	0.7252	0.6736	0.8454	0.7054	0.7602	0.6660
ROE-28A	9	0.4697	0.6597	0.6077	0.7007	0.5868	0.6273	0.5905
ROE-28A	10	0.4335	0.5941	0.5656	0.5961	0.4926	0.5031	0.5537
ROE-28A	12	0.7759	0.7838	0.7269	0.9165	0.8315	0.8508	0.9369
ROE-28A	13	0.5578	0.7226	0.6817	0.8181	0.7055	0.7639	0.7041
ROE-28A	14	0.4733	0.6571	0.6117	0.7037	0.5879	0.6538	0.5868
ROE-28A	15	0.4392	0.5915	0.5648	0.6084	0.4985	0.5281	0.5398
ROE-28B	2	0.6269	0.7349	0.7073	0.8623	0.8069	0.8099	0.6699
ROE-28B	3	0.3911	0.6737	0.6594	0.7418	0.6666	0.7151	0.5915
ROE-28B	4	0.3130	0.6125	0.5856	0.5752	0.5455	0.6294	0.5517
ROE-28B	5	0.2880	0.5513	0.5337	0.4343	0.4470	0.5544	0.5299
ROE-28B	7	0.5411	0.7367	0.6922	0.8517	0.8289	0.7802	0.7600
ROE-28B	8	0.3578	0.6755	0.6546	0.7513	0.6831	0.6931	0.6162
ROE-28B	9	0.2994	0.6143	0.5907	0.6203	0.5597	0.6186	0.5503
ROE-28B	10	0.2817	0.5487	0.5367	0.4890	0.4553	0.5480	0.5193
ROE-28B	12	0.5418	0.7297	0.7030	0.8327	0.8301	0.7872	0.8501
ROE-28B	13	0.3538	0.6728	0.6662	0.7391	0.6916	0.7257	0.6671
ROE-28B	14	0.2968	0.6117	0.5976	0.6295	0.5673	0.6522	0.5489
ROE-28B	15	0.2825	0.5461	0.5374	0.5110	0.4652	0.5680	0.5015

Appendix D4 Predictions of Resilient Modulus from Artificial Neural Network Models for Evaluation Dataset (Continued)

Sample I.D.	Seq. No.	Experiment M_R/P_a (10^3)	Predicted M_R/P_a (10^3)					
			LN	GRNN	RBFN	MLPN-1	MLPN-2	MLPN-3
ROE-29A	2	0.8413	0.6657	0.6735	0.7500	0.6252	0.6716	0.5636
ROE-29A	3	0.6794	0.6089	0.6249	0.6225	0.5022	0.5522	0.5131
ROE-29A	4	0.4994	0.5433	0.5427	0.4389	0.3754	0.4261	0.4869
ROE-29A	5	0.4306	0.4778	0.4883	0.3103	0.2726	0.3156	0.4734
ROE-29A	7	0.8234	0.6631	0.6624	0.7032	0.6440	0.6676	0.5751
ROE-29A	8	0.6768	0.6063	0.6194	0.5871	0.5194	0.5556	0.4869
ROE-29A	9	0.5025	0.5407	0.5453	0.4445	0.3936	0.4404	0.4550
ROE-29A	10	0.4391	0.4752	0.4915	0.3503	0.2949	0.3341	0.4480
ROE-29A	12	0.8520	0.6605	0.6797	0.7307	0.6621	0.6479	0.6951
ROE-29A	13	0.6980	0.6037	0.6345	0.5994	0.5365	0.5568	0.5072
ROE-29A	14	0.5092	0.5381	0.5541	0.4598	0.4126	0.4424	0.4465
ROE-29A	15	0.4434	0.4725	0.4943	0.3610	0.3189	0.3244	0.4391
ROE-29B	2	0.6158	0.5919	0.6428	0.6036	0.5618	0.5903	0.3794
ROE-29B	3	0.3779	0.5307	0.5848	0.4755	0.4161	0.5000	0.3615
ROE-29B	4	0.2924	0.4739	0.5087	0.3247	0.3011	0.4257	0.3658
ROE-29B	5	0.2598	0.4127	0.4505	0.1950	0.2013	0.3538	0.3737
ROE-29B	7	0.5380	0.5937	0.6332	0.5439	0.6057	0.5824	0.3409
ROE-29B	8	0.3568	0.5325	0.5846	0.4299	0.4557	0.5043	0.2779
ROE-29B	9	0.2919	0.4713	0.5109	0.3094	0.3310	0.4342	0.2928
ROE-29B	10	0.2642	0.4101	0.4539	0.2192	0.2330	0.3669	0.3199
ROE-29B	12	0.5590	0.5910	0.6527	0.5945	0.6400	0.5807	0.5356
ROE-29B	13	0.3572	0.5298	0.6027	0.4580	0.4874	0.5031	0.3236
ROE-29B	14	0.2899	0.4687	0.5219	0.3361	0.3628	0.4227	0.3093
ROE-29B	15	0.2623	0.4075	0.4570	0.2424	0.2672	0.3419	0.3355
WOE-1A	2	0.6444	0.6268	0.6779	0.8664	0.6630	0.5919	0.7311
WOE-1A	3	0.5655	0.5612	0.6283	0.7274	0.5393	0.5402	0.6286
WOE-1A	4	0.4892	0.4869	0.5568	0.5746	0.4582	0.4895	0.5742
WOE-1A	5	0.4713	0.4082	0.5329	0.5663	0.4438	0.4372	0.5453
WOE-1A	7	0.6437	0.6198	0.6644	0.8094	0.6736	0.5851	0.7486
WOE-1A	8	0.5500	0.5586	0.6285	0.6996	0.5560	0.5392	0.6151
WOE-1A	9	0.4882	0.4799	0.5613	0.5715	0.4719	0.4820	0.5465
WOE-1A	10	0.4753	0.4056	0.5334	0.5672	0.4586	0.4263	0.5221
WOE-1A	12	0.6457	0.6215	0.6755	0.7884	0.7100	0.5572	0.7652
WOE-1A	13	0.5535	0.5559	0.6396	0.6849	0.5782	0.5110	0.5937
WOE-1A	14	0.4916	0.4773	0.5689	0.5848	0.4935	0.4473	0.5211
WOE-1A	15	0.4824	0.4030	0.5360	0.5674	0.4783	0.3805	0.5033
WOE-1B	2	0.5885	0.5793	0.6684	0.7715	0.7274	0.5894	0.6882
WOE-1B	3	0.5036	0.5094	0.6167	0.6170	0.5708	0.5494	0.5820
WOE-1B	4	0.4499	0.4307	0.5341	0.4484	0.4641	0.5100	0.5381
WOE-1B	5	0.4459	0.3564	0.5092	0.4407	0.4361	0.4723	0.5202
WOE-1B	7	0.5682	0.5723	0.6586	0.7362	0.7561	0.5791	0.7342
WOE-1B	8	0.4782	0.5024	0.6178	0.5983	0.5943	0.5418	0.5809
WOE-1B	9	0.4475	0.4281	0.5466	0.4617	0.4903	0.5031	0.5266
WOE-1B	10	0.4448	0.3538	0.5117	0.4431	0.4589	0.4618	0.5085
WOE-1B	12	0.5632	0.5697	0.6748	0.7429	0.8037	0.5636	0.7394
WOE-1B	13	0.4814	0.5041	0.6388	0.6258	0.6412	0.5244	0.5822
WOE-1B	14	0.4526	0.4254	0.5582	0.5005	0.5228	0.4723	0.5124
WOE-1B	15	0.4514	0.3512	0.5160	0.4573	0.4874	0.4202	0.4972

Appendix D4 Predictions of Resilient Modulus from Artificial Neural Network Models for Evaluation Dataset (Continued)

Sample I.D.	Seq. No.	Experiment M_R/P_a (10^3)	Predicted M_R/P_a (10^3) LN	GRNN	RBFN	MLPN-1	MLPN-2	MLPN-3
WOE-2A	2	0.5888	0.5918	0.6612	0.8648	0.5582	0.4945	0.7060
WOE-2A	3	0.5122	0.5218	0.6123	0.7613	0.4572	0.4383	0.6185
WOE-2A	4	0.4569	0.4432	0.5481	0.6542	0.4122	0.3824	0.5734
WOE-2A	5	0.4477	0.3645	0.5358	0.6968	0.4173	0.3286	0.5490
WOE-2A	7	0.5880	0.5891	0.6383	0.7477	0.5764	0.4959	0.7179
WOE-2A	8	0.5021	0.5192	0.6038	0.6682	0.4753	0.4394	0.5948
WOE-2A	9	0.4609	0.4405	0.5468	0.6083	0.4323	0.3770	0.5438
WOE-2A	10	0.4560	0.3619	0.5280	0.6720	0.4336	0.3137	0.5229
WOE-2A	12	0.5964	0.5865	0.6360	0.6954	0.5989	0.4509	0.7222
WOE-2A	13	0.5043	0.5210	0.6052	0.6195	0.5019	0.3979	0.5768
WOE-2A	14	0.4610	0.4423	0.5456	0.5767	0.4568	0.3281	0.5200
WOE-2A	15	0.4627	0.3636	0.5197	0.6217	0.4536	0.2558	0.5043
WOE-2B	2	0.5390	0.5355	0.6467	0.7015	0.6023	0.4905	0.6397
WOE-2B	3	0.4569	0.4699	0.6004	0.5938	0.4868	0.4535	0.5674
WOE-2B	4	0.4123	0.3956	0.5289	0.4797	0.4190	0.4144	0.5356
WOE-2B	5	0.4131	0.3169	0.5055	0.5007	0.4160	0.3718	0.5199
WOE-2B	7	0.5283	0.5328	0.6274	0.6097	0.6381	0.4916	0.6754
WOE-2B	8	0.4461	0.4629	0.5924	0.5118	0.5111	0.4496	0.5592
WOE-2B	9	0.4166	0.3886	0.5301	0.4368	0.4452	0.4037	0.5209
WOE-2B	10	0.4193	0.3143	0.5012	0.4750	0.4400	0.3568	0.5073
WOE-2B	12	0.5369	0.5302	0.6310	0.5987	0.6801	0.4506	0.6869
WOE-2B	13	0.4539	0.4647	0.6002	0.5035	0.5532	0.4059	0.5585
WOE-2B	14	0.4262	0.3860	0.5310	0.4346	0.4782	0.3483	0.5084
WOE-2B	15	0.4275	0.3117	0.4968	0.4531	0.4681	0.2934	0.4971
WOE-3A	2	0.9412	1.0074	0.6755	0.7078	0.8751	0.9273	0.8590
WOE-3A	3	0.9946	0.9243	0.6072	0.6291	0.7782	0.8111	0.7256
WOE-3A	4	1.0037	0.8500	0.5656	0.5759	0.7332	0.7367	0.6615
WOE-3A	5	1.0220	0.7888	0.5496	0.6495	0.7317	0.6944	0.6250
WOE-3A	7	1.0247	1.0091	0.6615	0.6712	0.8446	0.8988	0.8353
WOE-3A	8	1.0185	0.9261	0.6066	0.6227	0.7440	0.8022	0.6832
WOE-3A	9	1.0266	0.8518	0.5668	0.5736	0.6980	0.7351	0.6225
WOE-3A	10	1.0439	0.7950	0.5521	0.6047	0.6943	0.6973	0.5931
WOE-3A	12	1.0618	1.0109	0.6605	0.6141	0.8179	0.9391	0.8516
WOE-3A	13	1.0333	0.9278	0.6125	0.6196	0.7151	0.8452	0.6766
WOE-3A	14	1.0394	0.8623	0.5750	0.6285	0.6723	0.7863	0.6185
WOE-3A	15	1.0601	0.8011	0.5540	0.6643	0.6654	0.7477	0.5871
WOE-3B	2	0.8698	0.9672	0.6730	0.6194	0.7645	0.8199	0.7391
WOE-3B	3	0.8683	0.8885	0.6018	0.5876	0.6599	0.7488	0.6350
WOE-3B	4	0.8503	0.8229	0.5506	0.5558	0.6065	0.7079	0.5957
WOE-3B	5	0.8208	0.7661	0.5311	0.5904	0.5953	0.6818	0.5739
WOE-3B	7	0.9067	0.9689	0.6553	0.5755	0.7413	0.7830	0.7840
WOE-3B	8	0.8542	0.8859	0.5964	0.5289	0.6280	0.7263	0.6262
WOE-3B	9	0.8425	0.8247	0.5530	0.4929	0.5778	0.6963	0.5845
WOE-3B	10	0.8219	0.7679	0.5319	0.5024	0.5658	0.6741	0.5623
WOE-3B	12	0.9319	0.9706	0.6546	0.5574	0.7239	0.8331	0.8492
WOE-3B	13	0.8636	0.8832	0.5980	0.5217	0.6026	0.7776	0.6382
WOE-3B	14	0.8519	0.8221	0.5554	0.5158	0.5546	0.7379	0.5873
WOE-3B	15	0.8253	0.7609	0.5307	0.5403	0.5458	0.7015	0.5616

Appendix D4 Predictions of Resilient Modulus from Artificial Neural Network Models for Evaluation Dataset (Continued)

Sample I.D.	Seq. No.	Experiment M_R/P_a (10^3)	Predicted M_R/P_a (10^3) LN	GRNN	RBFN	MLPN-1	MLPN-2	MLPN-3
WOE-4A	2	0.6835	0.8666	0.6997	0.7551	0.7994	0.8078	0.7053
WOE-4A	3	0.6543	0.7923	0.6310	0.6466	0.6925	0.7268	0.6142
WOE-4A	4	0.6416	0.7180	0.5755	0.5491	0.6288	0.6692	0.5752
WOE-4A	5	0.6432	0.6437	0.5628	0.6119	0.6227	0.6258	0.5531
WOE-4A	7	0.6403	0.8683	0.6850	0.7306	0.7810	0.7912	0.7447
WOE-4A	8	0.6430	0.7940	0.6311	0.6445	0.6696	0.7202	0.6015
WOE-4A	9	0.6608	0.7197	0.5789	0.5510	0.6042	0.6670	0.5564
WOE-4A	10	0.6690	0.6454	0.5622	0.5686	0.5964	0.6242	0.5356
WOE-4A	12	0.6757	0.8657	0.6846	0.6718	0.7602	0.8054	0.8117
WOE-4A	13	0.6758	0.7914	0.6327	0.6224	0.6474	0.7494	0.6023
WOE-4A	14	0.6848	0.7215	0.5817	0.5759	0.5866	0.7046	0.5517
WOE-4A	15	0.6935	0.6515	0.5603	0.5764	0.5776	0.6551	0.5319
WOE-4B	2	0.5109	0.5571	0.6989	0.8577	0.9142	0.6404	0.7816
WOE-4B	3	0.4101	0.4916	0.6363	0.6622	0.7189	0.6035	0.6433
WOE-4B	4	0.3663	0.4173	0.5469	0.4746	0.5691	0.5683	0.5674
WOE-4B	5	0.3487	0.3473	0.5183	0.4644	0.5019	0.5361	0.5348
WOE-4B	7	0.4424	0.5632	0.7104	0.9309	1.0134	0.6262	0.8673
WOE-4B	8	0.3784	0.4933	0.6616	0.7384	0.7837	0.5940	0.6725
WOE-4B	9	0.3502	0.4190	0.5756	0.5428	0.6166	0.5615	0.5606
WOE-4B	10	0.3435	0.3491	0.5299	0.4819	0.5361	0.5290	0.5223
WOE-4B	12	0.4682	0.5606	0.7458	0.9788	1.0918	0.6381	0.8879
WOE-4B	13	0.3855	0.4950	0.7013	0.8245	0.8599	0.5989	0.6895
WOE-4B	14	0.3504	0.4207	0.6077	0.6446	0.6747	0.5541	0.5462
WOE-4B	15	0.3423	0.3464	0.5453	0.5389	0.5770	0.5085	0.5051
WOE-5A	2	0.7260	0.6480	0.6354	0.6520	0.5983	0.6077	0.6095
WOE-5A	3	0.7197	0.5737	0.5815	0.6072	0.5143	0.5607	0.5619
WOE-5A	4	0.6816	0.5169	0.5366	0.5514	0.4868	0.5249	0.5437
WOE-5A	5	0.6041	0.4338	0.5154	0.5621	0.5025	0.4682	0.5274
WOE-5A	7	0.7364	0.6453	0.6210	0.6343	0.5897	0.6064	0.5748
WOE-5A	8	0.7055	0.5798	0.5846	0.5834	0.5144	0.5695	0.5339
WOE-5A	9	0.6562	0.5142	0.5391	0.5372	0.4831	0.5293	0.5181
WOE-5A	10	0.6072	0.4356	0.5148	0.5597	0.4986	0.4731	0.5084
WOE-5A	12	0.7579	0.6427	0.6263	0.6528	0.5857	0.5934	0.5658
WOE-5A	13	0.7102	0.5772	0.5903	0.5781	0.5116	0.5599	0.5232
WOE-5A	14	0.6523	0.5116	0.5440	0.5387	0.4839	0.5121	0.5088
WOE-5A	15	0.6061	0.4286	0.5194	0.5714	0.5018	0.4389	0.5006
WOE-5B	2	0.6597	0.5904	0.6098	0.4851	0.5963	0.5623	0.5562
WOE-5B	3	0.5923	0.5248	0.5645	0.4322	0.5071	0.5284	0.5275
WOE-5B	4	0.4755	0.4549	0.5055	0.3539	0.4579	0.4920	0.5145
WOE-5B	5	0.4300	0.3806	0.4827	0.3508	0.4640	0.4505	0.5067
WOE-5B	7	0.6014	0.5877	0.5967	0.5295	0.6062	0.5631	0.5429
WOE-5B	8	0.5118	0.5266	0.5641	0.4471	0.5181	0.5330	0.5152
WOE-5B	9	0.4333	0.4479	0.5064	0.3483	0.4616	0.4899	0.5036
WOE-5B	10	0.4053	0.3780	0.4827	0.3379	0.4686	0.4467	0.4987
WOE-5B	12	0.5773	0.5895	0.6036	0.6394	0.6307	0.5562	0.5261
WOE-5B	13	0.4768	0.5239	0.5713	0.5199	0.5303	0.5150	0.5079
WOE-5B	14	0.4098	0.4496	0.5140	0.4149	0.4736	0.4648	0.4991
WOE-5B	15	0.3912	0.3753	0.4862	0.3787	0.4784	0.4111	0.4947